

GLAXOSMITHKLINE

University of Strathclyde
Department of Pure and Applied Chemistry

*The synthesis & optimisation of irreversible ITK
inhibitors as a potential new treatment for severe
asthma*

Thesis submitted to the University of Strathclyde
in fulfilment of the requirements for the degree of
Doctor of Philosophy

by

Sébastien André Campos

2013

Declaration of Copyright

This thesis is the result of the author's original research. It has been composed by the author and has not been previously submitted for examination which has led to the award of a degree.

The copyright of this thesis belongs to the author under the terms of the United Kingdom Copyright Acts as qualified by University of Strathclyde Regulation 3.50. Due acknowledgement must always be made of the use of any material contained in, or derived from, this thesis.

Signed:

Date:

Abstract

Interleukin-2-inducible tyrosine kinase (ITK) is a member of the Tec family of non-receptor tyrosine kinases and plays an important role in T cell receptor signalling. Phosphorylation of ITK ultimately results in the release of several cytokines from T cells which are involved in the inflammatory response in asthmatic patients. ITK inhibitors could represent useful anti-inflammatory agents for severe asthma. This thesis describes the design and development of irreversible ITK inhibitors. It was envisaged that these compounds could provide a better duration of action *in vivo* compared to typical reversible inhibitors. After explaining first how irreversible ITK inhibition may be achieved, the medicinal chemistry undertaken to synthesise the designed molecules, and assess their activity profiles in various biological assays, is presented. Evidence of the covalent binding between some specific analogues and ITK is illustrated, the most explicit proof being a crystal structure of a kinase/inhibitor complex, clearly displaying a bond between the inhibitor and the cysteine residue present in the ITK active site. However, the early irreversible ITK inhibitors developed did not possess the required profile (cellular activity, duration of action) expected from an irreversible ITK inhibitor drug candidate.

Three approaches are then described to improve the cellular activity of these irreversible ITK inhibitors. Firstly, the nature of the electrophilic moieties was investigated. Compounds presenting improved irreversible ITK inhibitor profiles (activities and rate of the covalent reaction) have been developed but these species could not be progressed further due to their high probability of toxicity issues in the body. Secondly, the positioning of the electrophilic group with respect to the ITK active site cysteine is then discussed; this strategy did not lead to any improved compounds. Finally, moving to a chemically more challenging pyridine template provided inhibitors with enhanced non-covalent ITK recognition. Optimisation of the compounds from this series provided irreversible inhibitors with the required *in vitro* and *in vivo* activity profiles for a drug candidate within our laboratories. The progression of the lead covalent ITK inhibitor from this research programme was ultimately halted due to toxicology findings from a 14 day rat study.

The final part of the thesis studies the Buchwald-Hartwig amination reaction used in the synthetic route leading to the best covalent ITK inhibitors. This coupling required 30 mol % of palladium catalyst, which, on large scale, represents a significant amount of metal waste. The investigation of this coupling strongly suggested that the substrates involved in the reaction were poisoning the catalyst. The final results from this study indicate that an alternative palladium catalyst, allowing full conversion to the required product at room temperature, has been identified.

Acknowledgement

First of all, I would like to thank my academic supervisor, Prof William Kerr (a.k.a Billy), for his constant support and commitment into this novel and unusual joint PhD programme between GlaxoSmithKline and the University of Strathclyde, Glasgow. Collaborating with you has been a pleasure, an honour and a great learning experience. The scientific discussions we have had for the past four years have challenged and changed my way of thinking about chemistry and made me a more accomplished scientist. I will definitely miss those exchanges in the future but be assured that you will remain a great source of inspiration for the rest of my career. I also want to thank my internal examiner, Prof Jonathan Percy, for his thorough review of this work and important comments to improve this thesis.

Secondly, I am indebted to my two GSK supervisors, John Pritchard and Dr John Harling, a.k.a. the “two Johns”, who, four years ago, took the risk to be part of this programme, which involved a lot of mentoring, supporting and reviewing the many versions of this work. I am particularly grateful to my team leader, John Harling, for originally presenting me with the project and allowing me to work independently on this research programme over the length of my PhD. Many thanks to John Pritchard for committing to being my PhD supervisor, even when we went into two different directions within GSK. You might have regretted this choice, John, especially on the day of my thirty month *viva* when you had the luxury of spending a long night on the train from Glasgow to London. A massive thank you to both of you, I would not be writing the final lines of this thesis without you.

The next “merci” goes to Dr Harry Kelly, who has initiated this collaborative PhD programme between GlaxoSmithKline and the University of Strathclyde. I know that setting up this unusual programme has been a challenge and countless hours of hard work for Harry and his team but I believe they should be proud of what they have achieved. It is an exceptional development opportunity for graduates like me to be able to enter a four-year PhD while continuing working at GSK. For all the work you have done before, during and surely after my PhD, “un grand merci à toi, Harry”. I

am also grateful to Dave Allen, Head of Respiratory Therapy Area Unit, and to Dr Patrick Vallance, President of GSK pharmaceutical R&D, for their amazing support to this programme and for sparing some of their extremely valuable time discussing my progress, concerns and achievements.

Despite leading the medicinal chemistry of this research programme quite independently, I would not have been able to successfully develop these compounds without the amazing work performed by all the ITK project team. In particular, my thanks go to the project leader, Dr John Harling, for sharing his medicinal chemistry ideas, to Dr Angela Deakin, for the time she spent explaining biology to me, to Dr Michelle Heathcote and Fiona Lucas for running the biological assays, to Dr Rachel Grimley, Laiq Chaudry and Catherine Nye for the kinetic experiment data, to Dr Nick Barton for his help with the molecular modelling, to Becky Graves and John Barrett for the DMPK data, to Bob Gibbon for the SLF solubility, to Rob Willacy for his help during the recrystallisation, to Rob Wheeler, Dr Matthew Walker and Hugh Clark for their advice with large scale syntheses and to Ian Smith for his medicinal chemistry expertise on ITK reversible compounds. I am also thankful to Dr Roberto Solari, head of the Allergic Inflammation DPU at the time, for his support of this research programme, to Dr Amanda Gladwin, the programme patent attorney, for reading and approving all of my reports in amazing timelines and to Sean Lynn, who has always made himself available to discuss particularly complex NMR spectra. I am also indebted to my former GSK manager, Dr Vipul Patel, who kindly agreed to scientifically review this final thesis. Knowing your level of scientific rigour, I am relieved that you did not ask me to rewrite that many paragraphs.

The past four years in the laboratory were made fun and enjoyable in large parts due to the presence of a fantastic group of chemists: Afjal Miah, Ian Smith, Dr Jonhathan Shannon, Niall Anderson, Mubina Mohamed (nearly Dr), as well as industrial students (in particular Samson Perrot, Jothi Kothandaraman and Lola Beltran Molina), and all the other chemists who have spent some time in laboratory 2S113 from 2009 to 2013 and who are too numerous to name individually here. I am also thankful to the “petite France” group of chemists – and now friends – from GSK Stevenage, with whom I have spent most of my lunch breaks for the past four years.

You have made these breaks really enjoyable and relaxing and I am sure you will be happy to know that I have finished this PhD about which I am always talking. I am also grateful to all the fellow students from Billy's research team, who have made me feel part of their group every time I went to Strathclyde. Their suggestions have also been extremely valuable and important in the discovery of the cross-coupling amination conditions described in this thesis. Last but not least, I would like to thank all the GSK graduates who are part of this MPhil/PhD programme. Despite all working on different programmes, we have shared extremely useful information, which have helped me in the writing of this thesis. Good luck to all of you for the completion of your MPhil/PhDs.

Finally, I would like to thank my family, in particular my parents and my sister, for their incredible love and support during the past 33 years. I would not be the person I am now without the fantastic education given by my parents. The last words of this section have to go to my other half, Aude, who has been extremely supportive of this PhD during the past four years. I have spent countless hours, during evenings and weekends, working on this thesis and during these, you have had to look after our young son, Baptiste, on your own. Without your help and your understanding, I don't think I would have been able to finally finish it. Thank you for everything.

Contents

Declaration of Copyright	2
Abstract	3
Acknowledgement	5
Contents	8
Abbreviations	10
I. Biological background	14
II. Previous studies on ITK inhibitors	16
III. Early medicinal chemistry	18
IV. The ITK crystal structure	21
V. Covalent inhibitors in drug discovery	25
1. <i>Marketed covalent drugs</i>	25
2. <i>Safety concerns</i>	29
3. <i>Protein kinase irreversible inhibitors</i>	30
VI. Designing irreversible ITK inhibitors	35
1. <i>Computational molecular modelling</i>	35
2. <i>Biological assays used to characterize irreversible ITK inhibitors</i>	39
VII. Results and discussion	52
1. <i>The 6-methoxymethylpyrimidine template</i>	52
2. <i>The 6-morpholinylmethylpyrimidine template</i>	69
3. <i>Investigation of the nature of the electrophilic moiety</i>	86
4. <i>Investigation of the positioning of the electrophilic moiety</i>	101
5. <i>The 6-morpholinylmethylpyridine template</i>	115
6. <i>Replacement of the morpholine motif to improve solubility and activity</i> . 148	
7. <i>Progression of compound 107 and 101 to toxicology studies</i>	168
8. <i>Synthesis and genotoxicity data for compound 101</i>	170

1. Synthesis optimisation	170
2. Genotoxicity results	178
3. Substitutions to the acrylamide unit.....	181
4. MLA results for compound 117	189
9. <i>Synthesis and genotoxicity data for compound 107</i>	189
1. Synthesis optimisation	189
2. Genotoxicity results	201
3. Crystallisation work	202
4. Lung and DMPK data	206
5. 14 Day rat toxicology study results and inhaled in vivo pharmacodynamic (PD) model	207
6. Investigation of the Buchwald-Hartwig coupling.....	211
Conclusions	227
Experimental section	230
<i>General Methods</i>	230
1. <i>Synthetic procedures for the 6-methoxymethylpyrimidine series</i>	239
2. <i>Synthetic procedures for the 6-morpholinemethylpyrimidine series</i>	265
3. <i>Synthetic procedures for the investigation of the electrophilic moiety</i>	288
4. <i>Synthetic procedures for the investigation of the positioning of the electrophilic moiety</i>	298
5. <i>Synthetic procedures for the 6-morpholinemethylpyridine series</i>	309
6. <i>Synthetic procedures for the replacement of the morpholine motif to improve solubility and activity</i>	331
7. <i>Synthetic procedures for the synthesis of compound 101 for toxicology assessment</i>	352
8. <i>Synthetic procedures for the synthesis of compound 107 for toxicology assessment</i>	368
9. <i>Synthetic procedures for the investigation of the Buchwald-Hartwig coupling</i>	381
References	391

Abbreviations

Ac:	Acetate
acac:	Acetylacetonate
ATP:	Adenosine triphosphate
BLK:	B cell lymphocyte kinase
BMX:	Bone marrow tyrosine kinase gene in chromosome X
Boc:	<i>tert</i> -Butoxycarbonyl
BrettPhos:	2-(Dicyclohexylphosphino)-3,6-dimethoxy-2',4',6'- <i>tri-iso</i> -propyl-1,1'-biphenyl
BTK:	Bruton's tyrosine kinase
CDI:	1,1'-Carbonyldiimidazole
CD4:	Cluster of differentiation 4
CD8:	Cluster of differentiation 8
Chrom:	Chromatographic
clogD:	Calculated logD
COMU:	1-[(1-(Cyano-2-ethoxy-2-oxoethylideneaminoxy)dimethylaminomorph-olino)] uronium hexafluorophosphate
COX:	Cyclooxygenase
cpK _a :	Calculated pK _a
Cy:	Cyclohexane
Cys:	Cysteine
D:	Distribution coefficient
DavePhos:	2-(Dicyclohexylphosphino)-2'-(<i>N,N</i> -dimethylamino)biphenyl
dba:	Dibenzylideneacetone
DCM:	Dichloromethane
DIPEA:	<i>N,N</i> -Diisopropylethylamine
DMAP:	4- <i>N,N</i> -Dimethylaminopyridine
DME:	Dimethoxyethane
DMF:	<i>N,N</i> -Dimethylformamide
DMP:	Dess-Martin periodinane

DMPK:	Drug metabolism and pharmacokinetics
DMSO:	Dimethylsulfoxide
DSC:	Differential scanning calorimetry
E:	Enzyme
EGFR:	Epidermal growth factor receptor
EI:	Enzyme:inhibitor non-covalent complex
EI*:	Enzyme:inhibitor covalent complex
Eq:	Equivalent
FDA:	Food and Drug Administration
FRET:	Fluorescence resonance energy transfer
h:	Hour
HATU:	2-(7-Aza-1H-benzotriazole-1-yl)-1,1,3,3-tetramethyluronium hexafluoro-phosphate
HER:	Human epidermal growth factor receptor
hERG:	Human ether-a-go-go related gene
HMBC:	Heteronuclear multiple bond correlation
HPLC:	High-performance liquid chromatography
HSQC:	Heteronuclear multiple-quantum correlation
HTRF:	Homogeneous time resolved fluorescence
I:	Inhibitor
IADR:	Idiosyncratic adverse drug reaction
IFN- γ :	Interferon-gamma
IL:	Interleukin
IPA:	Isopropanol
ⁱ Pr:	Isopropyl
IPRL:	Isolated perfused rat lung
ITK:	Interleukin-2-inducible T cell kinase
JAK3:	Janus kinase 3
K _a :	Acid dissociation constant
k _c :	Rate of covalent binding constant
K _i :	Dissociation constant
k _{off} :	Off rate binding constant

k_{on} :	On rate binding constant
LCK:	Leukocyte-specific protein kinase
LCMS:	Liquid chromatography-mass spectrometry
LHMDS:	Lithium bis(trimethylsilyl)amide
MDAP:	Mass directed auto preparation
MDCK:	Mardin-Darby canine kidney
Met:	Methionine
MFI:	Median fluorescence intensity
Min:	Minute
MLA:	Mouse lymphoma assay
MOE:	Molecular Operating Environment
NHC:	<i>N</i> -Heterocyclic carbene
NK:	Natural killer
NMP:	<i>N</i> -Methyl-2-pyrrolidinone
NMR:	Nuclear magnetic resonance
NOE:	Nuclear Overhauser effect
NSAID:	Non-steroidal anti-inflammatory drug
NT:	Not tested
OVA:	Ovalbumin
PBMC:	Peripheral blood mononuclear cell
PD:	Pharmacodynamic
PEG:	Polyethylene glycol
Phe:	Phenylalanine
pIC_{50} =	$-\log(IC_{50})$. IC_{50} represents the compound/substance concentration required for 50 % inhibition
pK_i =	$-\log K_i$
PLC γ :	Phospholipase- γ
ppm:	Parts per million
PR:	Preincubation time
PyBOP [®] :	(Benzotriazol-1-yloxy)tripyrrolidinophosphonium hexafluorophosphate.
R:	Reaction time
RLK:	Resting lymphocyte kinase

Rt:	Retention time
rt:	Room temperature
SAR:	Structure activity relationship
SLF:	Simulated lung fluid
S _N 2:	Substitution Nucleophilic bimolecular
STK11:	Serine/threonine kinase 11
T:	Temperature
T _{1/2} :	Half-life
TBAF:	<i>tert</i> -Butylammonium fluoride
TBD:	1,5,7-Triazabicyclo[4.4.0]dec-5-ene
TBDMS:	<i>tert</i> -Butyldimethylsilane
TCI:	Targeted covalent inhibitor
^t Bu:	<i>tert</i> -Butyl
TCR:	T cell receptor
TEA:	Triethylamine
TEC:	Tyrosine kinase expressed in hepatocellular carcinoma
<i>Tert</i> :	Tertiary
TFA:	Trifluoroacetic acid
TGA:	Thermal gravimetric analysis
THF:	Tetrahydrofuran
T _H :	T helper
Trk:	Tropomyocin receptor kinase
T3P [®] :	2,4,6-Tripropyl-1,3,5,2,4,6-trioxatriphosphorinane-2,4,6-trioxide (also known as propylphosphonic anhydride)
UV:	Ultraviolet
VP:	Vinyl pyridine
v/v:	By volume
w/w:	By weight
Xphos:	2-Di- <i>t</i> -butylphosphino-2',4',6'-tri- <i>iso</i> -propyl-1,1'-biphenyl.
XRPD:	X-ray powder diffraction

I. Biological background

Interleukin-2-inducible tyrosine kinase (ITK) is a member of the tyrosine kinases expressed in the hepatocellular carcinoma (Tec) family. It is the predominant Tec kinase in T cells (CD4 and CD8 cells) but is also present in mast cells and human natural killer (NK) cells.^{1,2,3} As described in Figure 1, activation of the T cell receptor (TCR) by an antigen or an allergen leads to phosphorylation of ITK by the leukocyte-specific protein kinase (LCK).⁴ Activation of phospholipase- γ (PLC γ) by ITK leads to downstream activation of mitogen-activated protein kinases and other effectors that regulate gene transcription.

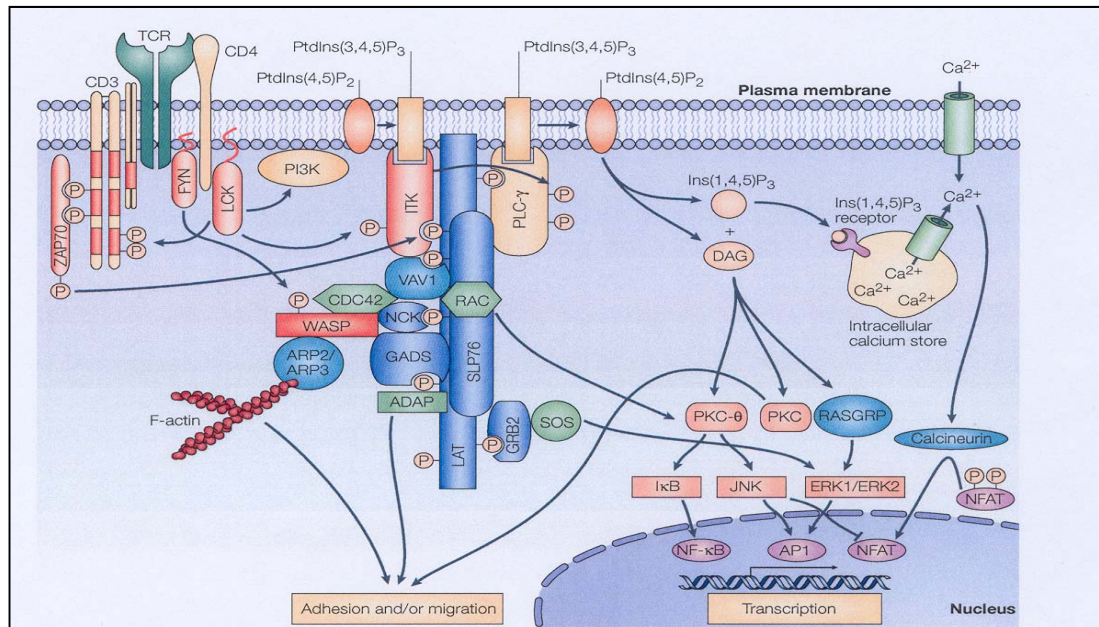


Figure 1. Role of ITK in signalling downstream of TCR activation⁵ (this reference was taken from the literature)

In patients with allergic asthma, exposure to allergen leads to an increase in T_H2 cells.⁶ The unbalanced expression of T_H1/T_H2 cells results in the T_H2 cells producing an excess of cytokines (Interleukin 4, 5, 9 and 13), which will induce proliferation of inflammatory cells and production of mucus (Figure 2). The accumulation of fluid

and cellular debris tends to clog up the airways of people with asthma contributing to breathing difficulties.

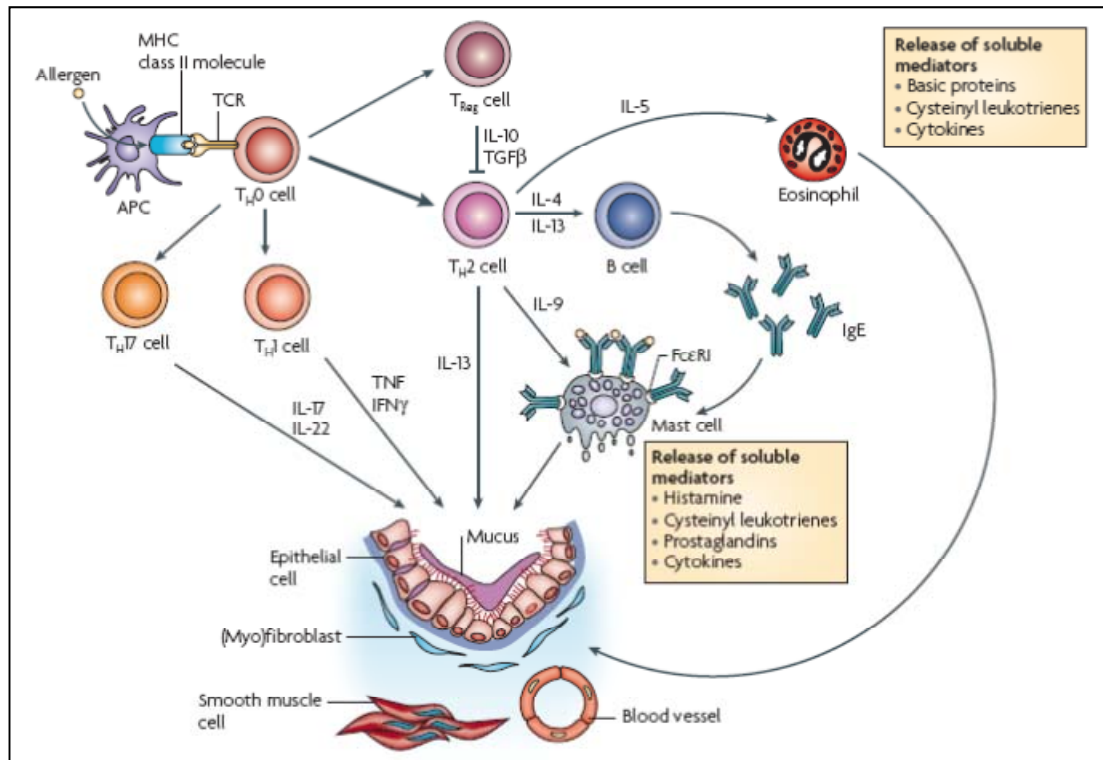


Figure 2. Inflammation cascade after activation of the TCR⁷ (this reference was taken from the literature)

ITK has been shown to be involved in the development of T_H2 cells.⁸ In ITK-deficient T cells, activation of the TCR gave a diminished production of IL-4, IL-5 and IL-13. Moreover, in ITK-deficient mice, a reduced inflammatory response was noted in an allergic asthma model induced by ovalbumin (OVA).⁹ These observations suggest that ITK plays a key role in activation of T cells and can be an ideal therapeutic target for the regulation of T_H2 cell-mediated diseases.¹⁰ Preventing the phosphorylation of ITK with inhibitors of the kinase should lead to a reduced proliferation of inflammatory cells in asthmatic patients. ITK inhibitors could thus be useful anti-inflammatory agents for asthma.¹¹

II. Previous studies on ITK inhibitors

Because of its important role in T cell signalling, ITK inhibitors have been extensively investigated in the past decade for the treatment of inflammatory diseases.¹¹ Since 2002, more than 21 patents including more than 16 different chemical structure classes of ITK inhibitors have been reported.¹² It is important to note that although some of these ITK inhibitors have shown some efficacy in various animal models, none of these species have been reported to have entered clinical trials.

In 2002, researchers from Bristol-Myers Squibb reported the first class of potent and selective ITK inhibitors based on an aminothiazole template.¹³ Optimisation of the ITK binding affinity, as well as the pharmacokinetic properties of the template, resulted in the discovery of BMS-509744 (Figure 3),^{14,15} which showed anti-inflammatory efficacy in a mouse model and an ovalbumin-induced lung inflammation model.¹⁶ However, because of its relatively poor bioavailability (6.4%),¹⁵ BMS-509744 had to be administered either subcutaneously or intraperitoneally. It has been postulated that the poor bioavailability of this template could have been the reason that prevented the progression of this class of ITK inhibitors to clinical studies.¹²

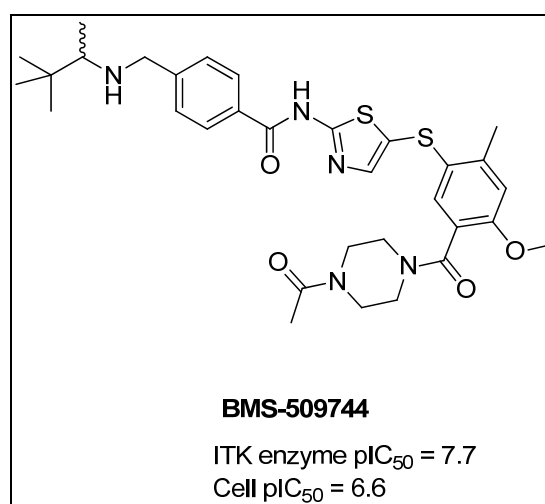


Figure 3. First ITK inhibitor with efficacy in an ovalbumin-induced lung inflammation model¹⁶

Boehringer Ingelheim published their first patent on aminobenzimidazole ITK inhibitors in 2004.¹⁷ Two subsequent patents were filed the following year^{18,19} and the SAR of this template was extensively described in peer-reviewed journals.^{20- 27} Using the information obtained from a crystal structure of their template in the ITK active site,²¹ these researchers developed the first oral ITK inhibitor with *in vivo* efficacy (Figure 4).²⁷

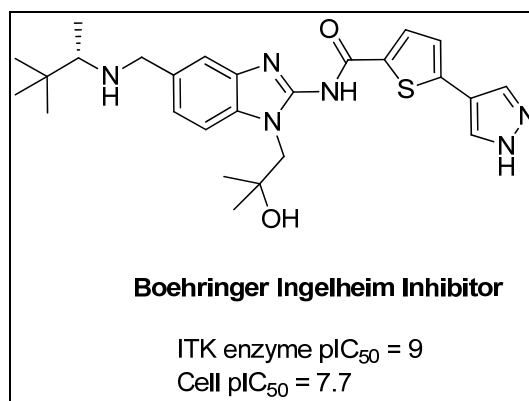


Figure 4. First orally administered ITK inhibitor with *in vivo* efficacy.

Around the same time as the communication outputs from Boehringer Ingelheim, Sanofi-Aventis reported a new class of potent ITK inhibitors based on an indole core.^{28,29} Their lead compound (Figure 5) showed good affinity towards ITK in an enzyme assay, as well as a potent reduction of cytokine production in a cellular experiment. Despite these encouraging data, these molecules have not been reported to be further progressed.

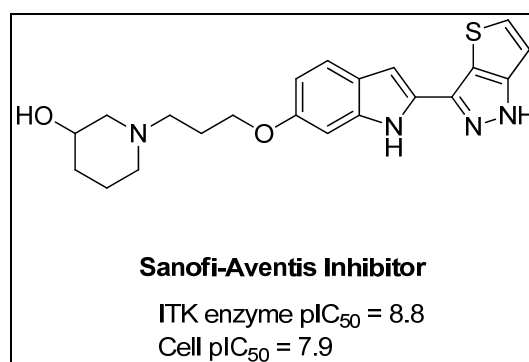


Figure 5. ITK inhibitor from Sanofi-Aventis.

Since 2002, four other research organisations have published various patents describing new classes of ITK inhibitors.¹² To our knowledge, these molecules are less potent than those described above and no *in vivo* data are reported.

In summary, for the past decade, ITK has been an extensively investigated target for the treatment of anti-inflammatory diseases. Some potent *in vitro* and *in vivo* inhibitors have been developed within various laboratories, nonetheless, the first ITK inhibitor has yet to reach clinical studies. It remains unclear why none of these compounds have progressed to the first time in human milestone. Nonetheless, this reinforces the potential importance and impact of this present programme of study.

III. Early medicinal chemistry

The initial target of this medicinal chemistry programme within our laboratory was to discover *reversible* ITK inhibitors suitable for inhaled administration. Like the previously accessed molecules described above, these compounds would bind reversibly to the adenosine triphosphate (ATP) binding site of ITK, preventing phosphorylation by the kinase and resulting in attenuation of the inflammatory cytokine release. Subsequently, a series of highly potent inhibitors were developed with good kinase selectivity based on an amino-benzothiazole template (Figure 6).^{30,31} Compound **1** displayed a good level of ITK activity in the high ATP concentration homogeneous time resolved fluorescence (HTRF) assay (*vide infra*), as well as a promising inhibition of interferon-gamma cytokines (IFN- γ) in the peripheral blood mononuclear cell (PBMC) assay.^{32,33}

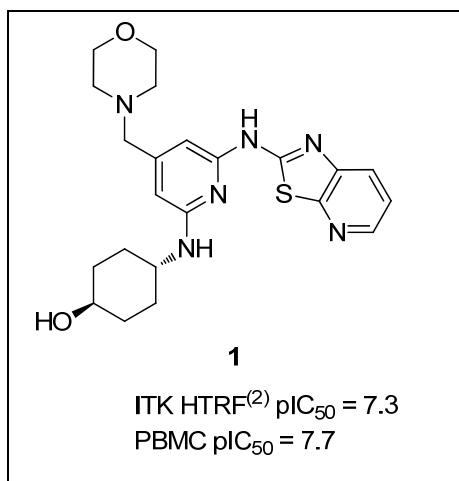


Figure 6. Structure and activity of compound **1**

Despite the good levels of enzyme and cellular potency observed in the *in vitro* (HTRF and PBMC) assays, none of these inhibitors showed evidence of significant efficacy in the OVA-inhaled disease mouse model.^{34,35} *In vitro* kinetic studies³⁶ performed on some of these amino-benzothiazole ITK inhibitors showed that the molecules had a very short residence time at the ITK active site (< 5 mins), which renders the species unable to drive any duration of action via their inhibition kinetics. Additionally, data obtained in the isolated perfused rat lung (IPRL) studies suggested that when these ITK inhibitors were dosed topically, if the soluble fraction rapidly perfused across the lung and was not retained in the lung tissues,³⁷ duration of action was not achieved. Therefore, it was postulated that the lack of efficacy in the inhaled *in vivo* model was due to a poor duration of action of the amino-benzothiazole compounds in the lungs and not to the mode of action of ITK. This hypothesis was confirmed by an *in vivo* study demonstrating that when compound **1** was administered subcutaneously in the same mouse *in vivo* model, a significant reduction in the levels of the anti-inflammatory cytokines released was observed (Figure 7).³⁴ Indeed, at the highest dose of 5 mg/mL, 99 % inhibition of the interleukin 4 (IL-4) cytokine release was observed. The analysis of the mice lungs after the study showed that 4.5 hours post-dose, compound **1** was distributed between the lung and the blood at a ratio of 1:1 across all three dose groups. This indicates that the amino-benzothiazole ITK inhibitors have the potential to work as anti-inflammatory agents for severe asthma when they reach T cells. However, when

delivered topically (inhaled), the combination of poor lung retention and short residence time at the ITK active site prevents them from demonstrating any appreciable efficacy.

It is worth noting here that the anti-inflammatory effect observed in the subcutaneous PD study could be due to a cumulative effect of the ITK inhibition from the T cells located in the systemic system, as well as in the lungs. It is not possible at this stage to prove that the same anti-inflammatory effect could be achieved by inhibiting ITK only in the lungs. It is however strongly believed that a significant effect would be observed from an inhaled ITK inhibitor if the compound was reaching the lung T cells.

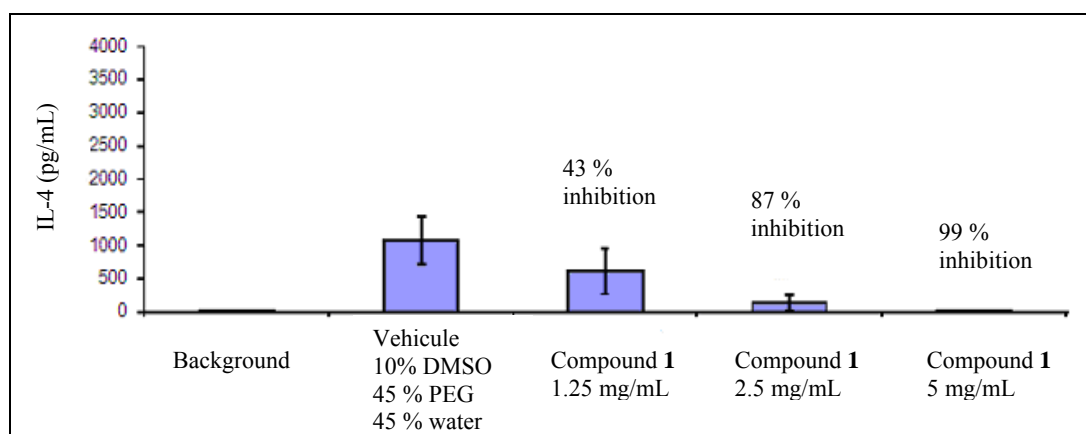


Figure 7. *In vivo* data obtained for compound 1 when administered subcutaneously

Analyzing these data, one could postulate that an orally administered ITK inhibitor from the amino-benzothiazole template would be more efficacious than an inhaled agent. However, the drug metabolism and pharmacokinetic (DMPK) properties of the compounds from this template proved to better suit inhaled administration, as most compounds tested showed low bioavailability after oral administration in rats.³⁷ Moreover, and perhaps most importantly, further profiling of these compounds has indicated a residual kinase selectivity issue against TrkA and TrkB.³⁸ TrkA and TrkB activities have been confirmed in cellular assays where activity was shown to be only 10 times lower than the ITK level of activity. To date, six different ITK inhibitor templates have been screened against TrkA and TrkB and, in all cases, undesirable potent inhibition was recorded for both kinases. The modification of the structure of

the amino-benzothiazole compounds to optimise both the DMPK and the TrkA/B selectivity profiles was believed to be extremely challenging to achieve. In contrast, developing an inhaled compound with poor oral bioavailability would result in low systemic levels of compound following topical administration, which would decrease any toxicity related to TrkA and TrkB selectivity issues. Therefore, the strategy of this programme was the improvement of the duration of action of the compounds in the lungs by *irreversible* inhibition, which was thought to be much more tractable. Accordingly, this approach is now delineated as part of this research programme.

IV. The ITK crystal structure

X-ray crystal structures of the phosphorylated and unphosphorylated ITK domains in ligand-bound and apo forms demonstrate that phosphorylation of tyrosine (Tyr) 512 does not induce order in the activation loop or promote rearrangement of protein side chains in the ATP binding site.³⁹ This finding suggests that an ITK inhibitor will bind with similar affinity to the unphosphorylated and phosphorylated kinase domain. A number of X-ray crystal structures have been determined for ITK with inhibitors based on the amino-benzothiazole template.⁴⁰ Although compound **1** could not be crystallised with ITK, the X-ray crystal structure of the structurally related compound **2**³⁰ (Figure 8 and Figure 9 - note that only the residues present in the active site are displayed) in the ITK active site provides key information about the binding mode of the template. Compound **2** presents key hydrogen bond interactions between the amino-benzothiazole and the methionine 438 (Met438) residue in the hinge region (Figure 9). Another interesting interaction can be observed between the NH of the *trans*-aminocyclohexanol and a water residue. The *trans*-aminocyclohexanol is situated in a solvated area of the binding site. The electron density surface of the active site presented in Figure 10 shows that the lipophilic cyclohexane unit is positioned between two lipophilic sidechains of the protein (green surfaces) and also in an area which is exposed to the solvent (red surface). The hydrophobic interaction between the cyclohexane unit and the kinase was believed to be associated with the release of water molecules from the protein active

site and the ligand, which plays an important role in the formation of the non-covalent complex.^{41,42} In contrast, the terminal alcohol functionality is solvated with water residues. Finally, the fluoropiperidyl motif does not seem to make any interaction with the kinase suggesting that other groups could be used at this position to improve the physico-chemical properties of the molecules (*e.g.* solubility).

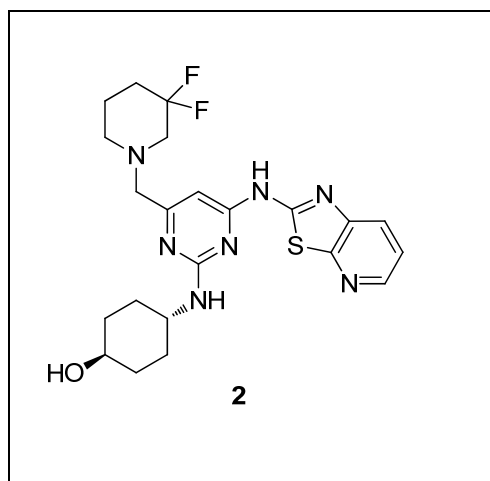


Figure 8. Structure of compound 2

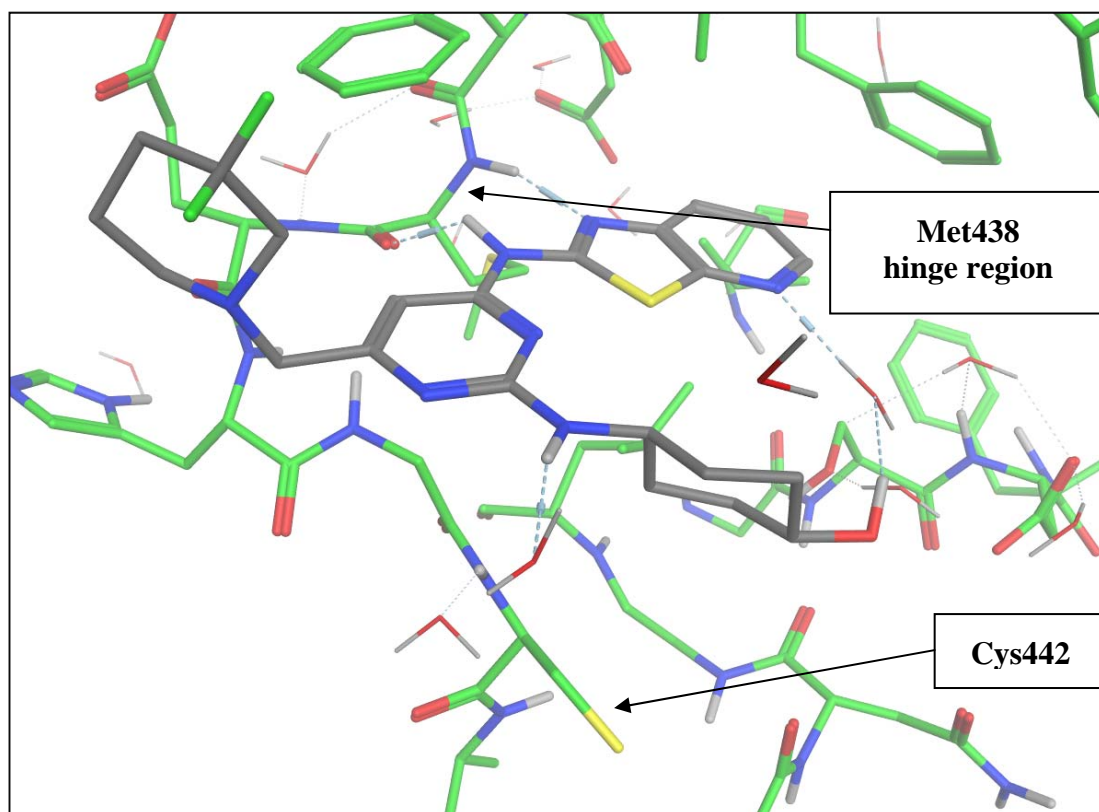


Figure 9. X-ray crystal structure of compound 2 in the ITK active site

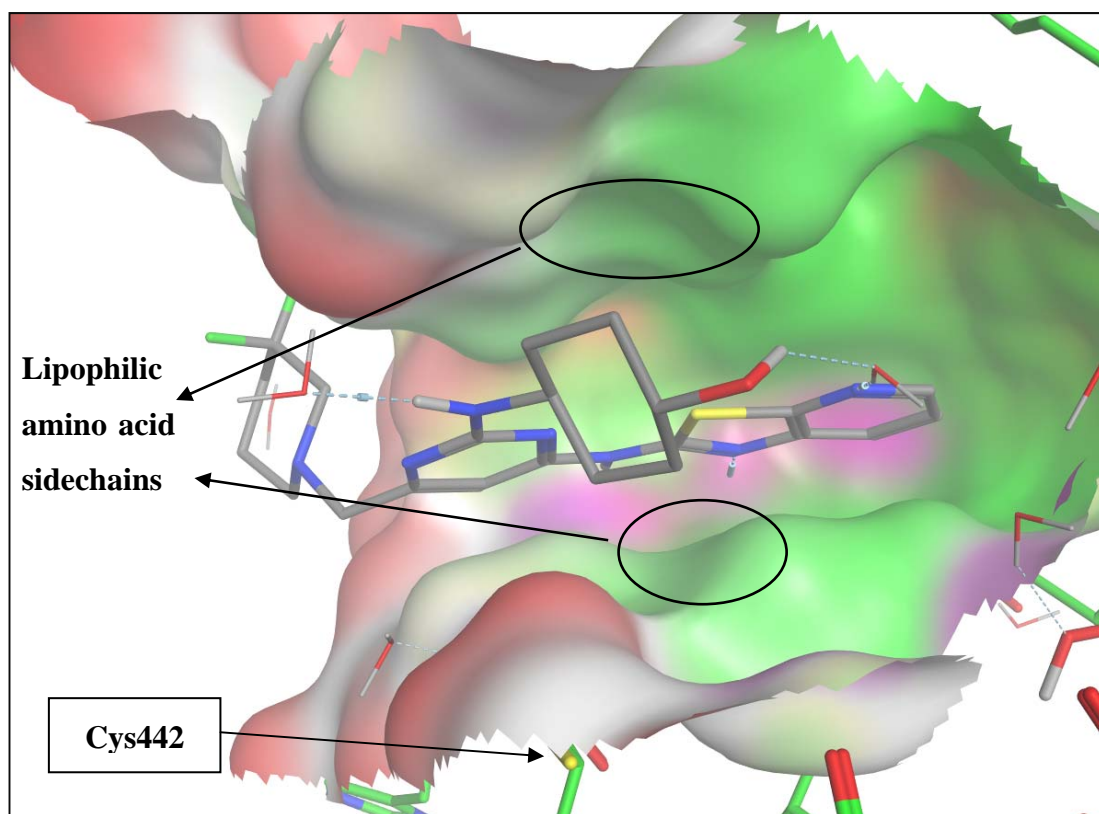


Figure 10. X-ray crystal structure of compound **2** in the ITK active site (electron density surface view. Surface colours: green represent the lipophilic areas, red represent the areas exposed to solvent and purple represent the areas of polar interactions)

One important residue of the active site which does not appear to make any interaction with the template is the cysteine 442 (Cys442), which resides underneath the *trans*-aminocyclohexanol (Figure 9). Although more than 200 kinases have a cysteine located in the vicinity of the ATP pocket,⁴³ only eleven of these kinases are known to possess a conserved cysteine residue situated in this region of the ATP pocket (Table 1). Figure 11 represents the crystal structure of the non-selective kinase inhibitor, staurosporine, in the ITK active site alongside the various positions occupied by these cysteines present in more than 200 kinase active sites.⁴³ The ITK Cys442 is located in the position F of Group 3.

Table 1. List of eleven kinases possessing a Cys residue in the Group 3 - position F of the ATP pocket⁴³

Tec family kinases	BTK	BMX	ITK	TEC	RLK	
Other kinases	BLK	HER-1	HER-2	HER-4	JAK3	STK11

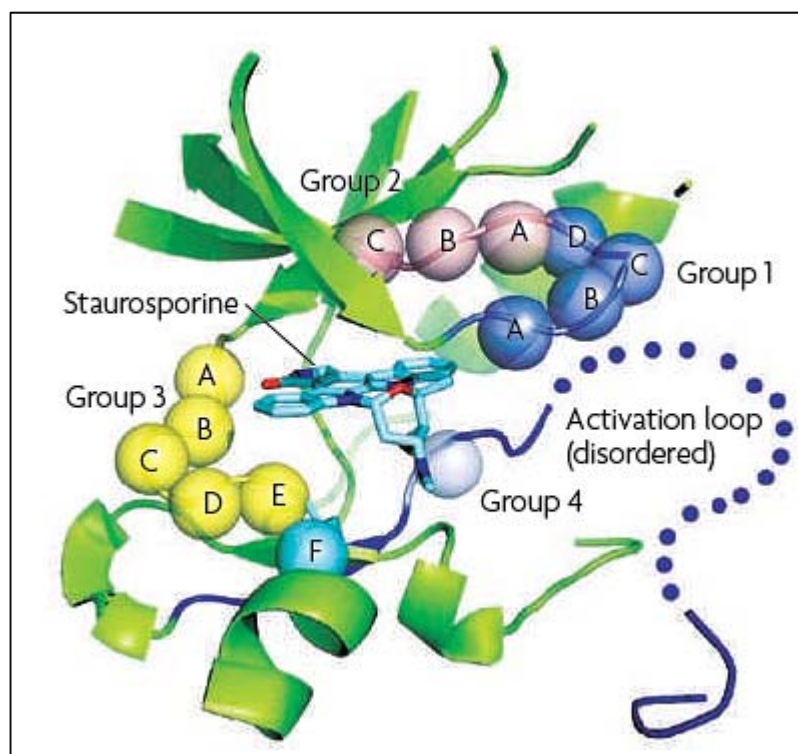


Figure 11. Location of the cysteines present in the ATP active site of more than 200 kinases.⁴³ The ITK Cys442 occupies the position F of Group 3 (cyan circle). (This reference was taken from the literature)

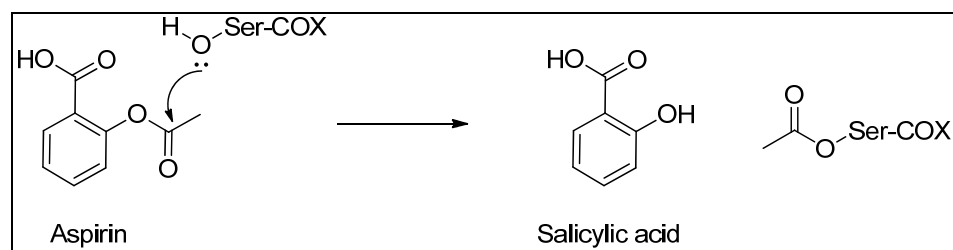
The cysteine residue has the potential to react with electrophilic groups and, in turn, generate a covalent bond between the kinase and the inhibitor. This would make the compounds irreversible inhibitors of the kinase. The main attraction of irreversible inhibitors is their perceived superior *in vivo* activity due to the long lasting inactivation of the enzyme.^{44- 47} An irreversible ITK inhibitor would also test the hypothesis that the short duration of action of the reversible ITK inhibitors developed so far was the main reason for the lack of *in vivo* efficacy.

V. Covalent inhibitors in drug discovery

1. Marketed covalent drugs

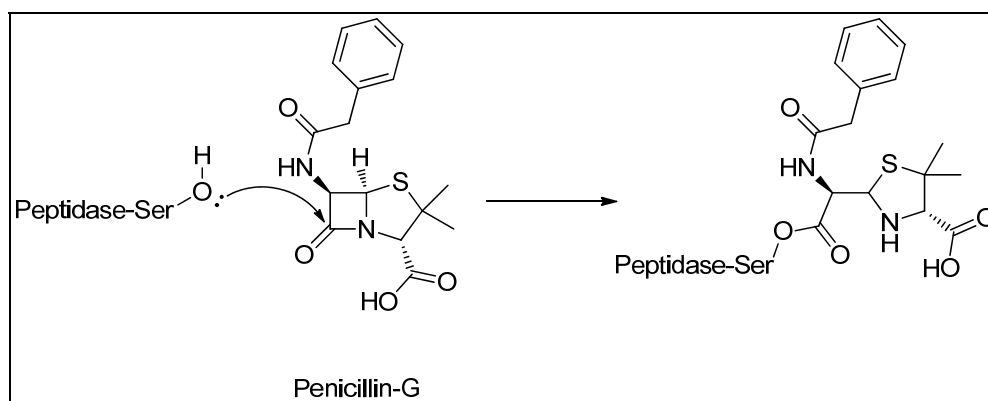
Covalently bound drugs are generally avoided by pharmaceutical research laboratories as they stimulate anxiety concerning their potential off-target reactivity leading to toxicity.^{48,49} However, over the years, many covalent drugs have been approved for the treatment of various diseases and have had a clear impact on human health.^{50,51} In fact, approximately one-third of the enzymes that are inhibited by marketed drugs have an example of an approved covalent drug.⁵¹ In 2009, three of the ten top selling drugs in the United States were covalent inhibitor drugs and all three achieved blockbuster status (clopidogrel, lansoprazole and esomeprazole). Despite the prevalence of covalent drugs on the market, most of these drugs were not discovered by design but by serendipity and the irreversible binding mechanism to their targets was only established years later, and after the compounds had revealed clinical utility. An excellent review by Potashman and Duggan describes in details the various mechanisms by which some marketed drugs and late stage clinical candidates modify their targets by covalent interactions.⁵⁰ In this section, only a selection of the most successful examples of covalent inhibitors and their mechanisms of action are described.

Aspirin, which was first distributed to patients in 1899 by Bayer, represents the earliest example of a covalent modifier. However, its mechanism of action was only discovered in the 1970s.^{52,53} Aspirin is part of a group of medications called non-steroidal anti-inflammatory drugs (NSAIDs) but differs from most other NSAIDs as it irreversibly acetylates a serine residue in the active site of the cyclooxygenases COX-1 and COX-2 (Scheme 1). The acetylation of the cyclooxygenases blocks the approach of the substrate to the active site and leads to irreversible inhibition of COX-1 and COX-2.⁵⁴ More than 100 years after its discovery, aspirin remains the most widely used medication worldwide, with more than 80 billion tablets being consumed every year in the United States alone.⁵⁵



Scheme 1. Mechanism of action of aspirin

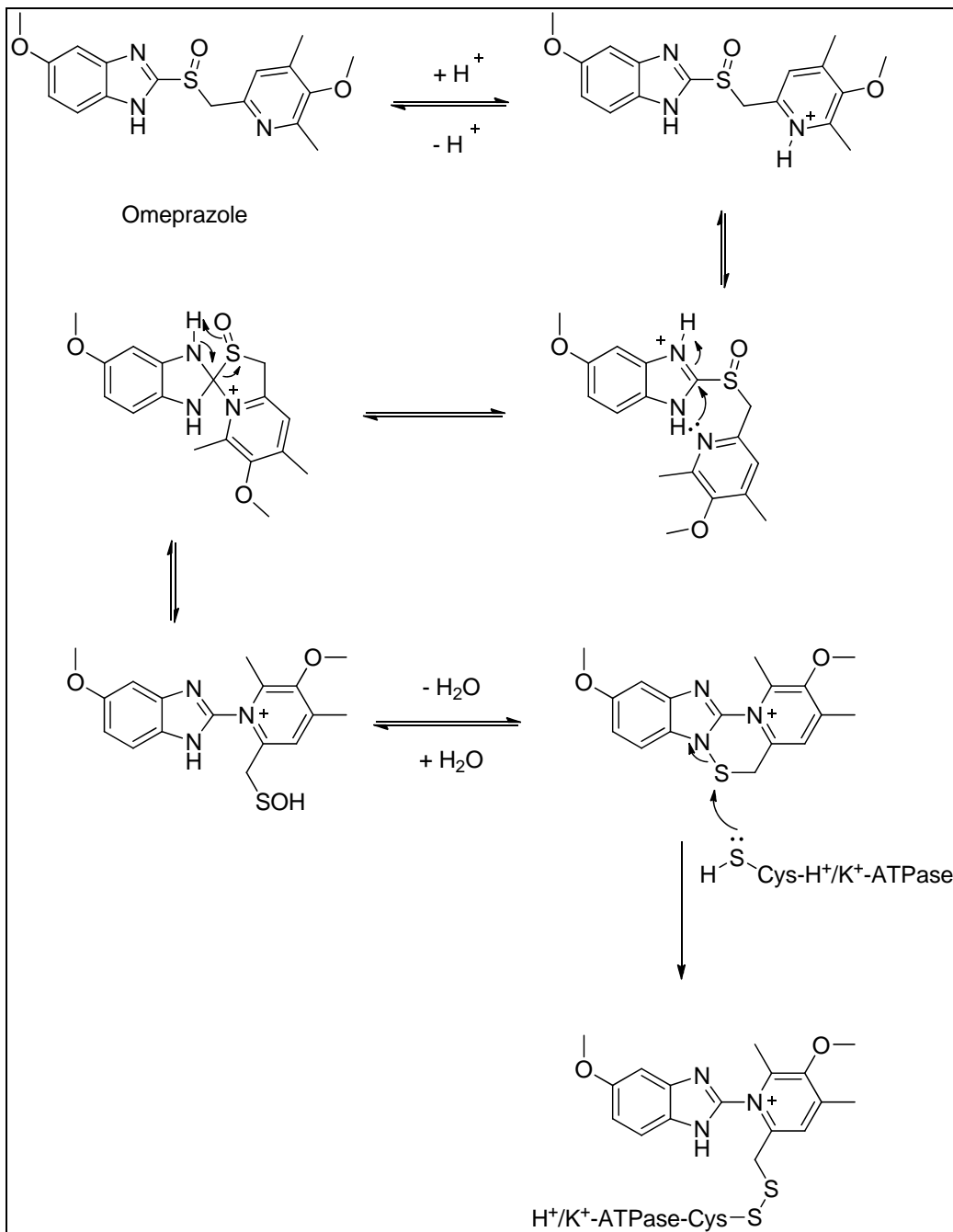
Penicillin antibiotics probably represent the most famous class of irreversible inhibitors. Benzylpenicillin, also known as penicillin-G, was discovered in 1928 by Alexander Fleming in a Petri dish.⁵⁶ Penicillin-G was used to treat patients during the Second World War and has since become the most widely used antibiotic to date. Penicillin-G (like other commonly used antibiotics such as amoxicillin and ampicillin) contains a β -lactam nucleus which covalently modifies a serine residue in the active site of a bacterial DD-transpeptidase (Scheme 2) and renders the enzyme unable to catalyse a key step in cell-wall synthesis, causing the cell to rapidly die.^{57,58}



Scheme 2. Mechanism of action of penicillin-G

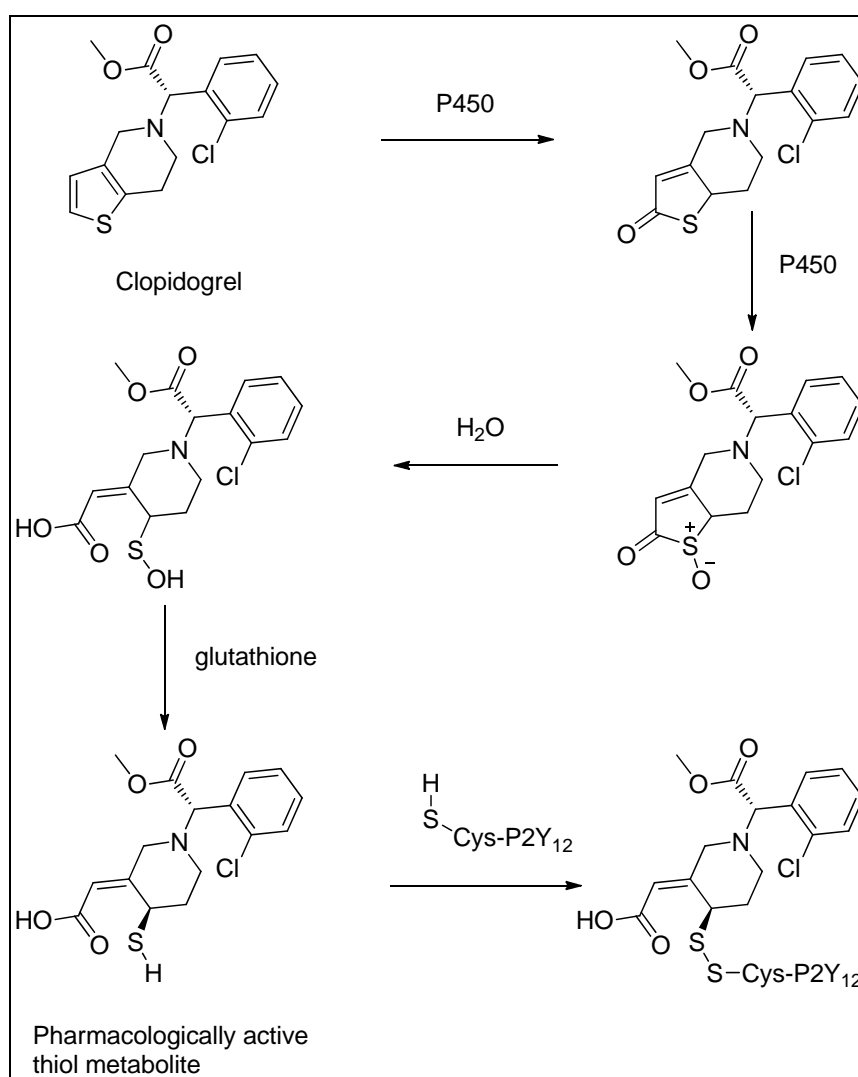
Proton pump inhibitors are another major class of successful covalent drug which were not discovered by design but by pharmacological screening.⁵⁹ Omeprazole, the first proton pump inhibitor used in clinical practice, was launched in the United States in 1990 by Astra (now AstraZeneca) and the drug has greatly improved the treatment of gastrointestinal reflux disease. Nearly ten years later, in 1999, Omeprazole global sales totaled \$5.91 billion (representing 40 % of AstraZeneca's

annual revenues), making it the best-selling drug on the market.⁶⁰ Omeprazole is a prodrug which, once activated by acid in the stomach to a tetracyclic sulfenamide intermediate, covalently binds to a cysteine residue of the gastric H^+/K^+ -ATPase to form disulfide adducts (Scheme 3).^{61,62}



Scheme 3. Mechanism of action of omeprazole

Clopidogrel is also a prodrug which, once activated by hepatic metabolism, covalently modifies the adenosine 5'-diphosphate receptor P2Y₁₂ resulting in irreversible inhibition of platelet aggregation.⁶³ Similarly to omeprazole, clopidogrel was discovered through pharmaceutical screening and not by design.⁶⁴ It was elucidated later that the compound reacts with liver P450 enzymes to form an activated thiol metabolite which inhibits platelet aggregation by covalently binding to a cysteine residue in the P2Y₁₂ receptor (Scheme 4).⁶⁴⁻⁶⁶ Clopidogrel represented a breakthrough in the treatment of vascular disorders,⁶⁷ and accounted for sales of \$4.67 billion in the United States during the year 2010 alone.⁶⁸



Scheme 4. Mechanism of action of clopidogrel

There are many more examples of covalent inhibitors which have reached late stage clinical trials or are even available to patients as marketed drugs and are targeting a wide range of enzymes and diseases.^{49,50,69} These compounds have displayed advantages over conventional non-covalent inhibitors, such as longer duration of action, increased biochemical potency, isoform selectivity, or lower drug dosing *in vivo*.^{48,69} However, despite the success of this irreversible inhibitor approach, there is a reluctance from pharmaceutical research laboratories to pursue covalent mechanisms of action, due to concerns over off-target reactivities leading to toxicity issues.

2. Safety concerns

Molecules possessing functionalities reactive enough to covalently bind to their targets stimulate anxiety from the medicinal chemist as they could also potentially react with other macromolecules or enzymes, which might trigger an immune response resulting in some form of idiosyncratic adverse drug reactions (IADRs). Protein covalent binding appeared as a mechanism of toxicity in the early 1970s as it was discovered that some marketed drugs, such as paracetamol, that were associated with IADRs, could form reactive metabolites, which had the potential to covalently bind to liver proteins that can cause hepatotoxicity.^{48,49,70} Although a clear relationship between covalent binding and toxicity remains to be demonstrated, most pharmaceutical research laboratories, in order to reduce attrition, became reluctant to develop inhibitors with parent structure or active metabolites that had the potential to covalently bind to off-target proteins.^{71,72} Efforts in the field of covalent drug design were then focused on developing mechanism-based enzyme inactivators (or suicide substrates) which first non-covalently bind to the target enzyme and only covalently react with the enzyme when it begins catalysis.⁷³⁻⁷⁵ This approach proved to be very challenging, with these compounds targeting a nucleophilic residue involved in the catalytic mode of action of the enzyme, which might induce selectivity issues with close related enzymes from the same family.⁴⁸

A different approach has recently been taken by various research laboratories still hoping to develop covalent drugs. These research groups have designed molecules,

often called targeted covalent inhibitors (TCIs),⁴⁸ with low reactivity electrophiles which would first non-covalently bind to the active site of the enzyme and then react covalently with a (non-catalytic) nucleophile which is poorly conserved across the target protein family.⁴⁸ These inhibitors have a high non-covalent target recognition, which allows sufficient residence time in the active site for the non-conserved nucleophilic residue and the mild electrophile to covalently react. High selectivity against off-target covalent reactions requires both high non-covalent target selectivity against enzymes from the same family, which also possess the poorly conserved nucleophile in their active site, and low intrinsic reactivity of the electrophile moiety to avoid off-target covalent reactions with macromolecules/enzymes present *in vivo*, even at high concentrations. In the perfect scenario, the electrophilic moiety will covalently react with a nucleophilic residue only when the molecule is non-covalently bound to the enzyme active site. In this configuration, the reacting groups are at distance and orientation which are highly favourable for reaction. It has already been described in the literature that close proximity between reacting functionalities can increase the rate of the reaction by many orders of magnitude,^{76,77} which can allow the bond formation between reactants for which the inherent biomolecular reaction in solution is low or negligible.

This latter approach should decrease the risks of IADRs and toxicity associated with covalent drug molecules. However, one cannot guarantee that, despite meticulous design, these inhibitors will not covalently react with any off-target macromolecules/enzymes. For that reason, the safety of these drugs has to be evaluated on a case by case basis.

3. Protein kinase irreversible inhibitors

Strategies focusing on the development of TCIs have mainly been investigated for protein kinases involved in life-threatening disease such as cancer.^{43,78-80} Since the first rationally designed irreversible HER-1 and HER-2 (HER-1 also commonly called EGFR kinase) inhibitor (PD168393, Figure 12) was reported in 1998,⁴⁵ a number of other irreversible inhibitors has been developed for these kinases.^{81,82} One of the furthest advanced irreversible HER-1 and -2 inhibitor, HKI-272 (Neratinib,

Figure 13), is currently in Phase III trials for breast and non-small cell lung cancer.⁴⁶ These analogues form covalent bonds with a poorly conserved cysteine residue in the ATP pocket of the kinase through incorporation of an electrophilic moiety; this is typically a Michael acceptor.

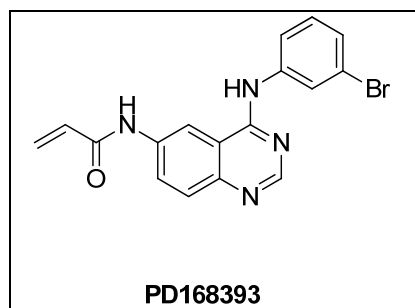


Figure 12. First irreversible EGFR and HER-2 inhibitor (PD168393)

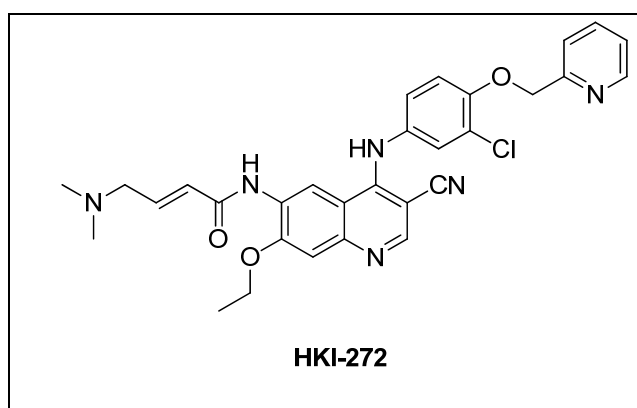
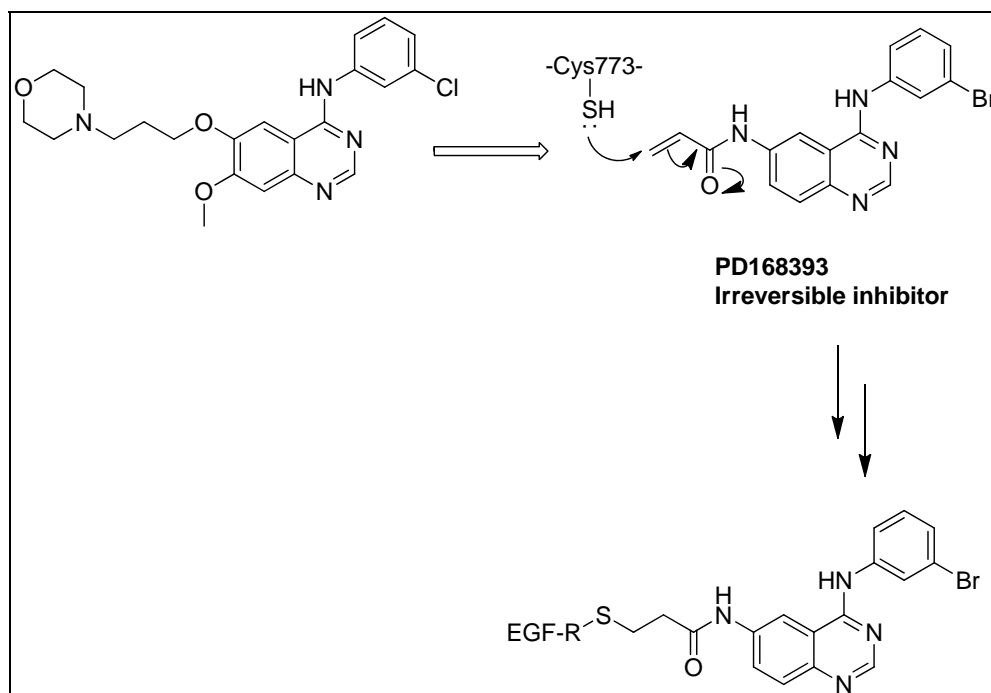


Figure 13. Structure of Neratinib (HKI-272)

The approach followed by various researchers to develop irreversible EGFR inhibitors consisted of using an existing potent reversible template and incorporating an electrophilic moiety in proximity to the Cys773 residue when the potential inhibitor resides in the ATP pocket (Scheme 5).⁴⁷ The non-covalent recognition features for the kinase of interest allow the compound to be locked in the ATP pocket long enough for the Michael addition between the cysteinyl sulfur and the electrophilic moiety to occur. Moreover, keeping the non-covalent recognition features for EGFR helps maintain the selectivity over the other kinases possessing a cysteine in the ATP binding pocket. In summary and as already described in the previous section, the reactivity of the electrophilic moiety is low enough to prevent

non-specific cysteine interactions; the attack of a sulfur nucleophile only occurs when the inhibitor is located in the active site of the kinase.



Scheme 5. Medicinal chemistry approach to design irreversible inhibitors

Covalent binding of the irreversible inhibitors to the kinase has been confirmed by mass spectrometry and enzyme digestion experiments,⁴⁵ as well as by obtaining an X-ray crystal structure of the inhibitor bound to the kinase (Figure 14).^{81,83} The main advantage of these irreversible inhibitors was seen in their ability to retain 80 % or greater inhibition after an 8 hour washout assay.^{47,84} In this assay, the inhibitor was incubated with the cells containing the kinase for one hour and then the cells were washed free of unbound drug. After 8 hours, the cells were stimulated and the inhibition of the response was measured. A potent reversible EGFR inhibitor was washed from the cells and no inhibition was observed at the 8 hour point. The improved duration of action of the irreversible inhibitors observed in these washout experiments was translated into the *in vivo* model,^{45,81,85,86} where a far superior efficacy compared to the reversible inhibitors was seen.

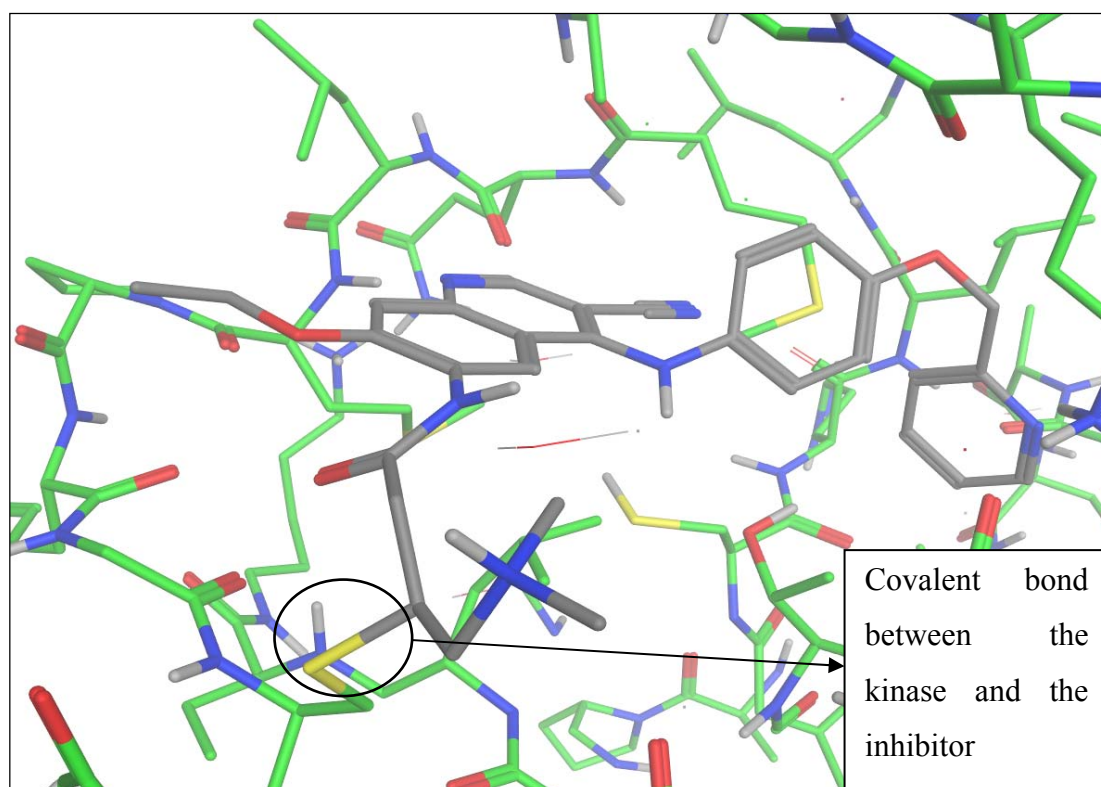


Figure 14. X-ray crystal structure indicating covalent bond formation between EGFR and HKI-272

Designing irreversible inhibitors for HER kinases has been investigated extensively for the past 10 years and, to date, five irreversible EGFR inhibitors have been evaluated in lung cancer clinical studies.^{43,82,87-89} The same approach has been recently followed by a medicinal chemistry team from Celera Genomics to discover irreversible inhibitors for the Bruton's Tyrosine Kinase (BTK),⁹⁰ which is part of the family of 11 kinases presenting a cysteine at a structurally equivalent position to that seen in EGFR (Table 1).⁴³ As described in Figure 15, the team used an existing potent reversible inhibitor of BTK and incorporated the Michael acceptor electrophile such that it was in proximity to the Cys481 unit present in the BTK active site. Compound **3** (Figure 15) was confirmed as an irreversible inhibitor using two methods similar to that already described for EGFR: firstly, a major peak corresponding to the molecular weight of the covalent complex between compound **3** and BTK was observed by mass spectrometry; secondly, after incubation of compound **3** with BTK, inhibition of the kinase was retained after multiple washings of the enzyme.⁹⁰

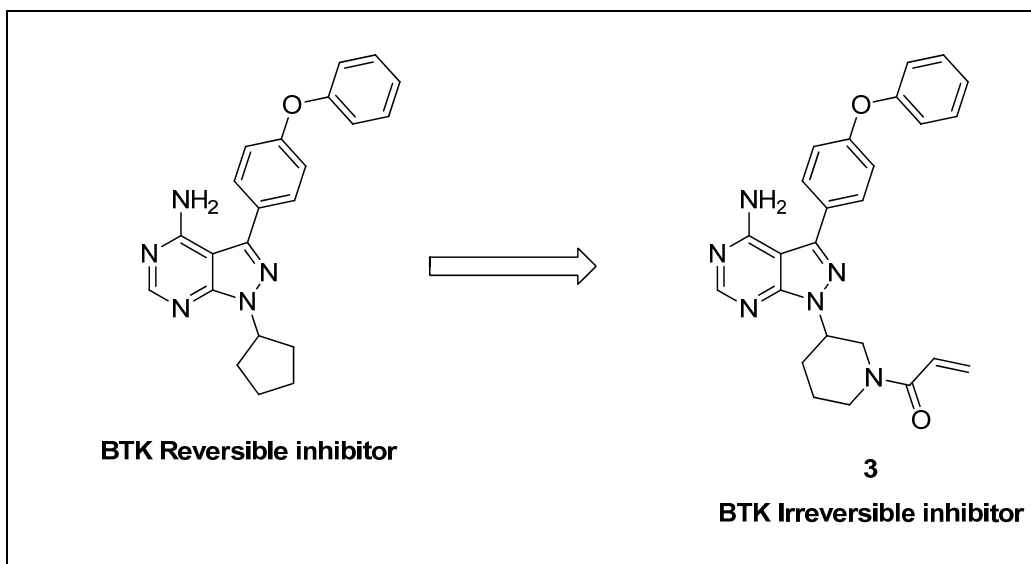


Figure 15. Medicinal chemistry approach to design irreversible inhibitors for BTK

The irreversible BTK inhibitor **3** showed acceptable selectivity over other kinases and demonstrated dose-dependent efficacy in the arthritis mouse *in vivo* model.⁸⁷ This compound has advanced into clinical trials for the treatment of haematological cancers and demonstrated potent inhibition of the target and prolonged duration of action.^{79,91} To our knowledge, the *R*-isomer of this inhibitor (Ibrutinib) is currently in Phase II clinical trials and is expected to enter two Phase III trials this year. Avila Therapeutics have also developed irreversible BTK inhibitors based on a 2,4-dianilinopyrimidine template.⁹² In the first quarter of 2012, Celgene acquired Avila Therapeutics for \$350 million, bringing the lead BTK covalent molecule (AVL-292, structure not disclosed), currently in Phase Ib clinical trial, into its portfolio.⁹³ This acquisition reinforces the potential and current interest in these kinase irreversible inhibitors.

Because of the success of the EGFR and BTK drug molecules currently in clinical studies, the TCI approach is rapidly evolving, with various research groups publishing evidence of irreversible inhibitors for kinases different to EGFR and BTK,^{78,94-97} with some appearing during the course of this research programme.

The literature on irreversible inhibitors suggests that this kind of inhibition could be achieved for, potentially, any kinase possessing a cysteine residue situated within the ATP pocket.^{43,80} As described previously, ITK is one of these kinases. Thus, it is

postulated that the discovery of irreversible ITK inhibitors would improve the duration of action of relevant active compounds and the *in vivo* efficacy in the inhaled mouse *in vivo* model. The duration of action would then depend on the turnover of ITK (*i.e.* how long it takes for the cell to regenerate new enzyme). Moreover, because TrkA and TrkB do not present any Cys residue in this region of the active site, non-selective irreversible ITK inhibitors would only inhibit TrkA/B reversibly. The extended duration of action would therefore not be observed for the TrkA and TrkB kinases resulting in functional selectivity in cellular assays for irreversible ITK inhibitors.^{48,90} In conclusion, an irreversible ITK inhibitor should allow the two major issues highlighted above to be overcome and for a suitably effective candidate molecule for ITK programmes within our laboratories to be realised.

VI. Designing irreversible ITK inhibitors

1. Computational molecular modelling

Structural analysis of X-ray data suggested that the ITK Cys442 unit is in a very similar position to the Cys773 in EGFR.⁹⁸ Therefore, accessing the Cys442 covalent interaction appeared to be possible if the electrophilic moiety was positioned in proximity to the cysteine residue. Taking the ITK X-ray crystal structure of compound **2** (Figure 9) as a starting point, Cys442 is situated under the *trans*-aminocyclohexanol. Following a similar strategy to that described earlier for the published EGFR and BTK programmes, the *trans*-aminocyclohexanol group could be replaced by electrophilic groups, while the remainder of the non-covalent interactions would be untouched to maintain the recognition for ITK. Starting from the highly potent template of compound **1**, the *trans*-aminocyclohexanol would first be replaced with a flexible acyclic chain possessing a terminal acrylamide Michael acceptor (compound **4**, Figure 16). [Note that the modelling was performed with various groups positioned in the morpholine area but they have been omitted in the visualisation as they do not play any role in the positioning of the acrylamide motif.]

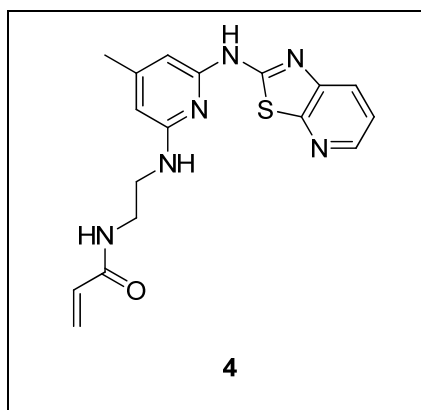


Figure 16. *Proposed irreversible ITK inhibitor*

As a general method developed by Dr Nick Barton, using the Molecular Operating Environment (MOE) modelling software,⁹⁹ the amino-benzothiazole and pyridine motifs of compound **4** were superimposed on the amino-benzothiazole and pyrimidine motifs within the crystal structure of compound **2** in the ITK binding site (Figure 9). This enabled compound **4** to make the critical interactions in the hinge region. The atom positions of these motifs were fixed for the rest of the modelling. Conformational searches were performed for the acyclic chain with the terminal acrylamide and for the cysteine sidechain (note that following this method, the rest of the protein was therefore treated as a rigid entity, even though it is flexible. For that reason, caution was required when interpreting the results from this approach as the inhibitors might have adopted different conformations with a fully flexible protein). The resulting low energy conformations were reviewed to identify acceptable conformations which may allow for covalent addition to the kinase. An example is shown in Figure 17 where Cys442 and the 4-position of the Michael acceptor are 4.23 Å away. This modelling demonstrates good ligand conformation but gives little indication of the ability of the ligand to react with the cysteine residue of the kinase. The ligand conformation presented in Figure 17 was then modified by saturating the alkene and bonding the 4-position carbon to the cysteine sidechain of ITK. The conformation of the covalently bound inhibitor was then energy minimised. The outcomes of this approach are presented in Figure 18: the conformation of the covalent complex appeared acceptable with no bond angles being distorted. It is interesting to note that Cys442 has to rotate from the conformation observed in the crystal structure of compound **2** (Figure 9 - same conformation also used in the

modelling presented in Figure 17) to allow the formation of the covalent bond. To assess whether this new conformation of Cys442 was realistic, the crystal structures of 21 small molecules non-covalently bound into the ITK active site were overlaid and compared.⁹⁸ For all 21 crystal structures, the structures were superposed on the backbone atoms of three residues; the gatekeeper phenylalanine 435 (Phe435), hinge residue Met438 and Cys442. This comparison identified a clear preference for two different sidechain conformations for Cys442 (Figure 19 - note that the crystal structure of compound **2** is also represented for clarity). This result confirmed that the C-S bond had the potential to rotate and adopt the required conformation presented in Figure 18 to react with electrophilic moieties and form the covalent complex.

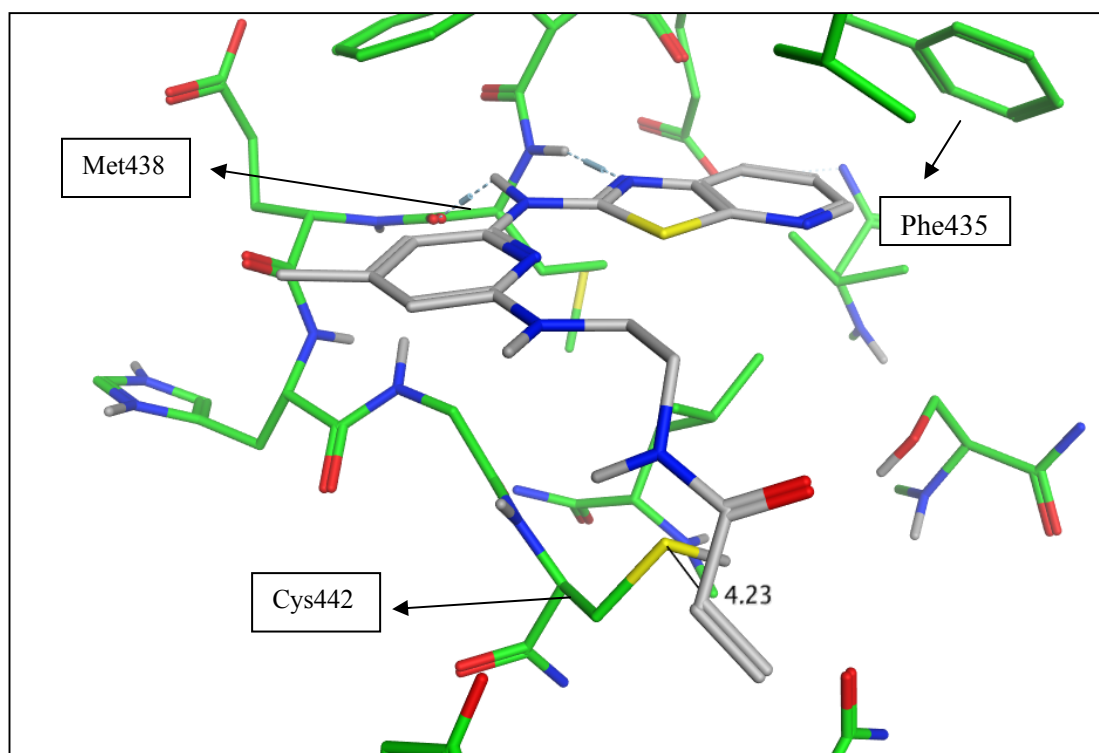


Figure 17. Potential conformation of compound **4** in the ITK active site

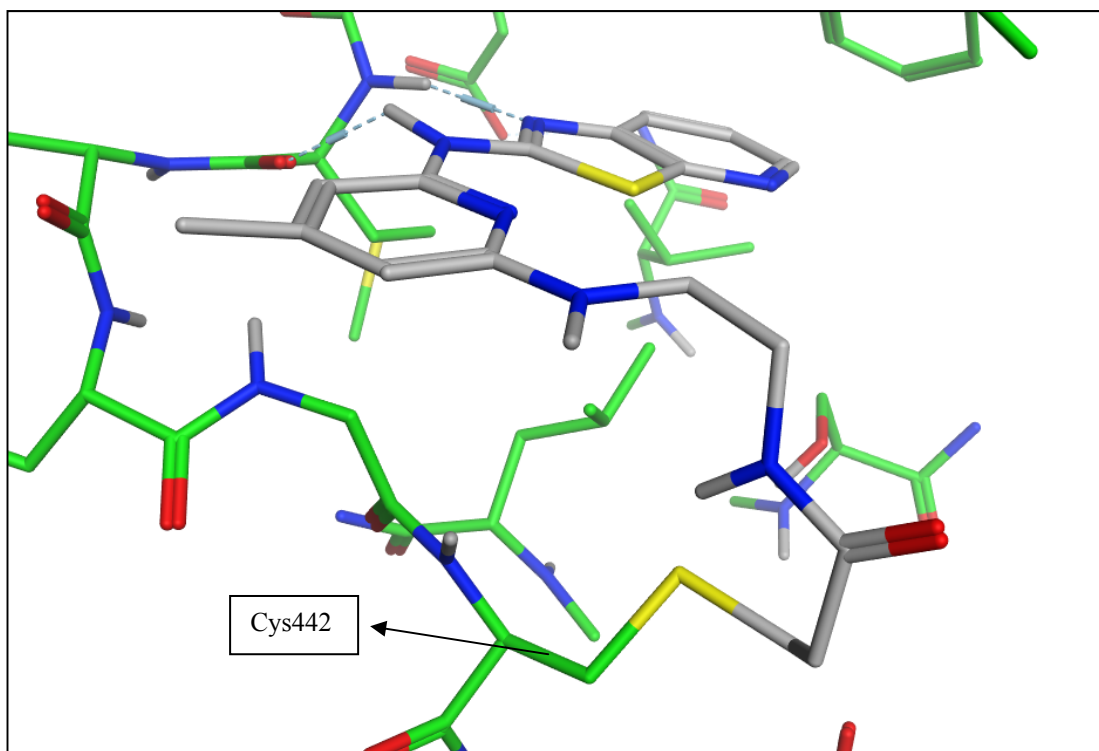


Figure 18. Modelling of compound **4** in the ITK active site presenting the potential covalent interaction between Cys442 and the acrylamide unit

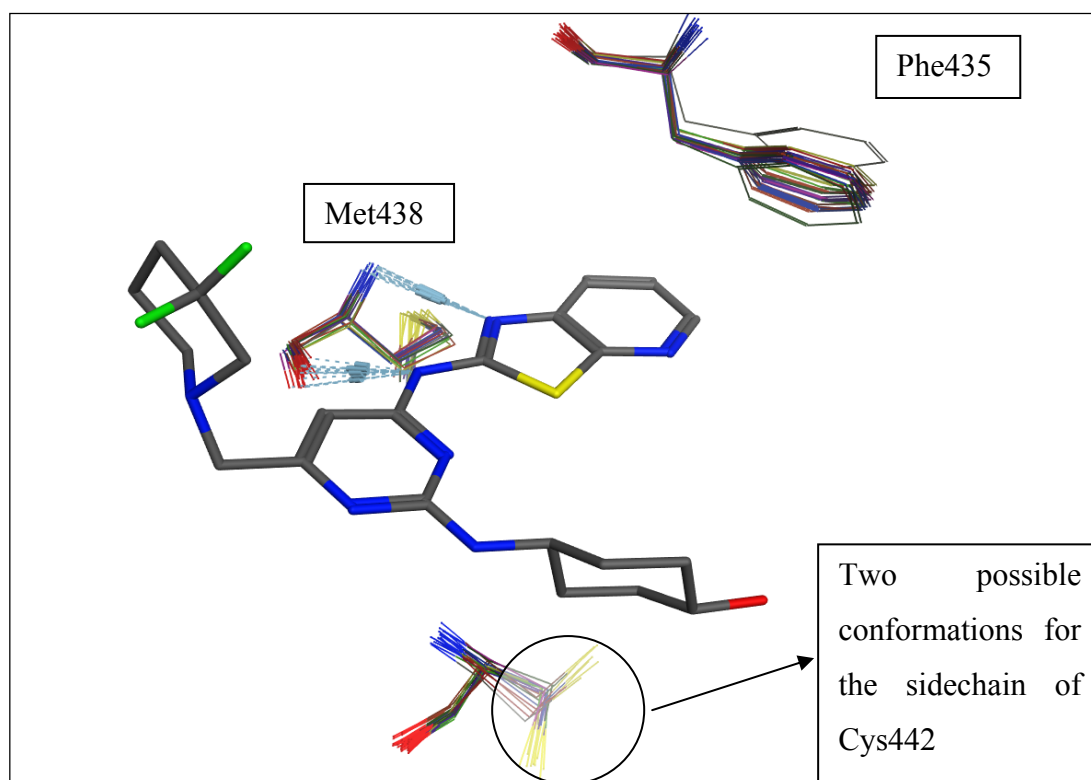


Figure 19. Comparison of 21 ITK crystal structures to assess the rotation potential of Cys442 in the ATP binding site

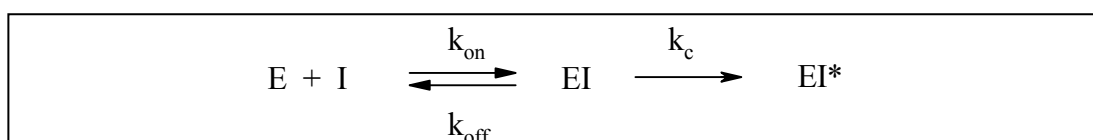
This molecular modelling supports the hypothesis that irreversible ITK inhibitors could be developed from the amino-benzothiazole non-covalent template.

2. Biological assays used to characterize irreversible ITK inhibitors

Based on all the reasoning detailed above, several objectives were set at the beginning of this programme:

- Investigating the effect on potency of replacing the important *trans*-aminocyclohexanol by the various groups containing an electrophilic moiety had to be performed. Before the Michael reaction can occur between the compound and Cys442, the inhibitor needs to non-covalently bind to ITK. Without sufficient non-covalent affinity to the kinase, the acrylamide and Cys442 may not be in close proximity long enough to react and make the covalent bond, as the electrophilic moiety is designed to be of low reactivity to avoid any unwanted reaction with

various nucleophiles present within the cells.⁴⁸ The kinetics of this time-dependent inhibition can be summarized by that described in Equation 1.¹⁰⁰ k_{on} and k_{off} represent the on and off rate constants for reversible or non-covalent binding of the compound to the kinase while k_c represents the rate constant for covalent bond formation between the kinase and the inhibitor: the greater the non-covalent binding (*i.e.* low K_i), the higher the concentration of the EI complex and the faster the rate of covalent bond formation. k_c is dependent on the type of electrophile and, more importantly, the position of the electrophilic moiety compared to Cys442 in the ATP pocket will dictate the rate of the required reaction.⁴⁵ For the same electrophilic moiety, the less spatial accommodation the Michael acceptor and the cysteine have to perform, to be in a position of reacting together, the quicker the reaction will be.



Equation 1. Kinetic representation of an irreversible kinase inhibitor¹⁰⁰

The kinase primary affinity will be measured using a HTRF binding assay between ITK and the suggested compounds.³² The principle of the assay is described in Figure 20: a commercial tyrosine kinase substrate¹⁰¹ is incubated with activated ITK, ATP and the ITK inhibitor for 25 minutes (no preincubation between the inhibitor and the kinase). After the reaction, the phosphorylation of the tyrosine kinase substrate is measured by fluorescence following the addition of Europium-labeled antibody and fluorochrome conjugate. This assay measures the concentration of inhibitor (IC_{50} or pIC_{50}) required to inhibit 50 % of the phosphorylation of substrate. Because of the way the assay is set-up (with no incubation between the inhibitor and the kinase), unless the covalent binding is rapid, the assay should mainly measure the non-covalent affinity to the kinase. Published literature^{45,82} confirms that irreversible inhibitors are not necessarily more potent than reversible agents in the primary enzyme assay. Comparing the pIC_{50} between the potential irreversible inhibitors and compound **1** will provide insight into whether the electrophilic moiety is tolerated in relation to the non-covalent binding affinity. However, one cannot ignore that for

irreversible inhibitors, even after a short 25 minute reaction, a fraction of the inhibitor has already covalently reacted with the kinase hence the pIC₅₀ reported is a measure of the non-covalent and covalent reactions with ITK at 25 minutes. For irreversible inhibitors, the HTRF pIC₅₀ is time dependent.

The initial HTRF ITK enzyme assay (HTRF⁽¹⁾) was set up using 4 nM of kinase and 20 μM of ATP. These conditions were used to assess the phosphorylation inhibition of the substrate up to a pIC₅₀ of 8.3, which represents the tight binding limit of the experiment. During the course of this research programme, potent ITK inhibitors reaching the tight binding limit of this assay were prepared, hence new conditions had to be developed to assess the affinity of the molecules to ITK. The second HTRF ITK enzyme assay (HTRF⁽²⁾) used a slightly lower amount of kinase (2.5 nM) but, more importantly, a much higher concentration of ATP (1 mM). These conditions reduced the pIC₅₀ of the inhibitors as they had to compete with a higher concentration of ATP to bind to the active site. This 1 mM concentration was selected because it represents approximately the amount of ATP found in cells (1-2 mM). The tight binding limit of this second HTRF assay was calculated at a pIC₅₀ approaching 8.5.¹⁰²

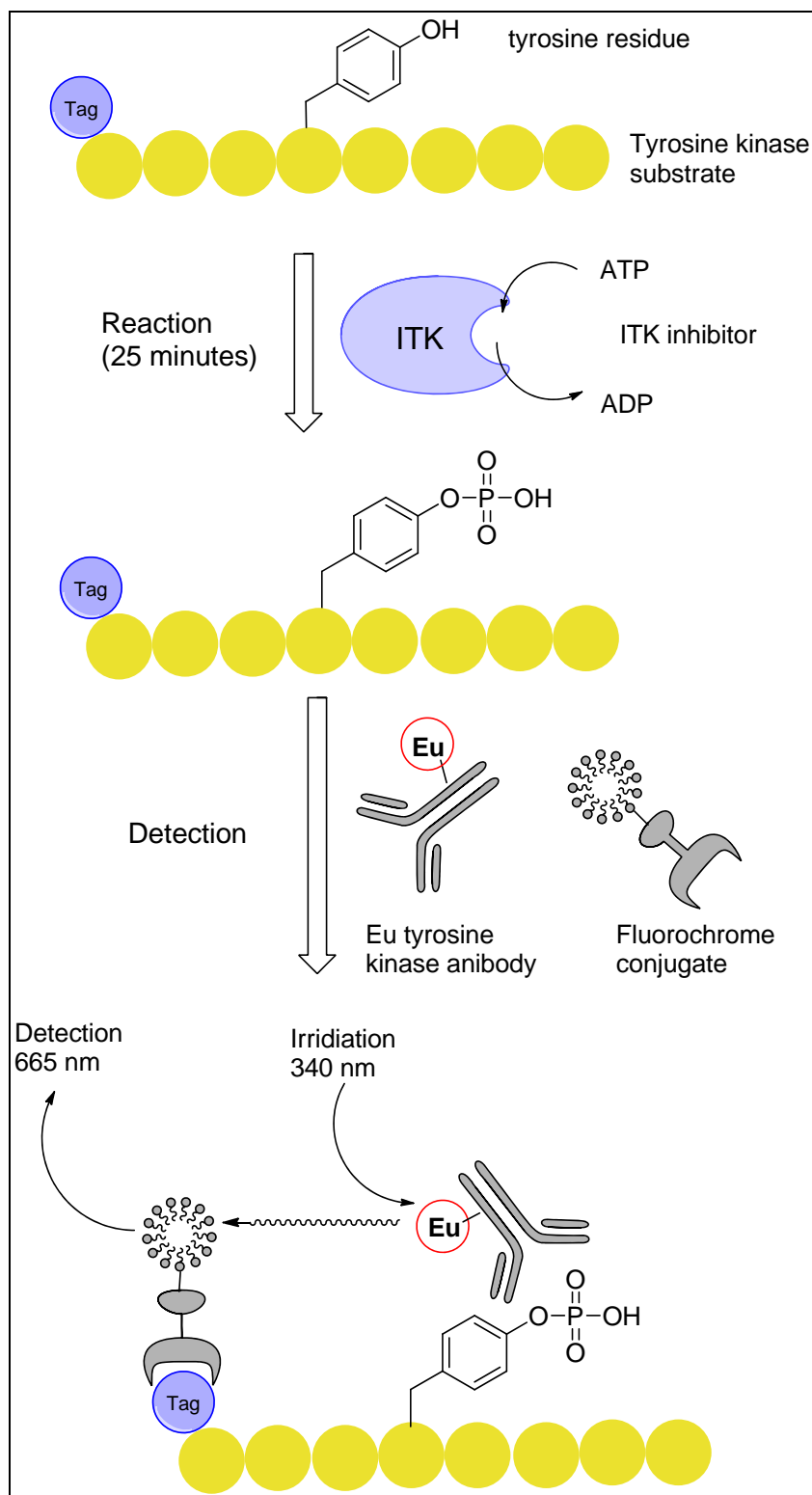


Figure 20. ITK HTRF enzyme assay principle

The activity of the compounds against ITK will then be measured in the more physiology relevant cellular PBMC assay. Contrary to the primary enzyme assay,

some reports in the literature tend to suggest that irreversible inhibitors start to display a greater activity profile compared to the corresponding reversible inhibitors in cellular assays.⁴⁵ This effect is potentially due to the longer incubation time often used in the cellular assays, allowing the covalent bond to be formed in the case of the irreversible inhibitors. The cells and the inhibitors are pre-incubated for one hour before being activated with an antibody-based reagent, Cytostim, designed to bind to the TCR. This leads to the activation of ITK and the release of inflammatory cytokines. The activity of the inhibitors is measured by their ability to reduce the production of IFN- γ cytokines 16 hours after the addition of Cytostim.

The activities of the compounds in these two assays are critical. As described previously, for the covalent interaction to occur selectively between the ITK Cys442 and the inhibitors, the compounds need to be firstly bound non-covalently into the ITK ATP pocket. A high pIC₅₀ in the 25 minute HTRF assay will indicate that the inhibitors bind to ITK, at least non-covalently. The level of activity in the cellular PBMC assay will indicate whether these irreversible inhibitors reduce the production of IFN- γ cytokines after 16 hour incubation at lower concentrations compared to the reversible molecules. The target of the ITK programme consists in achieving irreversible inhibitors displaying enzyme HTRF⁽²⁾ (1 mM ATP concentration) activity corresponding to pIC₅₀ > 7.7, whereas the crucial PBMC activities have to be greater than a pIC₅₀ of 8.5 (value never achieved by ITK reversible compounds from the amino-benzothiazole template) to be considered as potential drug candidate for inhaled administration.

Nevertheless, these assays do not provide direct information on the covalent binding of the compounds to ITK, which is expecting to deliver their desired extended duration of action.

- The initial stage was to confirm that replacing the *trans*-aminocyclohexanol by electrophilic moieties was tolerated for the kinase primary binding activity and whether the inhibitors were irreversibly bound to ITK. To this end, three methods were put in place:

(i) Mass spectrometry assay - The formation of a covalent bond between the kinase and the inhibitor can be detected using mass spectrometry experiments similar to

those described in the literature for the irreversible EGFR and BTK inhibitor programmes.^{45,90} An excess of compound is incubated with ITK protein. Any unreacted cysteine in the ITK protein is then labelled with iodoacetamide and the active site protein fragment of ITK is obtained by treatment with tryptic digests. Mass spectrometry analyses of this fragment subsequently determine the alkylation pattern of the kinase.¹⁰³ This active site protein fragment possesses three cysteine residues, including the targeted Cys442. When the mass spectrometry experiment was conducted with 4-vinylpyridine (VP) as the electrophile,¹⁰⁴ the labelling occurred at all three cysteine residues of the active site (Figure 21).

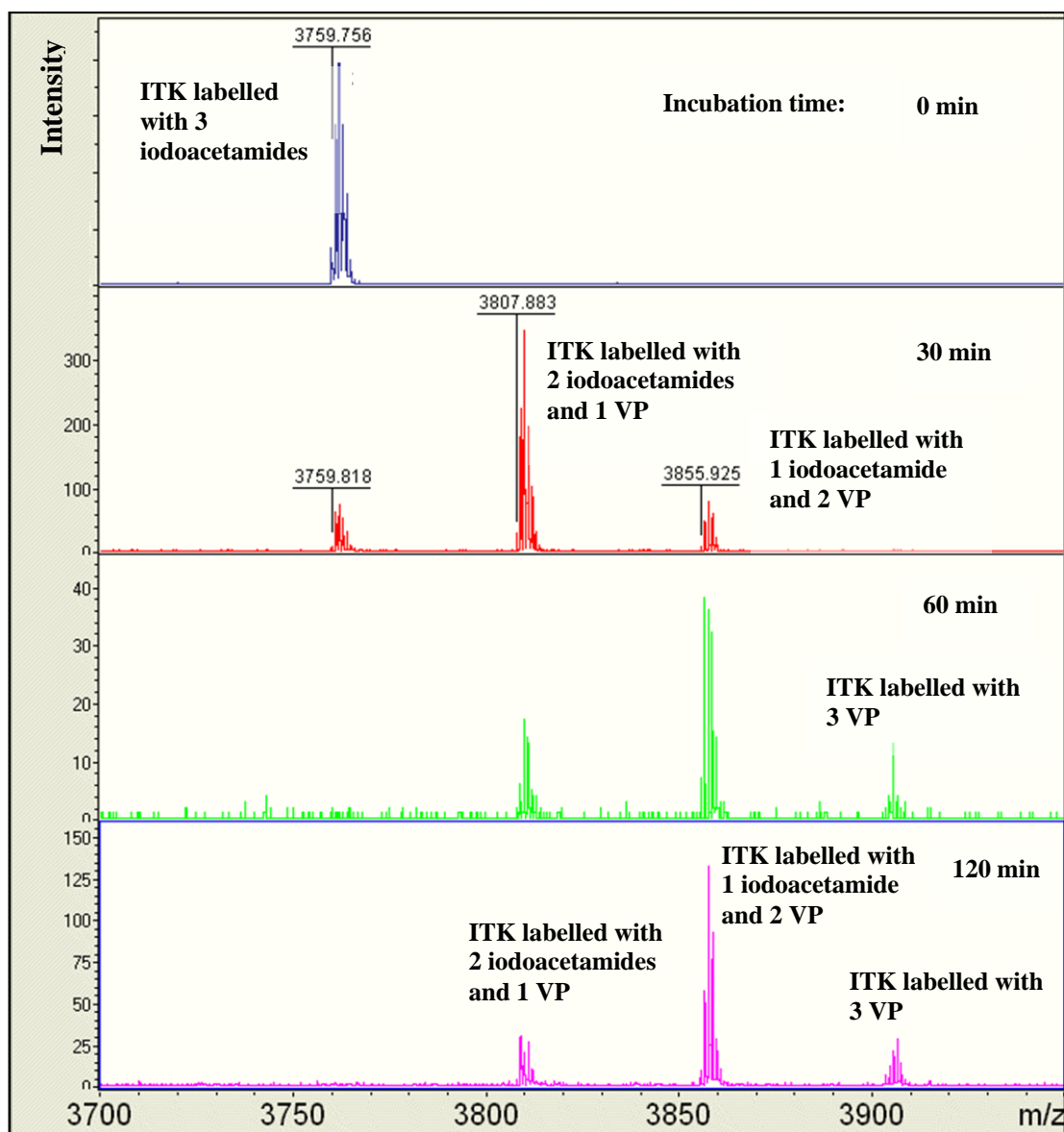


Figure 21. Mass spectrometry experiment using vinyl pyridine (VP) as the electrophile¹⁰³

With no incubation between the kinase and 4-vinylpyridine, all three Cys residues react with iodoacetamide and show a main peak at $m/z = 3759$. With the 30 minutes, 60 minutes, and 120 minutes incubation time, new peaks are observed in the mass spectrometry experiments. Mass analysis of the peaks provides information on the number of Cys residues alkylated with VP. After 30 minutes of incubation, a main peak at $m/z = 3807$ corresponds to one Cys labelled with VP, while a less intense second peak at $m/z = 3855$ corresponds to two Cys labelled with VP. The third Cys

residue has not reacted with VP in this timescale and therefore is labelled with iodoacetamide. After 60 and 120 minutes, all three Cys of the ITK ATP pocket start to be labelled with VP. This example proves that mass spectrometry can be used to determine alkylation reactions occurring in the active site of ITK.

(ii) Kinetic assay - The second assay used to determine the irreversible inhibition of ITK is a kinetic assay measuring the ability of the compound to bind to the kinase as a function of time.³⁶ As described in Figure 22, in the absence of inhibitor, the labelled tracer (ATP-competitive compound) binds to the active site of the kinase of interest and high fluorescence resonance energy transfer (FRET) is measured. In the presence of an inhibitor, the tracer and the compound compete to bind in the ATP pocket hence lower FRET is detected.

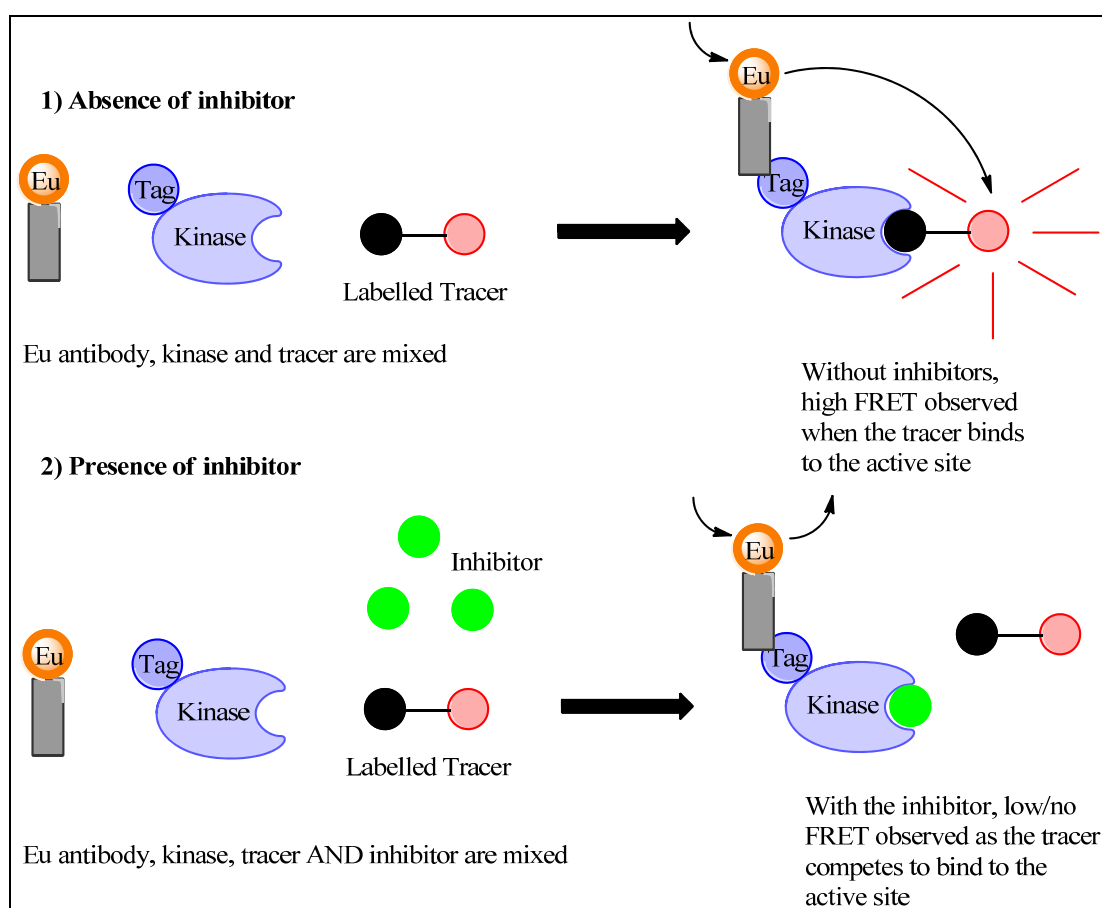


Figure 22. Principle of the binding assay used for kinetic studies¹⁰⁵

In the case of a reversible inhibitor, for a given concentration of the compound, the binding to the kinase (hence the FRET measured) should be constant as a function of time as the binding and release of the inhibitor to the kinase is an equilibrium (Figure 23). In the case of an irreversible inhibitor at a given concentration, the initial binding measured by the FRET will correspond to the non-covalent affinity to the kinase (formation of EI). With increasing time, the equilibrium should be driven towards the covalent formation of the compound-kinase complex (EI*) resulting in increased inhibition (corresponding to a decrease of the FRET measured).

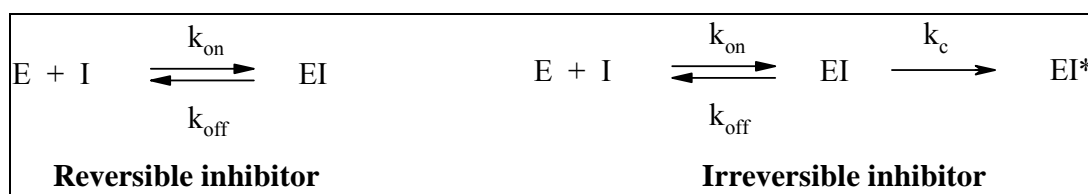


Figure 23. Kinetic equations for reversible and irreversible inhibitors¹⁰⁰

This assay was validated using known reversible and irreversible inhibitors.³⁶ For a typical reversible ITK inhibitor (Figure 24), the binding to ITK measured by FRET (Y axis) does not significantly vary (fluorescence signal within 0.005 units) with time (X axis) for the different concentrations of compound.

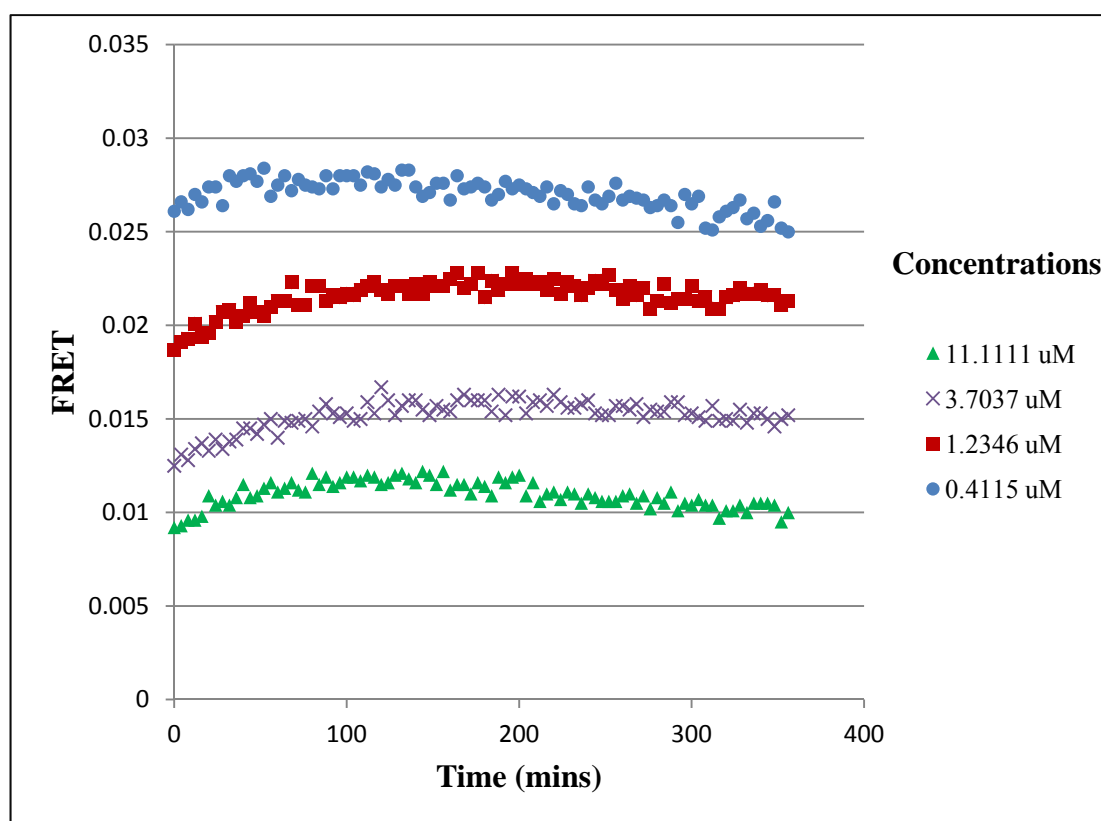


Figure 24. Binding kinetic data for an ITK reversible inhibitor³⁶

In the case of the literature irreversible BTK inhibitor **3** (Figure 15), using BTK protein in the experiment, for the concentrations represented in yellow, red and purple, a time dependent binding is observed by FRET (Figure 25). This is characteristic of an irreversible inhibitor: the formation of the covalent EI* complex drives the equilibrium towards the formation of the EI complex leading to the decrease in the observed fluorescence. However, another method is necessary to complement these data since the time dependent binding could also be consistent with slow-binding reversible inhibition. The “jump dilution” experiment consisted of mixing the kinase (for compound **3**, BTK; for the inhibitors developed as part of this research programme, ITK) and various concentrations of inhibitor for two hours to allow the formation of the complex (EI for a reversible inhibitor and EI* for an irreversible molecule). After that time, an excess of competitor tracer was added and the FRET was measured for a period of 6 hours at two minutes intervals. For irreversible inhibitors such as compound **3**, the FRET signal did not show an increase in binding over time of the competitor tracer, which is consistent with irreversible

complex formation between the inhibitor and the kinase. Moreover, after the addition of the competitor tracer and once the FRET signal was stable, the IC_{50} of the inhibitors was measured (usually at 60 minutes) and compared to the IC_{50} calculated using the Cheng-Prusoff equation, only valid for non-covalent inhibitors (Equation 2). For irreversible inhibitors, the measured IC_{50} should be significantly lower than predicted under the conditions of the assay according to the Cheng-Prusoff equation (*e.g.* for compound **3**, the measured IC_{50} was 11 times lower than predicted by the the Cheng-Prusoff equation. For the reversible inhibitor described in Figure 24, the measured and predicted IC_{50} were equivalent within experimental error).³⁶

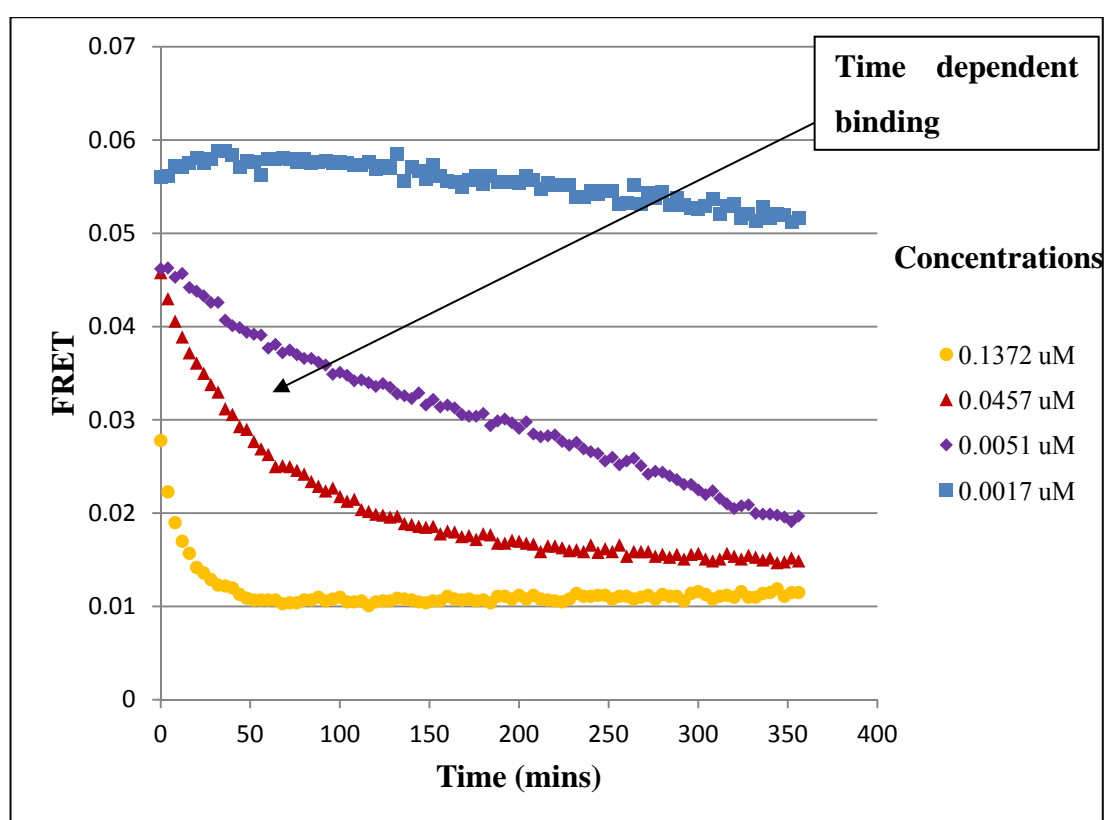


Figure 25. Binding kinetic data for the literature BTK irreversible inhibitor **3** (using BTK protein in the assay)³⁶

$$IC_{50} = K_i \left(1 + \frac{[L]}{K_d} \right)$$

[L] = concentration of tracer, K_d = affinity of tracer for ITK

Equation 2. Cheng-Prusoff equation for non-covalent inhibitors

The kinetic assay was initially used to assess qualitatively whether the inhibitors were covalently binding to ITK. However, when irreversible ITK inhibitors with the activity profile required for a drug candidate were obtained, the assay was refined to allow the precise quantification of the reversible binding constant K_i ($K_i = k_{off} / k_{on}$) and the rate of inactivation k_c (note that the initial kinetic assay was able to produce K_i and k_c values but the experimental errors were believed to be too high to be used to rank compounds with similar activities).¹⁰⁶ The various time dependent curves (such as the red and yellow curves in Figure 25) were fitted to Equation 3 for each compound concentration to obtain k_{obs} , the apparent first-order rate constant for the interconversion between the initial and final bound state.¹⁰⁷ The k_{obs} data were fitted using nonlinear regression analysis to Equation 4 to generate K_i and k_c .^{48,100,107} These values were critical to differentiate irreversible ITK inhibitors with similar potency profiles.

$$A = A_{\infty} + (A_0 - A_{\infty})e^{-k_{obs}t}$$

A = FRET signal at time t, A_{∞} = FRET signal at time infinity, A_0 = FRET signal at time zero

Equation 3. Exponential rate equation used to fit the kinetic data

$$k_{obs} = \frac{k_c[I]}{[I] + K_i \left(1 + \frac{[L]}{K_d} \right)}$$

[I] = concentration of compound, [L] = concentration of trace, K_d = affinity of tracer for the kinase

Equation 4. Mathematical relationship between k_{obs} , K_i and k_c

(iii) Crystal structure - The mass spectrometry and the kinetic assays are sufficient to identify irreversible ITK inhibitors. However, an X-ray crystal structure of the complex kinase-inhibitor, presenting the covalent bond between the electrophilic moiety and Cys442 would represent an excellent visual confirmation of the success of this approach. Moreover, it would indicate the conformation the inhibitor has to adopt for the covalent bond to be formed and this could be compared to the molecular modelling to assess the validity of the *in silico* predictions. Soakings and cocrystallisations⁴⁰ with the ITK protein were attempted to obtain crystal structures of the kinase-inhibitor complex. The success of these techniques is limited for ITK as many potent ITK reversible inhibitors failed to give crystals with good enough diffraction patterns to achieve high resolution and usable data. However, the technique will be attempted for the best compounds, as it would give extremely valuable information on the positions/conformations of the inhibitor/kinase to successfully form the requisite covalent bond.

(iv) Cellular wash-out experiment - Finally, but arguably the most important assay for further progression of the compounds, a cellular wash-out experiment was developed.¹⁰⁸ The inhibitors were incubated with the PBMC cells for an hour before being washed with aqueous media. The cells were then activated with an antibody-based reagent and the release of IL-2 cytokines was recorded. In the case of reversible inhibitors, no inhibition (hence full release of cytokines) should remain as the inhibitors would be washed from the cells. In contrast, irreversible inhibitors should retain ITK inhibition as the compounds will be covalently bound into the ATP binding site of the kinase. This assay is critical for the programme as it demonstrates the longer duration of action of the irreversible inhibitors in a cellular context. However, because of technical issues encountered during the set up this experiment, the assay was not available at the start of this research programme and was only validated by the biologists of our laboratory towards the middle of the medicinal chemistry effort.¹⁰⁸

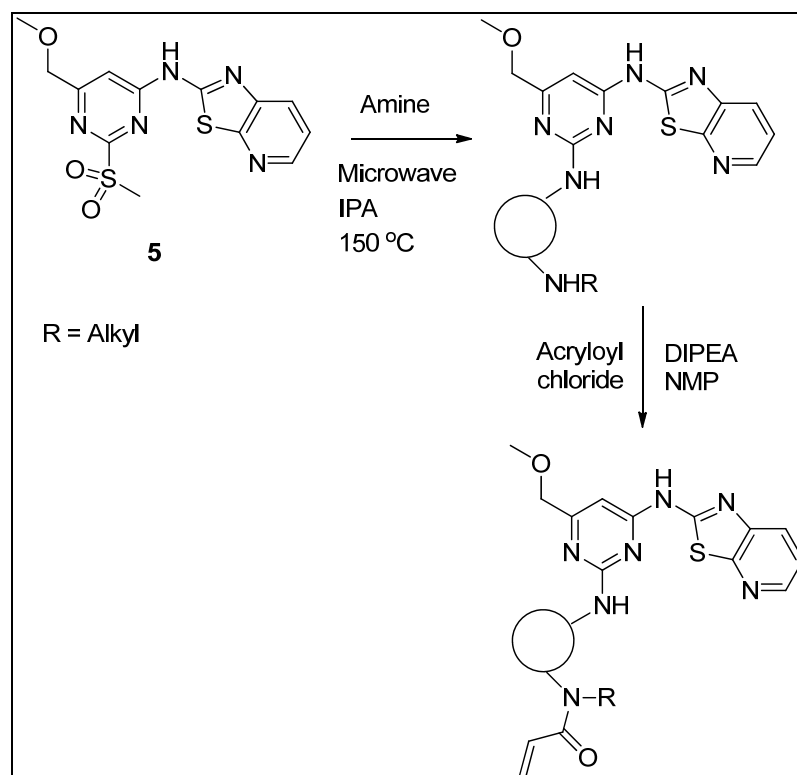
In summary, the molecular modelling predicts that irreversible ITK inhibitors are achievable by replacing the *trans*-aminocyclohexanol group with electrophilic moieties to investigate potential covalent interactions between the electrophilic unit

and the Cys442 residue. Furthermore, several assays are in place to assess whether the designed compounds are irreversible inhibitors of ITK. If these irreversible inhibitors are discovered, they should, in theory, overcome the two major issues highlighted previously with the ITK reversible amino-benzothiazole template (*i.e.* lack of *in vivo* efficacy and residual activity against TrkA and TrkB).

VII. Results and discussion

1. The 6-methoxymethylpyrimidine template

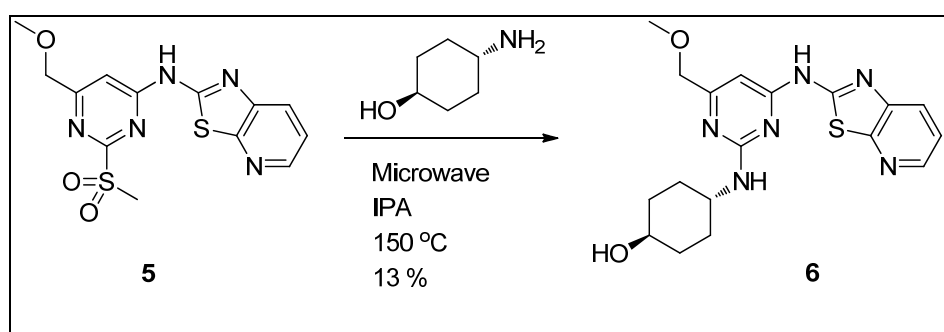
The primary medicinal chemistry target was to investigate the effect on ITK potency of replacing the important *trans*-aminocyclohexanol, by various groups containing an electrophilic moiety. To this end, it was decided to synthesise a range of potentially irreversible inhibitors using the intermediate compound **5** (Scheme 6), which is a legacy structure from the initial programme on reversible inhibitors within our laboratories.³⁰



Scheme 6. Target compounds to assess the effect of introducing the Michael acceptor on the ITK potency

It has been shown by the initial medicinal chemistry performed as part of this overall programme that the methoxymethyl group at the 6-position of the pyrimidine is not optimal for the solubility of the final compounds compared to the morpholine group found in the further advanced reversible inhibitor compound **1**.³⁸ In terms of the primary HTRF affinity (note that the HTRF⁽²⁾ assay is used in this comparison as compound **1** reached the tight binding limit of the HTRF⁽¹⁾ experiment), compound **6** (Scheme 7) is not as active as compound **1** (Figure 26). However, this species provides a good activity benchmark to study the effect of changing the *trans*-aminocyclohexanol by the various groups containing the electrophilic moiety. The slight increase in activity in the 1 mM ATP HTRF assay observed when adding the morpholine group (compound **7** compared to compound **6**, Figure 26) and when changing the pyrimidine to a pyridine motif (compound **1** compared to compound **7**, Figure 26) was previously studied when investigating this amino-benzothiazole template.³⁸ As a general trend, replacing the methoxy motif with a morpholine usually increases the HTRF binding activity by 0.8 log unit. In a similar way, moving

from the pyrimidine central ring to the pyridine ring found in compound **1** also increased the activity by approximately another 0.7 log unit (Note that the 0.7 log unit increment in activity between the pyrimidine and pyridine is an average for this series of compounds and not what is observed for compound **1** and compound **7**).³⁸ It is worth noting at this point that the increments in enzyme potency do not always translate into similar increments in the PBMC cellular assay. The reasons for this remain unclear but one can suggest that the permeability of the various compounds is playing an important role in their cellular potency. The cellular permeabilities of the three compounds described in Figure 26 have not been measured.



Scheme 7. Synthetic scheme for compound **6**

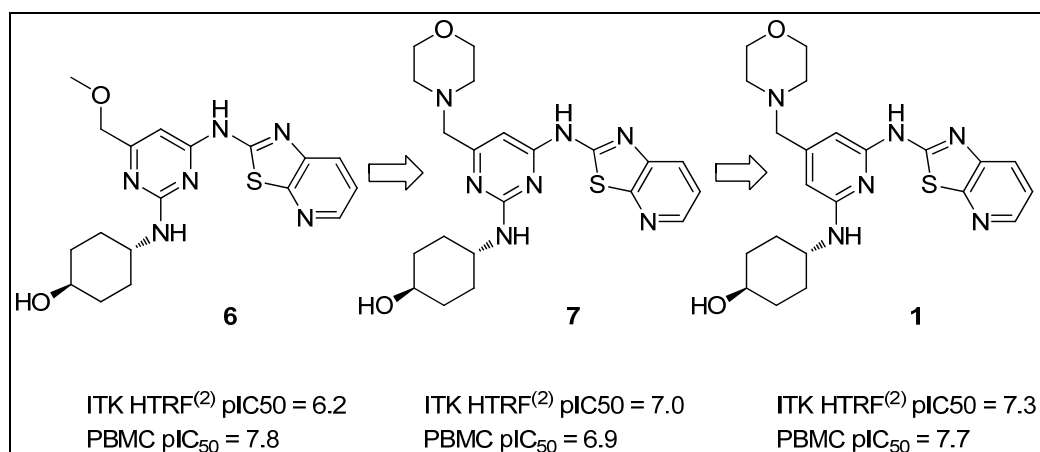


Figure 26. SAR optimisation of the amino-benzothiazole reversible template

The initial approach was aimed at investigating the effect on ITK activity of replacing the *trans*-aminocyclohexanol by the various groups containing the electrophilic moiety, using the intermediate compound **5**, with the synthetic strategy being shown in general terms in Scheme 6. Active compounds containing the novel

Michael acceptor motif would then be translated to the more active series (similar to compound **7** and compound **1**), where the chemistry was more challenging and time-consuming.

A range of amine linkers were selected to be attached to the 6-methoxymethylpyrimidine template to assess whether they would retain the important non-covalent recognition to ITK (Figure 27). These groups vary from flexible acyclic chains to more rigid and more lipophilic cyclic chains, all possessing a terminal acrylamide Michael acceptor. The flexible acyclic chains should have a better chance to place the Michael acceptor in a favourable position compared to Cys442 for the covalent reaction to occur, as already predicted by the computational molecular modelling described in Figure 17 and Figure 18. In contrast, the more rigid cyclic linkers will position the Michael acceptor in more precise area of the active site and some might end up being too far from Cys442 for any reaction to occur. Nonetheless, the more lipophilic character of the chain (similar to the *trans*-aminocyclohexanol) should deliver molecules with better non-covalent binding to ITK.^{41,42} The objective of this initial piece of work was to assess whether replacing the *trans*-aminocyclohexanol with these linkers would significantly affect the non-covalent binding to ITK. The best inhibitors from this series would thereafter be profiled in the complementary studies described in the previous section to assess whether they will covalently react with ITK.

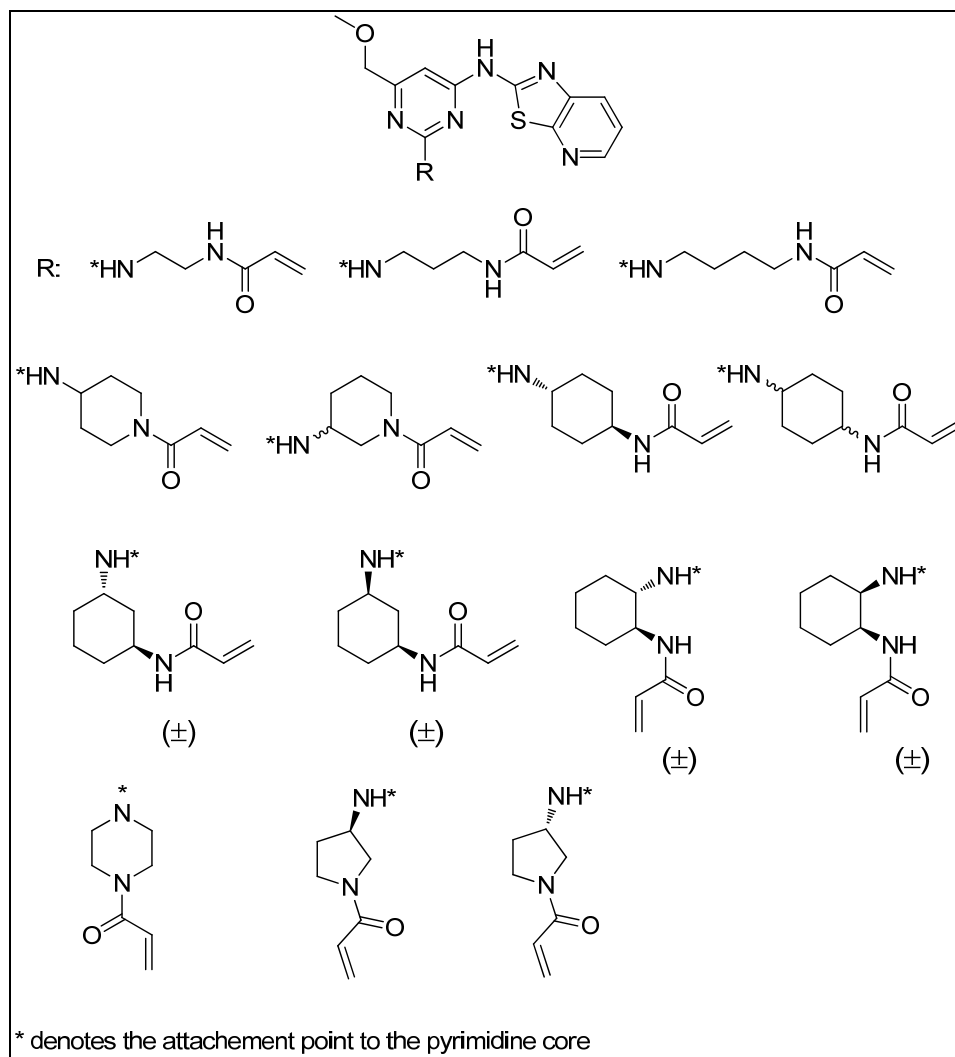
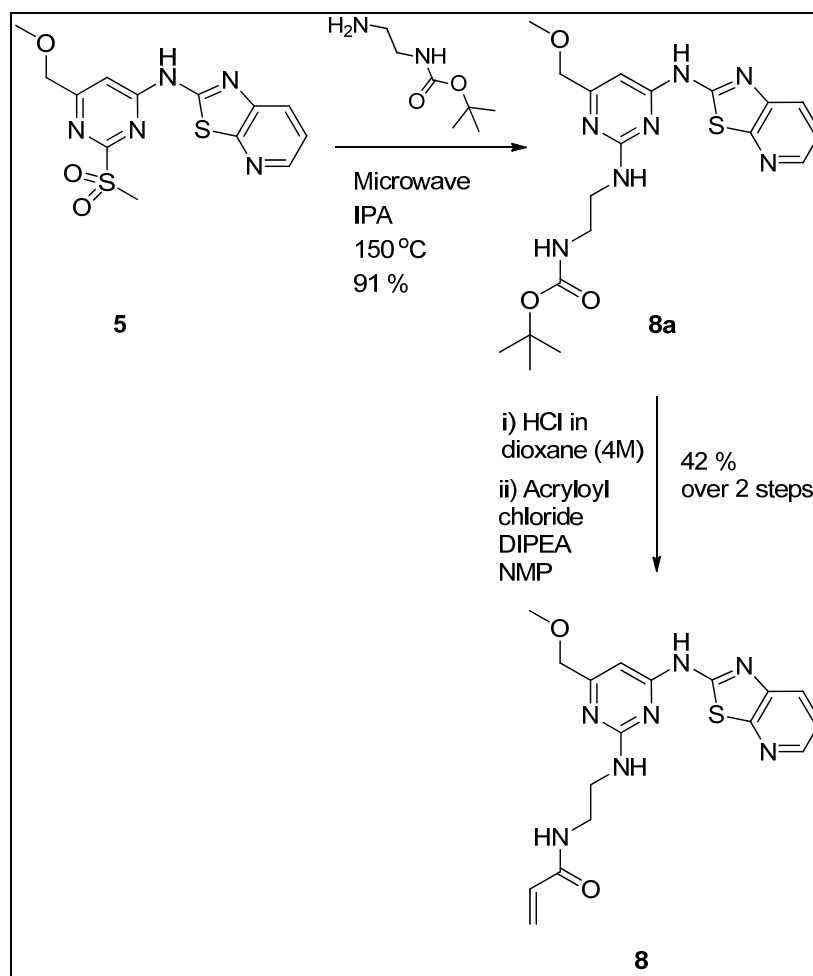


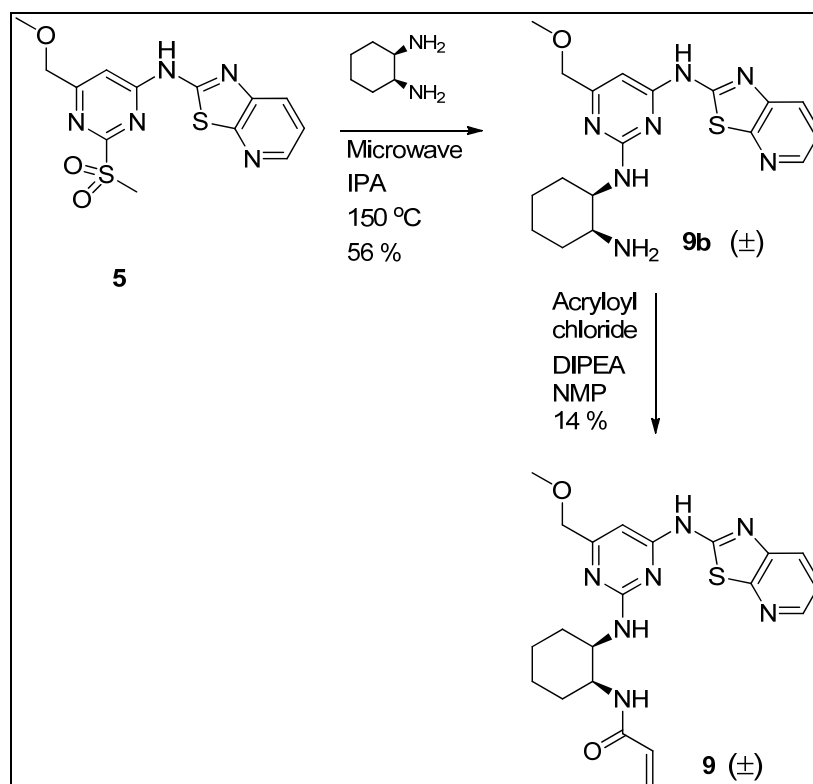
Figure 27. Range of amines selected to be attached to 6-methoxymethylpyrimidine template

The synthetic schemes presented in Scheme 8 and Scheme 9 summarise the two possible and closely related approaches followed to make the desired irreversible inhibitors. Depending on the availability of the amine or the reactivity requirements, the nucleophilic displacement was performed either with the diamine intermediate (Scheme 9) or the Boc protected diamine analogue (Scheme 8). In both synthetic schemes, the nucleophilic displacement on the methylsulfone **5** was performed using an excess of amine at 150 °C in a Biotage microwave system. In the first case, the Boc protected diamine intermediate **8a** was purified by normal phase chromatography before deprotecting the Boc group with HCl in dioxane (4 M). The HCl salt of the amine intermediate was then used in crude form and reacted with

acryloyl chloride at room temperature to yield compound **8**. In Scheme 9, the aromatic nucleophilic displacement with a diamine yielded the intermediate **9b** after mass directed autoprep (MDAP) purification. Compound **9b** was then reacted with acryloyl chloride in NMP to yield the desired Michael acceptor **9**. As a general trend, the first synthetic scheme (Scheme 8) was found to be more efficient for the synthesis of the required products and is the method of choice when accessing these species on a large scale. The aromatic nucleophilic displacement usually provides a clean profile and the intermediate can easily be purified by normal phase chromatography. The scheme presented in Scheme 9 is shorter in terms of the number of steps but the more polar intermediate, following the displacement with the diamine, requires purification by reverse phase chromatography. (The open access MDAP available in our laboratory is a straightforward automated reverse phase high pressure liquid chromatography system allowing purification of intermediates and products in a small scale (< 100 mg)). This type of purification is very effective for accessing clean compounds but the yield is often poor (< 70 % for the purification only). The moderate 56 % yield observed in Scheme 9 does not reflect the general profile of such reactions, which is comparable to the nucleophilic displacement performed with the Boc protected amines (Scheme 8). Finally, isolating the intermediates from the aromatic nucleophilic displacement in good purity was found not to be essential and the whole synthesis to the final products could be carried out without full characterization of the intermediate of the type of **8a** and **9b**.



Scheme 8. Synthesis of compound **8** using 1,1-dimethylethyl(2-aminoethyl)carbamate to perform the nucleophilic displacement

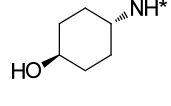
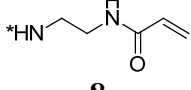
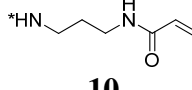
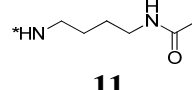
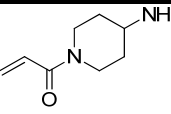
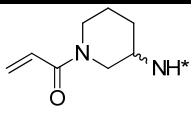
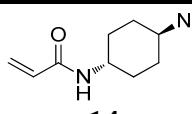
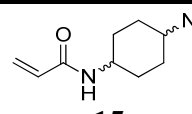
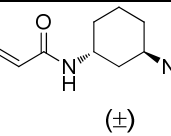
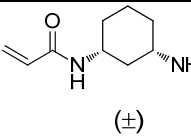
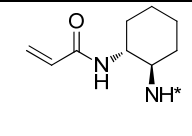
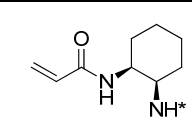
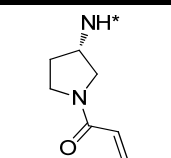
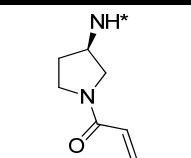
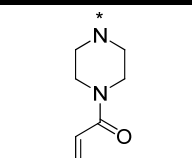


Scheme 9. Synthesis of compound **9** using *cis*-1,2-cyclohexanediamine to perform the nucleophilic displacement

The SAR analysis presented in Table 2 demonstrates that the Michael acceptor groups are tolerated in terms of retaining binding affinity to ITK (note that for this initial work, the low ATP concentration HTRF assay (HTRF⁽¹⁾) was used as these non-optimised compounds were not reaching the tight binding limit of the experiment). Indeed, although a small loss in binding activity to ITK is observed for the aliphatic amines (compounds **8**, **10** and **11**) compared to the *trans*-aminocyclohexanol **6** (approximately one log unit difference in the HTRF⁽¹⁾ assay), the gap in potency is much reduced with the more lipophilic cyclic amines (compounds **9**, **15** and **19**). This confirms the importance of the lipophilic cycloalkane ring which displaces water molecules from the active site and makes hydrophobic interactions with the protein, as observed in the crystal structure described in Figure 10. The molecular model of compound **19** in the ITK ATP binding site (Figure 28) shows positive contacts between the lipophilic pyrrolidine ring and the kinase, while the covalent interaction between the acrylamide and

Cys442 (Figure 29) remains available (refer to section VI.1 for the molecular modelling process).

Table 2. SAR analysis of the range of amines synthesised to access the Cys442 interaction

R	 6	 8	 10	 11
HTRF ⁽¹⁾ pIC ₅₀	7.8	6.6	6.8	7.0
PBMC pIC ₅₀	7.8	6.7	6.7	6.7
R	 12	 13	 14	 15
HTRF ⁽¹⁾ pIC ₅₀	7.2	7.4	7.3	7.7
PBMC pIC ₅₀	7.7	7.8	7.3	7.4
R	 (±) 16	 (±) 17	 (±) 18	 (±) 9
HTRF ⁽¹⁾ pIC ₅₀	6.8	7.5	6.4	7.6
PBMC pIC ₅₀	7.1	7.0	6.6	7.0
R	 19	 20	 21	
HTRF ⁽¹⁾ pIC ₅₀	7.5	6.6	6.9	
PBMC pIC ₅₀	7.7	6.1	7.2	

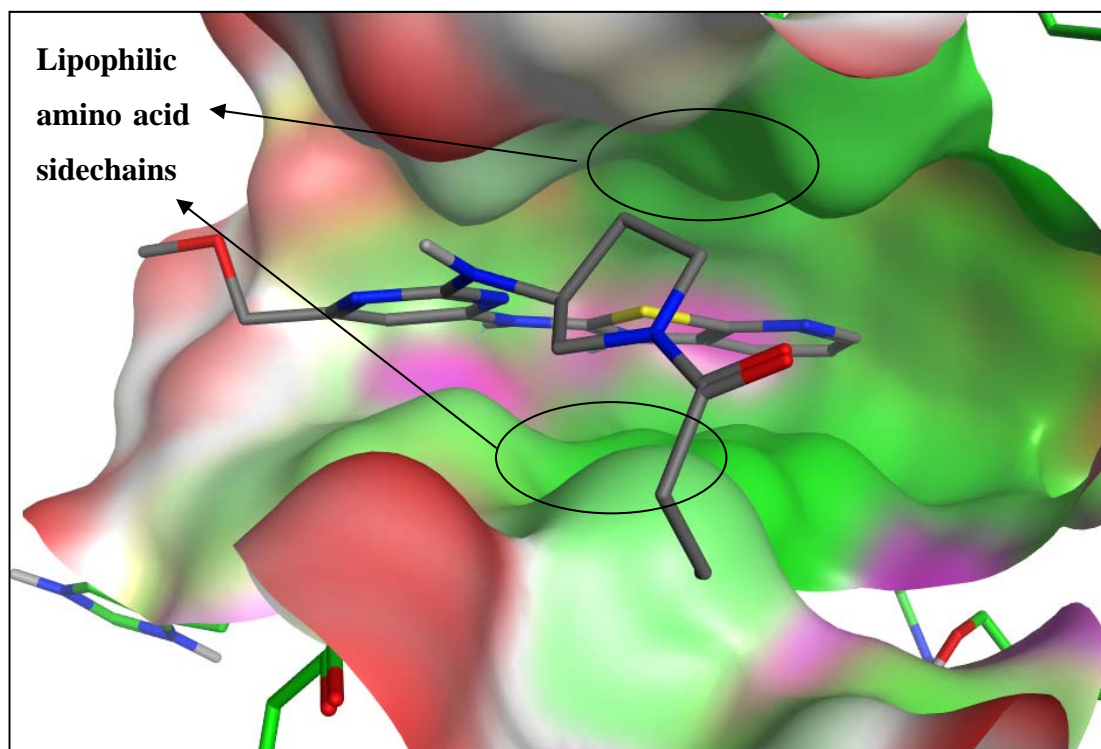


Figure 28. Molecular model of compound 19 in the ITK active site highlighting the importance of the lipophilic pyrrolidine ring (electron density surface view. Surface colours: green represent the lipophilic areas, red represent the areas exposed to solvent and purple represent the areas of polar interactions)

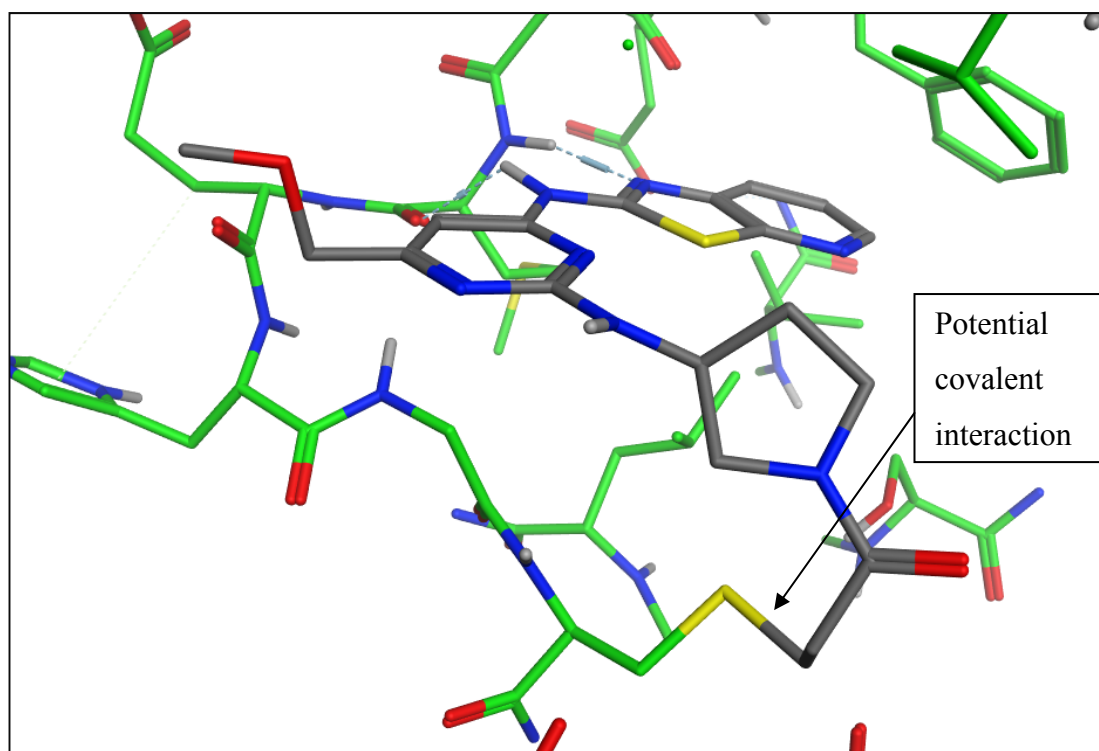


Figure 29. Molecular modelling of compound **19** in ITK presenting the potential interaction between the acrylamide and the cysteine residue

The reason for the difference in binding activities between the *cis*- and *trans*-isomers of the diaminocyclohexane analogues (compounds **14-15**, **16-17** and **18-9**) remains unknown. It is however interesting to note that the *cis*-isomers are, on average, 10 fold more active in the kinase binding assay than the *trans*-species. The increase in activity for the *cis*-compounds in the HTRF assay, unfortunately, does not automatically transfer into the PBMC assay. A similar one log unit difference is noticed in both the enzyme and the cellular assays between the *S*- and *R*-isomers of the pyrrolidine motif (compounds **19** and **20**). Once again, the computational molecular model cannot explain this observation. The model predicts that the more active *S*-enantiomer should present a better conformation for interacting with the cysteine residue. However, it has already been postulated that extra potency related to the covalent binding of the compounds to the kinase might not be visible in the short time course of the enzyme assay.

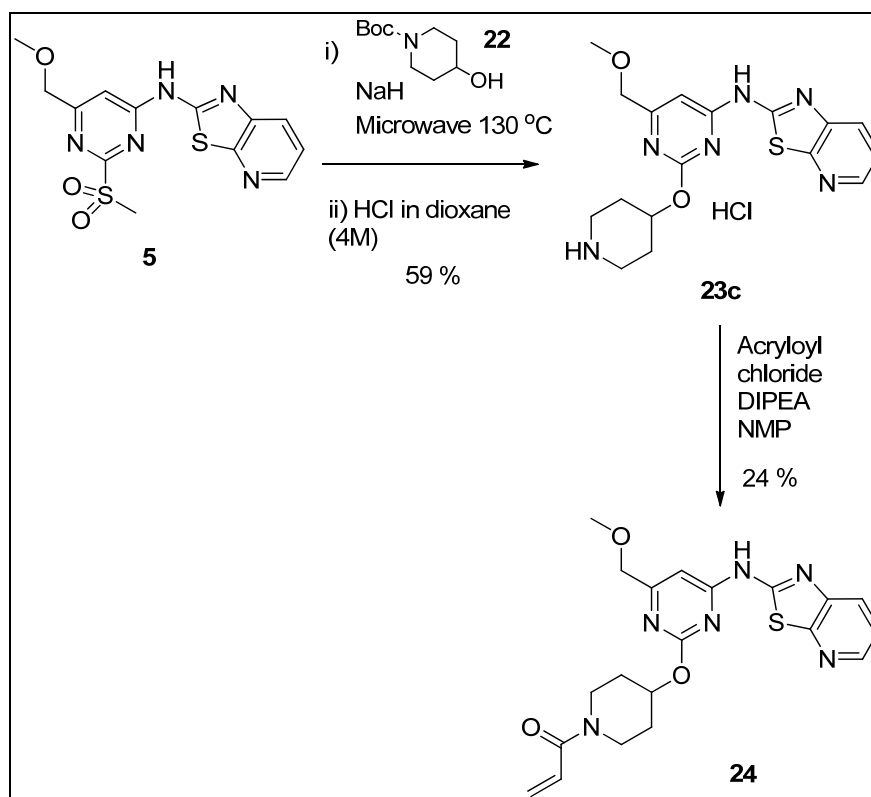
All compounds were also active in the cellular PBMC assay (Table 2). This demonstrates that the compounds can permeate cell membranes and gain access to

ITK within the cells. Looking at the difference between the HTRF and the PBMC assay, it is difficult to assess whether the compounds are making the covalent interaction with ITK. Indeed, as explained before, it has been shown in the literature that irreversible inhibitors start to present superior activity profiles compared to reversible compounds in cellular assays, which is mainly due to the longer incubation time present in the cellular experiments. The designed irreversible ITK inhibitors should start to be more potent in the PBMC assay than in the enzyme HTRF⁽¹⁾ assay as the reference non-covalent inhibitor **6** is equipotent in both experiments ($pIC_{50} = 7.8$, Table 2). Although it is observed that some cellular activities are greater than the enzyme values (compounds **8**, **12**, **13**, **16**, **18**, **19**, **21**), they are attributed more to the potential variation in data emerging from the assay (up to 0.5 log unit error not being uncommon) and to the differences in permeability of the compounds than to the irreversible character of the inhibitors. For all the compounds described in Table 2 the difference in potency between the enzyme and the cellular experiments does not provide insight into the reversible or irreversible binding of the compounds to the kinase. The only conclusions to draw from the SAR observed are that the non-covalent affinity to ITK is retained and that the slight enhanced cellular activities are encouraging in the view that some of these molecules might be covalently binding to the kinase. Further assays had to be performed to assess if irreversible inhibition had been achieved.

Finally, the importance of the NH linker to the pyrimidine ring was investigated by synthesizing compound **21** (Table 2). This tertiary amine compound does not possess the hydrogen required for interacting with the water residue in the X-ray crystal structure presented in Figure 9. Compound **21** is slightly less active than its closest analogues **13** and **19** in both the HTRF and the PBMC assays. Nevertheless, it is difficult to conclude that this difference in activity is due to the loss of the hydrogen bond interaction, as it could also be attributed to unfavoured lipophilic interactions with the protein. To confirm this hypothesis, it was decided to replace the NH linker with an oxygen (compound **24**, Scheme 10).

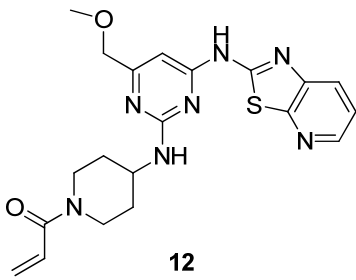
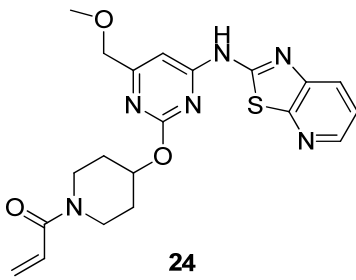
Intermediate **5** was reacted with the commercially available Boc-protected piperidine alcohol **22** in the presence of sodium hydride. Deprotection of the Boc group with

HCl in dioxane (4 M) yielded the intermediate **23c**, which was reacted, as previously, with acryloyl chloride and DIPEA in NMP to form the desired acrylamide product **24**.



Scheme 10. Synthesis and activity profile of compound **24**

Table 3. SAR analysis of compound **24**

Structure		
HTRF ⁽¹⁾ pIC ₅₀	7.2	6.4
PBMC pIC ₅₀	7.7	6.5

The HTRF and PBMC activities obtained for compound **24** (Table 3) confirmed the importance of the NH interaction with a water residue (Figure 9). Replacing the NH linker with an oxygen should not introduce a major change in the conformation of the compound. However, compound **24** is found to be less potent than its amine analogue **12** by nearly a log unit. Therefore, to increase the non-covalent recognition of the inhibitors to ITK, the secondary amines will remain the tethering groups of choice to link to the pyrimidine central ring.

The enzyme and cellular activities observed for the range of Michael acceptors successfully synthesised answer the first target set within this programme: the replacement of the *trans*-aminocyclohexanol by the various groups containing the electrophilic moiety did not dramatically reduce the binding activity to ITK, hence making the search for irreversible inhibitors feasible. Indeed, once the inhibitors are non-covalently bound to the kinase, a well-positioned Michael acceptor should interact with Cys442 to make the inhibitors irreversible.

To assess whether one of the inhibitors already synthesised has the potential to bind covalently to Cys442 in the ITK ATP binding site, a selection of compounds were tested in the mass spectrometry experiment described in the section VI.2. With this assay being low throughput in nature, only a relatively small number of compounds could be tested.

Compounds **8** and **13** were selected as candidates for the mass spectrometry experiment assessing the covalent binding of the inhibitors to ITK. These species were chosen for distinct reasons: compound **8** may not be the most active inhibitor synthesised for this series but the flexibility of the aliphatic chain might allow the Michael acceptor to be in proximity of the Cys442 residue without too much strain (Figure 17). Compound **13** is one of the most active compounds from the series (especially in the PBMC assay) hence an obvious choice for the assay. With compound **13**, the distance from the pyrimidine to the end of the Michael acceptor is also similar to compound **8** and its molecular modelling (for the *S*-isomer) is similar to that already described for compound **19** (Figure 29). Both compounds were incubated with the ITK kinase domain for one hour and the mass spectrometry data were collected using the protocol described in the previous section VI.2.¹⁰³ The

analyses of the data are presented in Figure 30. After one hour incubation at room temperature, compound **8** gave a clear single labelled species ($m/z = 4089.5$) for the active site peptide of interest, with only trace amounts of potential labelling of other cysteine-containing peptides. Mass spectrometry sequencing analysis of the m/z 4089 peptide confirmed labelling was at Cys442 in the peptide.¹⁰³ After the same incubation time, compound **13** also gave a peak corresponding to the 1:1 complex inhibitor:ITK active site ($m/z = 4129$). Moreover, the mass spectrum of compound **13** also presented a distinctive peak corresponding to another cysteine from the ITK protein (not in the active site) having reacted with the inhibitor. It is impossible to quantify how much compound has bound to this other cysteine using this assay. This reaction with a different cysteine being observed only for compound **13** was difficult to explain at this time, as it was believed that the two same Michael acceptors had similar reactivity toward various cysteine residues. This difference in reactivity will be investigated and discussed later in this thesis (section VII.3).



Figure 30. *Mass spectrometry experiments of compounds 8 and 13 after incubation with ITK for 1 hour*

These data clearly suggested that both compounds have covalently bound to the targeted Cys442 in the ITK active site. They also demonstrated that the covalent reaction between the inhibitor and ITK was somewhat selective to the cysteine of

interest (less selective for compound **13**) as none of the other cysteines present in the active site showed any reaction with the two inhibitors. However, the mass spectrometry assay was performed using an excess of inhibitor compared to ITK protein, which maximises the chance of forming the covalent interaction. Moreover, the assay does not allow the quantification of compound which has bound to the kinase. The peak corresponding to the 1:1 complex inhibitor:active site may only represent a small fraction of inhibitor initially incubated with the protein. This scenario would be the result of a slow Michael addition reaction, potentially due to the acrylamide motif and Cys442 not being favourably positioned for covalent reaction when the inhibitor is bound to ITK in the lowest energy conformation. In this case, both the cysteine and the inhibitor would have to accommodate and adopt potentially energetically disfavoured conformations to allow the covalent reaction to occur. Therefore, the irreversible character of the newly synthesised inhibitors has to be confirmed in a more physiological assay. The potential advantage of a longer duration of action for these irreversible inhibitors needs to be observed in a cellular experiment to validate the hypothesis which forms the foundation of this approach.

As the most active compound of the series in the PBMC assay (Table 2), the enantiomerically pure compound **19** was selected to be assayed in the ITK kinetic binding experiment. This compound, which is structurally similar to compound **13**, which has proven to covalently bind to the kinase in the mass spectrometry assay, was predicted to have the potential of covalently binding to Cys442 by the molecular model (Figure 29), while retaining most of the non-covalent binding to ITK (HTRF⁽¹⁾ pIC₅₀ = 7.5, Table 2) due to its lipophilic pyrrolidine unit. The kinetic binding profile of compound **19** presented in Figure 31³⁶ is clearly similar to the BTK irreversible inhibitor from the literature (Figure 25).⁹⁰ The binding to ITK is time-dependent which is consistent with irreversible inhibition of the kinase. The “jump dilution” experiment confirmed the irreversible character of compound **19**, with a measured IC₅₀ more than 40 times lower than the IC₅₀ predicted by the Cheng-Prusoff equation (refer to section VI.2 and Equation 2).

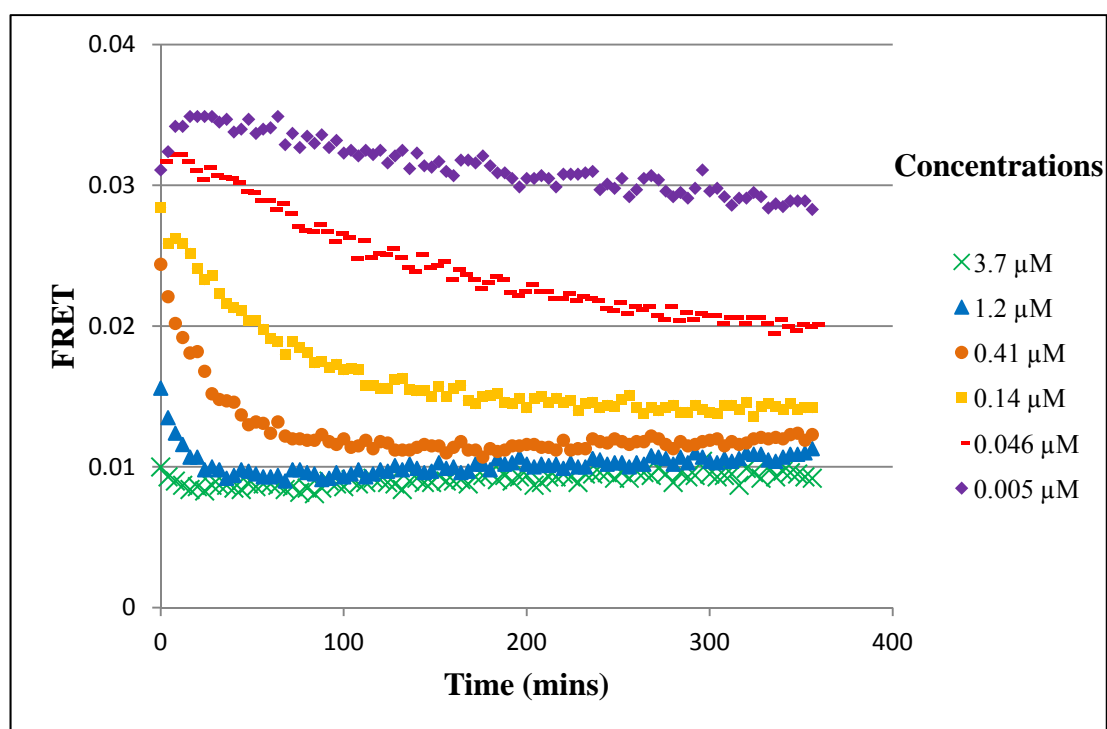


Figure 31. ITK binding kinetic data for compound **19**

Finally, to fully confirm that the inhibitors were binding covalently to Cys442, a crystallisation of compound **8** in the ITK active site was attempted. Unfortunately, both soakings and cocrystallizations experiments⁴⁰ failed to give any diffracting crystals. Two factors were thought to be responsible for the failure of the experiments: firstly, the compound was not potent enough, making it difficult to displace the existing molecule present in the ITK active site during the soaking experiment; and secondly, and perhaps more importantly, compound **8** (and the other compounds from this series) was found to be relatively insoluble, causing issues in both crystallization attempts. In conclusion, an X-ray crystal structure would have to be obtained with a more active and more soluble inhibitor in order to fully explore this option.

All the data gathered around the series of compounds presented in Figure 27 strongly suggested that potent irreversible inhibitors of ITK (compounds **8**, **13** and **19**) can be achieved by introducing a Michael acceptor motif in proximity to Cys442 in the active site using a known, active and selective, ITK reversible template. Two approaches are described to improve the irreversible binding of the compounds to

ITK: (i) increasing the non-covalent binding to the enzyme (low K_i) should increase the concentration of EI complex (Equation 1) and the rate of covalent binding; and (ii) increasing the reactivity and optimising the position of the Michael acceptor should improve the rate of the Michael addition reaction. Replacing the methoxymethyl group at the 6-position of the pyrimidine with the preferred morpholinomethyl motif present in compound **1** and compound **7** (Figure 26) should improve the non-covalent binding to ITK. If the morpholine motif does not disturb the binding mode of the inhibitors observed for the methoxymethyl template, the inhibitors should be more active in the HTRF assay (Figure 26), while maintaining the possibility of covalent interaction with Cys442 observed for compounds **8**, **13** and **19**. Moreover, introducing the morpholine motif will increase the solubility of the compounds, which will help in obtaining a crystal structure of the kinase:inhibitor complex, as well as in formulating the molecule in the inhaled *in vivo* model.

2. The 6-morpholinylmethylpyrimidine template

In the case of non-covalent ITK inhibitors,³⁸ replacing the methoxymethyl group at the 6-position of the pyrimidine with a morpholinylmethyl motif led to a 0.8 log unit increase in binding activity alongside a slight increase in polarity (lower measured LogD)¹⁰⁹ which should result in an improvement in the aqueous solubility of the molecules (Figure 32). It is important to note that as compound **7** was starting to reach the tight binding limit of the low ATP HTRF⁽¹⁾ enzyme assay, the 1 mM ATP HTRF⁽²⁾ assay was used to report primary enzyme activity. This assay was subsequently used to test all future compounds synthesized as part of this research programme. As designed, this high ATP assay lowered the pIC₅₀ of the inhibitors (*e.g.* the inhibition of the non-covalent compound **6** was reduced from pIC₅₀ of 7.8 in the HTRF⁽¹⁾ assay to pIC₅₀ of 6.2 in HTRF⁽²⁾ assay) allowing the assessment of SAR for more active ITK inhibitors. The small decrease in PBMC activity may be attributed to potential lower permeability and/or experimental error (typically 0.5 log unit) as, in some comparisons with other analogues, a 0.5 log unit increase in potency in this cellular assay is noticed for the morpholine series.

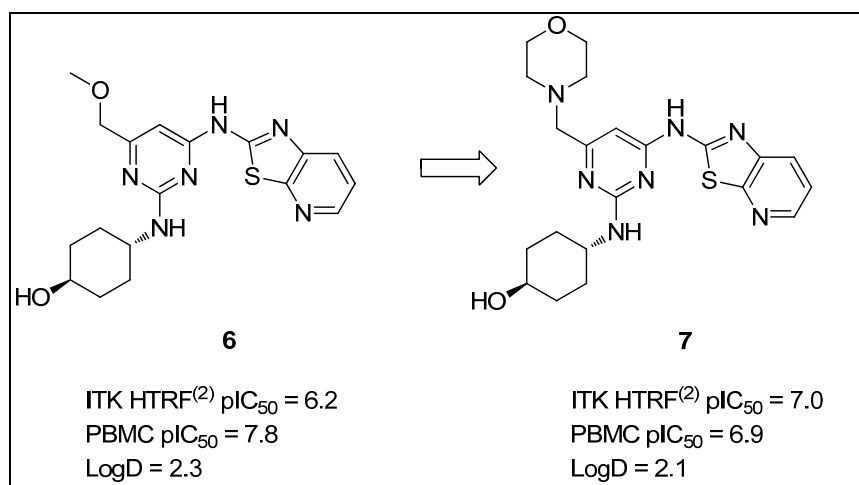
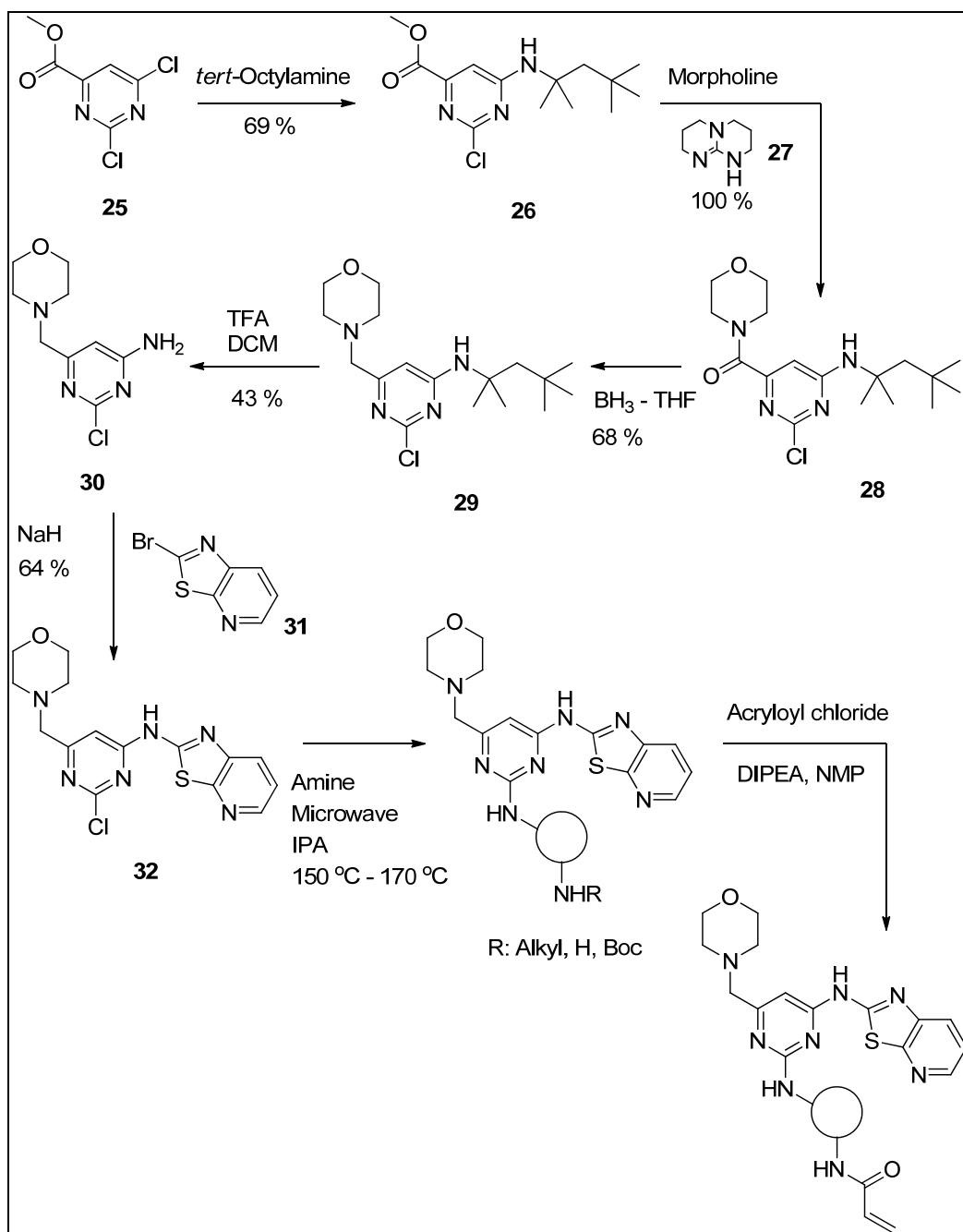


Figure 32. SAR comparison between the methoxymethyl and the morpholinylmethyl pyrimidine series

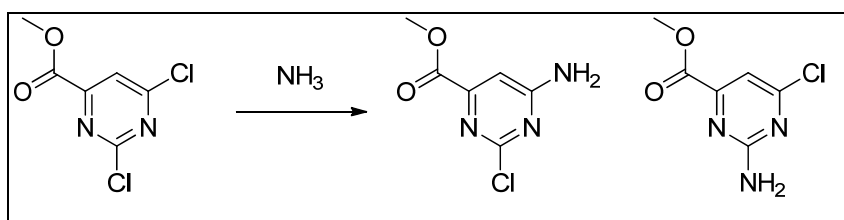
The same effect should be observed for the irreversible ITK inhibitors. The morpholine should disturb neither the hinge binding interaction nor the covalent interaction seen between the acrylamide and Cys442 in the methoxy series. Thus, an increase in activity and solubility might be anticipated for compounds **8-21** and **24** when moving to the morpholine template.

The synthetic transformation outlined in Scheme 11 presents the succession of reactions performed to create the irreversible inhibitors in this series. The commercially available methyl 2,6-dichloro-4-pyrimidinecarboxylate **25** was coupled with *tert*-octylamine at room temperature to yield the amino pyrimidine analogue **26**. The selectivity of the reaction for displacing the chlorine at the 4-position versus the chlorine at the 2-position is approximately 6:1 by LCMS. The same displacement performed with aqueous ammonia led to a mixture of the two isomers (3:2 by LCMS analysis), as presented in Scheme 12. The steric bulk of the *tert*-octylamine was believed to be responsible for the regioselectivity observed. Consequently, the methyl ester intermediate **26** was coupled with morpholine in the presence of TBD (**27**) at room temperature to quantitatively yield the amide **28**.¹¹⁰ The reaction temperature of this step is crucial as, if heated, the morpholine also displaces the chlorine at the 2-position. The amide **28** was reduced to the morpholine **29** with borane in THF complex. The *tert*-octylamine was deprotected by stirring compound **29** with an excess of TFA in refluxing DCM. The 4-aminopyrimidine **30** was then

coupled to the outsourced 2-bromo[1,3]thiazolo[5,4-*b*]pyridine **31**¹¹¹ to yield the important intermediate **32**. Following similar conditions to those described for the methoxymethyl series (Scheme 8 and Scheme 9), the chloropyrimidine **32** was reacted with a range of amines in a Biotage microwave system at temperatures between 150 °C and 170 °C for 30 minutes or longer. The higher microwave temperature is required for the 2-chloropyrimidine displacement compared to the methylsulfone aromatic displacement described section VII.1. This is believed to be due to the fact that the methylsulfone is more electronegative than the chlorine,^{112,113} facilitating the formation of the Meisenheimer complex in aromatic nucleophilic substitution. As presented previously, the newly formed amine is reacted with acryloyl chloride and DIPEA in NMP to yield the desired acrylamide products.



Scheme 11. Synthetic scheme to synthesise the irreversible ITK inhibitors in the 6-morpholinylmethylpyrimidine series



Scheme 12. Regioselectivity issue when performing the aromatic nucleophilic displacement with ammonia

To assess whether the SAR observed for the 6-methoxymethylpyrimidine series could be transferred to the morpholinylmethylpyrimidine series, a selection of the same amines was used to displace the 2-chloropyrimidine intermediate **32** (Figure 33).

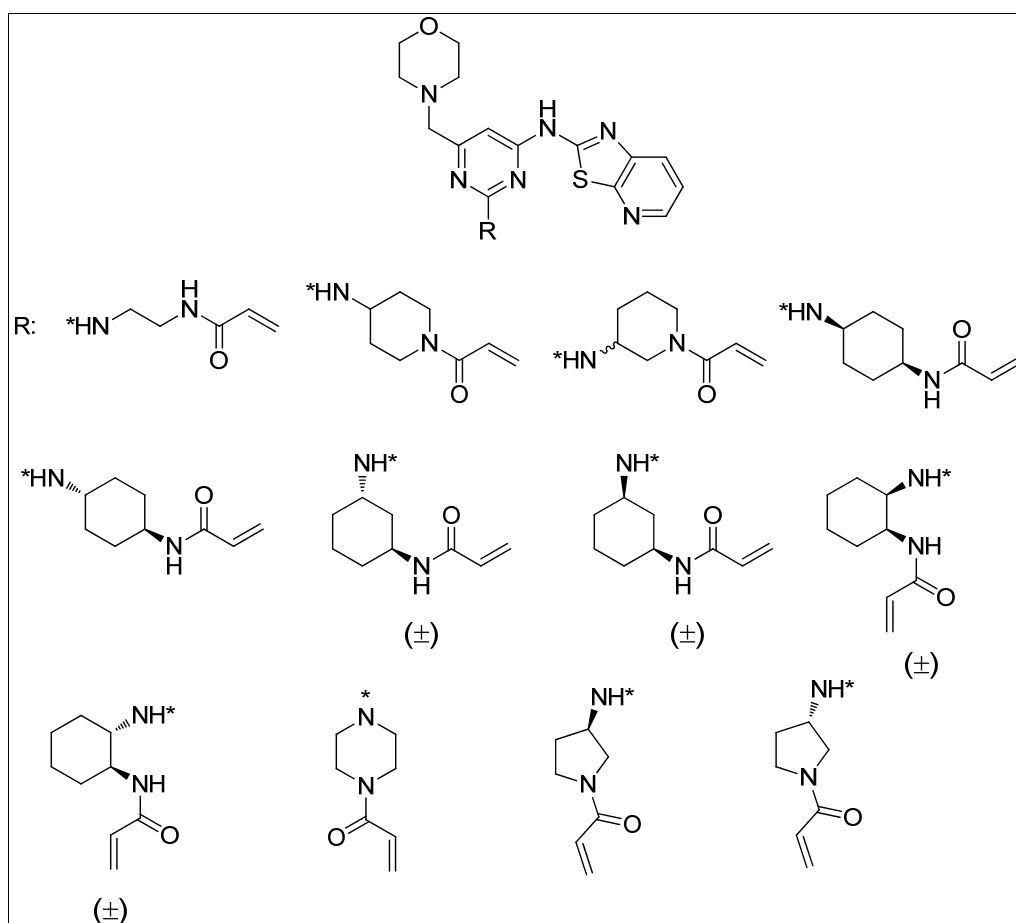
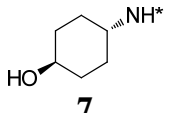
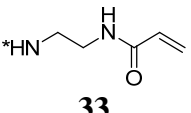
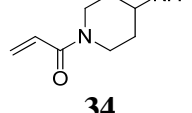
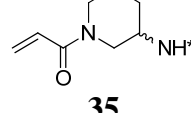
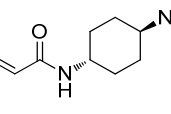
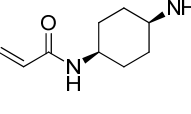
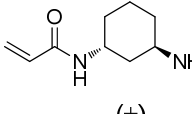
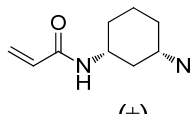
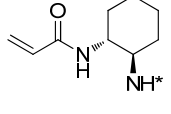
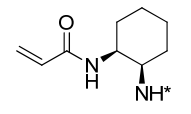
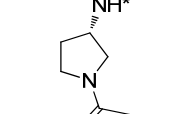
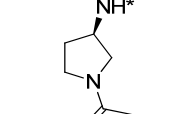
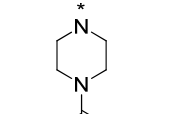


Figure 33. Range of amines synthesised to investigate the SAR of the morpholinylmethylpyrimidine template

The data obtained in the HTRF⁽²⁾ and PBMC assays for these inhibitors is summarized in Table 4. Despite the change of primary assay making the HTRF data interpretation slightly more difficult, the morpholine compounds are more potent than their analogues from the methoxymethyl series (Table 2) as the most potent compounds (*i.e.* compounds **35** and **37**) are almost equipotent to the non-covalent inhibitor **7**. In general, the morpholine compounds are also more potent in the cellular PBMC assay than the same analogues from the methoxymethyl template. Finally, the same SAR already discussed for the methoxymethyl template between the different amines is noted for the morpholine derivatives: the more lipophilic cyclic amines (**34**, **35**) are more active than the ethylenediamine species (**33**), whereas the *cis*-diaminocyclohexane analogues are more potent than the *trans*-compounds. Finally, the *S*-isomer of the pyrrolidine analogue (**42**) is, once again, a more active ITK inhibitor than the *R*-isomer (**43**) (note that the HTRF⁽²⁾ pIC₅₀ for compound **42** was slightly lower than one could have expected from the data described in the methoxymethylpyrimidine series; as the PBMC data for this compound was amongst the best value obtained within this series, the HTRF result was attributed to the experimental error within this assay).

This SAR matched what was predicted by the computational molecular model: the morpholine motif does not influence the hinge binding of the compounds hence the SAR observed for the methoxymethyl template can be transferred to the morpholine series. This observation would suggest that the position of the acrylamide motifs in the morpholine series should be the same as in the methoxy series. Therefore, some of these compounds, more particularly **33**, **35** and **42**, might be expected to be irreversible ITK inhibitors.

Table 4. SAR analysis of the range of amines synthesised in the morpholinylmethyl pyrimidine template

R				
HTRF ⁽²⁾ pIC ₅₀	7.0	5.9	6.5	6.9
PBMC pIC ₅₀	6.9	6.7	7.5	8.1
R				
HTRF ⁽²⁾ pIC ₅₀	5.7	6.8	5.9	6.6
PBMC pIC ₅₀	7.1	8.2	7.5	7.7
R				
HTRF ⁽²⁾ pIC ₅₀	5.0 ¹¹⁴	6.5	6.3	4.7
PBMC pIC ₅₀	6.7	7.6	8.0	6.2
R				
HTRF ⁽²⁾ pIC ₅₀	5.0			
PBMC pIC ₅₀	7.5			

From the SAR obtained in this 6-morpholinylmethylpyrimidine template, the most promising compounds for the programme were **34**, **35**, **37** and **42**. Indeed, these compounds demonstrated a good combination of enzyme and cellular activities; pIC₅₀s in this latter assay with these compounds were shown to be 7.5 – 8.2, providing values that were better than the non-covalent lead compound **1**. However,

such inhibition activities fell just short of the values targeted for an irreversible ITK drug candidate (HTRF⁽²⁾ pIC₅₀ > 7.7 and PBMC pIC₅₀ > 8.5).

While the increase in activity profile of the morpholine series had been confirmed, the irreversible character of these compounds remained to be assessed. The inhibitors were not tested in the mass spectrometry experiment, as the results from the first set of compounds showed that this assay was less relevant than the time dependent binding experiment. More specifically, the mass spectrometry based assay cannot be used to quantify the percentage of the irreversibly bound inhibitor:kinase complex. Consequently, it was thought that whilst inhibitors could be reported as irreversible inhibitors from this experiment, some of them might only partially covalently bind to the kinase. As the main advantage of irreversible inhibitors is the longer duration of action, the kinetic binding experiment was concluded to be more appropriate for the purpose of this research project.

Compound **33** was first tested in the time dependent binding experiment. Figure 34 clearly demonstrates that the binding of compound **33** to ITK is time dependent, suggesting that it is an irreversible inhibitor of ITK.³⁶ Compound **34** was also profiled in this experiment and was found to have a similar irreversible inhibitor profile. It should also be noted that: (i) both compounds were confirmed to be irreversible ITK inhibitors by the “jump dilution” experiment; and (ii) as various studies have confirmed that molecules with time dependent binding in the kinetic assay are irreversible inhibitors and not slow non-covalent binders, the “jump dilution” experiment results will not be reported on further in this overall study.

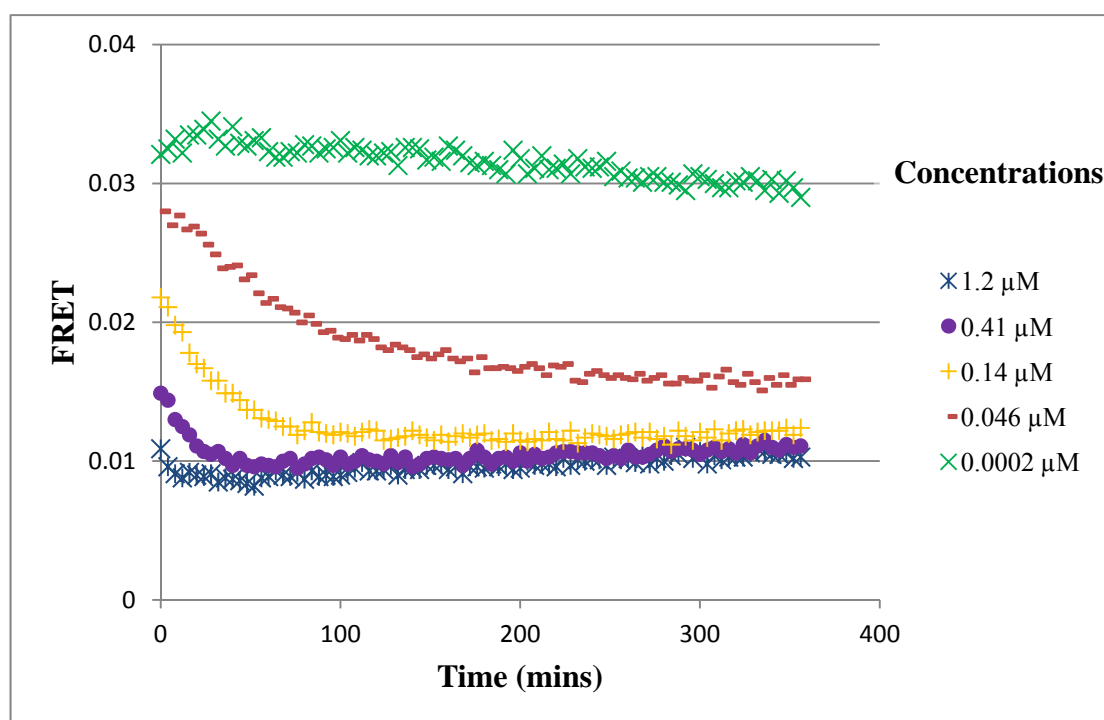


Figure 34. ITK binding kinetic data for compound 33

From these studies, it was assumed that the SAR observed for the methoxy series were likely to be transferable to the morpholine family of compounds. Therefore, compounds **35** and **42** were also believed to be irreversible inhibitors.

So far, all of the selected acrylamide compounds tested in the mass spectrometry and the kinetic experiments are believed to be acting as irreversible ITK inhibitors. These compounds had been selected for those experiments based on their potencies in ITK inhibition assays and on the predicted ability to form the covalent binding with Cys442. The docking of the selected inhibitors showed that none of them had to adopt unfavoured conformations to position the electrophilic moiety in close proximity of the cysteine residue. At this stage of the programme, it was decided to investigate how good the computational molecular modelling was at predicting the formation of the covalent interaction. Therefore, compounds which were predicted to have to adopt unfavoured conformations to position the Michael acceptor motif in proximity of the Cys442 residue were assayed in the kinetic experiment. The modelling indicated that the acrylamide motifs of compounds **36** and **37** were not optimally positioned to covalently interact with the cysteine residue while retaining

the hinge binding. In fact, from the lowest energy conformations of the inhibitor **36** non-covalently bound to the ITK active site, none of them could be used to make the covalent complex (refer to section VI.1 for the molecular modelling process), as the acrylamide unit and Cys442 were too far apart. As an example, the lowest energy conformation of compound **36**, which is presented in Figure 35 (note that the morpholine unit was omitted for the modelling), exhibits a 7.86 Å distance between the 4-position of the Michael acceptor and Cys442. From this conformation, the rotations of the cysteine and the acrylamide do not allow the formation of the covalent bond between the inhibitor and ITK. Therefore, despite having a Michael acceptor in the region of Cys442, this compound should only bind non-covalently to ITK (note that, as already explained in section VI.1, during the molecular modelling calculations, only the Cys442 sidechain from the protein was set as flexible. The rest of the protein was treated as a rigid entity, meaning that caution is required when interpreting the results from this approach, as the inhibitors could adopt different conformations with a fully flexible protein).

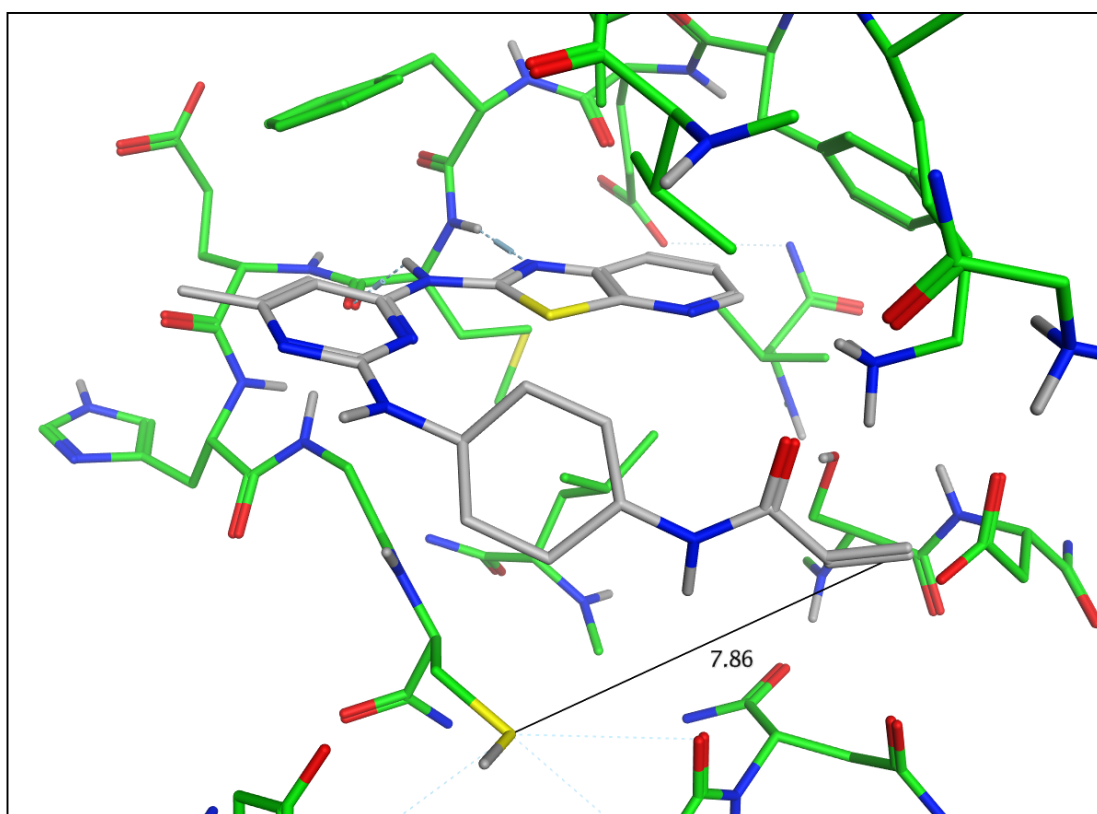


Figure 35. Molecular modelling of compound **36** in the ITK active site

As predicted, the ITK kinetic binding analysis of compound **36** indeed revealed that it was non-covalently binding to the kinase (Figure 36). The inhibitor did not present a clear time dependent binding to ITK. Kinetic data for compound **37** (Figure 37) demonstrated that the inhibition was time dependent but not as pronounced as for compound **33** (Figure 34) or compound **19** (Figure 31). This is characteristic of an inhibitor which covalently reacts slower with the kinase (smaller k_c , Equation 1), probably due, in this case, to the non-optimal positioning of the acrylamide and the cysteine residue, once the inhibitor is non-covalently bound to ITK. Therefore, at this stage of the programme, a good correlation between the computational molecular modelling predictions of irreversible inhibitors and the data gathered in the time dependent binding assay was observed. These observations enhanced the level of confidence in the use of molecular modelling to design novel irreversible inhibitors within this programme of research.

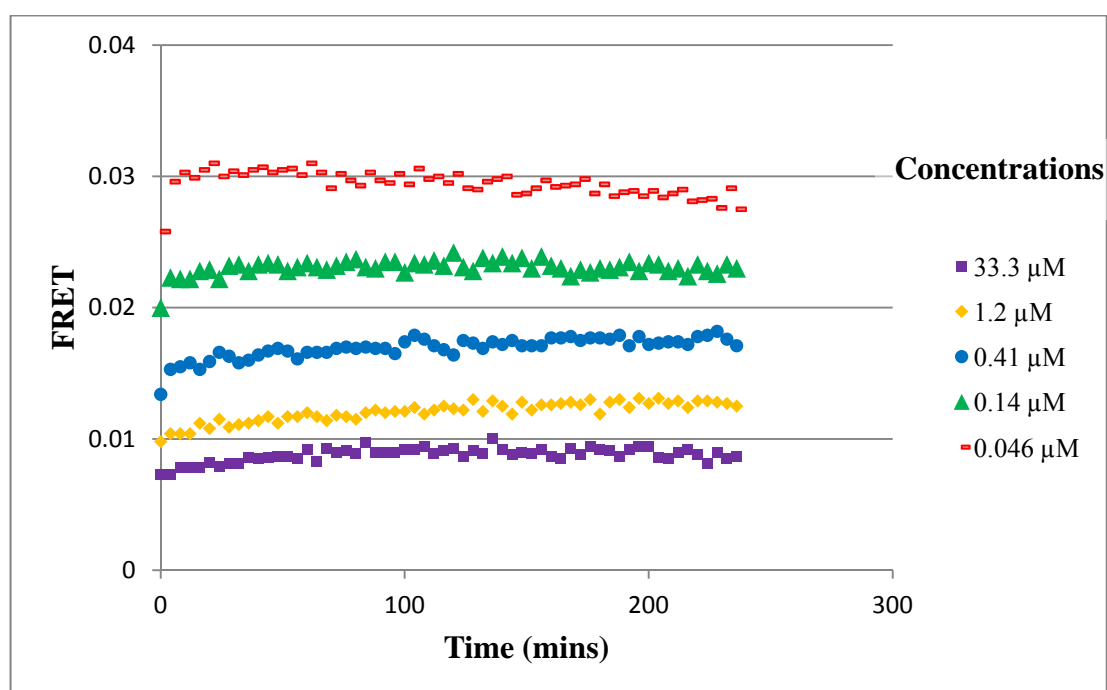


Figure 36. ITK binding kinetic data for compound **36**

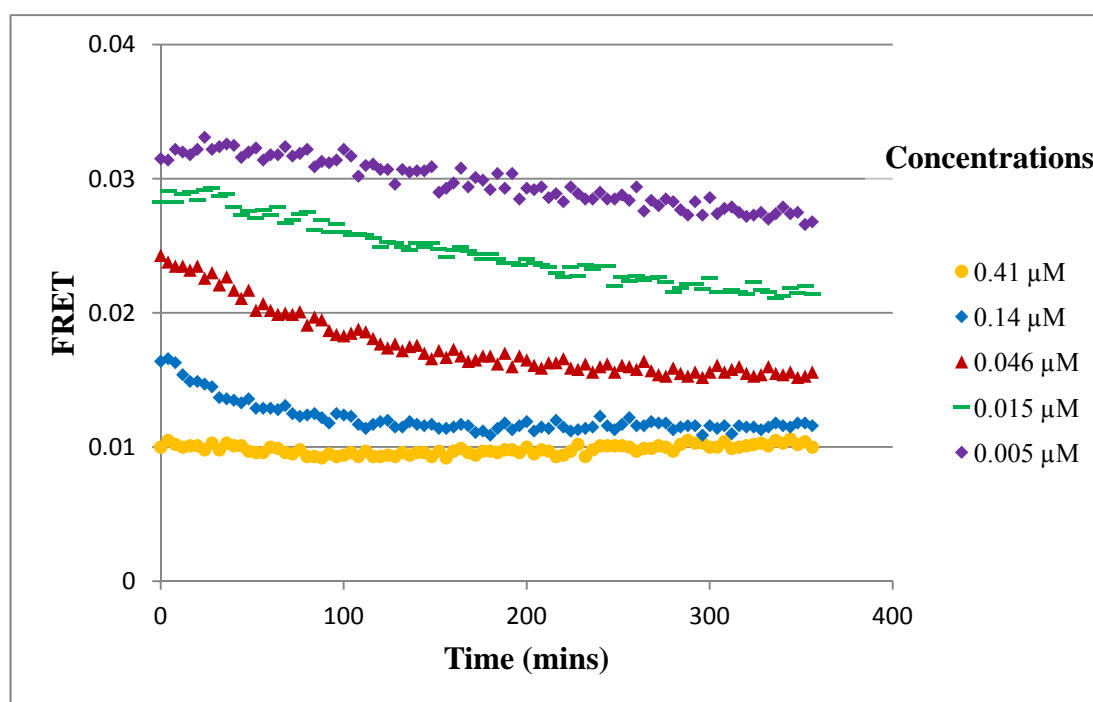


Figure 37. *ITK binding kinetic data for compound 37*

Interestingly, a correlation between the activity assays and the irreversible character of the inhibitors does not exist. Compound **37** was one of the most active compounds in both the HTRF⁽²⁾ and the PBMC assays but it did not prove to be acting optimally as an irreversible inhibitor of ITK. This observation emphasizes the importance of the kinetic assay in determining whether the designed inhibitors are binding irreversibly to the kinase.

The results obtained so far show clearly that potent irreversible ITK inhibitors have been identified from these series of compounds. However, even the compounds with the best irreversible ITK inhibitor profiles (compounds **34**, **35** and **42**) did not achieve the required activity profile for a drug candidate from this research programme (HTRF⁽²⁾ pIC₅₀ > 7.7 and PBMC pIC₅₀ > 8.5). Two main reasons were proposed for the slightly lower than expected activities of these compounds: (i) the non-covalent binding of the compounds was insufficient to drive the cellular activity over a pIC₅₀ of 8.5, even for irreversible inhibitors; and (ii) the covalent reaction between the inhibitor and Cys442 was too slow, which, once again, did not produce compounds with enhanced cellular activities compared to non-covalent inhibitors.

Two reasons for the relatively slow Michael addition reaction can be suggested. Firstly, the Michael acceptor might not be sufficiently reactive. Accordingly, other electrophilic moieties could be investigated to enhance the inhibitors reactivity towards Cys442. Whilst this approach will potentially allow the covalent bond to be formed faster, the inhibitors will also be more likely to react with the many other cysteines and nucleophilic residues found in cells. The inhibitors could thus lose their selectivity and potential off-target toxicity issues may arise. The second approach would consist of optimizing the position of the Michael acceptor compared to Cys442. The EGFR kinase literature^{45,82} also confirms that the positioning of the acrylamide motif will influence the reaction kinetics of the covalent bond. Kinetics studies proved that the 6-acrylamide analogue **45** (Figure 38) reacted rapidly with EGFR to form the covalent complex (half life < 2 mins), whereas the 7-acrylamide **46** covalently bound much more slowly with the same kinase (half life ~ 20 mins).⁸²

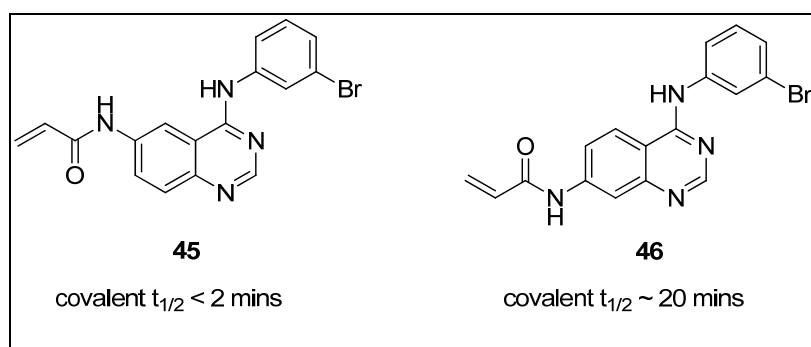


Figure 38. EGFR irreversible inhibitors presenting a different kinetic profile when reacting with the cysteine residue in the ATP binding site

To assess the position of the Michael acceptor compared to Cys442 and the conformation the inhibitor has to adopt to allow the reaction to occur, an X-ray crystal structure of the irreversible inhibitor **42** in the ITK ATP pocket was attempted. The increased solubility and binding activity of the molecule contributed to the success of the soaking experiment. The X-ray crystal structure of the ITK kinase domain in the complex with compound **42** was solved to a 2.18 Å resolution (Figure 39).^{40,115} Electron density clearly indicates a covalent bond between the acryloyl moiety and Cys442 in the active site of this crystal system (1.8 Å distance between the acryloyl moiety and Cys442). However, as shown in Figure 39 and

Figure 40, the cysteine presents two preferred rotamer conformations (in green and orange) and only the green conformation is involved in the covalent link to the inhibitor. The electron density around the electrophilic moiety indicates the overlay of two conformations of compound **42** (Figure 40). The major conformation is the acrylamide covalently linked to Cys442 (dark grey representation). The other conformation of the inhibitor (light grey representation) is a function of the alternative cysteine conformation in orange. In that case, the electrophilic moiety has not reacted with Cys442 hence the inhibitor is only non-covalently bound in the ATP binding pocket.

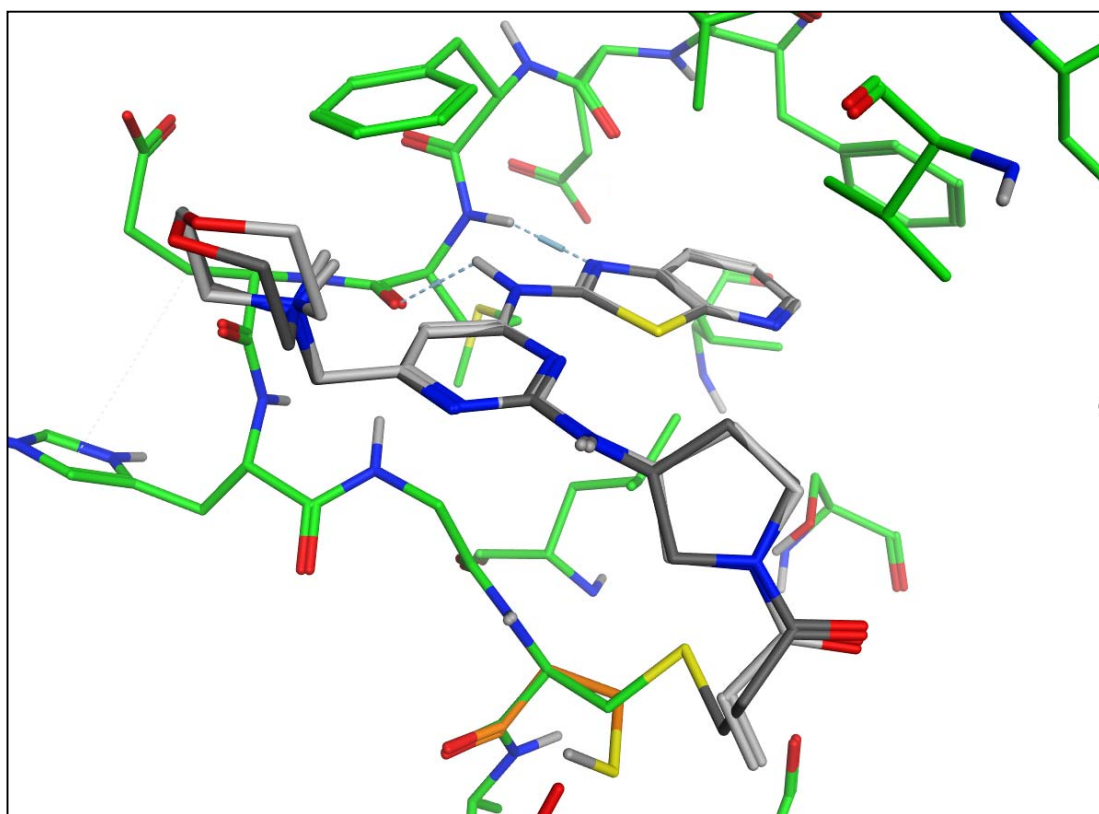


Figure 39. X-ray crystal structure of compound **42** in the ITK active site (dark grey: compound covalently bound to the kinase; light grey: compound non-covalently bound to the kinase; orange: conformation of Cys442 for the non-covalently bound compound)

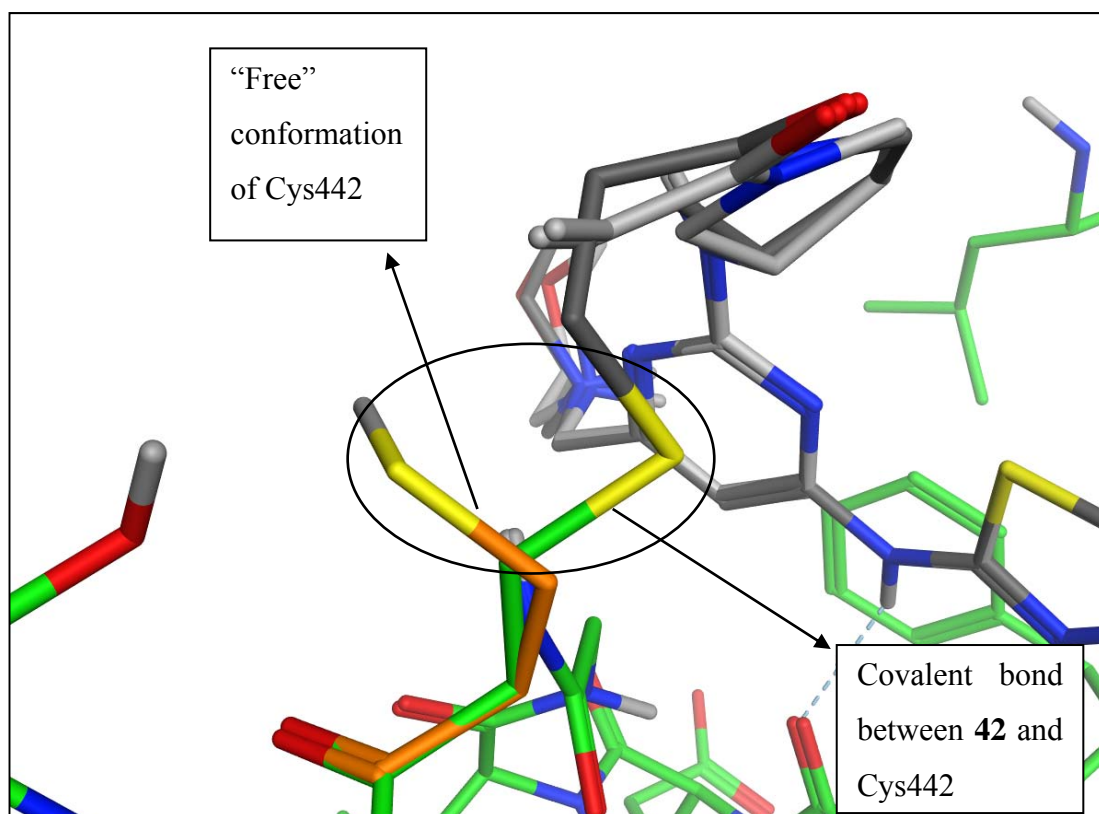


Figure 40. Two conformations of Cys442 observed in the X-ray crystal structure

The core template binding mode is as usually observed for this series, with key hydrogen bonding interactions made to the kinase hinge region. An overlay between compound **42** (irreversible inhibitor, dark grey - non-covalent inhibitor, light grey) and the molecular modelling already presented for the structurally related compound **19** in Figure 29 (covalent conformation displayed in brown) clearly shows that these contacts are unchanged (Figure 41). As the molecular modelling was based on the the crystal structure of compound **2** (Figure 9, refer to section VI.1 for the molecular modelling protocol), it demonstrates that the hinge hydrogen bond interactions are identical whether or not the inhibitor has covalently reacted with the kinase. The rest of the inhibitor is also nicely overlaid to the model of compound **19** (including the covalent interaction), confirming that the computational molecular modelling was predicting quite accurately the conformations adopted by the inhibitors in the ITK active site. Interestingly, the conformation of Cys442 in the X-ray crystal structure of compound **2** (Figure 9) is in the same position as the cysteine which does not interact with the acryloyl moiety (Cys442 in orange, Figure 40) in the crystal structure of

compound **42**. Therefore, as already postulated in the molecular modelling section VI.1, for the covalent reaction with compound **42** to occur, the cysteine residue has to adopt the “second conformation” presented in Figure 19.

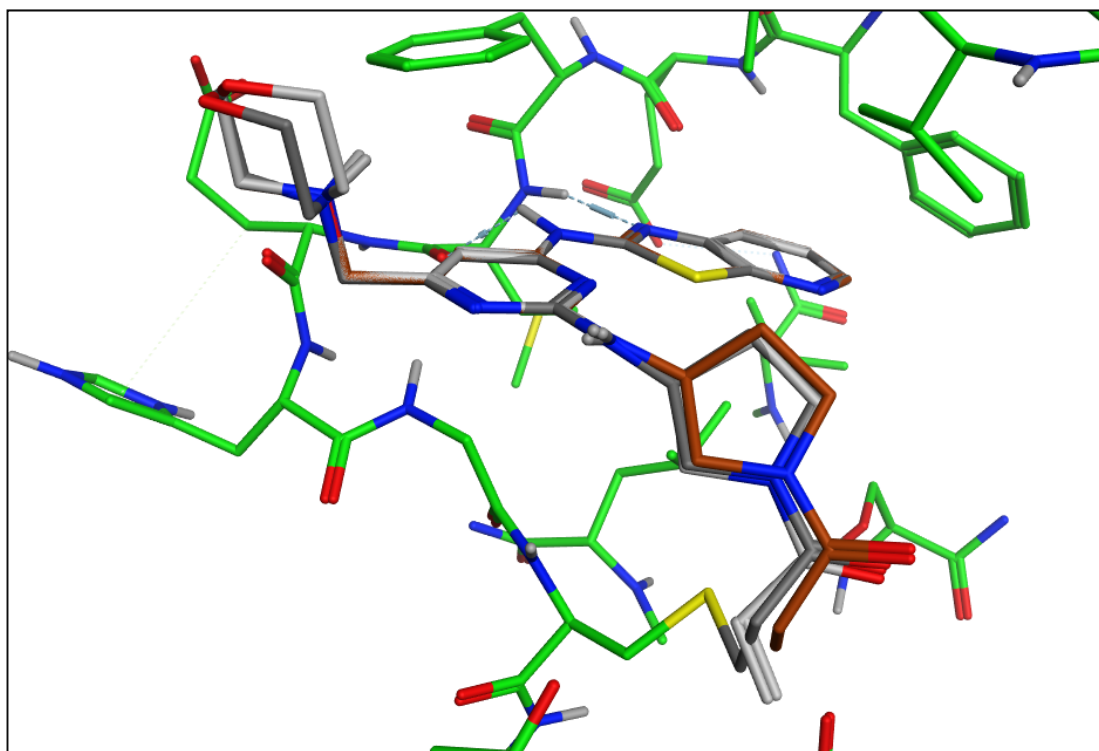


Figure 41. *Overlay of the X-ray crystal structure of compound **42** (irreversible inhibitor, dark grey - non-covalent inhibitor, light grey) and the molecular modelling obtained for compound **19** (covalently bound to ITK, brown)*

The X-ray crystal structure obtained for compound **42** in the ITK active site supports the hypothesis previously discussed: compound **42** is an irreversible ITK inhibitor but the formation of the covalent bond is relatively slow as one conformation of the inhibitor is only non-covalently bound to the active site. This supports the slow rate of the covalent reaction. If the covalent binding had been fast, the conformation where compound **42** is only reversibly bound to the kinase would not be visible. At this stage, the rationale behind the slow rate of the reaction remained unknown. However, one can postulate that once the inhibitor is present in the ATP binding pocket, the cysteine can no longer freely rotate to adopt the conformation required to make the covalent bond (Figure 40). The position of the Michael acceptor on top of the residue prevents the required free rotation. For the reaction to occur, the inhibitor

would have to adopt an unfavoured conformation to allow the Cys442 rotation or would have to unbind from the ATP pocket and bind again with the cysteine residue positioned in the required conformation for covalent binding. In contrast, the movement of a cysteine moiety to react with an acryloyl unit is observed for EGFR inhibitors (Figure 42). In the X-ray crystal structure of PD168393 in EGFR kinase (in grey), Cys773 has moved to make the covalent interaction compared to its position (in orange) when a non-covalent inhibitor (*e.g.* Gefitinib) is bound into the active site. This rotation is believed to be energetically permitted as PD168393 has proved to react covalently with the kinase within two minutes.⁴⁵

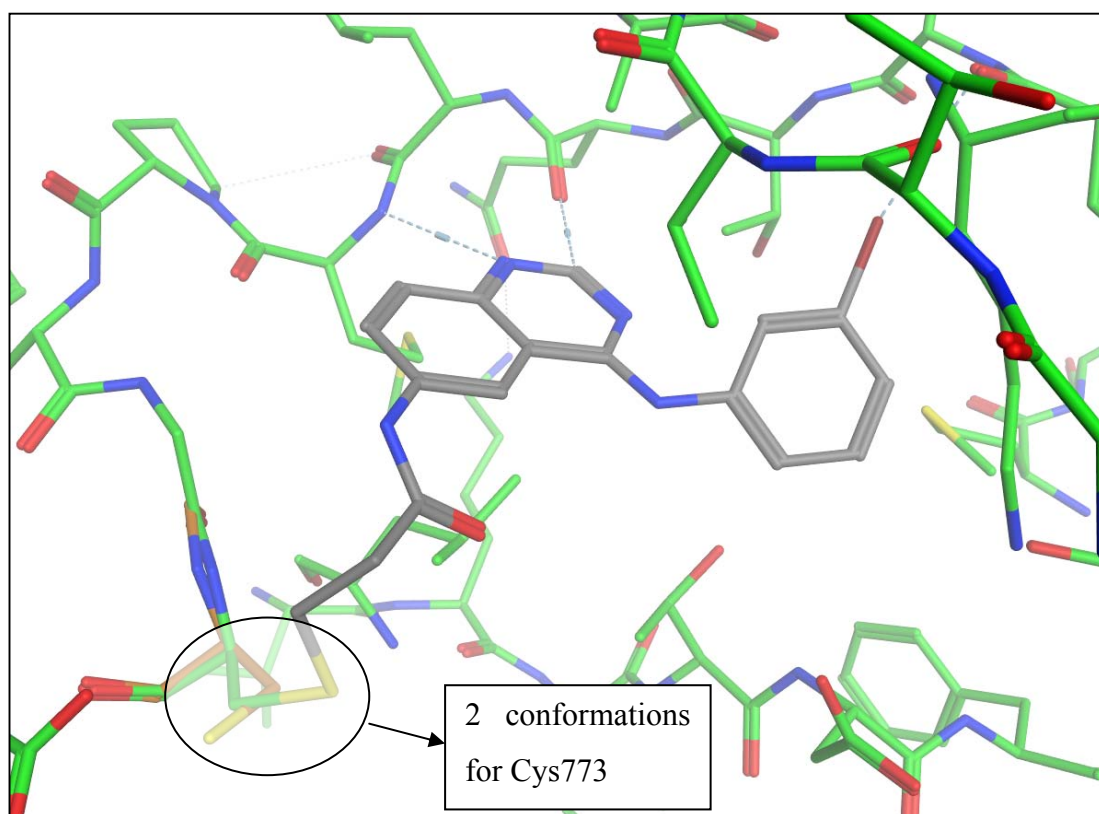


Figure 42. X-ray crystal structure of PD168393 in the EGFR active site (grey) overlaid with the conformation of Cys443 (orange) found in some non-covalent inhibitor crystal structures

A similar movement is required for ITK to react with compound **42**. However, the main difference between the positions of the two inhibitors (**42** and PD168393) relative to the cysteine residues hinges on the acryloyl moiety being in a restrictive position on top of the two conformations of Cys442 in the case of compound **42**.

This prevents the cysteine from freely rotating from one conformation to the other without removal of the inhibitor. In the case of PD168393, in the initial acceptor conformation, the Michael acceptor does not reach Cys773; the cysteine residue then flips to its other conformation, which is favourable for the covalent reaction with the acrylamide. Thus, it was postulated that the Michael acceptor of compound **42** could be too deep in the pocket, disfavoured the free rotation of the cysteine residue, resulting in the covalent reaction with the inhibitor being slow. Therefore, optimizing the position/conformation of the electrophile compared to the cysteine residue should increase the rate of the reaction.

In summary, potent irreversible ITK inhibitors have been discovered from the 6-morpholinylmethylpyrimidine template, with, in particular, compounds **34**, **35** and **42**. However, these compounds do not demonstrate the levels of activity (HTRF and PBMC) required for an ITK inhaled drug candidate. The relative slow covalent rate with Cys442 and/or the insufficient non-covalent binding of the compounds do not confer the enhanced activity profile expected for irreversible inhibitors.

3. Investigation of the nature of the electrophilic moiety

The combination of the data obtained from the mass spectrometry and the kinetic and crystallography assays supported the concept that the newly designed inhibitors were irreversibly binding to ITK. However, the covalent bond was believed to be formed relatively slowly resulting in the irreversible inhibitors not displaying the expected improved profile in the cellular assays. The acrylamide motif was initially selected to be included in these inhibitors as it is known to chemically react with nucleophilic sulphur units but its reactivity is relatively low. Indeed, the acrylamide was designed to react with Cys442 because it was placed in proximity of the nucleophilic sulfur when bound in the ITK ATP pocket but not to react with many other nucleophilic residues present elsewhere in the body.

However, although the acrylamide unit has been the electrophilic group of choice for kinase irreversible inhibitors,^{44,45-47,81,82,90} it has been demonstrated that other electrophilic moieties can also be used to design irreversible inhibitors.^{90,116} To

investigate if the nature of the electrophilic moiety was affecting the rate of the covalent reaction for this family of ITK inhibitors, various electrophilic units, described in Figure 43, were synthesised. The 2-chloroacetamide was believed to be the most reactive electrophile of all. However, the enhanced electrophilicity delivered could be detrimental to the selectivity in relation to other cysteines. Nonetheless, this compound, if sufficiently stable to be assayed within the different biological experiments should provide useful information regarding the kinetics of the covalent reaction. The 2-(4-fluorophenoxy)acetamide unit could potentially undergo the same nucleophilic displacement (S_N2) as the 2-chloroacetamide but its reactivity is significantly lower. However, the size of the 4-fluorophenoxy group might be detrimental for the binding activity to ITK as this large motif may unfavourably interact with the ATP binding pocket. Regarding the trifluoromethylacrylamide unit, it is predicted that the electrophilicity of the Michael acceptor would be enhanced compared to the acrylamide due to the electron-withdrawing CF_3 group. However, the Michael acceptor motif is now more hindered and this steric effect might reduce the rate of the covalent bond-forming reaction.⁸⁶ Finally, the (*E*)-4-(dimethylamino)but-2-enamide is the electrophilic moiety found in the most advanced EGFR irreversible inhibitor, Neratinib (Figure 13). This Michael acceptor was found to increase the rate of the reaction with Cys773^{86,117} due to the reaction mechanism described in Figure 44. The Michael addition may be catalysed by the dimethylamino group which deprotonates the thiol to thiolate enhancing its reactivity. Another possible explanation for the higher reactivity of this (*E*)-4-(dimethylamino)but-2-enamide is the fact that the (dimethylamino)methyl could be already protonated at physiological pH. The presence of a cationic hydrogen bond donor may favour the approach of the thiol or thiolate, turning a repulsive steric interaction into an attractive electrostatic interaction. However, as the local pH around the (dimethylamino)methyl in the active site is not known, it is impossible to distinguish between these explanations.

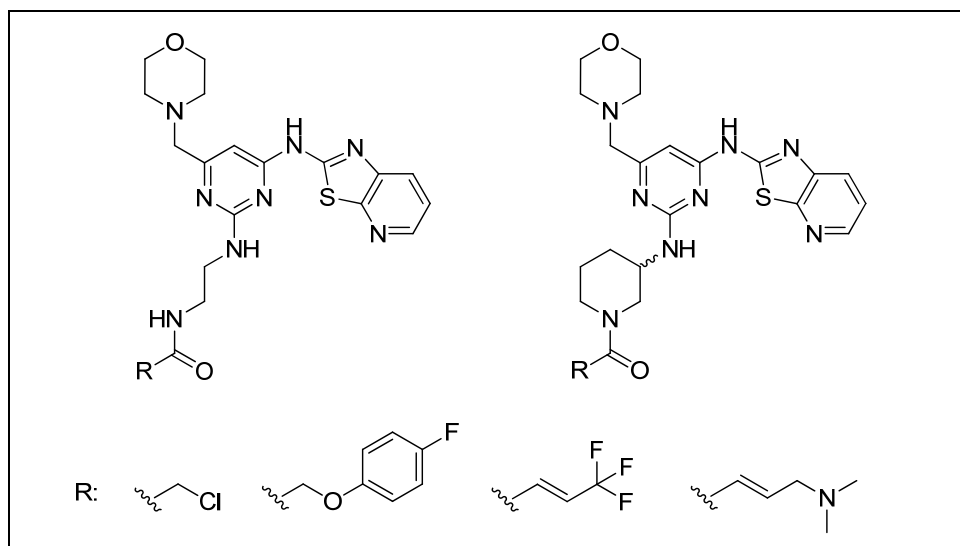


Figure 43. Range of electrophilic units selected to investigate the rate of the covalent reaction

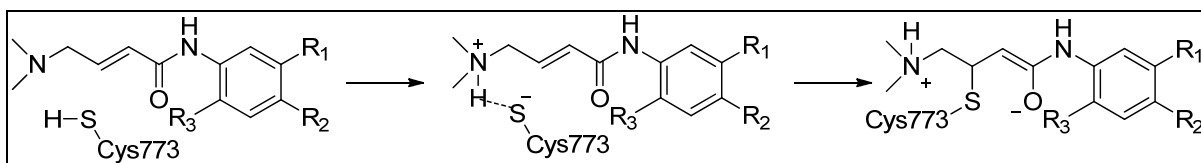
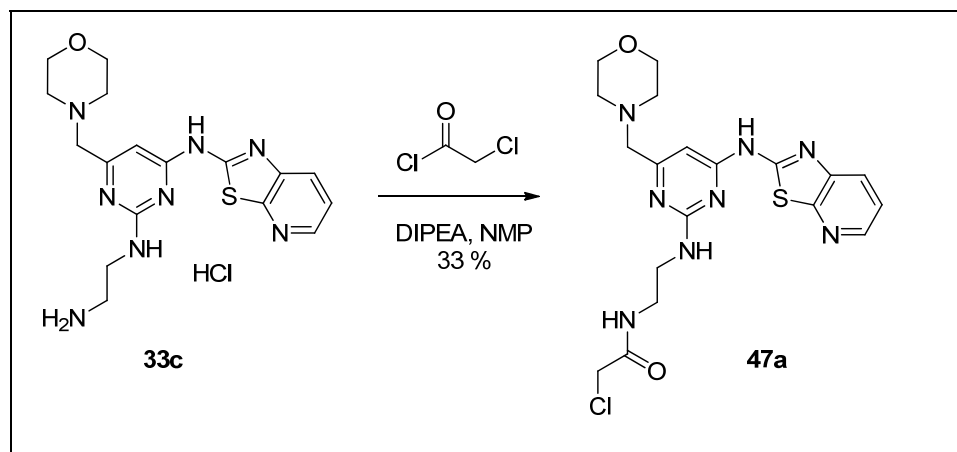


Figure 44. Potential explanation for the increased reactivity of the (*E*)-4-(dimethylamino)but-2-enamide towards Cys773 for EGFR inhibitors¹¹⁷

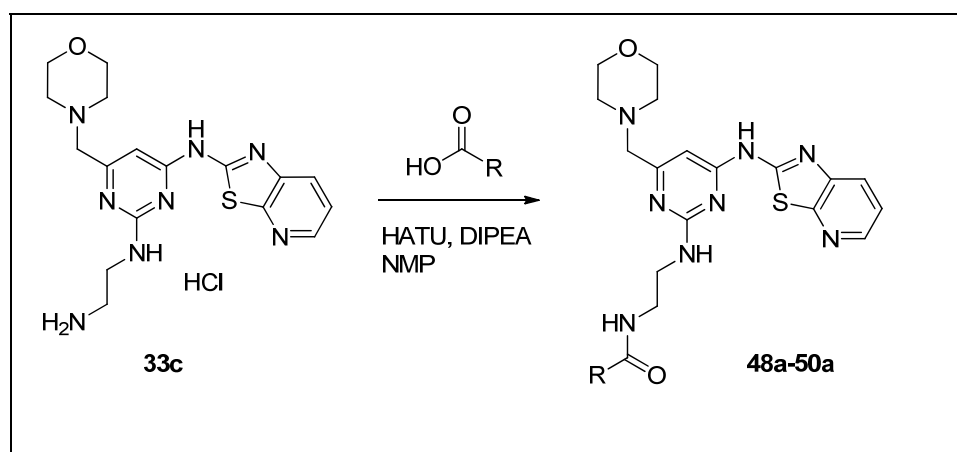
The four newly designed electrophilic moieties were synthesised as part of the diaminoethyl and the 3-aminopiperidyl series. The flexibility of the diaminoethyl unit might be required for all electrophilic moieties to adopt the desired conformations to react with Cys442, while the more active 3-aminopiperidyl unit should provide some promising molecules if the covalent reaction is achieved.

The 2-chloroacetamide motif was introduced to the molecule by reacting the amino intermediate **33c** with commercially available chloroacetyl chloride and DIPEA in NMP at 0 °C (Scheme 13).

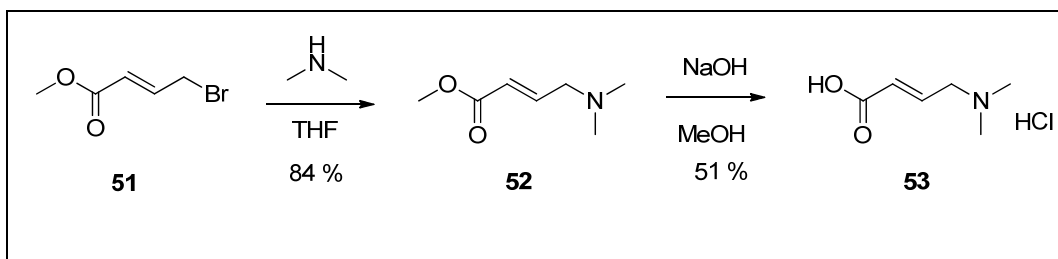


Scheme 13. Synthetic scheme for compound **47a**

The other three electrophilic moieties were synthesised by performing amide coupling reactions between **33c** and the respective carboxylic acids in the presence of HATU and DIPEA (Scheme 14). The 4-fluorophenoxyacetic acid and the (*E*)-4,4,4-trifluorobut-2-enoic acid were commercially available whereas the (*2E*)-4-(dimethylamino)-2-butenoic acid **53** had to be synthesised (Scheme 15).¹¹⁸ The commercially available methyl (*2E*)-4-bromo-2-butenoate **51** was reacted with dimethylamine in THF (2 M) at 45 °C to yield the ester **52**, which was hydrolysed to the desired carboxylic acid **53** in methanolic sodium hydroxide.



Scheme 14. Amide coupling reactions with HATU for compounds **48a-50a**



Scheme 15. Synthetic scheme for the carboxylic acid **53**¹¹⁸

The same class of reactions was performed to synthesise these electrophilic moieties with the 3-aminopiperidyl template. The reaction yields are summarised in Table 5. It is worth noting that none of these reaction conditions were optimised. However, the reaction profiles of the amide couplings were generally clean when monitored by LCMS. Therefore, the moderate yields obtained were likely to be due to the open access mass directed autoprep reverse phase purifications. Nonetheless, all the desired compounds were obtained in sufficient quantities to be assayed in biology. The data from the HTRF⁽²⁾ and the PBMC assays are presented in Table 6.

Table 5. Summary of the yields obtained for the amide coupling reactions

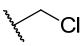
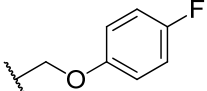
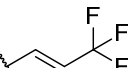
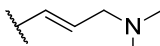
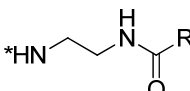
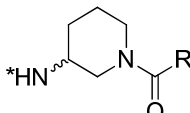
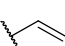
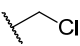
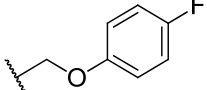
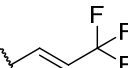
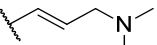
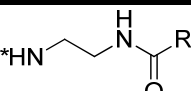
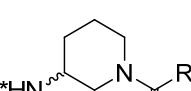
Template \ R				
	33 %	48 %	39 %	30 %
	23 %	55 %	10 %	46 %

Table 6. SAR analysis of the various electrophilic moieties

Template \ R					
	33	47a	48a	49a	50a
HTRF ⁽²⁾ pIC ₅₀	5.9	7.1	4.8 ¹¹⁴	6.3	5.5
PBMC pIC ₅₀	6.7	8.3	5.3	7.1	< 5
	35	47b	48b	49b	50b
HTRF ⁽²⁾ pIC ₅₀	6.9	7.0	4.8	6.0	6.2
PBMC pIC ₅₀	8.1	8.4	NT	7.5	5.6

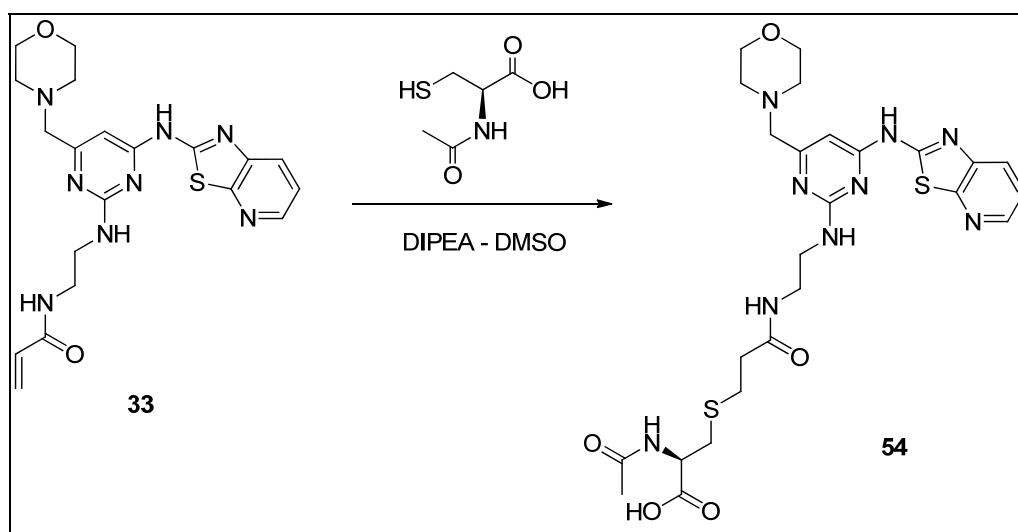
The SAR obtained so far for the various electrophilic moieties (Table 6) demonstrate that the highly reactive chloroacetamides **47a** and **47b** are the most potent compounds in both the HTRF⁽²⁾ and the PBMC assays. The improved enzyme activities of both compounds compared to the acrylamides **33** and **35** are believed to

be caused by the rapid irreversible binding of the molecules to ITK. In the 25 minute course of the HTRF assay, compounds **47a** and **47b** are thought to covalently bind, at least partially, to Cys442, driving the enzyme inhibition to $pIC_{50} \geq 7$. The less reactive and more bulky 4-fluorophenoxyacetamide **48a** and **48b** are tolerated less well in the ATP pocket, giving reduced ITK affinities in the HTRF⁽²⁾ assays. The trifluorobut-2-enamide compounds **49a** and **49b** do not display significantly better PBMC inhibitions compared to compounds **33** and **35**, which would tend to suggest that they do not react dramatically faster with Cys442. However, full data from the kinetic assays are required to confirm this hypothesis. Finally, the HTRF⁽²⁾ data obtained for the (2*E*)-4-(dimethylamino)-2-butenamide compounds **50a** and **50b** suggested that, despite a small reduction of enzyme activity, the dimethylamino motif was tolerated in this area on the active site. However, the data from PBMC assays indicated that both compounds were hardly inhibiting the release of IFN- γ in a cellular environment (respectively, $pIC_{50} < 5$ and $pIC_{50} = 5.6$). This major loss of activity from the enzyme to the cellular assay was attributed to the predicted lower permeability of these molecules possessing the polar dimethylamino unit, which will be protonated at physiological pH ($pK_a = 8.15$).¹¹⁹ The increase of polarity induced by the introduction of the dimethylamino unit was confirmed by the logD calculations¹²⁰ (Table 7): on average, the basic motif reduced the clogD by 1.6 units which translated in a larger enzyme/cell activity difference. These permeability differences make it impossible to establish whether the dimethylamine motif had the potential to deprotonate Cys442 and accelerate the covalent reaction with ITK. Nevertheless, the similar activities measured in the enzyme assays between compounds **33** and **50a** and compounds **35** and **50b** would suggest that the reactivity is not dramatically improved, at least not in the 25 minute course of the assay.

Table 7. Comparison between the enzyme/cell drop-off and the clogD for compounds **33**, **50a**, **35** and **50b**.

Compound	Enzyme/cell difference	clogD pH = 7.4 ¹²⁰
33	-0.8	1.78
50a	> 0.5	0.18
35	-1.2	2.47
50b	0.6	0.86

Before testing some of these compounds in the kinetic assay, the reactivity of these species towards cysteine residues was assessed by reacting them, in turn, with excess of *N*-acetylcysteine in DMSO (Scheme 16).



Scheme 16. Reaction between compound **33** and *N*-acetylcysteine

Compound **33** was reacted at room temperature with 10 equivalents of *N*-acetylcysteine and 20 equivalents of DIPEA in DMSO. The reaction was stirred at room temperature and monitored by LCMS. An excess of *N*-acetylcysteine was used in the reaction to mimic the large local concentration of Cys442 seen by the inhibitor in the ITK active site. After 30 minutes, only traces of the Michael addition product

54 was observed by LCMS. After overnight reaction, 46 % conversion towards the product **54** was seen. These data confirmed the low reactivity of the acrylamide group towards attack by sulfur nucleophiles.

The tertiary amide **35** was then tested in this *N*-acetylcysteine reactivity assay alongside the structurally similar amide of the BTK irreversible inhibitor **3** (Figure 45), which has been reported in the literature to demonstrate an enhanced *in vivo* efficacy compare to the corresponding BTK reversible analogues.⁹⁰ Both compounds were expected to have the same reactivity towards *N*-acetylcysteine as they possess the same acrylamide motif.

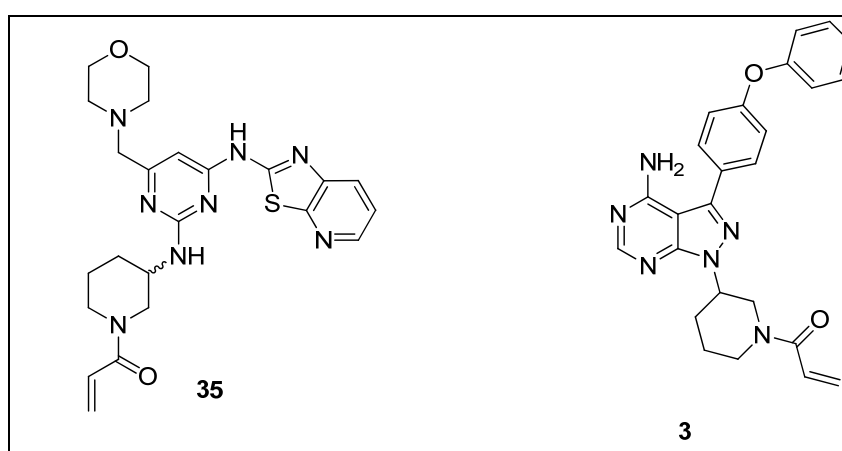


Figure 45. Compounds tested in the *N*-acetylcysteine assay

Compound **35** and **3** were reacted, as described previously, with 10 equivalents of *N*-acetylcysteine and 20 equivalents of DIPEA in DMSO. LCMS analyses after three hours showed that 39 % of compound **35** had reacted with *N*-acetylcysteine whereas 64 % of compound **3** had been consumed (Table 8). After overnight reaction, compound **3** had fully reacted with *N*-acetylcysteine whereas the reaction with compound **35** had nearly reached completion. Overall, both compounds showed similar reactivities towards *N*-acetylcysteine.

Table 8. Extent of the reaction between *N*-acetylcysteine and compound **3** and **35**

Formation of Michael adduct with	30 mins	1 hour	3 hours	20 hours
Compound 3	19 %	33 %	64 %	100 %
Compound 35	9 %	17 %	39 %	92 %

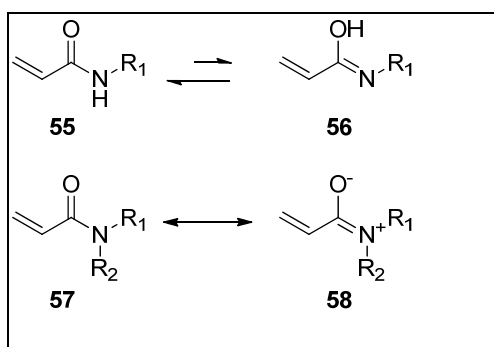
It was intriguing to notice that the tertiary amide **35** was significantly more reactive towards *N*-acetylcysteine than the secondary amide **33**. This finding was confirmed by performing the *N*-acetylcysteine experiment with compounds **8** and **13**. The tertiary amide compound **13** reacted much faster with the *N*-acetylcysteine than the secondary amide compound **8** (Table 9). This would suggest that a tertiary acrylamide positioned in a similar position to a secondary amide in the ITK ATP pocket would react faster with Cys442.

Table 9. Extent of the reaction between *N*-acetylcysteine and compound **8** and **13**

Formation of Michael adduct with	30 mins	1 hour	3 hours	20 hours
Compound 8	1 %	2 %	7 %	34 %
Compound 13	10 %	18 %	39 %	93 %

The rationale behind the difference of reactivity between secondary and tertiary acrylamides towards *N*-acetylcysteine remains unknown. However, these unexpected reactivities have previously been reported in the literature when the kinetics of the addition of alcohols to activated vinyl compounds was studied.¹²¹ In this paper, the authors also report that tertiary acrylamides undergo the 1,4-addition of alcohols more rapidly than secondary and primary acrylamides do. No explanation is

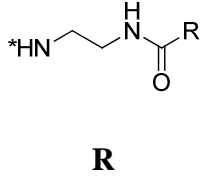
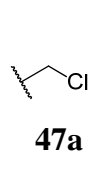
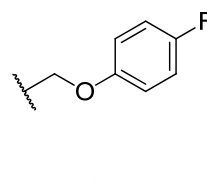
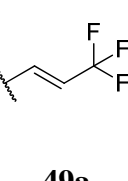
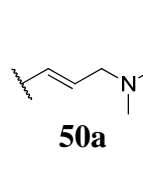
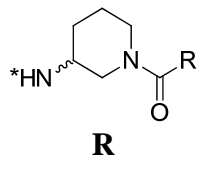
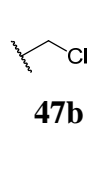
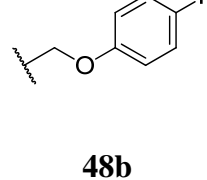
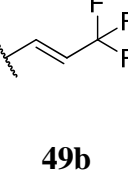
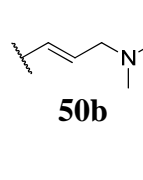
disclosed but one can postulate that the different tautomeric and mesomeric forms of the two amides, presented in Scheme 17, could explain the difference in reactivity observed. Indeed, although it is difficult to imagine any reactivity difference towards a cysteine residue when looking at the major tautomeric/mesomeric forms **55** and **57**, the minor forms **56** and **58** are believed to react differently to Michael 1,4-addition. The α,β -unsaturated imine **56** is less reactive than the α,β -unsaturated iminium ion **58** towards cysteine nucleophilic attack: 1,4-addition to compound **58** is driven by the quench of the positive charge on the nitrogen. Therefore, overall, the secondary acrylamide is less reactive than the tertiary acrylamide towards Michael 1,4-addition. This finding somewhat explains the data presented in the mass spectrometry experiment for the methoxymethyl series (section VII.1). The tertiary amide **13** was found to mainly react with Cys442 in the ITK active site but residual covalent reaction with another ITK cysteine was also observed. This was not the case for the less reactive secondary amide **8**.



Scheme 17. Different tautomeric/mesomeric forms of primary and secondary acrylamides

A selection of the newly synthesised electrophilic moieties were also assessed in the *N*-acetylcysteine experiment. The nucleophilic attack of the *N*-acetylcysteine was monitored by LCMS and the data are summarized in Table 10.

Table 10. Extent of the reaction between *N*-acetylcysteine and the different electrophilic moieties

 <p style="text-align: center;">R</p>	 <p style="text-align: center;">47a</p>	 <p style="text-align: center;">48a</p>	 <p style="text-align: center;">49a</p>	 <p style="text-align: center;">50a</p>
Formation of Michael adduct after 1 h	85 %	0 %	7 %	NT
Formation of Michael adduct after 3 h	100 %	0 %	22 %	NT
Formation of Michael adduct after 20 h	NT	0 %	74 %	NT
 <p style="text-align: center;">R</p>	 <p style="text-align: center;">47b</p>	 <p style="text-align: center;">48b</p>	 <p style="text-align: center;">49b</p>	 <p style="text-align: center;">50b</p>
Formation of Michael adduct after 1 h	100 %	0 %	68 %	NT
Formation of Michael adduct after 3 h	NT	0 %	89 %	NT
Formation of Michael adduct after 20 h	NT	0 %	100 %	NT

As expected, the chloroacetamides **47a** and **47b** reacted fastest with *N*-acetylcysteine, with full conversion achieved within three hours using these reaction conditions. Interestingly, the 4-fluorophenoxy group was not displaced by the cysteine in the assay; no conversion to the Michael adduct was observed by LCMS (Table 10). This result was somewhat surprising as such functionality has been reported in the literature¹¹⁶ as a possible electrophilic moiety for EGFR irreversible inhibitors. The trifluorobut-2-enamides **49a/49b** indicated that the trifluorobut-2-enamide was a better Michael acceptor than the acrylamide toward cysteine

nucleophilic attack. However, the difference in reactivity did not translate into better activities in the primary assays (Table 6). Interestingly, the difference in reactivity between secondary and tertiary amides was also demonstrated between the two trifluorobut-2-enamide **49a** and **49b**. The tertiary amide **49b** reacted faster with *N*-acetylcysteine than the secondary species **49a**. The inhibitors **50a** and **50b**, which did not demonstrate promising cellular activities (Table 6), were not tested in this reactivity experiment. However, Tsou *et al.*⁸⁶ have already studied the difference in reactivity between the unsubstituted acrylamide unit and the the (*E*)-4-(dimethylamino)but-2-enamide unit. In a competitive reactivity experiment with a pair of EGFR inhibitors possessing these two motifs and using glutathione in the absence of external base catalyst (such as triethylamine or DIPEA), 10 times more glutathione adduct was formed with the Michael acceptor possessing the (dimethylamino)methyl group. In our amino-benzothiazole ITK template, the introduction of this dimethylamino motif was assumed to lower the permeability of the compounds to such extent that they hardly demonstrate activity in the cellular assay. For that reason, this basic motif was not investigated further at this stage of the research project.

The data from the primary assays (Table 6) and *N*-acetylcysteine reactivity assay (Table 10) demonstrated that the 4-fluorophenoxyacetamide was not suitable as an electrophilic moiety for the ITK template. Consequently, compounds **48a** and **48b** were also not pursued any further. At this stage, compounds **47a**, **47b** and **49a** were selected to be tested in the kinetics assay. The data for the chloroacetamides **47a** and **47b** highlighted that both compounds were presenting time-dependent inhibition of ITK (Figure 46).¹²² Close analysis of the kinetic data indicated that these compounds were binding faster than all the acrylamide compounds tested previously. Indeed, when analysing the 0.14 μ M concentration curve (blue plots, Figure 46), the full inhibition of the kinase, corresponding to the covalent binding of all ITK to compound **47a**, was achieved after 30 minutes. For the acrylamide **33**, the similar inhibition was only reached after around 70 minutes (Figure 34). Therefore, the high reactivity of these chloroacetamides towards cysteines observed in the *N*-acetylcysteine experiment was confirmed in the kinetic assay.

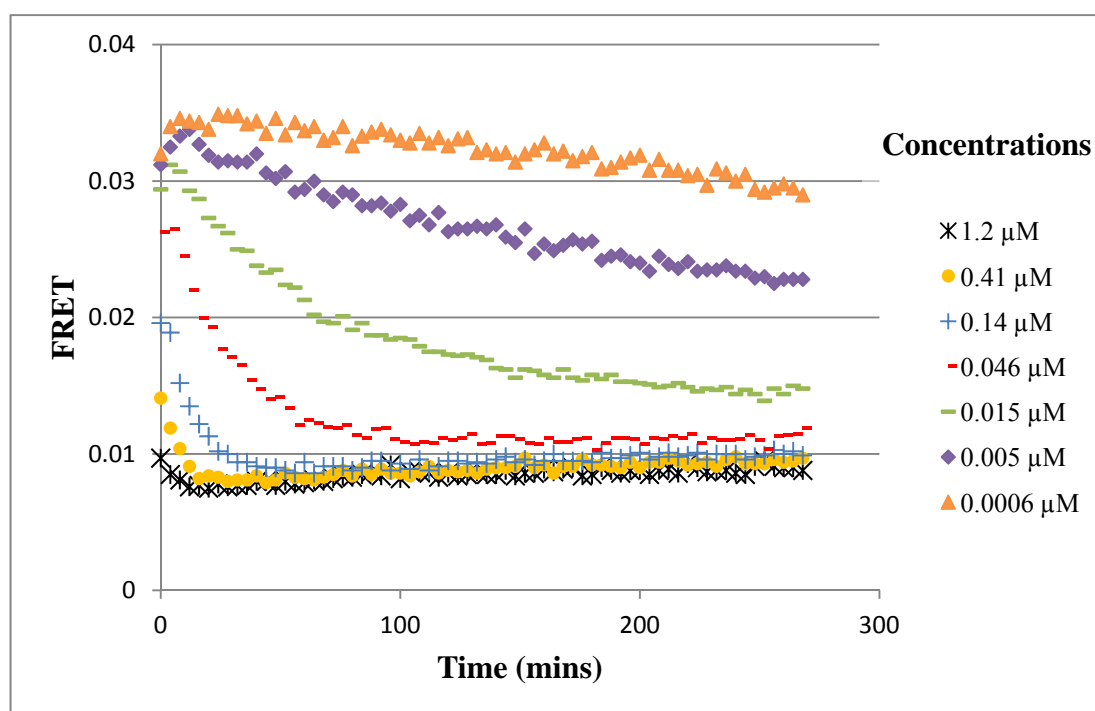


Figure 46. Kinetics data for compound **47a**

The kinetic data for the trifluorobut-2-enamide **49a** (Figure 47) revealed that, although the compound was irreversibly binding to ITK, the rate of covalent binding was slower than for the acrylamide **33**. Indeed, even at the concentration of 0.41 μM (yellow circles, Figure 47), full inhibition of ITK was only reached after 120 minutes. Contradictory evidence from the *N*-acetylcysteine assay had predicted that compound **49a** was reacting faster towards cysteines than the acrylamide compound **33**. However, once in the ITK ATP pocket, the steric bulk of the CF_3 group may disfavour the movement of the Cys442 motif, reducing the rate of the Michael addition reaction. Therefore, such an electrophile was not suitable for the ITK programme and compounds **49a** and **49b** were not profiled any further.

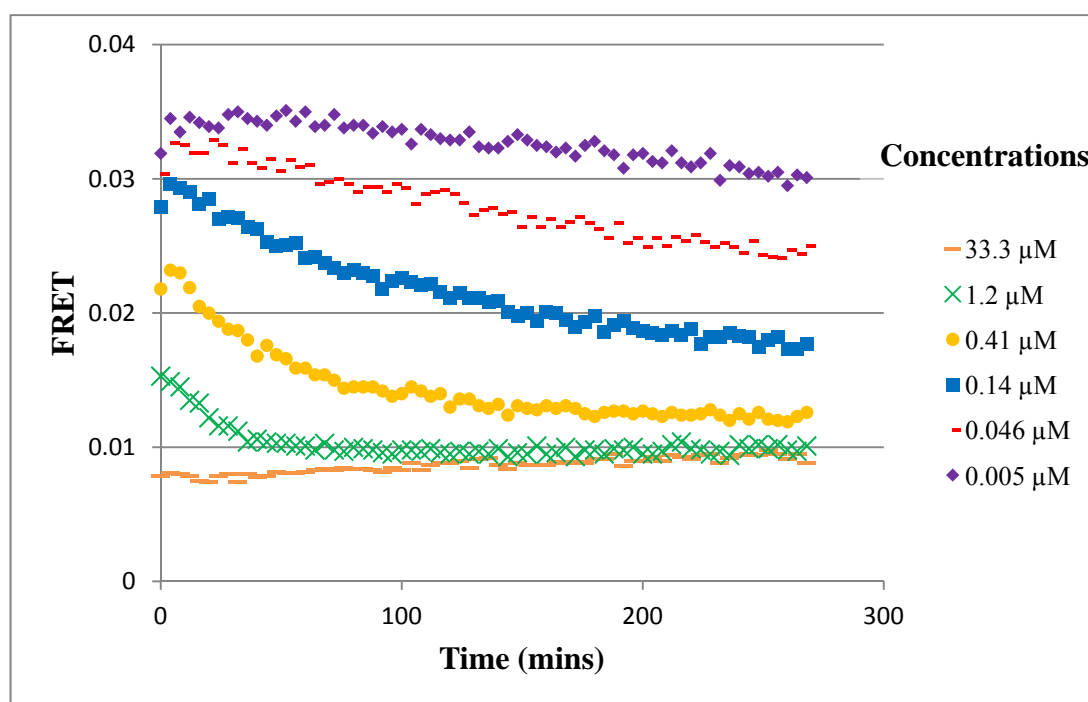


Figure 47. Kinetic data for compound **49a**

From the range of electrophilic moieties investigated so far, only the chloroacetamides have indicated an improved irreversible profile compared to the acrylamides previously tested. The chloroacetamides **47a** and **47b** have been demonstrated to covalently react faster with Cys442, with rapid irreversible binding resulting in enhanced activities in the primary assays. However, these compounds were only tools for the programme, as their high reactivity towards cysteine residues (confirmed in the *N*-acetylcysteine experiment) are likely to raise toxicity issues in humans.

Increasing the reactivity of the electrophilic moieties led to the discovery of compounds **47a** and **47b**, presenting better irreversible ITK profiles. Such compounds were, however, not progressable within this research programme. Moreover, the increase in reactivity did not always translate into faster covalent reaction with Cys442 (compounds **49a** and **49b**), as the newly introduced motifs may sterically disfavour the attack of Cys442 once the compounds are located in the ITK active site. Therefore, the reactivity findings from the *N*-acetylcysteine experiments do not always directly align with the data observed from the ITK kinetic binding

assays. However, the *N*-acetylcysteine experiment can provide useful information on the reactivity and potential toxicity of the electrophilic moieties.

The results from this investigation indicated that the acrylamide represented the most suitable electrophilic group for the needs of the ITK research programme. Different strategies aimed at increasing the rate of the covalent reaction were investigated in order to develop irreversible ITK inhibitors with improved cellular activities and duration of action.

4. Investigation of the positioning of the electrophilic moiety

The X-ray crystal structure obtained for compound **42** (Figure 39) indicates the formation of the desired covalent bond between the Cys442 of ITK and the inhibitor. However, it also clearly shows that the Michael acceptor hinges deeper into the pocket compared to the EGFR analogue, PD168393 (Figure 39, Figure 42). As discussed in section VII.2, the acrylamide unit is positioned on top of the two existing conformations of cysteine and might prevent the residue from moving from one conformation to the other. This could potentially explain why the covalent reaction is relatively slow with the compounds tested to date. Therefore, changing the position of the electrophilic moiety, to allow Cys442 to move without any steric hindrance, should optimise the interaction between the Michael acceptor and the nucleophilic sulfur, in turn increasing the reaction rate.

Positioning the Michael acceptor at a more shallow location of the pocket requires a reduction in the length of the alkyl chain linking the pyrimidine central ring to the acrylamide. This should allow the cysteine to rotate freely. The downside of this approach could be that the compound would miss the important interactions associated with the cyclic lipophilic unit, as presented in Figure 28. To maintain the required high activity towards ITK, the shorter inhibitors would have to quickly make the covalently bond with Cys442 to drive the binding equilibrium, presented in Equation 1, towards EI*, as the non-covalent binding affinity should be weaker.

The compounds presented in Figure 48 were designed to keep the low reactivity of the acrylamide unit while allowing Cys442 to adopt the two observed conformations

without restricted interactions with the inhibitor. Compounds **59-61** were first synthesised in the pyrimidine series and would be transferred into the more potent pyridine template if they displayed the required potency profiles.

Compounds **59** and **60** present the same atom length from the pyrimidine ring to the acrylamide. Compound **59** is more flexible than compound **60** and possesses the hydrogen bond donor NH, attached to the aromatic ring, which has already proven to be important for the binding activity to the ITK active site (Scheme 10, Table 3). However, compound **60** is more lipophilic than compound **59**, which could have a beneficial effect for the non-covalent recognition within the ATP binding pocket. Finally, the acrylamide unit of compound **61** is one atom closer to the pyrimidine ring compared to compounds **59** and **60**. This positioning was predicted to be outside of the optimal range for covalent interaction with Cys442 by the computational molecular modelling.⁹⁸

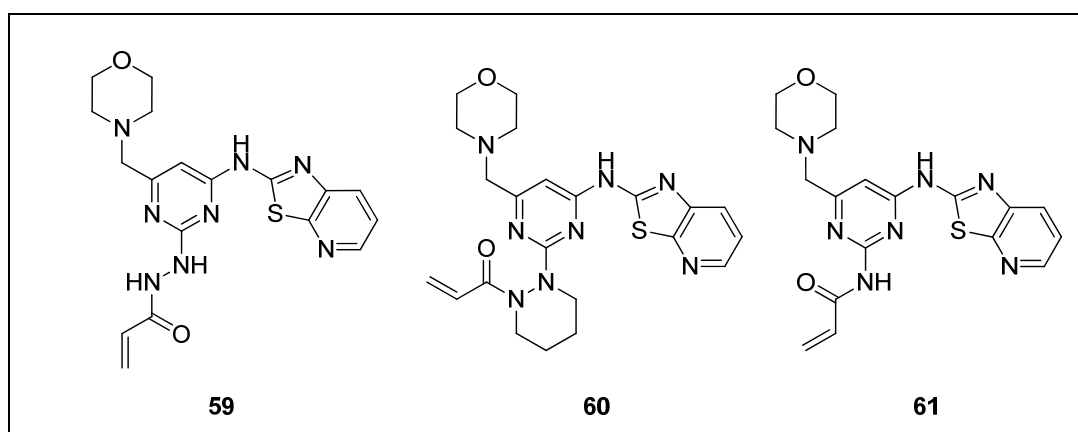
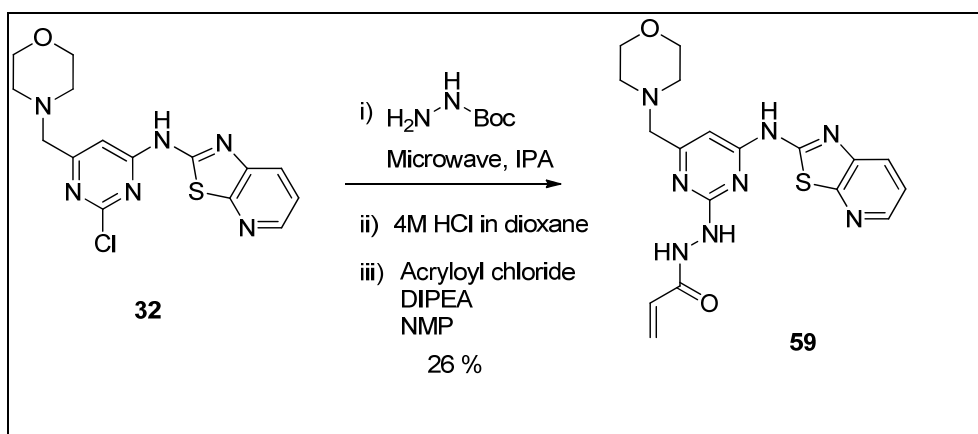
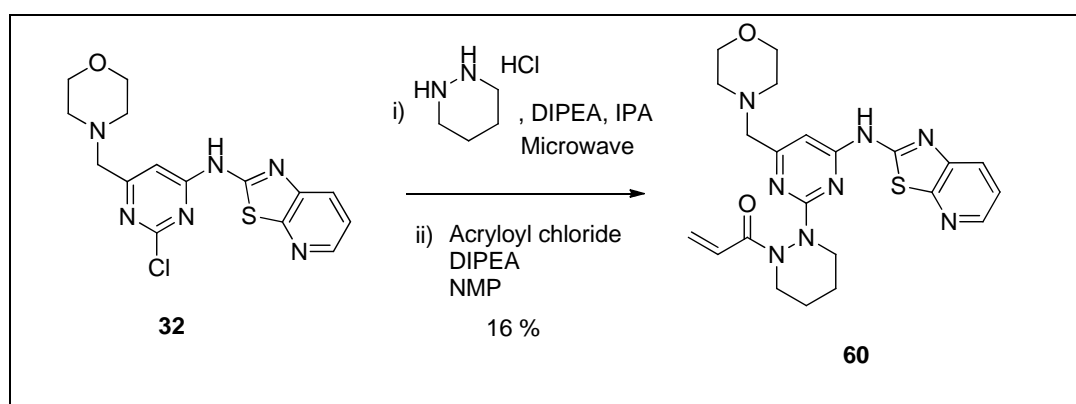


Figure 48. Proposed ITK inhibitors allowing Cys442 to freely rotate

Compounds **59** and **60** were synthesised by aromatic nucleophilic displacement in the microwave from the intermediate **32** (Scheme 18, Scheme 19). Subsequent Boc deprotection and amide coupling with acryloyl chloride gave the desired compounds **59** and **60**. Both compounds were synthesised without isolation of the intermediates; only the two final products were carefully purified before biological testing.

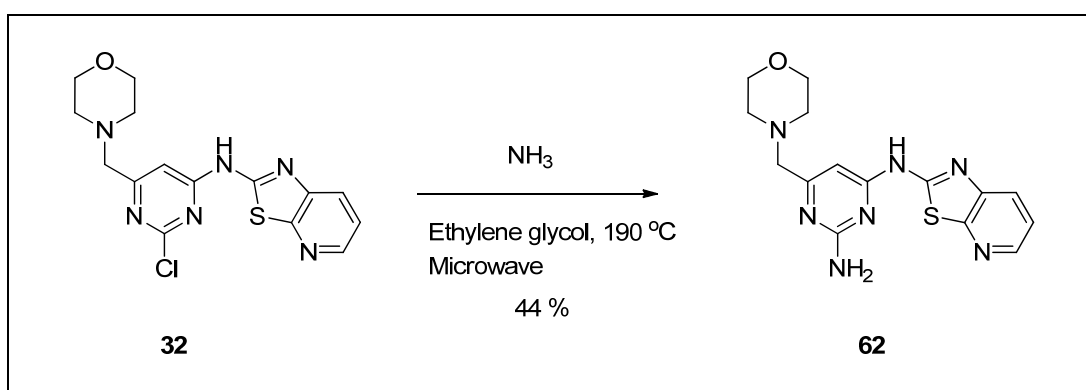


Scheme 18. Synthetic scheme for compound 59



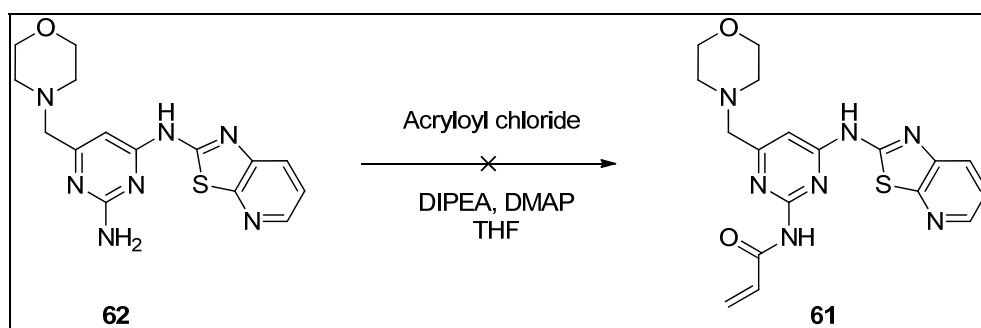
Scheme 19. Synthetic scheme for compound 60

The synthesis of compound **61** proved to be much more challenging. Aromatic nucleophilic displacement of the intermediate **32**, in the microwave, with concentrated aqueous ammonia yielded 44 % of the amino intermediate **62** (Scheme 20). The reaction temperature had to be increased to 190 °C to allow the displacement to occur, due to the weaker nucleophilicity of ammonia. Therefore, the solvent was changed from isopropanol to ethylene glycol, which has a higher boiling point (197 °C) and is more suitable to use in the Biotage microwave system at such temperatures.



Scheme 20. Synthetic scheme for compound **62**

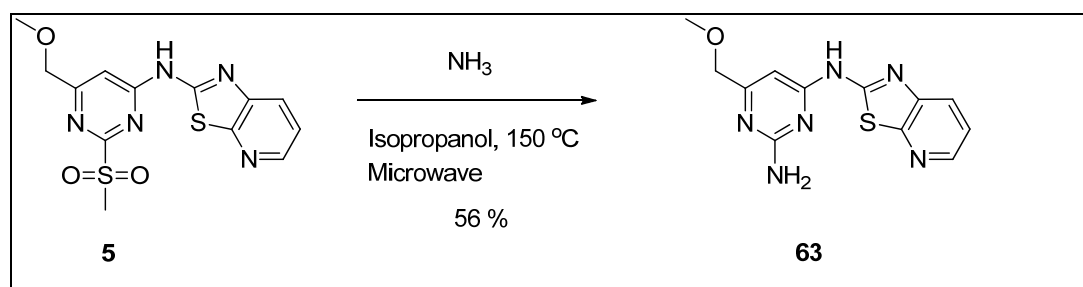
The amide coupling reaction between compound **62** and acryloyl chloride (Scheme 21) did not yield the desired product **61**. With 3 equivalents of acryloyl chloride, 3 equivalents of DIPEA and catalytic amount of DMAP in THF at room temperature, the LCMS profile of the reaction mixture, after 30 minutes, showed mainly the starting material **62** and poor conversion to the expected product **61**. Adding excess of acryloyl chloride and DIPEA or heating the reaction mixture to 50 °C improved the conversion but only the starting material **62** was recovered after MDAP purification (acetonitrile:water with ammonium carbonate modifier eluent).



Scheme 21. Amide coupling conditions failed to provide compound **61**

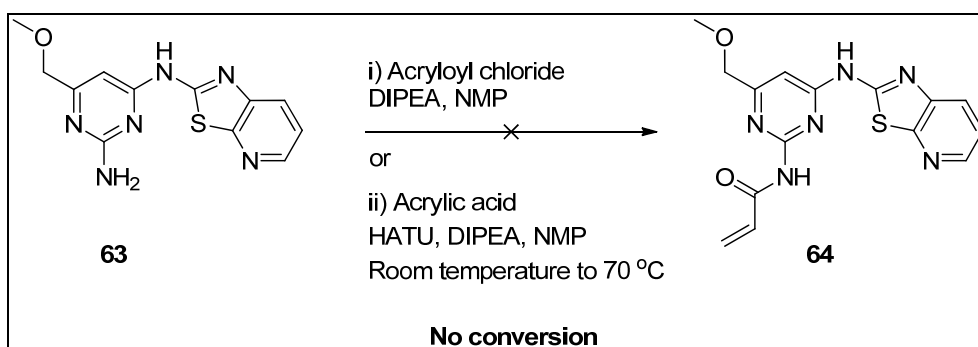
Instead of using the desirable intermediate **62**, which was obtained in 6 steps from the commercially available pyrimidine **25** (Scheme 11), the chemistry was investigated using the less active and less desirable 6-methoxymethylpyrimidine template. Compound **5** was reacted with aqueous ammonia in the microwave system to yield the amine **63**. As described previously, the greater electronegativity of the

methylsulfonyl group allowed the reaction to occur at 150 °C in isopropanol, compared to 190 °C in ethylene glycol for the chloro intermediate **32** (Scheme 20).



Scheme 22. Synthetic scheme for compound **63**

The amide coupling reaction, attempted with compound **63**, using acryloyl chloride and DIPEA in NMP at room temperature (Scheme 23), failed to give any useful conversion to the product **64**. Adding a catalytic amount of DMAP and changing the temperature of the reaction did not improve the profile of this transformation. Amide coupling conditions using acrylic acid and HATU (Scheme 23) also failed to give any useful conversion to compound **64**.



Scheme 23. Amide coupling conditions failed to provide compound **64**

The amide coupling was repeated with acryloyl chloride and DIPEA in THF at room temperature, and the minor peak, corresponding to the mass ion of compound **64** by LCMS, was purified. The mass directed autoprep equipment clearly collected a UV peak with a mass ion corresponding to compound **64**, but after concentration of the solvent (acetonitrile:water with ammonium carbonate modifier) under reduced pressure, NMR and LCMS analysis of the white solid obtained, supported the structure of the starting material **63**. The purification was also attempted with the

acidic media (acetonitrile:water with formic acid modifier) mass directed autoprep but both experiments resulted in degradation to the compound **63** after evaporation of the solvent under reduced pressure or nitrogen blowdown at room temperature. This indicated that the product with the mass ion corresponding to compound **64** was not stable in the solvents used by the LCMS system. This finding explained why the conversion of the amide coupling was always poor as the product was partially reversing to the starting material when analysed by LCMS. To confirm this hypothesis, the amide coupling using acryloyl chloride was repeated and the complex reaction mixture was, once again, purified by mass directed autoprep. Instead of evaporating the acetonitrile/aqueous mixture of solvents, the collected fractions were extracted with DCM. The organic extracts were dried, concentrated under reduced pressure and analysed by NMR. ¹H NMR and NOE experiments (Figure 49) supported the structure of the product **65** (Scheme 24). ¹H NMR clearly showed a singlet at 7.18 ppm (a, Figure 49), integrating for two protons and corresponding to the amino group. NOE irradiation of the pyrimidine proton labelled b (Figure 49) revealed coupling with the proton labelled c (Figure 49), which is part of the acrylamide unit. Both pieces of information supported the fact that the Michael acceptor was linked to the nitrogen at the 4-position of the pyrimidine.

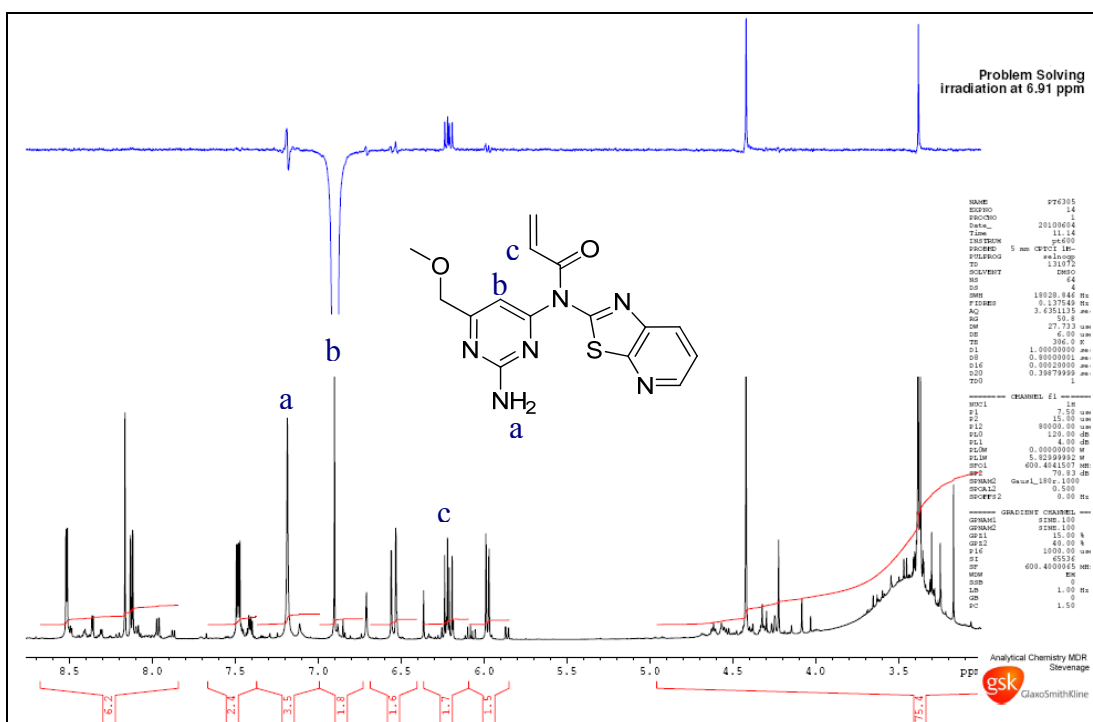
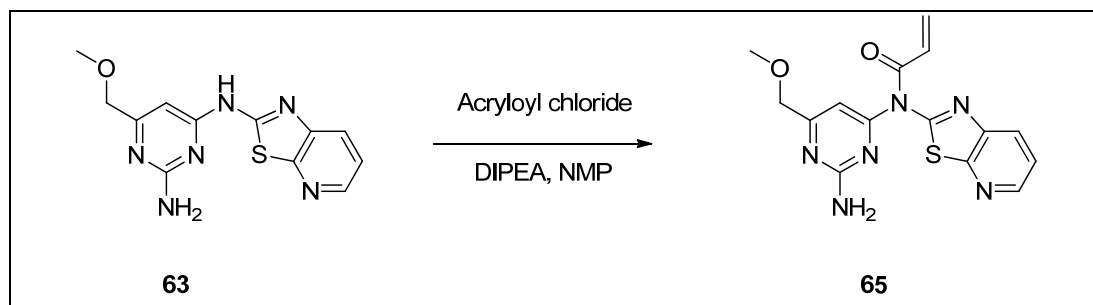


Figure 49. NMR analysis proving the structure of compound **65**

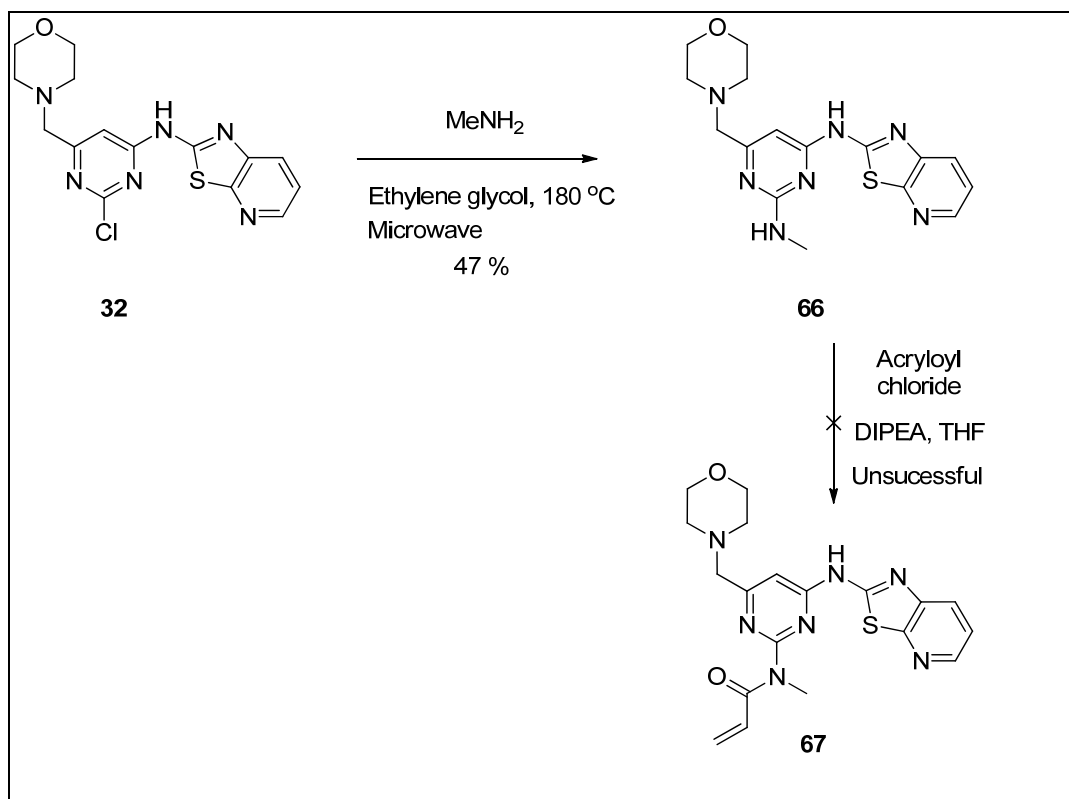


Scheme 24. Formation of compound **65** during the amide coupling

The formation of compound **65** instead of compound **64**, under these acid chloride coupling conditions, indicated the weak nucleophilicity of the amino group at the 2-position of the pyrimidine.

To increase the nucleophilicity of the desired amine, compound **32** was reacted with methylamine at 180 °C in the microwave to give the 2-methylamino intermediate **66**, with a 47 % yield (Scheme 25). However, reacting compound **66** with an excess of acryloyl chloride and DIPEA did not allow the isolation of the desired product **67**. Once again, a species with the mass ion corresponding to the product **67** was observed in the LCMS of the reaction mixture but the product was not isolated after

reverse phase purification. This suggested that the amide had not formed at the required position, as previously described in Scheme 24.

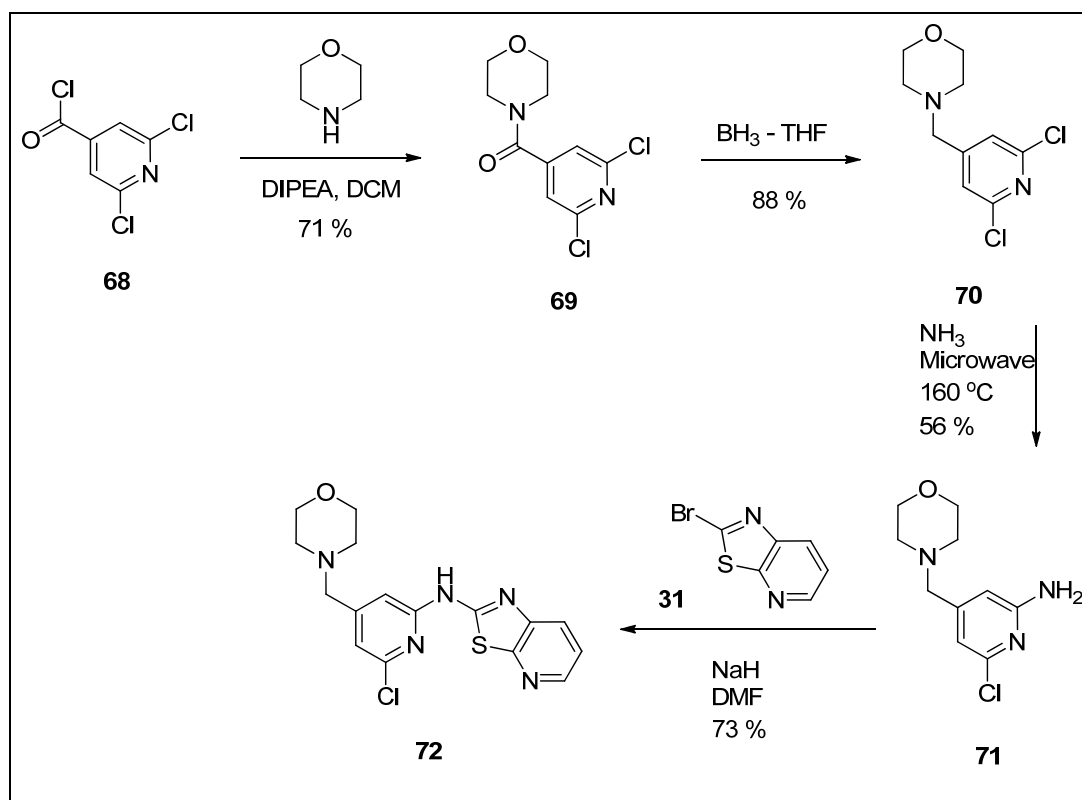


Scheme 25. Synthetic scheme to attempt making compound **67**

The challenging target compound **61** was transferred to the pyridine series, as the final amide coupling step was believed to be more accessible due to the higher nucleophilic character of the 2-aminopyridine compared to the 2-aminopyrimidine. The pyridine template had the additional advantage that it should have provided the best affinity to the ITK active site according to the data previously obtained on this programme (Figure 26).

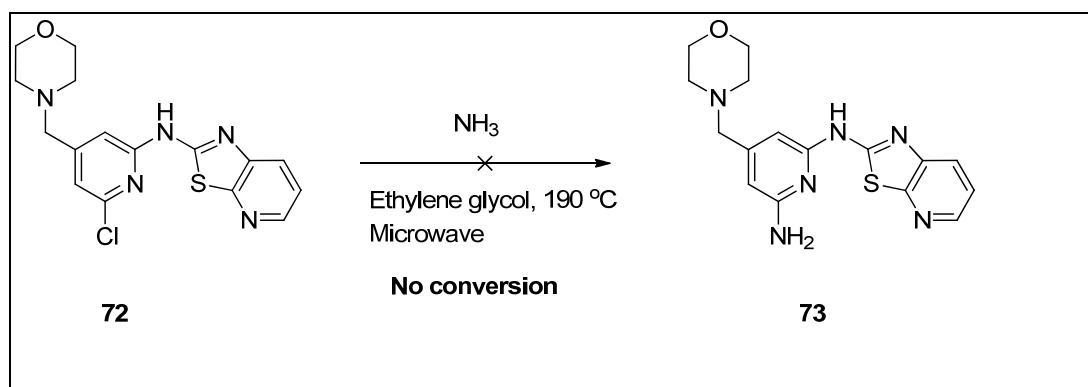
The synthesis of the pyridine template started with an amide coupling reaction to attach the morpholine to the template (Scheme 26). The amide was then reduced with borane in THF to provide compound **70** in an 88 % yield. The symmetrical dichloropyridine **70** was reacted with an excess of aqueous ammonia at $160\text{ }^\circ\text{C}$ for 15 hours in the microwave system. At such temperature, with the excess of ammonia, the pressure inside the microwave vial reached 18 bar, which was close to the 20 bar upper limit of the equipment. However, even under such forcing conditions, only

mono displacement of the bis-chloropyrimidine was observed by LCMS. This already suggested that the aromatic nucleophilic displacement of the second chlorine was going to be more challenging than in the pyrimidine series. Nucleophilic displacement of the 2-bromo[1,3]thiazolo[5,4-*b*]pyridine **31** with the chloro-aminopyridine intermediate **71** in the presence of sodium hydride finally gave the required chloro intermediate **72**.

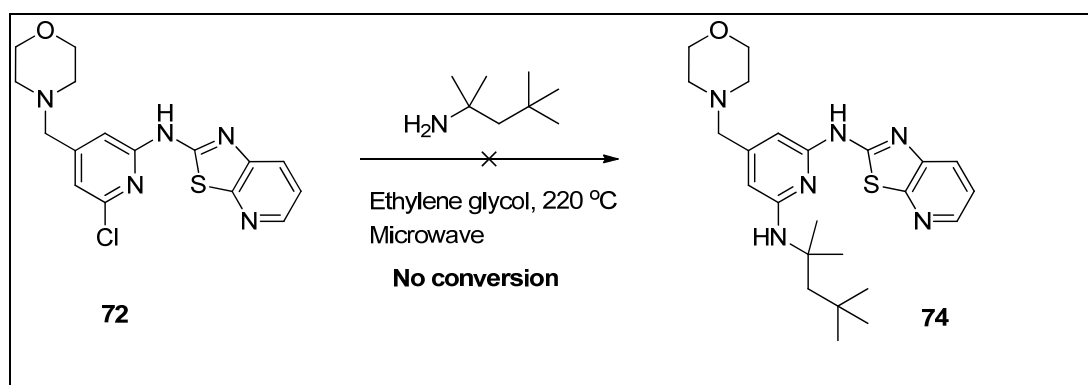


Scheme 26. Synthetic scheme for the intermediate compound **72**

Aromatic nucleophilic displacement of the chloropyridine intermediate **72** to give the desired aminopyridine compound **73** proved, as expected, to be difficult to achieve (Scheme 27). Microwave irradiation of compound **72** with excess ammonia up to the temperature of 190 °C (20 bar pressure) did not show any conversion to the desired product **73**. Similarly, nucleophilic displacement of the intermediate **72** with *tert*-octylamine at 220 °C failed to provide any conversion to compound **74** (Scheme 28). The steric hindrance of *tert*-octylamine was believed to be the main reason preventing the displacement to occur at such high temperatures.

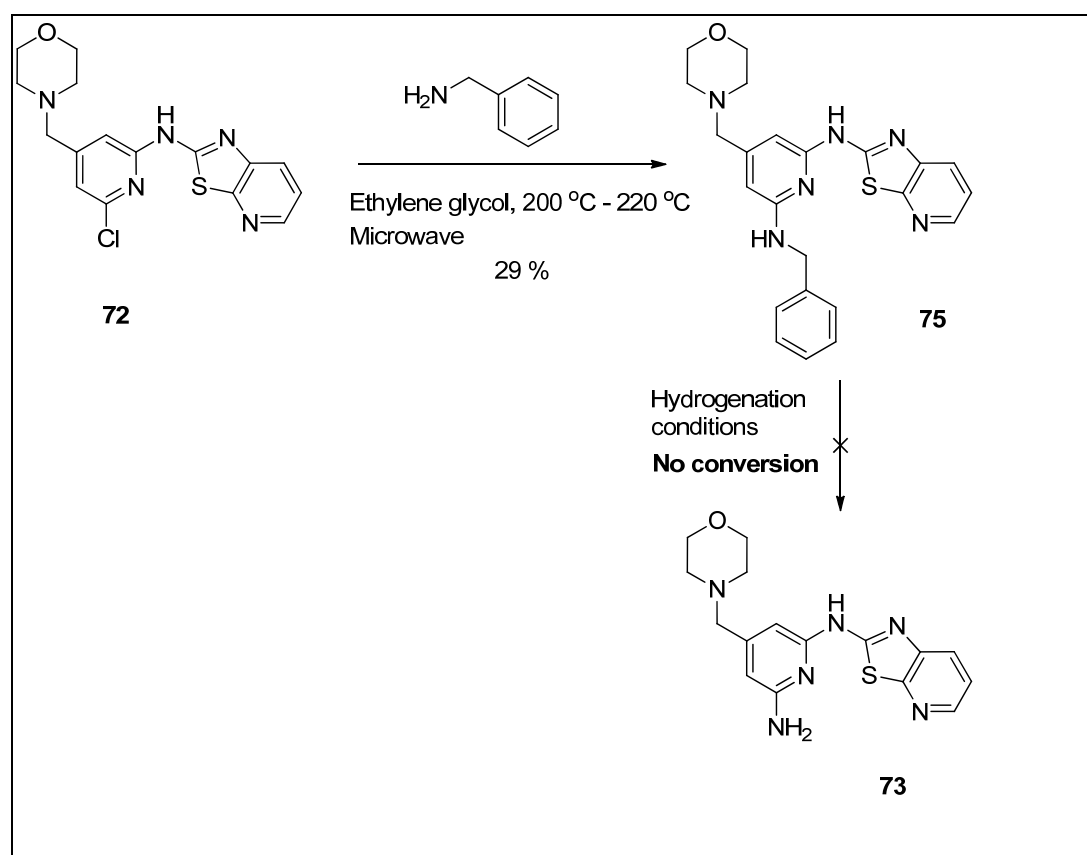


Scheme 27. Displacement of the chloropyridine intermediate 72 with ammonia failed to give any conversion towards compound 73



Scheme 28. Displacement of the chloropyridine intermediate 72 with tert-octylamine failed to give any conversion towards compound 74

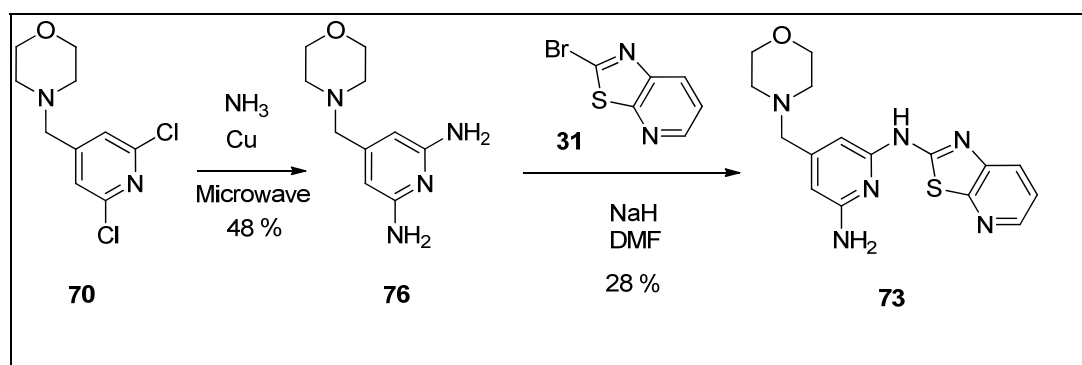
This hypothesis was confirmed when compound **72** was successfully reacted with benzylamine, under microwave irradiation (200 °C - 220 °C), to give the intermediate **75** in a moderate 29 % yield (Scheme 29). However, hydrogenation of the benzyl unit with 10 % palladium on charcoal either at room temperature (with and without acetic acid) or at 70 °C in the ThalesNano H-cube[®] equipment failed to convert the intermediate **75** into the required compound **73** (Scheme 29).



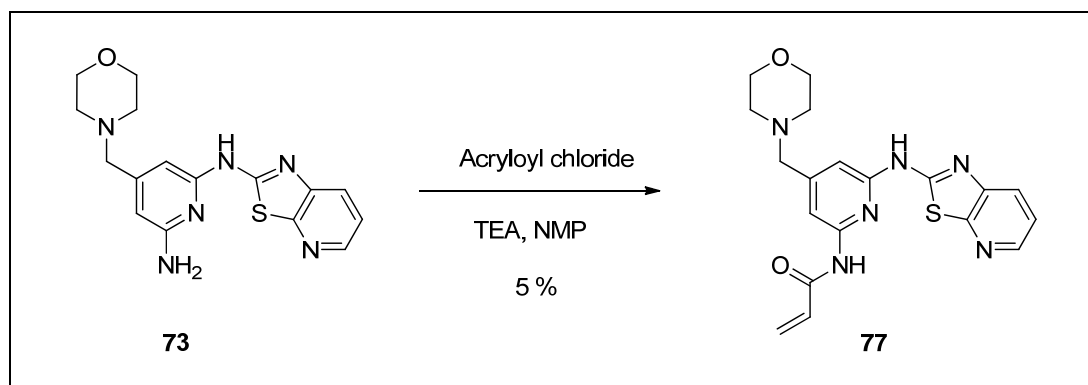
Scheme 29. Nucleophilic displacement with benzylamine provided compound **75** which could not be transformed into compound **73**

None of these methods proved to be efficient at transforming compound **72** into compound **73** by aromatic nucleophilic displacement reactions. Consideration was therefore given as to whether the amino group should be introduced earlier in the synthesis, or whether Buchwald cross-coupling conditions to introduce the amino group from the intermediate **72** should be attempted.¹²³ The first approach was investigated initially. A literature review of 2,6-diaminopyridine compounds revealed that bis displacement of 2,6-dichloroisonicotinic acid with ammonia, in the presence of copper powder, could be achieved at 200 °C under pressure.¹²⁴ Therefore, compound **70** was reacted with excess of ammonia and 0.3 equivalents of copper powder, at 170 °C, under microwave irradiation (pressure 18 bar) for 15 hours in the microwave system (Scheme 30). The copper catalyst allowed the formation of the desired diaminopyridine **76** in a 48 % yield, whereas similar conditions, without the catalyst, only yielded the mono aminopyridine compound **71** (Scheme 26). Subsequent aromatic nucleophilic displacement of 2-

bromo[1,3]thiazolo[5,4-*b*]pyridine **31** with compound **76** yielded the required product **73**. The moderate yield of this last reaction did not reflect the relatively clean LCMS profile of the reaction mixture, upon full consumption of the starting material **76**. This moderate yield was most likely due to the inadequate chromatography purification on basic silica column (aminopropyl column). Indeed, even using this column, the polar compound **73** streaked on the column leading to many impure fractions which were not collected and used. If repeated, the purification would be attempted using reverse phase chromatography conditions. However, sufficient quantities of compound **73** were obtained to attempt the synthesis of the required molecule **77** (Scheme 31), hence the synthesis and purification of compound **73** was not repeated at this stage.



Scheme 30. Synthetic scheme for compound 73



Scheme 31. Synthetic scheme for compound 77

Compound **73** was reacted with excess of acryloyl chloride and triethylamine in NMP at room temperature (Scheme 31). The reaction profile of the reaction was complicated and a large excess of reagents were required to observe full conversion

of the starting material **73**. However, a peak corresponding to the mass ion of compound **77** was observed by LCMS. After work-up, the reaction mixture was purified by mass directed autoprep. Evaporation of the desired fraction and NMR analysis of the residue obtained confirmed the structure of compound **77** (Figure 50). Clear signals for the two NH protons (a and b, Figure 50) were observed at 11.5 ppm and 10.3 ppm, whereas no signal corresponding to an NH₂ group was displayed. This supported the formation of compound **77** and not a similar by-product to compound **65** obtained in the pyrimidine series.

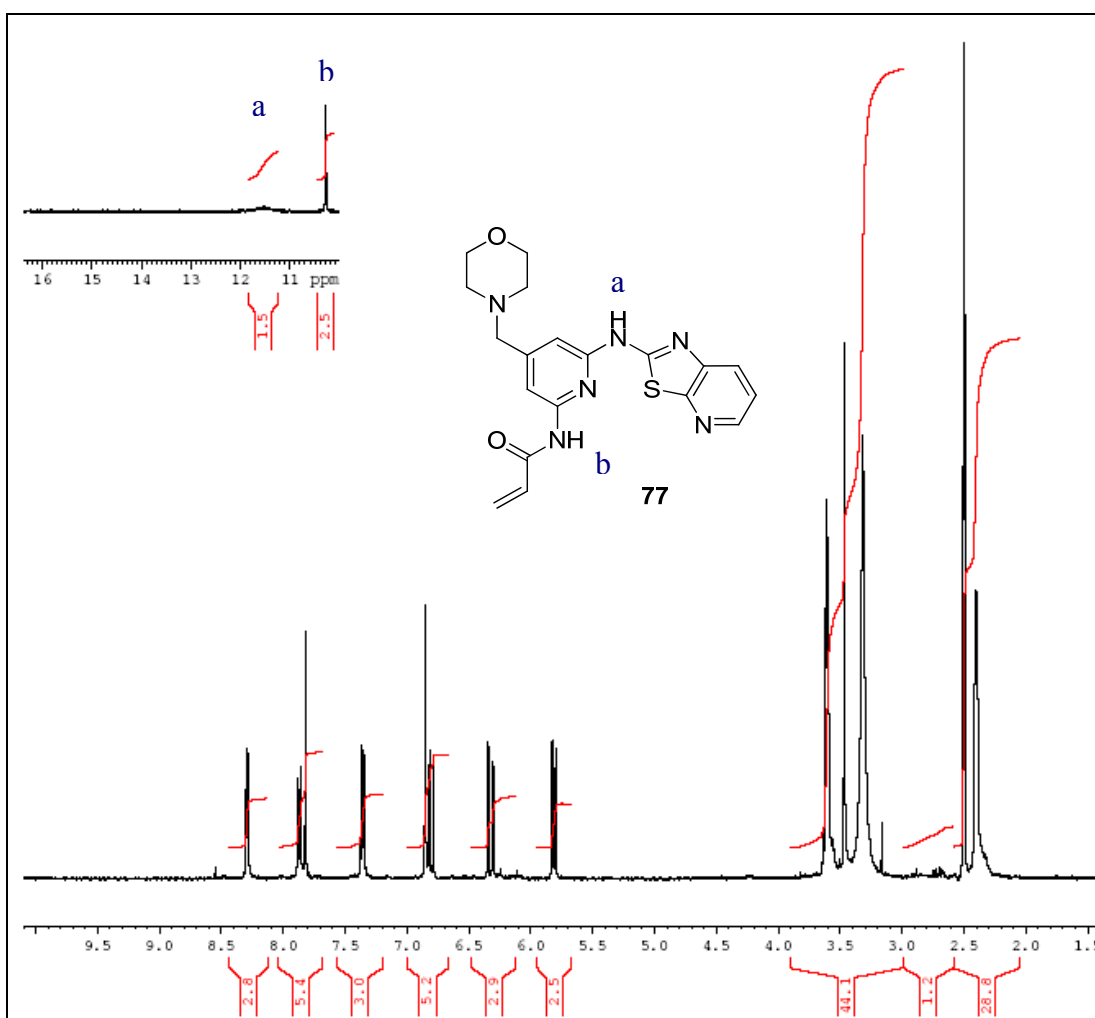


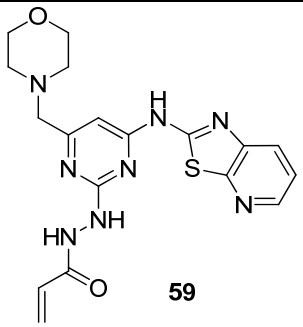
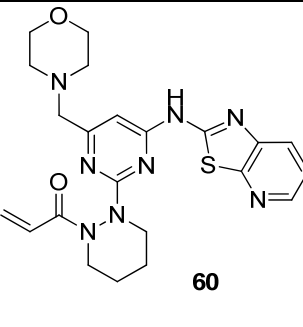
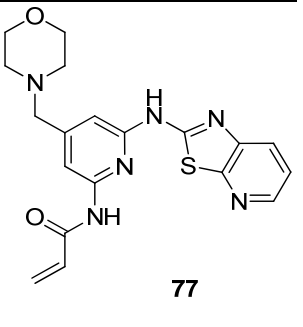
Figure 50. NMR analysis confirmed the structure of compound **77**

Despite the confirmation that compound **77** had been synthesised, the yield of the transformation was low (5 %). Although the amino group was more nucleophilic in the pyridine series than in the pyrimidine series, the reaction still required a large

excess of acid chloride to reach full conversion of the starting material. An attempt to improve the reaction conditions by modifying the amount of base used was performed but the profile of the reaction was similar or even worse than that obtained previously. Before committing more effort towards enhancing the reaction yield, compound **77** was tested in the various biological assays to assess whether it displayed a better irreversible profile compared to the longer amine linkers described in the previous section VII.2.

Table 11 summarises the biological data obtained for compounds **59**, **60** and **77**. All three compounds were significantly less active than the best amine linkers previously investigated (Table 4). Compounds **59** and **60** were recorded as being inactive ($pIC_{50} < 4.6$) in the 1 mM ATP HTRF⁽²⁾ assay. These compounds were therefore tested in the HTRF⁽¹⁾ assay and they demonstrated some low level of binding to ITK, with the observed pIC_{50} in this assay being lower than the values obtained for the compounds from the initial 6-methoxymethylpyrimidine series (Table 2). The extra lipophilicity of compound **60** did not improve the HTRF binding affinity. This was believed to be due to the loss of the important NH attached the pyrimidine ring. Compound **77** was more active than compounds **59** and **60** in both the HTRF and PBMC assays. However, it remained difficult to conclude that the amine linker was better than the hydrazine unit as the two compounds were synthesised in two different series (pyridine and pyrimidine). Previous SARs on both templates revealed that the pyridine series is on average 0.7 log unit better than the pyrimidine family in both assays (section VII.1 and Figure 26). Therefore, these SARs did not clearly demonstrate that the linker of compound **77** was more suitable for ITK inhibition than the hydrazine units found in compound **59** and **60**, as most of the increase in activity might have been related to the preferred pyridine template. To truly compare the linkers, compound **59** and **60** would, of course, have to be synthesised in the pyridine series and assayed in both biological tests.

Table 11. SAR analysis of the new acrylamide linkers

	 59	 60	 77
HTRF ⁽²⁾ pIC ₅₀	<4.5	<4.6	5.7
HTRF ⁽¹⁾ pIC ₅₀	6.3	5.6	7.3
PBMC pIC ₅₀	5.8	6.6	7.5

In conclusion, compound containing the three linkers, designed to allow the cysteine residue to move freely between conformations and react faster with the acrylamide moiety, displayed significantly lower activities in the primary assays (HTRF and PBMC) compared to the amines previously investigated, hence were not pursued any further. Efforts were then focused on strengthening the non-covalent binding to ITK to favour the formation of the requisite covalent bond.

5. The 6-morpholinylmethylpyridine template

The two previous approaches aimed at increasing the rate of the covalent reaction between the electrophilic moiety and Cys442 failed to improve on the compounds described in the section VII.2. The next target was to improve the non-covalent binding to ITK to drive the equilibrium presented in Equation 1 towards EI, which in turn should facilitate the formation of the covalent EI* complex. Moving from the pyrimidine to the pyridine template should increase the ITK binding affinity of the compounds (Figure 26) and may result in compounds presenting the required profile for the irreversible ITK research programme. Using SAR generated in the series that

have been explored to date, a range of amines (Figure 51) were selected for synthesis as they represented the best chances to obtain potent irreversible ITK inhibitors.

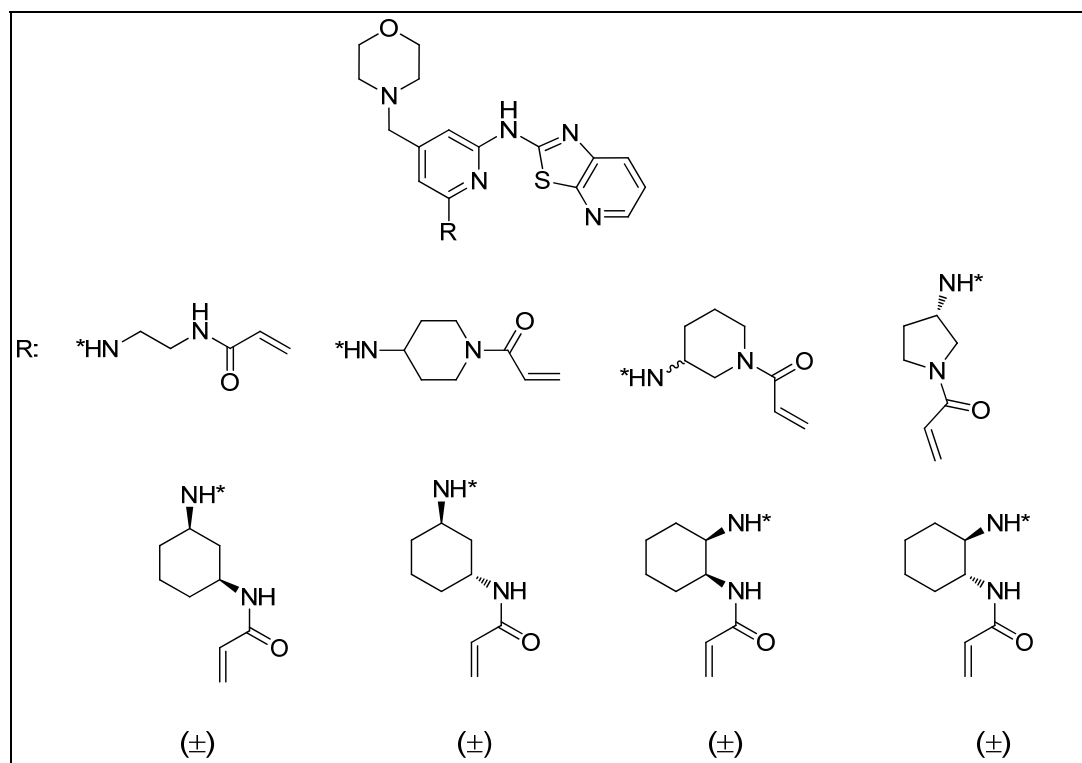
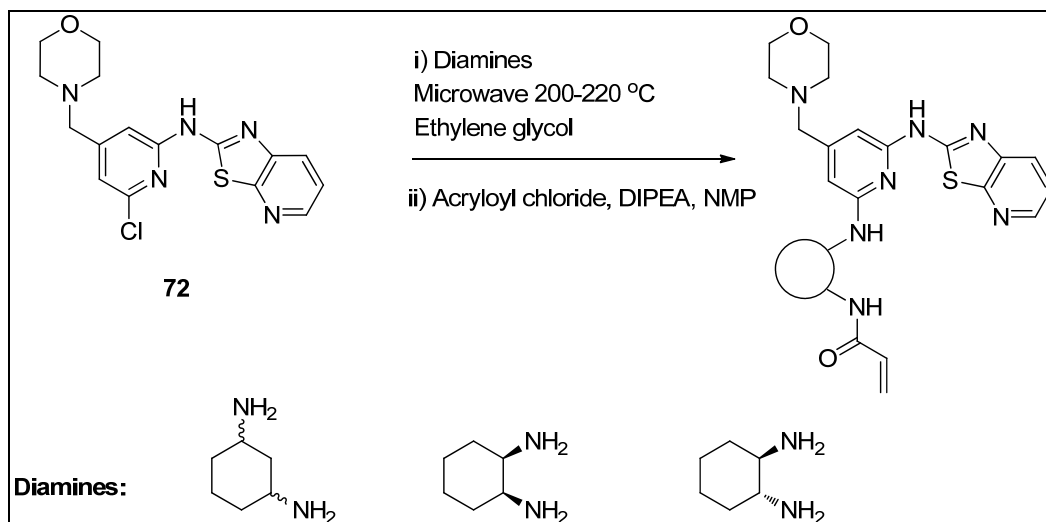


Figure 51. Range of amines synthesised to investigate the SAR of the morpholinylmethylpyridine template

These molecules were synthesised using the intermediate **72**, the synthesis of which was described in Scheme 26. Previous work suggested that these pyridine compounds would be preparatively more challenging than their direct analogues from the pyrimidine series (Figure 33), due to more difficult aromatic nucleophilic displacement between compound **72** and primary amines. The issue of displacing the 2-chloropyridine **72** with primary amines has already been discussed in section VII.4. The nucleophilic substitution reaction with benzylamine required microwave temperatures of 200 °C - 220 °C, at which the profile of the reaction became complicated and resulted in a moderate yield (Scheme 29).

The nucleophilic displacement was attempted with the cyclic diamines presented in Scheme 32. Compound **72** was reacted with an excess of diamine at 200 °C or 220 °C, in the microwave equipment for one to three hours. The amine intermediates

were reacted with acryloyl chloride and DIPEA to yield the desired compounds presented in Table 12. The yields of the reactions were, as expected, moderate to very low but the compounds were obtained in just sufficient amounts to be tested in the primary assays (HTRF and PBMC).



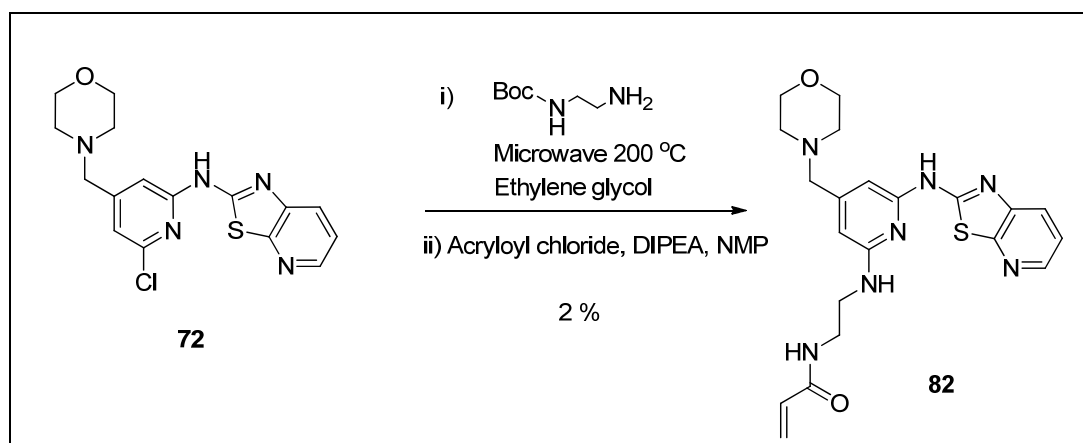
Scheme 32. Nucleophilic displacement using diamines to synthesise some desired compounds in the pyridine series

<p>R:</p>	<p>(±) 78</p>	<p>(±) 79</p>	<p>(±) 80</p>	<p>(±) 81</p>
Yield from compound 72	34 %	10 %	3 %	12 %

Table 12. Summary of the compounds obtained from the nucleophilic displacement using diamines

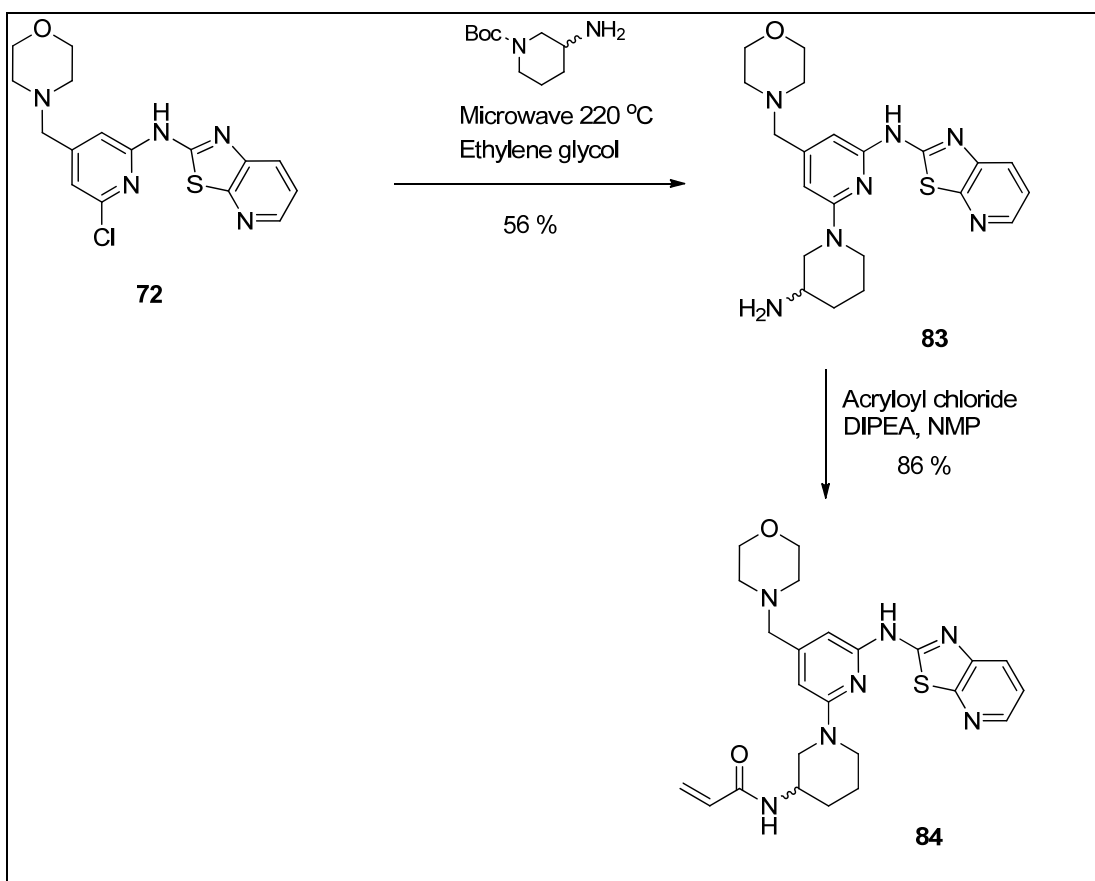
The same reaction was performed with *tert*-butyl 2-aminoethylcarbamate (Scheme 33). After microwave irradiation at 200 °C for one hour, the complicated LCMS profile showed a peak with a mass ion corresponding to the expected intermediate without the Boc group. An amide coupling reaction with acryloyl chloride yielded

the desired product **82**. The poor yield of the reaction was not the only issue here: the Boc group on the amine was not stable at such high temperature in the microwave. This suggested that the Boc group had possibly been removed before the nucleophilic substitution had occurred. This observation did not create issues in the synthesis of compound **82**, but for the desired piperidine and pyrrolidine compounds (Figure 51), it meant that the nucleophiles could potentially react via the more nucleophilic secondary amine should Boc deprotection occur *in situ* (*vide infra*).



Scheme 33. Synthetic scheme for compound **82**

The nucleophilic displacement reaction was attempted with *tert*-butyl 4-aminopiperidine-1-carboxylate (Scheme 34). Heating compound **72** with excess of *tert*-butyl 4-aminopiperidine-1-carboxylate in the microwave system for one hour at 180 °C provided little conversion of the starting material to a more polar product whose molecular weight corresponded to compound **83** (loss of the Boc group). Increasing the temperature to 220 °C led to full conversion to compound **83**, whose structure was confirmed by NMR. The intermediate **83** was reacted with acryloyl chloride to synthesise the final product **84**. This last compound was not expected to be as potent as the desired piperidine compound as it was missing the important NH unit attached to the aromatic ring. This anticipated reduced binding activity to ITK was later confirmed in the HTRF and PBMC assays (Table 17).

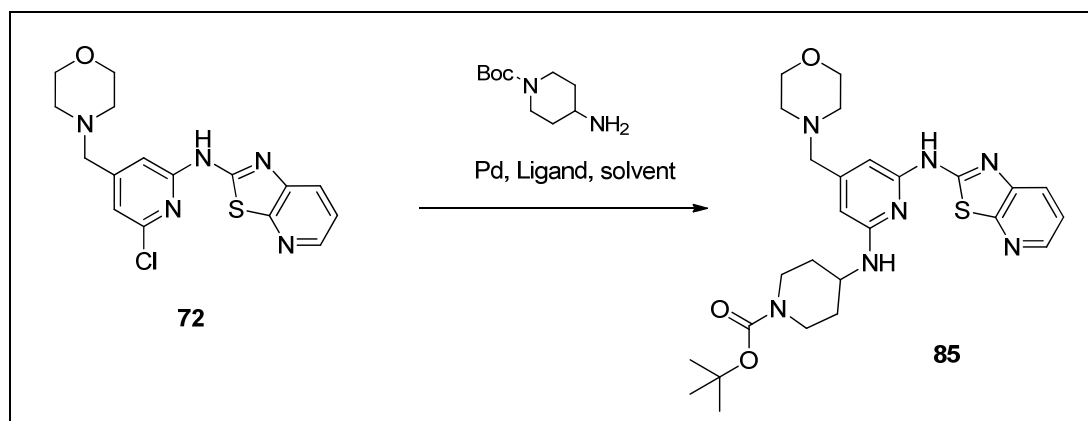


Scheme 34. Synthetic scheme for compound **84** proving that the nucleophilic displacement was not suitable for the aminopiperidine compounds

Taking into account the moderate to poor yields obtained with the diamine nucleophilic displacement (which would not be suitable for chemistry scale-up) and the associated difficulties in synthesising the most interesting piperidine and pyrrolidine desired compounds, new reaction conditions had to be developed to introduce the amine groups to the pyridine central ring. Palladium-catalysed Buchwald-Hartwig cross-coupling reactions were therefore investigated (Scheme 35).

Since the discovery¹²⁵⁻¹²⁷ in 1995 of this amination reaction between aryl halides and amines in the presence of a catalytic amount of palladium, the transformation has been investigated by numerous research groups.¹²⁸⁻¹³⁰ Major progress in the area has been enabled by the development of new classes of ligands,^{128,131} resulting in a wide range of nitrogen nucleophiles being successfully used in this reaction. However, the optimal combination of ligand, palladium source, base, solvent and temperature can

vary depending on the substrates and finding the right combinations of reaction parameters can often be a challenge.



Scheme 35. Buchwald-Hartwig amination reaction attempted to synthesise compound **85**

The amination reaction was investigated using the intermediate **72** and *tert*-butyl 4-aminopiperidine-1-carboxylate (Scheme 35). A range of reactions conditions were probed and the conversion to the product **85** was monitored by LCMS (Table 13). The initial conditions using DavePhos (Figure 52),¹³² Pd₂(dba)₃ and NaO^tBu in toluene or DMF (this latter solvent improved the solubility of the reactants), under an atmosphere of nitrogen, did not give any conversion of the intermediate **72**. Moving to the XPhos ligand (Figure 52), which has shown an improved reactivity in a diversity of amination reactions,¹³³ in combination with Pd₂(dba)₃ and Cs₂CO₃ in dioxane, did not show any improvement (entry 3, Table 13). Increasing the microwave reaction temperature to 180 °C did not change the profile of the reaction either (entry 4, Table 13). Although Pd₂(dba)₃ has been commonly used in amination reactions,¹³³⁻¹³⁵ the coordination of the dba ligand to the metal can decrease the reactivity of the palladium catalyst.^{136,137} Therefore, Pd₂(dba)₃ was replaced by Pd(OAc)₂, which, in contrast to Pd₂(dba)₃, needs to be reduced from Pd^(II) to Pd⁽⁰⁾ before the cross coupling reaction can take place. In this case, *tert*-butyl 4-aminopiperidine-1-carboxylate possesses one hydrogen, α to the amino group, allowing the Pd^(II) complex to undergo β -hydride elimination to form the desired Pd⁽⁰⁾ species (Scheme 36). The first reaction conditions attempted with Pd(OAc)₂, XPhos, NaO^tBu and toluene, heating thermally overnight, did not indicate any conversion of

the compound **72** (entry 5, Table 13). The same quantities of reagents were added to the previously used mixture, the vial was transferred into a microwave system and was heated at 160 °C for one hour (entry 6, Table 13). For the first time since the start of the investigation of the amination reaction, traces (~ 5 %) of product **85** were observed by LCMS. Screening of the reaction solvent (entry 6-9, Table 13) demonstrated that the conversion of the intermediate **72** into the compound **85** was only observed in toluene and DME, with the conversion being slightly better and more reproducible in DME. The better reproducibility of the conversion into compound **85** in DME was attributed to the higher solubility of the reagents in this solvent, whereas in toluene the mixture of reagents was in suspension (even at 100 °C, thermal heating), which could potentially explain the less reproducible conversions of the starting material. For this reason, DME was chosen as the solvent for the next series of conditions investigated (Table 14).

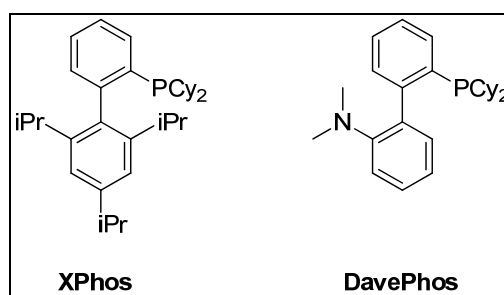
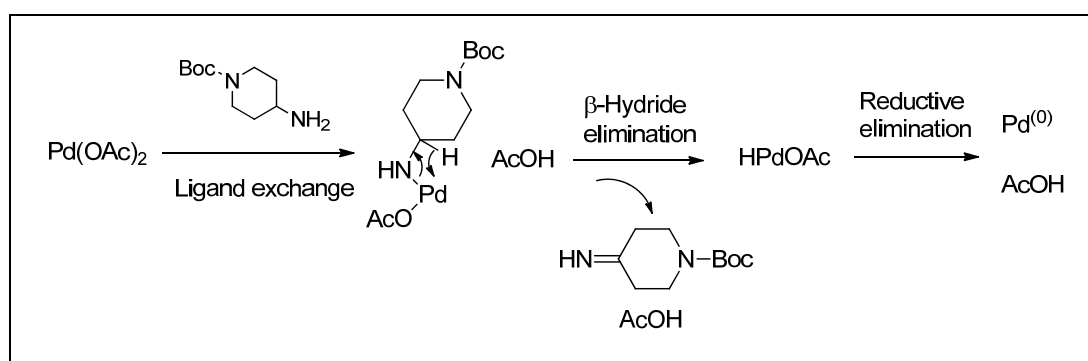


Figure 52. Structure of the XPhos and DavePhos ligands

Table 13. Investigation of the Buchwald-Hartwig amination coupling for the pyridine series

Entry	Amine eq	Pd (eq)	Ligand (eq)	Base (eq)	Solvent	T (°C)		Heating time	% conversion
						a = microwave	b = thermal		
1	1.5	Pd ₂ (dba) ₃ (0.1)	DavePhos (0.2)	NaO ^t Bu (4)	Toluene	150 (a)		1 h	-
2	1.5	Pd ₂ (dba) ₃ (0.1)	DavePhos (0.2)	NaO ^t Bu (4)	DMF	150 (a)		1 h	-
3	1.5	Pd ₂ (dba) ₃ (0.1)	XPhos (0.2)	Cs ₂ CO ₃ (2)	Dioxane	150 (a)		30 mins	-
4	1.5	Pd ₂ (dba) ₃ (0.1)	XPhos (0.2)	Cs ₂ CO ₃ (2)	Dioxane	180 (a)		30 mins	-
5	1	Pd(OAc) ₂ (0.1)	XPhos (0.2)	NaO ^t Bu (2)	Toluene	100 (b)		16 h	-
6	2	Pd(OAc) ₂ (0.2)	XPhos (0.4)	NaO ^t Bu (4)	Toluene	160 (a)		1 h	Traces
7	2	Pd(OAc) ₂ (0.2)	XPhos (0.4)	NaO ^t Bu (3)	Dioxane	160(a)		1 h	-
8	2	Pd(OAc) ₂ (0.2)	XPhos (0.4)	NaO ^t Bu (3)	DMF	160(a)		1 h	-
9	2	Pd(OAc) ₂ (0.2)	XPhos (0.4)	NaO ^t Bu (3)	DME	160(a)		1 h	Traces



Scheme 36. Reduction of Pd(OAc)₂ to Pd⁽⁰⁾ with, *tert*-butyl 4-aminopiperidine-1-carboxylate

In their latest review of amination reactions,¹³¹ Buchwald and Surry claim that the possible causes of low conversion could be attributed either to a low rate of the reaction or to inefficient formation of the active catalyst. The suggested solution to improve the rate of the transformation is to increase the temperature of the reaction.¹³¹ In this case, it has already been described that the temperature of the reaction could not be raised above 180 °C, as, at temperatures of 200 °C and 220 °C, degradation of the *tert*-butyl 4-aminopiperidine-1-carboxylate (loss of the Boc group) led to undesirable reactions (Scheme 34). Nonetheless, the microwave temperature was increased to 170 °C and 180 °C but no improvement in the conversion to the product **85** was observed (entry 1-3, Table 14). Hence, further work was focused on optimizing the formation of the active catalyst. To this end, the investigation of the catalyst and ligand loading was performed. The reaction was carried out using the conditions described in entry 4 (Table 14). As previously, only traces (< 5 %) of the compound **85** were seen by LCMS. Accordingly, further amounts of reagents (2 eq of amine, 0.2 eq of Pd(OAc)₂, 0.4 eq of XPhos and 3 eq of NaO^tBu) were added to the reaction mixture of entry 4 and the vial was irradiated in the microwave at 170 °C for another hour (entry 5). LCMS showed 17 % of the compound **85** (entry 5, Table 14). The reaction mixture was heated at 170 °C for one more hour without adding any reagents (entry 6, Table 14). LCMS analysis indicated no improvement in the formation of the compound **85**, with still 17 % observed in the HPLC spectrum. This finding indicated that after one hour at 170 °C in the microwave, the palladium catalyst was no longer effective. Further amounts of Pd(OAc)₂ and XPhos ligand needed to be added to the reaction mixture to drive the conversion to the product **85** to completion (entry 7, Table 14). [Note that entries 5, 6 and 7 were obtained by successively adding reagents to the reaction mixture of entry 4. The total amount of reagents in the microwave vial for each entry is recorded in the table.] This experiment confirmed that the low conversion observed in this reaction was due to the inefficient formation of the active catalyst. The active Pd⁽⁰⁾ species was believed to degrade into inactive Pd black before the amination reaction could completely occur.

Based on the outcomes to date, as recommended by Buchwald and Surry, the readily activated precatalyst **86** (Figure 53), which has produced excellent results with primary amines, was considered.¹³¹

Table 14: Investigation of the Buchwald-Hartwig amination coupling in DME

Entry	Amine eq	Pd (eq)	Ligand (eq)	Base (eq)	Solvent	T (°C) microwave	Heating time	% conversion
1	1.5	Pd(OAc) ₂ (0.2)	XPhos (0.2)	NaO ^t Bu (2)	DME	160	1 h	Traces
2	1.5	Pd(OAc) ₂ (0.2)	XPhos (0.2)	NaO ^t Bu (2)	DME	170	1 h	Traces
3	1.5	Pd(OAc) ₂ (0.2)	XPhos (0.2)	NaO ^t Bu (2)	DME	180	1 h	Traces
4	2	Pd(OAc) ₂ (0.2)	XPhos (0.4)	NaO ^t Bu (3)	DME	160	1 h	Traces
5	4	Pd(OAc) ₂ (0.4)	XPhos (0.8)	NaO ^t Bu (6)	DME	170	1 h	17 %
6	4	Pd(OAc) ₂ (0.4)	XPhos (0.8)	NaO ^t Bu (6)	DME	170	1 h	17 %
7	4	Pd(OAc) ₂ (0.6)	XPhos (1.2)	NaO ^t Bu (6)	DME	170	1 h	Full conversion

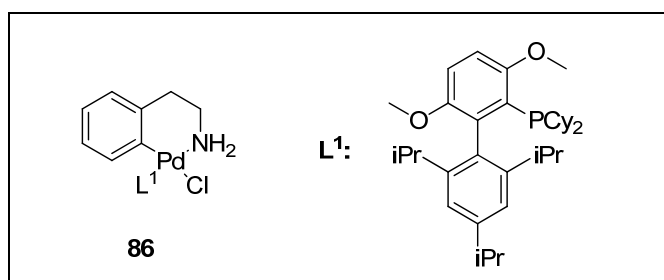
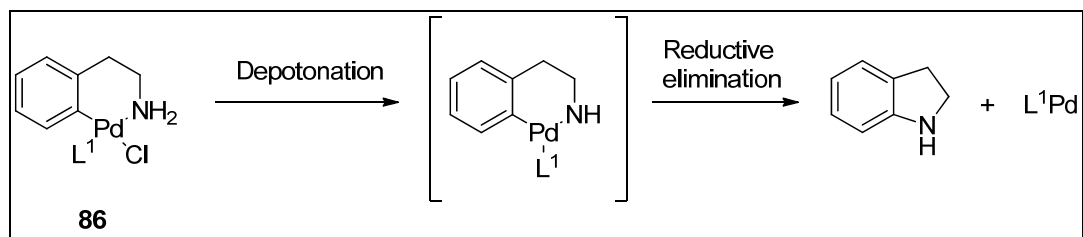


Figure 53. Readily activated precatalyst recommended by Buchwald and Surry¹³¹

The precatalyst **86** is deprotonated by a strong base and the Pd amido intermediate undergoes rapid reductive elimination to form the desired L¹Pd⁽⁰⁾ and indoline (Scheme 37). The active catalyst L¹Pd⁽⁰⁾ is generated at room temperature with a strong base, such as NaO^tBu or lithium bis(trimethylsilyl)amide (LHMDS), in less than three minutes.¹³¹



Scheme 37. Activation of the precatalyst **86**¹³¹

Following the recent reaction conditions recommended by Buchwald's research team for such a template,^{131,138} the amination transformation was performed with the precatalyst **86**, the ligand L^1 (also called BrettPhos)¹³⁹ and LHMDS in THF (entry 1, Table 15). After thermal heating at 80 °C for two hours, the reaction had reached completion by LCMS. Subsequent work-up and purification provided the desired intermediate **85** in an encouraging 55 % yield. The importance of the precatalyst **86** to the success of the reaction was illustrated when similar conditions were attempted with Pd(OAc)₂. Even with the more active BrettPhos ligand,¹³⁹ the conversion to the product **85** was only 12 % after 20 hours (entry 2-3, Table 15). This confirmed once again that the low conversion of the reaction, observed with Pd(OAc)₂, was due to the inefficient formation of the active catalyst. LHMDS was used in excess for the reaction, as the first equivalent was believed to deprotonate the NH proton of the substrate **72**. The use of excess LHMDS has been shown to allow the successful amination of aryl halides possessing labile NH groups.^{135,138,140}

In recent years, a similar approach of synthesising active precatalyst species, has been investigated using *N*-heterocyclic carbene (NHC) ligands.¹⁴¹ Complexes of the type of (NHC)Pd(R-allyl)Cl were first reported by Caddick and Cloke in 2001¹⁴² and have since been successfully used in amine arylation, Suzuki coupling and ketone arylation.¹⁴³⁻¹⁴⁶ It has been postulated that the Pd⁽⁰⁾ active species is formed from nucleophilic attack at the allyl moiety or through a chloride/alkoxide exchange, followed by reductive elimination (Figure 54).¹⁴⁷ Recently, Caddick's research group developed a novel and conveniently prepared (NHC)Pd(R-allyl)Cl catalyst allowing the use of mild Buchwald-Hartwig amination reaction conditions.¹⁴⁸ With suitable catalyst loading and heating (up to 70 °C), a wide range of aryl halides (including

aryl chlorides) were successfully coupled to primary and secondary amines. LHMDS was shown to be essential to the success of the reaction and the highest yields were obtained in THF. Overall, these reaction conditions were believed to be suitable for the desired amination transformation presented in Scheme 35. The precatalyst **87** was synthesised according to the conditions described by the Caddick's group (Scheme 38).¹⁴⁸ Deprotonation of 1,3-bis(2,6-diisopropylphenyl)-4,5-dihydro-1H-imidazol-3-ium chloride with KO^tBu at 80 °C formed the NHC, which was reacted *in situ* with palladium (methallyl)chloride dimer at room temperature for two hours. Aqueous work-up followed by silica chromatography yielded the desired precatalyst **87** in a good 71 % yield (literature¹⁴⁸ 72 %). The amination reaction was then carried out using 0.3 equivalents of precatalyst **87** and excess of LHMDS in THF (1 M, 3.6 eq) at 80 °C for one hour (entry 4, Table 15). LCMS indicated full conversion to the desired product **85**, with a clean profile. Further purifications provided the compound **85** with a satisfying 72 % yield. The reaction conditions were not optimised any further as the conversion to the desired product was achieved rapidly and in good yield. For any future scale-up work, reducing the loading of the precatalyst **87** should be investigated (*vide infra*).

Table 15. Investigation of the Buchwald-Hartwig amination coupling using preactivated catalyst

Entry	Amine eq	Pd (eq)	Ligand (eq)	Base (eq)	Solvent	T (°C) thermal	Heating time	% conversion (isolated yield)
1	1.5	86 (0.1)	L ¹ (0.1)	LHMDS (3)	THF	80	2 h	Full conversion (55 %)
2	1.5	Pd(OAc) ₂ (0.1)	L ¹ (0.2)	LHMDS (3)	THF	80	2 h	7 %
3	1.5	Pd(OAc) ₂ (0.1)	L ¹ (0.2)	LHMDS (3)	THF	100	20 h	12 %
4	1.5	87 (0.3)		LHMDS (3.6 eq)	THF	80	1 h	Full conversion (72 %)

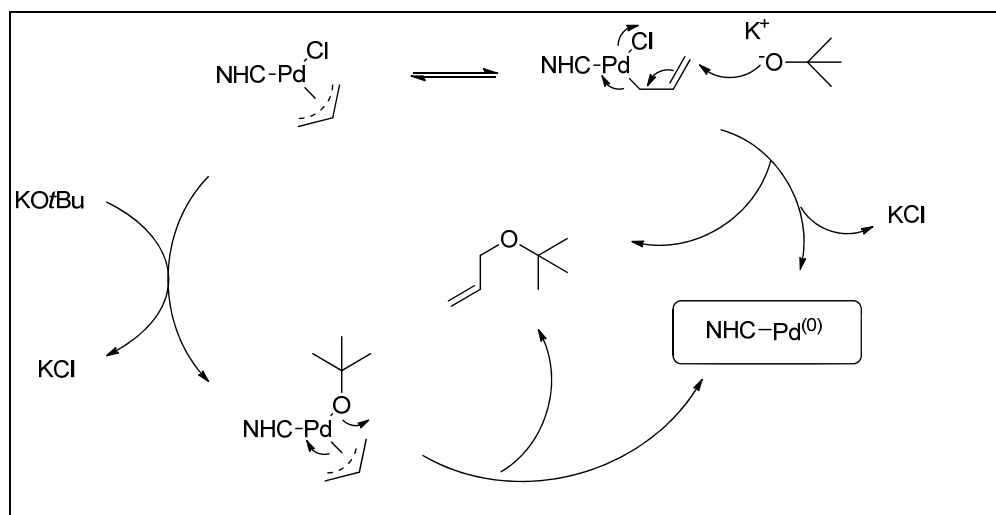
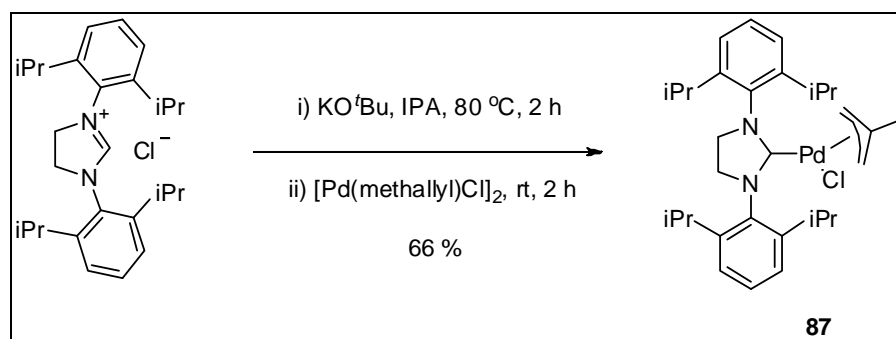


Figure 54. Postulated activation of $(\text{NHC})\text{Pd}(\text{R-allyl})\text{Cl}^{147}$

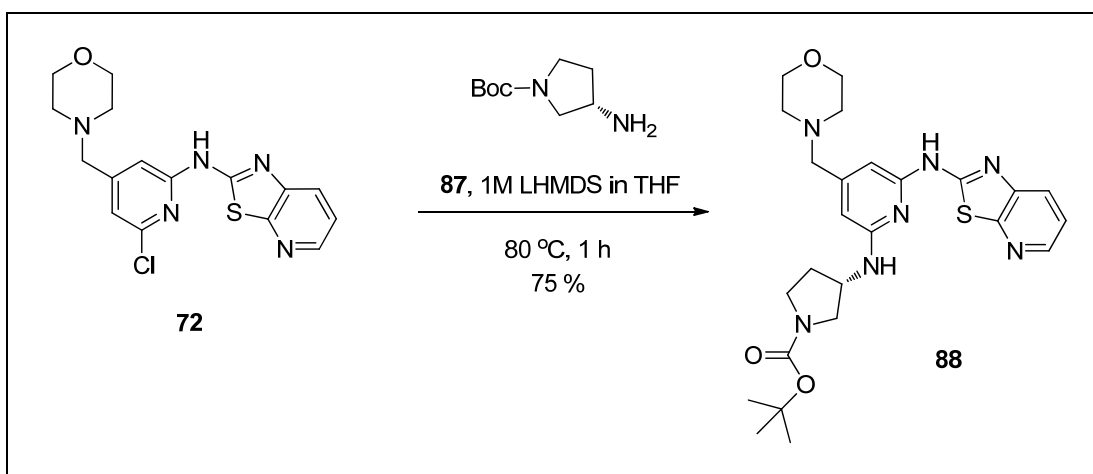


Scheme 38. Preparation of the precatalyst **87**

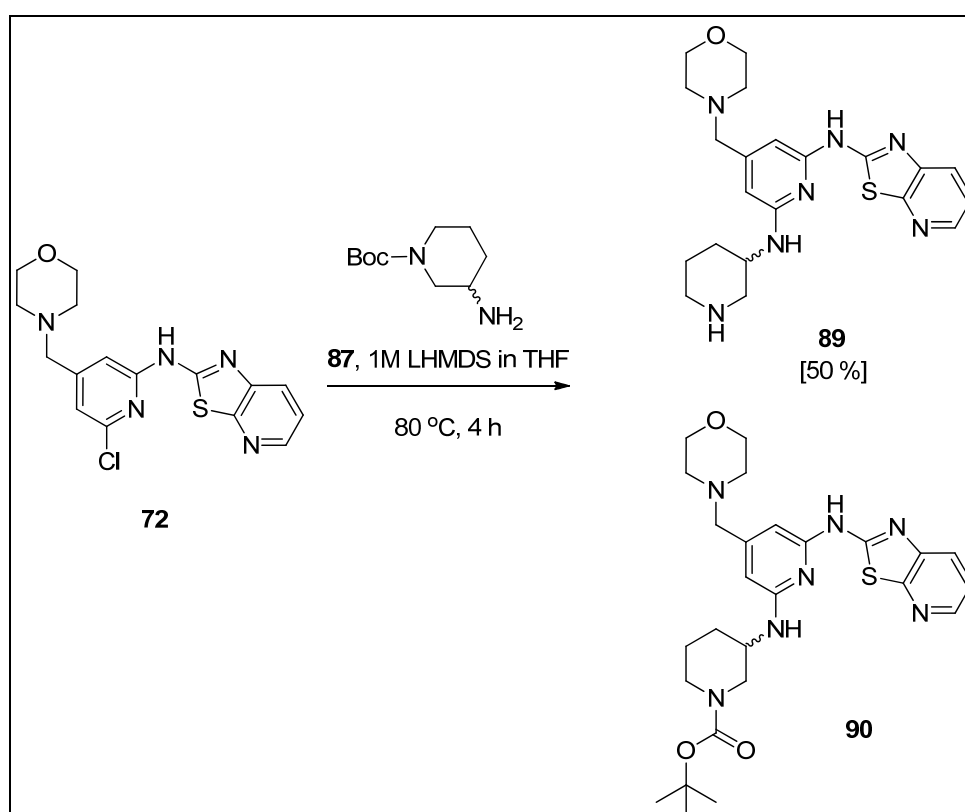
Both amination conditions using the precatalysts developed by the Buchwald and the Caddick research groups (respectively, entry 1 and entry 4 in Table 15) were considered suitable for the desired transformation as the lower yield obtained with the precatalyst **86** was obtained from unoptimized reaction conditions. However, the advantage of the precatalyst **87** relied on its relatively easy preparation from commercially available reagents. The good yield of the transformation allowed the synthesis of a large amount of precatalyst which could be used in many reactions. On the other hand, the precatalyst **86** could be either prepared in three steps,¹³¹ or purchased in small quantities from Strem chemicals[®] (100 mg bottles at the time of writing). The BrettPhos ligand was also sold by Strem chemicals[®] (1 g for \$264) but the relative limited availabilities of both latter reagents could restrict their use if the reaction needed to be performed on larger scale. Synthesising the precatalyst **86** and

the BrettPhos ligand would have required more synthetic effort than using the protocol involving the species **87**, without offering any clear advantages. Therefore, the reaction protocol developed with the precatalyst **87** was chosen to synthesise the required compounds in the pyridine series.

These reaction conditions were used with the (*S*)-*tert*-butyl 3-aminopyrrolidine-1-carboxylate substrate and the intermediate **88** was obtained with a 75 % yield (Scheme 39). However, when the same conditions were attempted with *tert*-butyl 3-aminopiperidine-1-carboxylate (Scheme 40), after 4 hours at 80 °C, the reaction had reached a 1:1 ratio of compound **89** and **90** with 13 % of intermediate **72** remaining by LCMS. The reasons for the longer reaction time and the deprotection of the Boc group for this substrate remain unexplained. The quality of the *tert*-butyl 3-aminopiperidine-1-carboxylate was confirmed by NMR and could not have been the cause of the results observed. Deprotection of the Boc group during the course of the reaction was also observed for the *tert*-butyl 4-aminopiperidine-1-carboxylate (entry 4, Table 15) but only traces of the amine product (< 5 %) were seen by LCMS. The effect of the temperature of the reaction on the rate of conversion to the desired product and the stability of the Boc protecting group is investigated later in this thesis. Nevertheless, the amino intermediate **89** was obtained in a moderate 50 % yield (from that originally observed by LCMS and additional deprotection of compound **90** during work-up and purification), whereas the intermediate **90** failed to be separated from the starting material **72** after silica chromatography. Compound **90** was found to be only 60 % pure by LCMS and NMR analyses. As sufficient quantities of compound **89** were obtained to synthesise the final product, the impure intermediate **90** was discarded.



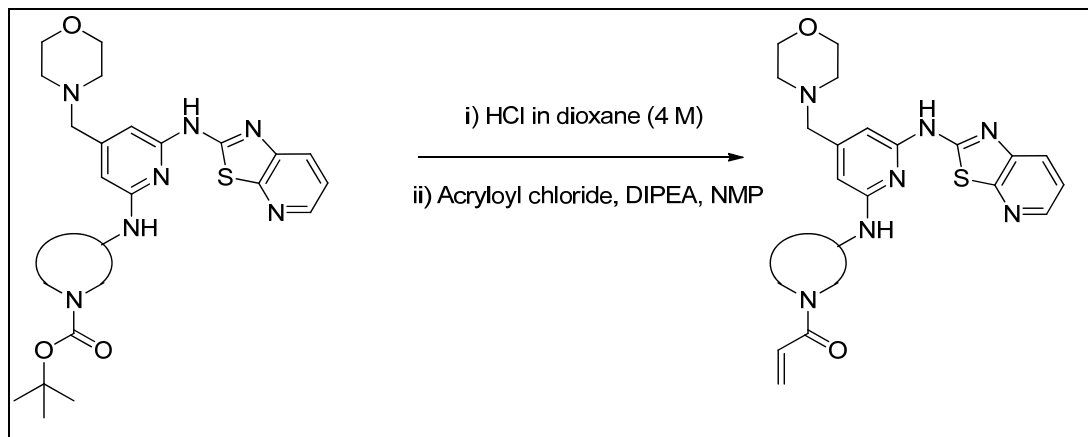
Scheme 39. Synthesis of compound 88



Scheme 40. Synthesis of compound 89

As described in previous sections, the Boc intermediates **85** and **88** were deprotected with HCl in dioxane and the crude amine residues were coupled with acryloyl chloride to synthesise the desired product **91** and **92** (Scheme 41 and Table 16). The Boc deprotected compound **89** was only reacted with acryloyl chloride to give the required product **93** (Table 16). The moderate yields obtained for these final steps

may well be due to the open access reverse phase mass directed autoprep purification. Compound **93** had to be purified twice by mass directed autoprep due to an undesirable small impurity seen in the NMR spectrum after the first column, hence the 29 % yield obtained.



Scheme 41. General scheme describing the synthesis of the final products in the pyridine series

Table 16. Summary of the final compounds obtained from the Buchwald-Hartwig coupling in the pyridine series

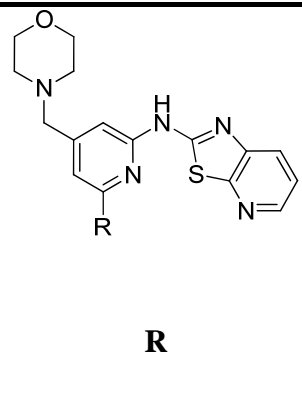
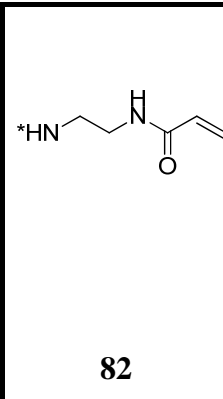
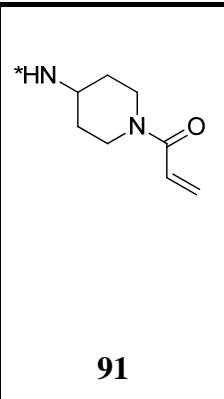
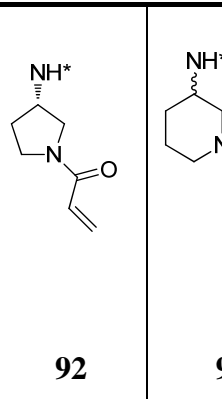
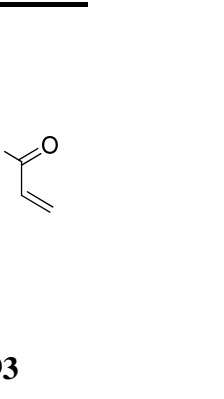
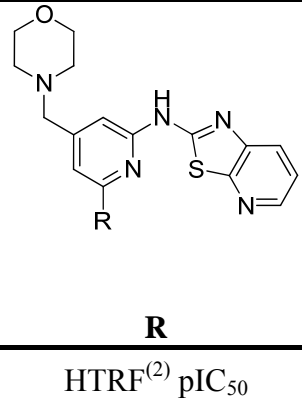
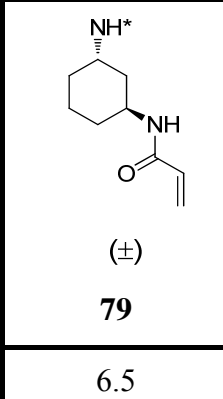
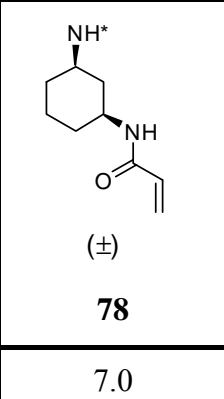
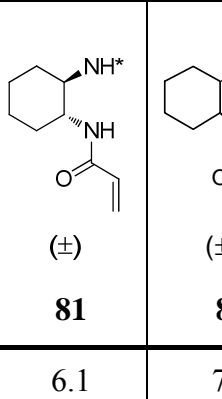
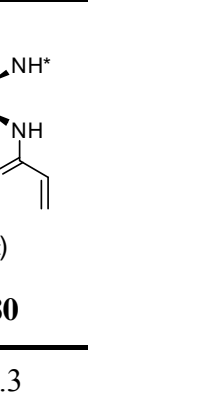
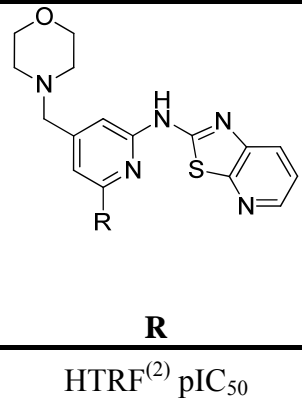
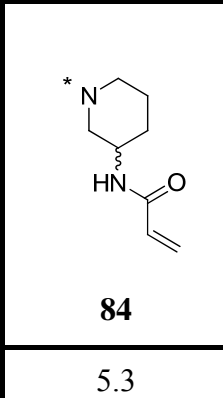
 R:	 91	 92	 93
Yield (deprotection and amide coupling)	51 %	57 %	29 % ^(a)

(a) yield from the amide coupling only

Enzyme and cellular primary data for the compounds from the pyridine series are summarised in Table 17. The HTRF⁽²⁾ assay clearly indicates improved binding affinities of these pyridine compounds compared to the pyrimidine analogues (Table 4). As previously discussed for the pyrimidine series, the cyclic amines **91**, **92** and **93** are more potent than the ethylene species **82**, while the *cis*-diaminocyclohexane

analogues are more active than the *trans*-compounds. The secondary amine compound **84** was found to be the least potent of the series, confirming once again, the importance of the NH functionality at the 2-position of the pyridine. The cellular data obtained for this series of compounds were in accordance with the results from the HTRF⁽²⁾, with the cyclic amines **91**, **92** and **93** displaying anti-inflammatory activities with $\text{pIC}_{50} \geq 8.2$. For the first time in this research programme, inhibitors such as compounds **92** and **93** were satisfying the potencies required for an ITK drug candidate (HTRF⁽²⁾ $\text{pIC}_{50} > 7.7$ and PBMC $\text{pIC}_{50} > 8.5$).

Table 17. SAR analysis of the pyridine series

 <p style="text-align: center;">R</p>	 <p style="text-align: center;">82</p>	 <p style="text-align: center;">91</p>	 <p style="text-align: center;">92</p>	 <p style="text-align: center;">93</p>
HTRF ⁽²⁾ pIC ₅₀	6.3	7.3	7.9 ¹⁴⁹	7.7
PBMC pIC ₅₀	7.8	8.2	8.7	8.6
 <p style="text-align: center;">R</p>	 <p style="text-align: center;">(±) 79</p>	 <p style="text-align: center;">(±) 78</p>	 <p style="text-align: center;">(±) 81</p>	 <p style="text-align: center;">(±) 80</p>
HTRF ⁽²⁾ pIC ₅₀	6.5	7.0	6.1	7.3
PBMC pIC ₅₀	7.7	7.9	7.4	8.3
 <p style="text-align: center;">R</p>	 <p style="text-align: center;">84</p>			
HTRF ⁽²⁾ pIC ₅₀	5.3			
PBMC pIC ₅₀	6.4			

The rationale behind the enhanced binding affinity of the pyridine series is not fully understood. The computational molecular modelling derived from the various ITK

analyses of the X-ray crystal structures obtained does not provide an explanation for the improved activity of the pyridine template. However, one can postulate that the difference in activity between the two aromatic central rings may be due to the unfavoured conformation the pyrimidine compound can adopt, when the morpholine is protonated (Figure 55). The conformation presenting the 5-membered ring, involving an H-bond interaction of the protonated morpholine with the pyrimidine nitrogen, would not favour the binding of the molecule in the ITK ATP pocket. Indeed, such a conformation would disturb the positioning of the amine group at the 2-position of the pyrimidine observed in the X-ray crystal structure of compound **42** (Figure 39). Such an arrangement cannot be formed in the pyridine series leading the morpholine group to be positioned in the sterically preferred desired conformation.

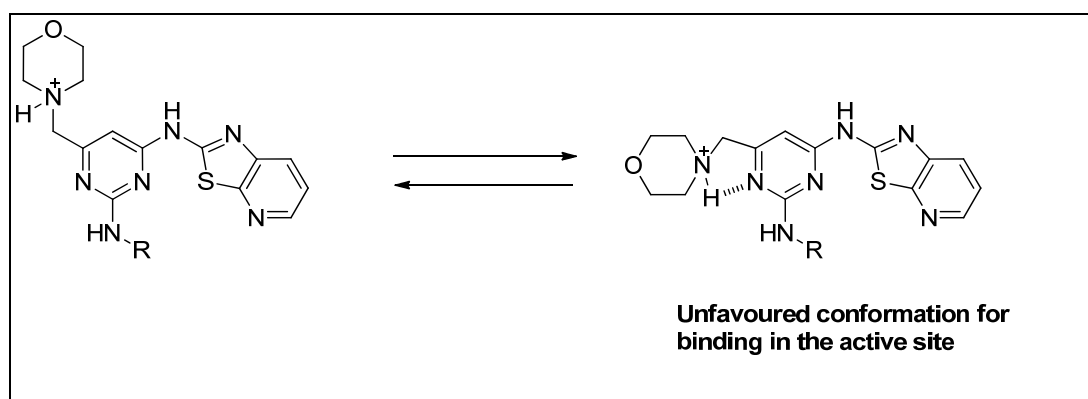
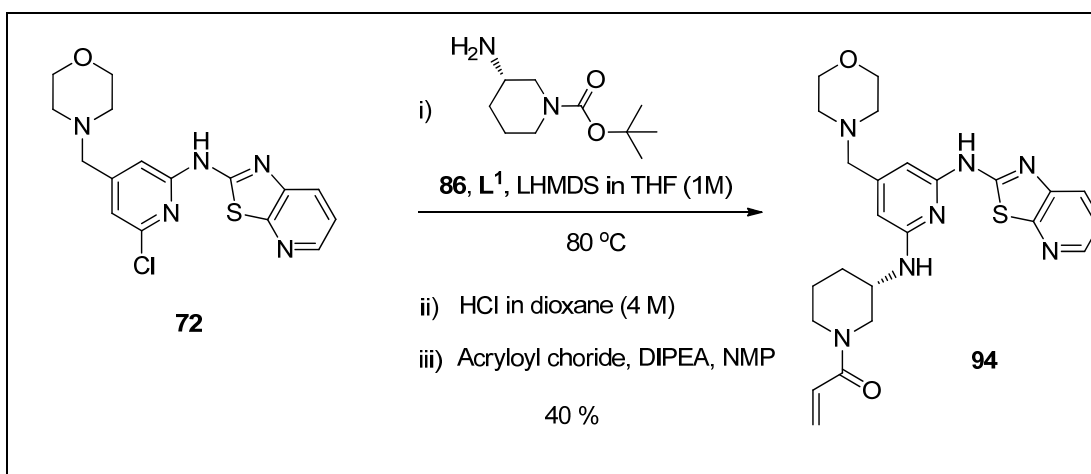


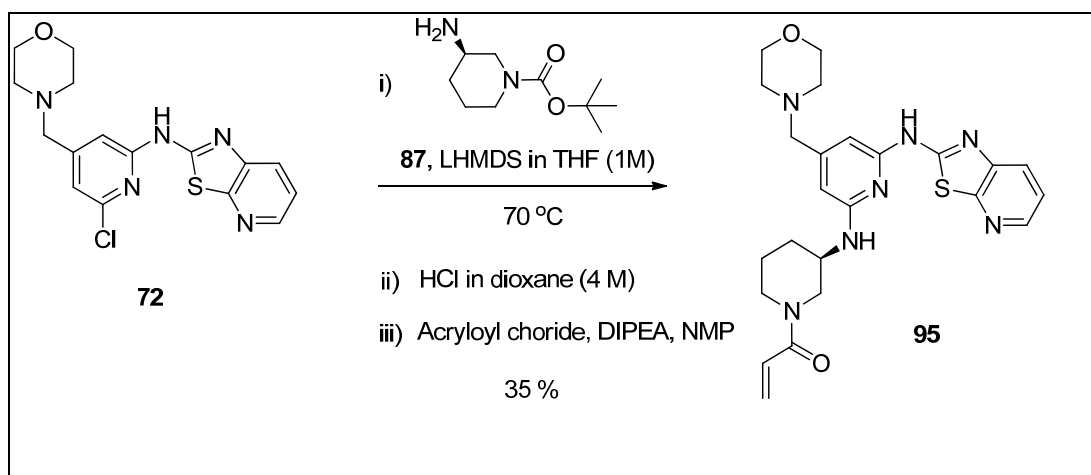
Figure 55. Potential unfavoured conformation adopted by the morpholine pyrimidine series

Compound **93** was initially synthesised as a racemic mixture of *R*- and *S*-enantiomers. Because of the encouraging activity profile of this racemic mixture, the two enantiomerically pure molecules were prepared. The *S*-enantiomer, compound **94**, was obtained by reacting compound **72** with the commercially available (*S*)-*tert*-butyl 3-aminopiperidine-1-carboxylate, in the presence of the precatalyst **86** and BrettPhos (Scheme 42).¹³⁸ Subsequent Boc deprotection under acidic conditions and amide coupling with acryloyl chloride provided the required product **94** with an overall 40 % yield.



Scheme 42. Synthesis of compound **94**

The *R*-enantiomer, compound **95**, was synthesised following a similar protocol (Scheme 43) but instead of the Buchwald catalyst **86** and ligand **L¹**, the conditions developed by the Caddick research group were employed.¹⁴⁸



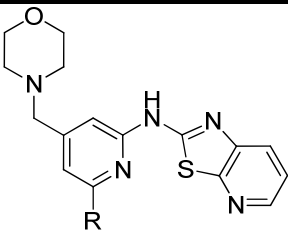
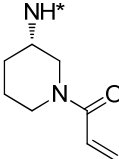
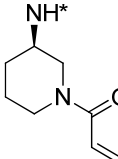
Scheme 43. Synthesis of compound **95**

The yields obtained for both syntheses supported the view that both cross-coupling reaction conditions were suitable for the amination transformation. However, during the course of both coupling reactions, significant amounts of deprotected piperidine intermediates (similar to compound **89**, Scheme 5) were observed by LCMS. The 3-amino-Boc-protected piperidine analogues were not believed to be stable under the reflux conditions in the presence of LHMDS. Nonetheless, the crude materials,

containing mixtures of protected and deprotected amine products, were used, without purification, in the hydrochloric acid Boc cleavage.

The data presented in Table 18 confirmed the SAR observed for the pyrrolidine motif (Table 4 and Table 17): as with the 3-aminopyrrolidine moiety, the *S*-enantiomer provides a better geometry to interact with ITK: a 1.5 log unit difference is observed in the HTRF⁽²⁾ assay between the two enantiomers and the inhibition superiority of compound **94** is verified in the cellular assay.

Table 18. Primary activity data for compound **94** and **95**

 <p>R</p>	 <p>94</p>	 <p>95</p>
HTRF ⁽²⁾ pIC ₅₀	7.8	6.3
PBMC ¹⁵⁰ pIC ₅₀	8.7	7.1

From the start of this research programme, regardless of the template, the three amine linkers present in compounds **91**, **92** and **93** have demonstrated similar levels of activities, both in the HTRF and the PBMC assays. Moreover, so far, the data from the kinetic assays had not been able to quantify any difference in irreversible inhibition for the three motifs. Such similar profiles are unsurprising for compounds **92** and **93**, as it is not difficult to envisage how both compounds could overlap and present the Michael acceptor in comparable positions to the cysteine residue. However, when comparing the 4-aminopiperidine and the (*S*)-3-aminopyrrolidine (or the (*S*)-3-aminopiperidine), the electrophilic moieties were believed to be delivered along slightly different vectors, resulting in the covalent reaction being more or less optimized. Close analysis of the kinetic assay protocol and the data obtained indicated that the reproducibility of the experiment, hence the precision of the data

produced, was not sufficient to assess which of the three groups were optimal for the covalent binding with Cys442.³⁶ Accordingly, the assay was optimised and the standard deviation reduced.¹⁰⁶ Using the newly developed experimental protocol, reproducible K_i and k_c values were obtained (Equation 1), allowing the more accurate assessment of both the non-covalent binding of the compounds to ITK and the rate of covalent binding. As described in the literature,¹⁰⁰ the best measure of inhibitory potency for an irreversible inhibitor is the second-order rate constant obtained from the ratio k_c/K_i : the greater this ratio, the better the profile of the inhibitor.

The kinetic data obtained for compound **91** and **92** are summarized in Table 19.

Table 19. Kinetic data for compound **91** and **92**¹⁰⁶

Compound	K_i (μM)	k_c (s^{-1})	k_c/K_i ($\text{s}^{-1}\cdot\mu\text{M}^{-1}$)
91	0.0168	0.0010	0.060
92	0.0129	0.0024	0.186

Although both molecules have similar non-covalent binding to ITK (K_i of 0.0129 μM and 0.0168 μM), the pyrrolidine analogue **92** covalently binds to the kinase 2.4 times faster than the piperidine compound **91** (respective k_c of 0.0024 s^{-1} and 0.0010 s^{-1}). This finding explains the data observed in the HTRF and PBMC assays (Table 17): the faster covalent binding of compound **92** to ITK confers slightly better inhibitory activities in both experiments. Therefore, all the data observed for these two compounds are in agreement with the ratios k_c/K_i described in Table 19: the (*S*)-3-aminopyrrolidine linker is a better motif for irreversible ITK inhibition than the 4-aminopiperidine unit. This difference in rate of kinase inactivation can also be visualised in the graph presented in Figure 56. At the same 0.019 μM concentration, the slope of the red curve (compound **92**) is greater than the slope of the blue curve (compound **91**): the rate of covalent binding for compound **92** is faster than for compound **91**. It is, however, important to note that while the kinetic data appear to support the hypothesis presented, errors cannot be estimated from the assay methods

used and it is possible that the relatively small variations in K_i and k_c may be fortuitous.

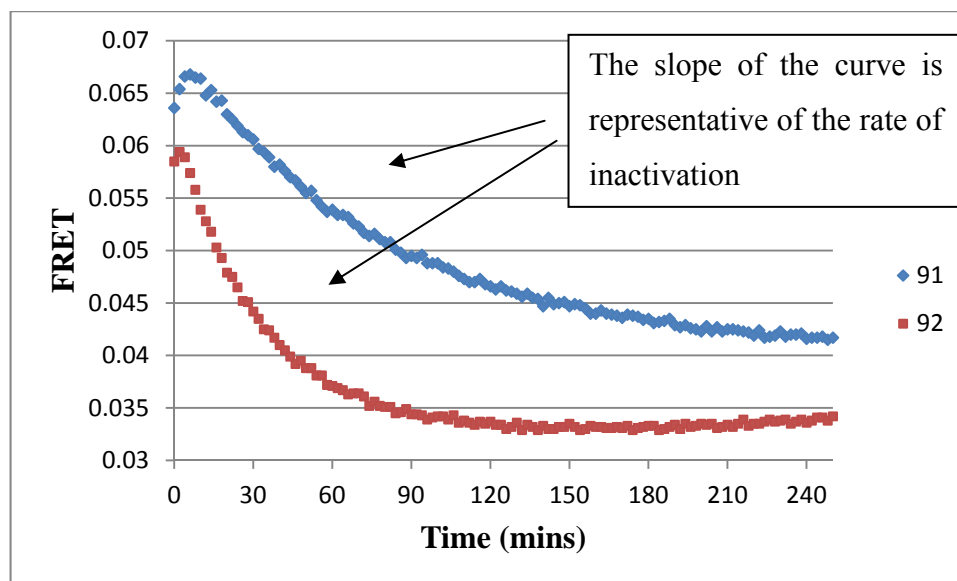


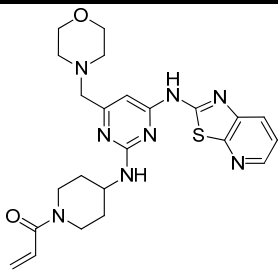
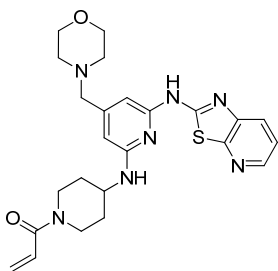
Figure 56. Kinetic data for compound **91** and **92** at the same $0.019 \mu\text{M}$ concentration

The (*S*)-3-aminopiperidine analogue **94** was not tested in the kinetic assay at this stage of the programme but due to its comparable geometrical arrangement to the (*S*)-3-aminopyrrolidine, the molecule was believed to have similar irreversible affinity towards ITK as that of compound **92**. This hypothesis will be confirmed in the next section (VII.6, Table 29).

At the start of this section VII.5, it was postulated that the improved non-covalent binding affinity conferred on the inhibitor by the pyridine unit might enhance the rate of the covalent reaction, as the inhibitor might stay longer in the active site (slower k_{off}). To assess the validity of this hypothesis, the optimized kinetic assay was used to determine the K_i and k_c of the pyrimidine **34** (Table 4) and compare them to the values already reported for the structurally related pyridine **91** (Table 19). The results are presented in Table 20: although the non-covalent affinity of the pyridine analogue is more than double that of the pyrimidine inhibitor (K_i of $0.0168 \mu\text{M}$ and $0.0410 \mu\text{M}$, respectively), the rate of covalent reaction remains the same for both compounds (k_c of 0.0010 s^{-1}). Therefore, the improved activity profile observed in

both the HTRF and PBMC assays for the pyridine series (Table 17) is the result of an increased non-covalent binding to ITK and not a faster covalent reaction rate (note that while the kinetic data appear to support the hypothesis presented, errors cannot be estimated from the assay methods used and it is possible that the relatively small variations in K_i and k_c may be fortuitous).

Table 20. Comparison of the kinetic data for compound **34** and **91**¹⁰⁶

Compound	K_i (μM)	k_c (s^{-1})	k_c/K_i ($\text{s}^{-1}\cdot\mu\text{M}^{-1}$)
 <p style="text-align: right;">34</p>	0.0410	0.0010	0.024
 <p style="text-align: right;">91</p>	0.0168	0.0010	0.060

The data generated so far for compound **92** suggested that, for the first time in this programme, the overall profile obtained was close to the desired candidate profile required. However, evidence of the longer duration of action of this compound in a cellular assay was required for progression of the molecule. After a few months of optimisation,¹⁰⁸ the PBMC wash-out assay was available to assess the benefits of these irreversible ITK inhibitors in physiological systems. As already described in section VI, compounds were incubated in PBMC for one hour before the cells were washed with aqueous media. Activation of the inflammatory response was performed after two hours and release of IL-2 cytokines was measured. Representative PBMC wash-out results for compound **92** are presented in Figure 57. The black curve represents the dose-response inhibition of the compound without the washing of the

cells. This is the reference inhibition curve and for compound **92**, the pIC_{50} without washing of the cells was measured at 8.4. The red plot represents the dose-response inhibition of compound **92** after wash-out of the cells. The pIC_{50} is slightly lower than the reference curve ($pIC_{50} = 8.0$) but most of the inhibition was still present which confirmed the benefits of this irreversible ITK inhibitor.

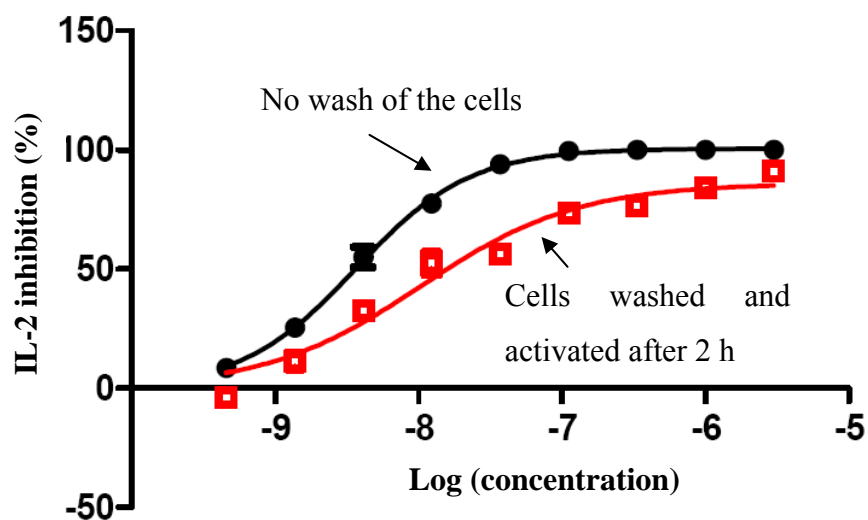


Figure 57. Representative wash-out data for compound **92**¹⁰⁸

To demonstrate the validity of this assay, an ITK reversible compound had to be tested. The ITK inhibitor **36** described in section VII.2 was selected. Indeed, previous data for this molecule indicated that the compound was inhibiting ITK with a moderate level of potency (Table 4, HTRF⁽²⁾ $pIC_{50} = 5.7$, PBMC $pIC_{50} = 7.1$) but it was believed that the Michael acceptor was unfavourably positioned to interact with Cys442 (Figure 35). The kinetic data (Figure 36) highlighted this compound as a reversible ITK inhibitor. The wash-out experiment for compound **36** (Figure 58) supported the data from the kinetic assay. All the IL-2 inhibition (pIC_{50} without wash = 6.2 - black curve) was lost after the cell wash with aqueous media (red curve - no inhibition response): the reversible inhibitor was removed from the PBMC during the wash of the cells with aqueous media.

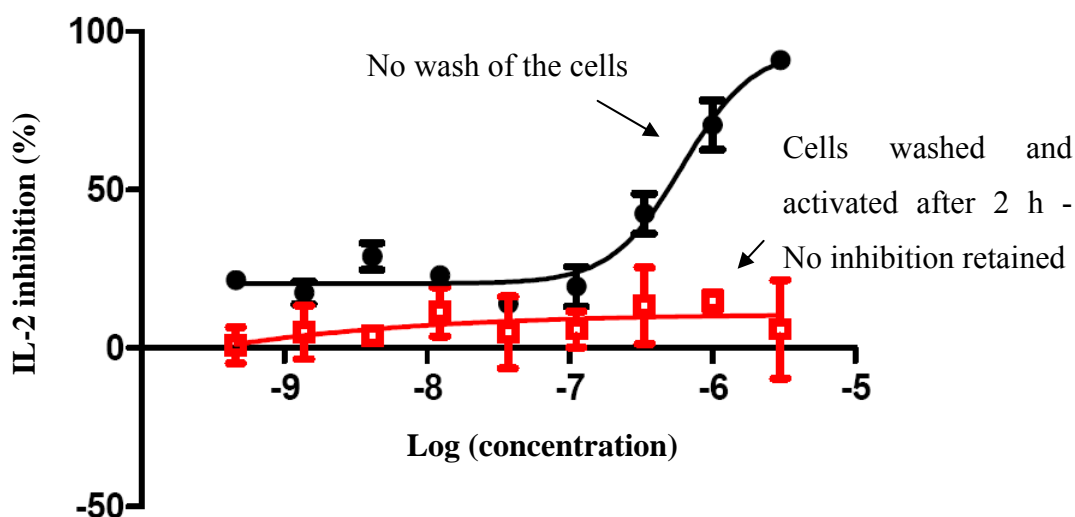


Figure 58. Representative wash-out data for compound **36**¹⁰⁸

Finally, compound **91** was evaluated in this experiment. Although this molecule was predicted to irreversibly inhibit the release of IL-2 cytokines, the pIC₅₀ drop-off between the reference (no wash) and the wash-out experiments was forecast to be higher than for compound **92**. Indeed, as this compound was covalently binding more slowly to ITK (Table 19), after the one hour incubation time, a lower proportion of compound would be irreversibly bound to Cys442, resulting in a larger inhibition difference with the reference potency (no wash). The PBMC wash-out data for compound **91** are presented in Figure 59 and are supportive of the expectations. The pIC₅₀ before wash was measured at 8.0 whereas the pIC₅₀ after washing of the cells was measured at 7.1. The compound was confirmed as an irreversible ITK inhibitor but was not as effective as the pyrrolidine analogue **92**.

The slight variation in the positioning of the Michael acceptor to Cys442, once the compounds are in the ATP active site, leads to significant differences in terms of potency and rate of inactivation. It is also important to note that a good correlation between the data from this cellular experiment and the original PBMC assay (measuring IFN- γ inhibition and not IL-2) was observed: in both assays, the (*S*)-3-aminopyrrolidine **92** was slightly more active than the 4-aminopiperidine compound **91**. This finding provided even greater confidence for the results obtained from these wash-out experiments and the benefits provided by irreversible ITK inhibitors.

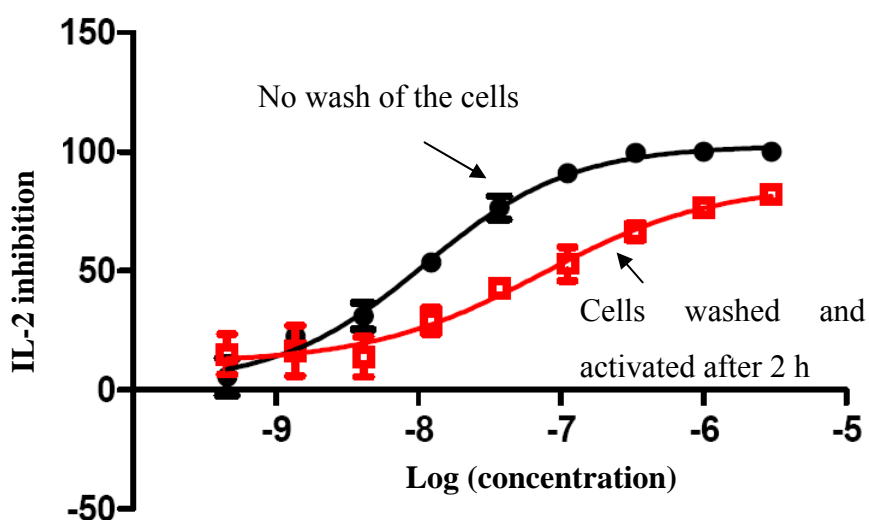


Figure 59. Representative wash-out data for compound **91**¹⁰⁸

Although the ITK irreversible inhibition profile presented by compound **92** was satisfactory for a drug candidate for the programme, the molecule had to be tested in other experiments (*e.g.* selectivity, solubility, permeability, DMPK, toxicology) to ensure that it could be developed further as an inhaled drug.

In reversible kinase programmes, compounds are tested for inhibition activities against various kinases. An acceptable selectivity window for a compound is typically 100 fold for the target of interest. For irreversible inhibitors, 100 fold selectivity is desirable against all kinases but the main off-target activity issues will be found for kinases to which the compound can bind irreversibly. In the case of this ITK programme, the selectivity against the other ten kinases possessing a Cys residue in the same area of the active site (Table 1) is important. Assessing the selectivity of covalent inhibitors should be performed using kinetic assays (such as the experiment used in this research programme for ITK) with the various kinases to which the compound can irreversibly bind to.⁴⁸ Such assays would inform on the non-covalent affinity (K_i) to the various kinases and the rate of covalent reaction (k_c). The different K_i and k_c would give clear indications of the selectivity of the inhibitor for the target of interest. These kinetic assays were not available in our laboratories and were thought to be challenging to set-up in the timecourse of this research programme. Instead, the enzyme binding assay for EGFR and BTK, which were available within our laboratories,¹⁵¹ were selected to qualitatively assess the

selectivity against kinases possessing similarly positioned cysteine residue in the ATP pocket. As described previously, the selectivity against these kinases was believed to be achievable from the non-covalent affinity of the compound to the various kinase. Although our compounds had the potential to covalently bind to these two kinases, a poor non-covalent affinity (high K_i) should prevent them from significantly covalently reacting with the cysteine residue and driving the inhibition of the kinase.

Assessing kinase selectivity data for a non-covalent inhibitor by just comparing pIC_{50} values can be misleading as the measured activities depend on the ATP concentrations used in the experiments. For example, the difference in ATP concentrations in the two ITK HTRF assays reduced the activity of the non-covalent inhibitor **6** from a pIC_{50} of 7.8 (HTRF⁽¹⁾, Table 2) to a pIC_{50} of 6.2 (HTRF⁽²⁾, Figure 32). A similar 1.6 log unit difference between the two assays was observed for compound **77** (Table 11). To standardise the reporting of data, the binding constants (K_i s) are often calculated using the Cheng-Prusoff equation (Equation 2). Comparing the K_i s of a non-covalent inhibitor towards different kinases allows its kinase selectivity to be established independently of the conditions (*i.e.* ATP concentrations) employed in the various assays. However, this equation does not technically apply to irreversible inhibitors and the binding constants K_i s can only be determined from kinetic binding studies.⁴⁸ In addition, for covalent inhibitors, the preincubation/reaction times before measuring the kinase inhibition are critical as the activities are time dependent. To obtain a more representative view of the selectivity of inhibitors which have the potential to covalently bind to kinases, the protocols (preincubation/incubation times and ATP concentrations) have to be identical.

Close analysis of the protocols for each binding assays revealed that the ATP concentrations in the assays and the preincubation/incubation times before measuring the kinase inhibition were different for the three kinases (Table 21).

Table 21. Enzyme assay protocols

Kinase	ITK		EGFR		BTK	
ATP assay concentration	1 mM		10 μ M		150 μ M	
Enzyme assay protocol	PI*	R*	PI*	R*	PI*	R*
	0 mins	25 mins	30 mins	40 mins	0 mins	90 mins

*: PI - Preincubation time. R - Incubation time.

The enzyme selectivity data of compound **92** against EGFR and BTK (Table 22) was initially assessed using these standard protocols developed in our laboratories. The activity towards EGFR was more than 10 times lower than the activity against ITK. However, the selectivity versus BTK appeared relatively poor, with only a 0.4 log unit difference in activity between the two kinases.

Table 22. Selectivity data of compound **92** versus EGFR and BTK¹⁵¹

Kinase	ITK	EGFR	BTK
pIC ₅₀	7.9	6.7	7.5

From the various assay protocols described in Table 21, the concentration of ATP in the ITK experiment (1 mM) is significantly higher than the concentrations used in the other tests (note that if the assay was run at lower concentration of ATP (*i.e.* 20 μ M - HTRF⁽¹⁾ assay), the inhibitor **92** would reach the tight binding limit of the experiment). Therefore, the activity of compound **92** in the EGFR and BTK assays would be reduced compared to the values reported in Table 22 if the selectivity experiments were run at 1 mM ATP concentrations. Unfortunately, changing the ATP concentrations in these assays, which had been optimised for assessing the activities of reversible compounds within our laboratories, was not straightforward and could not be delivered as part of this research programme. Instead, it was qualitatively assumed, from the data obtained between the ITK HTRF⁽¹⁾ and HTRF⁽²⁾

assays, that the values reported from the selectivity for EGFR (10 μ M ATP concentration) should be reduced by around 1.5 log unit to be compared to the ITK values from the 1 mM ATP enzyme test. For BTK (ATP concentration in the assay at 150 μ M), the value should be qualitatively reduced by at least 0.5 log unit to be compared for selectivity to the ITK assay. Therefore, the EGFR selectivity was qualitatively assessed to be more than 100 fold compared to ITK, whereas the BTK selectivity was believed to be around 10 fold.

To confirm that the preincubation/incubation times before measuring the kinase inhibition were also extremely important factors in these assays, the BTK protocol was changed to a 25 minute incubation time, matching the ITK experiment set-up.¹⁵¹ The selectivity data using the new BTK assay is presented in Table 23: the measured pIC₅₀ decreased to 7.1, confirming that the inhibition is time dependent. Taking into account the ATP concentration and the incubation time considerations, the BTK selectivity was qualitatively assessed to be around 1.3 log unit, which, although not ideal, was still worthy of progressing compound **92** to further investigation (Note that in the later section VII.6, the lead compound from this research programme **107** was tested in a BTK cellular assay to confirm the ITK/BTK selectivity in a more physiological environment).

Table 23. Selectivity data for compound **92** using similar reaction times for BTK and ITK assays¹⁵¹

Kinase	ITK	BTK
pIC ₅₀	7.9	7.1

The permeability of compound **92** was assessed via efflux through Mardin-Darby canine kidney (MDCK) cells. In this experiment, the permeability of the inhibitor **92** was measured at 141 nm/s,³⁷ which is classified as high and is fully acceptable for cellular penetration. The *in vitro* clearance of this compound suggested an *in vivo* clearance in human in the region of 50 % of the liver blood flow,³⁷ which once again is perfectly satisfactory for an inhaled drug. All of the data gathered so far for compound **92** were indicating that the molecule was suitable as an irreversible ITK

inhibitor for inhaled administration. Unfortunately, the simulated lung fluid (SLF) solubility of the compound was measured at 81 $\mu\text{g/mL}$ (30 minute time point),¹⁵² which was classified as low to moderate. This solubility was a concern for the progression of compound **92**, as the GSK inhaled science group had demonstrated a correlation between low solubility and lung macrophage activation for inhaled molecules. Macrophages are a normal feature of lungs and play a central role in host defence, immunity, inflammation and repair. The study revealed that molecules with SLF solubility less than 250 $\mu\text{g/mL}$ had a higher probability to induce macrophage activation in the lungs. This activation can result in the macrophages taking a vacuolated appearance (called foamy macrophages), often related to toxicity.¹⁵³ As a consequence, this presented the challenge of improving the solubility of the lead compound **92** to reduce any early risks of toxicity due to deposition of solid compound in the lungs.

Salt formation has become the most commonly applied technique of increasing solubility and dissolution rate in drug product development.¹⁵⁴ Therefore, this was the technique first attempted to improve the solubility of compound **92**. As a result of the measured basic pK_a of the morpholine motif ($\text{pK}_a = 6.0$),¹⁵⁵ salts can be formed with acidic counterparts. However, because no structure-solubility relationships for pharmaceutical salts have yet been established,¹⁵⁶ a salt screening had to be performed in order to assess which salt versions of compound **92** could potentially improve the SLF solubility.

Analysing the recent salt screenings performed within the GSK Particle Science Department for inhaled medicines,¹⁵⁷ six acids were initially selected to form salts with compound **92** in attempts to increase the aqueous solubility of the molecule (Table 24). The experiment performed to assess the solubilising benefits of the salts in water was straightforward: 1 mg of compound **92** was suspended in 1 mL of water; 25 μL of each acid solution (0.1 M in water) was added and the suspension was shaken gently at room temperature. The improvement in solubility of the suspension was monitored visually over time. The results are described in Table 24.

Table 24. Salt screening to increase the solubility of compound **92**

Salts	HCl	Citric acid	Maleic acid	Fumaric acid	Mandelic acid	Acetic acid
Solubility results	Suspension after 16 h	Clear solution after 15 min	Clear solution after 30 min	Mainly in solution after 3 h	Mainly in solution after 3 h	Suspension after 16 h

The citric and maleic acid salts clearly gave the best solubility results with the compound fully solubilising in less than 30 minutes. These salt versions of compound **92** were selected to be synthesised and assessed in the SLF solubility assay. It is worth noting at this stage that the pH of the solution was not controlled during the experiment. The pH of the aqueous solution was likely to become acidic after the addition of the acid, influencing the solubility of compound **92**.¹⁵⁴

Compound **92a** and **92b** (Figure 60) were obtained by simply dissolving compound **92** in a mixture of acetonitrile and water and reacting with one equivalent of the acid for 16 hours. The formation of the salts was confirmed by NMR analysis.

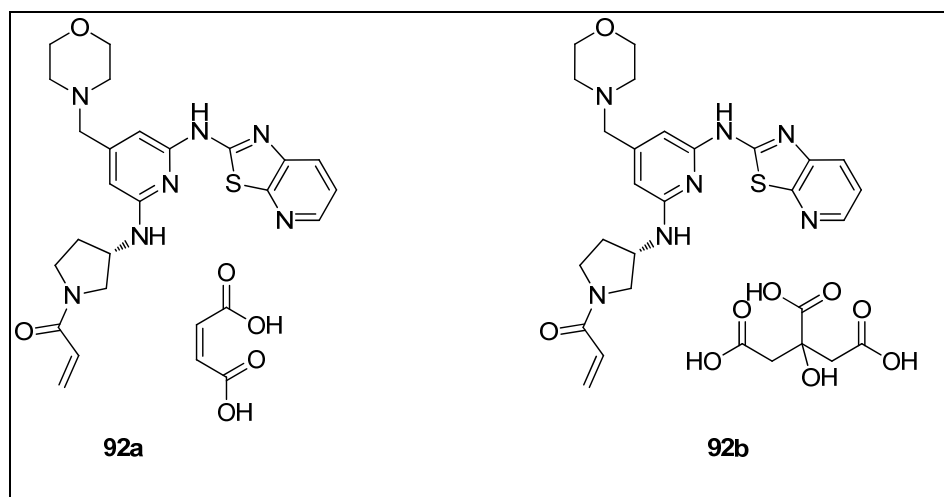


Figure 60. Salt versions of compound **92** synthesised to improve SLF solubility

The salts **92a** and **92b** were measured for SLF solubility¹⁵² over a 24 hour period and compared to the free base **92**. The data are summarized in Table 25.

Table 25. SLF solubility data for compound **92** and its salts forms¹⁵²

Time (hours)	Solubility (µg/mL)		
	92	92a	92b
0.5	81	99	109
4	84	71	71
24	62	60	62

The SLF solubility was marginally better for both salts when measured at 30 minutes, the citrate salt **92b** presenting the greatest value. However, the solubility of both analogues **92a** and **92b** was found to be well below the targeted 250 µg/mL SLF solubility desired for inhaled drugs. The main explanation for the disappointing SLF solubility data of both compounds is believed to be the relatively quick disproportion of both salts in the 6.9 pH buffer of the assay. Indeed, to mimic the pH of the lungs which is believed to be around 6.9,¹⁵⁸ the solubility in the SLF assay is measured in a buffer solution. Therefore, at pH 6.9, the salts disproportionate rapidly to produce the free base of compound **92**, which has a low solubility in that assay. The disproportion effect was confirmed by the SLF solubility data obtained after 4 and 24 hours. The solubility measured for **92a** and **92b** decreased over time to reach similar values to the free base compound **92** of around 60 µg/mL.

To confirm the disproportion hypothesis and conclude that the salt approach was not suitable to improve the solubility of our lead compound, the solubility of compound **92a** was measured in water¹⁵² without the pH 6.9 buffer. The data presented in Table 26 supported the high aqueous solubility of the compound observed during the salt screening. However, it also demonstrated that the high solubility of both salts was related to the decrease in pH of the aqueous solution induced by the maleic and citric acid. This finding ended the endeavours to increase the SLF solubility of compound **92** by forming a salt with the morpholine unit.

Table 26. SLF solubility data for compound **92a** with and without pH buffer¹⁵²

Time (hours)	Solubility ($\mu\text{g/mL}$)	
	SLF pH 6.9	water (no buffer)
0.5	99	> 700
4	71	> 700
24	60	> 700

Although the activity/selectivity profile of compound **92** was acceptable, the solubility criteria required for an irreversible ITK inhibitor was not believed to be sufficient to develop this species as an inhaled drug. The attempt to improve the solubility by forming salts did not prove to be successful. As a consequence, a different approach was envisaged: replacing the morpholine unit with motifs possessing slightly higher pK_a was anticipated to improve the SLF solubility measured at pH 6.9.

6. Replacement of the morpholine motif to improve solubility and activity

As already described in section VII.2, the morpholine unit provides a useful handle to increase the solubility of our ITK template. The motif also led to slightly increased non-covalent ITK binding of the molecules compared to the initial methoxymethyl group. The beneficial effects on potency of the morpholine group cannot be rationalised using the existing ITK crystal structures, as this part of the structure has always been less resolved and difficult to analyse. However, early SAR performed during the optimisation of reversible compounds^{30,31} suggested that changes to the morpholine group were tolerated for ITK activity. Various other research groups investigating ITK reversible inhibitors have also demonstrated that this area of the ITK active site could accommodate a wide range of functional groups, including basic amines.^{12,14,15,20-23,27} Crystal structures of some ITK inhibitors from Bristol-Myers Squibb and Boehringer Ingelheim (Figure 61) have been published in the literature^{23,159} and the overlay of these structures with compound **42**, in the ITK active site, indicates that the 3,3-dimethylbutan-2-amine, the cyclohexane and the morpholine motifs are positioned in the same area of the ATP pocket (Figure 62).

Therefore, replacing the morpholine motif with more basic functionalities has the potential to produce more soluble compounds while retaining the overall irreversible ITK inhibitor profile observed for compound **92**.

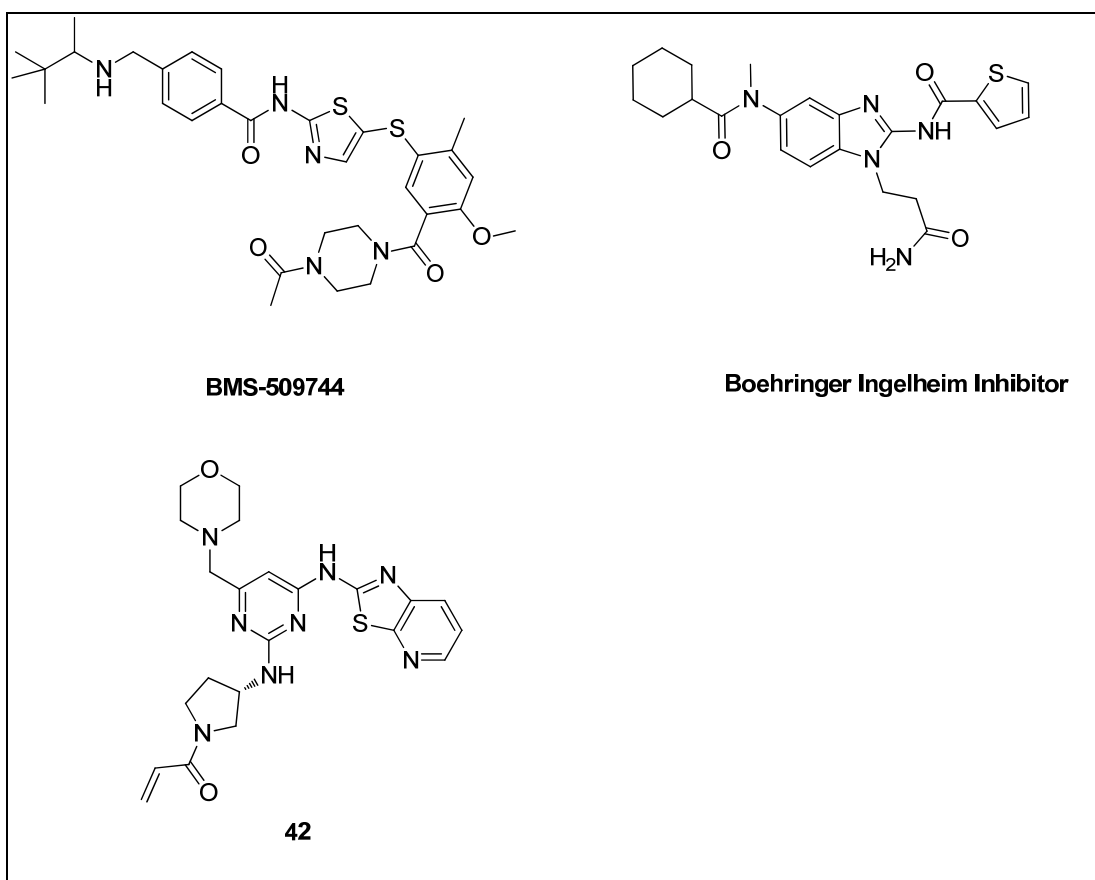


Figure 61. ITK inhibitors from Bristol-Myers Squibb and Boehringer Ingelheim compared to compound **42**

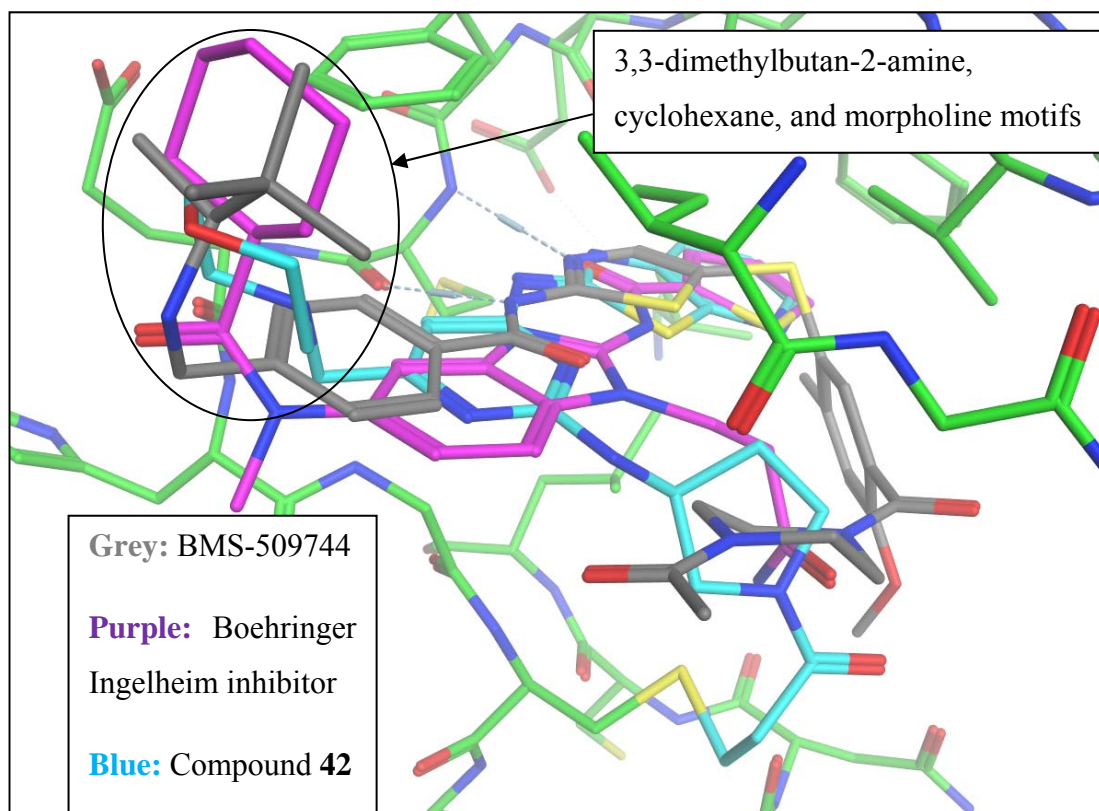


Figure 62. *Overlay of inhibitors from Bristol-Myers Squibb and Boehringer Ingelheim with compound 42*

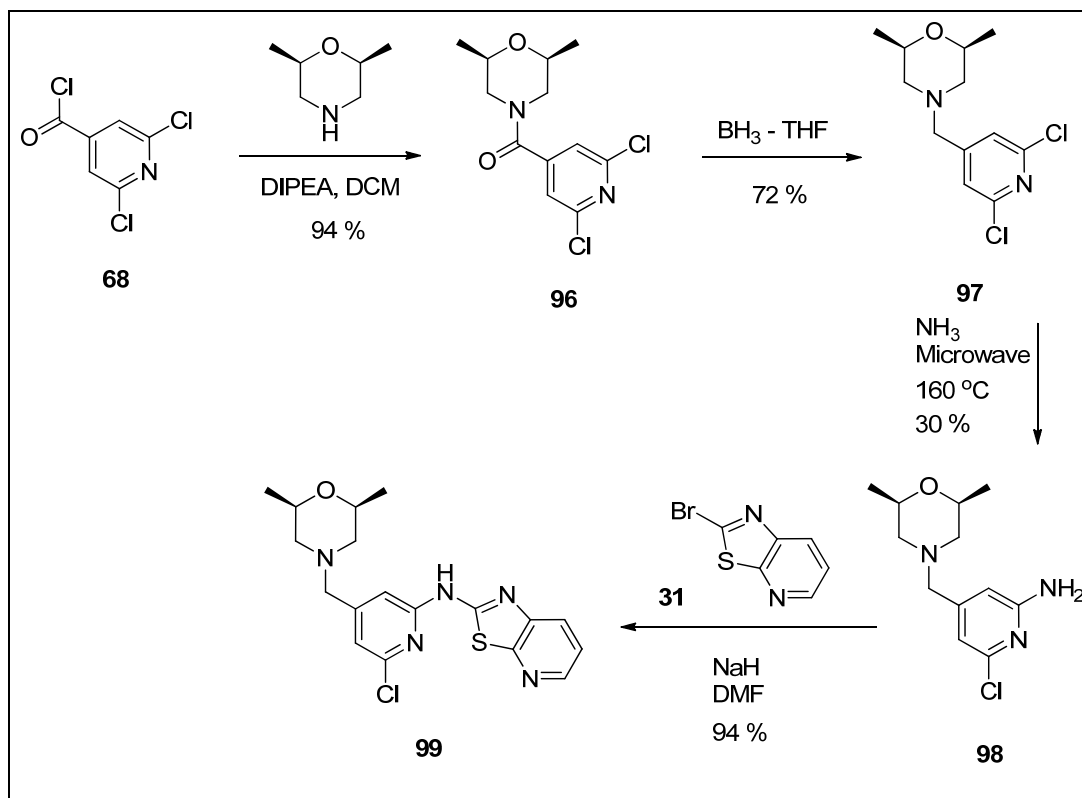
Although this approach holds some promise in relation to improving the SLF solubility to the required 250 $\mu\text{g/mL}$ guideline, increasing the basicity of lipophilic molecules could also be detrimental for the safety profile of the potential ITK drug candidate. The impact of lipophilicity and basicity on the human ether-a-go-go related gene (hERG) ion channel activity has indeed been demonstrated in the recent literature¹⁶⁰⁻¹⁶³ and the inhibition of this hERG encoded cardiac potassium channel represents a significant safety concern,^{164,165} which could halt the development of a drug candidate. Lipophilic and basic small molecules have also been shown to induce excess accumulation of phospholipids in tissues, called phospholipidosis.¹⁶⁶⁻¹⁶⁸ Therefore, the right balance between improving the solubility of the irreversible ITK inhibitors, by incorporating more basic amines into the template, and inducing hERG and phospholipidosis liabilities had to be found.

The initial strategy centred on replacement of the morpholine unit with a *cis*-2,6-dimethylmorpholine motif (Scheme 44). This functionality was chosen for two reasons: firstly, the pK_a of our final irreversible ITK inhibitors was calculated at 5.78 with such a group,¹¹⁹ a value just higher than with the morpholine (calculated pK_a = 5.38;¹¹⁹ note that the measured pK_a of the morpholine motif was found to be slightly higher at 6.0).¹⁵⁵ By slightly increasing the pK_a of the compounds, it was assumed that the salt disproportion would occur more slowly, leading to the compounds being more soluble in the pH 6.9 buffer solution. Moreover, such a small change in pK_a was not predicted to trigger hERG or phospholipidosis issues. Secondly, the two methyl groups were designed to add lipophilicity in the area where the hydrophobic (*S*)-3,3-dimethylbutan-2-amine and cyclohexane groups from the competitor compounds are found (Figure 62). The enhanced hydrophobic interaction was anticipated to be associated with the release of water molecules from the kinase active site on association with the compound, which should improve the non-covalent affinity of the molecules to ITK.⁴¹

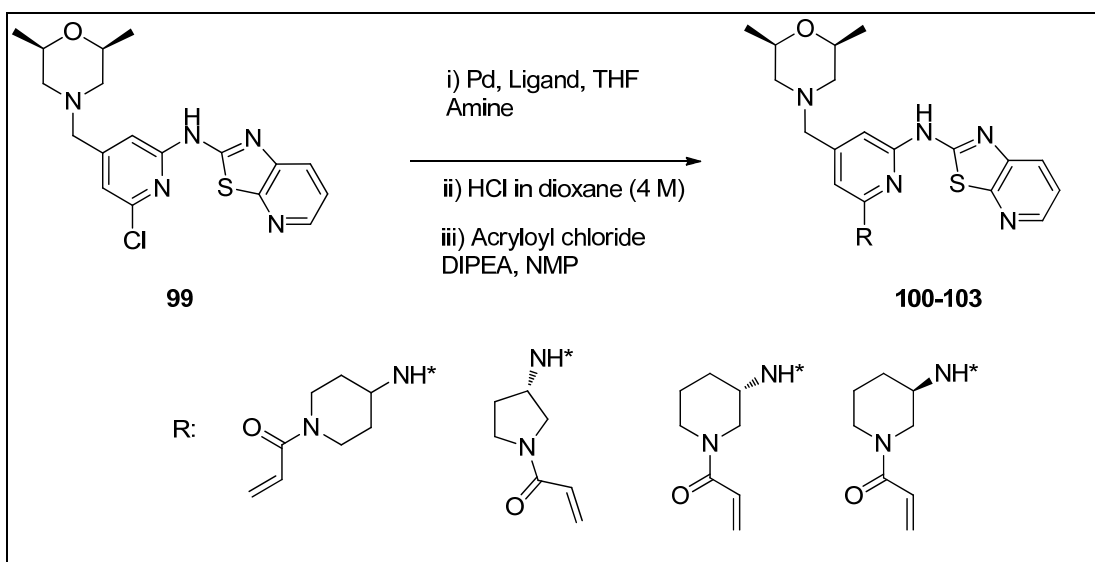
The *cis*-2,6-dimethylmorpholine motif was introduced in our ITK template following the preparative pathway which proved to be successful for the morpholine (Scheme 44). *Cis*-2,6-dimethylmorpholine was first reacted with the acid chloride **68** to yield the amide **96**. Reduction of the carbonyl group and displacement of one of the chloride groups with concentrated ammonia led to intermediate **98**, in a modest 30 % yield, which was attributed to the reaction not reaching completion even after 30 hours heating at 160 °C (18 bar pressure build up) in the microwave system. Aromatic nucleophilic substitution with the 2-bromothiazolo[5,4-*b*]pyridine **31** yielded the chloro analogue **99**.

To confirm the SAR observed in the pyridine series and to ensure that small changes into the non-covalent binding of the template to ITK were not affecting the irreversible interaction between the Michael acceptor and Cys442, the three amine linkers (4-aminopiperidine, (*S*)-3-aminopyrrolidine and (*S*)- and (*R*)-3-aminopiperidine) were synthesised in this template (Scheme 45). Three compounds (**100**, **101**, and **103**) were prepared using the conditions related to those developed by the Caddick research group,¹⁴⁸ whereas the analogue **102** was obtained from the

amination reaction employing the Buchwald catalyst **86** and ligand **L**^{1.131}. The overall yields for the sequence of reactions described in Scheme 45 are summarized in Table 27 and corroborate the outcomes obtained from the 6-morpholinylmethylpyridine template.

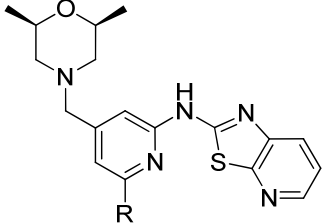
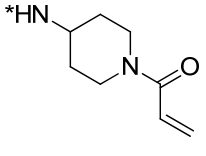
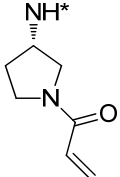
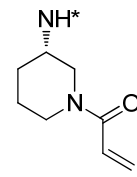
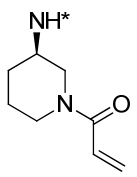


Scheme 44. Synthesis scheme to the intermediate 99



Scheme 45. Synthesis of compounds **100**, **101**, **102** and **103**

Table 27. Yield summary for the final steps of the synthesis of compounds **100**, **101**, **102** and **103**

 R	 100	 101	 102	 103
Overall yields from intermediate 99	37 %	38 %	25 %	21 %

The activities measured in both ITK primary assays are presented in Table 28. The potency ranking of all four compounds is similar to the results from the 6-morpholinylmethylpyridine template, with the two most active compounds possessing the (*S*)-3-aminopyrrolidine and (*S*)-3-aminopiperidine motifs (compounds **101** and **102**, respectively). Moreover, these molecules demonstrate improved ITK inhibitions compared to their direct analogues from the 6-morpholinylmethylpyridine template (Table 17 and Table 18), indicating that the increased lipophilicity from the

cis-2,6-dimethylmorpholine motif was indeed beneficial for the non-covalent affinity. ITK HTRF binding activity for compound **102** was the highest ever measured for this programme, with a value reaching the tight binding limit of the enzyme assay.

Table 28. ITK primary data for compounds **100**, **101**, **102** and **103**¹⁵¹

Compound number	100	101	102	103
HTRF ⁽²⁾ pIC ₅₀	7.9	8.3	8.5*	6.8
PBMC pIC ₅₀	8.4	9.2	9.3	7.7

*: values reaching the tight binding limit of the enzyme assay

The SAR described in Table 28 tend to suggest that the *cis*-2,6-dimethylmorpholine motif had no effect on the positioning of the Michael acceptor compared to Cys442, with the most potent compounds **101** and **102** from the series presenting the optimal geometries to covalently bind with ITK. To confirm this hypothesis, all four compounds were profiled in the kinetic assay¹⁰⁶ and the data are recorded in Table 29. As expected from the data presented for the 6-morpholinylmethylpyridine template (Table 19), despite compound **100** presenting a slightly better non-covalent binding to ITK than compound **101** (respective K_i of 0.003 μM and 0.0085 μM), the (*S*)-3-aminopyrrolidine unit positions the Michael acceptor more optimally for the reaction with Cys442, leading to rate of inactivation being nearly six times faster than for the 4-aminopiperidine motif (respective k_c of 0.0028 s⁻¹ and 0.0005 s⁻¹). Overall, compound **101** is a better ITK inhibitor than compound **100** (respective k_cK_i of 0.311 s⁻¹/μM and 0.167 s⁻¹/μM).

As already postulated from their structural similarities, the (*S*)-3-aminopyrrolidine and (*S*)-3-aminopiperidine compounds **101** and **102** are equivalent irreversible ITK inhibitors: the kinetic data measured for both compounds are identical within experimental errors (Table 29), translating into comparable activities in the PBMC assays (Table 28). The extra lipophilicity of compound **102** does not contribute to any favorable lipophilic contacts with the protein, and consequently results in no further increase in ITK affinity. Finally, the (*R*)-3-aminopiperidine analogue **103** is

clearly less optimal in terms of non-covalent binding (higher K_i) and covalent binding (lower k_c) than the *S*-enantiomer. The kinetic data for compound **103** correlate with the reduced cellular inhibition (PBMC) when compared to compound **102** (Table 28. Note that while the kinetic data appear to support the hypothesis presented, errors cannot be estimated from the assay methods used and it is possible that the relatively small variations in K_i and k_c may be fortuitous).

Table 29. Kinetic data for compound **100**, **101**, **102** and **103**¹⁰⁶

Compound	K_i (μM)	k_c (s^{-1})	k_c/K_i ($\text{s}^{-1}\cdot\mu\text{M}^{-1}$)
100	0.003	0.0005	0.167
101	0.0085	0.0028	0.311
102	0.0073	0.0027	0.386
103	0.0436	0.0004	0.009

Figure 63 visually describes the kinetic values presented in Table 29 for compounds **100**, **101** and **102**. At the concentration of $0.012\ \mu\text{M}$, the time dependent inhibition curves for the inhibitors **101** and **102** are identical and both compounds reach full inhibition of ITK after just 30 minutes. In contrast, the ITK irreversible compound **100** covalently binds to the kinase much more slowly, characterised by a shallower rate of inactivation curve. Even after 180 minutes, at such concentration, the time dependent inhibition is still increasing but has not attained the saturation of the kinase observed for compounds **101** and **102**.

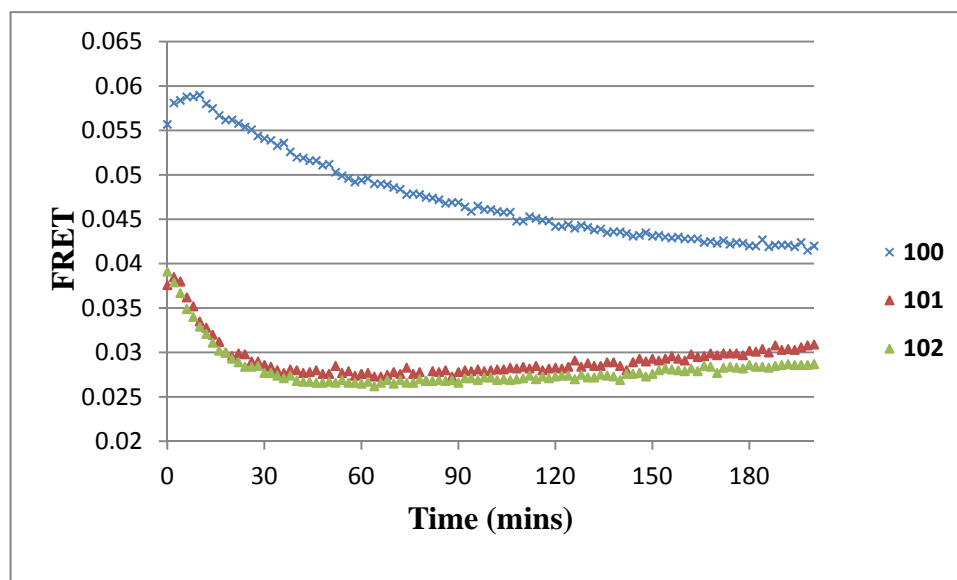


Figure 63. Kinetic data for compounds **100**, **101** and **102** at the $0.012 \mu\text{M}$ concentration

Similarly, the kinetic measurements of the binding of the (*S*)- and (*R*)-3-aminopiperidine analogues **102** and **103** to ITK clearly indicate that a small change in the positioning of the Michael acceptor in the ATP active site can be detrimental for both the non-covalent binding to ITK and the covalent binding to Cys442. As presented in Figure 64, at the concentration of $0.06 \mu\text{M}$, compound **102** reaches saturation of the ITK ATP binding site within minutes whereas the rate of inactivation of the inhibitor **103** is much slower.

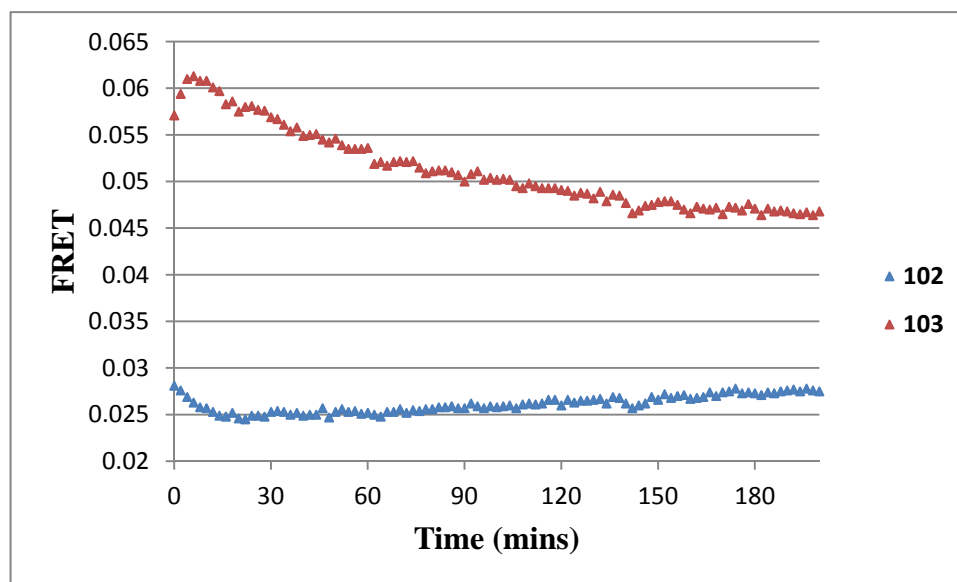


Figure 64. Kinetic data for compounds **102** and **103** at the $0.06 \mu\text{M}$ concentration

As the best two compounds from this series, the inhibitors **101** and **102** were profiled in the SLF solubility assay. The salt screen was not performed at this stage for both compounds. However, to give them the best chance of exhibiting improved solubility compared to the initial lead molecule **92**, the maleic acid versions of both compounds (Figure 65) were prepared and tested in the SLF solubility assay.

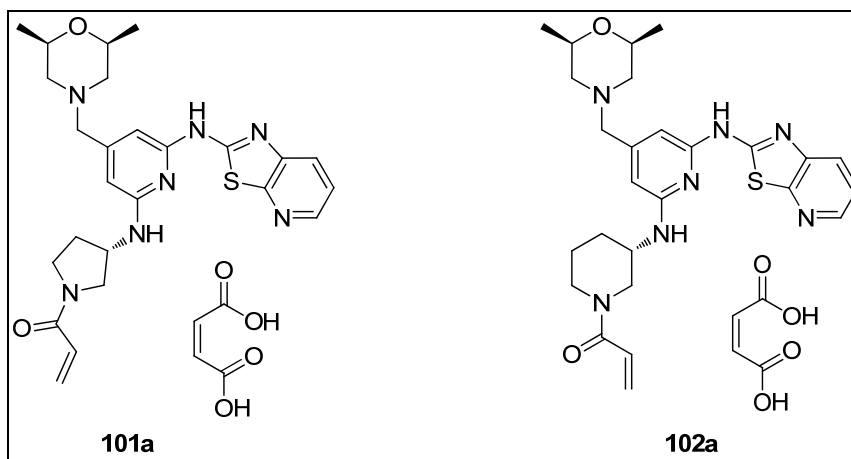


Figure 65. Maleic acid versions of the inhibitors **101** and **102**

The SLF solubility data obtained for compounds **101a** and **102a** are recorded in Table 30.¹⁵² The solubility of the inhibitor **101a** was measured at $105 \mu\text{g/mL}$ after 30 minutes and was found to be constant over 24 hours. This suggested that the salt was

either not disproportionating over time or the solubility measured was related to the free base compound **101**. At the 30 minutes time point, the SLF solubility of compound **102a** was evaluated at 155 $\mu\text{g/mL}$, which is an improvement compared to compound **101a**. However, over time, the slightly more lipophilic compound **102a** disproportionated to reach the relatively low solubility of 45 $\mu\text{g/mL}$ after 24 hours. This finding, coupled to the fact that compound **102** does not offer any activity improvement towards ITK, established that the less lipophilic and lower molecular weight inhibitor **101** possesses the preferred profile from this series.

Table 30. SLF solubility data for compounds **101a** and **102a**¹⁵²

Time (hours)	Solubility ($\mu\text{g/mL}$)	
	101a	102a
0.5	105	155
4	105	71
24	106	45

In relation to these advances, not only does compound **101** demonstrates better affinity and rate of inactivation towards ITK than the initial lead inhibitor **92**, the SLF solubility conferred by the *cis*-2,6-dimethylmorpholine motif was also marginally better and did not decrease over time. The inhibitor **101** hence became the lead compound from this research programme.

The SLF solubility of the template increased, as expected, with the pK_a of the basic motif (the pK_a of the *cis*-2,6-dimethylmorpholine unit was measured at 6.1).¹⁵⁵ However, although the solubility values of compound **101a** was found to be slightly better, it remained below the 250 $\mu\text{g/mL}$ target set as part as this overall programme. As a consequence, the decision was taken to incorporate different amines into the pyridine template with the aim of improving the SLF solubility and also ITK affinity.

The following range of compounds, varying the key amino group, was selected to be prepared (Figure 66). As variation at this position had not indicated any alteration of the non-covalent binding mode to ITK, it was assumed that the positioning of the Michael acceptor would not be affected by these modifications. As a consequence,

all of these compounds were prepared only with the preferred (*S*)-3-aminopyrrolidine linker.¹⁶⁹

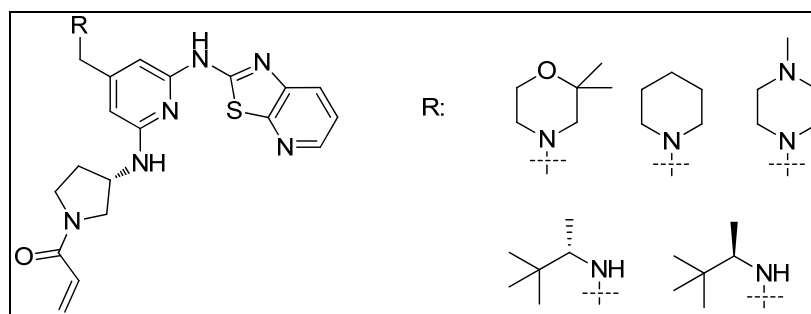
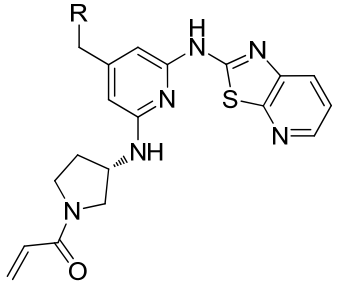
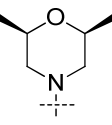
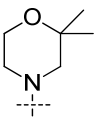
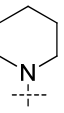
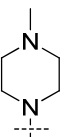
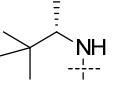
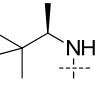


Figure 66. Range of amines selected to increase the solubility of the inhibitors

These amine units were selected for different reasons: firstly, all five compounds have a calculated pK_a greater than that for the *cis*-2,6-dimethylmorpholine unit (Table 31). Although the calculated pK_a of the 2,2-dimethylmorpholine found in compound **104** is similar to the *cis*-2,6-dimethylmorpholine motif, the position of the lipophilic methyl groups is different and could have a positive influence on the non-covalent binding to ITK. The piperidine and piperazine units were chosen for their structural similarities to the morpholine moiety, as well as their increased basicity. Finally, the most basic 3,3-dimethylbutan-2-amine group of the selection is found in potent ITK inhibitors from Bristol-Myers Squibb^{14,15} and Boehringer Ingelheim,²⁷ and the crystal structures presented in Figure 62 indicate that this motif fills the same area of the active site as the morpholine unit within our template. As it was unclear as to which enantiomer would fit the active site more effectively, both compounds **107** and **108** were prepared. If the risk of significant hERG and phospholipidosis activities was believed to be minimal for the less basic molecules **101** and **104**, it was likely to be higher with the pK_a of the molecules increasing to values up to 8.53. Potencies towards hERG and phospholipidosis would be assessed carefully to discharge any toxicity risks at this early stage of development.

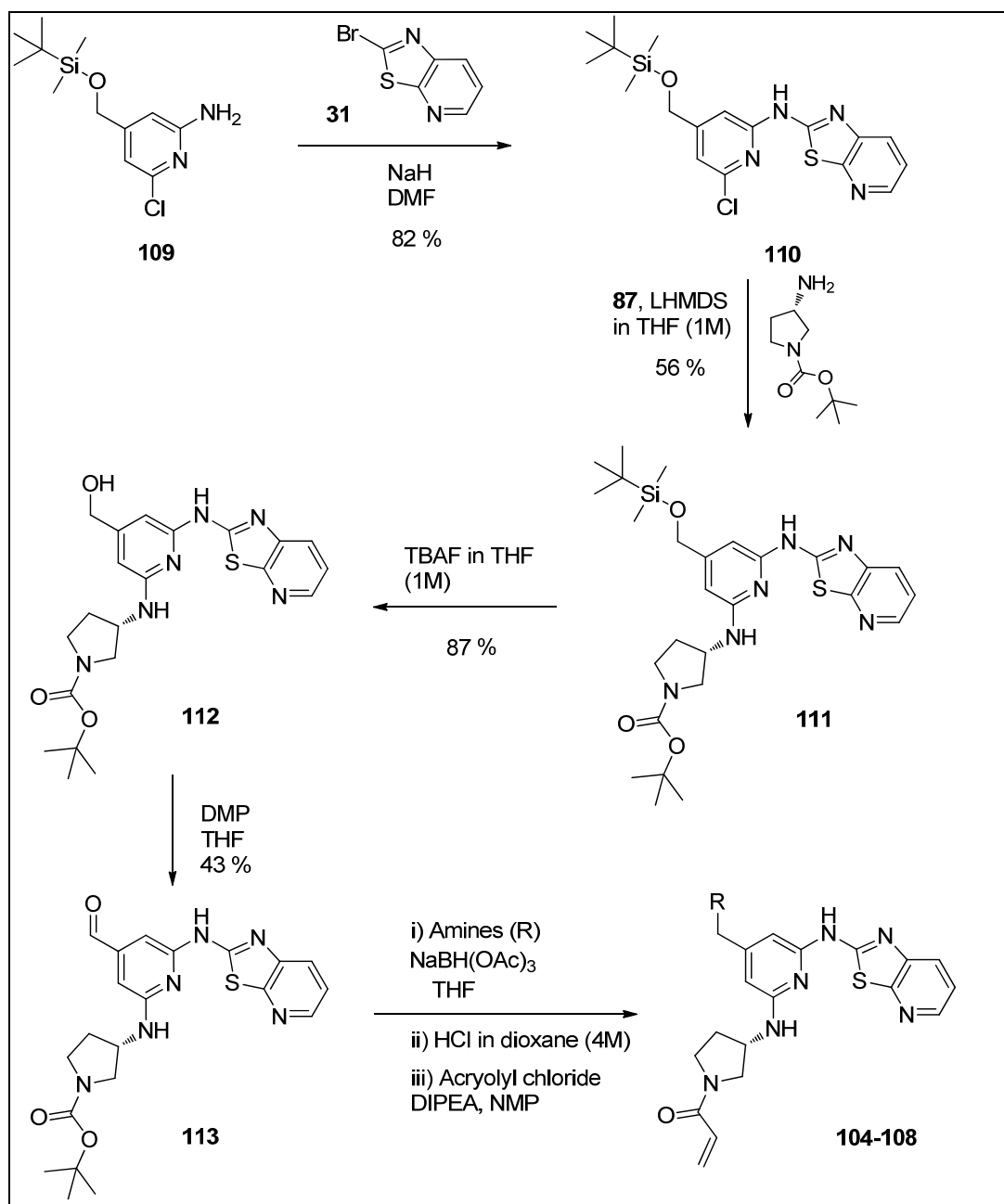
Table 31. Calculated pK_a for the various morpholine replacements¹¹⁹

 R	 101	 104	 105	 106	 107	 108
pK_a	5.78	5.82	7.22	7.5	8.53	8.53

The synthesis of these five compounds could have been performed using the existing route described in Scheme 44 and Scheme 45 for the *cis*-2,6-dimethylmorpholine unit. However, as the introduction of the amine motif was performed during the first step of the synthetic scheme, the preparation of five different compounds would have been extremely time consuming and inefficient. Therefore, an alternative synthetic route was designed (Scheme 46) to allow the addition of the amino units later in the sequence of reactions.

The *tert*-butyldimethylsilyl- (TBDMS) protected (2-amino-6-chloropyridin-4-yl)methanol intermediate **109**, a legacy structure from the initial programme on reversible inhibitors,³¹ was reacted with the 2-bromothiazolo[5,4-*b*]pyridine **31** in the presence of sodium hydride to yield the intermediate **110**. The newly developed palladium cross coupling reaction employing the catalyst developed by the Caddick research group,¹⁴⁸ **87**, was used to link the Boc-protected (*S*)-3-aminopyrrolidine to our pyridine template. Deprotection of the TBDMS group with *tert*-butylammonium fluoride (TBAF) produced the alcohol intermediate **112**, which was oxidised to the aldehyde **113** with the Dess-Martin periodinane (DMP) reagent. The oxidation was also attempted using MnO_2 but no product could be observed by LCMS. The aldehyde functionality was then used to introduce the various amines by reductive amination. Without purification, the amines were treated with HCl to free the pyrrolidine of the Boc protecting group and subsequent amide coupling with acryloyl chloride yielded the final products **104-108** (Table 32). It is worth noting that for the

secondary amines **107** and **108**, the final amide coupling reaction was slightly more complicated as the acryloyl chloride reacted with the 3,3-dimethylbutan-2-amine motif, as well as with the desired pyrrolidine. The formation of the side products **114** and **115** (Figure 67) were observed by LCMS but these peaks were minor compared to the products **107** and **108** (NB: the isolation of compound **114** is described in section VII.9.1). The amide reaction for these two amine monomers was not optimised at this stage as enough quantities of products were obtained for the initial biological assays. Details of the optimisation of this sequence to decrease the amount of side product formed during the reaction are described in the later section VII.9.1.



Scheme 46. Synthetic scheme for compounds **104-108**

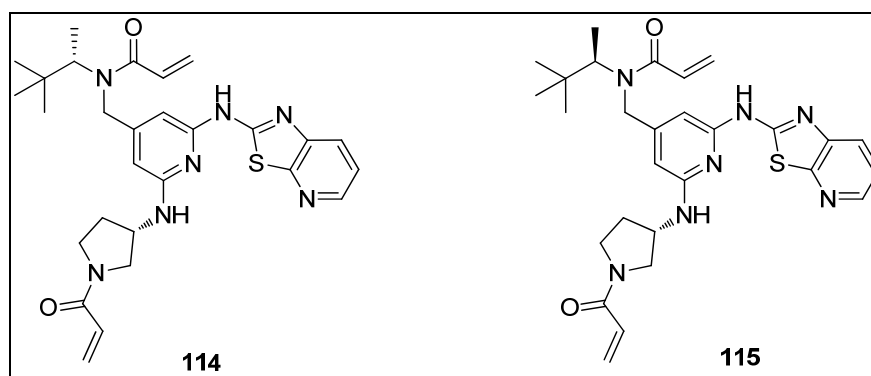
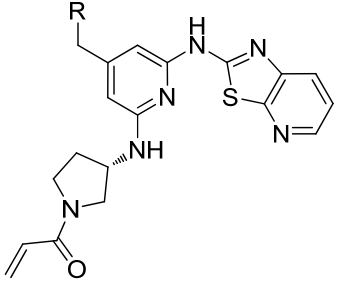
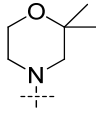
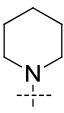
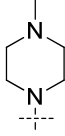
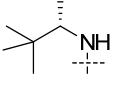
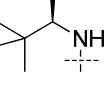


Figure 67. Side products observed by LCMS during the amide coupling to prepare compounds **114** and **115**

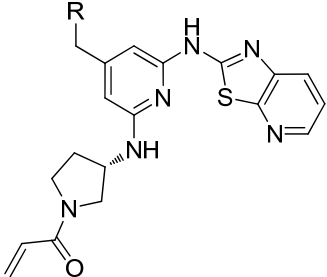
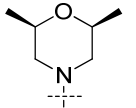
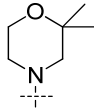
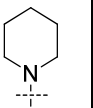
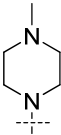
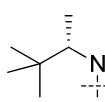
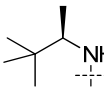
Table 32. Synthetic yields for compounds **104-108** from the intermediate **112**

					
R	104	105	106	107	108
Yield from intermediate 112	48 %	55 %	59 %	46 %	77 %

This newly developed synthetic scheme enabled the preparation of compounds **104-108** in a rapid turnaround. The primary SAR, presented in Table 33, indicates that all amine units were tolerated for ITK binding. Compound **104** presented a similar profile to the *cis*-2,6-dimethylmorpholine analogue **101**: the PBMC activity was not significantly improved compared to compound **101** and as the calculated pK_a of both motifs were equivalent, compound **104** was not taken any further at this stage, as it was unlikely to provide any SLF solubility enhancement. Out of the other four more basic amines, the (*S*)-3,3-dimethylbutan-2-amine analogue **107** clearly demonstrated the best profile with a PBMC pIC₅₀ of 9.5. It is interesting to note that the (*S*)-3,3-dimethylbutan-2-amine unit is marginally better in both assays compared to the (*R*)-enantiomer. This finding was also described by Boehringer Ingelheim when they reported the optimisation and discovery of the first ITK inhibitor (Figure 68) which

displayed *in vivo* efficacy after oral administration.²⁷ As the (*R*)-enantiomer **108** was not predicted to offer any solubility advantages compared to the more active (*S*)-enantiomer **107**, it was not further profiled. Finally, the piperidine and *N*-methylpiperazine compounds **105** and **106** showed excellent HTRF potencies but the cellular inhibitions were not as good as the other four compounds from this series.

Table 33. Primary SAR for the various different amine motifs aimed at replacing the initial morpholine unit to improve SFL solubility¹⁵¹

						
R	101	104	105	106	107	108
HTRF ⁽²⁾ pIC ₅₀	8.3	8.1	8.2	7.9	8.3	8.1
PBMC pIC ₅₀	9.2	9.3	8.7	8.3	9.5	9.1

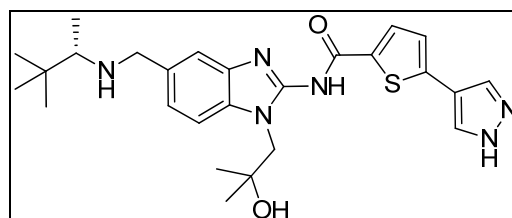


Figure 68. Orally active ITK inhibitor from Boehringer Ingelheim²⁷

Although compounds **105** and **106** were not as potent as the analogue **107** in the cellular PBMC assay, all three compounds were selected to be assayed for SLF solubility. Indeed, as the aim of this study was to obtain a molecule with the required 250 µg/mL solubility in SLF, a less active but soluble irreversible ITK inhibitor, such as compound **105** or **106**, would still have been considered for development if none of the most active species (such as compound **107**) would have passed the solubility criteria. The SLF solubility was assessed for the maleate versions of

compounds **105** and **107** (respectively **105a** and **107a**) and for the free base of compound **106** (Table 34). (NB: the maleate version of compound **106** was not prepared in sufficient time for the SLF solubility study hence the free base was used to give an initial indication of solubility). As designed, the solubility of all three compounds was higher than the less basic compound **101**. More importantly, the measured solubilities were well over the required 250 µg/mL target and no significant disproportion was observed even after 24 hours. Finally, the most basic compound **107a** provided the best SLF solubility values measured as part of this ITK programme. These SLF data, combined with the primary activities measured in the HTRF and PBMC assays (Table 33), indicated that compound **107** presents the most promising profile for an irreversible ITK inhibitor drug candidate.

Table 34. SLF solubility data for compounds **105a**, **106** and **107a**¹⁵²

Time (hours)	Solubility (µg/mL)		
	105a	106	107a
0.5	690	872	1430
4	690	864	1440
24	606	786	1320

The kinetic data for compound **107** (Table 35) confirmed the molecule was covalently binding to ITK. The ratio k_c/K_i was the highest value ever measured within this programme, supporting the progression of that particular molecule as a drug candidate. It is interesting to note that, as already described in Table 20, despite variation in the non-covalent binding affinity to the kinase K_i , the rate of inactivation k_c remains constant (within experimental error) between compounds **92**, **101** and **107** (Table 19, Table 29 and Table 35), which all possess the same pyrrolidine linker. This implies that the improved activity profile of compound **107** is driven by the superior non-covalent affinity to ITK, which is the result of the incorporation of the (*S*)-3,3-dimethylbutan-2-amine unit into the compound template (note that while the kinetic data appear to support the hypothesis presented, errors cannot be estimated from the assay methods used and it is possible that the relatively small variations in K_i and k_c may be fortuitous).

Table 35. Kinetic data for the lead compound **107**^{106,170}

Compound	K _i (μM)	k _c (s ⁻¹)	k _c /K _i (s ⁻¹ .μM ⁻¹)
107	0.0054	0.0026	0.481

The PBMC wash-out data also indicated the benefit of this inhibitor in a more physiological assay (Figure 69). Most of the cellular activity (pIC₅₀ without wash of 8.7) was retained after washing the cells at the one hour point and activation after two and nineteen hours (respective pIC₅₀ of 8.3 and 7.9). These data confirmed that compound **107** was irreversibly inhibiting ITK. After the one hour incubation period, most of the compound was covalently bound to Cys442 as the wash of the cells with aqueous media did not remove the cellular activity. Finally but quite importantly, maintaining the activity after nineteen hours demonstrated that these cells were not capable of fully regenerating new ITK within this time frame. This is a key factor of the success of irreversible ITK inhibitors as potential drugs, as it confirms the long duration of action of these molecules. In the event that the cells had been able to resynthesise the kinase within the nineteen hours, the activity would have dropped dramatically as no compound, after the wash, would have been able to inhibit the newly formed ITK. If the cellular turnover of the targeted kinase had been too rapid, irreversible inhibitors could not have exhibited their main advantage, which is their longer duration of action compared to reversible molecules.

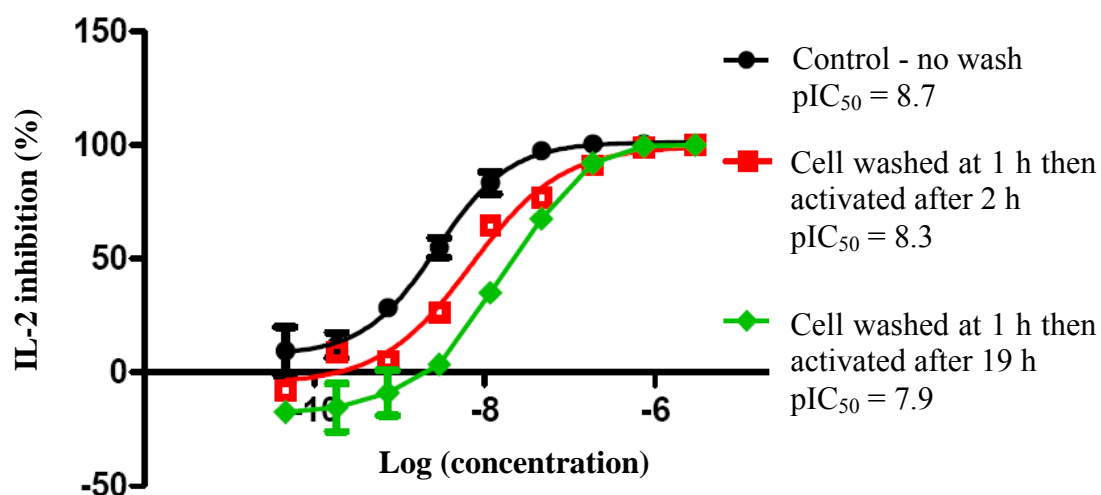


Figure 69. Representative wash-out data for compound **107a**¹⁰⁸

The selectivity profile of compound **107** was assessed versus a panel of kinases and receptors available within our laboratories. No major off-target activities were found to be within a 100 fold window of the ITK activity of compound **107** and the selectivity of compound **107** with respect to EGFR and BTK (both containing a cysteine residue in the same area of the ATP pocket) was judged to be acceptable (Table 36). It is important to mention that the value recorded in Table 36 for EGFR is using the longer preincubation and reaction times described in Table 21. In contrast, the BTK selectivity data reported here were generated using the redesigned 25 minutes reaction time without preincubation, which allows a more accurate comparison of the difference of binding affinity between BTK and ITK. The EGFR and BTK assays were, however, performed using the lower ATP concentration compared to the ITK experiment (Table 21), hence the confidence that the inhibitor **107** is selective towards the target of interest. It is important to notice from these data that the selectivity of compound **107** (Table 36) towards EGFR and BTK has improved over that observed with the inhibitor **92** (Table 22 and Table 23). The enzyme activity of compound **107** to ITK has increased compared to compound **92**, whereas the potencies to EGFR and BTK remained similar. This finding corroborates the initial hypothesis asserted in the design of irreversible inhibitors at the outset of this research programme: the selectivity towards other kinases possessing a cysteine residue in the same position of the active site can be achieved though non-covalent binding to the desired kinase. Indeed, as indicated by the kinetic binding studies, compound **107** presents a better non-covalent binding to ITK ($K_i = 0.0054 \mu\text{M}$, Table 35) compared to compound **92** ($K_i = 0.0129$, Table 19). The introduction of the (*S*)-3,3-dimethylbutan-2-amine unit did not increase the non-covalent activity to EGFR and BTK, resulting in compound **107** being more selective with regards these important kinases. To confirm that these enzyme selectivity data were translating into a more relevant physiological cellular environment, compound **107** was tested in a cellular B cell BTK assay. Although compound **107** did produce a concentration-dependent inhibition of a B cell marker involved in cytokine secretion with a pIC_{50} of 7.25, this is 100 fold less potent than its effect on IFN- γ production in PBMCs activated by Cytostim (Table 33).

Table 36. Selectivity data for compound **107** against EGFR and BTK¹⁵¹

Kinase	ITK	EGFR	BTK (25 mins)
pIC ₅₀	8.3	6.4	7.1

Finally, increasing the pK_a of the molecule to improve the solubility initially caused a concern regarding hERG and phospholipidosis liabilities. The activities against both targets did not highlight any issues at this stage of the programme (Table 37). The activity for the hERG potassium channel was recorded with a pIC₅₀ of 4.9, 1000 times lower than the affinity towards ITK, whereas no indication of phospholipidosis could be measured in our assay.

Table 37. hERG and phospholipidosis activities for the lead compound **107**¹⁷⁰

	hERG pIC50	Phospholipidosis pEC50
Compound 107	4.9	< 4

All the data gathered so far for compound **107** indicated that the molecule possessed all the criteria required for an irreversible ITK drug candidate.

7. Progression of compound 107 and 101 to toxicology studies

Despite the excellent cellular PBMC measured for compound **107** (Table 33), the MDCK permeability was measured at 33 nm/s (Table 38),^{37,170} which is classified as low to medium. In contrast, the permeability of the potent inhibitor **101** was measured at 279 nm/s,³⁷ which is classified as high. Moreover, the human plasma protein binding of both compounds were similar (94 % and 97 %, Table 38) and suggested an acceptable free fraction of compound available *in vivo* to deliver the required inhibition of the kinase. The much better solubility of compound **107** reduced liability towards the accumulation of solid in the lungs, which could result in unwanted toxicity. However, the higher permeability of compound **101** might lead to a better distribution in the lungs hence a superior efficiency of the molecule at

finding and inhibiting ITK in T cells. Because of the similar inhibition profiles of both molecules and because it was not fully understood which compound would deliver better efficacy when administrated by inhalation into the lungs (the two analogues were covering different physicochemical space), the analogue **101** was progressed to toxicity studies alongside the lead irreversible ITK inhibitor **107**.

A summary of the various biological and physicochemical data obtained for both molecules is presented in Table 38.

Table 38. Full profiling data for compounds **107** and **101**

Compound number	107	101
HTRF ⁽²⁾ pIC ₅₀	8.3	8.3
PBMC pIC ₅₀	9.5	9.2
Selectivity (BTK and EGFR)	acceptable	acceptable
ITK kinetic binding (K _i , k _c)	0.0054 μM, 0.0026 s ⁻¹	0.0085 μM, 0.0028 s ⁻¹
PBMC wash-out pIC ₅₀ prior to wash - 2 h after wash	8.7 - 8.3 ¹⁷¹	8.8 - 8.0
SLF solubility at 30 mins	1430 μg/mL (maleate)	105 μg/mL (maleate)
HERG pIC ₅₀	4.9	4.4
Phospholipidosis pIC ₅₀	<4	<4
MDCK permeability	33 nm.s ⁻¹	279 nm.s ⁻¹
Human plasma protein binding	94 % ¹⁷⁰	97 %
Chrom LogD (pH = 7.4) ^{109,172}	4.1	3.4

The inhaled *in vivo* disease model would usually be used to differentiate molecules at this stage of such a programme but the model was not delivering constant results for standard compounds³⁴ so it was decided not to use this method any further to assess

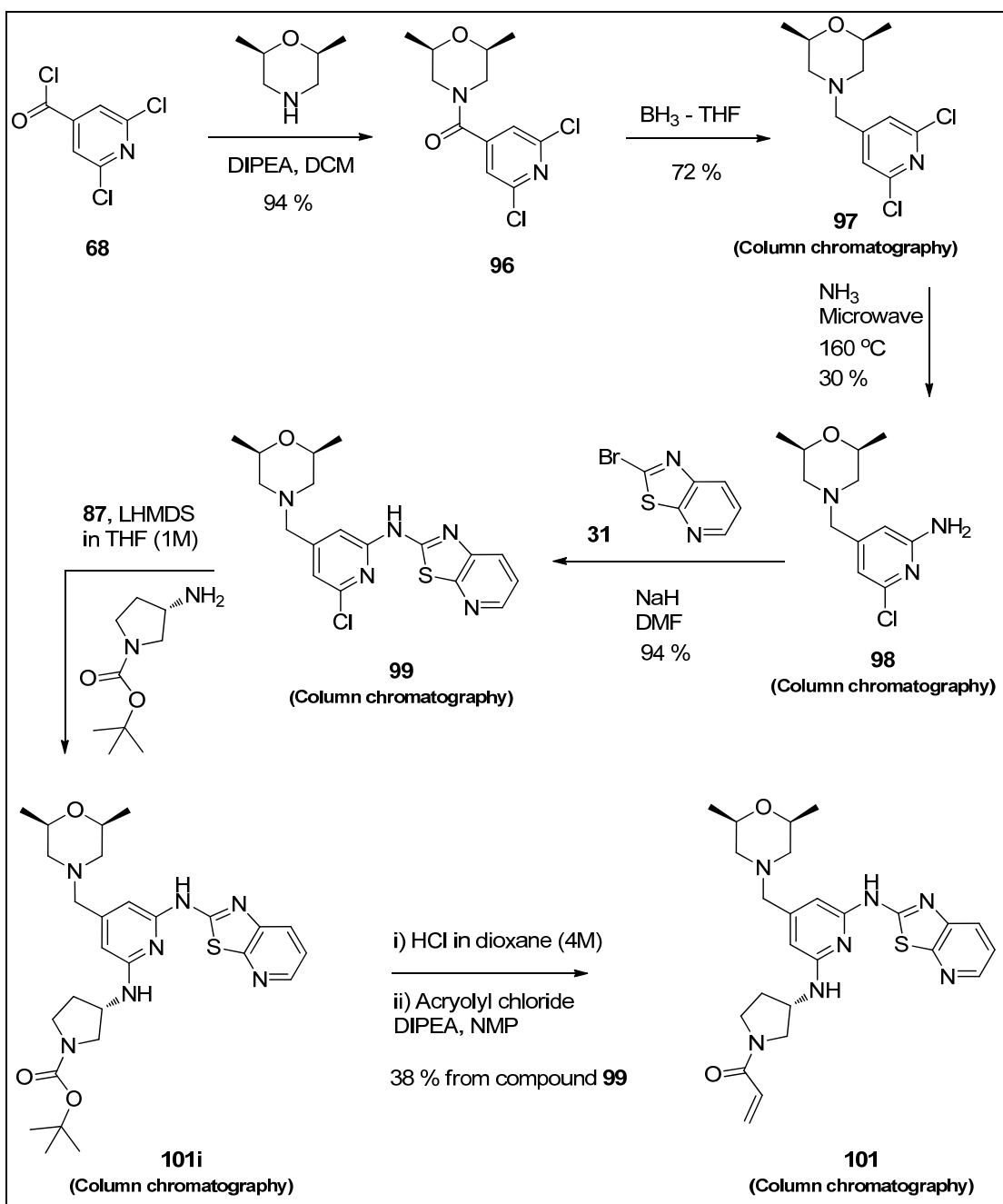
the efficacy of our lead compounds. Instead, the anti-inflammatory inhibition of these molecules in human lung tissues combined with rat inhaled DMPK experiments studying the lung retention and distribution of the drugs were proposed to be measured to assess the efficacy and duration of action of the lead molecules. This new progression criteria for the research project were believed to deliver better predictions for the potential clinical doses of compound required to observe the desired anti-inflammatory effects of our ITK inhibitors.

Before putting both compounds in the human lung tissues and rat inhaled DMPK experiments, the Safety Assessment Department of our laboratories¹⁷³ required their potential genotoxicity in the Ames test¹⁷⁴ and the mouse lymphoma assay (MLA) to be probed.¹⁷⁵ The optimisation of the synthetic routes to these compounds was undertaken because large amounts of materials were required for these studies (around one gram of active substance for both experiments) and for further potential *in vivo* experiments (rat inhaled DMPK experiments, and rat and dog 14 day toxicology studies).

8. Synthesis and genotoxicity data for compound 101

1. Synthesis optimisation

Compound **101** was synthesised first for the Ames test and the MLA. The original chemistry used to prepare this molecule (Scheme 47) consisted of a seven step linear synthesis requiring five column chromatography purifications for the species **97**, **98**, **99**, **101i** and **101**. In order to provide the material to meet the required timelines, the route to the product **101** was kept unchanged but each step had to be optimised. With a view to later scale-up, the following modifications were targeted: (i) an alternative to the microwave amination reaction by replacement with an autoclave system, (ii) changing the NaH base, which has a high risk of flammability on large scale, and, (iii) reducing the number of chromatography purifications to a minimum. The latter modification was given the highest priority.



Scheme 47. Original synthesis to prepare compound **101**

The first amide coupling reaction was successfully repeated on 65 g scale, achieving a nearly quantitative yield of 97 %, without the need of purification beyond routine aqueous work-up (Scheme 48). The reduction reaction with borane in THF was performed with 34 g of compound **96**. After work-up, the analogue **97** was suspended in dichloromethane and acidification with aqueous HCl resulted in the precipitation of the hydrochloride product. Filtration of the white solid followed by

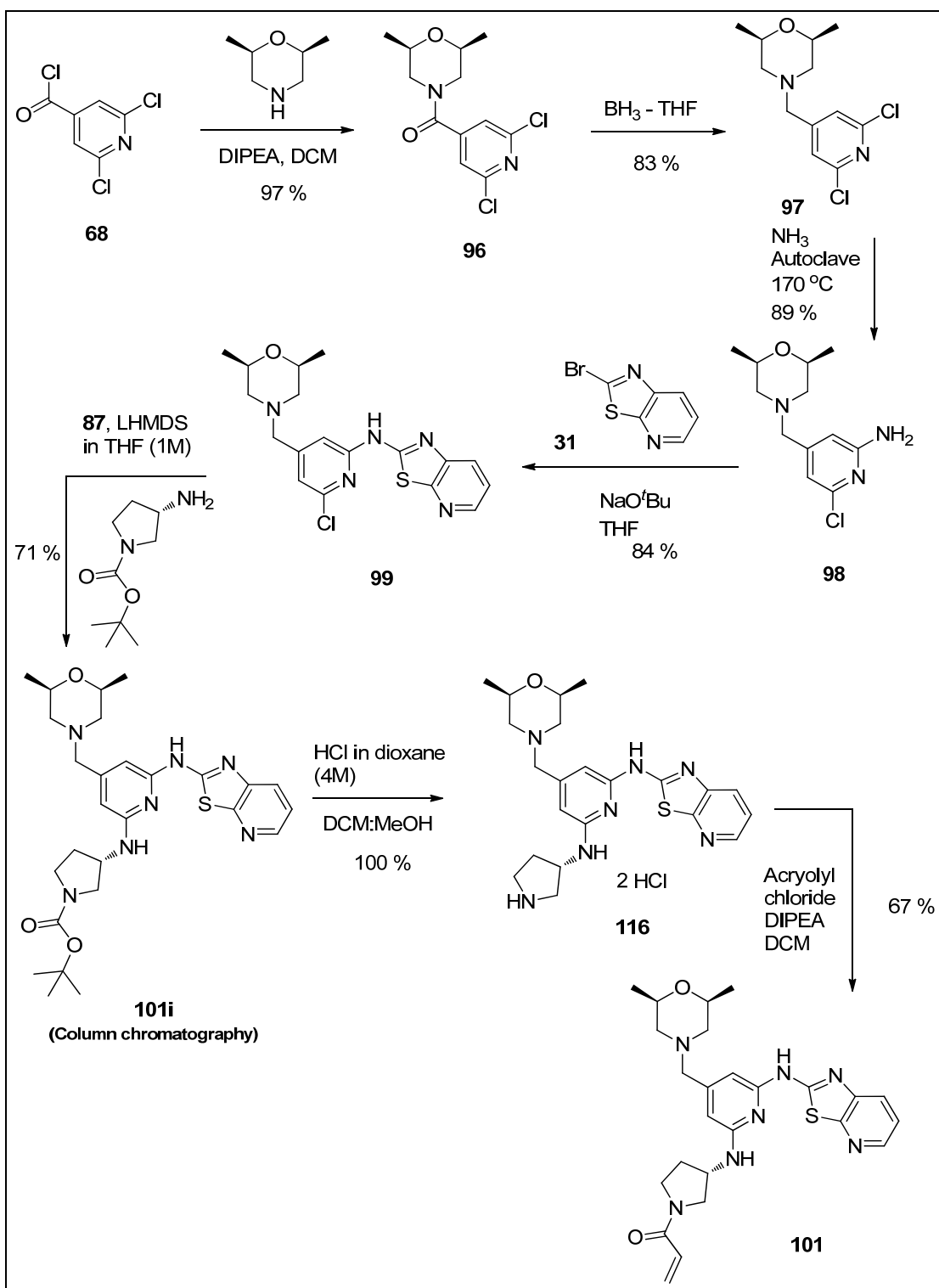
basification with concentrated NaOH produced the required free base which was extracted with DCM. After concentration under reduced pressure, the intermediate **97** was obtained in an encouraging 83 % yield and without the need of column chromatography purification.

The aromatic nucleophilic displacement with ammonia, originally performed in the Biotage microwave, was successfully carried out in a steel alloy autoclave. Optimisation of this reaction indicated that the transformation was slow and required heating for days at 170 °C, with a 20 bar pressure, to achieve the depletion of the starting material **97**. When performed on a close to 35 g scale, the reaction was left heating under these conditions for 66 hours. The white solid obtained after the work-up was triturated with diethyl ether, which dissolved both the impurities and the unreacted starting material. Filtration of the white suspension provided the amino-pyridine **98** in an excellent 89 % yield.

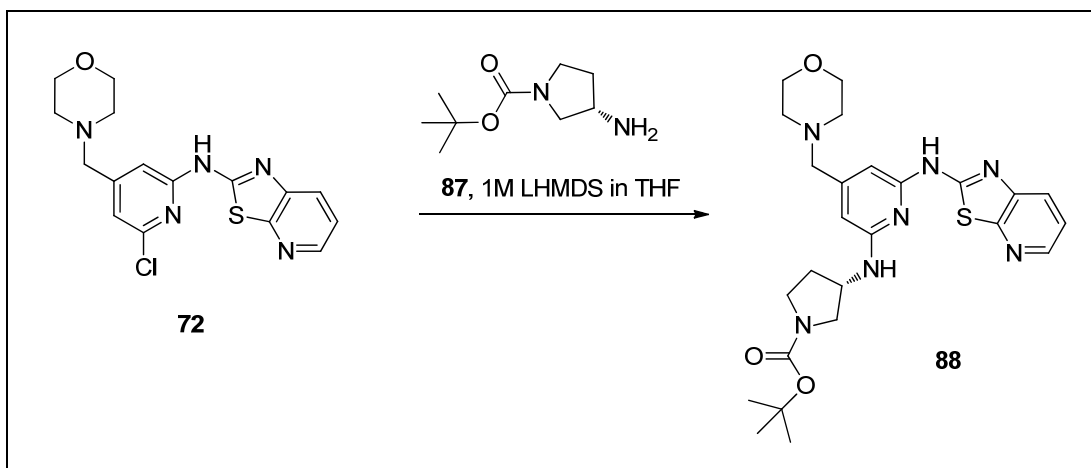
To avoid the risks involved with the use of the flammable solid, NaH, on large scale, NaO^tBu was employed instead for the transformation from compound **98** to compound **99**. The reaction profile with NaO^tBu, as base, and THF, as solvent, was extremely close to that previously observed with the NaH and DMF system. After work-up, the solid was triturated with diethyl ether or acetonitrile to obtain the required product **99**. On a 45.7 g scale and trituration with diethyl ether, the reaction resulted in an excellent 84 % yield and high purity of product. Although the yield of compound **99** was slightly lower than the 94 % obtained on smaller scale with the NaH/DMF process, this was outweighed by the removal of the column chromatography and the elevated level of product purity.

The subsequent Buchwald-Hartwig coupling was performed with the palladium catalyst **87**. The investigation of this reaction was carried out with the less precious morpholine intermediate **72** (Scheme 49) as the data were thought to be reproducible on the *cis*-2,6-dimethylmorpholine analogue **99**. When this reaction was first developed on our template, the typical conditions used a high loading of palladium catalyst (30 mol %), excess of LHMDS in THF (1M, typically 3.6 equivalents), 1.5 equivalents of (*S*)-*tert*-butyl 3-aminopyrrolidine-1-carboxylate and heating of the mixture at 80 °C for one hour (Table 39, entry 1. Note that the % conversion refers to

the formation of product relative to starting material. The % of impurities formed were not taken into account). Reducing the temperature to 70 °C (Table 39, entry 2) or 50 °C (Table 39, entry 3) did not prove detrimental to the turnover of the reaction, with completion achieved within one hour. However, lowering further the temperature to 20 °C resulted in only 40 % conversion to the product **88**, even after 16 hours (Table 39, entry 4). For further optimisation, the temperature was then set at 50 °C leading to 100 % conversion even with only 1.1 equivalents of amine (Table 39, entry 5). Reducing the palladium loading to 20 % or 10 % of catalyst **87** (Table 40, entry 2 and 3) resulted in incomplete reaction, regardless of the length of time the reaction was heated for. It was also important to note that the numbers and the amounts of impurities increased with the reaction times for the incomplete reactions with 20 % or 10 % of catalyst loading (Table 40, entry 2 and 3). Due to timeline related issues, the reaction was not investigated any further and was performed with 30 % loading of **87** to allow full conversion of the intermediate **99**. On large scales, to consistently obtain completion of the reaction, the precatalyst **87** and LHMDS (3 equivalents) were premixed in THF before being added to a solution of chloropyridine analogue and amine in THF. The addition was performed dropwise to maintain the temperature of the reaction around 50 °C. After work-up, various triturations and recrystallisations of the crude product were attempted but none provided the analogue **101i** with acceptable purity. Therefore, the crude material had to be purified by column chromatography on silica. The brown solid obtained after the column was recrystallised from acetonitrile to provide 27.2 g of the intermediate **101i** (71 % yield) as a white solid.



Scheme 48. Optimised synthesis to prepare compound **101** on large scale



Scheme 49. Investigation of the Buchwald-Hartwig reaction using the intermediate **72**

Table 39. Effect of the reaction temperature for the Buchwald-Hartwig coupling with 0.3 equivalents of **87**, 3.6 equivalents of LHMDS in THF (1M), 1.5 equivalents of (*S*)-*tert*-butyl 3-aminopyrrolidine-1-carboxylate (unless stated in the comment box), 1 h reaction time

Entry	Temperature (°C)	Conversion to 88 (%) ^a	Comments
1	80	100	
2	70	100	
3	50	100	
4	20	40 ^b	
5	50	100	1.1 eq of amine used

^a Determined by LCMS analysis; ^b 16 h reaction time

Table 40. Effect of the palladium catalyst loading for the Buchwald-Hartwig coupling with 3.6 equivalents of LHMDS in THF (1M), 1.5 equivalents of (S)-tert-butyl 3-aminopyrrolidine-1-carboxylate at 50 °C

Entry	Catalyst 87 loading (%)	Conversion to 88 (%) ^a		
		1 h	3 h	18 h
1	30	100	-	-
2	20	62	70 ^b	71 ^b
3	10	37	30 ^b	31 ^b

^a Determined by LCMS analysis; ^b more impurities observed

Boc deprotection was performed with HCl in dioxane in 25:1 DCM:MeOH as solvent. This solvent ratio was able to dissolve the intermediate **101i** but not the hydrochloride product **116**, which was filtered under reduced pressure after completion of the reaction to obtain 37 g of product. On a 2.8 g scale, the final amide formation step was performed using acryloyl chloride and DIPEA in DCM. The addition of acryloyl chloride was carried out dropwise at 0 °C to prevent any side reactions. After an aqueous work up, the product was recrystallised from acetonitrile to yield 67 % of the inhibitor **101**. The purity was assessed by the usual LCMS and NMR techniques but also by high resolution HPLC to ensure the product passed the criteria required for these high sensibility genotoxicity assays (*i.e.* purity > 98 % with no impurities more than 0.5 %). No impurities could be observed by NMR and LCMS and the purity by HPLC was assigned to 99.7 % (area/area by UV absorbance detection at 220 nM, Figure 70).

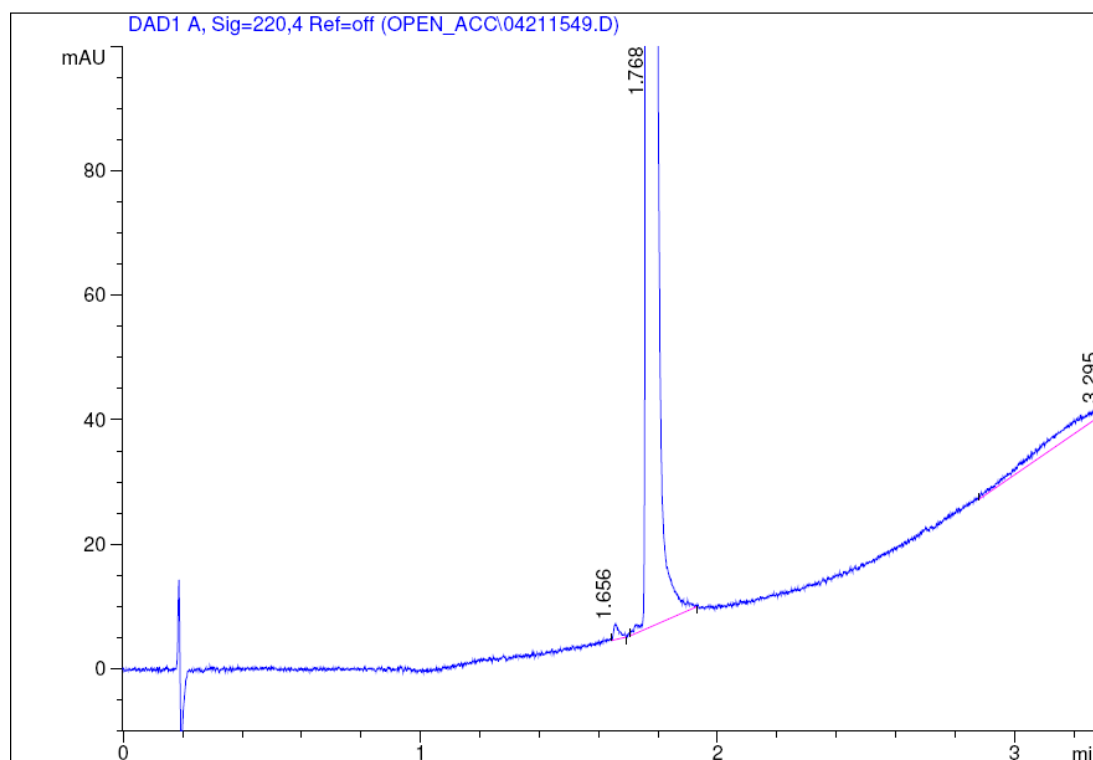


Figure 70. HPLC spectrum for compound **101** after acetonitrile recrystallisation. The product (1.768 mins) was found to be 99.7 % pure with only one impurity at 1.656 mins integrating for less than 0.3 %

Overall, the chemistry route to prepare the irreversible ITK inhibitor **101** was vastly improved with only one chromatographic purification remaining in the whole sequence of reactions (Scheme 48). All transformations were performed on a reasonable scale, indicating that the chemistry was suitable to provide the required material for the 14 day rat and dog studies (~ 26 g for each study). The overall yield to prepare compound **101** from commercially available starting material **68** was calculated at 29 %.

However, although the desired intermediates were obtained in good yields, two steps remained less than optimal for the scale up work: firstly, the amination reaction in the autoclave required at least 66 hours of heating at 170 °C and 20 bar to reach close to full conversion of the starting material **97**. This reaction was also difficult to monitor as the steel alloy autoclave had to be left cooling to room temperature for hours before it could be opened to allow TLC or LCMS analyses. Ideally, a shorter reaction time to reach completion of the reaction and a reduced pressure (20 bar

being the pressure limit allowed in our laboratories) would have been preferred for this transformation. Secondly, the Buchwald-Hartwig coupling step required high loading of catalyst **87** (30 %) for completion of the reaction. Reducing the catalyst loading was necessary for two reasons: (i) decreasing the palladium waste, and (ii) reducing the amount of palladium catalyst **87** requiring to be synthesised. Reducing the amount of palladium side products present in the mixture after aqueous work up would assist in establishing a suitable recrystallisation method which might remove the need for the column chromatography on silica. It is worth noting that lower palladium loadings were previously successfully developed with the precatalyst **86** and ligand **L**¹ system (Table 15, entry 1 and Figure 53). However, the relatively limited availabilities of both reagents from commercial sources prevented their use in the preparation of large quantities of ITK inhibitors. This work was, nonetheless, encouraging and supported future efforts dedicated towards decreasing the loading of precatalyst **87** in the amination reaction.

2. Genotoxicity results

To ensure the genotoxicity experiments were not limited by the compound precipitating from solution at the highest test concentrations, the more soluble maleic acid version of compound **101** was prepared following the method described previously. The purity of the final material **101a** was assessed to 99.4 % by high resolution HPLC (Figure 71).

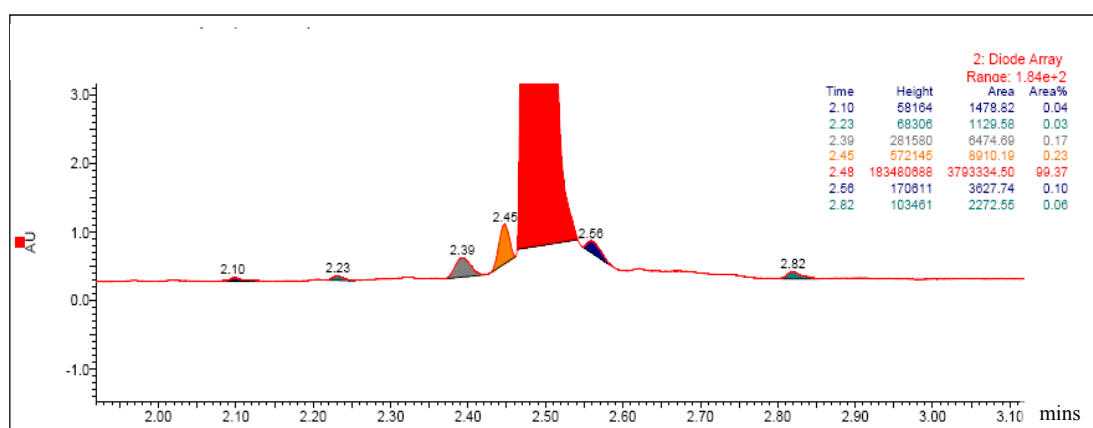


Figure 71. High resolution HPLC for compound **101a** which was submitted to genotoxicology assays

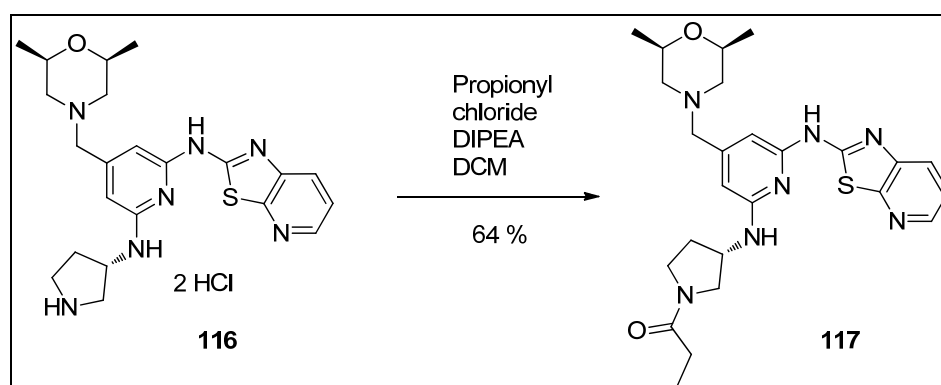
The Ames test uses a variety of *Salmonella typhimurium* strains with pre-existing mutations that render the bacteria unable to synthesise histidine, which is essential for its growth. The experiment tests the ability of a compound to induce new mutations at the site of these preexisting mutations, which would restore the gene's function and allow the cells to synthesise histidine. The Ames test is commonly used as an initial screen to assess the mutagenic potential of new chemicals as a good correlation exists between rodent carcinogenicity and a mutagenic response from this test.¹⁷⁶ The MLA is complementary to the Ames test and also widely used to determine the genotoxic potential of a chemical. The MLA detects the mutations induced by a chemical at the thymidine kinase locus caused by base pair changes, frameshift, and small deletions. Mutant cells are resistant to the cytotoxic effect of pyrimidine analogues such as trifluorothymidine.¹⁷⁵ Rat liver enzymes can be added to both tests to mimic the mammalian metabolic conditions and assess the mutagenicity of compound metabolites.¹⁷⁷

The compound **101a** did not trigger any mutagenic response from the Ames experiment, at any of the test concentrations.¹⁷⁸ However, the compound was reported positive from the MLA,¹⁷⁹ resulting in major concerns relating to potential genotoxicity effects of this ITK inhibitor.

The progression of this molecule was halted at this stage in an attempt to understand the reasons behind the positive results from the MLA and the mutagenic risks of this potential drug. The initial rationale for these results pointed at the reactive Michael acceptor unit which could potentially cause mutagenicity.¹⁸⁰ No MLA data were found within our laboratory's internal safety database for these type of motifs and no conclusions could be taken from the kinase irreversible inhibitors currently in clinical trials,^{48,50} as compounds can carry a higher toxicology risk when treating life-threatening diseases (oncology area). Therefore, it was crucial to determine whether the positive data from the MLA were due to the Michael acceptor or the overall template of compound. Indeed, if the genotoxicity risk observed in the MLA was assigned to the acrylamide unit, it would seriously retard the progresses of this programme as non-toxic electrophilic moieties, with the required ITK potencies, would have to be developed. It would also seriously question the validity of this

kinase irreversible inhibitor approach for non-oncology targets, as the acrylamide motif was initially chosen for its relative weak reactivity towards nucleophilic attack.

To interrogate this issue, the propanamide **117** was selected to be tested in the MLA (Scheme 50). This molecule possesses the overall template of the potent irreversible ITK inhibitor **101** but the potentially mutagenic acrylamide unit has been replaced by a simple propanamide functionality. To prepare this material, the intermediate **116** was coupled with propionyl chloride in the presence of DIPEA. Recrystallisation of the crude product from acetonitrile only yielded the product in a 97 % pure state by HPLC. Further purification by reverse phase chromatography provided compound **117**, after basification with ammonia, with an acceptable purity for genotoxicity assays, quantified at 99.8 % by HPLC (Figure 72).



Scheme 50. Synthesis of compound 117

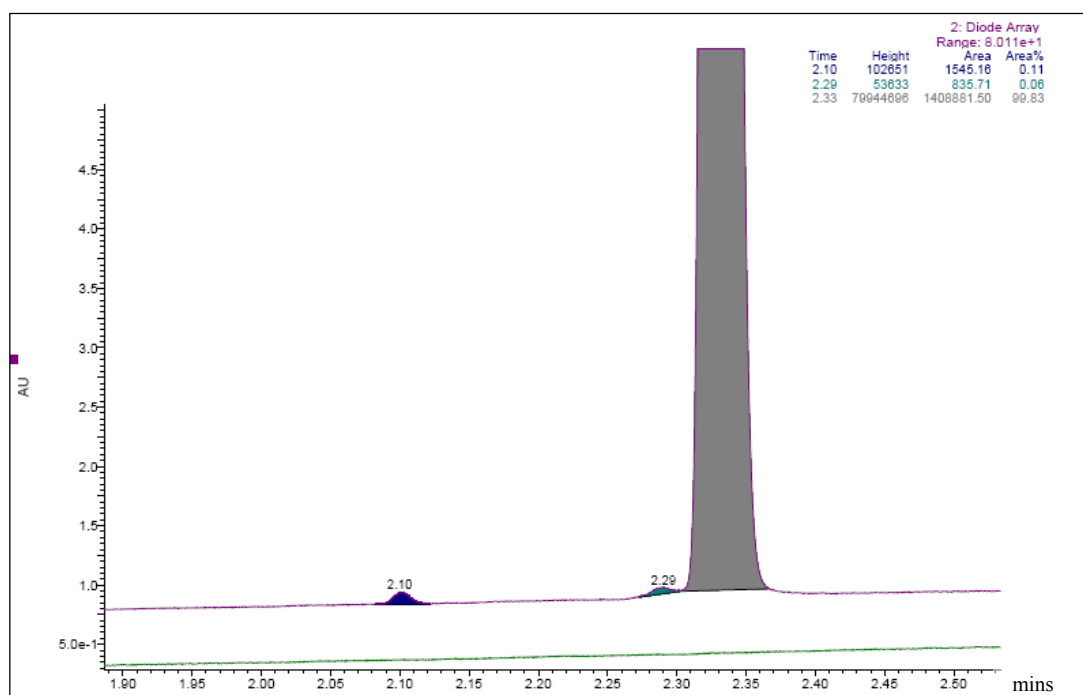


Figure 72. High resolution HPLC for compound **117** which was sent to the MLA

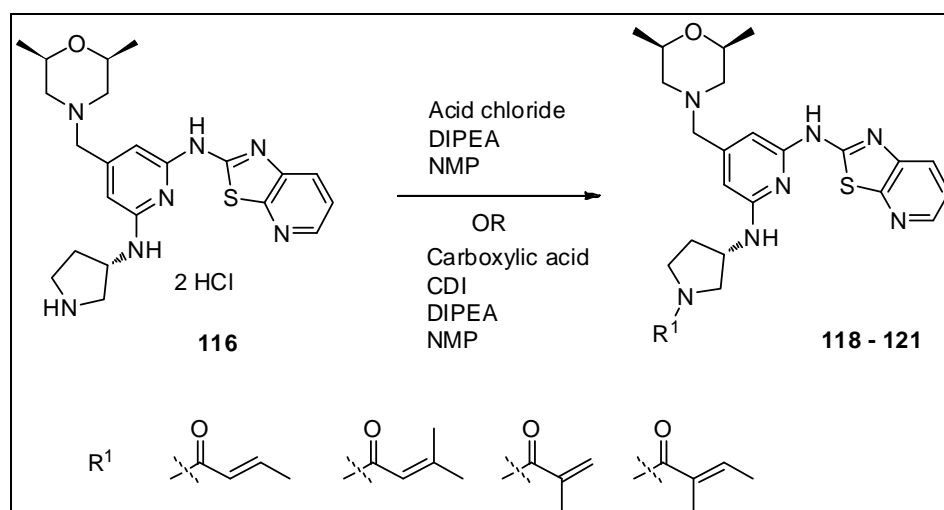
Primary enzyme ITK data for compound **117** indicated, as expected, a good non-covalent binding of the molecule in the ITK ATP pocket, with an HRTF⁽²⁾ pIC₅₀ of 7.0.¹⁵¹ It was, however, more than one log unit lower than the value obtained for **101** (pIC₅₀ = 8.3), demonstrating the potency advantages of irreversible inhibitors of this series. While the MLA for compound **117** was being performed (the data are reported in next section VII.8.4) and in preparation for the event that the reactive acrylamide unit was assigned as the cause of mutagenicity, modifications of the Michael acceptors were investigated.

3. Substitutions to the acrylamide unit

The aim of this endeavour was to decrease the reactivity of the acrylamide unit to reduce the chances of off-target reactivity potentially causing the positive data measured in the MLA. Recent work from Houk *et al.*¹⁸¹ demonstrated that substitution at the 3- and 4-positions of a Michael acceptor diminished the reactivity towards nucleophilic addition of thiols. The same observation was made by Tsou *et al.*⁸⁶ when they optimised the reactivity of their EGFR irreversible inhibitors by reacting these species with glutathione. Therefore, small alkyl groups were to be incorporated onto the acrylamide motif of compound **101** to reduce any potential off-

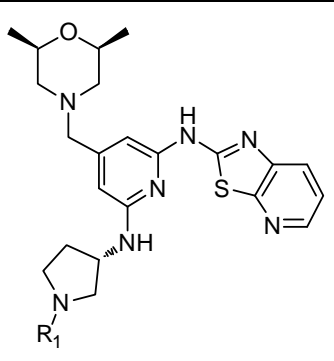
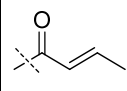
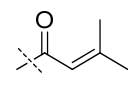
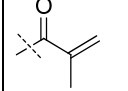
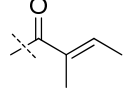
target reactivity of the molecule. However, this approach was also likely to decrease the rate of the reaction with Cys442 in the ITK active site, hence reducing the compounds' activities.

Houk *et al.* compared the reactivity of the unsubstituted 3-buten-2-one to five other substituted Michael acceptors. It was also desired to keep the lipophilicity of the overall molecule as close as possible to compound **101**, hence the lipophilic (2*E*)-3-phenyl-2-propenamide unit¹⁸¹ was not synthesised. Moreover, as already observed for compounds **48a** and **48b** (section VII.3, Table 6), a bulky phenyl group was detrimental for activity in this position of the active site. Four substituted acrylamide analogues (Scheme 51) were prepared using coupling between the intermediate **116** and either the corresponding acid chlorides (method 1) or the carboxylic acids in the presence of 1,1'-carbonyldiimidazole (CDI) (method 2). All four reaction mixtures were purified by MDAP to yield the desired products **118-121** (Table 41).



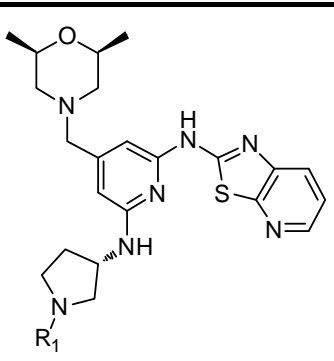
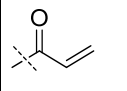
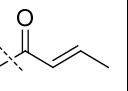
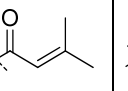
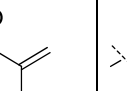
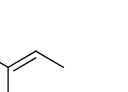
Scheme 51. Synthesis of the substituted acrylamide analogues **118-121**

Table 41. Synthetic yields for compounds **118-121**

 R₁	 118	 119	 120	 121
Coupling method	1	1	2	2
Yield	61 %	79 %	46 %	50 %

Primary enzyme activity for compounds **118-121** (Table 42) indicated that the incorporation of the methyl groups to the Michael acceptor was tolerated in the ITK active site, although all compounds were less potent than the unsubstituted acrylamide analogue **101**. These compounds were, at least, as potent as the non-covalent inhibitor **117** ($pIC_{50} = 7.0$), which was encouraging for the potential irreversible character of these inhibitors. However, the enzyme activities did not translate into the PBMC assay with pIC_{50} s lower than 7.5.

Table 42. Primary SAR for compounds **118-121**¹⁵¹

 R₁	 101	 118	 119	 120	 121
HTRF ⁽²⁾ pIC_{50}	8.3	7.4	7.6	7.0	7.1
PBMC pIC_{50}	9.2	7.2	7.5	7.3	6.4 ^{182,183}

ITK kinetic data for compounds **118** and **120** demonstrated that both analogues were only inhibiting ITK reversibly.¹⁰⁶ Compounds **119** and **121** were not tested in the kinetic experiment but were also believed to be reversible as a result of their similar activities. Therefore, although the introduction of the methyl groups to the Michael acceptor had only small effects on the non-covalent binding to the ITK active site, they prevented the Cys442 residue from covalently reacting with the inhibitors. This finding could be due to a steric clash between the lipophilic methyls and the cysteine residue in the active site or the lower reactivity of these Michael acceptors towards thiol nucleophilic attack, as described by Houk *et al.*¹⁸¹

Interestingly, the (*E*)-4-(dimethylamino)but-2-enamide motif found in the irreversible EGFR inhibitor, Neratinib (Figure 13), was reported to increase the rate of the reaction with Cys773,^{86,117} due to the deprotonation of the cysteine thiol by the amine, increasing its reactivity (Figure 73). It was also discussed in section VII.3, that the enhanced reactivity of this acrylamide unit could also be due the fact that the (dimethylamino)methyl might already be protonated at physiological pH, resulting in the presence of a cationic hydrogen bond donor favouring the approach of the thiol or thiolate. The results obtained for compounds **118-121** tend to suggest that without deprotonation of the cysteine, this (*E*)-4-(dimethylamino)but-2-enamide unit would be less reactive towards nucleophilic attack than the unsubstituted acrylamide functionality. Therefore, the (dimethylamino)methyl group needs to be perfectly positioned in the kinase active site relative to the cysteine residue to allow the activation described in Figure 73 to occur.

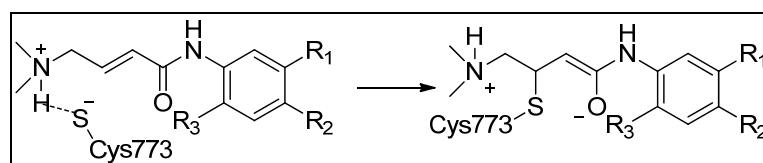


Figure 73. Potential explanation for the increased reactivity of the (*E*)-4-(dimethylamino)but-2-enamide towards thiol attack of Cys773 for Neratinib¹¹⁷

This rationale would explain the data observed for compounds **50a** and **50b** (Figure 74). Indeed, the poor cellular activity, which was initially attributed to the predicted poor permeability of the molecules (Table 7, Figure 74), is also likely to be due to

the fact that both compounds are only reversible ITK inhibitors. In the ITK active site, the dimethylamine might not be in a position to deprotonate Cys442, making this Michael acceptor less reactive towards nucleophilic attack. Indeed, as already described (Figure 39, Figure 40 and Figure 41), the crystal structure of compound **42** indicates that the acrylamide unit has already passed Cys442 in the ITK active site. As a consequence, the dimethylamine group of compound **50a** and **50b** must be located deeper in the pocket, and more remote from the cysteine residue.

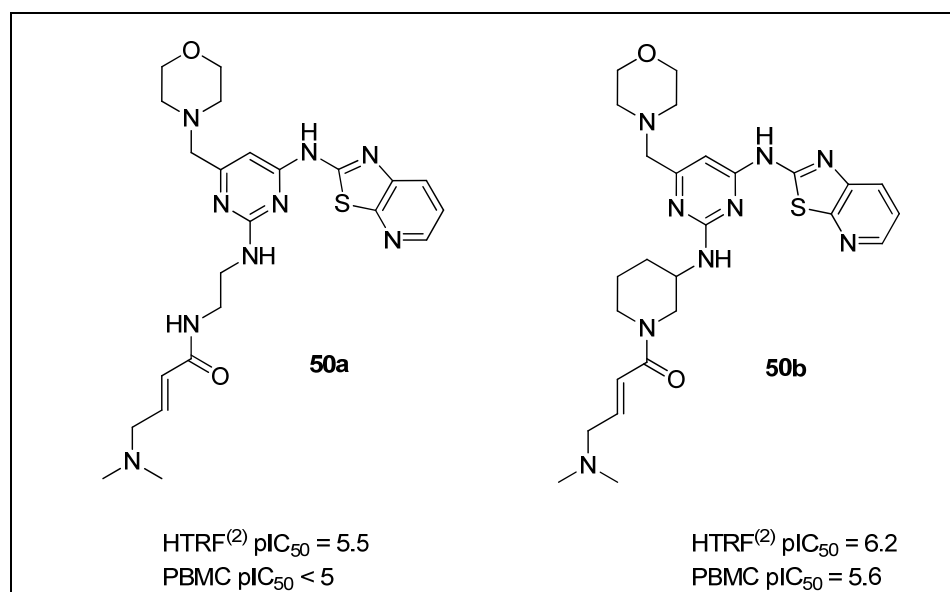


Figure 74. Primary SAR for compound **50a** and **50b**

In their search for the optimal electrophilic moiety, Tsou *et al.*⁸⁶ have demonstrated that a (morpholino)methyl group attached at the 3-position of the Michael acceptor was also able to catalyse the deprotonation and 1,4-addition of glutathione onto the acrylamide motif. In their glutathione assay, this (morpholino)methyl compound was more reactive than the (*E*)-4-(dimethylamino)but-2-enamide lead molecule. However, the (morpholino)methyl at this 3-position of the Michael acceptor may not have been as well tolerated in the EGFR active site or might not have been positioned optimally compared the Cys773 in the active site as the compound was less active than the molecule containing the preferred (*E*)-4-(dimethylamino)but-2-enamide motif. In our ITK template, such a (morpholino)methyl group substituted at that position of the acrylamide might have a better arrangement in the active site to deprotonate Cys442 and catalyse the covalent reaction between the inhibitor and the

kinase. Moreover, the less basic morpholine group should confer on the compound a better permeability than the dimethylamine motif, which should improve the inhibition measured in the PBMC assay. To confirm this hypothesis, the two compounds **122** and **123** were synthesised.

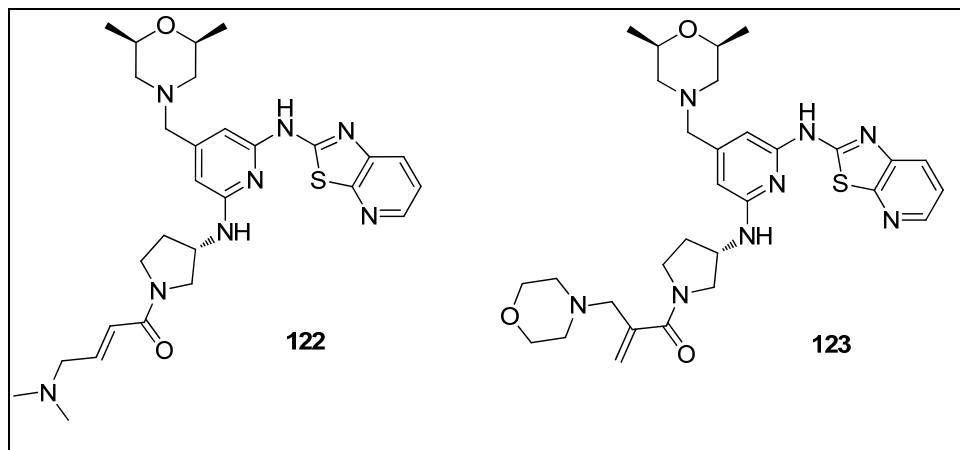
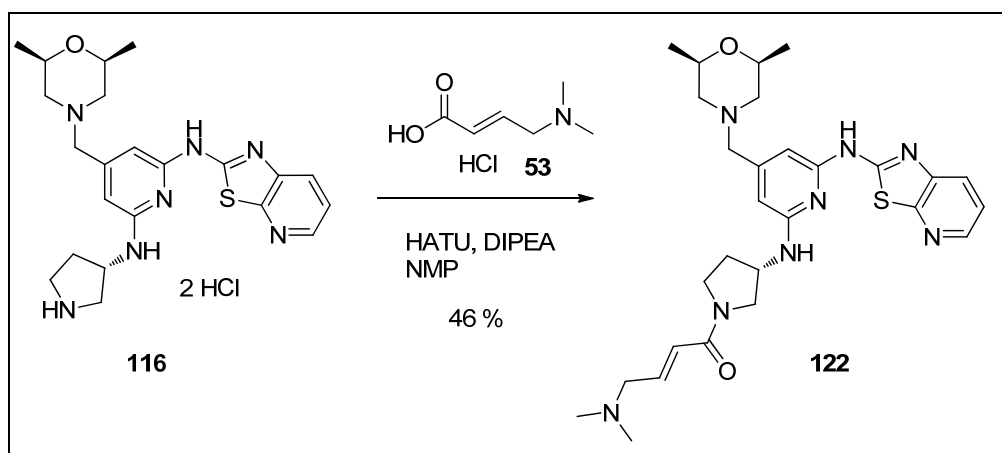


Figure 75. Structures of compounds **122** and **123**

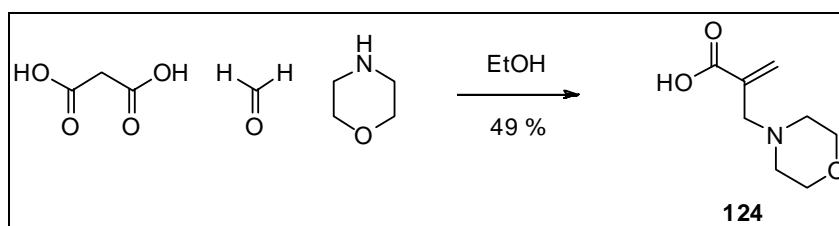
Compound **122** was prepared following the HATU coupling conditions already used to synthesise the analogues **50a** and **50b** (Scheme 52).



Scheme 52. Synthesis of compound **122**

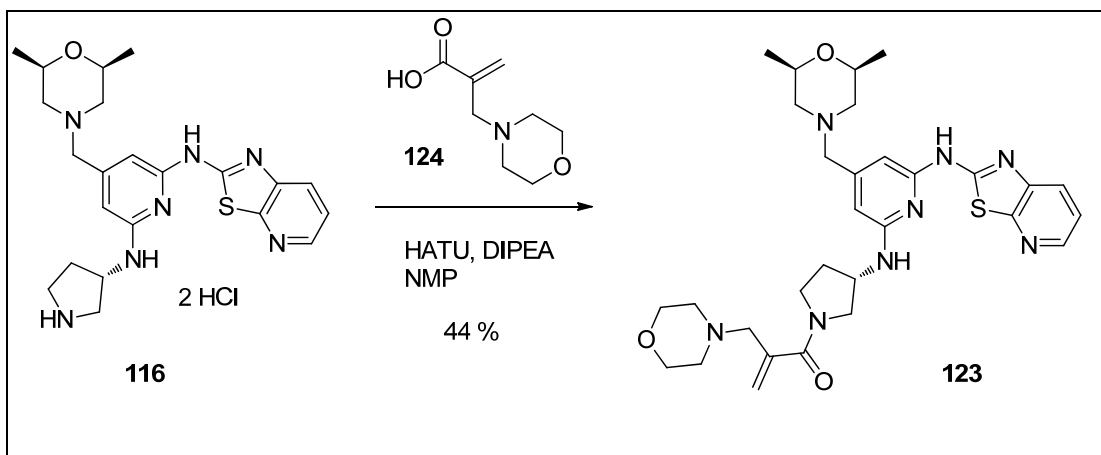
The 2-(morpholinomethyl)acrylic acid monomer was prepared following literature conditions¹⁸⁴ by refluxing a mixture of malonic acid, paraformaldehyde and morpholine in ethanol (Scheme 53). The product did not crystallise on standing, as described in the literature reference, so it had to be purified by chromatography on silica and was obtained with a 49 % yield. This yield was lower than that reported by

Krawczyk (80 %) ¹⁸⁴ but slightly higher than the same preparation, this time in 1,4-dioxane, described in a Wyeth patent (32 %), ¹⁸⁵ in which column chromatography was also required to produce the desired intermediate **124**.



Scheme 53. Preparation of the intermediate 124

The intermediate **124** was then coupled to the pyrrolidine derivative **116** in the presence of HATU to yield, after purification, the required product **123** in a 44 % yield (Scheme 54).



Scheme 54. Synthesis of compound 123

While both compounds **122** and **123** were found to be equipotent in the HTRF assay, with pIC₅₀ of 6.9, a 1.3 log unit difference was observed between the two compounds in the cellular assay (Table 43). This major variation in PBMC potency was believed to be not only due to the potential permeability difference between the two compounds (respective Chrom logD of 2.4 and 3.5) ¹⁰⁹ but also to their reversible and irreversible characters as ITK inhibitors. Indeed, the activity profile of compound **122**, clearly resembles that observed for the reversible inhibitors **118** and **120** (reversible character demonstrated by the kinetic assay), with no significant gain of activity shown in the cellular assay. This compound was assumed to only reversibly

inhibit ITK, the (dimethylamino)methyl unit reducing the reactivity of the Michael acceptor as the basic group was not positioned optimally to deprotonate Cys442 in the active site. On the contrary, the improved cellular activity observed for compound **123**, suggested that the inhibitor could be irreversibly binding to ITK. In this case, the newly positioned basic group was potentially able to deprotonate Cys442 to catalyse the 1,4-Michael addition and transform the reversible molecule **120** into an irreversible ITK inhibitor.

Table 43. Primary SAR for compounds **122** and **123**¹⁵¹

Compound number	101	122	123
HTRF ⁽²⁾ pIC ₅₀	8.3	6.9	6.9
PBMC pIC ₅₀	9.2	6.4	7.7 ¹⁸⁶

The irreversible character of compound **123** was confirmed in the kinetic assay (Table 44). The non-covalent binding to the kinase, K_i , and the rate of inactivation, k_c , were, however, significantly inferior to the values obtained for the unsubstituted analogue **101**. Although the morpholine motif appeared to be able to activate the Michael addition by deprotonating Cys442, the arrangement that compound **123** and the cysteine residue have to adopt in the active site may not be optimal, resulting in reduced potency values being obtained compared to the inhibitor **101** (Table 43, Table 44. Note that while the kinetic data appear to support the hypothesis presented, errors cannot be estimated from the assay methods used and it is possible that the relatively small variations in K_i and k_c may be fortuitous).

Table 44. Kinetic data for compound **123**¹⁰⁶

Compound number	K_i (μM)	k_c (s^{-1})	k_c/K_i ($\text{s}^{-1}/\mu\text{M}$)
101	0.0085	0.0028	0.311
123	0.022	0.0012	0.055

Introducing the (morpholino)methyl at the 2-position of the acrylamide restored the covalent binding to Cys442. Nonetheless, the activity profile measured for compound **123** was weaker than the profile observed for the unsubstituted acrylamide **101**. The kinetic data revealed that the (morpholino)methyl motif was not optimal for both the non-covalent affinity to ITK and the Michael addition reaction with Cys442. The effect of the amine functionality on the activity/reactivity profile with ITK could have represented a new area of research. However, the MLA data for compound **117** (*vide infra*) inspired a renewed focus on the compounds possessing the most reactive unsubstituted acrylamide unit.

4. MLA results for compound 117

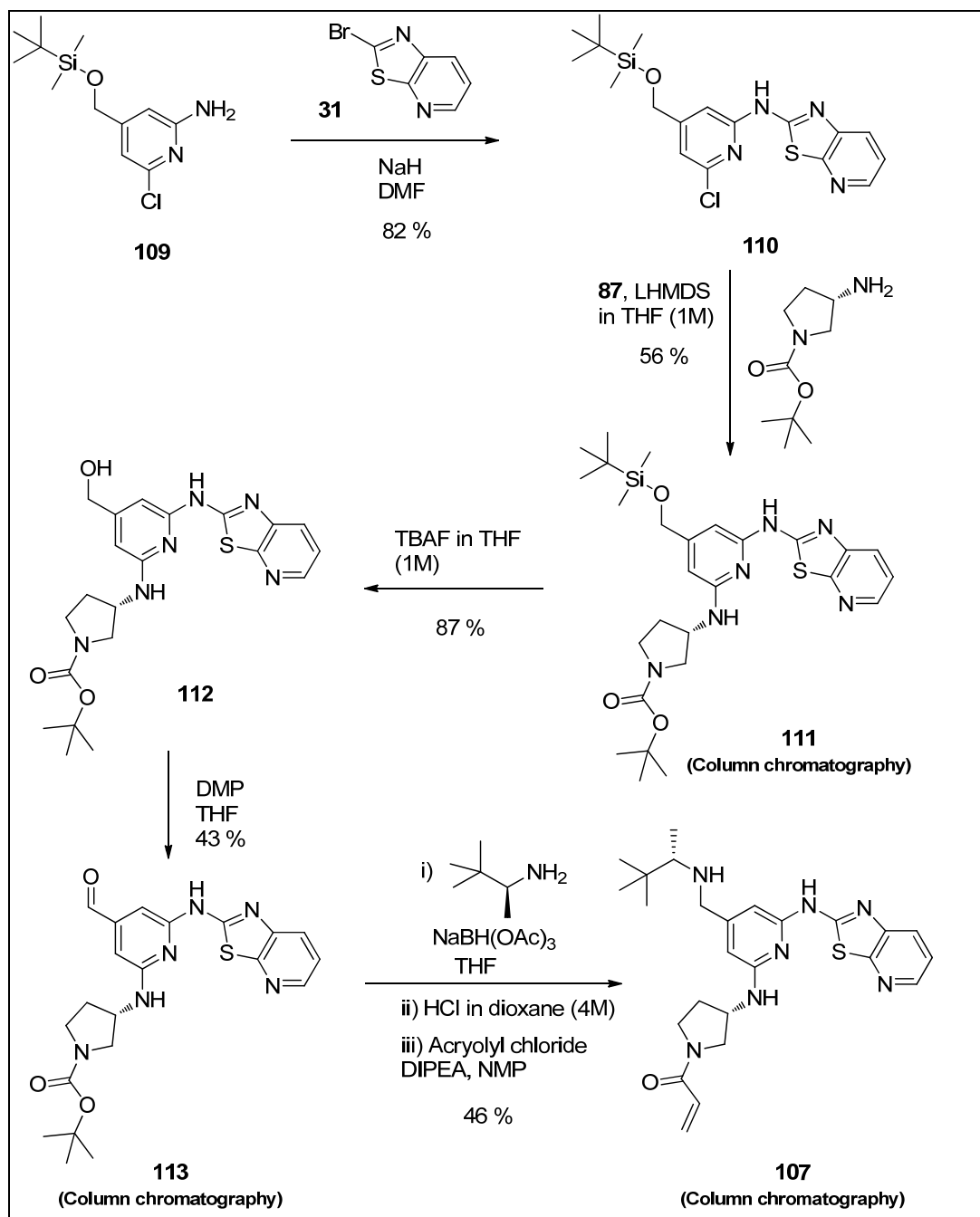
The reversible ITK inhibitor **117**, which does not possess the potentially mutagenic acrylamide unit, was still reported positive in the MLA.¹⁷⁹ The dose/response profile for both compounds **101** and **117** was very similar, suggesting that the mutagenicity observed in these experiments was not related specifically to the acrylamide unit. This result was somewhat positive as the irreversible inhibitor approach was not thought to be responsible for the genotoxicity measured in the MLA. However, it also meant that the structural template of compound **101** was conferring mutagenicity issues to the molecule. The causes of the positive data observed in the MLA for this molecule remain unknown but it was postulated that small changes to the structure of the compound might have an effect on the properties (*i.e.* selectivity) of the inhibitor, resulting in loss of this mutagenicity issue. For that reason, the development of the synthetic chemistry to prepare compound **107** was investigated.

9. Synthesis and genotoxicity data for compound 107

1. Synthesis optimisation

The synthetic route initially used to prepare the lead compound **107** (Scheme 55) consisted in a seven step synthesis, starting from the intermediate **109**, which required three steps to be made.³¹ Although three stages required column chromatography purifications (compounds **111**, **113** and **107**), the main issue of this synthetic scheme was the high catalyst loading (30 % of catalyst **87**) needed for the Buchwald-Hartwig coupling in the second step of the route. The scale up chemistry

to provide 26 g of compound **107** for the 14 day rat toxicology study would require a significant amount of precatalyst **87** (95 g if all yields remained the same). Additionally, the use of the Dess-Martin periodinane is restricted in our laboratories, resulting in the necessity to change the oxidation conditions for the formation of the aldehyde **113** on large scale. Taking all these factors into consideration, this synthetic route to the inhibitor **107** was not believed to be suitable for large scale development.



Scheme 55. Original synthesis to prepare compound 107

The sequence of reactions optimised for compound **101** (Scheme 48) was predicted to be appropriate for the synthesis of compound **107**, simply by replacing *cis*-2,6-dimethylmorpholine with (2*S*)-3,3-dimethyl-2-butanamine. The amination reaction performed in the autoclave with ammonia had, however, to be modified to decrease the reaction time and allow better conversion to the aminopyridine analogue. Ideally, the catalyst loading of the Buchwald-Hartwig transformation should also be reduced.

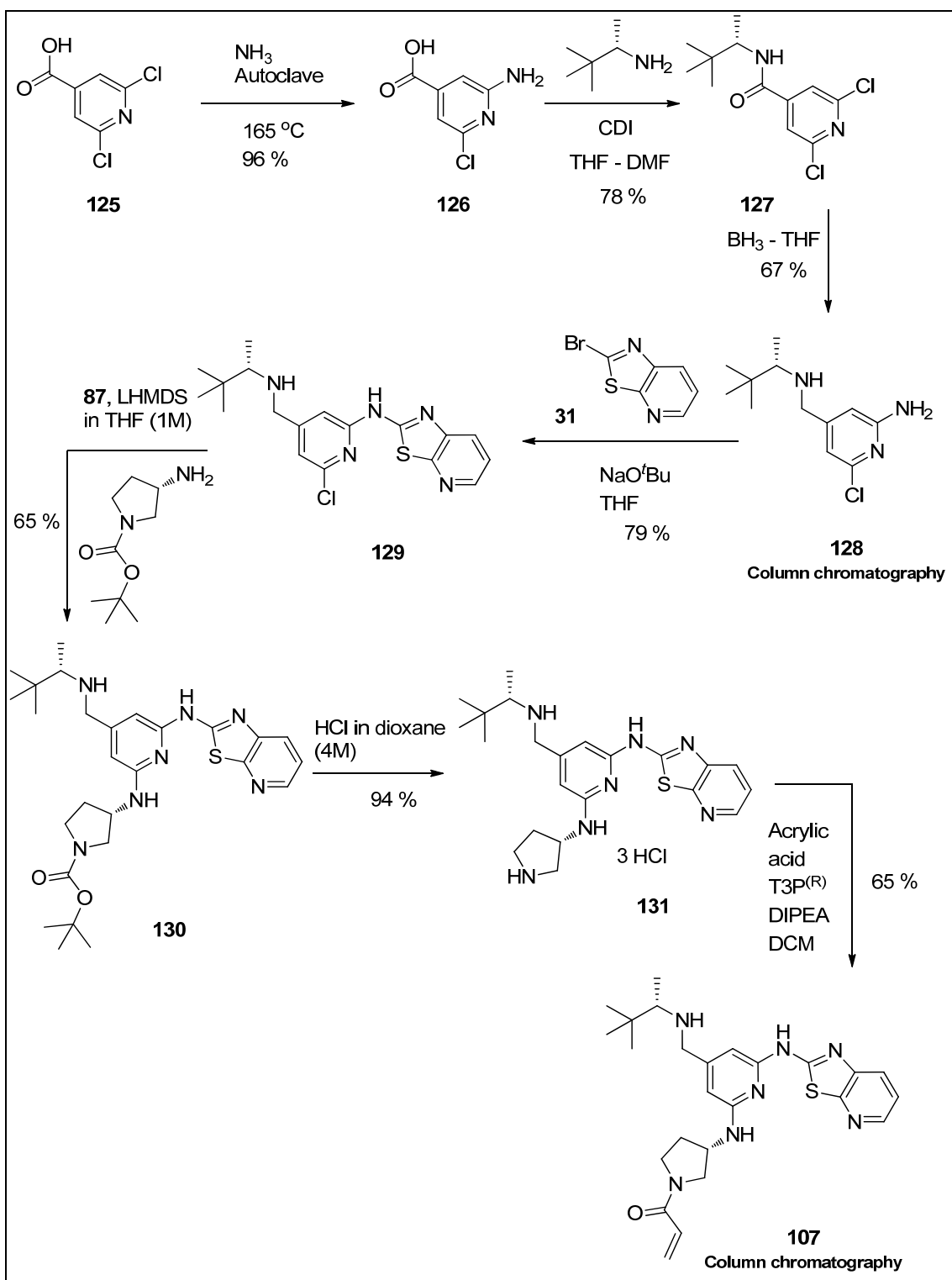
The amination reaction now became the first step of the synthesis (Scheme 56). Reacting the 2,6-dichloro-4-pyridinecarboxylic acid **125** with ammonia in the autoclave at 165 °C for 16 hours (pressure 17 bar) provided full conversion of the starting material to the product **126**. As predicted, the electron delocalisation on the carboxylic acid motif enhanced the aromatic nucleophilic displacement. The amination reaction was reproducibly completed after overnight heating. After evaporation of the excess of ammonia, the residue was suspended in water and acidified to pH 3. The product was isolated by filtration in an excellent 96 % yield on 50 g scale.

The carboxylic acid **126** was coupled at room temperature with (2*S*)-3,3-dimethyl-2-butanamine, in the presence of CDI. Aqueous work up was sufficient to provide compound **127** in 78 % yield. Borane reduction of the amide **127** was first attempted at room temperature. However, even with excess of borane, the reaction only reached 50 % completion after 24 hours and was still not completed after 48 hours. Heating the reaction mixture at 40 °C increased the conversion to the desired intermediate **128**, keeping the reaction profile relatively clean by LCMS. After 24 hours at 40 °C, the starting material **127** was fully consumed. A succession of aqueous work up manipulations followed by a column chromatography afforded the compound **128** with an acceptable 67 % yield. Further optimisations of the reaction¹⁸⁷ demonstrated that column chromatography proved unnecessary as the crude product **128** could be stirred in *tert*-butyl methyl ether, filtered and the filtrate concentrated under reduced pressure to afford the compound with sufficient purity (~ 90 %) to perform the next step.

The aromatic nucleophilic displacement between the aminopyridine **128** and the bromo analogue **31** was performed using the previously optimised NaO^tBu/THF

system. Trituration with diethyl ether yielded the intermediate **129** in 79 % yield and high purity. The Buchwald-Hartwig conditions employing 30 % of catalyst **87** and 3 equivalents of LHDMS at 50 °C also proved to be successful on this template. Contrary to the optimised synthesis of the inhibitor **101**, the crude product was successfully triturated with DCM-diethyl ether to afford compound **130** with an acceptable 65 % yield. It is worth noting that although the trituration provided the desired intermediate **130** with high purity, there was more product, by LCMS, in the mother liquors but it was not possible to isolate pure material by triturating further.

Boc deprotection with HCl in DCM-MeOH yielded the intermediate **131**, which precipitated out of the reaction mixture and was collected by filtration. Up to this stage, the synthesis was successfully developed without the need of any column chromatography purifications to isolate the intermediates cleanly. After filtration, the hydrochloride pyrrolidine analogue **131** was assessed to a purity of 99.6 % by HPLC (Figure 76) and the overall yield over six steps was 16 %. All reactions had also been performed on scales greater than 10 g, suggesting that the route was suitable to provide large quantities of material.



Scheme 56. Optimised synthesis to prepare compound **107** on large scale

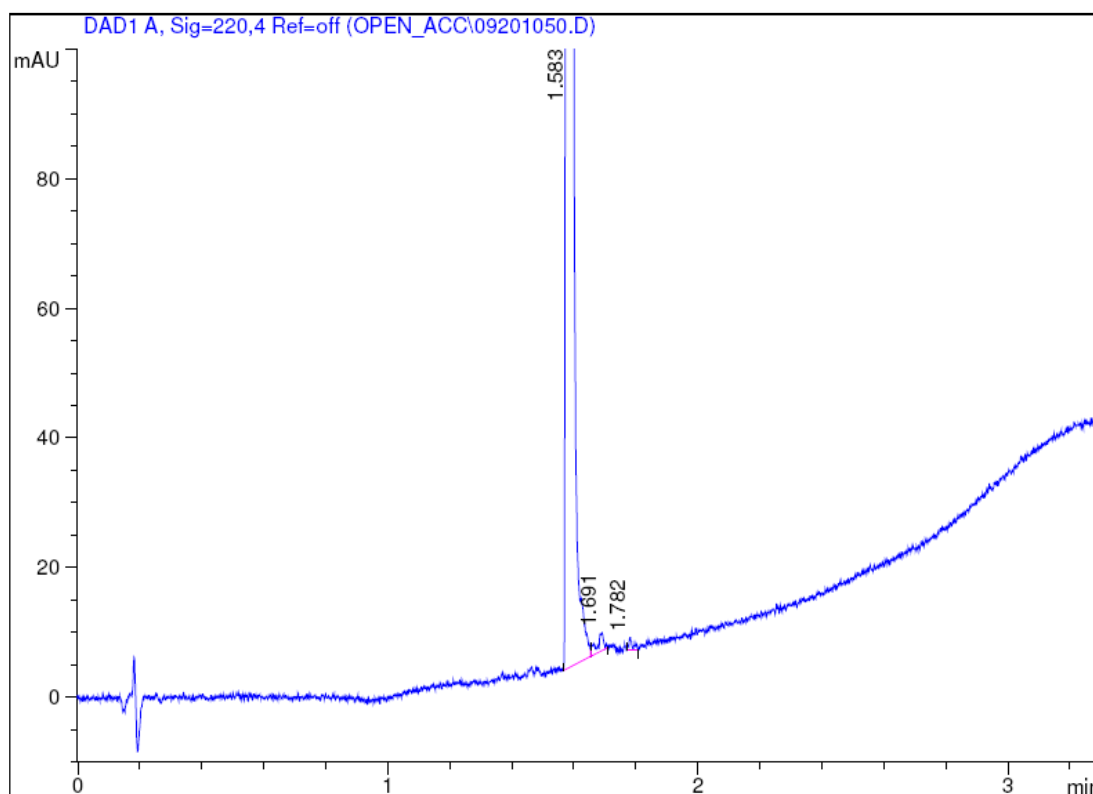
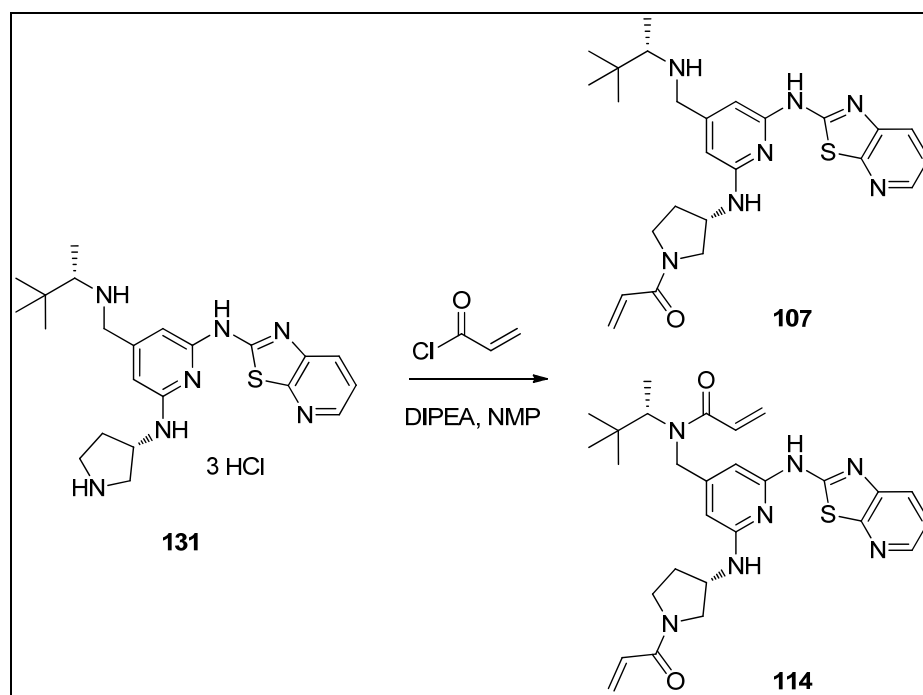


Figure 76. HPLC spectrum for compound **131**

The final amide coupling to attach the acrylamide unit to the pyrrolidine had already been shown to generate issues (section VII.6) with over reaction of acryloyl chloride with the (2*S*)-3,3-dimethyl-2-butanamine which produced the side product **114** (Scheme 57). The formation of the analogue **114** was observed by LCMS before complete depletion of the starting material **131**. Typically, after full conversion of compound **131**, around 20 % of side product **114** was observed by LCMS.



Scheme 57. Formation of the sideproduct **114** during the amide coupling between compound **131** and acryloyl chloride

The temperature was lowered to 0 °C and -30 °C in an attempt to reduce the amount of side product **114** produced during the reaction. Although the reaction profiles were slightly better at these lower temperatures (LCMS and HPLC traces), the formation of compound **114** could not be prevented. The acryloyl chloride was thought to be too reactive to totally stop the reaction with the (2*S*)-3,3-dimethyl-2-butanamine unit. A range of amide coupling reagents were used to react the acrylic acid with compound **131** with the aim of reducing the formation of the side product **114** (Table 45). These reagents were chosen as they are considered to possess the best balance of properties between safety and environmental impact for this type of reaction in our laboratories.¹⁸⁸ Formation of the desired product **107** was observed by LCMS for the reactions with propylphosphonic anhydride (T3P[®]),^{189,190,191} (benzotriazol-1-yloxy)tripyrrolidinophosphonium hexafluorophosphate (PyBOP[®])¹⁹² and (1-cyano-2-ethoxy-2-oxoethylideneaminoxy)dimethylamino-morpholino-carbenium hexafluorophosphate (COMU)¹⁹³ (Table 45, entry 1, 2, 3). The quantity of side product **114** measured by HPLC analyses (LCMS was not sensitive enough to detect compound **114**) was reduced compared to the 20 % seen in the reaction with acryloyl chloride (LCMS detection). It is worth noting that the solvent of the reaction was

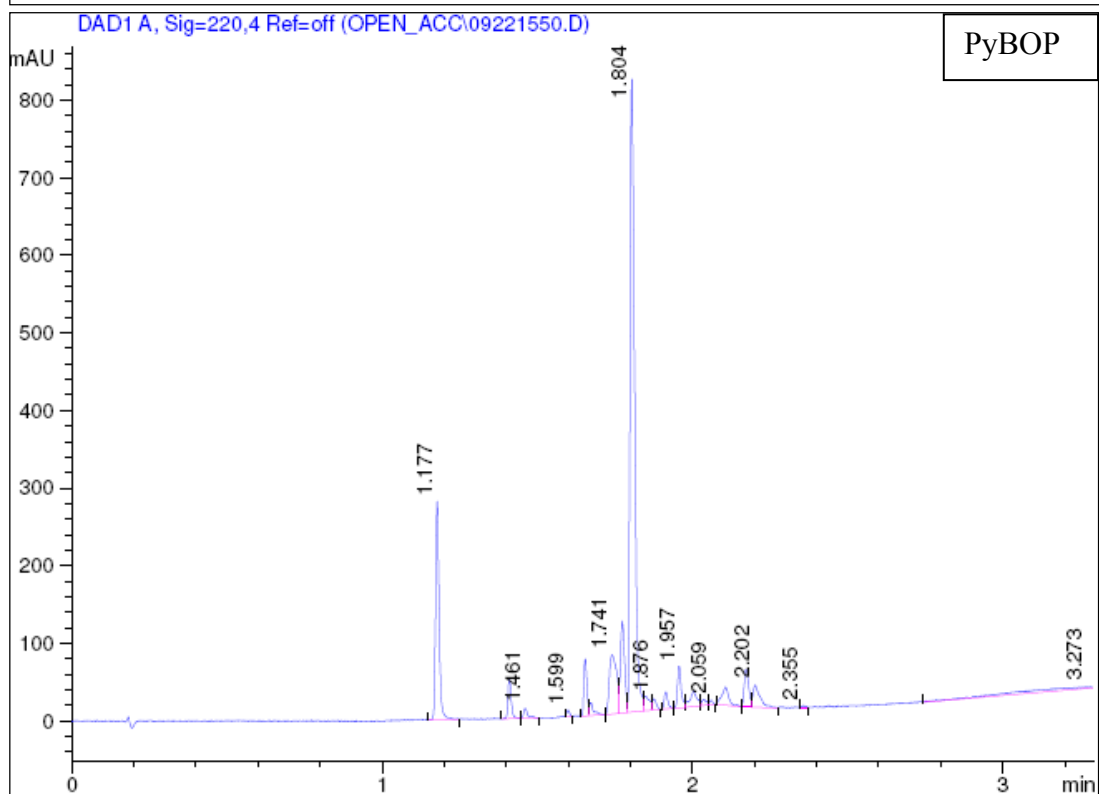
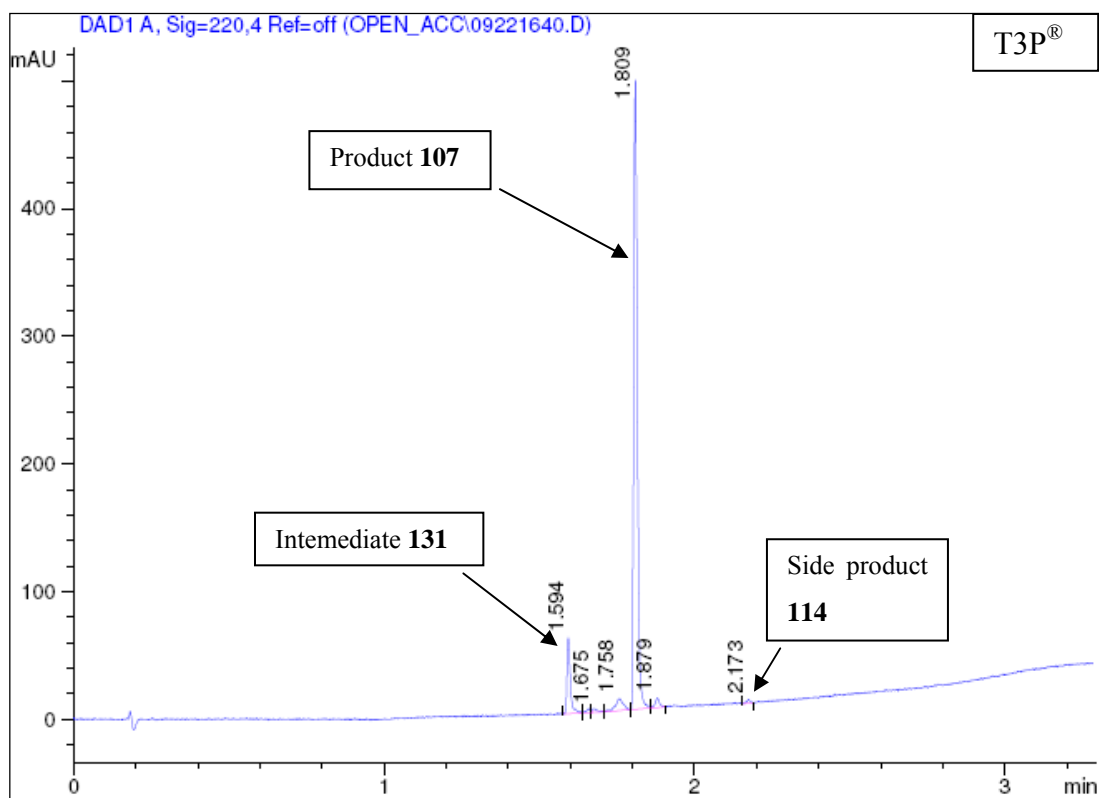
changed from NMP (used in the coupling with acryloyl chloride) to DCM. NMP was typically used for the final step of the synthesis as, on small scale, the mixture was directly injected into the MDAP. On larger scale, the reaction would have to be worked up and the crude product dried before purification hence the need of a lower boiling point solvent. The modification of the solvent was, however, not thought to play a major role in the formation of the side product **114** (solvent screening discussed later in Table 46). Examinations of the rest of the HPLC traces indicated that the reaction with T3P[®] clearly presented the cleaner profile (Figure 77), despite the fact the reaction had not reached full completion. In the reaction with CDI, consumption of the substrate **131** was observed but the structure of the product isolated after purification was assigned to the analogue **132** and not the compound **107** (Scheme 58). During the course of the reaction, the imidazole released had reacted with the acrylamide unit. This observation confirmed the reactivity analysis of the Michael acceptor described previously (section 3). Indeed, with the less reactive substituted acrylamides (compound **120** and **121**, Scheme 51), no reaction was observed by LCMS with the imidazole released from CDI.

Overall, T3P[®] was considered as the most appropriate coupling reagent for this amide reaction. As a consequence, further optimisation of the reaction was performed with T3P[®].

Table 45. Investigation of the amide reaction to prepare compound **107** using T3P[®], PuBOP[®], COMU and CDI as coupling agents

Entry	Coupling agent	Amount of side product 114 ^a	Comments
1	T3P [®]	0.53 %	Still 10 % of 131 remaining
2	PyBOP [®]	2.8 %	Only 0.3 % of 131 remaining Messy mixture
3	COMU	10 %	< 0.1 % of 131 remaining Messy mixture
4	CDI	NA	No product

^a Determined by HPLC analysis.



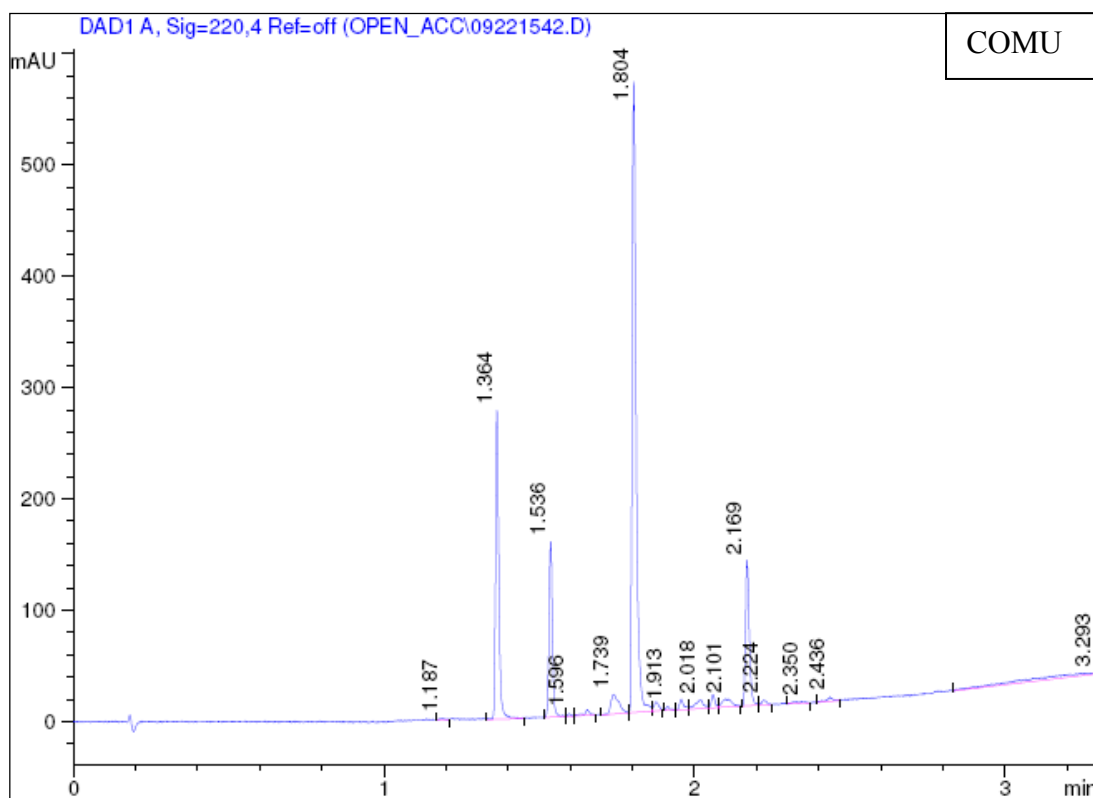
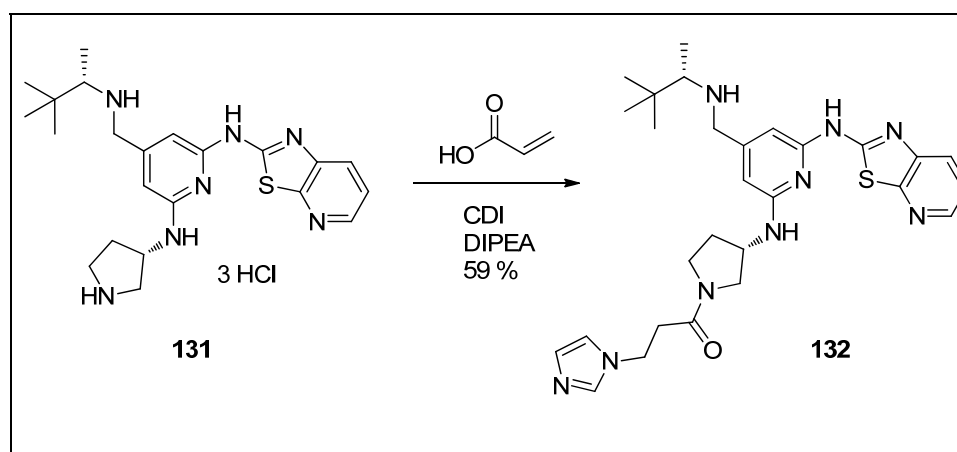


Figure 77. HPLC profiles of the various amide coupling reactions to prepare compound **107**, with, from top to bottom, T3P[®], PyBOP[®] and COMU



Scheme 58. Side product formed during the amide coupling with CDI

Investigation of the amide coupling with T3P[®] revealed that if excess of acrylic acid and coupling reagents were used, an increasing amount of side product **114** was formed, whatever the temperature of the reaction. Using 1.1 equivalents of acrylic acid and T3P[®] with 5 equivalents of DIPEA provided the best compromise between

completion of the reaction and formation of the side product **114**. Various attempts at recrystallizing the crude material failed to remove the impurities seen at 1.758 and 1.879 minutes in the HPLC trace (Figure 77). In collaboration with the purification department of our laboratories,¹⁹⁴ a reverse phase chromatography method, using TFA modifier, was developed to provide the product **107** with purity greater than 99 % by HPLC (Figure 78). A 65 % yield was obtained for the overall reaction, limited by the difficult purification required to provide material with high purity.

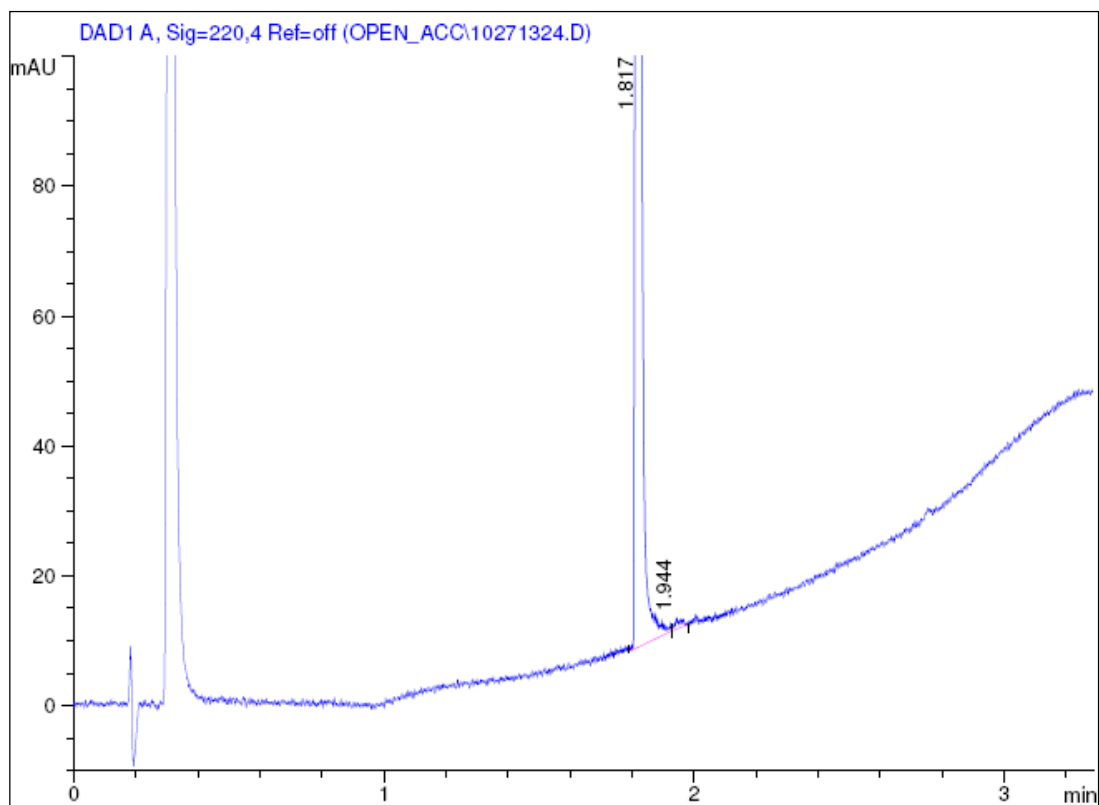


Figure 78. HPLC spectrum for compound **107** after reverse phase purification

A solvent screening of the amide coupling reaction with T3P[®] was performed to attempt to remove the impurities seen at 1.758 and 1.879 minutes (Figure 77) and eliminate the need for reverse phase purification. A range of solvents were tested (Table 46) and the reactions were monitored by HPLC and compared to the profile obtained in DCM (entry 1). The amount (%) of both impurities were normalised to the amount of product formed. No major changes in the ratio of product **107**:impurities were observed in THF and acetonitrile (Table 46, entries 2 and 3). However, in THF, the solubility of the starting material **131** was lower resulting in

incomplete reaction. In acetonitrile, many other baselines impurities were seen compared to the clean profile in DCM. Finally, the intermediate **131** was found to be quite insoluble in MeTHF and 1,4-dioxane leading to poor conversion to compound **107** (Table 46, entries 4 and 5). The results obtained in DCM, THF and MeCN indicate that the rate of the formation of the impurities at 1.76 mins and 1.88 mins is independent of the solvent used. DCM remained the solvent providing the cleanest profile for that reaction. Hence, no improvement was delivered when compared to the 65 % yield reported previously for the transformation.

Table 46. Solvent screen for the amide coupling to prepare compound **107**

Entry	Solvent	% impurity at 1.76 mins ^a	% impurity at 1.88 mins ^a	Comment
1	DCM	4	1.3	Still 5 % of 131 no other impurity > 1 %
2	THF	5.7	1.6	Still 19 % of 131 no other impurity > 1.5 %
3	MeCN	5.6	1.3	Still 4 % of 131 Many baselines impurities
4	MeTHF	NA	NA	131 not soluble - 54 % conversion
5	1,4-dioxane	NA	NA	131 not soluble - 14 % conversion

^a Determined by HPLC analysis

The new synthesis of the irreversible ITK inhibitor **107** (Scheme 56) proved to be more suitable to large scale operation than the initial route developed during the optimisation of the top amine motif (Scheme 55). Indeed, the key Buchwald-Hartwig coupling requiring 30 % of precatalyst **87** is currently three steps before the isolation of the final product **107** compared to six steps for the original synthesis. The number of column chromatography purifications has been reduced from three to two (note that it was later discovered¹⁸⁷ that the column chromatography used to purify **138** was unnecessary, leaving only one column purification in the whole synthetic scheme) and the number of reaction steps from ten to seven. Finally, the difficult amination reaction described during the synthesis of compound **101** (synthesis of

intermediate **98**, Scheme 48) was performed in the first step of the synthetic scheme. This allowed a much better turnover of the reaction while the pressure required in the autoclave decreased from 20 to 17 bar. Overall, although this succession of reactions was suitable to prepare quantities of compound **107** for 14 day rat and dog safety studies (26 g of product for each study), should the inhibitor progress to clinical studies (usually requiring > 500 g of material) then the high catalyst loading for the Buchwald-Hartwig coupling and the HPLC purification for compound **107** would need to be addressed.

2. Genotoxicity results

The maleic acid salt of compound **107** was prepared and submitted to the Ames test and the MLA (Figure 79).

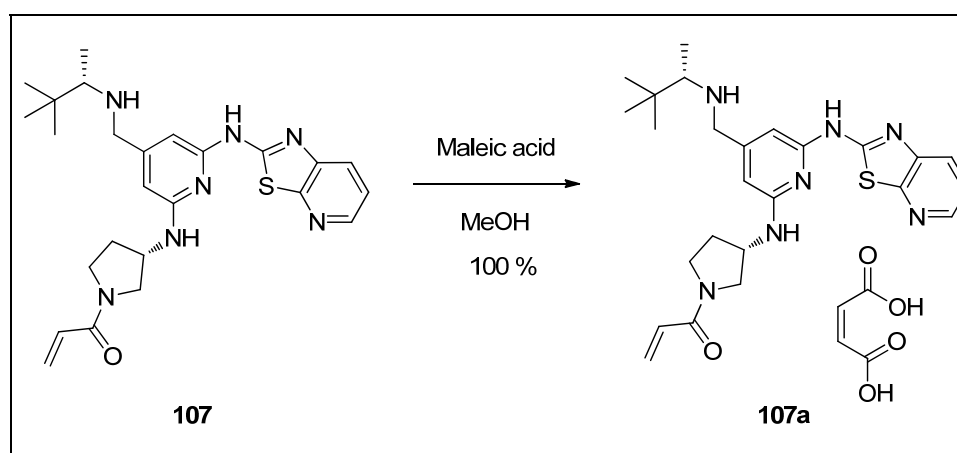


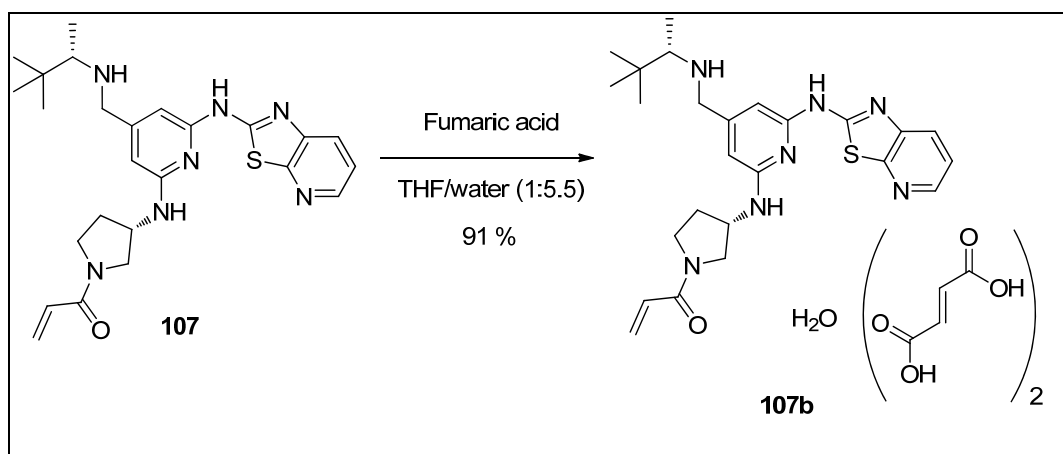
Figure 79. Synthesis of compound **107a**

In agreement with the data measured for compound **101a** (section 2), no mutagenic response was observed in the Ames assay during the testing of the inhibitor **107a**.¹⁷⁸ Interestingly, this compound was also reported negative from the MLA and was therefore considered safe from any mutagenic risks.¹⁷⁹ With regards the rationale behind the difference in mutagenicity effects seen in the MLA for compounds **101a** and **107a**, one can postulate that the various top amines (*cis*-2,6-dimethylmorpholine and (2*S*)-3,3-dimethyl-2-butanamine) confer different selectivity profiles to the molecules which could contribute to the difference of data seen in the MLA.

The discharge of mutagenicity risks obtained for compound **107** resulted in further progression of the potential drug towards candidate selection.

3. *Crystallisation work*

The development of a drug for inhaled administration requires identification of a crystalline form of the final active substance. The crystalline material requires micronization to obtain homogeneous particles with suitable size for inhalation.¹⁹⁵ Particle sizes between 0.5 and 8 μm are believed to have maximum chances to be delivered in the lower respiratory tract while particles larger than 10 μm are usually deposited in the upper respiratory tract.¹⁹⁶⁻¹⁹⁸ Therefore, to ensure compound **107** could be efficiently administered by inhalation *in vivo*, a crystalline form of the molecule had to be developed to allow reproducibility of the micronization process. Various attempts at recrystallising compound **107a** did not provide crystalline material when assessed by microscopy and X-Ray powder diffraction (XRPD). Further investigation of this recrystallisation by temperature cycling experiments¹⁵⁷ did not result in any improvements. Therefore, the decision to investigate the crystallisation of a different salt was taken. A salt screen performed in the Product Development Department of our laboratories¹⁹⁹ revealed that crystalline material of compound **107** was obtained with fumaric acid from a THF/water mixture (~ 1:5.5 ratio). Scale-up to 30 g of compound **107** yielded the desired crystalline material **107b** with a 91 % yield (Scheme 59).¹⁸⁷ The ¹H NMR spectrum indicated the compound was a difumaric acid salt while the differential scanning calorimetry (DSC)/thermal gravimetric analysis (TGA) analyses (Figure 80) showed evidence of the material to be the monohydrate. Finally, microscopy and XRPD measurements demonstrated the crystallinity of compound **107b** (Figure 81, Figure 82).



Scheme 59. Synthesis of the crystalline material 107b

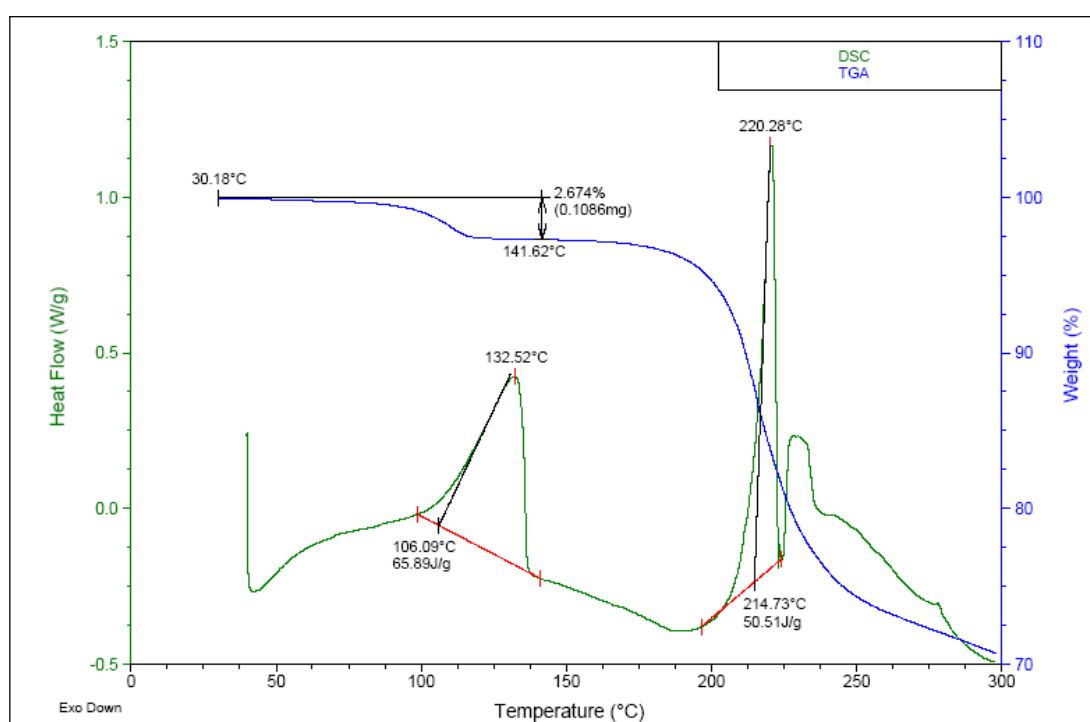


Figure 80. DSC (green curve) and TGA (blue curve) traces for compound 107b

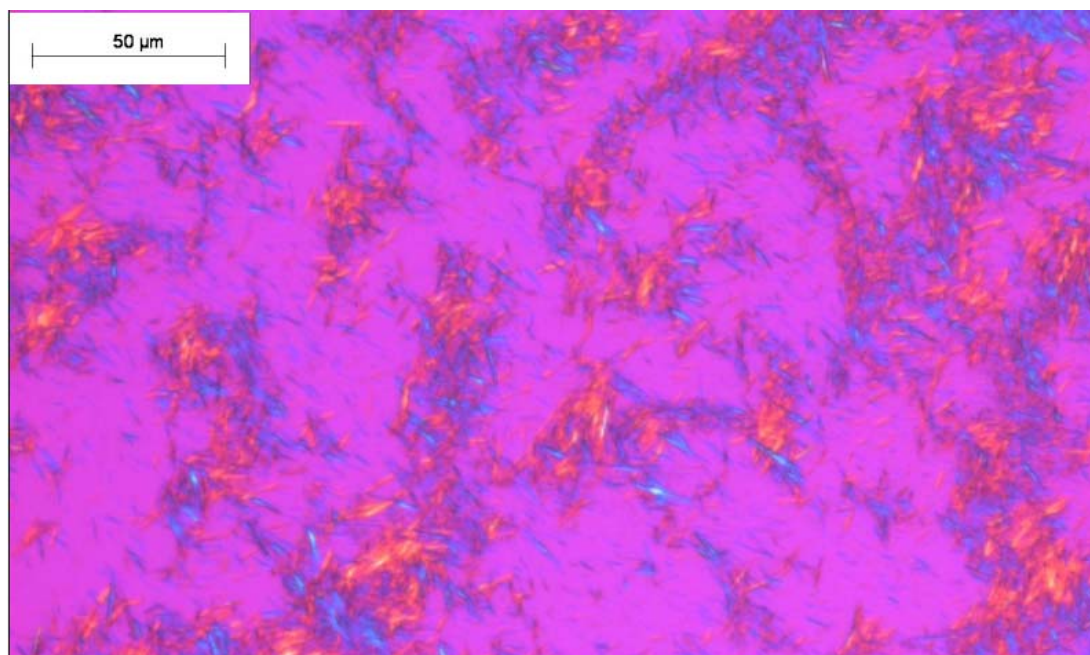


Figure 81. Microscopy image of compound **107b** displaying birefringent crystals

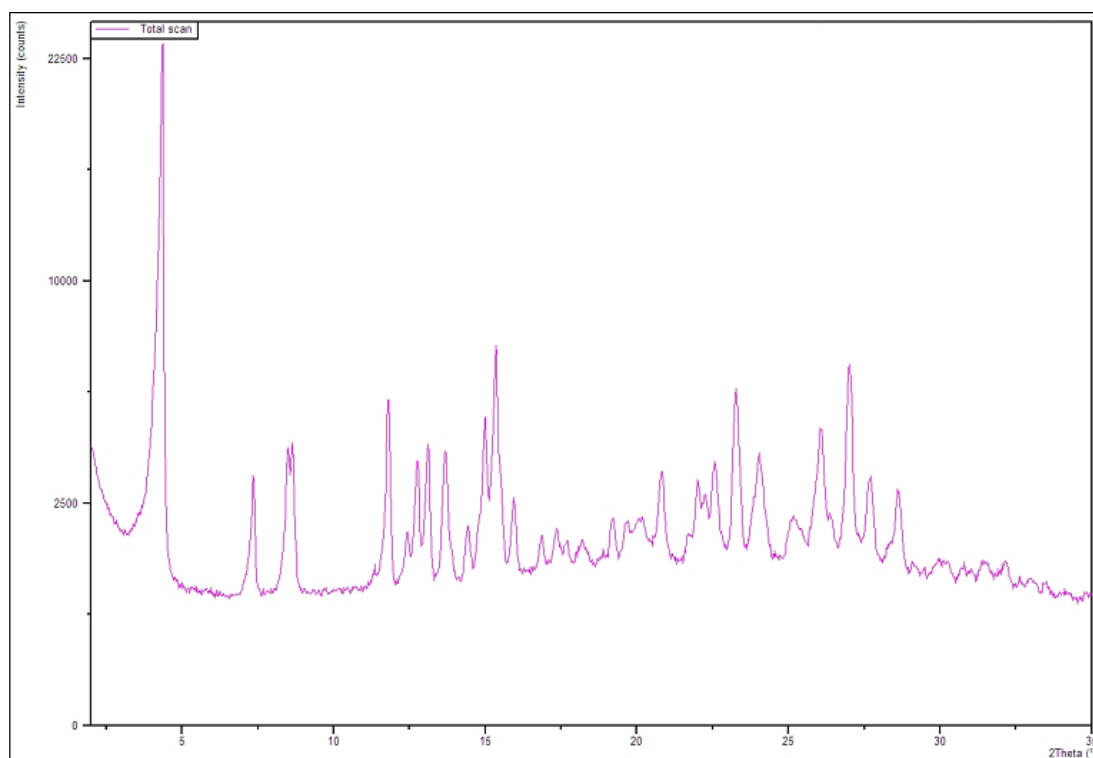


Figure 82. XRPD spectrum for compound **107b**

The SLF solubility of the compound **107b** was measured to ensure the new salt version and the crystalline arrangement did not dramatically decrease the solubility of the drug below the required 250 μg/mL.¹⁹⁹ As expected, the values were lower

than that measured for the amorphous maleic acid version **107a** (Table 47), but remained acceptable to avoid lung macrophage toxicity risks.¹⁹⁹ Moreover, it was envisaged that the reduction of the particle size of compound **107b** by micronization would have resulted in an increase of the SLF solubility over that reported in Table 47,^{200,201} further reducing any lung toxicity risks due to poor dissolution of the compound into lung fluid.

Table 47. SLF solubility data for compounds **107b**¹⁵²

Time (hours)	Solubility (µg/mL)	
	107a	107b
0.5	1430	423
4	1440	415
24	1320	398

The micronization of compound **107b** successfully yielded homogeneous crystals with particle sizes ranging between 1.1 and 1.3 µm.¹⁵²

The successful identification of a crystalline form for compound **107** prompted the investigation of the purification of the final amide coupling reaction by direct crystallisation of compound **107b**. Indeed, during the salt screen performed by the Product Development Department of our laboratories,¹⁵⁷ various attempts at recrystallising the free base **107** proved unsuccessful. As a consequence, the only opportunity left to remove the impurities seen at 1.758 and 1.879 minutes in the HPLC trace (Figure 77) without the need of column chromatography was to crystallise the crude product from the amide reaction directly into **107b** (Figure 83). Crystallisation of the crude product **107** following the method described in Scheme 59 did not successfully remove the desired impurities. A white solid was obtained from the crystallisation with a purity profile similar to the crude material from the amide reaction.

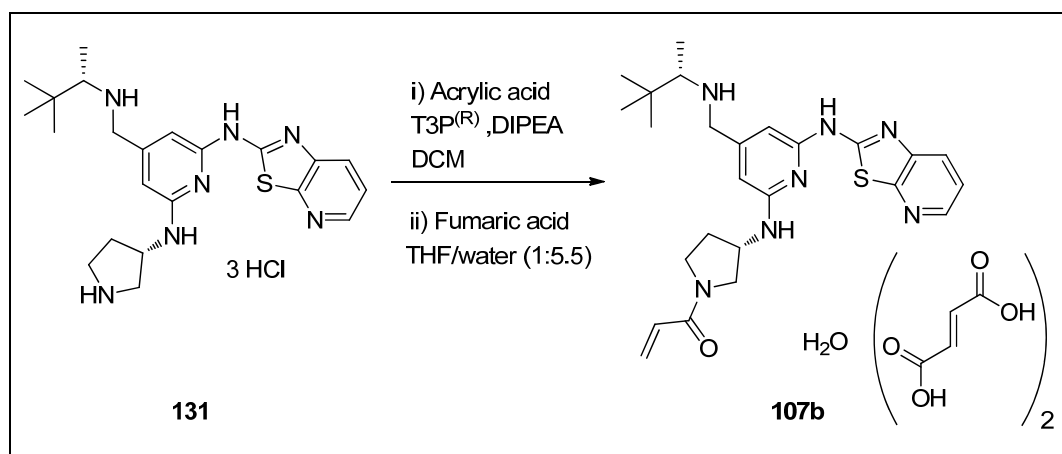


Figure 83. Attempt at purifying the amide coupling reaction by direct crystallisation of **107b**

As the desired crystalline material **107b** was required to be prepared with high purity for the 14 day animal toxicology studies (> 98 % purity with no impurities greater than 1 %) and the fact that the reverse phase chromatography could be performed on large scales, the optimisation of this reaction was not pursued any further. The amide coupling process described in Scheme 56 was used to prepare the required material for both safety studies.

4. Lung and DMPK data

Overall, compound **107b** exhibited the best irreversible ITK inhibitor overall profile from the amino-benzothiazole template. This profile was fulfilling the requirements for a drug candidate for the ITK programme. However, for the compound to be tested in the clinic, an effective dose had to be selected. The typical way of assessing clinical doses consists of analysing the efficacy data obtained in an *in vivo* model and combining them with the results from the DMPK studies in various species. Scaling models can then be used to predict the human pharmacokinetics hence the dose required to achieve inhibition.^{202- 207} As the inhaled *in vivo* disease model was not performing consistently for the programme, the efficacy of the compound was assessed by measuring inhibition in human lungs.

Compound **107** was tested for inhibition of the release of the IFN- γ in human lung tissues. Inhibition data obtained for the potent inhibitor demonstrated an encouraging pIC₅₀ of 7.5,¹⁰⁸ proving that the compound had anti-inflammatory efficacy in human

lung tissues. Moreover, the human lung tissue binding under these conditions was measured at 82 %, ³⁷ indicating that a good free fraction was available to inhibit ITK. Therefore, it was concluded that as long as the drug was reaching the site of action after inhaled administration, compound **107** should demonstrate anti-inflammatory efficacy *in vivo*.

The DMPK data recorded for compound **107a** after oral and intravenous administration³⁷ (at the time of the study compound **107b** was not available) highlighted acceptable parameters for an inhaled drug, with, in particular, a high clearance and no bioavailability measured after oral administration (Table 48).

Table 48. DMPK data for compound **107a** after oral and intravenous administration³⁷

Compound	Clearance (Cl)	T _{1/2}	V _{dss}	Bioavailability
107a	47 mL/min/kg (55 % of the liver blood flow)	2.2 h	5.6 L/h	negligible

Data from the human lung tissues and the DMPK studies supported the emerging evidence that the inhibitor **107** had the required profile of a potent inhaled drug. In the absence of an *in vivo* disease model, the inhibitor was directly subjected to the 14 day rat toxicology study.

5. 14 Day rat toxicology study results and inhaled *in vivo* pharmacodynamic (PD) model

The toxicology of the irreversible ITK inhibitor **107** was assessed in a 14 day rat inhalation study. The lack of a meaningful PD model for this programme did not allow calculation of the various clinical doses at which the inhibitor could be predicted to produce a beneficial anti-inflammatory effect. Therefore, the rat toxicology study had to be run at doses which would support for the administration of the maximum inhaled dose allowed in clinical studies by the Safety Assessment Department of our laboratories.¹⁷³ Various rats were administrated with the

micronized compound **107b** at doses of 120, 600 and 3000 µg/kg/day for 14 days. Daily observations, body weight and food intake were recorded during the time of the study, as well as a full clinical pathology at the end of the study.

No significant in-life indicators of toxicity were noted during the 14 days, at any of the doses. Although a slight reduction in food intake accompanied by reduced body weight gain was recorded in males at 3000 µg/kg/day, the compound was believed to be acceptable for further progression. However, at all doses, a significant irritation of the animal's larynx was observed which would not support the progression of the compound to the clinic at 1 mg per day. Moreover, an unexpected dose related inflammation throughout the airways was detected. These two main toxicology findings prevented the progression of the drug to further clinical studies.

Although the causes of these safety findings remain unknown, one can postulate that they are related to the high doses of compound administered to the rats. Indeed, these doses were selected to cover for the maximum inhaled dose allowed in clinical studies by our Safety Assessment Department,¹⁷³ as the absence of a PD model prevented the team from predicting the doses of compound required to produce the desired anti-inflammatory response. However, such high amounts of the irreversible inhibitor in the animals might have triggered some undesired selectivity issues, leading to inflammation in the lung. Moreover, at such doses, large numbers of inhibitor particles were more likely to deposit on the larynx, causing irritancy.

To understand these results, efforts were directed at developing an inhaled PD model with the aim of confirming the efficacy of the lead irreversible ITK inhibitor **107** at low doses. An *in vivo* rat PD model was developed by the biologists within our laboratories²⁰⁸ and the micronized compound **107b** was tested at the initial high dose of 2.3 mg/kg. This high inhaled dose was used to confirm the validity of the PD experiment. After administration of the drug by inhalation, the lung suspensions were activated *ex vivo* with anti-CD3 and the expression of CD25 (a cell surface marker of inflammation) was measured by flow cytometry in CD4 cells. The results from this study are presented in Figure 84. Without activation of the TCR with anti-CD3 (control), the median fluorescence intensity (MFI) of CD25 remained extremely low for both the rats administered with the inhibitor **107b** (red control bar) and those that

did not breathe the drug (blue control bar). Activation of the inflammation with anti-CD3 resulted in an expected increase of CD25 protein for the rats that were not treated with any compound (blue anti-CD3 bar). Interestingly, complete inhibition of CD25 was observed with the ITK inhibitor **107b** (red anti-CD3 bar), suggesting that, at this concentration, the compound totally blocked the T cell inflammation response.

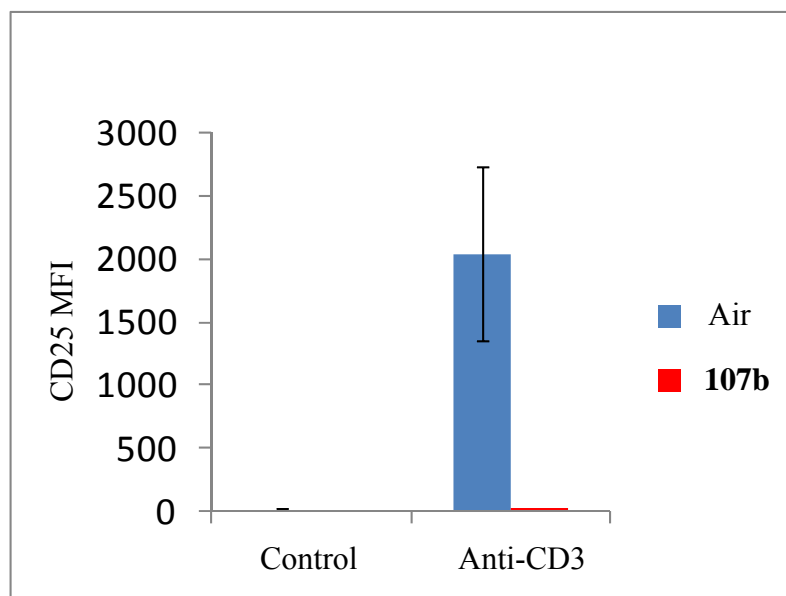


Figure 84. Rat *in vivo* PD model results following inhaled administration of micronized compound **107b** (2.3 mg/kg)

The results from this rat PD study were extremely encouraging as they prove that for the first time since the start of this ITK programme (both reversible and irreversible efforts), a significant anti-inflammatory response was measured after inhaled administration of an ITK inhibitor. To understand the levels of compound deposited in the lungs to achieve this efficacy, DMPK studies were performed during the PD experiments.³⁷ Analyses of the concentrations of compound located in the lung over time are presented in Figure 85. Over the 24 hour time of the experiment, the levels of inhibitor **107** in the lungs remained higher than the IC_{50} of 7.5 measured in the lung tissue (section VII.4) for at least 15 hours. As the *ex vivo* analysis was performed within the first 30 minutes of the study, the levels of inhibitor in the lungs were high (> 1000 ng/mL), well over the IC_{50} , explaining the near to complete inhibition of CD25 observed in Figure 84.

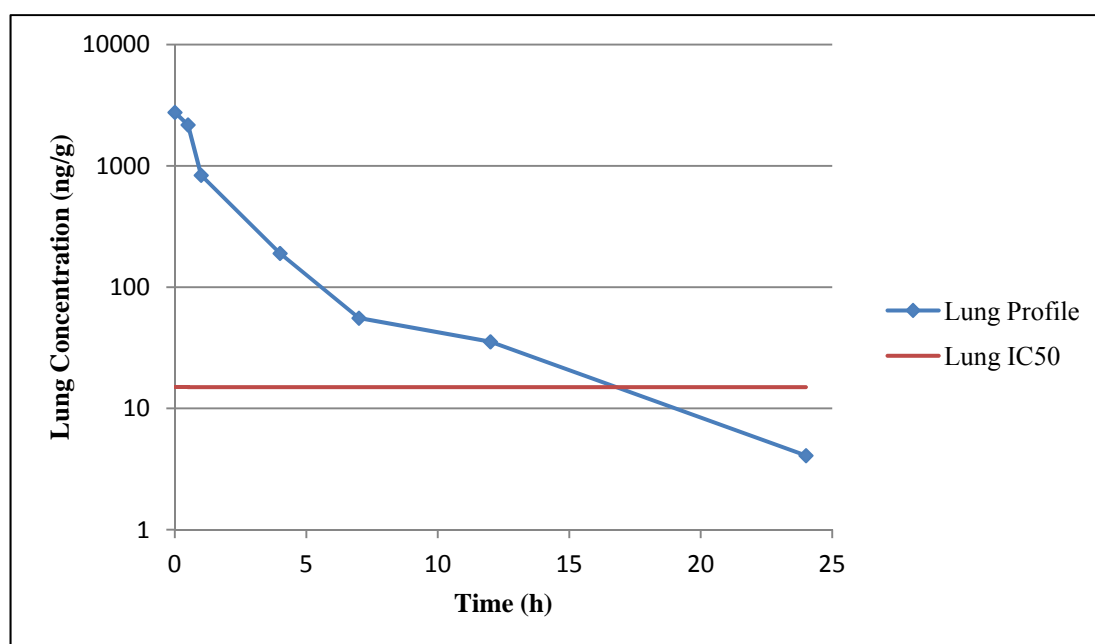


Figure 85. Rat lung concentrations of compound **107b** following inhaled dosing at 2.3 mg/kg

The inhibitor **107b** was then tested in the inhaled PD model at the lower dose of 3 $\mu\text{g}/\text{kg}$. This dose is significantly lower than the doses used in the 14 day rat toxicology studies and has the potential to provide a safe therapeutic window for the use of the inhibitor **107b**. From the data presented in Figure 86, a clear reduction of CD25 was achieved for the animals treated with the irreversible ITK inhibitor **107b** (red anti-CD3 bar) compared to the control animals (blue anti-CD3 bar). These results were extremely encouraging for this research programme as it demonstrated *in vivo* efficacy of the lead ITK inhibitor **107b** at extremely low doses. Nevertheless, for that compound to be of any use in clinical studies, its therapeutic index needs to be established using additional toxicity studies.

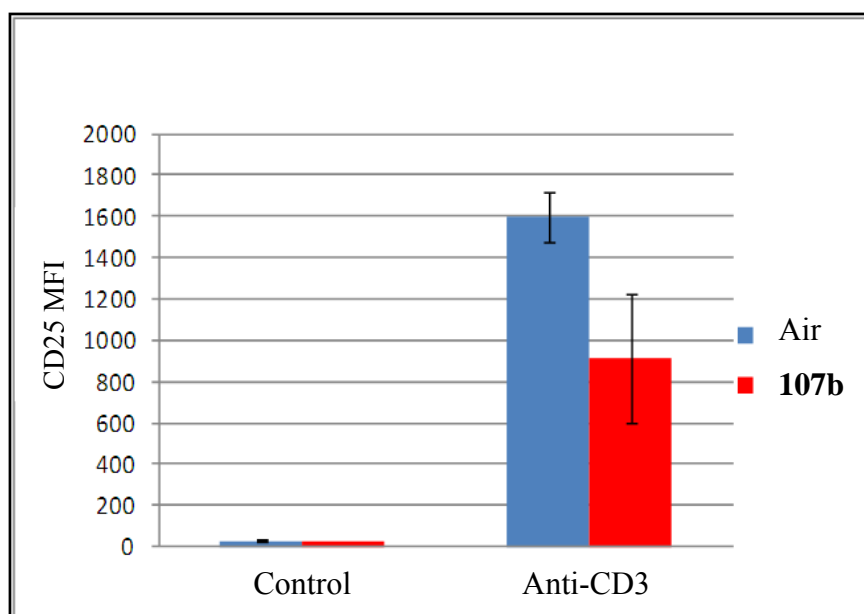


Figure 86. Rat *in vivo* PD model results following inhaled administration of micronized compound **107b** (3 $\mu\text{g}/\text{kg}$). Animals were dosed once daily for 3 days.

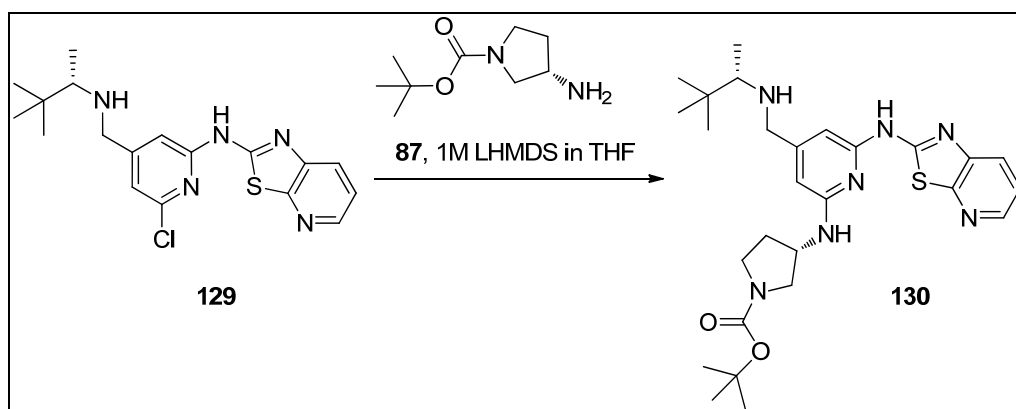
Despite the encouraging data presented in Figure 86, the repeat of the inhaled rat *in vivo* PD model at these technically challenging to deliver low doses (around 3 $\mu\text{g}/\text{kg}$) resulted in variable data with no clear anti-inflammatory effect of the compound on the treated animals. It was therefore decided to stop the progression of the compound at this stage of this research programme as a safe therapeutical window for the use of the inhibitor **107b** had not been clearly achieved.

6. Investigation of the Buchwald-Hartwig coupling

Compound **107b** was prepared for 14 day rat and dog studies (note that the dog toxicology study was not performed as the progression of the inhibitor was halted after the 14 day rat study) following the protocol described in Scheme 56 and in Scheme 59. A total of 86 g of material **107b** was obtained with sufficient purity (> 99 %) to be submitted to the rat safety studies.¹⁸⁷

However, the Buchwald-Hartwig amination reaction, used to convert the analogue **129** into the compound **130**, unexpectedly required 30 % of precatalyst **87** and was therefore further investigated.

The initial target consisted in reducing the amount of precatalyst **87** to 20 mol % and varying the rest of the conditions to allow full conversion of the starting material **129** into the desired analogue **130** (Scheme 60). The typical conditions employed with this template (1.1 eq of amine, 3 eq of LHMDS) resulted, after one hour at 50 °C, in 61 % conversion to compound **130** by LCMS analysis (Table 49, entry 1. Note that the % conversion refers to the formation of product relative to starting material. The % of impurities formed were not taken into account). Extending the reaction time to 16 hours under the same conditions did not improve the transformation (Table 49, entry 2), while sideproducts started to be observed in the LCMS spectrum. Studies of the reaction from the Caddick group revealed that THF as solvent and LHMDS as base were optimal for this transformation.¹⁴⁸ As a consequence, these two parameters were not changed in this reaction optimisation. On a large scale, premixing of the precatalyst **87** and LHMDS to form the active Pd⁽⁰⁾ species (Figure 54) before addition to the reaction mixture resulted, with 30 % catalyst, in consistent total conversion to the desired intermediate (section VII.8.1). Applying this technique to the desired transformation on small scale did not result in a dramatic improvement in the conversion of the intermediate **129** (Table 49, entry 3). Increasing the amount of amine, as suggested by the Caddick research group, resulted in the same conversion to the product (Table 49, entry 4). Decreasing the amount of LHMDS from 3 equivalents to 1.5 equivalents resulted in no reaction (Table 49, entry 5). This finding is in accordance with reports from the literature stating that excess LHMDS is required to couple amines to aryl and heteroaryl halides possessing protic functional groups.^{135,138,140,209-211} Increasing the excess of LHMDS to 6 equivalent unexpectedly decreased the conversion to the product (Table 49, entry 6). Finally, and once again in accordance with the reaction details provided by Caddick's group, the amination reaction was found to be rapid, with the maximum 72 % conversion obtained within 30 minutes (Table 49, entry 7). As already discussed in the section VII.8.1, increasing the temperature to 70 °C resulted in a more complex reaction profile without dramatically improving the conversion of the substrate **129**.



Scheme 60. Investigation of the amination coupling conditions to prepare the analogue **130**

Table 49. Optimisation of the Buchwald-Hartwig coupling to prepare compound **130** (the reaction temperature was set at 50 °C unless stated)

Entry	Amine (eq)	87 (eq)	LHMDS (eq)	Heating time	% conversion ^a
1	1.1	0.2	3	1 h	61 %
2	1.1	0.2	3	16 h	62 %
3	1.1	0.2 ^b	3 ^b	1 h	72 %
4	2	0.2 ^b	3 ^b	1 h	61 %
5	1.1	0.2 ^b	1.5 ^b	1 h	No product
6	1.1	0.2 ^b	6 ^b	1 h	45 %
7	1.1	0.2 ^b	3 ^b	30 mins	72 %
8	1.1	0.2 ^c	3 ^c	30 mins	75 %

^a Determined by LCMS analysis, ^b 87 and LHMDS premixed and added to the reaction, ^c Reaction temperature set at 70 °C

The data obtained so far for this amination coupling indicates that, after 30 minutes, the active Pd⁽⁰⁾ species is not available for the catalytic cycle. This tends to suggest

that it has been poisoned by one or various components of the reaction mixture. The substrate **129**, product **130** or the 1,1-dimethylethyl (3*S*)-3-amino-1-pyrrolidinecarboxylate could all be responsible for chelating and inactivating the Pd species. The chelation of the 1,1-dimethylethyl (3*S*)-3-amino-1-pyrrolidinecarboxylate analogue is feasible although unlikely as this amine has already been successfully used in Pd-mediated amination reactions using low quantities of catalyst and leading to high product yields.²¹²⁻²¹⁴ Therefore, species **129** and **130**, once deprotonated by LHMDS, were believed to chelate to the Pd catalyst and remove it from the amination catalytic cycle. Potential chelated species are presented in Figure 87. The Hartwig research group has already reported similar species, with heteroaryl substrates displacing phosphine ligands from the palladium catalyst through basic heterocyclic nitrogen units (*e.g.* pyridine).^{215,216} The newly formed pyridine complexes do not catalyse the amination reaction of aryl chloride. In the case of our reaction, the formation of these complexes could be competing with the oxidative addition of the Pd⁽⁰⁾ with the chloropyridine. With 30 % of precatalyst **87**, enough quantities of Pd⁽⁰⁾ could stay activated to allow the completion of the reaction.

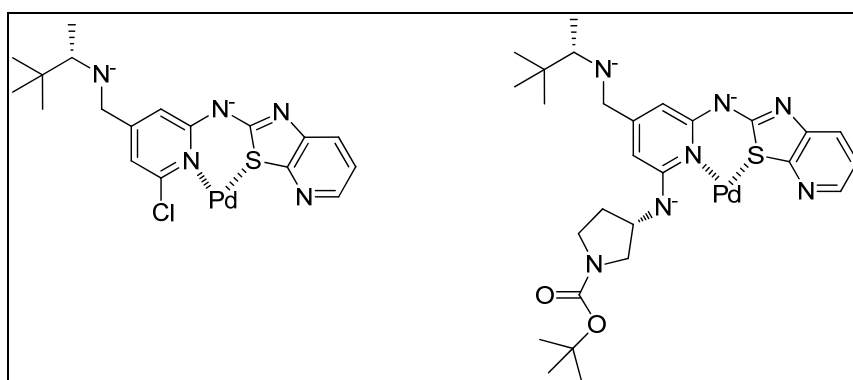
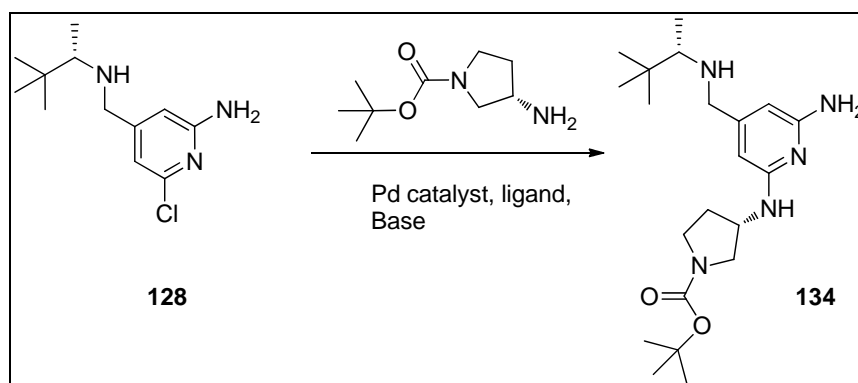


Figure 87. Potential chelated species obtained between the substrates **129** and **130** with Pd⁽⁰⁾

To test this hypothesis, the amination reaction was attempted between the intermediate **128** and the 1,1-dimethylethyl (3*S*)-3-amino-1-pyrrolidinecarboxylate analogue (Scheme 61). In relation to this, it was felt that, without the aminobenzothiazole unit, the palladium would be less likely to chelate to the pyridine analogues **128** and **134**. Therefore, the reaction should be able to reach completion

without the need of 30 % of precatalyst **87**. However, processing this amination reaction before adding the aminobenzothiazole unit had not been undertaken previously as two main side products, presented in Figure 88, were expected to be formed during the course of the reaction. The formation of these compounds would obviously decrease the yield of the desired transformation but would not affect the results associated with the chelation hypothesis, as active Pd⁽⁰⁾ is required to create both molecules.



Scheme 61. Preparation of compound **134** to confirm the chelation hypothesis between Pd⁽⁰⁾ and compounds **129** and **130**

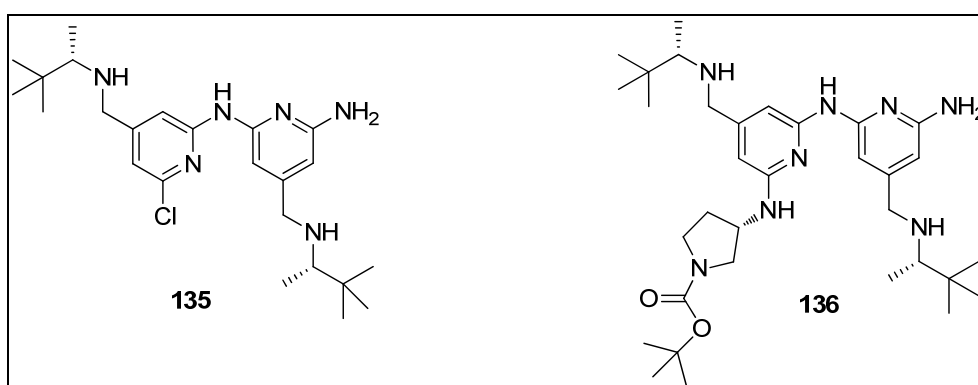


Figure 88. Potential sideproducts formed during the amination reaction described in Scheme 61

To reduce the coupling of compound **128** with itself (leading to the formation of the analogues **135** and **136**) and to encourage the desired amination reaction (Scheme 61), an excess of 1,1-dimethylethyl (3*S*)-3-amino-1-pyrrolidinecarboxylate (4 eq) was employed. The reaction was initially attempted with 10 % of precatalyst **87** and 3.1 equivalents of LHMDS. After one hour stirring at 70 °C, an encouraging 43 % of

product **134** was observed by LCMS (Table 50, entry 1. Note that the % conversion refers to the formation of product relative to starting material. The % of impurities formed were not taken into account). The same reaction was left heating and stirring overnight (20 hours) and resulted in full conversion of the intermediate **128** (Table 50, entry 2). The LCMS analysis also indicated the formation of the side product **136** at a level of 25 % (Note that the amount (%) of compound **136** was normalised to the amount of product formed). Purification of the product by MDAP provided compound **134** with a 43 % yield. The impurity **136** was later isolated (Table 50, entry 5) and its structure was confirmed by NMR. This result supported the chelation hypothesis between the palladium complexes and compounds **129** and **130** previously discussed. Indeed, without the aminobenzothiazole unit, the substrates **128** and **134** were not chelating the active Pd⁽⁰⁾ species allowing the catalyst (10 %) to remain active over time and consume all of the starting material **128**. The rate of the reaction was then further studied, this time at 50 °C (Table 50, entry 3, 4 and 5) to investigate whether the formation of the side product **136** was temperature related. The conversion to the product **134** gradually increased over time and reached completion overnight. The product was isolated with the same yield and the impurity **136** was formed with a similar ratio. Reducing the loading of precatalyst **87** to 5 % resulted in incomplete reaction, even after heating at 50 °C for 48 hours (Table 50, entry 6 and 7). Full conversion was restored by increasing the temperature to 70 °C (Table 50, entry 8). However, at such temperature with 5 % of precatalyst **87**, the isolated yield of compound **134** was lower than that obtained with 10 % of palladium (Table 50, entry 2 and 8).

Table 50. Investigation of the Buchwald-Hartwig amination reaction with the substrate **128**

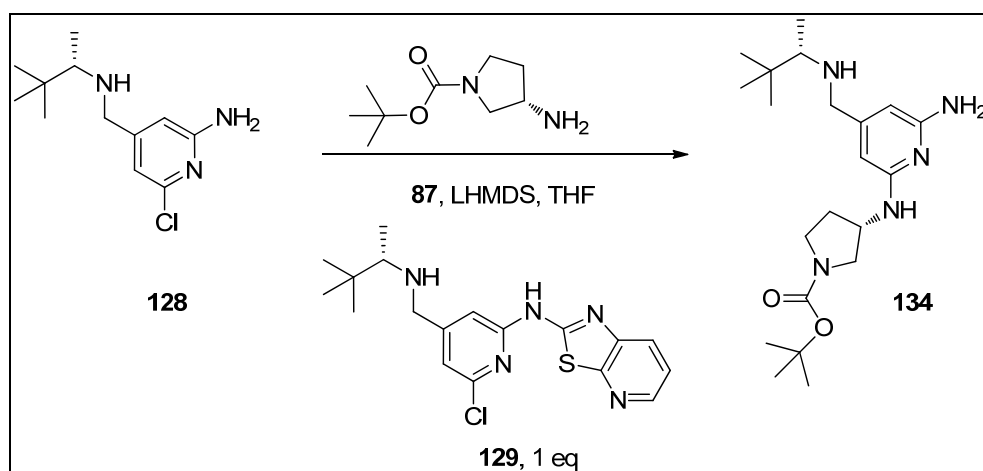
Entry	Pyrrolidine (eq)	87 (eq)	LHMDS (eq)	Heating time	T (°C)	% conversion ^a (isolated yield) ^b	Comment ^c
1	4	0.1	3.1	1 h	70 °C	43 %	
2	4	0.1	3.1	20 h	70 °C	100 % (43 %)	peak for 136 (25 % by LCMS)
3	4	0.1	3.1	3 h	50 °C	66 %	
4	4	0.1	3.1	8 h	50 °C	91 %	
5	4	0.1	3.1	24 h	50 °C	100 % (38 %)	peak for 136 (17 % by LCMS)
6	4	0.05	3.1	24 h	50 °C	65 %	
7	4	0.05	3.1	48 h	50 °C	80 % (17 %)	peak for 136 (13 % by LCMS)
8	4	0.05	3.1	24 h	70 °C	100 % (24 %)	peak for 136 (23 % by LCMS)

^a Determined by LCMS analysis. ^b Product isolated by MDAP. ^c The amount (%) of compound **136** was normalised to the amount of product formed

The conditions described in Table 50, entry 5 were scaled up to 540 mg of intermediate **128** and yielded, after 16 hours reaction time and column purification, 52 % of product **134**.

To confirm the chelation hypothesis described in Figure 87, the same conditions (Table 50, entry 2) were attempted but this time adding one equivalent of compound **129** to the reaction mixture (Scheme 62). Poisoning of the catalyst by the substrate **129** would prevent the turnover of compound **128** into compound **134**. LCMS analyses of the reaction mixture after one hour was similar to the profile observed after 4 hours, with only 10 - 15 % of product **130** being formed and no peaks

corresponding to compound **134**. Most of two starting materials **128** and **129** remained untransformed, characteristic of poisoning of the active Pd⁽⁰⁾ species.



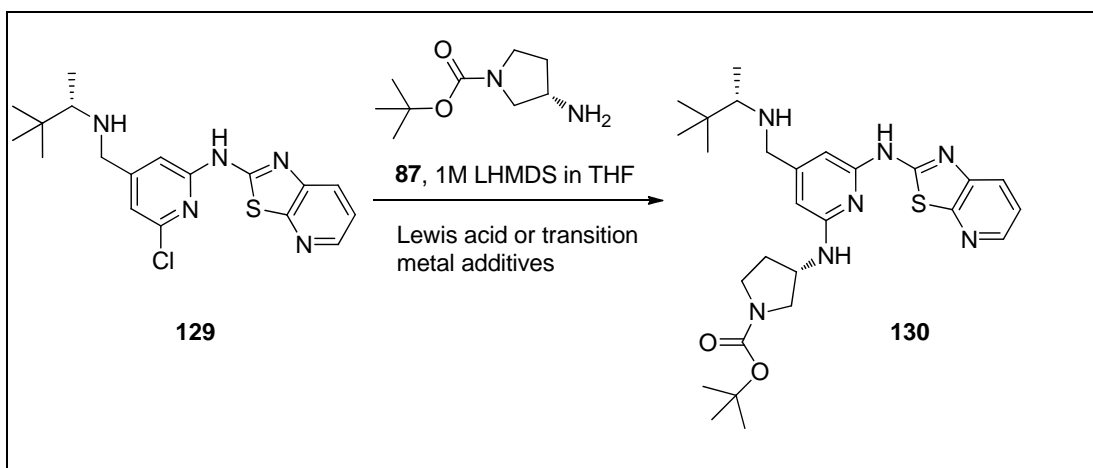
Scheme 62. Attempt to prepare compound **134** in the presence of the intermediate **129**

These studies indicated that 30 % of precatalyst **87** was necessary to allow full conversion of the substrate **129** within the transformation described in Scheme 60 potentially due to the chelation of the substrate **129** and the product **130** to the active palladium species. Performing the Buchwald-Hartwig amination coupling on the intermediate **128** yielded the desired product **134** with reduced amount of precatalyst **87** (10 % was found optimal, Table 50) but the transformation was not believed to add any advantages compared to the current process (Scheme 56) on large scales, as the product **134** had to be purified by column chromatography.

Two approaches were undertaken to prevent the poisoning of the Pd⁽⁰⁾ catalyst during the transformation of compound **129** into compound **130**: firstly, Lewis acids or other transition metals were added to the reaction mixture to force chelation of the two substrates to those and not the active Pd⁽⁰⁾; and secondly, the amination conditions developed by the Buchwald's research group,^{131,138} using of the precatalyst **86** and ligand **L¹** (Table 15, entry 1 and Figure 53), which achieved full conversion of the chloropyridine intermediate with only 10 % of catalyst were reconsidered. This system was not suitable for large scale synthesis as the precatalyst **86** and ligand **L¹** are not readily commercially available and require various steps to be prepared.^{131,139} However, these results indicate that the careful choice of the palladium catalyst could

reduce the chelation of the analogues **129** and **130**, allowing the reaction to be successful with lower loadings of catalyst. Therefore, investigating other palladium catalyst coupling reagents was also performed.

A range of Lewis acid and transition metals were investigated as additives to the amination reaction to prevent chelation of compounds **129** and **130** to the active palladium catalyst (Scheme 63).



Scheme 63. Investigation of additives to prevent poisoning of the precatalyst **87** during the Buchwald-Hartwig amination reaction

The reactions were all performed on 25 mg of substrate **129**, 10 mol % of precatalyst **87**, 1.1 equivalent of 1,1-dimethylethyl (3*S*)-3-amino-1-pyrrolidinecarboxylate and 3 equivalents of LHMDS in THF. One equivalent of each additive was added to the reactions which were monitored by LCMS after 1 and 16 hours stirring at 50 °C. In the absence of additives, around 30 % conversion to the product **130** was observed after 1 and 16 hours (Table 51, entry 1. Note that the % conversion refers to the formation of product relative to starting material. The % of impurities formed were not taken into account). LiCl and CuI did not prove to significantly affect the profile of the reaction (Table 51, entry 2 and 3). Although the conversion with CuI was slightly better, it did not change over time, characteristic of the inactivation of the Pd⁽⁰⁾ species. The reactions with the other additives (Fe(acac)₃ and ZnCl₂, (Table 51, entry 4 and 5)) did not produce any product **130**; the substrate **129** was the only

species observed in the LCMS analysis. These additives must have poisoned the precatalyst **87** before any reaction could have taken place.

Table 51. Investigation of additives to prevent poisoning of the precatalyst **87** during the Buchwald-Hartwig amination reaction

Entry	Additive	% conversion to 130 at 1 h ^a	% conversion to 130 at 16 h ^a
1	None	30 %	24 %
2	LiCl	35 %	35 %
3	CuI	44 %	41 %
4	Fe(acac) ₃	0 %	0 %
5	ZnCl ₂	0 %	0 %

^a Determined by LCMS analysis

Although other Lewis acids could have been investigated as additive (e.g. Ag₂CO₃), this approach did not seem to be providing fruitful results. Therefore, efforts turned to the development of a new catalytic system which would allow the coupling to occur without chelation of the compounds **129** and **130** to the active palladium species.

The hunt for suitable palladium catalysts for this transformation had, so far, indicated that only precatalysts able to rapidly form the active Pd⁽⁰⁾ species^{131,148} were effective at converting the intermediate **129** into the product **130**. In their review on palladium-catalysed amination reactions,¹³¹ Surry and Buchwald describe the precatalyst **86** and ligand **L**¹ system as one of the most effective at coupling primary amines to aryl or heteroaryl chlorides. As previously mentioned, their rationale for such enhanced level of reactivity relies on the fact the precatalyst **86** can be transformed into the active Pd⁽⁰⁾ species (Scheme 37) within minutes, allowing the catalytic cycle to start quickly and preventing any side reactions to occur. With Pd(OAc)₂ or Pd₂(dba)₃, the reduction of the Pd^(II) species or the dissociation of the

dba to provide the active Pd⁽⁰⁾ complex can be slow, even under heating conditions, leading to inefficiency of the catalytic reaction.^{136,137,217,218} Therefore, in the case of low conversion of the amination reaction, Surry and Buchwald advise that various precatalysts described in the review should be used, as they all should, in theory, be able to quickly form the Pd⁽⁰⁾ species. One such system is the precatalyst **137** (Figure 89), structurally similar to **86**, apart from the SPhos group which is replacing the BrettPhos ligand. This precatalyst **137** and SPhos are readily available from Aldrich, in contrast to compounds **86** and **L**¹.²¹⁹ The amination reaction to transform the chloropyridine **129** into the diaminopyridine **130** was attempted using the precatalyst **137** (10 %), SPhos (10 %), LHMDS (3 eq) and 1,1-dimethylethyl (3*S*)-3-amino-1-pyrrolidinecarboxylate (1.1 eq) (Scheme 64). The reaction was performed following similar conditions to the successful coupling employing the precatalyst **86** and ligand **L**¹ system (Table 15, entry 1). However, in this case, even after 16 hours at 70 °C, no traces of the desired product were detected by LCMS. This finding highlighted the fact that although the formation of the Pd⁽⁰⁾ was an important factor for the success of the reaction, the nature of the ligand attached to the palladium was also influencing the conversion to the required product.

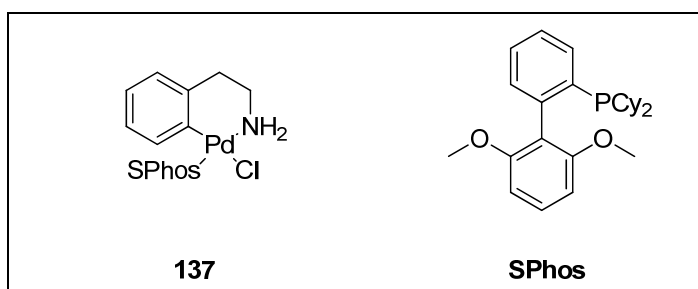
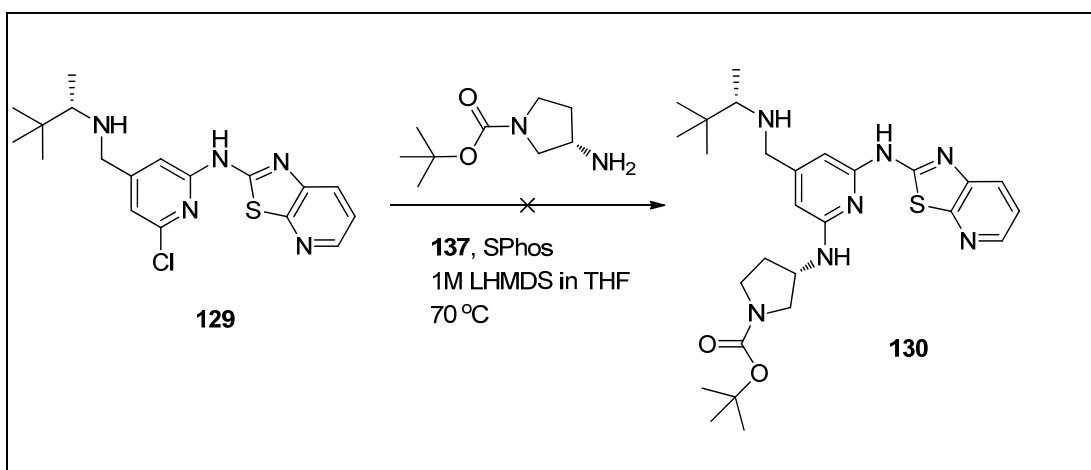


Figure 89. Structure of the precatalyst 133



Scheme 64. Attempt at synthesising the intermediate **130** with the precatalyst **130** and SPhos

The Hartwig research group has also developed efficient catalysts to couple primary amines to aryl or heteroaryl chlorides.^{211,216,220} Amination reactions with the air- and moisture-stable ligand from the Josiphos family (CyPF-*t*Bu, compound **138**) have been reported with a wide range of aryl or heteroaryl chlorides in high yields and low loadings of catalyst.^{211,216} The steric hinderance of this ligand combined to the strong phosphorous-palladium bond which it will create are believed to be the main reasons for its success.

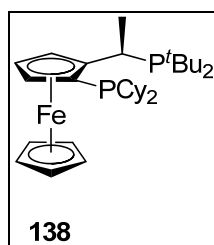
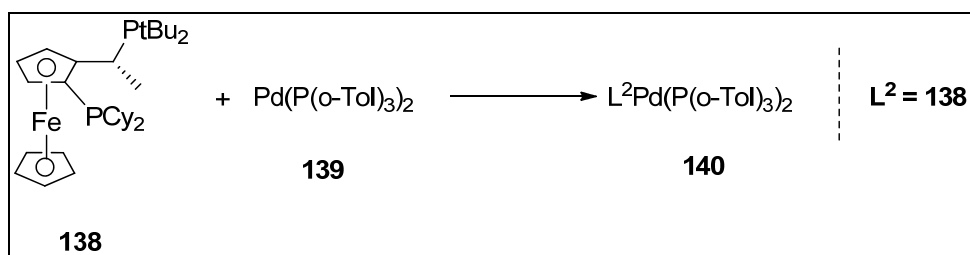


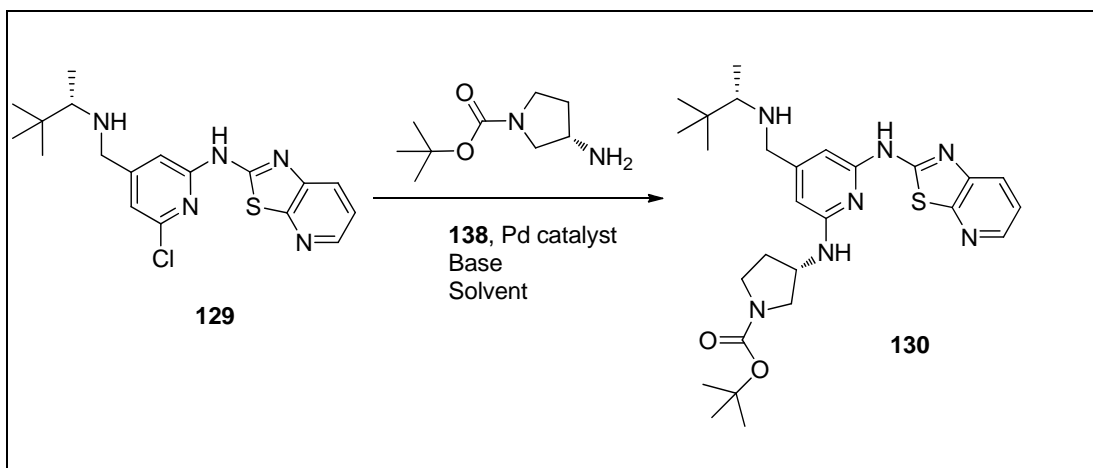
Figure 90. Structure of the Josiphos, CyPF-*t*Bu, ligand **138**

Initial studies reported in the literature^{211,216} successfully used this ligand with Pd(OAc)₂, as the formation of the Pd⁽⁰⁾ active species was believed to be more efficient than with Pd(dba)₂ or PdCl₂(PhCN)₂. However, although the oxidative addition and the reductive elimination steps of the catalytic cycle were efficient at room temperature,^{221,222} the reactions were reported to occur at higher temperatures, indicating that the formation of the active Pd⁽⁰⁾, even from Pd(OAc)₂, was requiring significant additional energy.²²³ Further reports from the Hartwig research group

described the development of a highly efficient, active and air-stable Pd⁽⁰⁾ precatalyst (compound **140**, Scheme 65), allowing amination reactions of aryl and heteroaryl tosylates at room temperature.²²¹ This precatalyst catalysed the coupling of ammonia and aryl chlorides, bromides, iodides and sulfonates efficiently.²²⁴ The active catalyst is generated in solution, at room temperature, from the reaction between the Josiphos ligand **138** and bis(tris(2-methylphenyl)phosphine)palladium (Pd(P(*o*-Tol)₃)₂) **139** (Scheme 65). It provides the advantages of the Josiphos ligand (steric hindrance and strong P-Pd bond reducing the replacement of the phosphine ligand by amines or basic heterocyclic nitrogen), as well as the possibility to perform the coupling at room temperature as the active Pd⁽⁰⁾ species is already formed. Mechanistic studies demonstrated that the oxidative addition between aryl chlorides and the catalyst **140** occurred at room temperature in less than 15 minutes, whereas no reaction occurred when Pd(OAc)₂ or Pd₂(dba)₃ were used.^{224,225} Such a catalyst was believed to have the potential to deliver positive results for the amination reaction transforming the chloropyridine **129** into the diaminopyridine **130** (Scheme 66).



Scheme 65. Structure and preparation of the precatalyst 140²²¹



Scheme 66. Preparation of compound **130** using the Josiphos type ligand, CyPF-*t*Bu, **138**

The typical conditions described to couple aryl and heteroaryl tosylates to amines with the catalyst **140** by Hartwig *et al.*²²¹ use small loadings of Pd(P(*o*-Tol)₃)₂ **139** catalyst and ligand **138**, in combination with NaO^{*t*}Bu and toluene. Repeat of this exact protocol using 10 mol % of compounds **138** and **139** did not produce any product **130** (Table 52, entry 1). This was not that surprising as it has been already demonstrated that NaO^{*t*}Bu was not a suitable base for this transformation. To our knowledge, LHMDS has never been reported with this combination of Pd and ligand. However, Hartwig *et al.* have described the use of LHMDS with Pd(OAc)₂ and the Josiphos type ligand, CyPF-*t*Bu, **138**.²¹¹ In line with the results presented in this thesis, they claim that LHMDS is a more suitable base to couple heteroaryl chlorides containing protic functionalities. As LHMDS was available as a 1 M solution in THF in our laboratories, the reaction solvent was modified from toluene to THF. With this stronger base, 41 % of product was detected by LCMS after stirring at room temperature for two hours (Table 52, entry 2. Note that the % conversion refers to the formation of product relative to starting material. The % of impurities formed were not taken into account). A longer reaction time (16 hours, Table 52, entry 3) provided a better conversion (65 %) to compound **130** but the reaction did not go any further. This result was, nonetheless, very encouraging as the gradual turnover of the starting material **129** suggested that the active Pd⁽⁰⁾ was still able to catalyse the reaction after 2 hours. Increasing the reaction temperature to 70 °C was less successful, resulting in a more complex reaction profile (34 % conversion, Table 52, entry 4). The reason for

this finding remains unknown but one can postulate that although the catalyst **140** had been used at high temperature to couple ammonia to aryl chloride,²²⁴ the combination of our protic template and LHMDS at 70 °C could have caused degradation of the active species **140**. Replacing the palladium **139** with Pd(OAc)₂ resulted in only 11 % conversion for the reaction at 70 °C over 24 hours. This confirmed the benefits of the rapid formation of the active species **140**. Finally, changing the amount of amine to 2.2 equivalents resulted in full conversion to the product **130** observed after 24 hours at room temperature (Table 52, entry 6) (note that the extents of reactions 3 and 4 were also assessed after 24 hours but no major improvements were observed). Reducing further the palladium loading (3 %, Table 52, entry 7) only produced 7 % of product by LCMS.

Table 52. Investigation of the amination reaction using the Josiphos type ligand **138**

Entry	Amine eq	Pd (eq)	Ligand (eq)	Base (eq)	Solvent	T (°C) thermal	Heating time	% conversion ^a
1	1.1	139 (0.1)	138 (0.1)	NaOtBu (3)	Toluene	room	16 h	0 %
2	1.1	139 (0.1)	138 (0.1)	LHMDS (3)	THF	room	2 h	41 %
3	1.1	139 (0.1)	138 (0.1)	LHMDS (3)	THF	room	16 h	65 %
4	1.1	139 (0.1)	138 (0.1)	LHMDS (3)	THF	70 °C	16 h	34 %
5	1.1	Pd(OAc) ₂ (0.1)	138 (0.1)	LHMDS (3)	THF	70 °C	24 h	11 %
6	2.2	139 (0.1)	138 (0.1)	LHMDS (3)	THF	room	24 h	100 %
7	2.2	139 (0.03)	138 (0.03)	LHMDS (3)	THF	room	24 h	7 %

^a Determined by LCMS analysis

In summary, the investigation of the Buchwald-Hartwig coupling strongly suggested that the substrates **129** and **130** were chelating the precatalyst **87** (or its active species). The search for other palladium complexes capable of catalysing the amination reaction with lower loading (ideally less than 10 %) led to the discovery of

the precatalyst Pd⁽⁰⁾ **140**, which can be prepared *in situ* from the Josiphos ligand **138** and the Pd species **139**. The reaction with LHMDS provided room temperature coupling with 10 mol % of palladium loading, which represents a significant improvement compared to the conditions used previously with 30 % of precatalyst **87**. However, these reaction conditions using the catalyst **140** were to be performed on larger scale with isolation of the product **130** to truly confirm the benefits of this approach compared to the conditions employing the precatalyst **87**. The termination of this research programme, due to the toxicity of the lead compound **107b** in the 14 day rat study, prevented the further optimisation of the reaction conditions employing the precatalyst Pd⁽⁰⁾ **140** catalyst. Nonetheless, these conditions are likely to be employed by other scientists from our research laboratories and elsewhere to perform challenging amination reactions on similar heteroaromatic templates.

Conclusions

This thesis highlights the discovery of potent inhaled irreversible ITK inhibitors for severe asthma. To our knowledge, this represents the first known evidence of irreversible ITK inhibitors in the literature.^{226,227} Six months after the publication of this patent, Zaft *et al.* published the discovery of a different series of irreversible ITK inhibitors.²²⁸ Their strategy was radically different to that described in this thesis, as they used the template from the irreversible BTK inhibitor **3** to design their ITK covalent compounds. This prevented this research team from developing compounds which selectively inhibit ITK (the best compounds were equipotent at ITK and BTK), and, to our knowledge, these compounds were not progressed to clinical studies. Our inhibitors were designed from a potent non-covalent amino-benzothiazole template, to which were added electrophilic acrylamide motifs, carefully positioned to interact with a cysteine residue present in the ITK active site. The irreversible binding of the early inhibitors was confirmed by mass spectrometry, kinetics, and crystallography studies. Although the early pyrimidine compounds **34** and **35** did not present the level of activities required for an ITK inhaled drug candidate, the analysis of the kinetics and crystallography results indicated that the covalent bond between the kinase and the electrophilic moiety was formed relatively slowly, resulting in the irreversible character of the compound not being able to drive the ITK inhibition to the required levels. From the three strategies aimed at improving the activity profile of the compounds, improving the non-covalent affinity to ITK by moving to the more active pyridine core was the most successful, as the investigations of the nature and positioning of the electrophilic moiety did not produce better irreversible ITK inhibitors than compounds **34** and **35**. Compounds with subnanomolar potency (*i.e.* compound **92**) were synthesised in the pyridine series thanks to the development of relatively mild Buchwald-Hartwig amination conditions. The improvement of the kinetic assay demonstrated that the (*S*)-3-aminopyrrolidine linker was optimal for the non-covalent binding and the rate of inactivation (covalent binding to Cys442) of ITK. Further profiling of the lead compound **92** proved, however, that the SLF solubility was not adequate for inhaled

administration and could result in deposition of the compound in the lung, triggering undesired toxicity. Optimisation of the solubility of compound **92** by investigating salt versions of the molecule did not lead to any useful results as the salt was believed to disproportionate rapidly in the SLF buffer solution.

Replacement of the morpholine motif with more basic amines led to the discovery of compound **107** which presents improved solubility and inhibition activity compared to the analogue **92**. From this study, two irreversible ITK inhibitors (compounds **101** and **107**), possessing different physicochemical properties (solubility and permeability), were selected to be progressed to mutagenicity experiments. These compounds were nearly 100 times more potent in our cellular assay than the lead reversible analogue **1**, and this level of activity was retained over time, despite washing the cells and removing any non-covalently bound compound. To cover the eventuality that both compounds could be progressed to 14 day animal toxicology studies, the chemistry routes to prepare the inhibitors in large quantities were optimized. In particular, the number of column purifications were vastly reduced and both final molecules were obtained in sufficient purity and quantities for toxicology studies. Unfortunately, MLA data demonstrated a mutagenic risk for the analogue **101**. Further investigation of this liability indicated that the acrylamide Michael acceptor was not the cause of the positive results, which proved that the irreversible inhibitor approach was still viable. Nonetheless, the progression of the inhibitor **101** was halted. Mutagenic studies on compound **107** did not trigger any risks hence this inhibitor was solely pursued towards drug candidate selection. A suitable crystalline form of the inhibitor was developed to allow the required micronization of the material for *in vivo* inhaled administration. The inhibition human lung data and the DMPK profile obtained for compound **107b** were suitable for an inhaled candidate molecule but the absence of a PD model dictated that the inhibitor be assessed in the 14 day rat toxicology study at the highest doses tolerated in clinical studies. The results from this rat toxicology study revealed a severe irritation of the trachea combined with inflammatory effects, which halted the compound from further progression. The development of a new rat *in vivo* PD model revealed that, at the inhaled dose of 2.3 mg/kg, the inhibitor **107b** was fully inhibiting the inflammatory response in CD4 cells. Repeat of this rat *in vivo* study suggested that the compound

was able to reduce inflammation at lower doses (*i.e.* 3 µg/kg) but these data remained difficult to reproduce, which prompted the decision of halting the progression of this compound to clinical studies, as a safe therapeutical window was not demonstrated.

Finally, the Buchwald-Hartwig amination reaction used as part of the synthesis of compound **107** was further investigated. Although the current method was successfully employed to prepare 86 g of final drug material **107b**, it required 30 % of precatalyst which is not preparatively acceptable or cost effective. Extensive studies of the reaction strongly suggested that our chemical template was poisoning the catalyst hence the large amount (30 %) necessary to reach completion of the reaction. Supported by the various literature reviews on this type of transformations, a suitable combination of palladium species and ligand was developed to allow the total conversion to the product at room temperature with a reduced 10 mol % quantity required. Further work would be required to fully optimise the reaction conditions and assess whether they are suitable for large scale synthesis. Nonetheless, the optimization of this coupling has been thoroughly transformative compared to the initial conditions used at the start of this programme. The aromatic nucleophilic displacement was initially carried out at 220 °C for hours in the Biotage® microwave system. The yield of the transformation was, not surprisingly, poor at such a temperature and the synthesis was restricted to small scale reactions. The fact the coupling can be performed at room temperature with only 10 % of catalyst represents a major improvement.

Overall, despite the termination of this research programme before clinical evaluation, this work has delivered a landmark irreversible ITK inhibitor and has established a novel conceptual approach in this area, with the potential to assist in the strategic design of related medicinal chemistry programmes.

Experimental section

General Methods

All temperatures are in °C.

Nuclear Magnetic Resonance (NMR)

NMR spectra were recorded using a Bruker DPX250, DPX400, DPX500, AV400 or AVIII600 (with cryoprobe). Chemical shifts (δ) are reported in parts per million (ppm) relative to tetramethylsilane and coupling constants (J) in Hz. The following abbreviations are used for multiplicities: s = singlet; br. s = broad singlet; d = doublet; t = triplet; q = quartet; m = multiplet; dd = doublet of doublets. If not specifically stated, the NMR experiments were run at 30 °C.

Liquid Chromatography Mass Spectroscopy (LCMS)

LCMS Method A:

The analysis was conducted on an Acquity UPLC BEH C18 column (50 mm x 2.1 mm internal diameter 1.7 μ m packing diameter) at 40 °C.

The solvents employed were:

A = 0.1 % v/v solution of formic acid in water.

B = 0.1 % v/v solution of formic acid in acetonitrile.

The gradient employed was as follows:

Time (minutes)	Flow Rate (mL/min)	% A	% B
0	1	97	3
1.5	1	0	100
1.9	1	0	100
2.0	1	97	3

The UV detection was an averaged signal from wavelength of 210 nm to 350 nm and mass spectra were recorded on a Waters ZQ mass spectrometer using alternate-scan positive and negative mode electrospray ionisation (ES +ve and ES -ve).

LCMS Method B:

The analysis was conducted on an XBridge C18 column (50 mm x 4.6 mm internal diameter 3.5 µm packing diameter) at 30 °C.

The solvents employed were:

A = 10 mM ammonium bicarbonate in water adjusted to pH 10 with ammonia solution.

B = acetonitrile.

The typical gradient employed was as follows:

Time (minutes)	Flow Rate (mL/min)	% A	% B
0	3	99	1
0.1	3	99	1
4.0	3	3	97
5.0	3	3	97

The UV detection was an averaged signal from wavelength of 210 nm to 350 nm and mass spectra were recorded on a Waters ZQ mass spectrometer using alternate-scan positive and negative mode electrospray ionisation (ES +ve and ES -ve).

LCMS Method C:

The analysis was conducted on an a Sunfire C18 column (30 mm x 4.6 mm i.d. 3.5 µm

packing diameter) at 30 °C.

The solvents employed were:

A = 0.1 % v/v solution of formic acid in water.

B = 0.1 % v/v solution of formic acid in acetonitrile.

The gradient employed was as follows:

Time (minutes)	Flow Rate (mL/min)	% A	% B
0	3	97	3
0.1	3	97	3
4.2	3	0	100
4.8	3	0	100
4.9	3	97	3
5.0	3	97	3

The UV detection was an averaged signal from wavelength of 210 nm to 350 nm and mass spectra were recorded on a Waters ZQ mass spectrometer using alternate-scan positive and negative mode electrospray ionisation (ES +ve and ES -ve).

LCMS Method D:

The analysis was conducted on an Acquity UPLC BEH C18 column (50 mm x 2.1 mm internal diameter 1.7 µm packing diameter) at 40 °C.

The solvents employed were:

A = 10 mM ammonium bicarbonate in water adjusted to pH 10 with ammonia solution.

B = acetonitrile.

The gradient employed was as follows:

Time (minutes)	Flow Rate (mL/min)	% A	% B
0	1	99	1
1.5	1	3	97
1.9	1	3	97
2.0	1	0	100

The UV detection was an averaged signal from wavelength of 210 nm to 350 nm and mass spectra were recorded on a Waters ZQ mass spectrometer using alternate-scan positive and negative mode electrospray ionisation (ES +ve and ES -ve).

LCMS Method E:

The analysis was conducted on an Acquity UPLC BEH C18 column (50 mm x 2.1 mm internal diameter 1.7 μ m packing diameter) at 40 °C.

The solvents employed were:

A = 0.1 % v/v solution of trifluoroacetic acid in water.

B = 0.1 % v/v solution of trifluoroacetic acid in acetonitrile.

The gradient employed was as follows:

Time (minutes)	Flow Rate (mL/min)	% A	% B
0	1	97	3
1.5	1	0	100
1.9	1	0	100
2.0	1	97	3

The UV detection was an averaged signal from wavelength of 210 nm to 350 nm and mass spectra were recorded on a Waters ZQ mass spectrometer using alternate-scan positive and negative mode electrospray ionisation (ES +ve and ES -ve).

LCMS Method F:

The analysis was conducted on an Acquity UPLC BEH C18 column (100 mm x 2.1 mm internal diameter 1.7 μ m packing diameter) at 50 °C.

The solvents employed were:

A = 0.1 % v/v solution of trifluoroacetic acid in water.

B = 0.1 % v/v solution of trifluoroacetic acid in acetonitrile.

The gradient employed was as follows:

Time (minutes)	Flow Rate (mL/min)	% A	% B
0	0.8	97	3
8.5	0.8	0	100
9.0	0.8	0	100
9.5	0.8	97	3
10.0	0.8	97	3

The UV detection was an averaged signal from wavelength of 210 nm to 350 nm and mass spectra were recorded on a Waters ZQ mass spectrometer using alternate-scan positive and negative mode electrospray ionisation (ES +ve and ES -ve).

High-performance liquid chromatography (HPLC)

HPLC Method A:

The UPLC analysis was conducted on a Zorbax SB-C18 column at 40 °C.

The solvents employed were:

A = 0.1 % v/v solution of trifluoroacetic acid in water.

B = 0.1 % v/v solution of trifluoroacetic acid in acetonitrile.

The gradient employed was as follows:

Time (minutes)	Flow Rate (mL/min)	% A	% B
0	1	97	3
2.5	1	0	100
2.9	1	0	100
3.0	1	97	3

The UV detection was a signal from wavelength of 220 nm.

HPLC Method B:

The analysis was conducted on an Acquity UPLC BEH C18 column (100 mm x 2.1 mm internal diameter 1.7 µm packing diameter) at 50 °C.

The solvents employed were:

A = 0.1 % v/v solution of trifluoroacetic acid in water.

B = 0.1 % v/v solution of trifluoroacetic acid in acetonitrile.

The gradient employed was as follows:

Time (minutes)	Flow Rate (mL/min)	% A	% B
0	0.8	97	3
8.5	0.8	0	100
9.0	0.8	0	100
9.5	0.8	97	3
10.0	0.8	97	3

The UV detection was an averaged signal from wavelength of 210 nm to 350 nm.

Chiral HPLC

Chiral HPLC analysis was conducted on a Chiralpak IA column (250 x 4.6mm, 5micron) at 50 °C and with a flowrate of 1.5 mL/min. The UV detection was a signal from wavelength of 300 nm.

Mobile Phase A: Heptane (Containing 0.2% isopropylamine). Mobile Phase B: Ethanol (Containing 0.2% isopropylamine).

Isocratic system: 95:5 Mobile phase A: B. Runtime: 40 minutes.

High resolution mass spectroscopy (HRMS)

ESI (+) high resolution mass spectra were obtained on a Micromass Q-ToF 2 hybrid quadrupole time-of-flight mass spectrometer, equipped with a Z-spray interface, over a mass range of 100 - 1100 Da, with a scan time of 0.9 s and an interscan delay of 0.1 s. Reserpine was used as the external mass calibrant ($[M + H]^+ = 609.2812$ Da). The Q-ToF 2 mass spectrometer was operated in W reflectron mode to give a resolution (FWHM) of 16000 - 20000. Ionisation was achieved with a spray voltage of 3.2 kV, a cone voltage of 50 V, with cone and desolvation gas flows of 10-20 and 600 L/h,

respectively. The source block and desolvation temperatures were maintained at 120 °C and 250 °C, respectively. The elemental composition was calculated using MassLynx v4.1 for the $[M + H]^+$ and the mass error quoted as ppm.

An Agilent 1100 Liquid Chromatograph equipped with a model G1367A autosampler, a model G1312A binary pump and a HP1100 model G1315B diode array detector was used. The method used was generic for all experiments. All separations were achieved using a Phenomenex Luna C18 (2) reversed phase column (100 x 2.1 mm, 3 μ m particle size). Gradient elution was carried out with the mobile phases as (A) water containing 0.1 % (v/v) formic acid and (B) acetonitrile containing 0.1 % (v/v) formic acid. The conditions for the gradient elution were initially 5 % B, increasing linearly to 100 % B over 6 minutes, remaining at 100 % B for 2.5 min then decreasing linearly to 5 % B over 1 min followed by an equilibration period of 2.5 min prior to the next injection. The flow rate was 0.5 mL/min, temperature controlled at 35 °C with an injection volume of between 2 to 5 μ L. All samples were diluted with DMSO (99.9 %) prior to LCMS analysis.

Mass Directed Auto-Preparative (MDAP)

“Mass directed automated preparative HPLC” (MDAP) was conducted on a system such as a Waters FractionLynx system comprising of a Waters 600 pump with extended pump heads, Waters 2700 autosampler, Waters 996 diode array and Gilson 202 fraction collector on an XBridge C18 column (100 mm x 30 mm i.d. 5 μ m packing diameter) at ambient temperature, eluting with 10 mM ammonium bicarbonate in water adjusted to pH 10 with ammonia solution (solvent A) and acetonitrile (solvent B) using the appropriate elution gradient. The UV detection was a summed signal from wavelength of 210 nm to 350 nm. The mass spectra were recorded on a Waters ZQ spectrometer using electrospray positive and negative mode (ES +ve and ES -ve). The software used was MassLynx 3.5 with OpenLynx and FractionLynx option or using equivalent alternative systems. Similar systems using Sunfire C18 columns and gradient of solvents such as formic acid (or TFA) in water (solvent A) and acetonitrile (solvent B) were also employed.

Infrared

IR spectra were recorded from solid samples using a Perkin Elmer Spectrum One FTIR spectrometer fitted with a Perkin Elmer Universal ATR (attenuated total reflectance) sampling accessory. Absorption frequencies are reported in wavenumbers (cm^{-1}).

Melting point

Melting points were measured on a Stuart automatic melting point apparatus, SMP40.

Note that most the compounds assayed for melting point appeared to decompose (transform into gums or change colours) before melting.

Optical rotation

Optical rotations were measured with an Optical Activity AA100 digital polarimeter.

Phase separators

“Hydrophobic frits” refers to filtration tubes sold by Whatman. SPE (solid phase extraction) refers to the use of cartridges sold by International Sorbent Technology Ltd.

Purification by column chromatography

The Flashmaster II is an automated multi-user flash chromatography system, available from Argonaut Technologies Ltd, which utilises disposable, normal phase, SPE cartridges. It provides quaternary on-line solvent mixing to enable gradient methods to be run. Samples are queued using the multi-functional open access software, which manages solvents, flow-rates, gradient profile, and collection conditions. The system is equipped with a Knauer variable wavelength UV-detector and two Gilson FC204 fraction-collectors enabling automated peak cutting, collection and tracking.

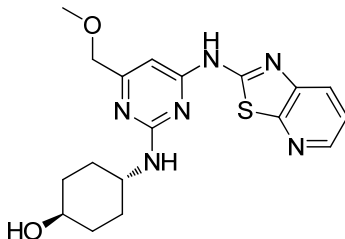
Silica chromatography techniques include either automated (Flashmaster) techniques or manual chromatography on pre-packed cartridges (SPE) or manually-packed flash columns.

Microwave

Microwave chemistry was typically performed in sealed vessels, irradiating with a suitable microwave reactor system, such as a Biotage InitiatorTM Microwave Synthesiser.

1. Synthetic procedures for the 6-methoxymethylpyrimidine series

***Trans*-4-{{4-[(methoxy)methyl]-6-[[1,3]thiazolo[5,4-*b*]pyridin-2-ylamino)-2-pyrimidinyl]amino}cyclohexanol (6)**



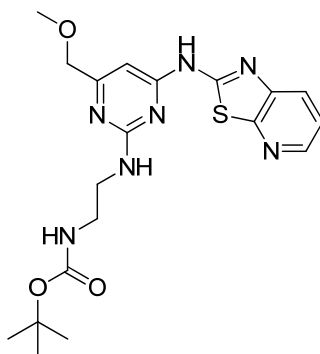
A microwave vial was charged with *N*-[6-[(methoxy)methyl]-2-(methylsulfonyl)-4-pyrimidinyl][1,3]thiazolo[5,4-*b*]pyridin-2-amine **5** (250 mg, 0.711 mmol), *trans*-4-aminocyclohexanol (246 mg, 2.13 mmol) and isopropanol (5 mL). The vial was sealed and was heated in a Biotage Initiator microwave to 150 °C for 45 minutes. After cooling, the reaction was filtered under reduced pressure and the solid was washed with isopropanol. The filtrate was evaporated to dryness. The residue was subjected to purification by mass directed automated preparative HPLC to afford the title compound as a white solid (36 mg, 13 % yield). **LCMS** (Method D) (ES +ve) m/z 387 ($M + H$)⁺ Rt 0.75 minutes. **¹H NMR** (400 MHz, DMSO-*d*₆) δ 11.62 (br. s, 1H), 8.36 (dd, $J = 1.3, 4.8$ Hz, 1H), 7.98 (dd, $J = 1.3, 8.0$ Hz, 1H), 7.42 (dd, $J = 4.8, 8.0$ Hz, 1H), 7.19 (d, $J = 7.0$ Hz, 1H), 6.31 (s, 1H), 4.71 - 4.57 (br. s, 1H), 4.21 (s, 2H), 3.97 - 3.78 (br. s, 1H), 3.51 - 3.39 (br. s, 1H), 3.36 (s, 3H), 2.09 - 1.96 (m, 2H), 1.97 - 1.80 (m, 2H), 1.49 - 1.19 (m, 4H).

General procedure A for the aromatic nucleophilic displacement reaction:

A microwave vial was charged with *N*-[6-[(methoxy)methyl]-2-(methylsulfonyl)-4-pyrimidinyl][1,3]thiazolo[5,4-*b*]pyridin-2-amine **5**, the amine analogue and isopropanol. The vial was sealed and was heated in the Biotage Initiator microwave system at 150 °C until the reaction had reached completion. Unless stated otherwise, the residue was then evaporated to dryness and the product was purified either by chromatography on silica or by mass directed automated preparative HPLC.

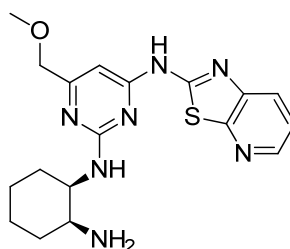
Following the general procedure A for the nucleophilic displacement reaction, data are presented as (a) amount of compound **5**, (b) amount of amine, (c) volume of isopropanol, (d) reaction time, (e) purification system.

1,1-Dimethylethyl (2-{[4-[(methoxy)methyl]-6-([1,3]thiazolo[5,4-*b*]pyridin-2-ylamino)-2-pyrimidinyl]amino}ethyl)carbamate (8a**)**



(a) 450 mg, 1.28 mmol, (b) 1,1-dimethylethyl (2-aminoethyl)carbamate, 308 mg, 1.92 mmol, (c) 10 mL, (d) 30 minutes, (e) purification by Flashmaster chromatography on silica (gradient elution from 0 to 30 % methanol (+1 % triethylamine) in dichloromethane). Off-white solid. Yield: 504 mg, 91 %. **LCMS** (Method B) (ES +ve) m/z 432 ($M + H$)⁺ Rt 2.37 minutes. **¹H NMR** (400 MHz, DMSO-*d*₆) δ 11.74 (br. s, 1H), 8.36 (dd, $J = 1.3, 4.5$ Hz, 1H), 7.98 (dd, $J = 1.3, 8.0$ Hz, 1H), 7.42 (dd, $J = 4.5, 8.0$ Hz, 1H), 7.20 - 7.13 (m, 1H), 6.89 (d, $J = 2.0$ Hz, 1H), 6.36 (s, 1H), 4.23 (s, 2H), 3.58 - 3.45 (br. s, 2H), 3.37 (s, 3H), 3.20 (br. s, 2H), 1.37 (s, 9H).

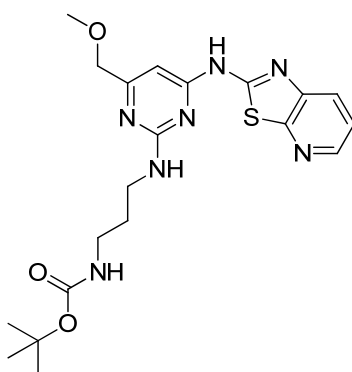
***N*²-[*Cis*-2-aminocyclohexyl]-6-[(methoxy)methyl]-*N*⁴-[1,3]thiazolo[5,4-*b*]pyridin-2-yl-2,4-pyrimidinediamine (**9b**)**



(±)

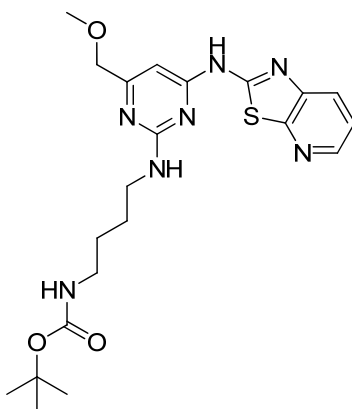
(a) 200 mg, 0.569 mmol, (b) *cis*-1,2-cyclohexanediamine, 97 mg, 0.85 mmol, (c) 4 mL, (d) 30 minutes, (e) purification by mass directed automated preparative HPLC. White solid. Yield: 124 mg, 56 %. **LCMS** (Method B) (ES +ve) m/z 386 ($M + H$)⁺ Rt 2.11 minutes. **¹H NMR** (400 MHz, DMSO- d_6) δ 8.37 (dd, $J = 1.4, 4.6$ Hz, 1H), 7.99 (dd, $J = 1.4, 8.0$ Hz, 1H), 7.43 (dd, $J = 4.6, 8.0$ Hz, 1H), 7.12 (br. s, 1H), 6.41 (s, 1H), 4.33 - 4.20 (m, 3H), 3.48 (br. s, 1H), 3.38 (s, 3H), 1.92 - 1.77 (m, 2H), 1.77 - 1.55 (m, 4H), 1.51 - 1.34 (m, 2H).

1,1-Dimethylethyl (3-[[4-[(methoxy)methyl]-6-([1,3]thiazolo[5,4-*b*]pyridin-2-ylamino)-2-pyrimidinyl]amino}propyl]carbamate (10a)



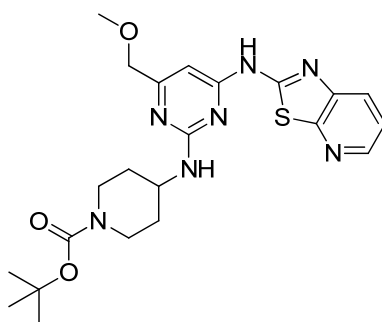
(a) 150 mg, 0.427 mmol, (b) 1,1-dimethylethyl (3-aminopropyl)carbamate 0.224 mL, 1.28 mmol, (c) 4 mL, (d) 45 minutes. After the reaction mixture had cooled to room temperature, the suspension was filtered under reduced pressure and washed with isopropanol. The solid was collected and the filtrate was evaporated under reduced pressure and purified. (e) purification by Flashmaster chromatography on silica (gradient elution from 0 to 30 % methanol (+1 % triethylamine) in dichloromethane). Both solids were combined to give a yellow solid. Yield: 138 mg, 73 %. **LCMS** (Method B) (ES +ve) m/z 446 ($M + H$)⁺ Rt 2.48 minutes. **¹H NMR** (400 MHz, DMSO- d_6) δ 11.60 (br. s, 1H), 8.36 (dd, $J = 1.4, 4.6$ Hz, 1H), 7.98 (dd, $J = 1.4, 8.2$ Hz, 1H), 7.42 (dd, $J = 4.6, 8.2$ Hz, 1H), 7.22 (br. s, 1H), 6.85 - 6.76 (m, 1H), 6.34 (s, 1H), 4.23 (s, 2H), 3.46 (br. s, 2H), 3.37 (s, 3H), 3.03 (br. s, 2H), 1.72 (br. s, 2H), 1.36 (s, 9H).

1,1-Dimethylethyl 4-{[4-[(methyloxy)methyl]-6-([1,3]thiazolo[5,4-*b*]pyridin-2-ylamino)-2-pyrimidinyl]amino}butyl)carbamate (11a)



(a) 150 mg, 0.427 mmol, (b) 1,1-dimethylethyl (4-aminobutyl)carbamate, 0.245 mL, 1.28 mmol, (c) 4 mL, (d) 45 minutes. After the reaction mixture had cooled to room temperature, the suspension was filtered under reduced pressure and washed with isopropanol. (e) Purification by Flashmaster chromatography on silica (gradient elution from 0 to 30 % methanol (+1 % triethylamine) in dichloromethane). Yellow solid. Yield: 146 mg, 74 %. **LCMS** (Method C) (ES +ve) m/z 460 ($M + H$)⁺ Rt 1.79 minutes. **¹H NMR** (400 MHz, DMSO-*d*₆) δ 11.70 (br. s, 1H), 8.36 (dd, $J = 1.4, 4.6$ Hz, 1H), 7.98 (dd, $J = 1.4, 8.0$ Hz, 1H), 7.42 (dd, $J = 4.6, 8.0$ Hz, 1H), 7.31 (br. s, 1H), 6.77 (t, $J = 5.4$ Hz, 1H), 6.33 (s, 1H), 4.22 (s, 2H), 3.41 (br. s, 2H), 3.37 (s, 3H), 2.99 - 2.90 (m, 2H), 1.65 - 1.42 (m, 4H), 1.33 (s, 9H).

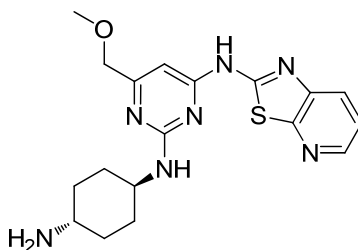
1,1-Dimethylethyl 4-{[4-[(methyloxy)methyl]-6-([1,3]thiazolo[5,4-*b*]pyridin-2-ylamino)-2-pyrimidinyl]amino}-1-piperidinecarboxylate (12a)



(a) 500 mg, 1.42 mmol, (b) 1,1-dimethylethyl 4-amino-1-piperidinecarboxylate, 427

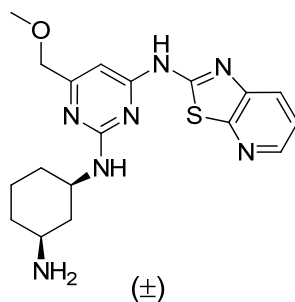
mg, 2.13 mmol, (c) 5 mL, (d) 45 minutes. After the reaction mixture had cooled to room temperature, the yellow solid was filtered under reduced pressure and was purified. (e) Purification by FlashMaster chromatography on silica (gradient elution from 0 to 25 % methanol in dichloromethane). Light brown solid. Yield: 287 mg, 75 % pure, 32 %. **LCMS** (Method A) (ES +ve) m/z 472 (M + H)⁺ Rt 0.84 minutes. **¹H NMR** (400 MHz, DMSO-*d*₆) δ 11.77 (br. s, 1H), 8.37 (dd, $J = 1.5, 4.8$ Hz, 1H), 7.99 (dd, $J = 1.5, 8.0$ Hz, 1H), 7.43 (dd, $J = 4.8, 8.0$ Hz, 1H), 7.38 - 7.31 (m, 1H), 6.35 (s, 1H), 4.23 (s, 2H), 4.15 - 3.91 (m, 3H), 3.37 (s, 3H), 2.93 (br. s, 2H), 2.06 - 1.90 (m, 2H), 1.42 (s, 9H), 1.40 - 1.33 (m, 2H).

***N*²-(*Trans*-4-aminocyclohexyl)-6-[(methoxy)methyl]-*N*⁴-[1,3]thiazolo[5,4-*b*]pyridin-2-yl-2,4-pyrimidinediamine (14b)**



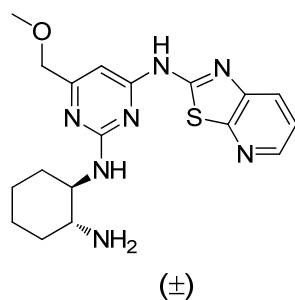
(a) 200 mg, 0.569 mmol, (b) *trans*-1,4-cyclohexanediamine, 65 mg, 0.57 mmol, (c) 4 mL, (d) 30 minutes. After the reaction mixture had cooled to room temperature, the suspension was filtered under reduced pressure and washed with isopropanol. The filtrate was evaporated under reduced pressure and purified. (e) Purification by mass directed automated preparative HPLC. White solid. Yield: 93 mg, 42 %. **LCMS** (Method C) (ES +ve) m/z 386 (M + H)⁺ Rt 1.02 minutes. **¹H NMR** (400 MHz, DMSO-*d*₆) δ 8.35 (dd, $J = 1.4, 4.6$ Hz, 1H), 7.95 (dd, $J = 1.4, 8.0$ Hz, 1H), 7.41 (dd, $J = 4.6, 8.0$ Hz, 1H), 7.09 (br. s, 1H), 6.29 (s, 1H), 4.20 (s, 2H), 3.84 (br. s, 1H), 3.36 (s, 3H), 2.72 - 2.55 (m, 1H), 2.13 - 1.95 (m, 2H), 1.92 - 1.76 (m, 2H), 1.48 - 1.08 (m, 4H).

***N*²-[*Cis*-3-aminocyclohexyl]-6-[(methoxy)methyl]-*N*⁴-[1,3]thiazolo[5,4-*b*]pyridin-2-yl-2,4-pyrimidinediamine (17b)**



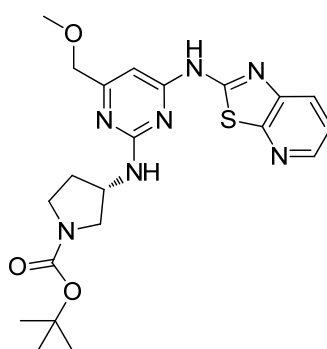
(a) 200 mg, 0.569 mmol, (b) 1,3-cyclohexanediamine (mixture of *cis*- and *trans*-isomers), 97 mg, 0.85 mmol, (c) 4 mL, (d) 30 minutes. After the reaction mixture had cooled to room temperature, the suspension was filtered under reduced pressure and washed with isopropanol. The filtrate was evaporated under reduced pressure and purified. (e) Purification by mass directed automated preparative HPLC. White solid. Yield: 73 mg, 33 %. **LCMS** (Method B) (ES +ve) *m/z* 386 (*M* + *H*)⁺ *R*_t 1.91 minutes. **¹H NMR** (400 MHz, DMSO-*d*₆) δ 8.35 (dd, *J* = 1.3, 4.5 Hz, 1H), 7.96 (dd, *J* = 1.3, 8.0 Hz, 1H), 7.41 (dd, *J* = 4.5, 8.0 Hz, 1H), 7.32 - 7.20 (m, 1H), 6.31 (s, 1H), 4.21 (s, 2H), 3.99 (br. s, 1H), 3.37 (s, 3H), 2.88 - 2.69 (m, 1H), 2.19 - 1.92 (m, 2H), 1.91 - 1.66 (m, 2H), 1.53 - 0.91 (m, 4H). NOE experiments of the final compound **17** established the *cis*-geometry of this compound. Note that the MDAP enabled the isolation of this *cis*-isomer. The fraction containing the *trans*-isomer was contaminated with impurities hence was used crude to prepare the product **16** (*vide infra*).

***N*²-[*Trans*-2-aminocyclohexyl]-6-[(methoxy)methyl]-*N*⁴-[1,3]thiazolo[5,4-*b*]pyridin-2-yl-2,4-pyrimidinediamine (18b)**



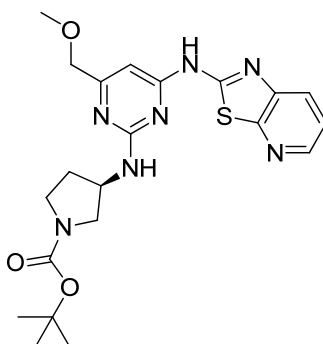
(a) 200 mg, 0.569 mmol, (b) *trans*-1,2-cyclohexanediamine, 97 mg, 0.85 mmol, (c) 4 mL, (d) 30 minutes (e) purification by mass directed automated preparative HPLC. White solid. Yield: 117 mg, 53 %. **LCMS** (Method B) (ES +ve) m/z 386 (M + H)⁺ Rt 2.07 minutes. **¹H NMR** (400 MHz, DMSO-*d*₆) δ 8.32 (dd, $J = 1.3, 4.8$ Hz, 1H), 7.93 (dd, $J = 1.3, 8.0$ Hz, 1H), 7.37 (dd, $J = 4.8, 8.0$ Hz, 1H), 7.16 (br. s, 1H), 6.28 (s, 1H), 4.18 (s, 2H), 3.68 - 3.54 (m, 1H), 3.33 (s, 3H), 2.63 - 2.53 (m, 1H), 2.21 - 2.06 (m, 1H), 1.94 - 1.81 (m, 1H), 1.78 - 1.59 (m, 2H), 1.53 - 0.98 (m, 4H).

1,1-Dimethylethyl (3*S*)-3-{[4-[(methoxy)methyl]-6-([1,3]thiazolo[5,4-*b*]pyridin-2-ylamino)-2-pyrimidinyl]amino}-1-pyrrolidinecarboxylate (19a)



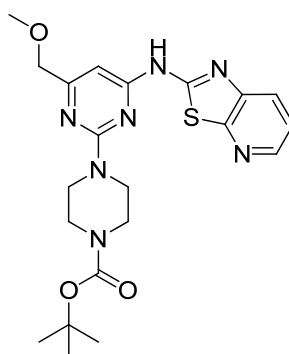
(a) 200 mg, 0.569 mmol, (b) (3*S*)-3-amino-1-pyrrolidinecarboxylate, 159 mg, 0.854 mmol, (c) 4 mL, (d) 30 minutes. LCMS analysis revealed that some starting material remained in the reaction mixture. Therefore, a second portion of (3*S*)-3-amino-1-pyrrolidinecarboxylate (159 mg, 0.854 mmol) was added to the reaction mixture and the vial was heated in the Biotage Initiator microwave system at 150 °C for further 30 minutes. (e) Purification by mass directed automated preparative HPLC. Off-white solid. Yield: 86 mg, 33 %. **LCMS** (Method D) (ES +ve) m/z 458 (M + H)⁺ Rt 1.05 minutes. **¹H NMR** (400 MHz, DMSO-*d*₆) δ 8.36 (dd, $J = 1.3, 4.8$ Hz, 1H), 7.99 (dd, $J = 1.3, 8.0$ Hz, 1H), 7.58 (br. s, 1H), 7.42 (dd, $J = 4.8, 8.0$ Hz, 1H), 6.39 (s, 1H), 4.56 (br. s, 1H), 4.24 (s, 2H), 3.78 - 3.44 (m, 3H), 3.37 (s, 3H), 3.24 - 3.15 (m, 1H), 2.30 - 2.10 (m, 1H), 1.92 (br. s, 1H), 1.49 - 1.27 (s, 9H).

1,1-Dimethylethyl (3R)-3-{[4-[(methoxy)methyl]-6-([1,3]thiazolo[5,4-*b*]pyridin-2-ylamino)-2-pyrimidinyl]amino}-1-pyrrolidinecarboxylate (20a)



(a) 200 mg, 0.569 mmol, (b) (3R)-3-amino-1-pyrrolidinecarboxylate, 159 mg, 0.854 mmol, (c) 4 mL, (d) 30 minutes. LCMS analysis revealed that some starting material remained in the reaction mixture. Therefore, a second portion of (3R)-3-amino-1-pyrrolidinecarboxylate (159 mg, 0.854 mmol) was added to the reaction mixture and the vial was heated in the Biotage Initiator microwave system at 150 °C for further 30 minutes. (e) Purification by mass directed automated preparative HPLC. Off-white solid. Yield: 80 mg, 31 %. **LCMS** (Method D) (ES +ve) m/z 458 (M + H)⁺ Rt 1.05 minutes. **¹H NMR** (400 MHz, DMSO-*d*₆) δ 11.59 (br. s, 1H), 8.36 (dd, $J = 1.3$, 4.6 Hz, 1H), 7.99 (dd, $J = 1.3$, 8.0 Hz, 1H), 7.60 (br. s, 1H), 7.42 (dd, $J = 4.6$, 8.0 Hz, 1H), 6.40 (s, 1H), 4.56 (br. s, 1H), 4.25 (s, 2H), 3.79 - 3.41 (m, 3H), 3.38 (s, 3H), 3.25 - 3.14 (m, 1H), 2.21 (br. s, 1H), 2.01 - 1.84 (m, 1H), 1.39 (s, 9H).

1,1-Dimethylethyl 4-[4-[(methoxy)methyl]-6-([1,3]thiazolo[5,4-*b*]pyridin-2-ylamino)-2-pyrimidinyl]-1-piperazinecarboxylate (21a)



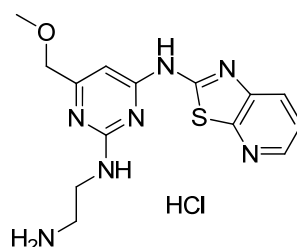
(a) 200 mg, 0.569 mmol, (b) 1,1-dimethylethyl 1-piperazinecarboxylate, 159 mg, 0.854 mmol, (c) 4 mL, (d) 30 minutes. LCMS analysis revealed that some starting material remained in the reaction mixture. Therefore, a second portion of 1,1-dimethylethyl 1-piperazinecarboxylate (159 mg, 0.854 mmol) was added to the reaction mixture and the vial was heated in the Biotage Initiator microwave system at 150 °C for further 30 minutes. (e) Purification by mass directed automated preparative HPLC. Yellow solid. Yield: 72 mg, 28 %. **LCMS** (Method B) (ES +ve) m/z 458 (M + H)⁺ Rt 3.01 minutes. **¹H NMR** (400 MHz, DMSO-*d*₆) δ 11.81 (br. s, 1H), 8.38 (dd, *J* = 1.4, 4.6 Hz, 1H), 8.01 (dd, *J* = 1.4, 8.1 Hz, 1H), 7.44 (dd, *J* = 4.6, 8.1 Hz, 1H), 6.43 (s, 1H), 4.28 (s, 2H), 3.84 (br. s, 4H), 3.47 (br. s, 4H), 3.38 (s, 3H), 1.44 (s, 9H).

General procedure B to perform the Boc deprotection reactions.

A round bottom flask was charged with the Boc protected analogues (such as **8a**) and dichloromethane (or dichloromethane:methanol to improve solubility). Excess of HCl in dioxane (4 M) was added and the reaction was stirred at room temperature until it had reached completion. The mixture was either evaporated to dryness or filtered under reduced pressure to obtain the amine intermediates as HCl salts. These amines were not purified and were used, as such, in the following amide coupling reactions. For that reason, only LCMS analyses of the crude products were recorded.

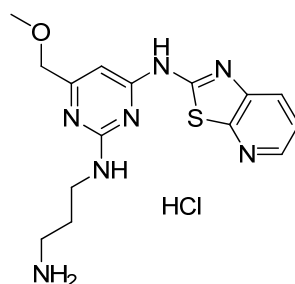
Following the general procedure B, data are presented as (a) amount of Boc protected analogues, (b) volume of solvent, (c) volume of HCl in dioxane (4 M), (d) reaction time, (e) isolation technique.

*N*²-(2-Aminoethyl)-6-[(methoxy)methyl]-*N*⁴-[1,3]thiazolo[5,4-*b*]pyridin-2-yl-2,4-pyrimidinediamine hydrochloride (**8c**)



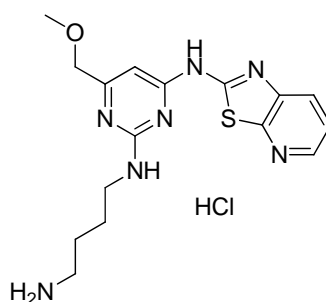
(a) **8a**, 500 mg, 1.16 mmol, (b) dichloromethane, 10 mL, (c) 1.45 mL, 5.79 mmol, (d) 16 hours. Another aliquot of HCl in dioxane (4 M, 1.45 mL, 5.79 mmol) was added and the reaction was stirred for further 3 hours. (e) solid filtered under reduced pressure. White solid. Yield: 400 mg, 94 %. **LCMS** (Method C) (ES +ve) m/z 332 (M + H)⁺ Rt 1.04 minutes.

***N*²-(3-Aminopropyl)-6-[(methoxy)methyl]-*N*⁴-[1,3]thiazolo[5,4-*b*]pyridin-2-yl-2,4-pyrimidinediamine hydrochloride (10c)**



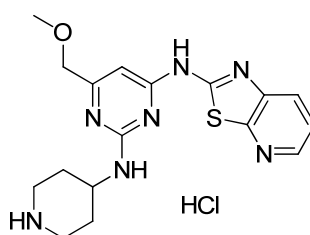
(a) **10a**, 115 mg, 0.258 mmol, (b) dichloromethane, 4 mL, methanol, 1 mL, (c) 0.400 mL, 1.60 mmol, (d) 16 hours, (e) solvent evaporated under reduced pressure. Yellow solid. Yield: 148 mg, > 100 %. **LCMS** (Method C) (ES +ve) m/z 346 (M + H)⁺ Rt 0.99 minutes.

***N*²-(4-Aminobutyl)-6-[(methoxy)methyl]-*N*⁴-[1,3]thiazolo[5,4-*b*]pyridin-2-yl-2,4-pyrimidinediamine hydrochloride (11c)**



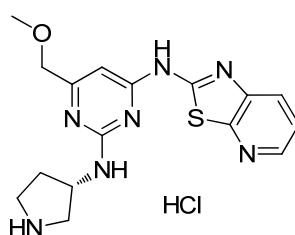
(a) **11a**, 146 mg, 0.318 mmol, (b) dichloromethane, 4 mL, methanol, 1 mL, (c) 0.318 mL, 1.27 mmol, (d) 16 hours, (e) solvent evaporated under reduced pressure. Yellow solid. Yield: 144 mg, > 100 %. **LCMS** (Method C) (ES +ve) m/z 360 (M + H)⁺ Rt 1.00 minutes.

6-[(Methoxy)methyl]-*N*²-4-piperidinyl-*N*⁴-[1,3]thiazolo[5,4-*b*]pyridin-2-yl-2,4-pyrimidinediamine hydrochloride (12c)



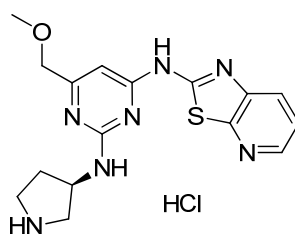
(a) **12a**, 237 mg, 0.503 mmol, (b) dichloromethane, 8 mL, (c) 0.600 mL, 2.40 mmol, (d) 16 hours, (e) solid filtered under reduced pressure. Yellow solid. Yield: 200 mg, 87 % pure, 84 %. **LCMS** (Method C) (ES +ve) *m/z* 372 (M + H)⁺ Rt 1.05 minutes.

6-[(Methoxy)methyl]-*N*²-[(3*S*)-3-pyrrolidinyl]-*N*⁴-[1,3]thiazolo[5,4-*b*]pyridin-2-yl-2,4-pyrimidinediamine hydrochloride (19c)



(a) **19a**, 80 mg, 0.18 mmol, (b) dichloromethane, 3 mL, (c) 0.262 mL, 1.05 mmol, (d) 16 hours, (e) solvent evaporated under reduced pressure. Brown solid. Yield: 84 mg, > 100 %. **LCMS** (Method B) (ES +ve) *m/z* 358 (M + H)⁺ Rt 1.73 minutes.

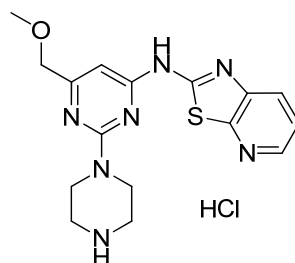
6-[(Methoxy)methyl]-*N*²-[(3*R*)-3-pyrrolidinyl]-*N*⁴-[1,3]thiazolo[5,4-*b*]pyridin-2-yl-2,4-pyrimidinediamine hydrochloride (20c)



(a) **20a**, 75 mg, 0.16 mmol, (b) dichloromethane, 3 mL, (c) 0.500 mL, 2.00 mmol, (d)

16 hours, (e) solvent evaporated under reduced pressure. Brown solid. Yield: 78 mg, > 100 %. **LCMS** (Method B) (ES +ve) m/z 358 (M + H)⁺ Rt 1.73 minutes.

***N*-[6-[(Methoxy)methyl]-2-(1-piperazinyl)-4-pyrimidinyl][1,3]thiazolo[5,4-*b*]pyridin-2-amine hydrochloride (21c)**



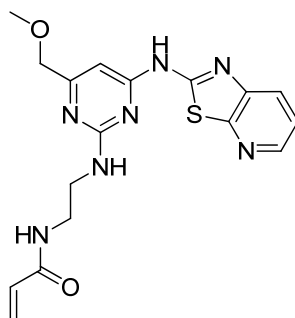
(a) **21a**, 67 mg, 0.15 mmol, (b) dichloromethane, 4 mL, (c) 0.227 mL, 0.908 mmol, (d) 16 hours, (e) solvent evaporated under reduced pressure. Yellow solid. Yield: 57 mg, 99 %. **LCMS** (Method B) (ES +ve) m/z 358 (M + H)⁺ Rt 1.91 minutes.

General procedure C to synthesise the final products from the amine intermediates (HCl salts or free bases):

A round bottom flask was charged with the amine intermediate (such as **8c** or **9b**), *N,N*-diisopropylethylamine and *N*-methyl-2-pyrrolidone. 2-Propenoyl chloride was added and the reaction was stirred at room temperature. The mixture was subjected to purification by mass directed automated preparative HPLC to afford the desired compounds.

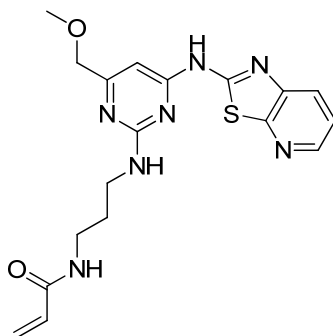
Following the general procedure C, data are presented as (a) amount of amine intermediate, (b) amount of *N,N*-diisopropylethylamine, (c) volume of solvent, (d) amount of 2-propenoyl chloride, (e) reaction time.

***N*-2-([4-[(Methoxy)methyl]-6-([1,3]thiazolo[5,4-*b*]pyridin-2-ylamino)-2-pyrimidinyl]amino)ethyl)-2-propenamide (8)**



(a) **8c**, 70 mg, 0.19 mmol, (b) 0.199 mL, 1.14 mmol, (c) 2 mL, (d) 0.022 mL, 0.27 mmol, (e) 72 hours. Off-white solid. Yield: 33 mg, 45 %. **LCMS** (Method B) (ES +ve) m/z 386 ($M + H$)⁺ Rt 1.87 minutes. **¹H NMR** (400 MHz, DMSO-*d*₆) δ 11.71 (br. s, 1H), 8.37 (dd, $J = 1.1, 4.6$ Hz, 1H), 8.23 (t, $J = 5.1$ Hz, 1H), 7.98 (dd, $J = 1.1, 8.0$ Hz, 1H), 7.42 (dd, $J = 4.6, 8.0$ Hz, 1H), 7.24 (br. s, 1H), 6.37 (s, 1H), 6.24 (dd, $J = 10.0, 17.1$ Hz, 1H), 6.08 (dd, $J = 2.3, 17.1$ Hz, 1H), 5.58 (dd, $J = 2.3, 10.0$ Hz, 1H), 4.24 (s, 2H), 3.58 (br. s, 2H), 3.48 - 3.39 (m, 2H), 3.37 (s, 3H).

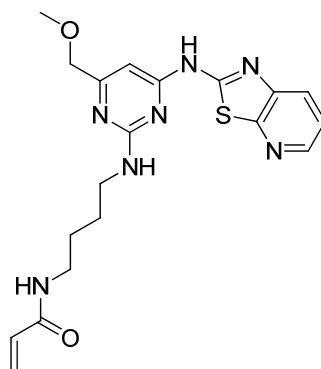
***N*-3-([4-[(Methoxy)methyl]-6-([1,3]thiazolo[5,4-*b*]pyridin-2-ylamino)-2-pyrimidinyl]amino)propyl)-2-propenamide (10)**



(a) **10c**, 50 mg, 0.13 mmol, (b) 0.152 mL, 0.869 mmol, (c) 2 mL, (d) 0.016 mL, 0.18 mmol, (e) 2 hours. Off-white solid. Yield: 13 mg, 25 %. **LCMS** (Method B) (ES +ve) m/z 400 ($M + H$)⁺ Rt 1.91 minutes. **¹H NMR** (400 MHz, DMSO-*d*₆) $\delta = 12.18 - 11.37$ (br. s, 1H), 8.35 (dd, $J = 1.3, 4.6$ Hz, 1H), 8.16 - 8.10 (m, 1H), 7.97 (dd, $J = 1.3, 8.1$ Hz, 1H), 7.41 (dd, $J = 4.6, 8.1$ Hz, 1H), 7.25 (br. s, 1H), 6.33 (s, 1H), 6.20

(dd, $J = 10.3, 17.1$ Hz, 1H), 6.06 (d, $J = 17.1$ Hz, 1H), 5.54 (d, $J = 10.3$ Hz, 1H), 4.23 (s, 2H), 3.56 - 3.42 (m, 2H), 3.37 (s, 3H), 3.28 - 3.18 (m, 2H), 1.78 (br. s, 2H). **IR** (cm^{-1}) 1519, 1554, 1620, 1634. **HRMS** (ES) calcd for $\text{C}_{18}\text{H}_{22}\text{N}_7\text{O}_2\text{S}$, ($\text{M} + \text{H}$)⁺ 400.1550, found 400.1546. **^{13}C NMR** (126 MHz, DMSO-d_6) δ 168.5, 165.1, 161.9, 158.5, 156.4, 144.3, 143.0, 132.3, 126.4, 125.3, 121.8, 92.8, 74.2, 58.8, 39.3, 37.0, 29.8. Note that the signals from two quaternary carbons are believed to be overlapping at 158.5 ppm. For comparison, these two signals are separated in the ^{13}C NMR spectrum of the structurally related compounds **9** (158.1 ppm and 158.2 ppm), **14** (158.3 ppm and 158.2 ppm), **39** (158.3 ppm and 158.2 ppm) and **40** (158.3 ppm and 158.1 ppm). Decomposition temperature 239 °C.

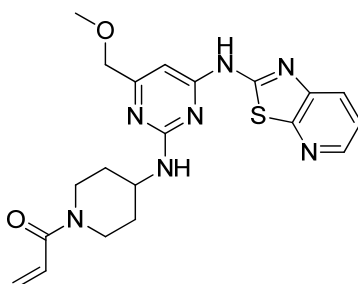
***N*-(4-{[4-[(Methoxy)methyl]-6-([1,3]thiazolo[5,4-*b*]pyridin-2-ylamino)-2-pyrimidinyl]amino}butyl)-2-propenamide (**11**)**



(a) **11c**, 50 mg, 0.13 mmol, (b) 0.146 mL, 0.835 mmol, (c) 2 mL, (d) 0.015 mL, 0.18 mmol, (e) 2 hours. Off-white solid. Yield: 13 mg, 25 %. **LCMS** (Method C) (ES +ve) m/z 414 ($\text{M} + \text{H}$)⁺ Rt 1.38 minutes. **^1H NMR** (400 MHz, DMSO-d_6) δ 11.69 (br. s, 1H), 8.36 (dd, $J = 1.3, 4.8$ Hz, 1H), 8.08 (t, $J = 5.4$ Hz, 1H), 7.98 (dd, $J = 1.3, 8.0$ Hz, 1H), 7.42 (dd, $J = 4.8, 8.0$ Hz, 1H), 7.35 - 7.25 (m, 1H), 6.33 (s, 1H), 6.19 (dd, $J = 10.0, 17.1$ Hz, 1H), 6.04 (dd, $J = 1.8, 17.1$ Hz, 1H), 5.54 (dd, $J = 1.8, 10.0$ Hz, 1H), 4.22 (s, 2H), 3.45 (br. s, 2H), 3.37 (s, 3H), 3.21 - 3.11 (m, 2H), 1.73 - 1.42 (m, 4H). **IR** (cm^{-1}) 1516, 1553, 1633, 1671. **HRMS** (ES) calcd for $\text{C}_{19}\text{H}_{24}\text{N}_7\text{O}_2\text{S}$, ($\text{M} + \text{H}$)⁺ 414.1707, found 414.1709. **^{13}C NMR** (126 MHz, DMSO-d_6) δ 168.6, 164.9, 161.9, 158.3, 156.4, 144.4, 143.0, 132.3, 126.5, 125.2, 121.9, 92.5, 74.1, 58.8, 41.4, 38.9, 27.3, 27.2. Note that the signals from two quaternary carbons are believed to be

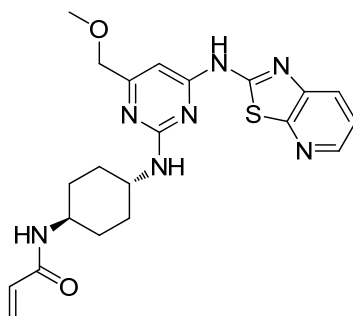
overlapping at 158.3 ppm. For comparison, these two signals are separated in the ^{13}C NMR spectrum of the structurally related compounds **9** (158.1 ppm and 158.2 ppm), **14** (158.3 ppm and 158.2 ppm), **39** (158.3 ppm and 158.2 ppm) and **40** (158.3 ppm and 158.1 ppm). Decomposition temperature 245 °C.

***N*²-(1-Acryloyl-4-piperidinyl)-6-[(methoxy)methyl]-*N*⁴-[1,3]thiazolo[5,4-*b*]pyridin-2-yl-2,4-pyrimidinediamine (**12**)**



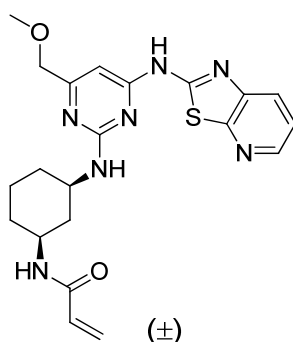
(a) **12c**, 50 mg, 0.12 mmol, (b) 0.141 ml, 0.808 mmol, (c) 1 mL, (d) 0.015 ml, 0.18 mmol, (e) 18 hours. Light brown solid. Yield: 13 mg, 24 %. **LCMS** (Method C) (ES +ve) m/z 426 ($M + H$)⁺ Rt 1.50 minutes. **¹H NMR** (400 MHz, DMSO- d_6) δ = 11.78 (br. s, 1H), 8.36 (dd, J = 1.3, 4.8 Hz, 1H), 7.99 (dd, J = 1.3, 8.1 Hz, 1H), 7.45 - 7.38 (br. s, 1H), 7.43 (dd, J = 4.8, 8.1 Hz, 1H), 6.87 (dd, J = 10.4, 16.7 Hz, 1H), 6.35 (s, 1H), 6.12 (dd, J = 2.3, 16.7 Hz, 1H), 5.68 (dd, J = 2.3, 10.4 Hz, 1H), 4.50 - 4.36 (m, 1H), 4.23 (s, 2H), 4.19 - 4.00 (m, 2H), 3.37 (s, 3H), 3.30 - 3.14 (m, 1H), 2.99 - 2.84 (m, 1H), 2.14 - 1.87 (m, 2H), 1.52 - 1.33 (m, 2H).

***N*-(*Trans*-4-{4-[(methoxy)methyl]-6-([1,3]thiazolo[5,4-*b*]pyridin-2-ylamino)-2-pyrimidinyl}amino)cyclohexyl)-2-propenamide (**14**)**



(a) **14b**, 50 mg, 0.13 mmol, (b) 0.136 mL, 0.778 mmol, (c) 2 mL, (d) 0.014 mL, 0.17 mmol, (e) 10 minutes. Light brown solid. Yield: 31 mg, 54 %. **LCMS** (Method C) (ES +ve) m/z 440 ($M + H$)⁺ Rt 1.55 minutes. **¹H NMR** (400 MHz, DMSO-*d*₆) δ 11.67 (br. s, 1H), 8.37 (dd, $J = 1.4, 4.6$ Hz, 1H), 8.16 (d, $J = 7.3$ Hz, 1H), 7.98 (dd, $J = 1.4, 8.0$ Hz, 1H), 7.43 (dd, $J = 4.6, 8.0$ Hz, 1H), 7.18 (d, $J = 7.3$ Hz, 1H), 6.33 (s, 1H), 6.24 (dd, $J = 10.3, 17.1$ Hz, 1H), 6.09 (dd, $J = 2.3, 17.1$ Hz, 1H), 5.57 (dd, $J = 2.3, 10.3$ Hz, 1H), 4.21 (s, 2H), 3.89 (br. s, 1H), 3.65 (br. s, 1H), 3.36 (s, 3H), 2.17 - 2.03 (m, 2H), 1.98 - 1.83 (m, 2H), 1.51 - 1.31 (m, 4H). **IR** (cm⁻¹) 1518, 1578, 1622, 1654. **HRMS** (ES) calcd for C₂₁H₂₆N₇O₂S, ($M + H$)⁺ 440.1863, found 440.1860. **¹³C NMR** (126 MHz, DMSO-*d*₆) δ 168.6, 164.2, 161.1, 158.3, 158.2, 156.3, 144.3, 142.9, 132.5, 126.5, 125.3, 121.9, 92.5, 74.1, 58.8, 49.7, 47.8, 31.9, 31.6. Decomposition temperature 271 °C.

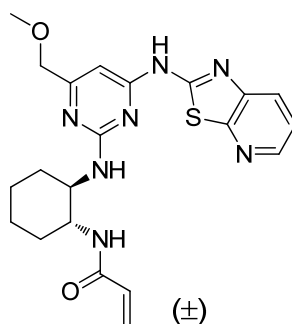
***N*-(*Cis*-3-{[4-[(methoxy)methyl]-6-([1,3]thiazolo[5,4-*b*]pyridin-2-ylamino)-2-pyrimidinyl]amino}cyclohexyl)-2-propenamide (17)**



(a) **17b**, 73 mg, 0.19 mmol, (b) 0.198 mL, 1.14 mmol, (c) 1 mL, (d) 0.021 mL, 0.25 mmol, (e) 10 minutes. White solid. Yield: 26 mg, 31 %. **LCMS** (Method B) (ES +ve) m/z 440 ($M + H$)⁺ Rt 2.10 minutes. **¹H NMR** (400 MHz, DMSO-*d*₆) δ 11.75 (br. s, 1H), 8.37 (dd, $J = 1.4, 4.7$ Hz, 1H), 8.10 (d, $J = 7.1$ Hz, 1H), 7.98 (dd, $J = 1.4, 8.1$ Hz, 1H), 7.42 (dd, $J = 4.7, 8.1$ Hz, 1H), 7.40 - 7.36 (m, 1H), 6.32 (s, 1H), 6.20 (dd, $J = 10.1, 17.1$ Hz, 1H), 6.06 (dd, $J = 2.0, 17.1$ Hz, 1H), 5.56 (dd, $J = 2.0, 10.1$ Hz, 1H), 4.22 (s, 2H), 4.02 (br. s, 1H), 3.76 (br. s, 1H), 3.37 (s, 3H), 2.17 - 2.00 (m, 2H), 1.95 - 1.72 (m, 2H), 1.56 - 1.23 (m, 2H), 1.20 - 1.02 (m, 2H); NOE coupling observed between the protons at 3.76 ppm and 4.02 ppm supported the

characterisation of the *cis*-geometry for this compound. **IR** (cm^{-1}) 1516, 1576, 1621, 1656. **HRMS** (ES) calcd for $\text{C}_{21}\text{H}_{26}\text{N}_7\text{O}_2\text{S}$, ($\text{M} + \text{H}$)⁺ 440.1863, found 440.1860. **¹³C NMR** (126 MHz, DMSO-d_6) δ 168.6, 164.0, 161.0, 158.3, 156.4, 144.4, 142.9, 132.4, 126.5, 125.4, 121.9, 92.6, 74.1, 58.8, 49.4, 47.8, 38.9, 32.5, 32.2, 23.5. Note that the signals from two quaternary carbons are believed to be overlapping at 158.3 ppm. For comparison, these two signals are separated in the ¹³C NMR spectrum of the structurally related compounds **9** (158.1 ppm and 158.2 ppm), **14** (158.3 ppm and 158.2 ppm), **39** (158.3 ppm and 158.2 ppm) and **40** (158.3 ppm and 158.1 ppm). Decomposition temperature 264 °C.

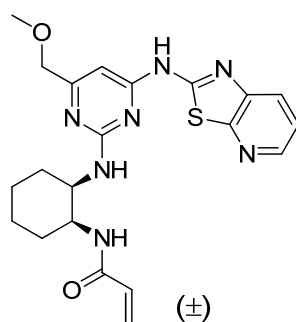
***N*-(*Trans*-2-[[4-[(methoxy)methyl]-6-([1,3]thiazolo[5,4-*b*]pyridin-2-ylamino)-2-pyrimidinyl]amino}cyclohexyl)-2-propenamamide (**18**)**



(a) **18b**, 112 mg, 0.291 mmol, (b) 0.101 mL, 0.581 mmol, (c) 1 mL, (d) 0.025 mL, 0.29 mmol, (e) 10 minutes. White solid. Yield: 24 mg, 19 %. **LCMS** (Method B) (ES +ve) m/z 440 ($\text{M} + \text{H}$)⁺ Rt 2.28 minutes. **¹H NMR** (400 MHz, DMSO-d_6) δ 11.75 (br. s, 1H), 8.37 (dd, $J = 1.3, 4.7$ Hz, 1H), 8.14 (d, $J = 7.0$ Hz, 1H), 7.99 (d, $J = 8.0$ Hz, 1H), 7.43 (dd, $J = 4.7, 8.0$ Hz, 1H), 6.76 (d, $J = 5.8$ Hz, 1H), 6.33 (s, 1H), 6.20 (dd, $J = 10.3, 16.6$ Hz, 1H), 6.07 (d, $J = 16.6$ Hz, 1H), 5.56 (d, $J = 10.3$ Hz, 1H), 4.19 (s, 2H), 3.94 - 3.74 (m, 2H), 3.35 (s, 3H), 2.42 - 2.29 (m, 1H), 2.04 - 1.91 (m, 1H), 1.84 - 1.64 (m, 2H), 1.55 - 1.16 (m, 4H). **IR** (cm^{-1}) 1521, 1576, 1612, 1649. **HRMS** (ES) calcd for $\text{C}_{21}\text{H}_{26}\text{N}_7\text{O}_2\text{S}$, ($\text{M} + \text{H}$)⁺ 440.1863, found 440.1860. **¹³C NMR** (126 MHz, DMSO-d_6) δ 168.7, 165.4, 161.3, 158.3, 156.4, 144.4, 143.0, 132.3, 126.5, 125.7, 121.9, 92.8, 74.1, 58.8, 55.9, 51.6, 32.6, 25.0. Note that (i) the HMQC data indicates that two ¹³C signals from the cyclohexane ring are overlapping at 32.6 ppm and at 25.0 ppm; (ii) the signals from two quaternary carbons are believed to be

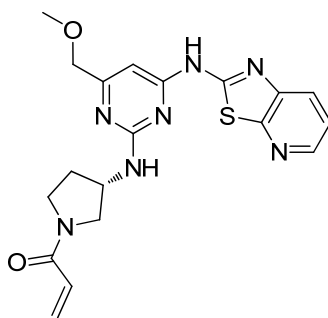
overlapping at 158.3 ppm. For comparison, these two signals are separated in the ^{13}C NMR spectrum of the structurally related compounds **9** (158.1 ppm and 158.2 ppm), **14** (158.3 ppm and 158.2 ppm), **39** (158.3 ppm and 158.2 ppm) and **40** (158.3 ppm and 158.1 ppm). Decomposition temperature 275 °C.

***N*-(*Cis*-2-{[4-[(methoxy)methyl]-6-([1,3]thiazolo[5,4-*b*]pyridin-2-ylamino)-2-pyrimidinyl]amino}cyclohexyl)-2-propenamide (**9**)**



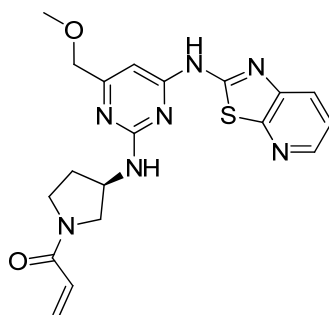
(a) **9b**, 70 mg, 0.18 mmol, (b) 0.063 mL, 0.36 mmol, (c) 1 mL, (d) 0.015 mL, 0.18 mmol, (e) 10 minutes. White solid. Yield: 11 mg, 14 %. **LCMS** (Method B) (ES +ve) m/z 440 ($M + H$)⁺ Rt 2.23 minutes. **^1H NMR** (400 MHz, DMSO- d_6) δ 11.74 (br. s, 1H), 8.37 (dd, $J = 1.4, 4.6$ Hz, 1H), 7.99 (dd, $J = 1.4, 8.2$ Hz, 1H), 7.76 (d, $J = 7.8$ Hz, 1H), 7.43 (dd, $J = 4.6, 8.2$ Hz, 1H), 6.85 (br. s, 1H), 6.38 (dd, $J = 10.3, 16.9$ Hz, 1H), 6.36 (s, 1H), 6.04 (dd, $J = 2.1, 16.9$ Hz, 1H), 5.57 (dd, $J = 2.1, 10.3$ Hz, 1H), 4.40 (br. s, 1H), 4.25 (br. s, 1H), 4.22 (s, 2H), 3.36 (s, 3H), 1.90 - 1.77 (m, 2H), 1.77 - 1.67 (m, 2H), 1.67 - 1.52 (m, 2H), 1.52 - 1.36 (m, 2H). **IR** (cm^{-1}) 1512, 1578, 1620, 1654. **HRMS** (ES) calcd for $\text{C}_{21}\text{H}_{26}\text{N}_7\text{O}_2\text{S}$, ($M + H$)⁺ 440.1863, found 440.1868. **^{13}C NMR** (126 MHz, DMSO- d_6) δ 168.6, 165.1, 161.1, 158.2, 158.1, 156.3, 144.5, 142.9, 132.5, 126.6, 125.6, 121.9, 92.9, 74.0, 58.8, 51.5, 48.2, 29.4, 27.8, 23.9, 21.1. Decomposition temperature 278 °C.

***N*²-[(3*S*)-1-Acryloyl-3-pyrrolidinyl]-6-[(methoxy)methyl]-*N*⁴-[1,3]thiazolo[5,4-*b*]pyridin-2-yl-2,4-pyrimidinediamine (19)**



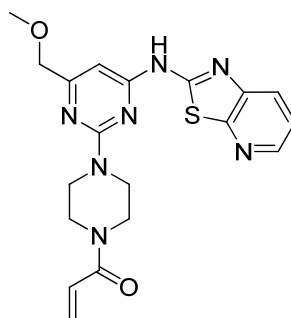
(a) **19c**, 79 mg, 0.20 mmol, (b) 0.070 mL, 0.40 mmol, (c) 1 mL, (d) 0.016 mL, 0.20 mmol, (e) 10 minutes. Light brown solid. Yield: 39 mg, 47 %. **LCMS** (Method B) (ES +ve) *m/z* 412 (*M* + *H*)⁺ Rt 1.96 minutes. **¹H NMR** (250 MHz, DMSO-*d*₆, 120 °C) δ 11.30 (br. s, 1H), 8.35 (d, *J* = 4.7 Hz, 1H), 7.94 (d, *J* = 7.9 Hz, 1H), 7.39 (dd, *J* = 4.7, 7.9 Hz, 1H), 7.04 (br. s, 1H), 6.55 (dd, *J* = 10.7, 16.8 Hz, 1H), 6.50 (s, 1H), 6.11 (d, *J* = 16.8 Hz, 1H), 5.61 (d, *J* = 10.7 Hz, 1H), 4.76 - 4.59 (m, 1H), 4.27 (s, 2H), 4.00 - 3.82 (m, 1H), 3.82 - 3.67 (m, 1H), 3.66 - 3.46 (m, 2H), 3.42 (s, 3H), 2.30 (br. s, 1H), 2.07 (br. s, 1H). **IR** (cm⁻¹) 1516, 1574, 1615, 1641. **HRMS** (ES) calcd for C₁₉H₂₂N₇O₂S, (*M* + *H*)⁺ 412.1550, found 412.1558. **¹³C NMR** (126 MHz, DMSO-*d*₆) δ 168.7, 163.9, 161.3, 158.3, 156.3, 144.4, 143.0, 130.2, 129.9, 127.2, 127.0, 126.6, 121.9, 93.2, 74.1, 58.8, 52.0, 50.2, 45.0, 44.4, 31.7, 30.0. Note: ¹³C NMR at room temperature displays the presence of rotamers for the compound. Decomposition temperature 222 °C.

***N*²-[(3*R*)-1-Acryloyl-3-pyrrolidinyl]-6-[(methoxy)methyl]-*N*⁴-[1,3]thiazolo[5,4-*b*]pyridin-2-yl-2,4-pyrimidinediamine (20)**



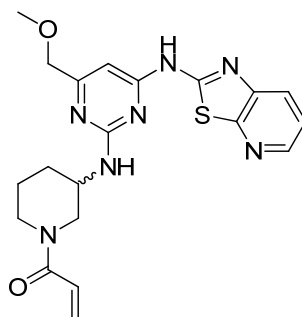
(a) **20c**, 73 mg, 0.19 mmol, (b) 0.071 mL, 0.41 mmol, (c) 1 mL, (d) 0.017 mL, 0.21 mmol, (e) 10 minutes. Off-white solid. Yield: 37 mg, 49 %. **LCMS** (Method B) (ES +ve) *m/z* 412 (*M* + *H*)⁺ *Rt* 1.96 minutes. **¹H NMR** (250 MHz, DMSO-*d*₆, 120 °C) δ = 11.28 (br. s, 1H), 8.34 (dd, *J* = 1.4, 4.7 Hz, 1H), 7.93 (dd, *J* = 1.4, 8.1 Hz, 1H), 7.38 (dd, *J* = 4.7, 8.1 Hz, 1H), 7.01 (d, *J* = 6.4 Hz, 1H), 6.55 (dd, *J* = 10.5, 16.9 Hz, 1H), 6.50 (s, 1H), 6.11 (dd, *J* = 2.4, 16.9 Hz, 1H), 5.61 (dd, *J* = 2.4, 10.5 Hz, 1H), 4.75 - 4.59 (m, 1H), 4.27 (s, 2H), 3.99 - 3.82 (m, 1H), 3.82 - 3.66 (m, 1H), 3.66 - 3.46 (m, 2H), 3.42 (s, 3H), 2.41 - 2.19 (m, 1H), 2.16 - 1.96 (m, 1H). **IR** (cm⁻¹) 1516, 1574, 1615, 1636. **HRMS** (ES) calcd for C₁₉H₂₂N₇O₂S, (*M* + *H*)⁺ 412.1550, found 412.1550. **¹³C NMR** (126 MHz, DMSO-*d*₆) δ 168.63, 163.91, 161.26, 158.31, 158.29, 156.26, 144.42, 142.98, 142.97, 130.18, 129.86, 127.15, 127.02, 126.56, 121.88, 93.21, 74.08, 58.79, 52.02, 50.25, 45.03, 44.45, 31.70, 30.03. Note: ¹³C NMR at room temperature displays the presence of rotamers for the compound. The data is reported with two decimal points to differentiate the signals. Decomposition temperature 225 °C.

***N*-{2-(4-Acryloyl-1-piperazinyl)-6-[(methoxy)methyl]-4-pyrimidinyl}[1,3]thiazolo[5,4-*b*]pyridin-2-amine (21)**



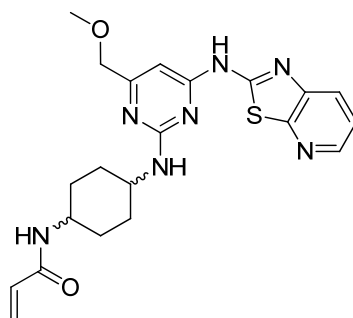
(a) **21c**, 49 mg, 0.12 mmol, (b) 0.048 mL, 0.27 mmol, (c) 1 mL, (d) 0.012 mL, 0.14 mmol, (e) 10 minutes. Light brown solid. Yield: 24 mg, 47 %. **LCMS** (Method B) (ES +ve) *m/z* 412 (*M* + *H*)⁺ *Rt* 2.17 minutes. **¹H NMR** (400 MHz, DMSO-*d*₆) δ 11.89 (br. s, 1H), 8.39 (dd, *J* = 1.3, 4.5 Hz, 1H), 8.01 (dd, *J* = 1.3, 8.1 Hz, 1H), 7.44 (dd, *J* = 4.5, 8.1 Hz, 1H), 6.91 (dd, *J* = 10.4, 16.5 Hz, 1H), 6.44 (s, 1H), 6.17 (dd, *J* = 2.0, 16.5 Hz, 1H), 5.73 (dd, *J* = 2.0, 10.4 Hz, 1H), 4.29 (s, 2H), 3.88 (m, 4H), 3.72 (m, 4H), 3.38 (s, 3H). **HRMS** (ES) calcd for C₁₉H₂₂N₇O₂S, (*M* + *H*)⁺ 412.1556, found 412.1552. **IR** (cm⁻¹) 1519, 1575, 1625, 1643. **¹³C NMR** (101 MHz, DMSO-*d*₆) δ 167.9, 164.4, 160.2, 158.0, 157.5, 155.5, 144.1, 142.6, 128.2, 127.5, 126.3, 121.5, 93.3, 73.8, 58.4, 44.7, 44.3, 43.6, 41.2. Note: ¹³C signals at 44.7, 44.3, 43.6 and 41.2 were very weak. Their assignments were however confirmed by the HSQC spectrum. Decomposition temperature 250 °C.

***N*²-(1-Acryloyl-3-piperidinyl)-6-[(methoxy)methyl]-*N*⁴-[1,3]thiazolo[5,4-*b*]pyridin-2-yl-2,4-pyrimidinediamine (13)**



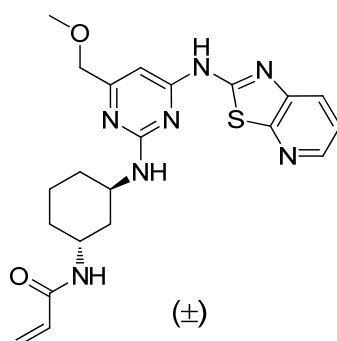
A microwave vial was charged with *N*-[6-[(methoxy)methyl]-2-(methylsulfonyl)-4-pyrimidinyl][1,3]thiazolo[5,4-*b*]pyridin-2-amine **5** (500 mg, 1.42 mmol), 1,1-dimethylethyl 3-amino-1-piperidinecarboxylate (570 mg, 2.85 mmol) and isopropanol (5 mL). The microwave vial was sealed and was heated in a Biotage Initiator microwave at 150 °C for 45 hours. The residue was purified by FlashMaster chromatography on silica using a gradient elution from 0 to 15 % methanol (+1 % triethylamine) in dichloromethane. After evaporation of the desired fractions to dryness, the residue was dissolved in dichloromethane and treated with HCl in dioxane (4 M, 0.60 mL, 2.4 mmol) at room temperature. The solution was stirred at room temperature overnight. The reaction mixture was filtered under reduced pressure and dried to give a solid (185 mg). A mixture of the obtained solid (50 mg only), 2-propenoyl chloride (0.015 ml, 0.18 mmol) and *N,N*-diisopropylethylamine (0.141 ml, 0.810 mmol) in *N*-methyl-2-pyrrolidone (1 ml) was stirred at room temperature for 2 hours. The mixture was subjected to purification by mass directed automated preparative HPLC to afford the title compound (12 mg, 2 % yield - note that only 50 mg of the intermediate solid was used for the amide coupling reaction) as an off-white solid. **LCMS** (Method C) (ES +ve) *m/z* 426 (*M* + *H*)⁺ *Rt* 1.54 minutes. **¹H NMR** (250 MHz, DMSO-*d*₆, 120 °C) δ 11.06 (br. s, 1H), 8.33 (dd, *J* = 1.4, 4.7 Hz, 1H), 7.92 (dd, *J* = 1.4, 8.1 Hz, 1H), 7.37 (dd, *J* = 4.7, 8.1 Hz, 1H), 6.67 (dd, *J* = 10.6, 16.9 Hz, 1H), 6.58 (d, *J* = 7.5 Hz, 1H), 6.48 (s, 1H), 6.01 (dd, *J* = 2.3, 16.9 Hz, 1H), 5.54 (dd, *J* = 2.3, 10.6 Hz, 1H), 4.26 (s, 2H), 4.21 - 3.88 (m, 3H), 3.42 (s, 3H), 3.27 - 3.05 (m, 2H), 2.19 - 2.04 (m, 1H), 1.93 - 1.78 (m, 1H), 1.78 - 1.45 (m, 2H).

***N*-[4-[[4-[(Methoxy)methyl]-6-([1,3]thiazolo[5,4-*b*]pyridin-2-ylamino)-2-pyrimidinyl]amino}cyclohexyl)-2-propenamide (15)**



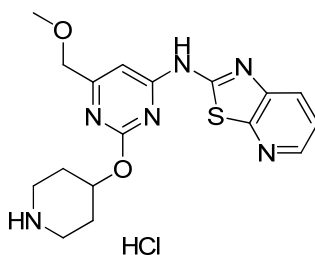
A microwave vial was charged with *N*-[6-[(methoxy)methyl]-2-(methylsulfonyl)-4-pyrimidinyl][1,3]thiazolo[5,4-*b*]pyridin-2-amine **5** (200 mg, 0.569 mmol), 1,4-cyclohexanediamine (mixture of *cis*- and *trans*-isomers, 97 mg, 0.85 mmol) and isopropanol (4 mL). The vial was sealed and was heated in a Biotage Initiator microwave at 150 °C for 30 minutes. After cooling, the reaction was filtered under reduced pressure and the solid was washed with isopropanol. The filtrate was evaporated to dryness to give a yellow solid. The solid was dissolved in *N*-methyl-2-pyrrolidone (3 mL) and treated with 2-propenoyl chloride (0.096 mL, 1.14 mmol) and *N,N*-diisopropylethylamine (0.596 mL, 3.41 mmol). The reaction was stirred at room temperature for 5 minutes. The mixture was subjected to purification twice by mass directed automated preparative HPLC to afford the title compound (45 mg, 18 % yield) as a light brown solid. **LCMS** (Method B) (ES +ve) *m/z* 440 (*M* + *H*)⁺ *Rt* 2.08 minutes. **¹H NMR** (400 MHz, DMSO-*d*₆) δ = 11.42 (br. s, 1H), 8.36 (dd, *J* = 1.4, 4.6 Hz, 1H), 7.97 (dd, *J* = 1.4, 8.0 Hz, 1H), 7.96 - 7.94 (m, 1H), 7.42 (dd, *J* = 4.6, 8.0 Hz, 1H), 7.26 - 7.15 (m, 1H), 6.40 - 6.30 (m, 2H), 6.08 (dd, *J* = 2.3, 17.1 Hz, 1H), 5.56 (dd, *J* = 2.3, 10.0 Hz, 1H), 4.23 (s, 2H), 4.15 - 3.95 (m, 1H), 3.85 (br. s, 1H), 3.37 (s, 3 H), 2.13 - 1.33 (m, 8H).

***N*-(*Trans*-3-{[4-[(methoxy)methyl]-6-([1,3]thiazolo[5,4-*b*]pyridin-2-ylamino)-2-pyrimidinyl]amino}cyclohexyl)-2-propenamide (16)**



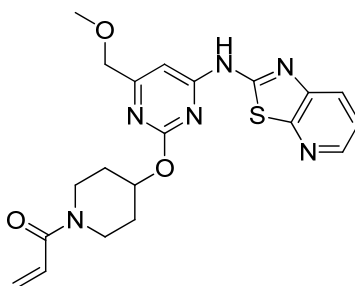
A microwave vial was charged with *N*-[6-[(methoxy)methyl]-2-(methylsulfonyl)-4-pyrimidinyl][1,3]thiazolo[5,4-*b*]pyridin-2-amine **5** (200 mg, 0.569 mmol), 1,3-cyclohexanediamine (mixture of *cis*- and *trans*-isomers, 97 mg, 0.85 mmol) and isopropanol (4 mL). The vial was sealed and was heated in a Biotage Initiator microwave at 150 °C for 30 minutes. After cooling, the reaction was filtered under reduced pressure and the solid was washed with isopropanol. The filtrate was evaporated to dryness to give a yellow solid. The solid was subjected to purification by mass directed automated preparative HPLC. The obtained intermediate, 2-propenoyl chloride (7.14 μL, 0.0843 mmol) and *N,N*-diisopropylethylamine (0.068 mL, 0.39 mmol) in *N*-methyl-2-pyrrolidone (1 mL) were stirred at room temperature for 10 minutes. The mixture was subjected to purification by mass directed automated preparative HPLC to afford the title compound (5 mg, 2 % yield) as an off-white solid. **LCMS** (Method B) (ES +ve) *m/z* 440 (*M* + *H*)⁺ *Rt* 2.15 minutes. **¹H NMR** (400 MHz, DMSO-*d*₆) δ 11.66 (br. s, 1H), 8.33 (d, *J* = 4.8 Hz, 1H), 7.99 (d, *J* = 7.3 Hz, 1H), 7.94 (d, *J* = 8.0 Hz, 1H), 7.39 (dd, *J* = 4.8, 8.0 Hz, 1H), 7.20 (br. s, 1H), 6.32 (s, 1H), 6.24 (dd, *J* = 10.1, 16.7 Hz, 1H), 6.00 (d, *J* = 16.7 Hz, 1H), 5.45 (d, 10.1 Hz, 1H), 4.37 (br. s, 1H), 4.23 (s, 2H), 4.05 (br. s, 1H), 3.37 (s, 3H), 2.00 - 1.86 (m, 1H), 1.85 - 1.74 (m, 2H), 1.74 - 1.59 (m, 3H), 1.59 - 1.48 (m, 1H), 1.45 - 1.32 (m, 1H); NMR (including NOE couplings) comparisons with compound **17** supported the characterisation of the *trans*-geometry for this compound.

***N*-[6-[(Methoxy)methyl]-2-(4-piperidinyloxy)-4-pyrimidinyl][1,3]thiazolo[5,4-*b*]pyridin-2-amine hydrochloride (23c)**



A microwave vial was charged with *N*-[6-[(methoxy)methyl]-2-(methylsulfonyl)-4-pyrimidinyl][1,3]thiazolo[5,4-*b*]pyridin-2-amine **5** (200 mg, 0.569 mmol), 1,1-dimethylethyl 4-hydroxy-1-piperidinecarboxylate (229 mg, 1.14 mmol) and sodium hydride (60 % w/w in mineral oil, 68 mg, 1.7 mmol) in tetrahydrofuran (3 mL). The vial was sealed and was heated in a Biotage Initiator microwave at 130 °C for 30 minutes. The reaction mixture was partitioned between dichloromethane and water. The organic layer was dried using a hydrophobic frit and evaporated to dryness. The intermediate was dissolved in dichloromethane (3 mL) and methanol (1 mL) and was treated with HCl in dioxane (4 M, 0.711 mL, 2.85 mmol). The reaction was stirred at room temperature overnight. The reaction mixture was evaporated to dryness to afford the title compound (160 mg, 85 % pure by LCMS and NMR, 59 % yield) as a brown solid. **LCMS** (Method B) (ES +ve) *m/z* 373 (*M* + *H*)⁺ *Rt* 1.69 minutes. **¹H NMR** (400 MHz, DMSO-*d*₆) δ 12.28 (br. s, 1H), 9.10 (br. s, 1H), 8.45 (dd, *J* = 1.4, 4.8 Hz, 1H), 8.10 (dd, *J* = 1.4, 8.2 Hz, 1H), 7.51 (dd, *J* = 4.8, 8.2 Hz, 1H), 6.86 (s, 1H), 5.37 - 5.30 (m, 1H), 4.37 (s, 2H), 3.41 (s, 3H), 3.32 - 3.14 (m, 4H), 2.35 - 2.23 (m, 2H), 2.10 - 1.96 (m, 2H).

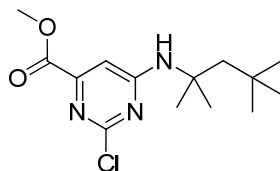
***N*-{2-[(1-Acryloyl-4-piperidinyloxy)-6-[(methoxy)methyl]-4-pyrimidinyl][1,3]thiazolo [5,4-*b*]pyridin-2-amine (24)**



A mixture of *N*-[6-[(methoxy)methyl]-2-(4-piperidinyloxy)-4-pyrimidinyl][1,3]thiazolo[5,4-*b*]pyridin-2-amine hydrochloride **24** (80 mg, 85 % pure, 0.17 mmol), 2-propenoyl chloride (0.017 mL, 0.20 mmol) and *N,N*-diisopropylethylamine (0.068 mL, 0.39 mmol) in *N*-methyl-2-pyrrolidone (1 mL) was stirred at room temperature for 10 minutes. The mixture was subjected to purification by mass directed automated preparative HPLC to afford the title compound (20 mg, 24 % yield) as an off-white solid. **LCMS** (Method D) (ES +ve) *m/z* 427 (M + H)⁺ Rt 0.78 minutes. **¹H NMR** (400 MHz, DMSO-*d*₆) δ 12.17 (br. s, 1H), 8.40 (dd, *J* = 1.4, 4.7 Hz, 1H), 8.04 (dd, *J* = 1.4, 8.2 Hz, 1H), 7.46 (dd, *J* = 4.7, 8.2 Hz, 1H), 6.87 (dd, *J* = 10.4, 16.7 Hz, 1H), 6.80 (s, 1H), 6.13 (dd, *J* = 2.5, 16.7 Hz, 1H), 5.69 (dd, *J* = 2.5, 10.4 Hz, 1H), 5.37 - 5.29 (m, 1H), 4.36 (s, 2H), 4.06 - 3.87 (m, 2H), 3.57 - 3.46 (m, 1H), 3.45 - 3.37 (m, 4H), 2.20 - 2.06 (m, 2H), 1.81 - 1.61 (m, 2H). **IR** (cm⁻¹) 1518, 1575, 1589, 1615. **HRMS** (ES) calcd for C₂₀H₂₃N₆O₃S, (M + H)⁺ 427.1547, found 427.1548. **¹³C NMR** (126 MHz, DMSO-*d*₆) δ 170.2, 164.8, 163.4, 159.6, 157.9, 156.1, 144.9, 142.9, 128.9, 127.7, 127.0, 122.1, 97.9, 73.8, 72.5, 58.9, 43.0, 31.8, 30.8. Note that the HMQC data revealed that one ¹³C signal was present at around 40 ppm. In the ¹³C spectrum, this peak is overlapping with the DMSO signals hence can not be seen. Decomposition temperature 151 °C.

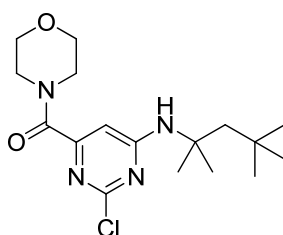
2. Synthetic procedures for the 6-morpholinemethylpyrimidine series

Methyl 2-chloro-6-[(1,1,3,3-tetramethylbutyl)amino]-4-pyrimidinecarboxylate (26)



A mixture of methyl 2,6-dichloro-4-pyrimidinecarboxylate **25** (10 g, 48 mmol), *tert*-octylamine (11.6 mL, 72.5 mmol) and *N,N*-diisopropylethylamine (12.7 mL, 72.5 mmol) in tetrahydrofuran (10 mL) was stirred at room temperature for 96 hours. The reaction mixture was evaporated to dryness. The residue was partitioned between dichloromethane (200 mL) and saturated aqueous NaHCO₃ (150 mL). After separation, the organic extract was dried using a hydrophobic frit and evaporated to dryness. The residue was purified by FlashMaster chromatography on silica using a gradient elution from 0 to 60 % ethyl acetate in cyclohexane to afford the title compound (10.01 g, 69 % yield) as a white solid. LCMS (Method B) (ES +ve) *m/z* 300 (M + H)⁺ Rt 3.32 minutes. ¹H NMR (400MHz, DMSO-d₆) δ 7.93 (s, 1H), 7.13 (s, 1H), 3.83 (s, 3H), 1.87 (s, 2H), 1.42 (s, 6H), 0.91 (s, 9H).

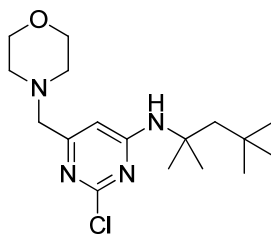
2-Chloro-6-(4-morpholinylcarbonyl)-*N*-(1,1,3,3-tetramethylbutyl)-4-pyrimidinamine (28)



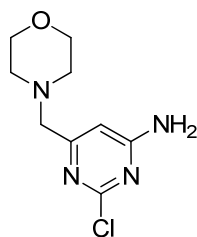
A mixture of methyl 2-chloro-6-[(1,1,3,3-tetramethylbutyl)amino]-4-pyrimidinecarboxylate **26** (5.00 g, 16.7 mmol), TBD (0.696 g, 5.00 mmol) and morpholine (1.453 mL, 16.68 mmol) in tetrahydrofuran (30 mL) was stirred at room temperature for 3 hours. The reaction mixture was partitioned between

dichloromethane (100 mL) and saturated aqueous Na₂CO₃ (100 mL). After separation, the organic extract was dried using a hydrophobic frit and evaporated to dryness to afford the title compound (5.9 g, 100 % yield) as a white solid. **LCMS** (Method B) (ES +ve) m/z 355 (M + H)⁺ Rt 3.07 minutes. **¹H NMR** (400 MHz, DMSO-d₆) δ 7.75 (s, 1H), 6.55 (s, 1H), 3.65 - 3.59 (m, 2H), 3.59 - 3.51 (m, 4H), 3.47 - 3.35 (m, 2H), 1.87 (s, 2H), 1.42 (s, 6H), 0.91 (s, 9H).

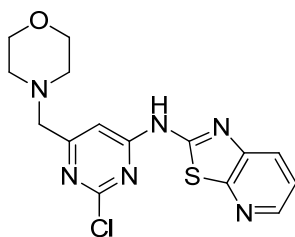
2-Chloro-6-(4-morpholinylmethyl)-N-(1,1,3,3-tetramethylbutyl)-4-pyrimidinamine (29)



Borane in tetrahydrofuran (1M, 41.4 mL, 41.4 mmol) was added dropwise to a solution of 2-chloro-6-(4-morpholinylcarbonyl)-N-(1,1,3,3-tetramethylbutyl)-4-pyrimidinamine **28** (4.90 g, 13.8 mmol) stirring at 0 °C in tetrahydrofuran (20 mL) under a nitrogen atmosphere. The reaction mixture was stirred at 0 °C for 20 minutes then warmed to room temperature and continued stirring under a nitrogen atmosphere for 48 hours. Further borane in tetrahydrofuran (1M, 20 mL, 20 mmol) was added dropwise and the reaction mixture was heated at 30 °C for 2 hours. The reaction was cooled to room temperature and aqueous HCl (5 M) was carefully added until a clear solution was obtained. The reaction was stirred for 30 minutes. The reaction mixture was basified with aqueous NaOH (10 M) to reach pH 14 and the aqueous layer was extracted with dichloromethane:ethyl acetate (1:1, 2 x 100 mL). The combined organic layers were dried and evaporated to dryness. The residue was purified by FlashMaster chromatography on silica using a gradient elution from 0 to 100 % ethyl acetate in cyclohexane to afford the title compound (3.2 g, 68 % yield) as a colourless oil. **LCMS** (Method B) (ES +ve) m/z 341 (M + H)⁺ Rt 3.22 minutes. **¹H NMR** (400 MHz, DMSO-d₆) δ 7.43 (br. s, 1H), 6.54 (s, 1H), 3.64 - 3.56 (m, 4H), 3.29 (s, 2H), 2.43 - 2.37 (m, 4H), 1.86 (s, 2H), 1.40 (s, 6H), 0.90 (s, 9H).

2-Chloro-6-(4-morpholinylmethyl)-4-pyrimidinamine (30)

A mixture of 2-chloro-6-(4-morpholinylmethyl)-*N*-(1,1,3,3-tetramethylbutyl)-4-pyrimidinamine **29** (3.2 g, 9.4 mmol) in trifluoroacetic acid (20 mL, 260 mmol) and dichloromethane (20 mL) was heated at 50 °C for 16 hours. The reaction mixture was evaporated to dryness. The residue was partitioned between ethyl acetate:dichloromethane (1:1, 100 mL) and saturated aqueous Na₂CO₃ (100 mL). The pH of the aqueous phase was adjusted to 14 with aqueous NaOH (10 M). After separation, the aqueous phase was extracted with ethyl acetate:dichloromethane (1:1, 2 x 100 mL). The organic extracts were combined, dried using a hydrophobic frit and evaporated to dryness. The solid was triturated with dichloromethane and filtered under reduced pressure to afford the title compound (915 mg, 43 % yield) as a white solid. LCMS (Method B) (ES +ve) *m/z* 229 (M + H)⁺ Rt 1.32 minutes. ¹H NMR (400 MHz, DMSO-d₆) δ 7.30 (br. s, 2H), 6.48 (s, 1H), 3.63 - 3.56 (m, 4H), 3.32 (s, 2H), 2.44 - 2.39 (m, 4H).

***N*-[2-Chloro-6-(4-morpholinylmethyl)-4-pyrimidinyl][1,3]thiazolo[5,4-*b*]pyridin-2-amine (32)**

Under an atmosphere of nitrogen, an ice-cooled solution of a mixture of 2-chloro-6-(4-morpholinylmethyl)-4-pyrimidinamine **30** (1.14 g, 4.99 mmol) and 2-bromo[1,3]thiazolo[5,4-*b*]pyridine **31** (1.18 g, 5.48 mmol) in dry *N,N*-

dimethylformamide (20 mL) was treated portionwise over 5 minutes with sodium hydride (60 % w/w in mineral oil, 0.399 g, 9.97 mmol). The reaction mixture was stirred with cooling for 1 hour and at ambient temperature for a further 1 hour. The mixture was treated cautiously with saturated ammonium chloride (5 mL). Saturated aqueous Na₂CO₃ was added to reach pH 9 and the product was extracted with dichloromethane (2 x 100 mL). The organic extracts were combined, dried using a hydrophobic frit and evaporated to dryness. The residue was purified by FlashMaster chromatography on silica using a gradient elution from 0 to 100 % ethyl acetate in cyclohexane followed by a methanol wash to afford the title compound (1.15 g, 64 % yield) as an off-white solid. **LCMS** (Method B) (ES +ve) m/z 363 (M + H)⁺ Rt 1.82 minutes. **¹H NMR** (400 MHz, DMSO-d₆) δ 8.43 (dd, *J* = 1.5, 4.8 Hz, 1H), 8.06 (dd, *J* = 1.5, 8.2 Hz, 1H), 7.47 (dd, *J* = 4.8, 8.2 Hz, 1H), 7.32 (s, 1H), 3.66 - 3.61 (m, 4H), 3.54 (s, 2H), 2.49 - 2.46 (m, 4H).

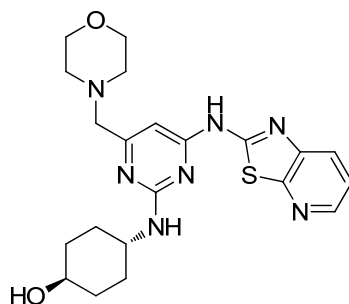
General procedure D for the aromatic nucleophilic displacement reaction:

A microwave vial was charged with *N*-[2-chloro-6-(4-morpholinylmethyl)-4-pyrimidinyl][1,3]thiazolo[5,4-*b*]pyridin-2-amine **32**, the amine analogue and isopropanol. The vial was sealed and was heated in the Biotage Initiator microwave at the temperature stated until the reaction had reached completion. The reaction mixture was evaporated to dryness. The product was purified either by chromatography on silica or by mass directed automated preparative HPLC.

Following the general procedure D for the nucleophilic displacement reaction, data are presented as (a) amount of compound **32**, (b) amount of amine analogue, (c) volume of isopropanol, (d) reaction temperature, (e) reaction time, (f) purification system.

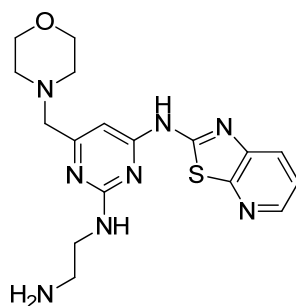
Note that as the same chemistry had already been performed in the methoxymethyl series, some of these intermediates were only analysed by LCMS and used, as such, in the subsequent steps.

***Trans*-4-((4-(morpholinomethyl)-6-(thiazolo[5,4-*b*]pyridin-2-ylamino)pyrimidin-2-yl)amino)cyclohexanol (7)**



(a) 50 mg, 0.14 mmol, (b) *trans*-4-aminocyclohexanol, 48 mg, 0.42 mmol, (c) 4 mL, (d) 170 °C, (e) 1 hour, (f) purification by mass directed automated preparative HPLC. Off-white solid. Yield: 25 mg, 41 %. **LCMS** (Method D) (ES +ve) m/z 442 (M + H)⁺ Rt 0.74 minutes. **¹H NMR** (400 MHz, DMSO-*d*₆, 120 °C) δ 8.34 (dd, J = 4.5, 1.5 Hz, 1H), 7.91 (dd, J = 8.1, 1.5 Hz, 1H), 7.37 (dd, J = 8.1, 4.5 Hz, 1H), 6.49 (s, 1H), 6.32 (d, J = 7.6 Hz, 1H), 4.07 - 3.87 (m, 2H), 3.68 - 3.61 (m, 4H), 3.57 - 3.47 (m, 1H), 3.35 (s, 2H), 2.52 - 2.49 (m, 4H), 2.11- 2.02 (m, 2H), 1.99 - 1.91 (m, 2H), 1.47 - 1.34 (m, 4H).

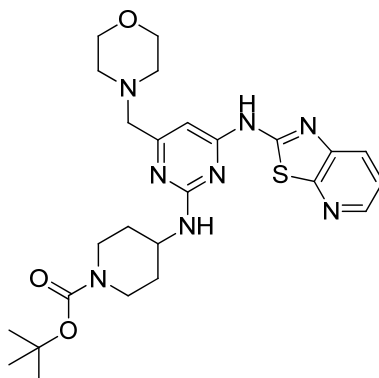
***N*²-(2-Aminoethyl)-6-(4-morpholinylmethyl)-*N*⁴-[1,3]thiazolo[5,4-*b*]pyridin-2-yl-2,4-pyrimidinediamine (33b)**



(a) 115 mg, 0.317 mmol, (b) (2-aminoethyl)amine, 0.023 mL, 0.35 mmol, (c) 5 mL, (d) 160 °C, (e) 30 minutes, (f) purification by mass directed automated preparative HPLC. Colourless glass. Yield: 31 mg, 25 %. **LCMS** (Method B) (ES +ve) m/z 387 (M + H)⁺ Rt 1.67 minutes. **¹H NMR** (400 MHz, DMSO-*d*₆) δ 8.34 (dd, J = 1.2, 4.5 Hz, 1H), 7.95 (dd, J = 1.2, 8.0 Hz, 1H), 7.40 (dd, J = 4.5, 8.0 Hz, 1H), 7.16 (br. s,

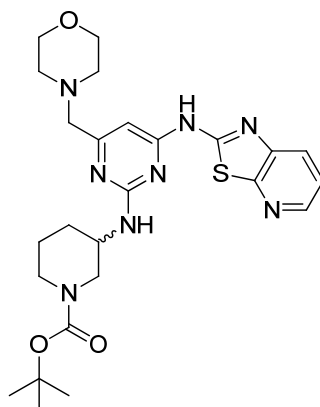
1H), 6.41 (s, 1H), 3.67 - 3.57 (m, 4H), 3.51 - 3.39 (m, 2H), 3.33 (s, 2H), 2.82 - 2.74 (m, 2H), 2.46 - 2.40 (m, 4H).

1,1-Dimethylethyl 4-[[4-(4-morpholinylmethyl)-6-([1,3]thiazolo[5,4-*b*]pyridin-2-ylamino)-2-pyrimidinyl]amino]-1-piperidinecarboxylate (34a)



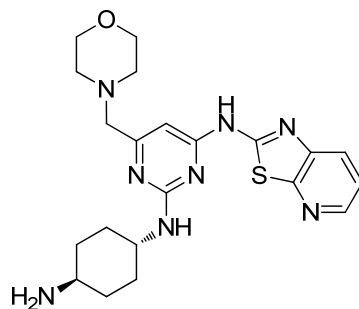
(a) 200 mg, 0.551 mmol, (b) 1,1-dimethylethyl 4-amino-1-piperidinecarboxylate, 331 mg, 1.65 mmol, (c) 3 mL, (d) 170 °C, (e) 1 hour, (f) Purification by FlashMaster chromatography on silica (gradient elution from 0 to 15 % methanol (+1 % triethylamine) in dichloromethane). Brown solid. Yield: 206 mg, 71 %. **LCMS** (Method D) (ES +ve) m/z 527 (M + H)⁺ Rt 1.05 minutes. **¹H NMR** (400 MHz, DMSO-*d*₆, 120 °C) δ 11.21 (br. s, 1H), 8.35 (dd, $J = 1.4, 4.7$ Hz, 1H), 7.93 (dd, $J = 1.4, 8.1$ Hz, 1H), 7.38 (dd, $J = 4.7, 8.1$ Hz, 1H), 6.66 (d, $J = 7.6$ Hz, 1H), 6.52 (s, 1H), 4.20 - 4.08 (m, 1H), 4.03 - 3.94 (m, 2H), 3.67 - 3.62 (m, 4H), 3.36 (s, 2H), 3.05 - 2.95 (m, 2H), 2.54 - 2.50 (m, 4H), 2.05 - 1.95 (m, 2H), 1.57 - 1.45 (m, 2H), 1.46 (s, 9H).

1,1-Dimethylethyl 3-[[4-(4-morpholinylmethyl)-6-([1,3]thiazolo[5,4-*b*]pyridin-2-ylamino)-2-pyrimidinyl]amino]-1-piperidinecarboxylate (35a)



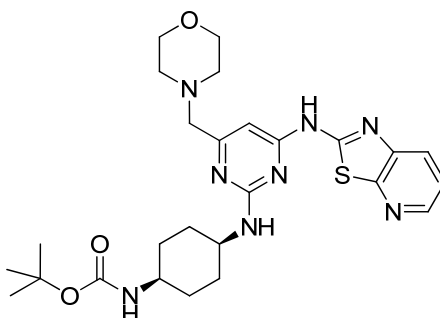
(a) 200 mg, 0.551 mmol, (b) 1,1-dimethylethyl 3-amino-1-piperidinecarboxylate, 221 mg, 1.10 mmol, (c) 5 mL, (d) 170 °C, (e) 40 minutes. LCMS analysis revealed that some starting material remained in the reaction mixture. Therefore, a second portion of 1,1-dimethylethyl 3-amino-1-piperidinecarboxylate (110 mg, 0.549 mmol) was added to the reaction mixture and the vial was heated in the Biotage Initiator microwave system at 170 °C for further 20 minutes. (f) Purification by FlashMaster chromatography on silica (gradient elution from 0 to 15 % methanol (+1 % triethylamine) in dichloromethane). Brown solid. Yield: 225 mg, 86 % pure, 67 %. **LCMS** (Method B) (ES +ve) m/z 527 ($M + H$)⁺ Rt 2.54 minutes. **¹H NMR** (400 MHz, DMSO-*d*₆, 120 °C) δ 10.26 (br. s, 1H), 8.33 (dd, $J = 1.4, 4.7$ Hz, 1H), 7.92 (dd, $J = 1.4, 8.1$ Hz, 1H), 7.37 (dd, $J = 4.7, 8.1$ Hz, 1H), 6.56 (s, 1H), 6.40 (d, $J = 7.6$ Hz, 1H), 4.11 - 4.01 (m, 1H), 3.92 (m, 1H), 3.72 - 3.59 (m, 5H), 3.38 (s, 2H), 3.15 - 3.00 (m, 2H), 2.54 - 2.51 (m, 4H), 2.12 - 2.02 (m, 1H), 1.85 - 1.75 (m, 1H), 1.69 - 1.48 (m, 2H), 1.36 (s, 9H).

***N*²-(*Trans*-4-aminocyclohexyl)-6-(4-morpholinylmethyl)-*N*⁴-[1,3]thiazolo[5,4-*b*]pyridin-2-yl-2,4-pyrimidinediamine (36b)**



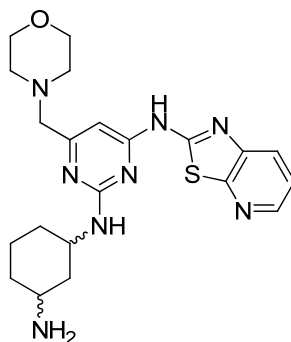
(a) 200 mg, 0.551 mmol, (b) *trans*-1,4-cyclohexanediamine, 63 mg, 0.55 mmol, (c) 4 mL, (d) 170 °C, (e) 60 minutes, (f) Purification by mass directed automated preparative HPLC. Colourless glass. Yield: 55 mg, 85 % pure, 20 %. **LCMS** (Method B) (ES +ve) *m/z* 441 (M + H)⁺ Rt 1.81 minutes.

1,1-Dimethylethyl (cis-4-{[4-(4-morpholinylmethyl)-6-([1,3]thiazolo[5,4-*b*]pyridin-2-ylamino)-2-pyrimidinyl]amino}cyclohexyl)carbamate (37a)



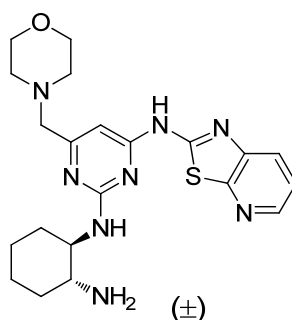
(a) 200 mg, 0.551 mmol, (b) 1,1-dimethylethyl (*cis*-4-aminocyclohexyl)carbamate, 354 mg, 1.65 mmol, (c) 4 mL, (d) 170 °C, (e) 60 minutes, (f) purification by mass directed automated preparative HPLC. White solid. Yield: 135 mg, 45 %. **LCMS** (Method D) (ES +ve) *m/z* 541 (M + H)⁺ Rt 1.07 minutes.

***N*²-(3-Aminocyclohexyl)-6-(4-morpholinylmethyl)-*N*⁴-[1,3]thiazolo[5,4-*b*]pyridin-2-yl-2,4-pyrimidinediamine (38b)**



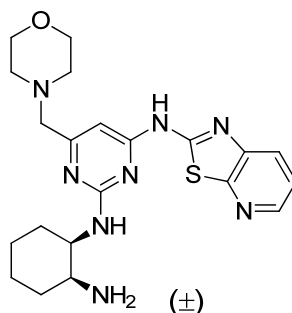
(a) 150 mg, 0.413 mmol, (b) 1,3-cyclohexanediamine (mixture of *cis*- and *trans*-isomers), 118 mg, 1.03 mmol, (c) 4 mL, (d) 170 °C, (e) 30 minutes, (f) purification by mass directed automated preparative HPLC. Colourless glass. Yield: 94 mg, 52 %. **LCMS** (Method B) (ES +ve) *m/z* 441 (M + H)⁺ Rt 1.90 minutes.

***N*²-[*Trans*-2-aminocyclohexyl]-6-(4-morpholinylmethyl)-*N*⁴-[1,3]thiazolo[5,4-*b*]pyridin-2-yl-2,4-pyrimidinediamine (40b)**



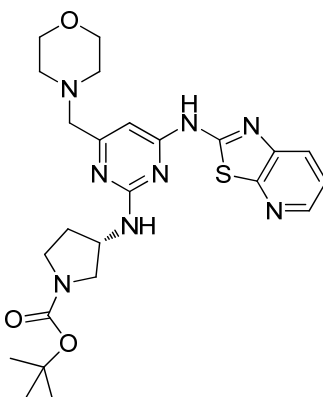
(a) 100 mg, 0.276 mmol, (b) *trans*-1,2-diaminocyclohexane, 79 mg, 0.69 mmol, (c) 4 mL, (d) 170 °C, (e) 30 minutes, (f) purification by mass directed automated preparative HPLC. Colourless glass. Yield: 45 mg, 37 %. **LCMS** (Method B) (ES +ve) *m/z* 441 (M + H)⁺ Rt 2.06 minutes.

***N*²-[*Cis*-2-aminocyclohexyl]-6-(4-morpholinylmethyl)-*N*⁴-[1,3]thiazolo[5,4-*b*]pyridin-2-yl-2,4-pyrimidinediamine (41b)**



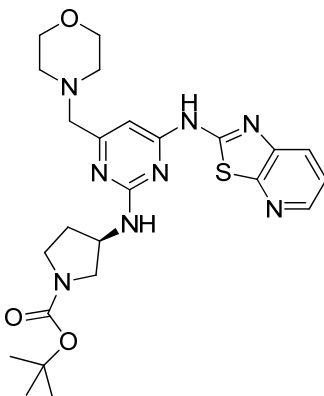
(a) 100 mg, 0.276 mmol, (b) *cis*-1,2-diamino-cyclohexane, 79 mg, 0.69 mmol, (c) 4 mL, (d) 170 °C, (e) 40 minutes, (f) purification by mass directed automated preparative HPLC. Colourless glass. Yield: 51 mg, 42 %. **LCMS** (Method B) (ES +ve) *m/z* 441 (M + H)⁺ Rt 2.08 minutes.

1,1-Dimethylethyl (3*S*)-3-[[4-(4-morpholinylmethyl)-6-([1,3]thiazolo[5,4-*b*]pyridin-2-ylamino)-2-pyrimidinyl]amino]-1-pyrrolidinecarboxylate (42a)



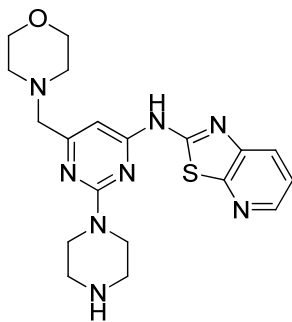
(a) 200 mg, 0.551 mmol, (b) 1,1-dimethylethyl (3*S*)-3-amino-1-pyrrolidinecarboxylate, 308 mg, 1.65 mmol, (c) 4 mL, (d) 170 °C, (e) 60 minutes, (f) purification by mass directed automated preparative HPLC. Light brown solid. Yield: 105 mg, 84 % pure, 31 %. **LCMS** (Method B) (ES +ve) *m/z* 513 (M + H)⁺ Rt 2.53 minutes.

1,1-Dimethylethyl (3R)-3-[[4-(4-morpholinylmethyl)-6-([1,3]thiazolo[5,4-*b*]pyridin-2-ylamino)-2-pyrimidinyl]amino]-1-pyrrolidinecarboxylate (43a)



(a) 200 mg, 0.551 mmol, (b) 1,1-dimethylethyl (3R)-3-amino-1-pyrrolidinecarboxylate, 308 mg, 1.65 mmol, (c) 4 mL, (d) 170 °C, (e) 60 minutes, (f) purification by mass directed automated preparative HPLC. Light brown solid. Yield: 97 mg, 34 %. **LCMS** (Method B) (ES +ve) m/z 513 ($M + H$)⁺ Rt 2.53 minutes.

***N*-[6-(4-Morpholinylmethyl)-2-(1-piperazinyl)-4-pyrimidinyl][1,3]thiazolo[5,4-*b*]pyridin-2-amine (44b)**



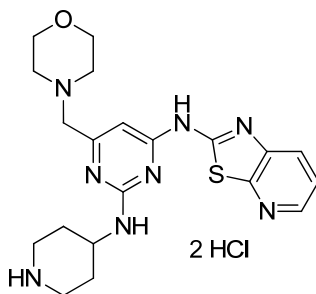
(a) 115 mg, 0.317 mmol, (b) piperazine, 41 mg, 0.48 mmol, (c) 4 mL, (d) 150 °C, (e) 30 minutes, (f) purification by mass directed automated preparative HPLC. Off-white solid. Yield: 50 mg, 38 %. **LCMS** (Method D) (ES +ve) m/z 413 ($M + H$)⁺ Rt 0.73 minutes.

General procedure E to perform the Boc deprotection reactions.

A round bottom flask was charged with the Boc protected analogues (such as **34a**) and dichloromethane (or dichloromethane:methanol). Excess of HCl in dioxane (4 M) was added and the reaction was stirred at room temperature until it had reached completion. The mixture was either evaporated to dryness or filtered under reduced pressure to obtain the amine intermediates as HCl salts. These amines were not purified and were used in the following amide coupling reactions. For that reason, only LCMS analyses of the crude products were recorded.

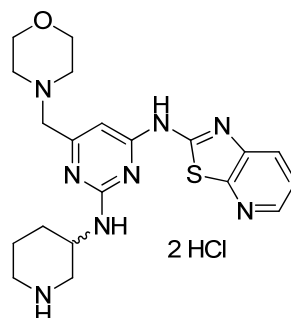
Following the general procedure E, data are presented as (a) amount of Boc protected analogue, (b) volume of solvent, (c) volume of HCl in dioxane (4 M), (d) reaction time, (e) isolation technique.

6-(4-Morpholinylmethyl)-N²-4-piperidinyl-N⁴-[1,3]thiazolo[5,4-*b*]pyridin-2-yl-2,4-pyrimidinediamine dihydrochloride (34c**)**



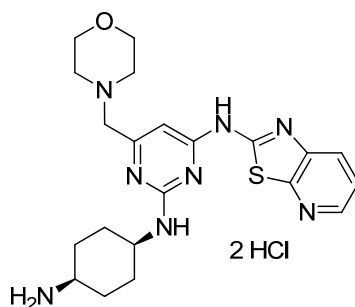
(a) **34a**, 235 mg, 0.446 mmol, (b) dichloromethane, 5 mL, (c) 1 mL, 4 mmol, (d) 16 hours, (e) the solid was filtered under reduced pressure. Yellow solid. Yield: 240 mg, 83 % pure, 90 %. LCMS (Method B) (ES +ve) m/z 427 (M + H)⁺ Rt 1.76 minutes.

6-(4-Morpholinylmethyl)-*N*²-3-piperidinyl-*N*⁴-[1,3]thiazolo[5,4-*b*]pyridin-2-yl-2,4-pyrimidinediamine dihydrochloride (35c)



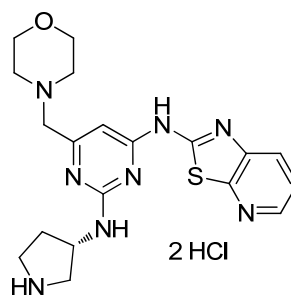
(a) **35a**, 230 mg, 0.437 mmol, (b) dichloromethane, 5 mL, (c) 1 mL, 4 mmol, (d) 1.5 hours, (e) the solvent was concentrated under reduced pressure. White solid. Yield: 214 mg, 98 %. **LCMS** (Method D) (ES +ve) *m/z* 427 (*M* + *H*)⁺ *Rt* 0.72 minutes. **¹H NMR** (400 MHz, DMSO-*d*₆, 120 °C) δ 9.33 (br. s, 1H), 8.39 (dd, *J* = 1.5, 4.5 Hz, 1H), 7.98 (dd, *J* = 1.5, 8.1 Hz, 1H), 7.42 (dd, *J* = 4.5, 8.1 Hz, 1H), 6.61 (s, 1H), 4.65 - 4.54 (m, 1H), 4.15 (s, 2H), 4.01 - 3.96 (m, 4H), 3.33 - 3.20 (m, 6H), 2.94 (m, 2H), 2.16 - 1.68 (m, 4H).

***N*²-(*Cis*-4-aminocyclohexyl)-6-(4-morpholinylmethyl)-*N*⁴-[1,3]thiazolo[5,4-*b*]pyridin-2-yl-2,4-pyrimidinediamine dihydrochloride (37c)**



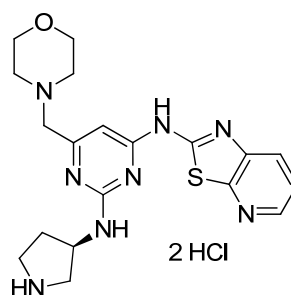
(a) **37a**, 135 mg, 0.250 mmol, (b) dichloromethane, 3 mL, (c) 0.375 mL, 1.50 mmol, (d) 16 hours, (e) the solvent was evaporated under reduced pressure. Brown solid. Yield: 146 mg, > 100 %. **LCMS** (Method D) (ES +ve) *m/z* 441 (*M* + *H*)⁺ *Rt* 0.85 minutes.

6-(4-Morpholinylmethyl)-*N*²-[(3*S*)-3-pyrrolidinyl]-*N*⁴-[1,3]thiazolo[5,4-*b*]pyridin-2-yl-2,4-pyrimidinediamine dihydrochloride (42c)



(a) **42a**, 105 mg, 0.205 mmol, (b) dichloromethane, 3 mL, methanol, 1 mL, (c) 0.307 mL, 1.23 mmol, (d) 16 hours, (e) the solvent was evaporated under reduced pressure. Brown solid. Yield: 106 mg, 88 % pure, 94 %. **LCMS** (Method D) (ES +ve) *m/z* 413 (M + H)⁺ Rt 0.77 minutes.

6-(4-Morpholinylmethyl)-*N*²-[(3*R*)-3-pyrrolidinyl]-*N*⁴-[1,3]thiazolo[5,4-*b*]pyridin-2-yl-2,4-pyrimidinediamine dihydrochloride (43c)



(a) **43a**, 97 mg, 0.19 mmol, (b) dichloromethane, 3 mL, methanol, 1 mL, (c) 0.284 mL, 1.14 mmol, (d) 16 hours, (e) the solvent was evaporated under reduced pressure. Brown solid. Yield: 97 mg, > 100 %. **LCMS** (Method D) (ES +ve) *m/z* 413 (M + H)⁺ Rt 0.77 minutes.

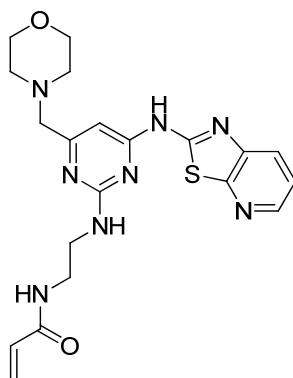
General procedure F to synthesise the final products from the amine intermediates (HCl salts or free bases):

A round bottom flask was charged with the amine intermediate (such as **33b** or **34c**), *N,N*-diisopropylethylamine, and *N*-methyl-2-pyrrolidone. 2-Propenoyl chloride was added and the reaction was stirred at room temperature. The mixture was subjected

to purification by mass directed automated preparative HPLC to afford the desired compounds.

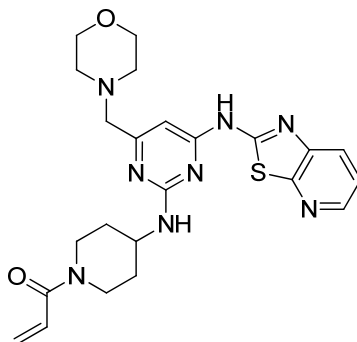
Following the general procedure F, data are presented as (a) amount of amine intermediates, (b) amount of *N,N*-diisopropylethylamine, (c) volume of solvent, (d) amount of 2-propenoyl chloride, (e) reaction time.

***N*-(2-{[4-(4-Morpholinylmethyl)-6-([1,3]thiazolo[5,4-*b*]pyridin-2-ylamino)-2-pyrimidinyl]amino}ethyl)-2-propenamamide (33)**



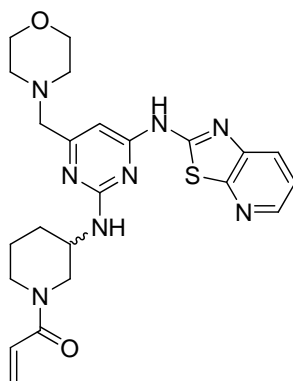
(a) **33b**, 31 mg, 0.080 mmol, (b) 0.028 mL, 0.16 mmol, (c) 0.8 mL, (d) 9.1 μ L, 0.11 mmol, (e) 30 minutes. Off-white solid. Yield: 22 mg, 62 %. **LCMS** (Method B) (ES +ve) m/z 441 ($M+H$)⁺ Rt 1.84 minutes. **¹H NMR** (400 MHz, DMSO-*d*₆) δ 11.64 (br. s, 1H), 8.36 (dd, $J = 1.0, 4.5$ Hz, 1H), 8.22 (t, $J = 5.0$ Hz, 1H), 7.97 (dd, $J = 1.0, 8.0$ Hz, 1H), 7.41 (dd, $J = 4.5, 8.0$ Hz, 1H), 7.22 (t, $J = 5.4$ Hz, 1H), 6.47 (s, 1H), 6.24 (dd, $J = 10.0, 17.1$ Hz, 1H), 6.08 (dd, $J = 2.1, 17.1$ Hz, 1H), 5.58 (dd, $J = 2.1, 10.0$ Hz, 1H), 3.65 - 3.52 (m, 6H), 3.42 (br. s, 2H), 3.33 (s, 2H), 2.47 - 2.40 (m, 4H).

***N*²-(1-Acryloyl-4-piperidinyl)-6-(4-morpholinylmethyl)-*N*⁴-[1,3]thiazolo[5,4-*b*]pyridin-2-yl-2,4-pyrimidinediamine (34)**



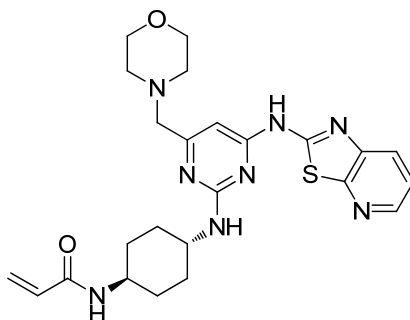
(a) **34c**, 70 mg, 0.14 mmol, (b) 0.147 mL, 0.841 mmol, (c) 0.6 mL, (d) 0.028 mL, 0.35 mmol, (e) 30 minutes. Off-white solid. Yield: 18 mg, 27 %. **LCMS** (Method B) (ES +ve) *m/z* 481 (*M* + *H*)⁺ *Rt* 1.98 minutes. **¹H NMR** (400 MHz, DMSO-*d*₆, 120 °C) δ 8.34 (dd, *J* = 1.4, 4.8 Hz, 1H), 7.93 (dd, *J* = 1.4, 8.2 Hz, 1H), 7.38 (dd, *J* = 4.8, 8.2 Hz, 1H), 6.74 (dd, *J* = 10.6, 16.9 Hz, 1H), 6.68 (d, *J* = 7.3 Hz, 1H), 6.53 (s, 1H), 6.06 (dd, *J* = 2.3, 16.9 Hz, 1H), 5.63 (dd, *J* = 2.3, 10.6 Hz, 1H), 4.28 - 4.16 (m, 3H), 3.69 - 3.61 (m, 4H), 3.36 (s, 2H), 3.21 - 3.09 (m, 2H), 2.50 - 2.53 (m, 4H), 2.12 - 2.02 (m, 2H), 1.61 - 1.47 (m, 2H). **IR** (cm⁻¹) 1516, 1573, 1620. **HRMS** (ES) calcd for C₂₃H₂₉N₈O₂S, (*M* + *H*)⁺ 481.2134, found 481.2138. **¹³C NMR** (151 MHz, DMSO-*d*₆) δ 168.7, 164.7, 161.2, 158.2, 156.3, 144.4, 143.0, 129.0, 127.6, 126.5, 121.9, 94.7, 66.7, 63.9, 53.9, 48.6, 44.7, 41.2, 32.9, 31.9. Note that the signals from two quaternary carbons are believed to be overlapping at 158.2 ppm. For comparison, these two signals are separated in the ¹³C NMR spectrum of the structurally related compounds **39** (158.3 ppm and 158.2 ppm) and **40** (158.3 ppm and 158.1 ppm). Decomposition temperature 164 °C.

***N*²-(1-Acryloyl-3-piperidinyl)-6-(4-morpholinylmethyl)-*N*⁴-[1,3]thiazolo[5,4-*b*]pyridin-2-yl-2,4-pyrimidinediamine (35)**



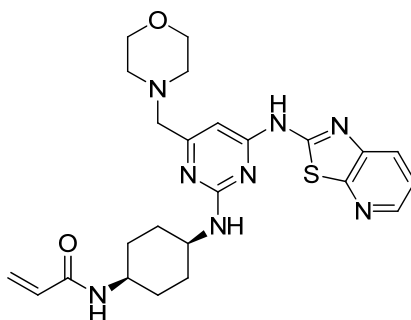
(a) **35c**, 75 mg, 0.15 mmol, (b) 0.079 mL, 0.45 mmol, (c) 1 mL, (d) 0.024 mL, 0.30 mmol, (e) 1 hour. Off-white solid. Yield: 40 mg, 55 %. **LCMS** (Method D) (ES +ve) *m/z* 481 (M + H)⁺ Rt 0.79 minutes. **¹H NMR** (400 MHz, DMSO-*d*₆, 120 °C) δ 10.72 (br. s, 1H), 8.34 (dd, *J* = 1.5, 4.8 Hz, 1H), 7.92 (dd, *J* = 1.5, 8.1 Hz, 1H), 7.37 (dd, *J* = 4.8, 8.1 Hz, 1H), 6.67 (dd, *J* = 10.8, 16.8 Hz, 1H), 6.59 (d, *J* = 7.5 Hz, 1H), 6.56 (s, 1H), 6.01 (dd, *J* = 2.3, 16.8 Hz, 1H), 5.53 (dd, *J* = 2.3, 10.8 Hz, 1H), 4.18 - 4.11 (m, 1H), 4.11 - 4.01 (m, 1H), 3.99 - 3.91 (m, 1H), 3.67 - 3.62 (m, 4H), 3.37 (s, 2H), 3.25 - 3.09 (m, 2H), 2.53 - 2.50 (m, 4H), 2.17 - 2.08 (m, 1H), 1.90 - 1.81 (m, 1H), 1.75 - 1.64 (m, 1H), 1.62 - 1.50 (m, 1H). **HRMS** (ES) calcd for C₂₃H₂₉N₈O₂S, (M + H)⁺ 481.2131, found 481.2134. **IR** (cm⁻¹) 1512, 1575, 1618. **¹³C NMR** (151 MHz, DMSO-*d*₆) δ 168.1, 164.6, 160.9, 157.8, 155.9, 143.9, 142.5, 128.7, 128.4, 127.0, 126.7, 126.0, 121.3, 94.5, 66.2, 63.4, 53.5, 49.7, 47.3, 47.8, 46.2, 45.3, 41.6, 30.5, 30.2, 24.4, 23.1. Note: ¹³C NMR at room temperature displays the presence of rotamers for the compound. Decomposition temperature 158 °C.

***N*-(*Trans*-4-{{4-(4-morpholinylmethyl)-6-([1,3]thiazolo[5,4-*b*]pyridin-2-ylamino)-2-pyrimidinyl}amino}cyclohexyl)-2-propenamide (36)**



(a) **36b**, 54 mg, 0.12 mmol, (b) 0.043 mL, 0.245 mmol, (c) 1 mL, (d) 0.020 mL, 0.245 mmol, (e) 10 minutes. Light brown solid. Yield: 27 mg, 44 %. **LCMS** (Method B) (ES +ve) m/z 495 ($M + H$)⁺ Rt 2.06 minutes. **¹H NMR** (250 MHz, DMSO-*d*₆, 120 °C) δ 8.34 (dd, $J = 1.4, 4.7$ Hz, 1H), 7.92 (dd, $J = 1.4, 8.1$ Hz, 1H), 7.62 (d, $J = 6.9$ Hz, 1H), 7.38 (dd, $J = 4.7, 8.1$ Hz, 1H), 6.51 - 6.44 (m, 2H), 6.26 (dd, $J = 10.2, 17.1$ Hz, 1H), 6.08 (dd, $J = 2.3, 17.1$ Hz, 1H), 5.53 (dd, $J = 2.3, 10.2$ Hz, 1H), 3.95 (m, 1H), 3.78 - 3.69 (m, 1H), 3.69 - 3.60 (m, 4H), 3.35 (s, 2H), 2.53 - 2.50 (m, 4H), 2.19 - 2.07 (m, 2H), 2.03 - 1.89 (m, 2H), 1.46 (t, $J = 9.7$ Hz, 4H).

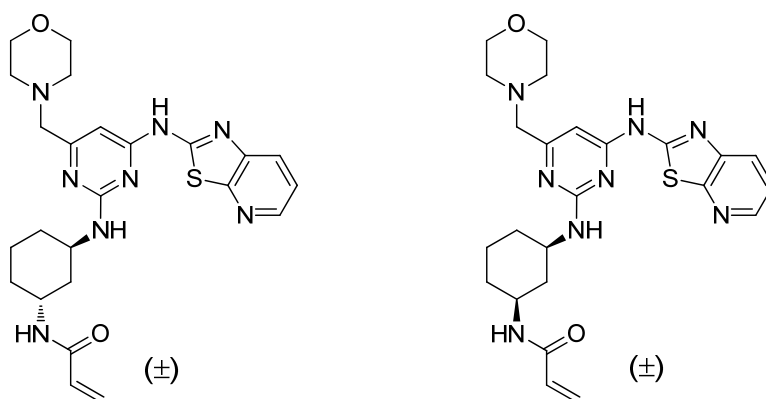
***N*-(*Cis*-4-{{4-(4-morpholinylmethyl)-6-([1,3]thiazolo[5,4-*b*]pyridin-2-ylamino)-2-pyrimidinyl}amino}cyclohexyl)-2-propenamide (37)**



(a) **37c**, 70 mg, 0.15 mmol, (b) 0.071 mL, 0.41 mmol, (c) 1 mL, (d) 0.022 mL, 0.27 mmol, (e) 10 minutes. Light brown solid. Yield: 17 mg, 25 %. **LCMS** (Method B) (ES +ve) m/z 495 ($M + H$)⁺ Rt 2.03 minutes. **¹H NMR** (400 MHz, DMSO-*d*₆) δ

11.73 - 11.45 (m, 1H), 8.36 (dd, $J = 1.3, 4.8$ Hz, 1H), 7.98 (dd, $J = 1.3, 8.1$ Hz, 1H), 7.96 - 7.94 (m, 1H), 7.42 (dd, $J = 4.8, 8.1$ Hz, 1H), 7.24 (br. s, 1H), 6.43 (s, 1H), 6.35 (dd, $J = 10.2, 17.0$ Hz, 1H), 6.08 (dd, $J = 2.4, 17.0$ Hz, 1H), 5.56 (dd, $J = 2.4, 10.2$ Hz, 1H), 4.00 (br. s, 1H), 3.85 (br. s, 1H), 3.66 - 3.56 (m, 4H), 3.31 (s, 2H), 2.46 - 2.40 (m, 4H), 1.91 - 1.53 (m, 8H).

***N*-(*Trans*-3-{{4-(4-morpholinylmethyl)-6-([1,3]thiazolo[5,4-*b*]pyridin-2-ylamino)-2-pyrimidinyl}amino}cyclohexyl)-2-propenamide (38) and *N*-(*cis*-3-{{4-(4-morpholinylmethyl)-6-([1,3]thiazolo[5,4-*b*]pyridin-2-ylamino)-2-pyrimidinyl}amino}cyclohexyl)-2-propenamide (39)**

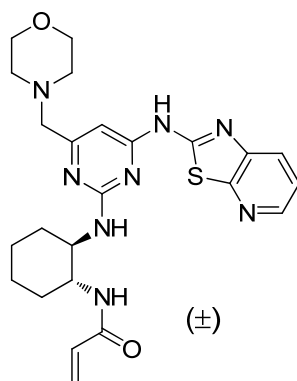


(a) **38b**, 94 mg, 0.21 mmol, (b) 0.112 mL, 0.640 mmol, (c) 0.8 mL, (d) 0.034 mL, 0.43 mmol, (e) 1.5 hours. The reverse phase purification (MDAP) allowed the separation of the 2 isomers.

38. Light brown solid. Yield: 10 mg, 20 %. **LCMS** (Method B) (ES +ve) m/z 495 ($M + H$)⁺ Rt 2.11 minutes. **¹H NMR** (400 MHz, DMSO- d_6) δ 11.52 (br. s, 1H), 8.35 (dd, $J = 1.4, 4.6$ Hz, 1H), 8.01 - 7.93 (m, 2H), 7.40 (dd, $J = 4.6, 8.0$ Hz, 1H), 7.23 (br. s, 1H), 6.43 (s, 1H), 6.26 (dd, $J = 10.0, 16.8$ Hz, 1H), 5.99 (d, $J = 16.8$ Hz, 1H), 5.45 (d, $J = 10.0$ Hz, 1H), 4.36 (br. s, 1H), 4.03 (br. s, 1H), 3.65 - 3.57 (m, 4H), 3.35 (s, 2H), 2.47 - 2.40 (m, 4H), 2.00 - 1.49 (m, 8H). NMR (including NOE couplings) comparisons with compound **39** supported the characterisation of the *trans*-geometry for this compound.

39. Light brown solid. Yield: 21 mg, 40 %. **LCMS** (Method B) (ES +ve) m/z 495 (M + H)⁺ Rt 2.05 minutes. **¹H NMR** (400 MHz, DMSO-d₆) δ 11.41 (br. s, 1H), 8.35 (dd, *J* = 1.5, 4.8 Hz, 1H), 8.06 (d, *J* = 7.5 Hz, 1H), 7.97 (dd, *J* = 1.5, 8.0 Hz, 1H), 7.41 (dd, *J* = 4.8, 8.0 Hz, 1H), 7.33 (br. s, 1H), 6.42 (s, 1H), 6.20 (dd, *J* = 10.0, 17.1 Hz, 1H), 6.06 (dd, *J* = 2.3, 17.1 Hz, 1H), 5.55 (dd, *J* = 2.3, 10.0 Hz, 1H), 4.01 (br. s, 1H), 3.76 (br. s, 1H), 3.65 - 3.58 (m, 4H), 3.36 (s, 2H), 2.47 - 2.39 (m, 4H), 2.18 - 2.00 (m, 2H), 1.96 - 1.74 (m, 2H), 1.56 - 1.26 (m, 2H), 1.22 - 1.05 (m, 2H). NOE coupling between the protons at 3.76 ppm and 4.01 ppm supported the characterisation of the *cis*-geometry for this compound. **HRMS** (ES) calcd for C₂₄H₃₁N₈O₂S, (M + H)⁺ 495.2285, found 495.2291. **IR** (cm⁻¹) 1518, 1545, 1573, 1628, 1655. **¹³C NMR** (126 MHz, DMSO-d₆) δ 168.5, 164.0, 161.2, 158.3, 158.2, 156.4, 144.3, 143.0, 132.4, 126.4, 125.4, 121.8, 94.5, 66.7, 63.9, 53.9, 49.4, 47.8, 38.9, 32.5, 32.2, 23.6. Decomposition temperature 227 °C.

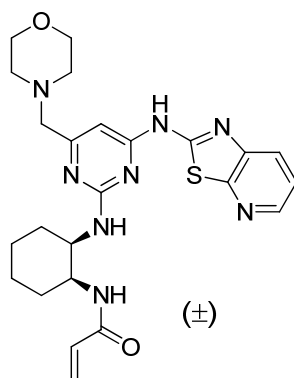
***N*-(*Trans*-2-[[4-(4-morpholinylmethyl)-6-([1,3]thiazolo[5,4-*b*]pyridin-2-ylamino)-2-pyrimidinyl]amino}cyclohexyl)-2-propenamide (40)**



(a) **40b**, 45 mg, 0.10 mmol, (b) 0.021 mL, 0.12 mmol, (c) 0.8 mL, (d) 9.1 μL, 0.11 mmol, (e) 30 minutes. Off-white solid. Yield: 20 mg, 40 %. **LCMS** (Method B) (ES +ve) m/z 495 (M + H)⁺ Rt 2.22 minutes. **¹H NMR** (400 MHz, DMSO-d₆) δ 11.56 (br. s, 1H), 8.36 (dd, *J* = 1.4, 4.8 Hz, 1H), 8.12 (d, *J* = 7.0 Hz, 1H), 7.97 (d, *J* = 8.1 Hz, 1H), 7.42 (dd, *J* = 4.8, 8.1 Hz, 1H), 6.72 (d, *J* = 6.1 Hz, 1H), 6.42 (s, 1H), 6.20 (dd, *J* = 10.1, 16.9 Hz, 1H), 6.07 (dd, *J* = 2.0, 16.9 Hz, 1H), 5.56 (dd, *J* = 2.0, 10.1 Hz, 1H), 3.94 - 3.75 (m, 2H), 3.66 - 3.56 (m, 4H), 3.27 (s, 2H), 2.48 - 2.37 (m, 4H), 2.38 - 2.31 (m, 1H), 2.04 - 1.94 (m, 1H), 1.84 - 1.69 (m, 2H), 1.56 - 1.17 (m, 4H).

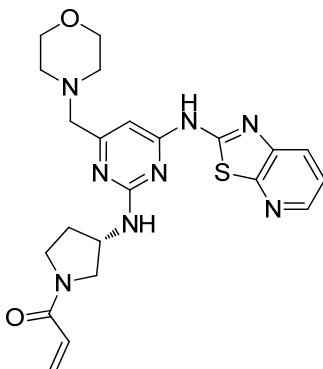
HRMS (ES) calcd for C₂₄H₃₁N₈O₂S, (M + H)⁺ 495.2285, found 495.2291. **IR** (cm⁻¹) 1508, 1578, 1616, 1658. **¹³C NMR** (126 MHz, DMSO-d₆) δ 168.6, 165.3, 161.5, 158.3, 158.1, 156.4, 144.4, 143.0, 132.3, 126.5, 125.7, 121.9, 94.6, 66.7, 63.8, 55.9, 53.9, 51.7, 32.7, 32.6, 25.0. Note that the HMQC data indicates that two ¹³C signals from the cyclohexane ring are overlapping at 25.0 ppm. Decomposition temperature 234 °C.

***N*-(*Cis*-2-[[4-(4-morpholinylmethyl)-6-([1,3]thiazolo[5,4-*b*]pyridin-2-ylamino)-2-pyrimidinyl]amino}cyclohexyl)-2-propenamide (41)**



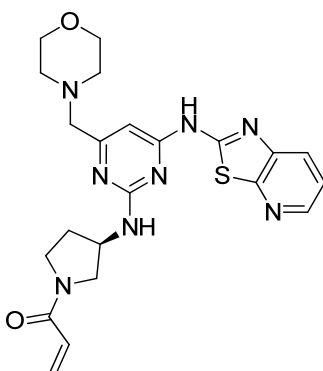
(a) **41b**, 51 mg, 0.12 mmol, (b) 0.024 mL, 0.14 mmol, (c) 0.8 mL, (d) 10.3 μL, 0.127 mmol, (e) 30 minutes. Brown solid. Yield: 23 mg, 40 %. **LCMS** (Method B) (ES +ve) m/z 495 (M + H)⁺ Rt 2.17 minutes. **¹H NMR** (400 MHz, DMSO-d₆) δ 11.54 (br. s, 1H), 8.36 (dd, *J* = 1.3, 4.8 Hz, 1H), 7.98 (dd, *J* = 1.3, 8.2 Hz, 1H), 7.78 (d, *J* = 7.8 Hz, 1H), 7.42 (dd, *J* = 4.8, 8.2 Hz, 1H), 6.85 (br. s, 1H), 6.44 (s, 1H), 6.38 (dd, *J* = 10.1, 17.2 Hz, 1H), 6.04 (dd, *J* = 2.0, 17.2 Hz, 1H), 5.57 (dd, *J* = 2.0, 10.1 Hz, 1H), 4.40 (br. s, 1H), 4.23 (br. s, 1H), 3.63 - 3.58 (m, 4H), 3.29 (br. s, 2H), 2.46 - 2.38 (m, 4H), 1.91 - 1.33 (m, 8H). **HRMS** (ES) calcd for C₂₄H₃₁N₈O₂S, (M + H)⁺ 495.2285, found 495.2281. **IR** (cm⁻¹) 1509, 1589, 1619, 1656. **¹³C NMR** (126 MHz, DMSO-d₆) δ 168.5, 165.1, 161.3, 158.2, 156.4, 144.3, 143.0, 132.5, 126.5, 125.5, 121.9, 94.9, 66.7, 63.8, 53.9, 51.5, 48.2, 29.4, 27.8, 24.0, 21.1. Note that the signals from two quaternary carbons are believed to be overlapping at 158.2 ppm. For comparison, these two signals are separated in the ¹³C NMR spectrum of the structurally related compounds **39** (158.3 ppm and 158.2 ppm) and **40** (158.3 ppm and 158.1 ppm). Decomposition temperature 234 °C.

***N*²-[(3*S*)-1-Acryloyl-3-pyrrolidinyl]-6-(4-morpholinylmethyl)-*N*⁴-
[1,3]thiazolo[5,4-*b*]pyridin-2-yl-2,4-pyrimidinediamine (42)**



(a) **42c**, 50 mg, 0.10 mmol, (b) 0.054 mL, 0.31 mmol, (c) 1 mL, (d) 0.017 mL, 0.21 mmol, (e) 10 minutes. Off-white solid. Yield: 13 mg, 27 %. **LCMS** (Method D) (ES +ve) *m/z* 467 (*M* + *H*)⁺ *Rt* 0.75 minutes. **¹H NMR** (250 MHz, DMSO-*d*₆, 120 °C) δ 8.34 (br. s, 1H), 7.92 (d, *J* = 8.0 Hz, 1H), 7.33 - 7.44 (m, 1H), 6.97 (d, *J* = 6.1 Hz, 1H), 6.47 - 6.65 (m, 2H), 6.12 (d, *J* = 16.9 Hz, 1H), 5.63 (d, *J* = 10.5 Hz, 1H), 4.58 - 4.76 (m, 1H), 3.85 - 4.01 (m, 1H), 3.71 - 3.83 (m, 1H), 3.65 (br. s, 4H), 3.47 - 3.60 (m, 2H), 3.38 (br. s, 2H), 2.49 (s, 4H), 2.20 - 2.42 (m, 1H), 1.97 - 2.17 (m, 1H).

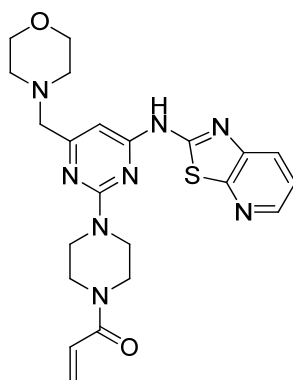
***N*²-[(3*R*)-1-Acryloyl-3-pyrrolidinyl]-6-(4-morpholinylmethyl)-*N*⁴-
[1,3]thiazolo[5,4-*b*]pyridin-2-yl-2,4-pyrimidinediamine (43)**



(a) **43c**, 48 mg, 0.99 mmol, (b) 0.052 mL, 0.30 mmol, (c) 1 mL, (d) 0.016 mL, 0.20 mmol, (e) 10 minutes. Light brown solid. Yield: 16 mg, 35 %. **LCMS** (Method D) (ES +ve) *m/z* 467 (*M* + *H*)⁺ *Rt* 0.75 minutes. **¹H NMR** (250 MHz, DMSO-*d*₆, 120 °C) δ 8.33 (br. s, 1H), 7.91 (d, *J* = 8.0 Hz, 1H), 7.37 (d, *J* = 8.0 Hz, 1H), 6.95 (br. s,

1H), 6.63 - 6.46 (m, 2H), 6.11 (d, $J = 16.4$ Hz, 1H), 5.61 (d, $J = 10.2$ Hz, 1H), 4.67 (br. s, 1H), 3.90 (br. s, 1H), 3.74 (br. s., 1H), 3.65 (br. s., 4H), 3.46 - 3.59 (m, 2H), 3.38 (br. s., 2H), 2.54 - 2.51 (m, 4H), 2.40 - 2.19 (m, 1H), 2.15 - 1.95 (m, 1H).. **IR** (cm^{-1}) 1514, 1576, 1619, 1641. **HRMS** (ES) calcd for $\text{C}_{22}\text{H}_{27}\text{N}_8\text{O}_2\text{S}$, ($\text{M} + \text{H}$)⁺ 467.1972, found 467.1970. **^{13}C NMR** (126 MHz, DMSO-d_6) δ 168.5, 163.9, 161.5, 158.3, 156.3, 144.3, 143.1, 130.2, 129.9, 127.2, 127.0, 126.5, 121.9, 95.2, 66.7, 63.8, 53.9, 52.1, 50.3, 45.0, 44.5, 31.7, 30.0. Note: ^{13}C NMR at room temperature displays the presence of rotamers for the compound. Decomposition temperature 157 °C.

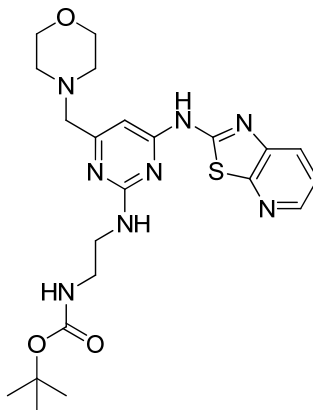
***N*-[2-(4-Acryloyl-1-piperazinyl)-6-(4-morpholinylmethyl)-4-pyrimidinyl][1,3]thiazolo [5,4-*b*]pyridin-2-amine (44)**



(a) **44b**, 50 mg, 0.12 mmol, (b) 0.042 mL, 0.24 mmol, (c) 1 mL, (d) 0.020 mL, 0.24 mmol, (e) 10 minutes. Off-white solid. Yield: 15 mg, 27 %. **LCMS** (Method B) (ES +ve) m/z 467 ($\text{M} + \text{H}$)⁺ Rt 2.10 minutes. **^1H NMR** (400 MHz, DMSO-d_6) δ 11.75 (br. s, 1H), 8.38 (dd, $J = 1.4, 4.6$ Hz, 1H), 8.00 (dd, $J = 1.4, 8.2$ Hz, 1H), 7.44 (dd, $J = 4.6, 8.2$ Hz, 1H), 6.90 (dd, $J = 10.5, 16.7$ Hz, 1H), 6.55 (s, 1H), 6.17 (dd, $J = 2.4, 16.7$ Hz, 1H), 5.72 (dd, $J = 2.4, 10.5$ Hz, 1H), 3.95 - 3.83 (m, 4H), 3.80 - 3.65 (m, 4H), 3.65 - 3.60 (m, 4H), 3.39 (s, 2H), 2.48 - 2.43 (m, 4H). **IR** (cm^{-1}) 1517, 1575, 1621, 1643. **HRMS** (ES) calcd for $\text{C}_{22}\text{H}_{27}\text{N}_8\text{O}_2\text{S}$, ($\text{M} + \text{H}$)⁺ 467.1972, found 467.1974. **^{13}C NMR** (126 MHz, DMSO-d_6) δ 168.3, 164.9, 160.8, 158.4, 158.0, 156.0, 144.5, 143.1, 128.7, 128.1, 126.7, 122.0, 95.5, 66.7, 63.9, 53.9, 45.2, 44.8, 44.1, 41.7. Decomposition temperature 227 °C.

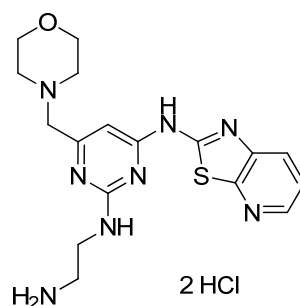
3. Synthetic procedures for the investigation of the electrophilic moiety

1,1-Dimethylethyl (2-{{[4-(4-morpholinylmethyl)-6-([1,3]thiazolo[5,4-*b*]pyridin-2-ylamino)-2-pyrimidinyl]amino}ethyl)carbamate (33b)



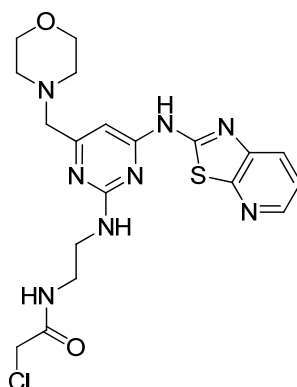
A microwave vial was charged with *N*-[2-chloro-6-(4-morpholinylmethyl)-4-pyrimidinyl][1,3]thiazolo[5,4-*b*]pyridin-2-amine **32** (200 mg, 0.551 mmol) and 1,1-dimethylethyl (2-aminoethyl)carbamate (0.131 mL, 0.827 mmol). The microwave vial was sealed and heated under microwave irradiation (Biotage Initiator system) at 170 °C for 45 minutes. The solvent was concentrated under reduced pressure. The product was purified by FlashMaster chromatography on silica using a gradient elution from 0 to 30 % methanol (+1 % triethylamine) in dichloromethane to afford the title compound (175 mg, 65 % yield) as a yellow solid. **LCMS** (Method D) (ES +ve) *m/z* 487 (*M* + *H*)⁺ *Rt* 0.91 minutes. **¹H NMR** (400 MHz, DMSO-*d*₆, 120 °C) δ 11.21 (br. s, 1H), 8.34 (dd, *J* = 1.5, 4.8 Hz, 1H), 7.92 (dd, *J* = 1.5, 8.2 Hz, 1H), 7.38 (dd, *J* = 4.8, 8.2 Hz, 1H), 6.63 (t, *J* = 6.0 Hz, 1H), 6.54 (s, 1H), 6.34 (br. s, 1H), 3.67 - 3.62 (m, 4H), 3.54 (q, *J* = 6.0 Hz, 2H), 3.37 (s, 2H), 3.27 (q, *J* = 6.0 Hz, 2H), 2.53 - 2.50 (m, 4H), 1.40 (s, 9H).

***N*²-(2-Aminoethyl)-6-(4-morpholinylmethyl)-*N*⁴-[1,3]thiazolo[5,4-*b*]pyridin-2-yl-2,4-pyrimidinediamine dihydrochloride (33c)**



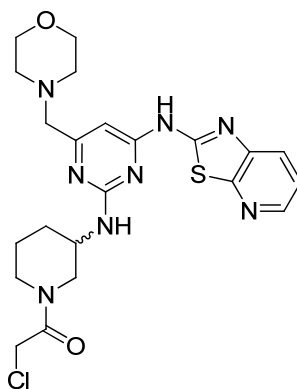
HCl in dioxane (4M, 0.385 mL, 1.54 mmol) was added to a solution of 1,1-dimethylethyl (2-([4-(4-morpholinylmethyl)-6-([1,3]thiazolo[5,4-*b*]pyridin-2-ylamino)-2-pyrimidinyl]amino)ethyl)carbamate **33b** (150 mg, 0.308 mmol) whilst stirring at room temperature in dichloromethane (5 mL) and methanol (1 mL). The reaction was stirred at room temperature for 48 hours. The solvent was removed under reduced pressure to give the title compound (137 mg, 97 % yield) as a white solid. **LCMS** (Method D) (ES +ve) *m/z* 387 (*M* + *H*)⁺ *Rt* 0.64 minutes. **¹H NMR** (400 MHz, DMSO-*d*₆, 120 °C) δ 8.39 (dd, *J* = 1.5, 4.8 Hz, 1H), 8.11 (br. s, 2H), 7.99 (dd, *J* = 1.5, 8.1 Hz, 1H), 7.42 (dd, *J* = 4.8, 8.1 Hz, 1H), 6.60 (s, 1H), 4.18 (br. s, 2H), 4.02 - 3.95 (m, 4H), 3.83 (t, *J* = 6.0 Hz, 2H), 3.59 (s, 2H), 3.33 - 3.25 (m, 4H), 3.12 (t, *J* = 6.0 Hz, 2H).

2-Chloro-*N*-(2-([4-(4-morpholinylmethyl)-6-([1,3]thiazolo[5,4-*b*]pyridin-2-ylamino)-2-pyrimidinyl]amino)ethyl)acetamide (47a)



Chloroacetyl chloride (0.013 mL, 0.16 mmol) was added to a cooled (0 °C, ice bath) solution of *N*²-(2-aminoethyl)-6-(4-morpholinylmethyl)-*N*⁴-[1,3]thiazolo[5,4-*b*]pyridin-2-yl-2,4-pyrimidinediamine dihydrochloride **33c** (75 mg, 0.16 mmol) and *N,N*-diisopropylethylamine (0.114 mL, 0.653 mmol) in *N*-methyl-2-pyrrolidone (0.8 mL). The reaction was stirred at 0 °C for 2 hours. The mixture was subjected to purification by mass directed automated preparative HPLC to afford the title compound (25 mg, 33 % yield) as a yellow solid. **LCMS** (Method B) (ES +ve) *m/z* 463 (M + H)⁺ Rt 1.89 minutes. **¹H NMR** (400 MHz, DMSO-*d*₆, 120 °C) δ 11.18 (br. s, 1H), 8.35 (dd, *J* = 1.4, 4.7 Hz, 1H), 7.93 (dd, *J* = 1.4, 8.1 Hz, 1H), 7.87 (br. s, 1H), 7.38 (dd, *J* = 4.7, 8.1 Hz, 1H), 6.72 - 6.66 (m, 1H), 6.55 (s, 1H), 4.04 (s, 2H), 3.67 - 3.63 (m, 4H), 3.60 (q, *J* = 6.0 Hz, 2H), 3.44 (q, *J* = 6.0 Hz, 2H), 3.38 (s, 2H), 2.54 - 2.51 (m, 4H). **HRMS** (ES) calcd for C₁₉H₂₄ClN₈O₂S, (M + H)⁺ 463.1431, found 463.1431. **IR** (cm⁻¹) 1520, 1582, 1623. **¹³C NMR** (151 MHz, DMSO-*d*₆) δ 168.1, 166.1, 161.5, 157.9, 157.7, 155.9, 143.9, 142.6, 126.1, 121.4, 94.4, 66.2, 63.4, 53.4, 42.7, 40.9, 39.1; Note: the ¹³C signal at 39.1 ppm (hidden by the DMSO) was assigned by HSQC. Decomposition temperature 155 °C.

***N*²-[1-(Chloroacetyl)-3-piperidinyl]-6-(4-morpholinylmethyl)-*N*⁴-[1,3]thiazolo[5,4-*b*]pyridin-2-yl-2,4-pyrimidinediamine (**47b**)**



Chloroacetyl chloride (8 μL, 0.1 mmol) was added to a cooled (0 °C, ice bath) solution of 6-(4-morpholinylmethyl)-*N*²-3-piperidinyl-*N*⁴-[1,3]thiazolo[5,4-*b*]pyridin-2-yl-2,4-pyrimidinediamine dihydrochloride **35c** (50 mg, 0.10 mmol) and *N,N*-diisopropylethylamine (0.07 mL, 0.4 mmol) in *N*-methyl-2-pyrrolidone (0.8 mL). The reaction was stirred at 0 °C for 2 hours. The mixture was subjected to

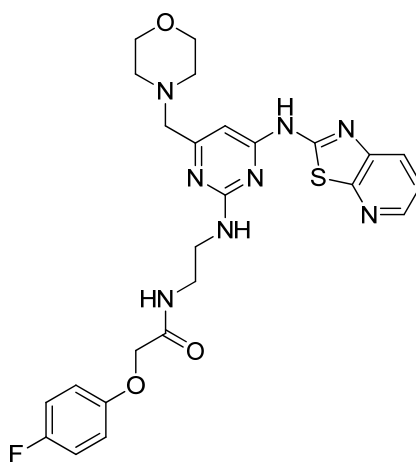
purification by mass directed automated preparative HPLC to afford the title compound (13 mg, 90 % pure, 23 % yield) as a yellow solid. **LCMS** (Method B) (ES +ve) m/z 503 ($M + H$)⁺ Rt 2.10 minutes. **¹H NMR** (250 MHz, DMSO- d_6 , 120 °C) δ 8.34 (dd, $J = 1.5, 4.7$ Hz, 1H), 7.93 (dd, $J = 1.5, 8.1$ Hz, 1H), 7.38 (dd, $J = 4.7, 8.1$ Hz, 1H), 6.70 - 6.60 (m, 1H), 6.57 (s, 1H), 4.28 (s, 2H), 4.13 - 3.99 (m, 2H), 3.93 - 3.79 (m, 1H), 3.69 - 3.61 (m, 4H), 3.38 (s, 2H), 3.27 - 3.06 (m, 2H), 2.53 - 2.51 (m, 4H), 2.09 (br. s, 1H), 1.94 - 1.79 (m, 1H), 1.77 - 1.50 (m, 2H).

General procedure F for the amide coupling with HATU:

A mixture of carboxylic acid analogue, *N,N*-diisopropylethylamine and *O*-(7-azabenzotriazol-1-yl)-*N,N,N',N'*-tetramethyluronium hexafluorophosphate (HATU) in *N*-methyl-2-pyrrolidone (1 mL) was stirred at room temperature for 2 minutes. A solution of amine dihydrochloride intermediate (**33c** or **35c**) and *N,N*-diisopropylethylamine in *N*-methyl-2-pyrrolidone (1 mL) was added to the previous solution and the reaction was stirred at room temperature until completion. The product was subjected to purification by mass directed automated preparative HPLC.

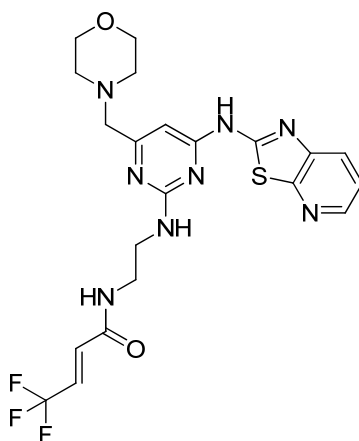
Following the general procedure F, data are presented as (a) amount of carboxylic acid analogue, (b) amount of *N,N*-diisopropylethylamine, (c) amount of HATU, (d) amount of amine intermediate, (e) amount of *N,N*-diisopropylethylamine, (f) reaction time.

2-[(4-Fluorophenyl)oxy]-*N*-(2-{[4-(4-morpholinylmethyl)-6-([1,3]thiazolo[5,4-*b*]pyridin-2-ylamino)-2-pyrimidinyl]amino}ethyl)acetamide (48a)



(a) 4-Fluorophenoxyacetic acid, 41.7 mg, 0.245 mmol, (b) 0.086 mL, 0.49 mmol, (c) 93 mg, 0.25 mmol, (d) **33c**, 75 mg, 0.16 mmol, (e) 0.086 mL, 0.49 mmol, (f) 16 hours. Off-white solid. Yield: 42 mg, 48 %. **LCMS** (Method B) (ES +ve) m/z 539 ($M + H$)⁺ Rt 2.23 minutes. **¹H NMR** (400 MHz, DMSO-*d*₆, 120 °C) δ 8.34 (dd, $J = 1.5, 4.8$ Hz, 1H), 7.92 (dd, $J = 1.5, 8.1$ Hz, 1H), 7.78 - 7.69 (m, 1H), 7.38 (dd, $J = 4.8, 8.1$ Hz, 1H), 7.08 - 6.94 (m, 4H), 6.73 - 6.66 (m, 1H), 6.54 (s, 1H), 4.45 (s, 2H), 3.68 - 3.59 (m, 6H), 3.52 - 3.45 (m, 2H), 3.36 (s, 2H), 2.52 - 2.50 (m, 4H). **IR** (cm⁻¹) 1508, 1555, 1580, 1636, 1658. **HRMS** (ES) calcd for C₂₅H₂₈FN₈O₃S, ($M + H$)⁺ 539.1984, found 539.1985. **¹³C NMR** (126 MHz, DMSO-*d*₆) δ 168.5, 168.3, 162.0, 158.3, 158.2, 156.7, 157.3 (d, $J = 237.0$ Hz), 154.5 (d, $J = 1.8$ Hz), 144.3, 143.0, 126.5, 121.8, 116.6 (d, $J = 8.3$ Hz), 116.3 (d, $J = 23.0$ Hz), 94.8, 68.1, 66.7, 63.8, 53.9, 41.6, 38.9. Decomposition temperature 197 °C.

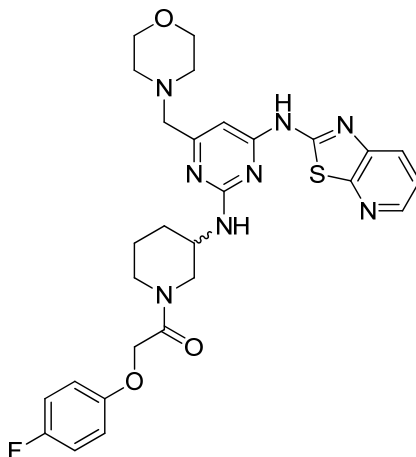
(2E)-4,4,4-Trifluoro-N-(2-([4-(4-morpholinylmethyl)-6-([1,3]thiazolo[5,4-*b*]pyridin-2-ylamino)-2-pyrimidinyl]amino)ethyl)-2-butenamide (49a)



(a) (2E)-4,4,4-Trifluoro-2-butenic acid, 34.3 mg, 0.245 mmol, (b) 0.086 mL, 0.49 mmol, (c) 93 mg, 0.25 mmol, (d) **33c**, 75 mg, 0.16 mmol, (e) 0.086 mL, 0.49 mmol, (f) 16 hours. Off-white solid. Yield: 32 mg, 39 %. **LCMS** (Method B) (ES +ve) m/z 509 ($M + H$)⁺ Rt 2.25 minutes. **¹H NMR** (400 MHz, DMSO-*d*₆, 120 °C) δ 8.34 (dd, $J = 1.5, 4.8$ Hz, 1H), 8.27 (br. s, 1H), 7.92 (dd, $J = 1.5, 8.0$ Hz, 1H), 7.38 (dd, $J = 4.8, 8.0$ Hz, 1H), 6.83 - 6.63 (m, 3H), 6.55 (s, 1H), 3.67 - 3.60 (m, 6H), 3.50 (q, $J = 6.0$ Hz, 2H), 3.37 (s, 2H), 2.53 - 2.50 (m, 4H). **IR** (cm⁻¹) 1508, 1552, 1620, 1657. **HRMS** (ES) calcd for C₂₁H₂₄F₃N₈O₂S, ($M + H$)⁺ 509.1690, found 509.1676. **¹³C**

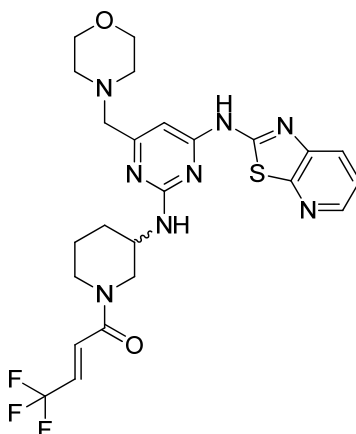
NMR (126 MHz, DMSO- d_6) δ 168.6, 162.6, 161.9, 158.4, 158.2, 156.3, 144.3, 143.0, 133.5 (q, $J = 6.1$ Hz), 126.5, 125.8 (q, $J = 34.0$ Hz), 121.8, 123.6 (q, $J = 271.0$ Hz), 94.8, 66.7, 63.9, 53.9, 41.2, 38.1. Decomposition temperature 169 °C.

***N*²-(1-[(4-Fluorophenyl)oxy]acetyl)-3-piperidiny]-6-(4-morpholinylmethyl)-*N*⁴-[1,3]thiazolo[5,4-*b*]pyridin-2-yl-2,4-pyrimidinediamine (48b)**



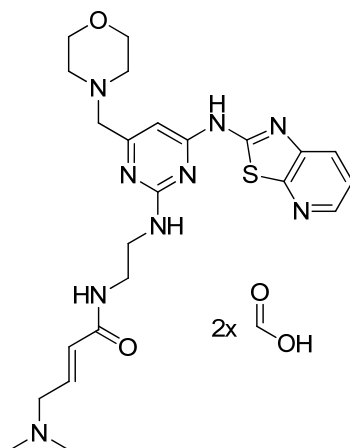
(a) 4-Fluorophenoxyacetic acid, 25.5 mg, 0.15 mmol, (b) 0.052 mL, 0.3 mmol, (c) 57.1 mg, 0.150 mmol, (d) **35c**, 50 mg, 0.10 mmol, (e) 0.052 mL, 0.30 mmol, (f) 1 hour. Off-white solid. Yield: 32 mg, 55 %. **LCMS** (Method B) (ES +ve) m/z 579 ($M + H$)⁺ Rt 2.37 minutes. **¹H NMR** (400 MHz, DMSO- d_6 , 120 °C) δ 8.34 (dd, $J = 1.4$, 4.7 Hz, 1H), 7.92 (dd, $J = 1.4$, 8.2 Hz, 1H), 7.38 (dd, $J = 4.7$, 8.2 Hz, 1H), 7.00 - 6.93 (m, 2H), 6.93 - 6.86 (m, 2H), 6.61 (d, $J = 7.1$ Hz, 1H), 6.55 (s, 1H), 4.73 (s, 2H), 4.14 - 3.97 (m, 2H), 3.88 - 3.78 (m, 1H), 3.66 - 3.59 (m, 4H), 3.35 (s, 2H), 3.28 - 3.23 (m, 1H), 3.20 - 3.11 (m, 1H), 2.49 - 2.46 (m, 4H), 2.17 - 2.07 (m, 1H), 1.92 - 1.81 (m, 1H), 1.77 - 1.65 (m, 1H), 1.64 - 1.52 (m, 1H).

6-(4-Morpholinylmethyl)-*N*⁴-[1,3]thiazolo[5,4-*b*]pyridin-2-yl-*N*²-{1-[(2*E*)-4,4,4-trifluoro-2-butenoyl]-3-piperidinyl}-2,4-pyrimidinediamine (49b)



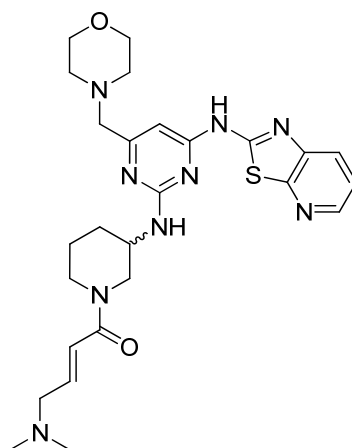
(a) (2*E*)-4,4,4-Trifluoro-2-butenic acid, 29.4 mg, 0.210 mmol, (b) 0.073 mL, 0.42 mmol, (c) 80 mg, 0.21 mmol, (d) **35c**, 70 mg, 0.14 mmol, (e) 0.073 mL, 0.42 mmol, (f) 2 hours. Off-white solid. Yield: 8 mg, 10 %. **LCMS** (Method B) (ES +ve) *m/z* 549 (M + H)⁺ Rt 2.33 minutes. **¹H NMR** (400 MHz, DMSO-*d*₆, 120 °C) δ 8.34 (dd, *J* = 1.4, 4.7 Hz, 1H), 7.93 (dd, *J* = 1.4, 8.2 Hz, 1H), 7.38 (dd, *J* = 4.7, 8.2 Hz, 1H), 7.16 (d, *J* = 15.1 Hz, 1H), 6.69 (d, *J* = 7.3 Hz, 1H), 6.66 - 6.59 (m, 1H), 6.58 (s, 1H), 4.11 (br. s, 2H), 3.94 - 3.84 (m, 1H), 3.68 - 3.63 (m, 4H), 3.37 (s, 2H), 3.31 - 3.21 (m, 2H), 2.53 - 2.51 (m, 4H), 2.16 - 2.07 (m, 1H), 1.96 - 1.86 (m, 1H), 1.80 - 1.69 (m, 1H), 1.66 - 1.52 (m, 1H).

(*E*)-4-(dimethylamino)-*N*-(2-((4-(morpholinomethyl)-6-(thiazolo[5,4-*b*]pyridin-2-ylamino)pyrimidin-2-yl)amino)ethyl)but-2-enamide, 2 formic acid salt (50a)



(a) (*E*)-4-(Dimethylamino)but-2-enoic acid hydrochloride **53**, 35 mg, 0.21 mmol, (b) 0.73 mL, 0.42 mmol, (c) 80 mg, 0.21 mmol, (d) **33c**, 64 mg, 0.14 mmol, (e) 0.73 mL, 0.42 mmol, (f) 1 hour. (Note formic acid MDAP yielded the diformic acid salt). Off-white solid. Yield: 25 mg, 30 %. **LCMS** (Method D) (ES +ve) m/z 498 ($M + H$)⁺ Rt 0.73 minutes. **¹H NMR** (400 MHz, DMSO-*d*₆, 120 °C) δ 8.34 (dd, $J = 1.4, 4.7$ Hz, 1H), 8.21 (br. s, 2H), 7.92 (dd, $J = 1.4, 8.2$ Hz, 1H), 7.68 (br. s, 1H), 7.38 (dd, $J = 4.7, 8.2$ Hz, 1H), 6.68 (br. s, 1H), 6.59 (dt, $J = 6.2, 15.6$ Hz, 1H), 6.55 (s, 1H), 6.04 (d, $J = 15.6$ Hz, 1H), 3.67 - 3.62 (m, 4H), 3.62 - 3.56 (m, 2H), 3.45 (q, $J = 6.0$ Hz, 2H), 3.37 (s, 2H), 3.01 (dd, $J = 1.3, 6.2$ Hz, 2H), 2.51 - 2.49 (m, 4H), 2.19 (s, 6H).

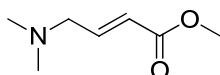
***N*²-{1-[(*E*)-4-(dimethylamino)-2-butenoyl]-3-piperidinyl}-6-(4-morpholinylmethyl)-*N*⁴-[1,3]thiazolo[5,4-*b*]pyridin-2-yl-2,4-pyrimidinediamine (**50b**)**



(a) (*E*)-4-(Dimethylamino)but-2-enoic acid hydrochloride **53**, 35 mg, 0.21 mmol, (b) 0.73 mL, 0.42 mmol, (c) 80 mg, 0.21 mmol, (d) **35c**, 70 mg, 0.14 mmol, (e) 0.73 mL, 0.42 mmol, (f) 1 hour. Off-white solid. Yield: 35 mg, 46 %. **LCMS** (Method D) (ES +ve) m/z 538 ($M + H$)⁺ Rt 0.78 minutes. **¹H NMR** (400 MHz, DMSO-*d*₆, 120 °C) δ 11.19 (br. s, 1H), 8.33 (dd, $J = 1.4, 4.7$ Hz, 1H), 7.91 (dd, $J = 1.4, 8.1$ Hz, 1H), 7.37 (dd, $J = 4.7, 8.1$ Hz, 1H), 6.60 - 6.48 (m, 3H), 6.43 (d, $J = 15.6$ Hz, 1H), 4.15 - 4.01 (m, 2H), 3.96 - 3.87 (m, 1H), 3.67 - 3.62 (m, 4H), 3.38 (s, 2H), 3.27 - 3.10 (m, 2H), 2.90 (d, $J = 5.5$ Hz, 2H), 2.53 - 2.51 (m, 4H), 2.15 - 2.11 (m, 1H), 2.10 (s, 6H), 1.90 - 1.80 (m, 1H), 1.75 - 1.64 (m, 1H), 1.61 - 1.48 (m, 1H). **IR** (cm⁻¹) 1514, 1576, 1618, 1655. **HRMS** (ES) calcd for C₂₆H₃₆N₉O₂S, ($M + H$)⁺ 538.2707, found 538.2697. **¹³C NMR** (126 MHz, DMSO-*d*₆) δ 168.6, 168.2, 164.8, 164.4, 161.3, 160.4, 158.9,

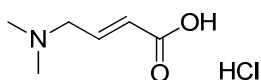
158.3, 156.8, 156.4, 156.1, 144.3, 143.0, 142.3, 141.7, 126.4, 123.1, 122.8, 121.8, 95.4, 95.0, 66.7, 64.2, 63.8, 60.8, 60.5, 60.2, 53.9, 50.2, 48.3, 47.9, 46.7, 45.8, 45.5, 45.2, 42.5, 42.0, 31.0, 30.4, 24.9, 24.1, 23.6. Note: ^{13}C NMR at room temperature displays the presence of rotamers for the compound. Decomposition temperature 154 °C.

(*E*)-Methyl 4-(dimethylamino)but-2-enoate (52)¹¹⁸



Dimethylamine in tetrahydrofuran (2 M, 69.8 mL, 140 mmol) was added dropwise to a solution of methyl (*2E*)-4-bromo-2-butenate **51** (6.68 mL, 55.9 mmol) in tetrahydrofuran (35 mL). The reaction mixture was stirred at room temperature under nitrogen atmosphere for 1 hour and at 45 °C for 45 minutes. The solid was filtered under reduced pressure and washed with tetrahydrofuran and dichloromethane. The filtrate was concentrated under reduced pressure. The residue was partitioned between dichloromethane (100 mL) and water (100 mL). The aqueous phase was back-extracted with dichloromethane (50 mL). The organic extracts were combined, dried using a hydrophobic frit and concentrated under reduced pressure to give the title compound (6.75 g, 84 % yield) as a yellow oil. ^1H NMR (400 MHz, DMSO- d_6) δ 6.82 (td, $J = 5.9, 15.7$ Hz, 1H), 6.00 (td, $J = 1.6, 15.7$ Hz, 1H), 3.66 (s, 3H), 3.04 (dd, $J = 1.6, 5.9$ Hz, 2H), 2.14 (s, 6H). No NMR details were provided in reference 118.

(*E*)-4-(Dimethylamino)but-2-enoic acid hydrochloride (53)¹¹⁸



Aqueous NaOH (3.3 M, 15.71 mL, 51.84 mmol) was added dropwise to a solution of methyl (*2E*)-4-(dimethylamino)-2-butenate **52** (6.75 g, 47.1 mmol) in methanol (30 mL). The reaction mixture was stirred at 45 °C under nitrogen atmosphere for 1 hour. Aqueous HCl (2 M) was added to reach pH 2. The solvent was evaporated to dryness

under reduced pressure. Anhydrous ethanol was added, the suspension stirred at room temperature and filtered under reduced pressure. The filtrate was evaporated to dryness and the solid triturated with isopropanol. The solid was filtered under reduced pressure, dried in the oven to give title compound (4 g, 51 % yield) as a white solid. ¹H NMR (400 MHz, DMSO-d₆) δ 12.75 (br. s, 1H), 11.36 (br. s, 1H), 6.84 (td, *J* = 7.0, 15.6 Hz, 1H), 6.18 (td, *J* = 1.3, 15.6 Hz, 1H), 3.88 (d, *J* = 7.0 Hz, 2H), 2.70 (s, 6H). No NMR details were provided in reference 118 but the NMR spectrum was in accordance with that described in reference 229.

Procedure for the investigation of the reactivity of compounds 3 and 35 with *N*-acetylcysteine:

A mixture of 1-(1-acryloyl-3-piperidiny)-3-[4-(phenyloxy)phenyl]-1H-pyrazolo[3,4-*d*]pyrimidin-4-amine **3** (4.1 mg, 9.3 μmol), *N,N*-diisopropylethylamine (32 μL, 0.183 mmol) and *N*-acetyl-L-cysteine (15 mg, 0.092 mmol) in DMSO (500 μL) was stirred at room temperature.

A mixture of *N*²-(1-acryloyl-3-piperidiny)-6-(4-morpholinylmethyl)-*N*⁴-[1,3]thiazolo[5,4-*b*]pyridin-2-yl-2,4-pyrimidinediamine **35** (4.4 mg, 9.2 μmol), DIPEA (32 μL, 0.183 mmol) and *N*-acetyl-L-cysteine (15 mg, 0.092 mmol) in DMSO (500 μL) was stirred at room temperature.

At the different time points stated in section VII.3, LCMS analyses of the reactions were recorded to measure the advancement of the Michael addition reactions. The results are detailed in section VII.3, Table 8. No products were isolated from these experiments.

General procedure G for the addition of *N*-acetylcysteine to the Michael acceptor analogues:

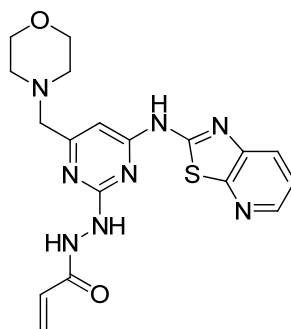
A mixture of the Michael acceptor analogues (such as **47a**, 9.19 μmol, see amount in table below), *N,N*-diisopropylethylamine (32 μL, 0.18 mmol) and *N*-acetyl-L-cysteine (15 mg, 92 μmol) in DMSO (500 μL) was stirred at room temperature. At the different time points stated in section VII.3, LCMS analyses of the reactions were recorded to measure the advancement of the Michael addition reactions. The results

are detailed in section VII.3, Table 10. No products were isolated from these experiments. Note that the reaction with **33** was performed on a slightly laterger scale (6 mg, 0.014 mmol) with *N,N*-diisopropylethylamine (47.6 μ L, 0.272 mmol) and *N*-acetyl-L-cysteine (22.2 mg, 0.136 μ mol).

Compound number	33	47a	48a	49a	47b	48b	49b
Amount of reagent used	6 mg	4.2 mg	5 mg	4.6 mg	2.5 mg	5.3 mg	5 mg
Compound number	8	13					
Amount of reagent used	3.5 mg	3.9 mg					

4. Synthetic procedures for the investigation of the positioning of the electrophilic moiety

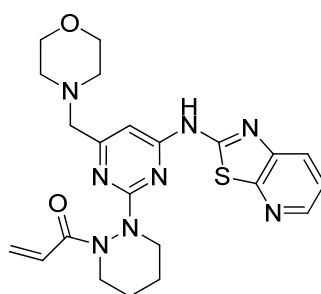
N'-(4-(Morpholinomethyl)-6-(thiazolo[5,4-*b*]pyridin-2-ylamino)pyrimidin-2-yl)acrylohydrazide (**59**)



A microwave vial was charged with *N*-[2-chloro-6-(4-morpholinylmethyl)-4-pyrimidinyl][1,3]thiazolo[5,4-*b*]pyridin-2-amine **32** (100 mg, 0.276 mmol), *tert*-butyl carbazate (109 mg, 0.827 mmol) and isopropanol (3 mL). The microwave vial was sealed and heated under microwave irradiation (Biotage Initiator system) at 170 °C for 45 minutes. Further *tert*-butyl carbazate (109 mg, 0.827 mmol) was added, the vial capped and heated in the microwave system at 170 °C for 30 minutes. The

mixture was evaporated to dryness under reduced pressure. The yellow solid was suspended in dichloromethane (5 mL) and treated with HCl in dioxane (4 M, 1 mL, 4 mmol). The reaction was stirred at room temperature for 16 hours. The mixture was evaporated to dryness under reduced pressure. The yellow solid was dissolved in *N*-methyl-2-pyrrolidone (2 mL) and treated with *N,N*-diisopropylethylamine (0.241 mL, 1.38 mmol) and 2-propenoyl chloride (0.045 mL, 0.55 mmol). The reaction was stirred at room temperature for 2 hours. Further portions of *N,N*-diisopropylethylamine (0.5 mL) and 2-propenoyl chloride (0.1 mL) were added and the reaction was stirred at room temperature for 2 hours. The mixture was purified by mass directed preparative HPLC to give the title compound (30 mg, 26 % yield) as an off-white solid. **LCMS** (Method D) (ES +ve) m/z 413 ($M + H$)⁺ Rt 0.63 minutes. **¹H NMR** (400 MHz, DMSO-*d*₆, 120 °C) δ 8.34 (d, $J = 4.7$ Hz, 1H), 7.92 (d, $J = 8.1$ Hz, 1H), 7.36 (dd, $J = 4.7, 8.1$ Hz, 1H), 6.71 (s, 1H), 6.47 (dd, $J = 10.7, 17.1$ Hz, 1H), 6.22 (dd, $J = 2.0, 17.1$ Hz, 1H), 5.70 (dd, $J = 2.0, 10.7$ Hz, 1H), 3.72 - 3.59 (m, 4H), 3.47 - 3.39 (m, 2H), 2.56 - 2.51 (m, 4H). **HRMS** (ES) calcd for C₁₈H₂₁N₈O₂S, ($M + H$)⁺ 413.1503, found 413.1512. **IR** (cm⁻¹) 1518, 1579, 1623, 1683. **¹³C NMR** (126 MHz, DMSO-*d*₆) δ 168.6, 164.9, 162.9, 158.8, 158.3, 156.7, 144.5, 142.9, 130.4, 126.9, 126.5, 121.7, 96.8, 66.7, 63.7, 53.9. Decomposition temperature 243 °C.

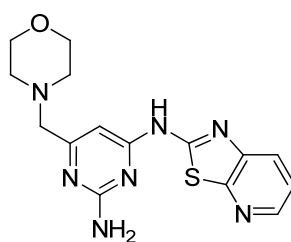
***N*-[2-(2-Acryloyltetrahydro-1(2H)-pyridazinyl)-6-(4-morpholinylmethyl)-4-pyrimidinyl][1,3]thiazolo[5,4-*b*]pyridin-2-amine (60)**



A microwave vial was charged with *N*-[2-chloro-6-(4-morpholinylmethyl)-4-pyrimidinyl][1,3]thiazolo[5,4-*b*]pyridin-2-amine **32** (100 mg, 0.276 mmol), hexahydropyridazine hydrochloride (132 mg, 0.827 mmol) and *N,N*-

diisopropylethylamine (0.144 mL, 0.827 mmol). The microwave vial was sealed and heated in the Biotage Initiator microwave system at 170 °C for 45 minutes. The solvent was evaporated to dryness. The brown residue was dissolved in *N*-methyl-2-pyrrolidone (2 mL). *N,N*-Diisopropylethylamine (0.289 mL, 1.65 mmol) and 2-propenoyl chloride (0.134 mL, 1.65 mmol) were added and the reaction was stirred at room temperature for 1 hour. The mixture was subjected to purification by mass directed automated preparative HPLC to afford the title compound (20 mg, 16 % yield) as an off-white solid. **LCMS** (Method B) (ES +ve) m/z 467 ($M + H$)⁺ Rt 2.22 minutes. **¹H NMR** (400 MHz, DMSO-*d*₆) δ 8.35 (dd, $J = 1.1, 4.6$ Hz, 1H), 7.98 (dd, $J = 1.1, 8.0$ Hz, 1H), 7.41 (dd, $J = 4.6, 8.0$ Hz, 1H), 6.73 (s, 1H), 6.60 (dd, $J = 10.3, 17.1$ Hz, 1H), 6.20 (dd, $J = 2.3, 17.1$ Hz, 1H), 5.63 (dd, $J = 2.3, 10.3$ Hz, 1H), 4.88 - 4.78 (m, 1H), 4.56 - 4.45 (m, 1H), 3.65 - 3.58 (m, 4H), 3.43 (s, 2H), 3.19 - 3.11 (m, 1H), 2.92 - 2.74 (m, 1H), 2.48 - 2.43 (m, 4H), 1.75 - 1.61 (m, 4H). **HRMS** (ES) calcd for C₂₂H₂₇N₈O₂S, ($M + H$)⁺ 467.1972, found 467.1960. **IR** (cm⁻¹) 1516, 1575, 1614, 1650. **¹³C NMR** (126 MHz, DMSO-*d*₆) δ 168.9, 166.5, 161.5, 159.2, 158.7, 156.4, 144.4, 143.0, 128.5, 128.0, 126.6, 121.9, 98.6, 66.7, 63.6, 53.8, 48.2, 23.9, 22.5. Note that the HMQC data revealed that one ¹³C signal was present at 40 ppm. In the ¹³C spectrum, this peak is overlapping with the DMSO signals hence can not be seen. Decomposition temperature 163 °C.

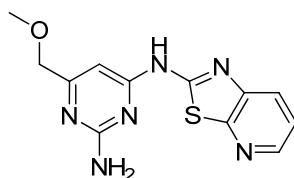
6-(Morpholinomethyl)-*N*⁴-(thiazolo[5,4-*b*]pyridin-2-yl)pyrimidine-2,4-diamine (62)



A microwave vial was charged with *N*-[2-chloro-6-(4-morpholinylmethyl)-4-pyrimidinyl][1,3]thiazolo[5,4-*b*]pyridin-2-amine **32** (500 mg, 1.378 mmol), aqueous ammonia (533 μl, 27.6 mmol) and ethylene glycol (4 mL). The microwave vial was sealed and heated under microwave irradiation (Biotage Initiator system) at 190 °C

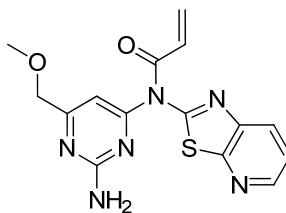
for 1 hour. The reaction mixture was filtered under reduced pressure and washed with water. The filtrate was concentrated under reduced pressure and purified by mass directed autopreparative HPLC to give the title product (210 mg, 44 % yield) as a white solid. **LCMS** (Method D) (ES +ve) m/z 344 ($M + H$)⁺ Rt 0.66 minutes. **¹H NMR** (400 MHz, DMSO- d_6) δ 11.57 (br. s, 1H), 8.35 (dd, $J = 1.4, 4.7$ Hz, 1H), 7.96 (dd, $J = 1.4, 8.1$ Hz, 1H), 7.40 (dd, $J = 4.8, 8.1$ Hz, 1H), 6.68 (s, 2H), 6.45 (s, 1H), 3.64 - 3.58 (m, 4H), 3.30 (s, 2H), 2.48 - 2.43 (m, 4H). **HRMS** (ES) calcd for $C_{15}H_{18}N_7OS$, ($M + H$)⁺ 344.1288, found 344.1294. **IR** (cm^{-1}) 1519, 1577, 1615, 1648. **¹³C NMR** (126 MHz, DMSO- d_6) δ 168.4, 162.4, 158.9, 158.3, 156.8, 144.3, 143.0, 126.3, 121.7, 95.1, 66.7, 63.8, 53.9. Decomposition temperature 269 °C.

6-(Methoxymethyl)-*N*⁴-(thiazolo[5,4-*b*]pyridin-2-yl)pyrimidine-2,4-diamine (63)



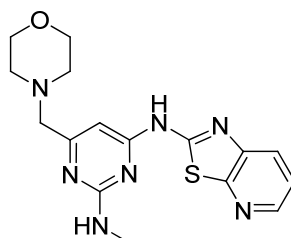
A microwave vial was charged with *N*-[6-[(methoxy)methyl]-2-(methylsulfonyl)-4-pyrimidinyl][1,3]thiazolo[5,4-*b*]pyridin-2-amine **5** (300 mg, 0.854 mmol), aqueous ammonia (0.165 mL, 8.54 mmol) and isopropanol (3 mL). The microwave vial was sealed and heated under microwave irradiation (Biotage Initiator system) at 150 °C for 35 minutes. A further portion of aqueous ammonia (0.165 mL, 8.54 mmol) was added. The microwave vial was sealed and heated under microwave irradiation at 150 °C for 35 minutes. Water was added and the solid was filtered under reduced pressure. The solid was dried in the oven under reduced pressure to give the title compound (168 mg, 82 % pure, 56 % yield) as a beige solid. **LCMS** (Method B) (ES +ve) m/z 289 ($M + H$)⁺ Rt 1.72 minutes. **¹H NMR** (400 MHz, DMSO- d_6) δ 11.65 (s, 1H), 8.36 (dd, $J = 1.4, 4.8$ Hz, 1H), 7.97 (dd, $J = 1.4, 8.0$ Hz, 1H), 7.41 (dd, $J = 4.8, 8.1$ Hz, 1H), 6.71 (s, 2H), 6.36 (s, 1H), 4.22 (s, 2H), 3.36 (s, 3H).

***N*-{2-Amino-6-[(methoxy)methyl]-4-pyrimidinyl}-*N*-[1,3]thiazolo[5,4-*b*]pyridin-2-yl-2-propenamide (65)**



A mixture of 6-(methoxymethyl)-*N*⁴-(thiazolo[5,4-*b*]pyridin-2-yl)pyrimidine-2,4-diamine **63** (50 mg, 0.17 mmol), *N,N*-diisopropylethylamine (0.121 mL, 0.694 mmol) and 2-propenoyl chloride (0.028 mL, 0.35 mmol) in *N*-methyl-2-pyrrolidone (1 mL) was stirred at room temperature for 1 hour. The mixture was subjected to purification by mass directed automated preparative HPLC (formic acid modifier). The desired fraction was extracted with dichloromethane. After separation, the organic extract was dried using a hydrophobic frit and concentrated under reduced pressure to afford the title compound (13 mg, 22 % yield) as a yellow glass. **LCMS** (Method B) (ES +ve) *m/z* 343 (*M* + *H*)⁺ *Rt* 2.01 minutes. **¹H NMR** (400 MHz, DMSO-*d*₆) δ 8.52 (dd, *J* = 1.5, 4.5 Hz, 1H), 8.13 (dd, *J* = 1.5, 8.0 Hz, 1H), 7.48 (dd, *J* = 4.5, 8.0 Hz, 1H), 7.18 (s, 2H), 6.90 (s, 1H), 6.55 (dd, *J* = 1.3, 16.6 Hz, 1H), 6.21 (dd, *J* = 10.3, 16.6 Hz, 1H), 5.98 (dd, *J* = 1.3, 10.3 Hz, 1H), 4.42 (s, 2H), 3.38 (s, 3H). NOE coupling observed between the protons at 6.90 ppm and 6.21 ppm supported the characterisation of this isomer. Purity < 80 %.

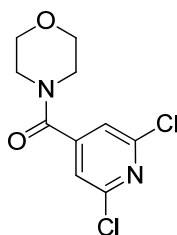
***N*²-Methyl-6-(morpholinomethyl)-*N*⁴-(thiazolo[5,4-*b*]pyridin-2-yl)pyrimidine-2,4-diamine (66)**



A microwave vial was charged with *N*-[2-chloro-6-(4-morpholinylmethyl)-4-pyrimidinyl][1,3]thiazolo[5,4-*b*]pyridin-2-amine **32** (100 mg, 0.276 mmol),

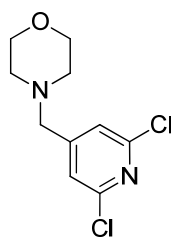
methylamine (40 % w/w in water, 428 mg, 5.51 mmol) and ethylene glycol (1 mL). The microwave vial was sealed and heated under microwave irradiation (Biotage Initiator system) at 180 °C for 1 hour. The mixture was purified by mass directed autopreparative HPLC to give the title compound (46 mg, 47 % yield) as a white solid. **LCMS** (Method D) (ES +ve) m/z 358 ($M + H$)⁺ Rt 0.77 minutes. **¹H NMR** (400 MHz, DMSO-*d*₆) δ 11.64 (br. s, 1H), 8.35 (dd, $J = 1.4, 4.6$ Hz, 1H), 7.97 (dd, $J = 1.4, 8.2$ Hz, 1H), 7.41 (dd, $J = 4.6, 8.2$ Hz, 1H), 7.20 (br. s, 1H), 6.43 (br. s, 1H), 3.66 - 3.57 (m, 4H), 3.32 (s, 2H), 2.99 (br. s, 3H), 2.48 - 2.43 (m, 4H). **IR** (cm⁻¹) 1515, 1559, 1580, 1629. **HRMS** (ES) calcd for C₁₆H₂₀N₇OS, ($M + H$)⁺ 358.1445, found 358.1445. **¹³C NMR** (126 MHz, DMSO-*d*₆) δ 168.3, 162.7, 158.5, 158.2, 156.5, 144.3, 143.0, 126.4, 121.8, 94.3, 66.7, 63.9, 53.9, 29.2. Decomposition temperature 243 °C.

(2,6-Dichloropyridin-4-yl)(morpholino)methanone (69)



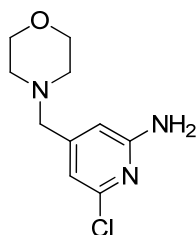
Morpholine (8.28 mL, 95 mmol) was added to a stirred, cooled (0 °C) mixture of 2,6-dichloro-4-pyridinecarbonyl chloride **68** (10 g, 48 mmol) and DIPEA (24.9 mL, 143 mmol) in dichloromethane (30 mL). The mixture was stirred at 0 °C for 2 hours and then at room temperature overnight. Aqueous saturated ammonium chloride (70 mL) was added to the reaction mixture and the product was extracted with ethyl acetate (2 x 100 mL). The organic fractions were combined, dried using a hydrophobic frit and concentrated under reduced pressure. The yellow sticky solid was purified by FlashMaster on silica using a gradient elution from 0 to 65 % ethyl acetate in cyclohexane to give the title compound (8.86 g, 71 % yield) as a yellow solid. **LCMS** (Method D) (ES +ve) m/z 261 ($M + H$)⁺ Rt 0.79 minutes. **¹H NMR** (400 MHz, DMSO-*d*₆) δ 7.66 (s, 2H), 3.63 - 3.70 (m, 2H), 3.58-3.63 (m, 2H), 3.55 (t, $J = 4.6$ Hz, 2H), 3.28 (t, $J = 4.6$ Hz, 2H).

4-((2,6-Dichloropyridin-4-yl)methyl)morpholine (70)



Borane in tetrahydrofuran (1 M, 140 mL, 140 mmol) was added dropwise to a cooled solution (0 °C) of 4-[(2,6-dichloro-4-pyridinyl)carbonyl]morpholine **69** (12.17 g, 46.61 mmol) in dichloromethane (50 mL). The reaction was stirred at 0 °C for 1 hour under nitrogen atmosphere. Aqueous HCl (5 M) was carefully added to the reaction, while still stirring at 0 °C, until a clear solution was obtained. After stirring for 30 minutes, the solution was basified with aqueous NaOH (10 M) to reach pH 14. The organic phase was dried (hydrophobic frit) and concentrated under reduced pressure. The residue was purified by FlashMaster chromatography on silica using a gradient elution from 0 to 100 % ethyl acetate in dichloromethane to afford the title compound (10.1 g, 88 % yield) as an off-white solid. **LCMS** (Method B) (ES +ve) m/z 247 ($M + H$)⁺ Rt 2.43 minutes. **¹H NMR** (400 MHz, DMSO- d_6) δ 7.50 (s, 2H), 3.62 - 3.56 (m, 4H), 3.54 (s, 2H), 2.40 - 2.36 (m, 4H).

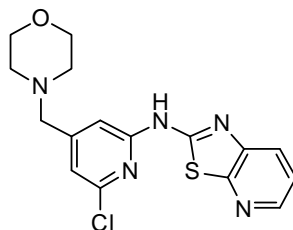
6-Chloro-4-(morpholinomethyl)pyridin-2-amine (71)



A solution of 4-((2,6-dichloropyridin-4-yl)methyl)morpholine **70** (3.5 g, 14 mmol) in isopropanol (3 mL) was treated with aqueous ammonia (7.0 mL, 323 mmol) and the mixture heated at 160 °C in the Biotage Initiator microwave for 15 hours (18 bar pressure build up). The reaction mixture was evaporated under reduced pressure to give a yellow solid. The mixture was purified by FlashMaster chromatography on

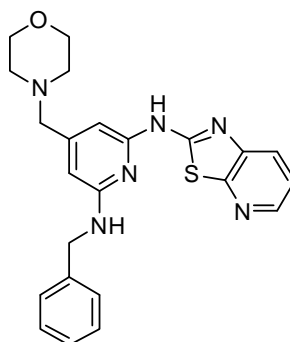
silica using a gradient elution from 0 to 100 % ethyl acetate in cyclohexane followed by a 0 to 20 % methanol in ethyl acetate to afford the title compound (1.8 g, 56 % yield) as an off-white solid. **LCMS** (Method D) (ES +ve) m/z 228 ($M + H$)⁺ Rt 0.70 minutes. **¹H NMR** (400 MHz, DMSO-*d*₆) δ 6.44 (s, 1H), 6.35 (s, 1H), 6.31 (s, 2H), 3.61 - 3.55 (m, 4H), 3.30 (s, 2H), 2.37 - 2.31 (m, 4H).

***N*-(6-Chloro-4-(morpholinomethyl)pyridin-2-yl)thiazolo[5,4-*b*]pyridin-2-amine (72)**



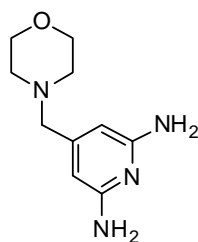
To an ice cooled solution of 6-chloro-4-(4-morpholinylmethyl)-2-pyridinamine **71** (1.8 g, 7.9 mmol) and 2-bromo[1,3]thiazolo[5,4-*b*]pyridine **31** (1.87 g, 8.70 mmol) in *N,N*-dimethylformamide (20 mL) was added sodium hydride (60 % w/w in mineral oil, 0.632 g, 15.8 mmol) portionwise. The reaction was stirred at 0 °C under nitrogen atmosphere for 1 hour and left stirring at room temperature overnight. Saturated aqueous ammonium chloride was added and the product was extracted with ethyl acetate. After separation, the organic extract was dried using a hydrophobic frit and concentrated under reduced pressure. The brown solid was suspended in dichloromethane and the suspension was filtered under reduced pressure. The white solid was dried in the oven to give the title compound (1.02 g). The filtrate was evaporated under vacuum. The brown solid was suspended in diethyl ether and the suspension filtered under vacuum. The light brown solid was dried in the oven to yield the title compound (1.05 g). Total amount obtained: 2.07 g, 73 % yield. **LCMS** (Method D) (ES +ve) m/z 362 ($M + H$)⁺ Rt 1.00 minutes. **¹H NMR** (400 MHz, DMSO-*d*₆) δ 11.91 (s, 1H), 8.36 (dd, $J = 1.5, 4.8$ Hz, 1H), 7.97 (dd, $J = 1.5, 8.2$ Hz, 1H), 7.42 (dd, $J = 4.8, 8.2$ Hz, 1H), 7.20 (s, 1H), 7.07 (s, 1H), 3.63 - 3.59 (m, 4H), 3.51 (s, 2H), 2.43 - 2.37 (m, 4H).

***N*²-Benzyl-4-(morpholinomethyl)-*N*⁶-(thiazolo[5,4-*b*]pyridin-2-yl)pyridine-2,6-diamine (75)**



A microwave vial was charged with *N*-[6-chloro-4-(4-morpholinylmethyl)-2-pyridinyl][1,3]thiazolo[5,4-*b*]pyridin-2-amine **72** (115 mg, 0.318 mmol), benzylamine (0.277 mL, 2.54 mmol) and ethylene glycol (1.5 mL). The microwave vial was sealed and heated under microwave irradiation (Biotage Initiator system) at 200 °C for 2 hours. The microwave vial was then heated under microwave irradiation at 220 °C for 1.5 hours. The product was purified by mass directed autopreparative HPLC to give the title compound (40 mg, 29 % yield) as a brown solid. **LCMS** (Method B) (ES +ve) *m/z* 433 (*M* + *H*)⁺ *Rt* 2.64 minutes. **¹H NMR** (400 MHz, DMSO-*d*₆) δ 11.26 (br. s, 1H), 8.25 (dd, *J* = 1.5, 4.8 Hz, 1H), 7.84 (dd, *J* = 1.5, 8.0 Hz, 1H), 7.42 - 7.37 (m, 2H), 7.36 - 7.29 (m, 3H), 7.26 - 7.19 (m, 2H), 6.26 (s, 1H), 6.18 (s, 1H), 4.71 (d, *J* = 6.0 Hz, 2H), 3.61 - 3.55 (m, 4H), 3.30 (s, 2H), 2.38 - 2.33 (m, 4H).

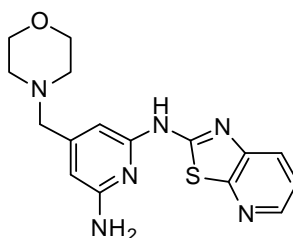
4-(Morpholinomethyl)pyridine-2,6-diamine (76)



A microwave vial was charged with 4-[(2,6-dichloro-4-pyridinyl)methyl]morpholine **70** (2.5 g, 10.1 mmol), copper powder (200 mg, 3.15 mmol) and aqueous ammonia (10.0 mL, 517 mmol). The vial was sealed and heated in the Biotage Initiator

microwave system at 170 °C, maximum pressure 18 bars, for 15 hours. An extra aliquot of copper powder (200 mg, 3.15 mmol) was added, the vial was sealed and heated in the Biotage Initiator microwave system at 170 °C, maximum pressure 18 bars, for further 15 hours. The reaction mixture was filtered on celite and the filtrate was evaporated under reduced pressure. The product was purified by reverse phase chromatography (C18) using a gradient elution from 0 to 50% acetonitrile in water with an ammonium carbonate modifier gradient to give the title compound (1.02 g, 48 % yield) as a brown solid. **LCMS** (Method D) (ES +ve) m/z 209 ($M + H$)⁺ Rt 0.47 minutes. **¹H NMR** (400MHz, DMSO- d_6) δ 5.62 (s, 2H), 5.26 (s, 4H), 3.60 - 3.53 (m, 4H), 3.13 (s, 2H), 2.35 - 2.28 (m, 4H).

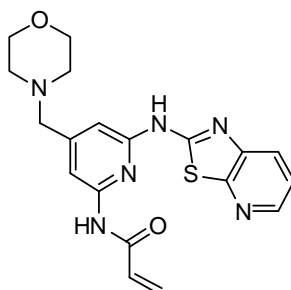
4-(Morpholinomethyl)-*N*²-(thiazolo[5,4-*b*]pyridin-2-yl)pyridine-2,6-diamine (73)



A round bottom flask was charged with 4-(4-morpholinylmethyl)-2,6-pyridinediamine **76** (900 mg, 4.32 mmol) and 2-bromo[1,3]thiazolo[5,4-*b*]pyridine **31** (1.022 g, 4.751 mmol) in anhydrous *N,N*-dimethylformamide (10 mL). The reaction was placed in an atmosphere of nitrogen and cooled in an ice bath. Sodium hydride (60% w/w in mineral oil, 519 mg, 13.0 mmol) was added portionwise over 5 minutes and the mixture was stirred for 1 hour whilst being allowed to warm at ambient temperature. The reaction mixture was stirred at room temperature for 16 hours. The reaction mixture was then partitioned between dichloromethane and water. The organic layer was dried using a hydrophobic frit and concentrated under reduced pressure to deliver a black oil. The sample was purified by FlashMaster chromatography on aminopropyl (NH₂) silica using a gradient elution from 0 to 100 % ethyl acetate in cyclohexane to give the title compound (417 mg, 28 % yield) as an off-white solid. **LCMS** (Method D) (ES +ve) m/z 343 ($M + H$)⁺ Rt 0.74 minutes. **¹H NMR** (400 MHz, DMSO- d_6) δ 11.22 (s, 1H), 8.28 (dd, $J = 1.5, 4.8$ Hz, 1H), 7.85

(dd, $J = 1.5, 8.0$ Hz, 1H), 7.34 (dd, $J = 4.8, 8.0$ Hz, 1H), 6.25 (s, 1H), 6.10 (s, 2H), 6.08 (s, 1H), 3.61 - 3.57 (m, 4H), 3.32 (s, 2H), 2.39 - 2.34 (m, 4H).

***N*-(4-(Morpholinomethyl)-6-(thiazolo[5,4-*b*]pyridin-2-ylamino)pyridin-2-yl)acrylamide (77)**

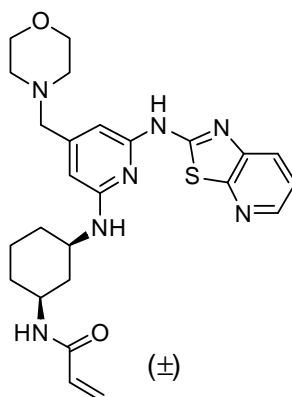


A reaction vessel was charged with 4-(4-morpholinylmethyl)-*N*-[1,3]thiazolo[5,4-*b*]pyridin-2-yl-2,6-pyridinediamine **73** (50 mg, 0.15 mmol) in anhydrous *N*-methyl-2-pyrrolidone (1 mL). Triethylamine (0.061 mL, 0.44 mmol) was added followed by 2-propenoyl chloride (0.035 mL, 0.44 mmol) and the reaction was stirred at room temperature for 16 hours. A second portion of triethylamine (0.061 mL, 0.44 mmol) and 2-propenoyl chloride (0.035 mL, 0.44 mmol) was added and the reaction was stirred at room temperature for 2 hours. A third portion of triethylamine (0.061 mL, 0.44 mmol) and 2-propenoyl chloride (0.035 mL, 0.44 mmol) was added and the reaction was stirred at room temperature for 2 hours. The reaction mixture was partitioned between dichloromethane (10 mL) and water (10 mL). After separation, the organic extract was dried using a hydrophobic frit and concentrated under reduced pressure. Saturated aqueous Na₂CO₃ was added to the aqueous phase and the product was extracted with dichloromethane (2 x 20 mL). The organic extracts were combined, dried using a hydrophobic frit and concentrated under reduced pressure. The residue was purified by mass directed autoperparative HPLC to give the title compound (3 mg, 5 % yield) as a brown solid. **LCMS** (Method D) (ES +ve) *m/z* 397 (M + H)⁺ Rt 0.85 minutes. **¹H NMR** (400 MHz, DMSO-*d*₆) δ 11.49 (br. s, 1H), 10.28 (s, 1H), 8.29 (dd, $J = 1.3, 4.8$ Hz, 1H), 7.87 (dd, $J = 1.3, 8.0$ Hz, 1H), 7.82 (s, 1H), 7.36 (dd, $J = 4.8, 8.0$ Hz, 1H), 6.85 (s, 1H), 6.82 (dd, $J = 10.0, 17.1$ Hz, 1H), 6.33

(dd, $J = 2.0, 17.1$ Hz, 1H), 5.81 (dd, $J = 2.0, 10.0$ Hz, 1H), 3.63 - 3.58 (m, 4H), 3.47 (s, 2H), 2.43 - 2.38 (m, 4H).

5. Synthetic procedures for the 6-morpholinemethylpyridine series

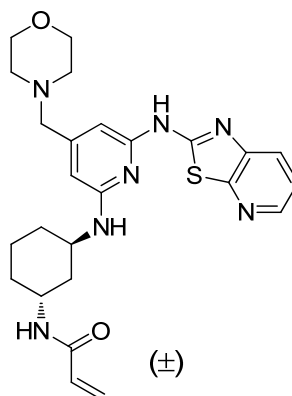
N-(*Cis*-3-{[4-(4-morpholinylmethyl)-6-([1,3]thiazolo[5,4-*b*]pyridin-2-ylamino)-2-pyridinyl]amino}cyclohexyl)-2-propenamide (78)



A microwave vial was charged with (3-aminocyclohexyl)amine (mixture of *cis*- and *trans*-isomers, 250 mg, 2.19 mmol), *N*-[6-chloro-4-(4-morpholinylmethyl)-2-pyridinyl][1,3]thiazolo[5,4-*b*]pyridin-2-amine **72** (59 mg, 0.16 mmol) and ethylene glycol (1 ml). The vial was sealed and was heated in a Biotage Initiator microwave at 200 °C for 1 hour. A second portion of (3-aminocyclohexyl)amine (mixture of *cis*- and *trans*-isomers, 250 mg, 2.19 mmol) was added to the reaction mixture and the microwave vial was heated in the Biotage Initiator microwave system for 1 hour at 220 °C. A third portion of (3-aminocyclohexyl)amine (mixture of *cis*- and *trans*-isomers, 250 mg, 2.19 mmol) was added to the reaction mixture and the microwave vial was heated in the Biotage Initiator microwave for 1 hour at 220 °C. The intermediate was purified by mass directed automated preparative HPLC. The residue (20 mg), 2-propenoyl chloride (4.4 μL, 0.055 mmol) and *N,N*-diisopropylethylamine (0.016 mL, 0.091 mmol) in *N*-methyl-2-pyrrolidone (1 mL) were stirred at room temperature for 10 minutes. The product was purified by mass directed automated preparative HPLC to afford the title compound (14 mg, 34 % yield) as a brown solid. LCMS (Method B) (ES +ve) m/z 494 ($M + H$)⁺ Rt 2.18

minutes. $^1\text{H NMR}$ (400 MHz, DMSO- d_6) δ 11.20 (br. s, 1H), 8.28 (dd, $J = 1.4, 4.8$ Hz, 1H), 8.05 (d, $J = 7.8$ Hz, 1H), 7.86 (dd, $J = 1.4, 8.0$ Hz, 1H), 7.36 (dd, $J = 4.8, 8.0$ Hz, 1H), 6.66 (d, $J = 8.0$ Hz, 1H), 6.20 (s, 1H), 6.19 (dd, $J = 10.2, 17.0$ Hz, 1H), 6.10 (s, 1H), 6.05 (dd, $J = 2.3, 17.0$ Hz, 1H), 5.55 (dd, $J = 2.3, 10.2$ Hz, 1H), 4.11 - 3.98 (m, 1H), 3.84 - 3.72 (m, 1H), 3.60 - 3.55 (m, 4H), 3.28 (s, 2H), 2.39 - 2.34 (m, 4H), 2.20 - 2.06 (m, 2H), 1.95 - 1.87 (m, 1H), 1.86 - 1.78 (m, 1H), 1.57 - 1.42 (m, 1H), 1.31 - 0.99 (m, 3H). NOE coupling between the protons at 4.11 - 3.98 ppm and 3.84 - 3.72 ppm supported the characterisation of the *cis*-geometry for this compound. **IR** (cm^{-1}) 1515, 1540, 1574, 1625, 1661. **HRMS** (ES) calcd for $\text{C}_{25}\text{H}_{32}\text{N}_7\text{O}_2\text{S}$, ($\text{M} + \text{H}$) $^+$ 494.2333, found 494.2332. $^{13}\text{C NMR}$ (126 MHz, DMSO- d_6) δ 164.0, 159.2, 157.5, 156.2, 150.5, 150.2, 143.5, 143.4, 132.4, 125.4, 125.3, 121.6, 101.4, 97.6, 66.7, 62.3, 53.8, 49.4, 47.8, 39.4, 32.9, 32.4, 23.6. Decomposition temperature 223 $^\circ\text{C}$.

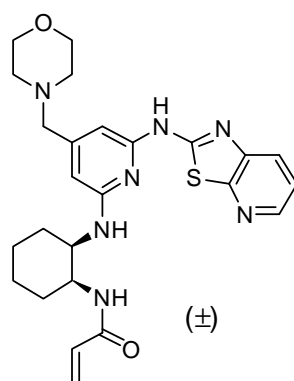
***N*-(*Trans*-3-{[4-(4-morpholinylmethyl)-6-([1,3]thiazolo[5,4-*b*]pyridin-2-ylamino)-2-pyridinyl]amino}cyclohexyl)-2-propenamide (79)**



A microwave vial was charged with (3-aminocyclohexyl)amine (mixture of *cis*- and *trans*-isomers, 250 mg, 2.19 mmol), *N*-[6-chloro-4-(4-morpholinylmethyl)-2-pyridinyl][1,3]thiazolo[5,4-*b*]pyridin-2-amine **72** (59 mg, 0.16 mmol) and ethylene glycol (1 ml). The vial was sealed and was heated in a Biotage Initiator microwave at 200 $^\circ\text{C}$ for 1 hour. A second portion of (3-aminocyclohexyl)amine (mixture of *cis*- and *trans*-isomers, 250 mg, 2.19 mmol) was added to the reaction mixture and the microwave vial was heated in the Biotage Initiator microwave system for 1 hour at 220 $^\circ\text{C}$. A third portion of (3-aminocyclohexyl)amine (mixture of *cis*- and *trans*-

isomers, 250 mg, 2.19 mmol) was added to the reaction mixture and the microwave vial was heated in the Biotage Initiator microwave for 1 hour at 220 °C. The intermediate was purified by mass directed automated preparative HPLC. The residue (10 mg), 2-propenoyl chloride (2.2 μL, 0.027 mmol) and *N,N*-diisopropylethylamine (7.95 μL, 0.0455 mmol) in *N*-methyl-2-pyrrolidone (1 mL) were stirred at room temperature for 10 minutes. The product was purified by mass directed automated preparative HPLC to afford the title compound (4 mg, 10 % yield) as a brown solid. **LCMS** (Method B) (ES +ve) *m/z* 494 (M + H)⁺ Rt 2.25 minutes. **¹H NMR** (400 MHz, DMSO-*d*₆) δ 11.22 (br. s, 1H), 8.26 (dd, *J* = 1.4, 4.8 Hz, 1H), 7.97 (d, *J* = 7.6 Hz, 1H), 7.85 (dd, *J* = 1.4, 8.1 Hz, 1H), 7.35 (dd, *J* = 4.8, 8.1 Hz, 1H), 6.74 (d, *J* = 7.6 Hz, 1H), 6.27 (s, 1H), 6.20 (s, 1H), 6.21 (dd, *J* = 10.1, 17.0 Hz, 1H), 6.01 (dd, *J* = 2.3, 17.0 Hz, 1H), 5.48 (dd, *J* = 2.3, 10.1 Hz, 1H), 4.49 - 4.40 (m, 1H), 4.07 - 3.97 (m, 1H), 3.62 - 3.57 (m, 4H), 3.28 (s, 2H), 2.40 - 2.35 (m, 4H), 2.01 - 1.91 (m, 1H), 1.83 - 1.58 (m, 6H), 1.36 - 1.24 (m, 1H). NMR (including NOE couplings) comparisons with compound **78** supported the characterisation of the *trans*-geometry for this compound.

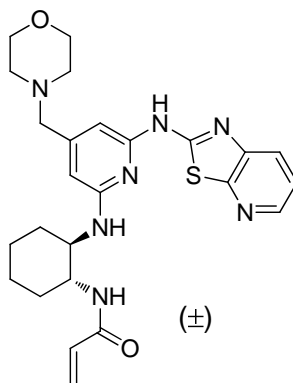
***N*-Cis-2-[[4-(4-morpholinylmethyl)-6-([1,3]thiazolo[5,4-*b*]pyridin-2-ylamino)-2-pyridinyl]amino}cyclohexyl)-2-propenamide (**80**)**



A microwave vial was charged with *N*-[6-chloro-4-(4-morpholinylmethyl)-2-pyridinyl][1,3]thiazolo[5,4-*b*]pyridin-2-amine **72** (100 mg, 0.276 mmol), *cis*-1,2-cyclohexanediamine (410 mg, 3.59 mmol) and ethylene glycol (1 ml). The vial was sealed and was heated in a Biotage Initiator microwave at 220 °C for 1 hour. The intermediate was purified by mass directed automated preparative HPLC. The

residue (18 mg), 2-propenoyl chloride (4.5 μ L, 0.049 mmol) and *N,N*-diisopropylethylamine (0.014 mL, 0.082 mmol) in *N*-methyl-2-pyrrolidone (1 mL) were stirred at room temperature for 10 minutes. The product was purified by mass directed automated preparative HPLC to afford the title compound (3.8 mg, 3 % yield) as a brown glass. **LCMS** (Method B) (ES +ve) m/z 494 ($M + H$)⁺ Rt 2.29 minutes. **¹H NMR** (400 MHz, DMSO- d_6) δ 8.27 (dd, $J = 1.3, 4.8$ Hz, 1H), 7.84 (dd, $J = 1.3, 8.2$ Hz, 1H), 7.75 (d, $J = 8.3$ Hz, 1H), 7.35 (dd, $J = 4.8, 8.2$ Hz, 1H), 6.46 - 6.34 (m, 2H), 6.20 (s, 1H), 6.18 (s, 1H), 6.02 (dd, $J = 2.3, 17.2$ Hz, 1H), 5.54 (dd, $J = 2.3, 10.3$ Hz, 1H), 4.44 - 4.23 (m, 2H), 3.63 - 3.53 (m, 4H), 3.27 (s, 2H), 2.39 - 2.34 (m, 4H), 1.85 - 1.40 (m, 8H).

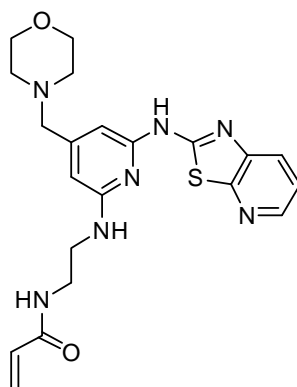
***N*-(*Trans*-2-[[4-(4-morpholinylmethyl)-6-([1,3]thiazolo[5,4-*b*]pyridin-2-ylamino)-2-pyridinyl]amino}cyclohexyl)-2-propenamide (81)**



A microwave vial was charged with *N*-[6-chloro-4-(4-morpholinylmethyl)-2-pyridinyl][1,3]thiazolo[5,4-*b*]pyridin-2-amine **72** (100 mg, 0.276 mmol), *trans*-1,2-cyclohexanediamine (31.6 mg, 0.276 mmol) and ethylene glycol (1 ml). The vial was sealed and was heated in a Biotage Initiator microwave at 220 °C for 1 hour. The intermediate was purified by mass directed automated preparative HPLC. The residue (20 mg), 2-propenoyl chloride (4.4 μ L, 0.055 mmol) and *N,N*-diisopropylethylamine (0.016 mL, 0.091 mmol) in *N*-methyl-2-pyrrolidone (1 mL) were stirred at room temperature for 10 minutes. The mixture was purified by mass directed automated preparative HPLC to afford the title compound (16 mg, 12 % yield) as a brown glass. **LCMS** (Method B) (ES +ve) m/z 494 ($M + H$)⁺ Rt 2.34 minutes. **¹H NMR** (400 MHz, DMSO- d_6) δ 8.27 (dd, $J = 1.4, 4.8$ Hz, 1H), 8.07 (d, J

= 7.8 Hz, 1H), 7.84 (dd, $J = 1.4, 8.0$ Hz, 1H), 7.35 (dd, $J = 4.8, 8.0$ Hz, 1H), 6.43 (d, $J = 7.3$ Hz, 1H), 6.20 (s, 1H), 6.18 (dd, $J = 10.0, 17.1$ Hz, 1H), 6.04 (s, 1H), 6.04 (dd, $J = 2.3, 17.1$ Hz, 1H), 5.52 (dd, $J = 2.3, 10.0$ Hz, 1H), 4.02 - 3.90 (m, 1H), 3.82 - 3.71 (m, 1H), 3.62 - 3.54 (m, 4H), 3.26 (s, 2H), 2.41 - 2.30 (m, 4H), 2.06 - 1.93 (m, 1H), 1.82 - 1.70 (m, 2H), 1.56 - 1.13 (m, 5H). **IR** (cm^{-1}) 1516, 1574, 1626, 1656. **HRMS** (ES) calcd for $\text{C}_{25}\text{H}_{32}\text{N}_7\text{O}_2\text{S}$, ($\text{M} + \text{H}$)⁺ 494.2333, found 494.2332. **¹³C NMR** (126 MHz, DMSO-d_6) δ 165.2, 159.2, 158.0, 156.2, 150.4, 150.1, 143.5, 143.4, 132.5, 125.4, 125.3, 121.6, 101.7, 97.6, 66.6, 62.2, 55.3, 53.8, 52.2, 33.1, 32.9, 25.1, 25.0. Decomposition temperature 214 °C.

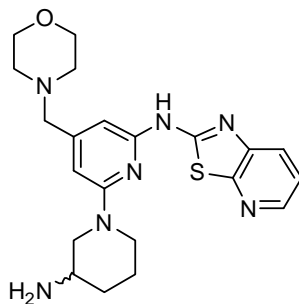
***N*-(2-{[4-(4-Morpholinylmethyl)-6-([1,3]thiazolo[5,4-*b*]pyridin-2-ylamino)-2-pyridinyl]amino}ethyl)-2-propenamamide (82)**



A microwave vial was charged with 1,1-dimethylethyl (2-aminoethyl)carbamate (443 mg, 2.76 mmol), *N*-[6-chloro-4-(4-morpholinylmethyl)-2-pyridinyl][1,3]thiazolo[5,4-*b*]pyridin-2-amine **72** (100 mg, 0.276 mmol) and ethylene glycol (1 ml). The vial was sealed and was heated in a Biotage Initiator microwave at 200 °C for 1 hour. The intermediate was purified by mass directed automated preparative HPLC. The intermediate (32 mg), 2-propenoyl chloride (8.09 μL , 0.100 mmol) and *N,N*-diisopropylethylamine (0.029 mL, 0.17 mmol) in *N*-methyl-2-pyrrolidone (1 mL) were stirred at room temperature for 10 minutes. The mixture was purified by mass directed automated preparative HPLC to afford the title compound (2.8 mg, 2 % yield) as a brown glass. **LCMS** (Method B) (ES +ve) m/z 440 ($\text{M} + \text{H}$)⁺ Rt 1.96 minutes. **¹H NMR** (400 MHz, DMSO-d_6) δ 8.26 (dd, $J = 1.5, 4.5$ Hz, 1H), 7.82 (dd, $J = 1.5, 8.1$ Hz, 1H), 7.80 - 7.72 (m, 1H), 7.32 (dd, $J = 4.5, 8.1$

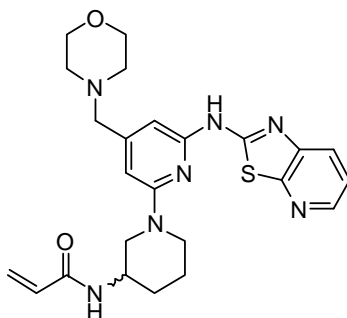
Hz, 1H), 6.38 (s, 1H), 6.27 - 6.25 (m, 1H), 6.25 (dd, $J = 10.2, 17.3$ Hz, 1H), 6.16 (s, 1H), 6.08 (dd, $J = 2.1, 17.3$ Hz, 1H), 5.55 (dd, $J = 2.1, 10.2$ Hz, 1H), 3.65 - 3.61 (m, 4H), 3.61 - 3.56 (m, 2H), 3.50 - 3.43 (m, 2H), 3.36 (s, 2H), 2.46 - 2.42 (m, 4H).

***N*-[6-(3-Amino-1-piperidiny)-4-(4-morpholinylmethyl)-2-pyridinyl][1,3]thiazolo[5,4-*b*]pyridin-2-amine (83)**



A microwave vial was charged with 1,1-dimethylethyl 3-amino-1-piperidinecarboxylate (221 mg, 1.11 mmol), *N*-[6-chloro-4-(4-morpholinylmethyl)-2-pyridinyl][1,3]thiazolo[5,4-*b*]pyridin-2-amine **72** (50 mg, 0.14 mmol) in ethylene glycol (1 ml). The vial was sealed and was heated in a Biotage Initiator microwave at 180 °C for 1 hour. A second portion of 1,1-dimethylethyl 3-amino-1-piperidinecarboxylate (221 mg, 1.11 mmol) was added and the vial was heated in the Biotage Initiator microwave at 220 °C for 1 hour. The product was purified by mass directed automated preparative HPLC to afford the title compound (33 mg, 56 % yield). **LCMS** (Method B) (ES +ve) m/z 426 ($M + H$)⁺ Rt 2.06 minutes. **¹H NMR** (400 MHz, DMSO- d_6) δ 8.28 (dd, $J = 1.1, 4.6$ Hz, 1H), 7.88 (dd, $J = 1.1, 8.2$ Hz, 1H), 7.37 (dd, $J = 4.6, 8.2$ Hz, 1H), 6.37 (s, 1H), 6.35 (s, 1H), 4.34 - 4.26 (m, 1H), 4.21 - 4.05 (m, 1H), 3.62 - 3.57 (m, 4H), 3.37 (s, 2H), 2.98 - 2.88 (m, 1H), 2.71 - 2.62 (m, 2H), 2.40 - 2.34 (m, 4H), 1.94 - 1.85 (m, 1H), 1.81 - 1.72 (m, 1H), 1.58 - 1.43 (m, 1H), 1.32 - 1.19 (m, 1H).

***N*-{1-[4-(4-Morpholinylmethyl)-6-([1,3]thiazolo[5,4-*b*]pyridin-2-ylamino)-2-pyridinyl]-3-piperidinyl}-2-propenamide (**84**)**



A mixture of *N*-[6-(3-amino-1-piperidinyl)-4-(4-morpholinylmethyl)-2-pyridinyl][1,3]thiazolo[5,4-*b*]pyridin-2-amine **83** (29 mg, 0.068 mmol), 2-propenoyl chloride (6.6 μ L, 0.082 mmol) and *N,N*-diisopropylethylamine (0.024 mL, 0.14 mmol) in *N*-methyl-2-pyrrolidone (1 mL) was stirred at room temperature for 10 minutes. The product was purified by mass directed automated preparative HPLC to afford the title compound (28 mg, 86 % yield) as an off-white solid. **LCMS** (Method B) (ES +ve) m/z 480 ($M + H$)⁺ Rt 2.20 minutes. **¹H NMR** (400 MHz, DMSO- d_6 , 120 $^{\circ}$ C) δ 8.26 (dd, $J = 1.2, 4.8$ Hz, 1H), 8.18 (d, $J = 7.5$ Hz, 1H), 7.85 (dd, $J = 1.2, 8.0$ Hz, 1H), 7.35 (dd, $J = 4.8, 8.0$ Hz, 1H), 6.41 (s, 1H), 6.36 (s, 1H), 6.27 (dd, $J = 10.0, 17.0$ Hz, 1H), 6.11 (dd, $J = 2.3, 17.0$ Hz, 1H), 5.59 (dd, $J = 2.3, 10.0$ Hz, 1H), 4.24 - 4.16 (m, 1H), 4.13 - 4.06 (m, 1H), 3.87 - 3.76 (m, 1H), 3.62 - 3.57 (m, 4H), 3.36 (s, 2H), 3.23 - 3.15 (m, 1H), 3.05 - 2.97 (m, 1H), 2.40 - 2.34 (m, 4H), 1.96 - 1.89 (m, 1H), 1.88 - 1.80 (m, 1H), 1.66 - 1.47 (m, 2H). **IR** (cm^{-1}) 1534, 1573, 1621, 1658. **HRMS** (ES) calcd for $\text{C}_{24}\text{H}_{30}\text{N}_7\text{O}_2\text{S}$, ($M + H$)⁺ 480.2176, found 480.2173. **¹³C NMR** (126 MHz, DMSO- d_6) δ 164.6, 159.1, 158.4, 155.8, 151.2, 150.6, 143.6, 143.4, 143.0, 132.6, 132.2, 129.7, 129.5, 128.4, 125.7, 125.4, 125.2, 121.7, 100.5, 99.9, 66.6, 62.3, 53.7, 50.9, 46.2, 46.2, 45.5, 30.6, 28.1, 23.5. Note: ¹³C NMR at room temperature displays the presence of rotamers for the compound. Decomposition temperature 134 $^{\circ}$ C.

General procedure H for the Buchwald-Hartwig amination trial reactions:

A microwave vial was charged with *N*-[6-chloro-4-(4-morpholinylmethyl)-2-pyridinyl][1,3]thiazolo[5,4-*b*]pyridin-2-amine **72**, 1,1-dimethylethyl 4-amino-1-piperidinecarboxylate, palladium catalyst, ligand, base and solvent. The vial was sealed and purged with nitrogen via vacuum. The vial was heated (thermal or microwave heating) at the stated temperature. The advancement of the reaction was monitored by LCMS analysis. The results were recorded in section VII.5. No products were isolated from these experiments.

Data from Table 13:

Entry	72	Amine	Pd	Ligand	Base	Solvent	T (°C)	
							a = microwave	b = thermal
1	100 mg	83 mg	Pd ₂ (dba) ₃ (25 mg)	DavePhos (22 mg)	NaOtBu (106 mg)	Toluene (2 mL)	150 (a)	1 h
2	100 mg	83 mg	Pd ₂ (dba) ₃ (25 mg)	DavePhos (22 mg)	NaOtBu (106 mg)	DMF (2 mL)	150 (a)	1 h
3	50 mg	41 mg	Pd ₂ (dba) ₃ (13 mg)	XPhos (13 mg)	Cs ₂ CO ₃ (90 mg)	Dioxane (3 mL)	150 (a)	30 mins
4	50 mg	41 mg	Pd ₂ (dba) ₃ (13 mg)	XPhos (13 mg)	Cs ₂ CO ₃ (90 mg)	Dioxane (3 mL)	180 (a)	30 mins
5	50 mg	28 mg	Pd(OAc) ₂ (3 mg)	XPhos (13 mg)	NaOtBu (27 mg)	Toluene (2 mL)	100 (b)	16 h
6*		28 mg	Pd(OAc) ₂ (3 mg)	XPhos (13 mg)	NaOtBu (27 mg)	Toluene (2 mL)	160 (a)	1 h
7	50 mg	56 mg	Pd(OAc) ₂ (6 mg)	XPhos (26 mg)	NaOtBu (40 mg)	Dioxane (2 mL)	160(a)	1 h
8	50 mg	56 mg	Pd(OAc) ₂ (6 mg)	XPhos (26 mg)	NaOtBu (40 mg)	DMF (2 mL)	160(a)	1 h
9	50 mg	56 mg	Pd(OAc) ₂ (6 mg)	XPhos (26 mg)	NaOtBu (40 mg)	DME (2 mL)	160(a)	1 h

*: As described in the Results and Discussion section, entry 6 was obtained by adding reagents to the reaction mixture from entry 5 and heating the vial in the

microwave system. The amount of reagents added to the reaction mixture of entry 5 (and to obtain entry 6) is recorded in this table.

Data from Table 14:

Entry	72	Amine	Pd	Ligand	Base	Solvent	T (°C) microwave	Heating time
1	50 mg	41 mg	Pd(OAc) ₂ (6 mg)	XPhos (13 mg)	NaOtBu (27 mg)	DME (2 mL)	160	1 h
2	50 mg	41 mg	Pd(OAc) ₂ (6 mg)	XPhos (13 mg)	NaOtBu (27 mg)	DME (2 mL)	170	1 h
3	50 mg	41 mg	Pd(OAc) ₂ (6 mg)	XPhos (13 mg)	NaOtBu (27 mg)	DME (2 mL)	180	1 h
4	50 mg	55 mg	Pd(OAc) ₂ (6 mg)	XPhos (26 mg)	NaOtBu (40 mg)	DME (2 mL)	170	1 h
5*	50 mg	55 mg	Pd(OAc) ₂ (6 mg)	XPhos (26 mg)	NaOtBu (40 mg)		170	1 h
6*							170	1 h
7*			Pd(OAc) ₂ (6 mg)	XPhos (26 mg)			170	1 h

*: As described in the Results and Discussion section, entries 5, 6 and 7 were obtained by successively adding reagents to the reaction mixture from entry 4. The amount of reagents added for each entry is recorded in this table.

General procedure I for the Buchwald-Hartwig amination trial reactions:

A microwave vial was charged with *N*-[6-chloro-4-(4-morpholinylmethyl)-2-pyridinyl][1,3]thiazolo[5,4-*b*]pyridin-2-amine **72**, 1,1-dimethylethyl 4-amino-1-piperidinecarboxylate, palladium catalyst, ligand (if stated) and THF (if stated). The vial was sealed and purged with nitrogen via vacuum. LHMDS in tetrahydrofuran (1 M) was added. The vial was stirred in a preheated oil bath at the stated temperature.

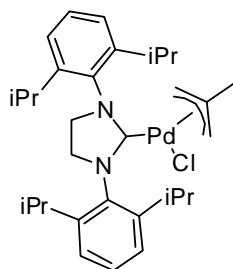
Data from Table 15:

Entry	72	Amine	Pd	Ligand	Base	Solvent	T (°C) thermal	Heating time
1*	50 mg	41 mg	86 (11 mg)	L ₁ (7.5 mg)	LHMDS (1 M, 415 µL)	THF (1 mL)	80	2 h
2	50 mg	41 mg	Pd(OAc) ₂ (3 mg)	L ₁ (15 mg)	LHMDS (1 M, 415 µL)	THF (1 mL)	80	2 h
3	50 mg	41 mg	Pd(OAc) ₂ (3 mg)	L ₁ (15 mg)	LHMDS (1 M, 415 µL)	THF (1 mL)	100	20 h
4**	50 mg	41 mg	87 (24 mg)		LHMDS (1 M, 500 µL)		80	1 h

*: After the 2 hours, the reaction was cooled to room temperature and partitioned between dichloromethane (10 mL) and saturated aqueous ammonium chloride (10 mL). The organic extract was dried using a hydrophobic frit and concentrated under reduced pressure. The product was purified by Flashmaster on silica using a gradient elution from 0 to 15 % methanol (+1 % triethylamine) in dichloromethane to afford compound **85** (40 mg, 55 % yield, 80 % pure) as a light brown solid. **LCMS** (Method D) (ES +ve) m/z 526 (M + H)⁺ Rt 1.13 minutes. **¹H NMR** (400 MHz, DMSO-d₆) δ 10.70 (br. s, 1H), 8.27 (dd, *J* = 1.5, 4.7 Hz, 1H), 7.81 (dd, *J* = 1.5, 8.1 Hz, 1H), 7.32 (dd, *J* = 4.7, 8.1 Hz, 1H), 6.35 (s, 1H), 6.18 (s, 1H), 6.14 (d, *J* = 7.3 Hz, 1H), 4.24 - 4.12 (m, 1H), 4.02 - 3.92 (m, 2H), 3.69 - 3.60 (m, 4H), 3.35 (s, 2H), 3.12 - 3.00 (m, 2H), 2.44 (m, 4H), 2.09 - 2.00 (m, 2H), 1.46 (s, 9H), 1.48 - 1.35 (m, 2H).

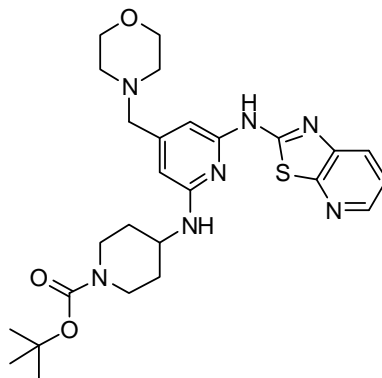
** : the full protocol for entry 4 is described below for the synthesis of compound **85**.

{1,3-Bis[2,6-bis(1-methylethyl)phenyl]-2-imidazolidinyl}(chloro)(2-methyl-2-propen-1-yl)palladium (87)¹⁴⁸



A 3-neck round bottom flask was charged with 1,3-bis[2,6-bis(1-methylethyl)phenyl]-4,5-dihydro-1H-imidazol-3-ium chloride (3.8 g, 8.9 mmol) and KO^tBu (0.887 g, 7.90 mmol). The flask was sealed and purged with nitrogen via vacuum. Under positive flow of nitrogen, isopropanol (70 ml) was added through the septum and the reaction was heated at 80 °C for 2 hours. After cooling to room temperature over 1 hour, palladium (methallyl)chloride dimer (1.24 g, 3.15 mmol) was added. The yellow mixture was stirred at room temp under nitrogen for 2 hours (over this time the reaction turned black). Water (200 mL) was added. The isopropanol was concentrated under reduced pressure. The product was extracted with ethyl acetate (200 mL). The organic extract was dried using a hydrophobic frit and concentrated under reduced pressure. The residue was triturated with diethyl ether (30 mL) and the grey solid was filtered under reduced pressure. The filtrate was concentrated under reduced pressure and the product was purified by Flashmaster on silica using a gradient elution from 0 to 100 % *tert*-butyl methyl ether in cyclohexane to afford the title compound (3.45 g, 66 % yield) as a yellow solid. ¹H NMR (400 MHz, CDCl₃) δ 7.35 (t, *J* = 7.7 Hz, 2H), 7.28 - 7.20 (m, 4H), 4.09 - 3.99 (m, 4H), 3.70 (d, *J* = 3.0 Hz, 1H), 3.53 - 3.40 (m, 4H), 2.70 (d, *J* = 3.3 Hz, 1H), 1.76 (s, 1H), 1.64 (br. s, 1H), 1.51 (d, *J* = 6.8 Hz, 6H), 1.36 (d, *J* = 6.8 Hz, 6H), 1.30 (d, *J* = 6.8 Hz, 6H), 1.23 (d, *J* = 6.8 Hz, 6H), 1.14 (s, 3H).

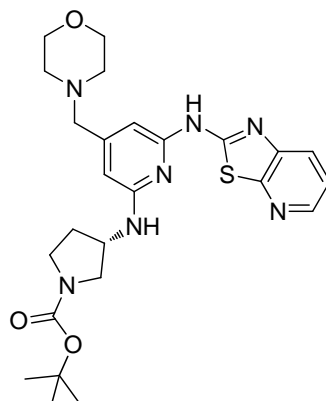
1,1-Dimethylethyl 4-{{[4-(4-morpholinylmethyl)-6-([1,3]thiazolo[5,4-*b*]pyridin-2-ylamino)-2-pyridinyl]amino}-1-piperidinecarboxylate (85)



A microwave vial was charged with *N*-[6-chloro-4-(4-morpholinylmethyl)-2-pyridinyl][1,3]thiazolo[5,4-*b*]pyridin-2-amine **72** (50 mg, 0.14 mmol), 1,1-dimethylethyl 4-amino-1-piperidinecarboxylate (41.5 mg, 0.207 mmol) and {1,3-bis[2,6-bis(1-methylethyl)phenyl]-2-imidazolidinyl}(chloro)(2-methyl-2-propen-1-yl)palladium **87** (24.4 mg, 0.0415 mmol). The vial was sealed and purged with nitrogen via vacuum. LHMDS in tetrahydrofuran (1 M, 0.5 mL, 0.5 mmol) was added. The vial was stirred in a preheated oil bath at 80 °C for 1 hour. The reaction was cooled to room temperature. The reaction mixture was partitioned between dichloromethane (10 mL) and saturated aqueous ammonium chloride (10 mL). After separation, the organic extract was dried using a hydrophobic frit and concentrated under reduced pressure. The product was purified by Flashmaster on silica using a gradient elution from 0 to 15 % methanol (+1 % triethylamine) in dichloromethane to afford the title compound (52 mg, 72 % yield) as a light brown solid. **LCMS** (Method D) (ES +ve) *m/z* 526 (M + H)⁺ Rt 1.11 minutes. **¹H NMR** (400 MHz, DMSO-*d*₆, 120 °C) δ 10.70 (br. s, 1H), 8.27 (dd, *J* = 1.4, 4.7 Hz, 1H), 7.81 (dd, *J* = 1.4, 8.1 Hz, 1H), 7.32 (dd, *J* = 4.7, 8.1 Hz, 1H), 6.35 (s, 1H), 6.18 (s, 1H), 6.15 (d, *J* = 7.3 Hz, 1H), 4.24 - 4.13 (m, 1H), 4.02 - 3.90 (m, 2H), 3.66 - 3.60 (m, 4H), 3.35 (s, 2H), 3.10 - 3.01 (m, 2H), 2.47 - 2.42 (m, 4H), 2.09 - 1.99 (m, 2H), 1.46 (s, 9H), 1.45 - 1.39 (m, 2H). **IR** (cm⁻¹) 1523, 1578, 1624, 1672. **HRMS** (ES) calcd for C₂₆H₃₆N₇O₃S, (M + H)⁺ 526.2600, found 526.2595. **¹³C NMR** (151 MHz, DMSO-*d*₆) δ 158.6, 157.0, 155.6, 153.9, 150.0, 149.7, 143.0, 142.9, 124.9, 121.1, 101.1, 97.2,

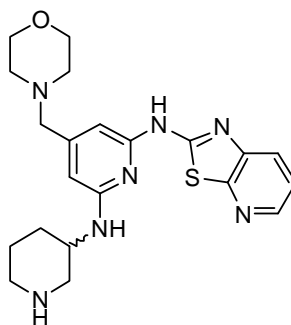
78.7, 66.2, 61.7, 53.3, 47.9, 43.1, 42.4, 31.9, 28.1. Decomposition temperature 246 °C.

1,1-Dimethylethyl (3S)-3-{{[4-(4-morpholinylmethyl)-6-([1,3]thiazolo[5,4-*b*]pyridin-2-ylamino)-2-pyridinyl]amino}-1-pyrrolidinecarboxylate (88)



A microwave vial was charged with *N*-[6-chloro-4-(4-morpholinylmethyl)-2-pyridinyl][1,3]thiazolo[5,4-*b*]pyridin-2-amine **72** (100 mg, 0.276 mmol), 1,1-dimethylethyl (3*S*)-3-amino-1-pyrrolidinecarboxylate (77 mg, 0.42 mmol) and {1,3-bis[2,6-bis(1-methylethyl)phenyl]-2-imidazolidinyl}(chloro)(2-methyl-2-propen-1-yl)palladium **87** (48.8 mg, 0.0829 mmol). The vial was sealed and purged with nitrogen via vacuum. LHMDS in tetrahydrofuran (1 M, 1 mL, 1 mmol) was added. The vial was stirred in a preheated oil bath at 80 °C for 1 hour. The reaction was cooled to room temperature. The reaction mixture was partitioned between dichloromethane (10 mL) and saturated aqueous ammonium chloride (10 mL). After separation, the organic extract was dried using a hydrophobic frit and concentrated under reduced pressure. The product was purified by Flashmaster on silica using a gradient elution from 0 to 15 % methanol (+1 % triethylamine) in dichloromethane to afford the crude title compound (133 mg, 80 % pure by NMR, 75 % yield) as a light brown solid. **LCMS** (Method D) (ES +ve) *m/z* 512 (M + H)⁺ Rt 1.06 minutes. **¹H NMR** (400 MHz, DMSO-*d*₆, 120 °C) δ 10.76 (br. s, 1H), 8.26 (dd, *J* = 1.4, 4.7 Hz, 1H), 7.82 (dd, *J* = 1.4, 8.1 Hz, 1H), 7.32 (dd, *J* = 4.7, 8.1 Hz, 1H), 6.47 (d, *J* = 7.0 Hz, 1H), 6.39 (s, 1H), 6.21 (s, 1H), 4.69 - 4.59 (m, 1H), 3.77 - 3.69 (m, 1H), 3.66 - 3.60 (m, 4H), 3.54 - 3.46 (m, 1H), 3.44 - 3.38 (m, 1H), 3.36 (s, 2H), 3.28 - 3.23 (m, 1H), 2.47 - 2.41 (m, 4H), 2.34 - 2.23 (m, 1H), 1.97 - 1.87 (m, 1H), 1.43 (s, 9H).

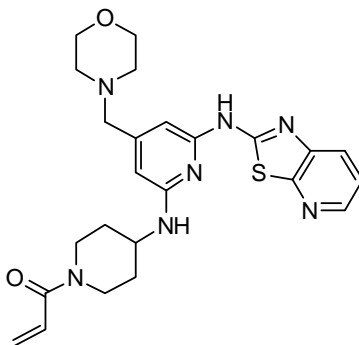
4-(4-Morpholinylmethyl)-*N*-3-piperidinyl-*N'*-[1,3]thiazolo[5,4-*b*]pyridin-2-yl-2,6-pyridinediamine (89**)**



A microwave vial was charged with *N*-[6-chloro-4-(4-morpholinylmethyl)-2-pyridinyl][1,3]thiazolo[5,4-*b*]pyridin-2-amine **72** (100 mg, 0.276 mmol), 1,1-dimethylethyl 3-amino-1-piperidinecarboxylate (83 mg, 0.42 mmol) and {1,3-bis[2,6-bis(1-methylethyl)phenyl]-2-imidazolidinyl}(chloro)(2-methyl-2-propen-1-yl)palladium **87** (48.8 mg, 0.0829 mmol). The vial was sealed and purged with nitrogen via vacuum. LHMDS in tetrahydrofuran (1 M, 1 mL, 1 mmol) was added. The vial was stirred in a preheated oil bath at 80 °C for 4 hours. The reaction was cooled to room temperature. The reaction mixture was partitioned between dichloromethane (10 mL) and saturated aqueous ammonium chloride (10 mL). The aqueous phase was basified to pH 13 with saturated sodium bicarbonate and was extracted with dichloromethane:methanol (9:1, 3 x 20 mL). The organic extracts were combined, dried using a hydrophobic frit and concentrated under reduced pressure to afford the title compound (58 mg, 50 % yield) as a yellow solid. LCMS (Method D) (ES +ve) m/z 426 ($M + H$)⁺ Rt 0.77 minutes. ¹H NMR (400 MHz, DMSO-*d*₆, 120 °C) δ 8.27 (dd, $J = 1.5, 4.8$ Hz, 1H), 7.82 (dd, $J = 1.5, 8.1$ Hz, 1H), 7.32 (dd, $J = 4.8, 8.1$ Hz, 1H), 6.33 (s, 1H), 6.18 (s, 1H), 6.10 (d, $J = 7.6$ Hz, 1H), 4.13 - 4.00 (m, 1H), 3.68 - 3.58 (m, 4H), 3.34 (s, 2H), 3.25 - 3.16 (m, 1H), 2.95 - 2.88 (m, 1H), 2.69 - 2.61 (m, 2H), 2.46 - 2.41 (m, 4H), 2.10 - 2.04 (m, 1H), 1.80 - 1.72 (m, 1H), 1.66 - 1.47 (m, 2H). Note that the LCMS monitoring of this reaction revealed a 1:1 ratio of compounds **89** and **90** with still 13 % of intermediate **72** remaining after 4 hours. Column chromatography separation difficulties only allowed the obtention of compound **90** with a 60 % purity assessed by LCMS and

NMR. As sufficient quantities of compound **89** were obtained for further reactions, the impure compound **90** was discarded.

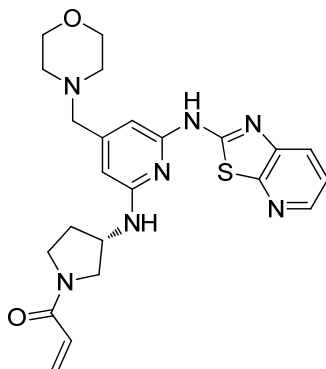
***N*-(1-Acryloyl-4-piperidiny)-4-(4-morpholinylmethyl)-*N'*-[1,3]thiazolo[5,4-*b*]pyridin-2-yl-2,6-pyridinediamine (**91**)**



A round bottom flask was charged with 1,1-dimethylethyl 4-{[4-(4-morpholinylmethyl)-6-([1,3]thiazolo[5,4-*b*]pyridin-2-ylamino)-2-pyridinyl]amino}-1-piperidinecarboxylate **85** (30 mg, 0.057 mmol) and HCl in dioxane (4 M, 0.30 mL, 1.2 mmol) in dichloromethane (3 mL) and methanol (1 mL). The reaction was stirred at room temperature for 2 hours. The solvent was evaporated under reduced pressure. The solid residue was dissolved in *N*-methyl-2-pyrrolidone (1 mL). *N,N*-Diisopropylethylamine (0.050 mL, 0.29 mmol) was added followed by 2-propenoyl chloride (0.014 mL, 0.17 mmol). The reaction was stirred at room temperature for 1 hour. The product was purified by mass directed automated preparative HPLC to afford the title compound (14 mg, 51 % yield) as a light brown solid. **LCMS** (Method D) (ES +ve) *m/z* 480 (M + H)⁺ Rt 0.83 minutes. **¹H NMR** (400 MHz, DMSO-*d*₆, 120 °C) δ 8.26 (dd, *J* = 1.5, 4.8 Hz, 1H), 7.81 (dd, *J* = 1.5, 8.1 Hz, 1H), 7.32 (dd, *J* = 4.8, 8.1 Hz, 1H), 6.75 (dd, *J* = 10.6, 16.8 Hz, 1H), 6.34 (s, 1H), 6.25 (d, *J* = 7.8 Hz, 1H), 6.18 (s, 1H), 6.07 (dd, *J* = 2.3, 16.8 Hz, 1H), 5.63 (dd, *J* = 2.3, 10.6 Hz, 1H), 4.32 - 4.24 (m, 1H), 4.23 - 4.15 (m, 2H), 3.65 - 3.61 (m, 4H), 3.35 (s, 2H), 3.24 - 3.15 (m, 2H), 2.46 - 2.41 (m, 4H), 2.15 - 2.07 (m, 2H), 1.54 - 1.41 (m, 2H). **IR** (cm⁻¹) 1519, 1573, 1607, 1632. **HRMS** (ES) calcd for C₂₄H₃₀N₇O₂S, (M + H)⁺ 480.2182, found 480.2180. **¹³C NMR** (151 MHz, DMSO-*d*₆) δ 164.3, 158.6, 157.0,

155.6, 150.1, 149.8, 143.0, 142.9, 128.5, 127.1, 124.8, 121.1, 101.1, 97.4, 66.2, 61.8, 53.3, 47.9, 44.3, 40.8, 32.8, 31.7. Decomposition temperature 178 °C.

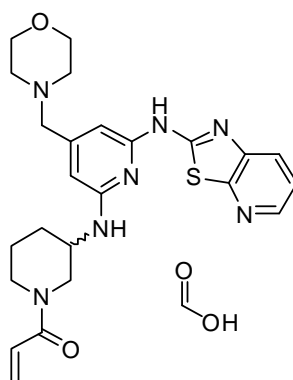
***N*-[(3*S*)-1-Acryloyl-3-pyrrolidinyl]-4-(4-morpholinylmethyl)-*N'*-[1,3]thiazolo[5,4-*b*]pyridin-2-yl-2,6-pyridinediamine (92)**



A round bottom flask was charged with 1,1-dimethylethyl (3*S*)-3-{[4-(4-morpholinylmethyl)-6-([1,3]thiazolo[5,4-*b*]pyridin-2-ylamino)-2-pyridinyl]amino}-1-pyrrolidinecarboxylate **88** (35 mg, 0.068 mmol), HCl in dioxane (4 M, 0.30 ml, 1.2 mmol) and dichloromethane (3 mL) and methanol (1 mL). The reaction was stirred at room temperature for 1 hour. The reaction mixture was concentrated under reduced pressure. The residue was dissolved in *N*-methyl-2-pyrrolidone (1 ml). *N,N*-Diisopropylethylamine (0.036 ml, 0.21 mmol) and 2-propenoyl chloride (0.011 ml, 0.14 mmol) were added and the reaction was stirred at room temperature for 1 hour. The product was purified by mass directed automated preparative HPLC to afford the title compound (18 mg, 57 % yield) as a light brown solid. **LCMS** (Method D) (ES +ve) *m/z* 466 (*M* + *H*)⁺ *Rt* 0.80 minutes. **¹H NMR** (400 MHz, DMSO-*d*₆, 120 °C) δ 8.26 (dd, *J* = 1.5, 4.7 Hz, 1H), 7.82 (dd, *J* = 1.5, 8.0 Hz, 1H), 7.32 (dd, *J* = 4.5, 8.0 Hz, 1H), 6.61 - 6.50 (m, 2H), 6.40 (s, 1H), 6.21 (s, 1H), 6.12 (dd, *J* = 2.3, 16.8 Hz, 1H), 5.61 (dd, *J* = 2.3, 10.4 Hz, 1H), 4.77 - 4.67 (m, 1H), 3.96 - 3.92 (m, 1H), 3.78 - 3.67 (m, 1H), 3.66 - 3.61 (m, 5H), 3.55 - 3.47 (m, 1H), 3.36 (s, 2H), 2.47 - 2.41 (m, 4H), 2.40 - 2.28 (m, 1H), 2.07 - 1.95 (m, 1H). **IR** (cm⁻¹) 1521, 1575, 1627, 1652. **HRMS** (ES) calcd for C₂₃H₂₈N₇O₂S, (*M* + *H*)⁺ 466.2025, found 466.2029. **¹³C NMR** (151 MHz, DMSO-*d*₆) δ 163.51, 163.46, 158.73, 158.72, 157.19, 157.14, 155.53, 155.51, 150.08, 150.06, 149.91, 149.84, 143.04, 143.02, 142.91, 142.89,

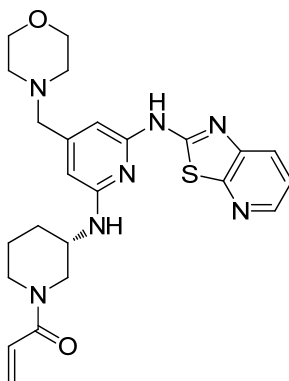
129.70, 129.44, 126.67, 126.56, 124.92, 121.16, 101.25, 101.15, 97.79, 97.73, 66.20, 61.69, 61.67, 53.29, 52.14, 51.73, 51.54, 49.84, 44.51, 43.96, 31.73, 29.97. Note: ^{13}C NMR at room temperature displays the presence of rotamers for the compound. The data is reported with two decimal points to differentiate the signals. Decomposition temperature 167 °C. $[\alpha]_{\text{D}}^{20} = -146$ ($c = 0.992$ in DMSO).

***N*-(1-Acryloyl-3-piperidiny)-4-(4-morpholinylmethyl)-*N'*-[1,3]thiazolo[5,4-*b*]pyridin-2-yl-2,6-pyridinediamine (formic acid salt) (93)**



A round bottom flask was charged with 4-(4-morpholinylmethyl)-*N*-3-piperidiny-*N'*-[1,3]thiazolo[5,4-*b*]pyridin-2-yl-2,6-pyridinediamine **89** (55 mg, 0.13 mmol), *N,N*-diisopropylethylamine (0.068 mL, 0.39 mmol) and *N*-methyl-2-pyrrolidone (1 mL). 2-Propenoyl chloride (0.021 mL, 0.26 mmol) was added. The reaction was stirred at room temperature for 1 hour. The product was purified by mass directed automated preparative HPLC to afford the title compound (20 mg, 29 % yield) as a light brown solid. LCMS (Method D) (ES +ve) m/z 480 ($\text{M} + \text{H}^+$) Rt 0.84 minutes. ^1H NMR (400 MHz, DMSO- d_6 , 120 °C) δ 8.25 (dd, $J = 1.5, 4.7$ Hz, 1H), 8.18 (br. s, 1H), 7.81 (dd, $J = 1.5, 8.1$ Hz, 1H), 7.31 (dd, $J = 4.7, 8.1$ Hz, 1H), 6.61 (dd, $J = 10.8, 16.8$ Hz, 1H), 6.37 (s, 1H), 6.21 (s, 1H), 6.19 (br. s, 1H), 5.97 (dd, $J = 2.3, 16.8$ Hz, 1H), 5.48 (dd, $J = 2.3, 10.8$ Hz, 1H), 4.20 - 4.10 (m, 1H), 4.10 - 4.02 (m, 1H), 3.88 - 3.80 (m, 1H), 3.66 - 3.61 (m, 4H), 3.35 (s, 2H), 3.32 - 3.24 (m, 2H), 2.46 - 2.41 (m, 4H), 2.20 - 2.12 (m, 1H), 1.91 - 1.82 (m, 1H), 1.69 - 1.53 (m, 2H).

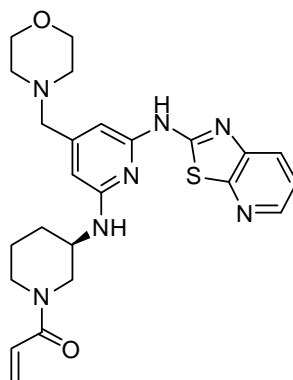
(S)-1-(3-((4-(Morpholinomethyl)-6-(thiazolo[5,4-*b*]pyridin-2-ylamino)pyridin-2-yl)amino)piperidin-1-yl)prop-2-en-1-one (94)



A microwave vial was charged with *N*-(6-chloro-4-(morpholinomethyl)pyridin-2-yl)thiazolo[5,4-*b*]pyridin-2-amine **72** (75 mg, 0.21 mmol), (*S*)-*tert*-butyl 3-aminopiperidine-1-carboxylate (62 mg, 0.31 mmol), 2-(dicyclohexylphosphino)-3,6-dimethoxy-2'-4'-6'-tri-*i*-propyl-1,1'-biphenyl **L**¹ (11 mg, 0.021 mmol), chloro[2-(dicyclohexylphosphino)-3,6-dimethoxy-2',4',6'-tri-*iso*-propyl-1,1'-biphenyl][2-(2-aminoethyl)phenyl]palladium(II) **86** (17 mg, 0.021 mmol) and tetrahydrofuran (1 mL). The vial was sealed and purged with nitrogen via vacuum. LHMDS in tetrahydrofuran (1 M, 0.622 mL, 0.622 mmol) was added and the vial was stirred at 80 °C in the preheated oil bath for 14 hours. The vial was cooled to room temperature and the reaction mixture was partitioned between dichloromethane (10 mL) and saturated ammonium chloride (10 mL). After separation, the organic extract was dried using a hydrophobic frit and evaporated under reduced pressure. The yellow residue was dissolved in dichloromethane (3 mL) and methanol (1 mL). The solution was treated with HCl in dioxane (4 M, 0.5 mL, 2 mmol) and stirred at room temperature overnight. The solvent was evaporated under reduced pressure. The yellow residue was dissolved in *N*-methyl-2-pyrrolidone (1 mL) and *N,N*-diisopropylethylamine (0.181 mL, 1.04 mmol). 2-Propenoyl chloride (0.034 mL, 0.42 mmol) was added and the reaction was stirred at room temperature for 1 hour. The mixture was purified by mass directed automated preparative HPLC to afford the title compound (40 mg, 40 % yield) as a brown solid. **LCMS** (Method D) (ES +ve) *m/z* 480 (*M* + *H*)⁺ *Rt* 0.85 minutes. **¹H NMR** (400 MHz, DMSO-*d*₆, 120 °C) δ 10.76 (br. s, 1H), 8.25 (dd, *J* = 1.5, 4.8 Hz, 1H), 7.81 (dd, *J* = 1.5, 8.1 Hz, 1H), 7.31

(dd, $J = 4.8, 8.1$ Hz, 1H), 6.61 (dd, $J = 10.6, 16.9$ Hz, 1H), 6.37 (s, 1H), 6.21 (s, 1H), 6.19 (d, $J = 7.8$ Hz, 1H), 5.97 (dd, $J = 2.3, 16.9$ Hz, 1H), 5.48 (dd, $J = 2.3, 10.6$ Hz, 1H), 4.20 - 4.10 (m, 1H), 4.10 - 4.02 (m, 1H), 3.88 - 3.80 (m, 1H), 3.65 - 3.61 (m, 4H), 3.35 (s, 2H), 3.33 - 3.23 (m, 2H), 2.46 - 2.42 (m, 4H), 2.20 - 2.11 (m, 1H), 1.90 - 1.82 (m, 1H), 1.68 - 1.54 (m, 2H). **IR** (cm^{-1}) 1517, 1574, 1626. **HRMS** (ES) calcd for $\text{C}_{24}\text{H}_{30}\text{N}_7\text{O}_2\text{S}$, ($\text{M} + \text{H}$)⁺ 480.2176, found 480.2159. **^{13}C NMR** (126 MHz, DMSO-d_6) δ 165.1, 159.3, 159.2, 157.5, 156.1, 155.9, 150.5, 150.3, 143.5, 143.4, 129.2, 128.8, 127.5, 126.9, 125.3, 121.6, 101.8, 101.5, 98.2, 98.1, 66.7, 62.2, 53.8, 50.3, 47.8, 47.7, 46.9, 45.8, 42.3, 31.4, 30.7, 24.8, 23.1. Note: ^{13}C NMR at room temperature displays the presence of rotamers for the compound. Decomposition temperature 149 °C.

(*R*)-1-(3-((4-(Morpholinomethyl)-6-(thiazolo[5,4-*b*]pyridin-2-ylamino)pyridin-2-yl)amino)piperidin-1-yl)prop-2-en-1-one (95)



A microwave vial was charged with *N*-[6-chloro-4-(4-morpholinylmethyl)-2-pyridinyl][1,3]thiazolo[5,4-*b*]pyridin-2-amine **72** (75 mg, 0.21 mmol), (*R*)-*tert*-butyl 3-aminopiperidine-1-carboxylate (62.3 mg, 0.311 mmol), {1,3-bis[2,6-bis(1-methylethyl)phenyl]-2-imidazolidinyl}(chloro)(2-methyl-2-propen-1-yl)palladium **87** (36.6 mg, 0.0622 mmol). The vial was sealed and purged with nitrogen via vacuum. LHMDS in tetrahydrofuran (1 M, 0.75 mL, 0.75 mmol) was added. The vial was stirred in the preheated oil bath at 70 °C for 2 hours. The vial was cooled to room temperature and the reaction mixture was partitioned between dichloromethane (10 mL) and saturated ammonium chloride (10 mL). After separation, the organic extract was dried using a hydrophobic frit and evaporated under reduced pressure.

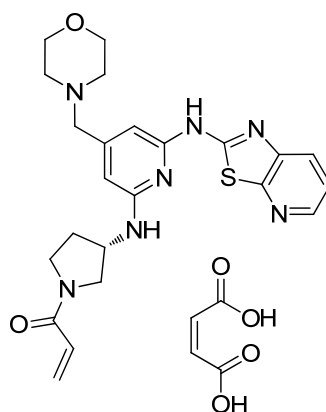
The residue was dissolved in dichloromethane (3 mL) and methanol (1 mL). The solution was treated with HCl in dioxane (4 M, 0.5 mL, 2 mmol) and stirred at room temperature overnight. The solvent was evaporated under reduced pressure. The yellow residue was dissolved in *N*-methyl-2-pyrrolidone (1 mL) and *N,N*-diisopropylethylamine (0.181 mL, 1.04 mmol). 2-Propenoyl chloride (0.034 mL, 0.42 mmol) was added and the reaction was stirred at room temperature for 1 hour. The mixture was purified by mass directed automated preparative HPLC to afford the title compound (35 mg, 35 % yield) as a brown solid. **LCMS** (Method D) (ES +ve) m/z 480 ($M + H$)⁺ Rt 0.85 minutes. **¹H NMR** (400 MHz, DMSO-*d*₆, 120 °C) δ 10.68 (br. s, 1H), 8.25 (dd, $J = 1.5, 4.8$ Hz, 1H), 7.81 (dd, $J = 1.5, 8.1$ Hz, 1H), 7.31 (dd, $J = 4.8, 8.1$ Hz, 1H), 6.61 (dd, $J = 10.7, 16.9$ Hz, 1H), 6.37 (s, 1H), 6.21 (s, 1H), 6.19 (d, $J = 8.1$ Hz, 1H), 5.97 (dd, $J = 2.5, 16.9$ Hz, 1H), 5.48 (dd, $J = 2.5, 10.7$ Hz, 1H), 4.20 - 4.10 (m, 1H), 4.09 - 4.02 (m, 1H), 3.88 - 3.80 (m, 1H), 3.65 - 3.61 (m, 4H), 3.35 (s, 2H), 3.32 - 3.21 (m, 2H), 2.46 - 2.42 (m, 4H), 2.20 - 2.12 (m, 1H), 1.90 - 1.82 (m, 1H), 1.68 - 1.54 (m, 2H). **IR** (cm⁻¹) 1517, 1574, 1627. **HRMS** (ES) calcd for C₂₄H₃₀N₇O₂S, ($M + H$)⁺ 480.2176, found 480.2159. **¹³C NMR** (126 MHz, DMSO-*d*₆) δ 165.1, 159.3, 159.1, 157.5, 156.1, 155.9, 150.5, 150.3, 143.5, 143.4, 129.2, 128.8, 127.5, 126.9, 125.3, 121.6, 101.8, 101.5, 98.2, 98.0, 66.7, 62.2, 53.8, 50.3, 47.8, 47.7, 46.9, 45.8, 42.3, 31.4, 30.7, 24.8, 23.1. Note: ¹³C NMR at room temperature displays the presence of rotamers for the compound. Decomposition temperature 155 °C.

Salt screening for compound 92

N-[(3*S*)-1-Acryloyl-3-pyrrolidinyl]-4-(4-morpholinylmethyl)-*N'*-[1,3]thiazolo[5,4-*b*]pyridin-2-yl-2,6-pyridinediamine **92** (1 mg, 0.002 mmol) was suspended and stirred in water (1 mL). The acidic solution (see table below, 0.1 M in water, 25 μ L) was added and the suspension was gently shaken at room temperature. The improvement in solubility of the suspension was monitored visually over time.

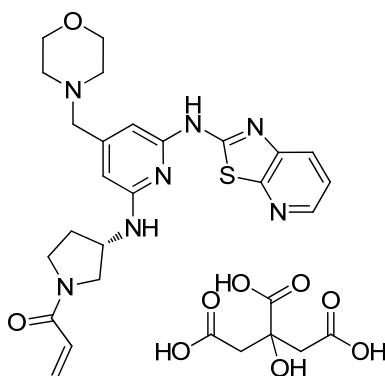
Salts	HCl	Citric acid	Maleic acid	Fumaric acid	Mandelic acid	Acetic acid
Solubility results	Suspension after 16 h	Clear solution after 15 min	Clear solution after 30 min	Mainly in solution after 3 h	Mainly in solution after 3 h	Suspension after 16 h

***N*-[(3*S*)-1-Acryloyl-3-pyrrolidinyl]-4-(4-morpholinylmethyl)-*N'*-[1,3]thiazolo[5,4-*b*]pyridin-2-yl-2,6-pyridinediamine, maleic acid salt (**92a**)**



A maleic acid solution in water (0.1 M, 0.451 mL, 0.0451 mmol) was added to a suspension of *N*-[(3*S*)-1-Acryloyl-3-pyrrolidinyl]-4-(4-morpholinylmethyl)-*N'*-[1,3]thiazolo[5,4-*b*]pyridin-2-yl-2,6-pyridinediamine **92** (20 mg, 0.043 mmol) in acetonitrile (2.5 mL) and water (2.5 mL). The reaction was stirred at room temperature for 16 hours. The solvent was concentrated under reduced pressure to give the title compound (27 mg, 96 % yield) as a yellow solid. **LCMS** (Method D) (ES +ve) *m/z* 466 (*M* + *H*)⁺ *Rt* 0.80 minutes. **¹H NMR** (400 MHz, DMSO-*d*₆, 120 °C) δ 8.27 (dd, *J* = 1.5, 4.8 Hz, 1H), 7.83 (dd, *J* = 1.5, 8.1 Hz, 1H), 7.34 (dd, *J* = 4.8, 8.1 Hz, 1H), 6.55 (dd, *J* = 10.6, 17.1 Hz, 1H), 6.48 (br. s, 1H), 6.43 (s, 1H), 6.23 (s, 1H), 6.17 (s, 2H), 6.11 (dd, *J* = 2.4, 17.1 Hz, 1H), 5.61 (dd, *J* = 2.4, 10.6 Hz, 1H), 4.76 - 4.67 (m, 1H), 3.98 - 3.88 (m, 1H), 3.78 - 3.71 (m, 1H), 3.70 - 3.66 (m, 4H), 3.66 - 3.59 (m, 1H), 3.52 (s, 2H), 3.50 (dd, *J* = 4.5, 11.3 Hz, 1H), 2.63 - 2.58 (m, 4H), 2.40 - 2.30 (m, 1H), 2.06 - 1.97 (m, 1H).

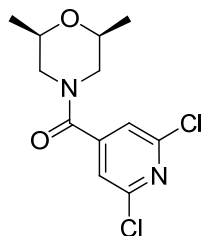
***N*-[(3*S*)-1-Acryloyl-3-pyrrolidinyl]-4-(4-morpholinylmethyl)-*N'*-[1,3]thiazolo[5,4-*b*]pyridin-2-yl-2,6-pyridinediamine, citric acid salt (**92b**)**



A citric acid solution in water (0.1 M, 0.451 mL, 0.0451 mmol) was added to a suspension of *N*-[(3*S*)-1-Acryloyl-3-pyrrolidinyl]-4-(4-morpholinylmethyl)-*N'*-[1,3]thiazolo[5,4-*b*]pyridin-2-yl-2,6-pyridinediamine **92** (20 mg, 0.043 mmol) in acetonitrile (2.5 mL) and water (2.5 mL). The reaction was stirred at room temperature for 16 hours. The solvent was concentrated under reduced pressure to give the title compound (25 mg, 100 % yield) as a yellow solid. **LCMS** (Method D) (ES +ve) m/z 466 ($M + H$)⁺ Rt 0.80 minutes. **¹H NMR** (400 MHz, DMSO-*d*₆, 120 °C) δ 8.26 (dd, $J = 1.5, 4.8$ Hz, 1H), 7.82 (dd, $J = 1.5, 8.1$ Hz, 1H), 7.32 (dd, $J = 4.8, 8.1$ Hz, 1H), 6.55 (dd, $J = 10.6, 16.9$ Hz, 1H), 6.47 (br. s, 1H), 6.42 (s, 1H), 6.22 (s, 1H), 6.11 (dd, $J = 2.5, 16.9$ Hz, 1H), 5.61 (dd, $J = 2.5, 10.6$ Hz, 1H), 4.76 - 4.67 (m, 1H), 3.98 - 3.88 (m, 1H), 3.77 - 3.67 (m, 1H), 3.67 - 3.57 (m, 5H), 3.49 (dd, $J = 4.8, 11.6$ Hz, 1H), 3.40 (s, 2H), 2.80 (d, $J = 15.4$ Hz, 2H), 2.72 (d, $J = 15.4$ Hz, 2H), 2.49 - 2.47 (m, 4H), 2.40 - 2.29 (m, 1H), 2.06 - 1.95 (m, 1H).

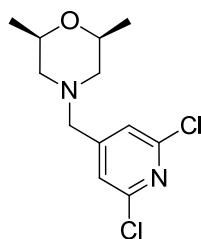
6. Synthetic procedures for the replacement of the morpholine motif to improve solubility and activity

4-[(2,6-Dichloro-4-pyridinyl)carbonyl]-(*cis*)-2,6-dimethylmorpholine (96)



Cis-2,6-dimethylmorpholine (7.06 mL, 57.0 mmol) was added dropwise to a stirred, cooled (0 °C) mixture of 2,6-dichloro-4-pyridinecarbonyl chloride **68** (10 g, 48 mmol) and *N,N*-diisopropylethylamine (24.9 mL, 143 mmol) in dichloromethane (30 mL). The reaction was stirred at 0 °C for 2 hours and then at room temperature for 16 hours. Aqueous saturated ammonium chloride (70 mL) was added and the product was extracted with dichloromethane (100 mL). The organic extract was washed with aqueous saturated ammonium chloride (70 mL), was dried using a hydrophobic frit and concentrated under reduced pressure to give the title compound (14.4 g, 90 % pure by NMR, 94 % yield) as a yellow solid. LCMS (Method D) (ES +ve) *m/z* 289 (M + H)⁺ Rt 0.97 minutes. ¹H NMR (400MHz, DMSO-d₆) δ 7.64 (s, 2H), 4.31 (d, *J* = 13.1 Hz, 1H), 3.62 - 3.48 (m, 2H), 3.35 (d, *J* = 13.3 Hz, 1H), 2.79 (dd, *J* = 10.9, 13.2 Hz, 1H), 2.46 (dd, *J* = 10.9, 13.2 Hz, 1H), 1.15 (d, *J* = 6.3 Hz, 3H), 1.00 (d, *J* = 6.3 Hz, 3H).

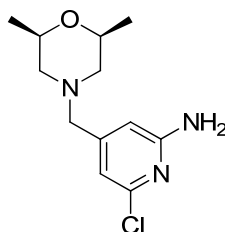
4-[(2,6-Dichloro-4-pyridinyl)methyl]-(*cis*)-2,6-dimethylmorpholine (97)



Borane in tetrahydrofuran (1 M, 149 mL, 149 mmol) was added dropwise to a cooled solution (0 °C) of 4-[(2,6-dichloro-4-pyridinyl)carbonyl]-(*cis*)-2,6-dimethylmorpholine (14.4 g, 49.8 mmol) in dichloromethane (50 mL). After the

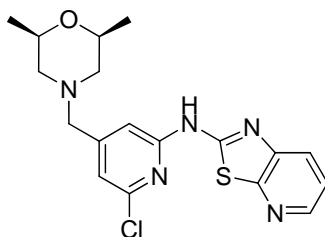
addition, the reaction was stirred at 0 °C for 1 hour under a nitrogen atmosphere. Aqueous HCl (5 M, 100 mL) was carefully added to the reaction while still stirring at 0 °C. After stirring for 2 hour, the solution was left standing at room temperature overnight. The mixture was basified with aqueous NaOH (10 M) to reach pH 14. The product was extracted with dichloromethane (50 mL). The organic extract was dried using a hydrophobic frit and concentrated under reduced pressure. The product was purified by Flashmaster on silica using a gradient elution from 0 to 100 % ethyl acetate in dichloromethane to afford the title compound (9.9 g, 72 %) as an off-white solid. **LCMS** (Method D) (ES +ve) m/z 275 (M + H)⁺ Rt 1.19 minutes. **¹H NMR** (400 MHz, DMSO-d₆) δ 7.49 (s, 2H), 3.63 - 3.54 (m, 2H), 3.52 (s, 2H), 2.66 (d, *J* = 10.5 Hz, 2H), 1.69 (t, *J* = 10.5 Hz, 2H), 1.03 (d, *J* = 6.3 Hz, 6H).

6-Chloro-4-((*cis*-2,6-dimethyl-4-morpholinyl)methyl)-2-pyridinamine (98)



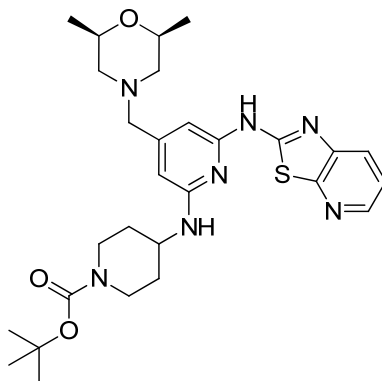
A microwave vessel was charged with (*cis*)-4-((2,6-dichloropyridin-4-yl)methyl)-2,6-dimethylmorpholine **97** (3.50 g, 12.7 mmol), isopropanol (3 mL) and concentrated ammonia (35 % in water, 7 mL, 323 mol). The vessel was sealed and was heated at 160 °C for 30 hours (18 bar pressure build up). The reaction was cooled to room temperature. The solvent was evaporated under reduced pressure. The product was purified by Flashmaster on silica using gradient elutions from 0 to 100 % ethyl acetate in cyclohexane and 0 to 20 % methanol in ethyl acetate to afford the title compound (960 mg, 30 % yield) as a white solid. **LCMS** (Method D) (ES +ve) m/z 256 (M + H)⁺ Rt 0.85 minutes. **¹H NMR** (400 MHz, DMSO-d₆) δ 6.43 (s, 1H), 6.35 - 6.32 (m, 3H), 3.60 - 3.52 (m, 2H), 3.28 (s, 2H), 2.64 (d, *J* = 10.0 Hz, 2H), 1.63 (t, *J* = 10.8 Hz, 2H), 1.03 (d, *J* = 6.3 Hz, 6H).

***N*-(6-Chloro-4-((*cis*-2,6-dimethyl-4-morpholino)methyl)pyridin-2-yl)thiazolo[5,4-*b*]pyridin-2-amine (99)**



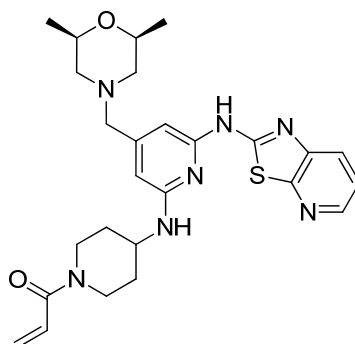
To an ice cooled solution of 6-chloro-4-((*cis*-2,6-dimethyl-4-morpholino)methyl)pyridin-2-amine **98** (960 mg, 3.75 mmol) and 2-bromo[1,3]thiazolo[5,4-*b*]pyridine **31** (888 mg, 4.13 mmol) in *N,N*-dimethylformamide (10 mL) was added sodium hydride (60 % w/w in mineral oil, 300 mg, 7.51 mmol) portionwise. The reaction was stirred at 0 °C under a nitrogen atmosphere for 1 hour and at room temperature for another 1 hour. Saturated aqueous ammonium chloride was added and the product was extracted with ethyl acetate. After separation, the organic extract was dried using a hydrophobic frit and evaporated under reduced pressure. The residue was purified by chromatography on silica using a gradient elution from 0 to 25 % methanol in dichloromethane to afford the title compound (1.38 g, 94 % yield) as a brown solid. **LCMS** (Method D) (ES +ve) *m/z* 390 (*M* + *H*)⁺ *Rt* 1.17 minutes. **¹H NMR** (400 MHz, DMSO-*d*₆) δ 11.92 (s, 1H), 8.37 (dd, *J* = 1.5, 4.7 Hz, 1H), 7.98 (dd, *J* = 1.5, 8.0 Hz, 1H), 7.43 (dd, *J* = 4.7, 8.0 Hz, 1H), 7.18 (s, 1H), 7.07 (s, 1H), 3.66 - 3.55 (m, 2H), 3.49 (s, 2H), 2.70 (d, *J* = 10.6 Hz, 2H), 1.71 (t, *J* = 10.6 Hz, 2H), 1.04 (d, *J* = 6.3 Hz, 6H).

tert-Butyl 4-((4-((*cis*-2,6-dimethyl-4-morpholino)methyl)-6-(thiazolo[5,4-*b*]pyridin-2-ylamino)pyridin-2-yl)amino)piperidine-1-carboxylate (100i)



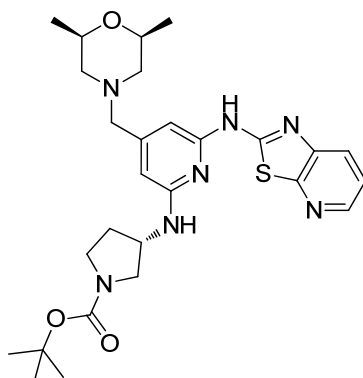
A microwave vial was charged with *N*-(6-chloro-4-((*cis*-2,6-dimethyl-4-morpholino)methyl)pyridin-2-yl)thiazolo[5,4-*b*]pyridin-2-amine **99** (150 mg, 0.385 mmol), *tert*-butyl 4-amino-1-piperidinecarboxylate (116 mg, 0.577 mmol) and {1,3-bis[2,6-bis(1-methylethyl)phenyl]-2-imidazolidinyl}(chloro)(2-methyl-2-propen-1-yl)palladium **87** (67.9 mg, 0.115 mmol). The vial was sealed and purged with nitrogen via vacuum. LHMDS in tetrahydrofuran (1 M, 1.5 mL, 1.5 mmol) was added. The vial was stirred in the preheated oil bath at 80 °C for 1 hour. The reaction mixture was cooled to room temperature. The reaction mixture was partitioned between dichloromethane (10 mL) and saturated aqueous ammonium chloride (10 mL). After separation, the organic extract was dried using a hydrophobic frit and evaporated under reduced pressure. The residue was purified by chromatography on silica using a gradient elution from 0 to 25 % methanol in dichloromethane to afford the title compound (213 mg, only 70 % pure by NMR, 70 % yield) as a brown solid. **LCMS** (Method D) (ES +ve) *m/z* 554 (*M* + *H*)⁺ *Rt* 1.22 minutes. **¹H NMR** (400 MHz, DMSO-*d*₆, 120 °C) δ 10.76 (br. s, 1H), 8.27 (dd, *J* = 1.5, 4.8 Hz, 1H), 7.82 (dd, *J* = 1.5, 8.1 Hz, 1H), 7.32 (dd, *J* = 4.8, 8.1 Hz, 1H), 6.32 (s, 1H), 6.22 (d, *J* = 7.6 Hz, 1H), 6.16 (s, 1H), 4.26 - 4.10 (m, 1H), 4.01 - 3.93 (m, 2H), 3.69 - 3.58 (m, 2H), 3.32 (s, 2H), 3.09 - 2.99 (m, 2H), 2.72 (d, *J* = 10.3 Hz, 2H), 2.10 - 1.99 (m, 2H), 1.73 (t, *J* = 10.7 Hz, 2H), 1.46 (s, 9H), 1.44 - 1.40 (m, 2H), 1.07 (d, *J* = 6.3 Hz, 6H).

***N*-(1-Acryloyl-4-piperidiny)-4-{{*cis*-2,6-dimethyl-4-morpholinyl}methyl}-*N'*-[1,3]thiazolo[5,4-*b*]pyridin-2-yl-2,6-pyridinediamine (100)**



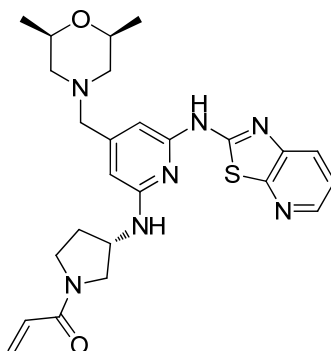
A round bottom flask was charged with *tert*-butyl 4-((4-((*cis*-2,6-dimethyl-4-morpholino)methyl)-6-(thiazolo[5,4-*b*]pyridin-2-ylamino)pyridin-2-yl)amino)piperidine-1-carboxylate **100i** (106 mg, 0.191 mmol), HCl in dioxane (4 M, 1.88 mL, 7.52 mmol), dichloromethane (3 mL) and methanol (2 mL). The reaction was stirred at room temperature for 1 hour. The solvent was evaporated under reduced pressure. The residue was dissolved in *N*-methyl-2-pyrrolidone (2 mL) and treated with *N,N*-diisopropylethylamine (0.167 mL, 0.957 mmol) and 2-propenoyl chloride (0.031 mL, 0.38 mmol). The reaction was stirred at room temperature for 1 hour. The mixture was purified by mass directed automated preparative HPLC to afford the title compound (36 mg, 37 % yield over the two previous steps) as an off-white solid. **LCMS** (Method D) (ES +ve) *m/z* 508 (M + H)⁺ Rt 0.93 minutes. **¹H NMR** (400 MHz, DMSO-*d*₆, 120 °C) δ 8.27 (dd, *J* = 1.5, 4.6 Hz, 1H), 7.82 (dd, *J* = 1.5, 8.1 Hz, 1H), 7.32 (dd, *J* = 4.6, 8.1 Hz, 1H), 6.75 (dd, *J* = 10.6, 16.7 Hz, 1H), 6.33 (s, 1H), 6.26 (d, *J* = 7.6 Hz, 1H), 6.17 (s, 1H), 6.07 (dd, *J* = 2.3, 16.7 Hz, 1H), 5.63 (dd, *J* = 2.3, 10.6 Hz, 1H), 4.32 - 4.23 (m, 1H), 4.24 - 4.14 (m, 2H), 3.69 - 3.57 (m, 2H), 3.32 (s, 2H), 3.25 - 3.13 (m, 2H), 2.72 (d, *J* = 10.3 Hz, 2H), 2.16 - 2.05 (m, 2H), 1.73 (t, *J* = 10.7 Hz, 2H), 1.54 - 1.41 (m, 2H), 1.07 (d, *J* = 6.3 Hz, 6H).

1,1-Dimethylethyl (3S)-3-[[4-[[*cis*-2,6-dimethyl-4-morpholinyl]methyl]-6-[[1,3]thiazolo[5,4-*b*]pyridin-2-ylamino)-2-pyridinyl]amino]-1-pyrrolidinecarboxylate (101i)



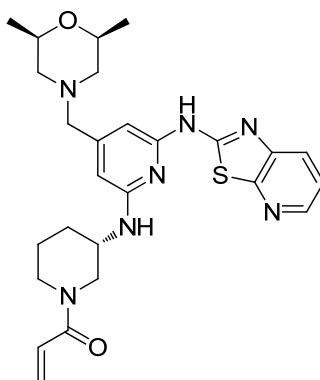
A microwave vial was charged with *N*-(6-chloro-4-((*cis*-2,6-dimethyl-4-morpholino)methyl)pyridin-2-yl)thiazolo[5,4-*b*]pyridin-2-amine **99** (150 mg, 0.385 mmol), (*S*)-*tert*-butyl 3-aminopyrrolidine-1-carboxylate (107 mg, 0.577 mmol) and {1,3-bis[2,6-bis(1-methylethyl)phenyl]-2-imidazolidinyl}(chloro)(2-methyl-2-propen-1-yl)palladium **87** (68 mg, 0.12 mmol). The vial was sealed and purged with nitrogen via vacuum. LHMDS in tetrahydrofuran (1 M, 1.5 mL, 1.5 mmol) was added. The vial was stirred in the preheated oil bath at 80 °C for 1 hour. The reaction was cooled to room temperature. The reaction mixture was partitioned between dichloromethane (10 mL) and saturated aqueous ammonium chloride (10 mL). After separation, the organic extract was dried using a hydrophobic frit and evaporated under reduced pressure. The residue was purified by chromatography on silica using a gradient elution from 0 to 25 % methanol in dichloromethane to afford the title compound (208 mg, 70 % pure by NMR, 70 % yield) as a brown solid. **LCMS** (Method D) (ES +ve) *m/z* 540 (*M* + *H*)⁺ *Rt* 1.16 minutes. **¹H NMR** (400 MHz, DMSO-*d*₆, 120 °C) δ 10.78 (br. s, 1H), 8.26 (dd, *J* = 1.4, 4.7 Hz, 1H), 7.82 (dd, *J* = 1.4, 8.1 Hz, 1H), 7.32 (dd, *J* = 4.7, 8.1 Hz, 1H), 6.47 (d, *J* = 6.5 Hz, 1H), 6.37 (s, 1H), 6.19 (s, 1H), 4.67 - 4.60 (m, 1H), 3.78 - 3.70 (m, 1H), 3.68 - 3.59 (m, 2H), 3.55 - 3.45 (m, 1H), 3.44 - 3.36 (m, 1H), 3.33 (s, 2H), 3.28 - 3.21 (m, 1H), 2.73 (d, *J* = 10.3 Hz, 2H), 2.34 - 2.23 (m, 1H), 1.97 - 1.87 (m, 1H), 1.74 (t, *J* = 10.7 Hz, 2H), 1.43 (s, 9H), 1.07 (d, *J* = 6.3 Hz, 6H).

1-((*S*)-3-((4-((*cis*-2,6-Dimethyl-4-morpholino)methyl)-6-(thiazolo[5,4-*b*]pyridin-2-ylamino)pyridin-2-yl)amino)pyrrolidin-1-yl)prop-2-en-1-one (101)



A round bottom flask was charged with 1,1-dimethylethyl (3*S*)-3-{[4-{[*cis*-2,6-dimethyl-4-morpholinyl]methyl}-6-([1,3]thiazolo[5,4-*b*]pyridin-2-ylamino)-2-pyridinyl]amino}-1-pyrrolidinecarboxylate **101i** (104 mg, 0.193 mmol), HCl in dioxane (4 M, 1.893 mL, 7.572 mmol), dichloromethane (3 mL) and methanol (2 mL). The reaction was stirred at room temperature for 1 hour. The solvent was evaporated under reduced pressure. The residue was dissolved in *N*-methyl-2-pyrrolidone (3 mL) and treated with *N,N*-diisopropylethylamine (0.168 mL, 0.964 mmol) and 2-propenoyl chloride (0.031 mL, 0.39 mmol). The reaction was stirred at room temperature for 1 hour. The mixture was purified by mass directed automated preparative HPLC to afford the title compound (36 mg, 38 % yield over the two previous steps) as an off-white solid. **LCMS** (Method D) (ES +ve) *m/z* 494 (M + H)⁺ Rt 0.89 minutes. **¹H NMR** (400 MHz, DMSO-*d*₆, 120 °C) δ 10.73 (br. s, 1H), 8.26 (dd, *J* = 1.4, 4.7 Hz, 1H), 7.82 (dd, *J* = 1.4, 8.2 Hz, 1H), 7.32 (dd, *J* = 4.7, 8.2 Hz, 1H), 6.55 (dd, *J* = 10.4, 17.0 Hz, 1H), 6.47 (d, *J* = 7.1 Hz, 1H), 6.40 (s, 1H), 6.20 (s, 1H), 6.11 (dd, *J* = 2.4, 17.0 Hz, 1H), 5.61 (dd, *J* = 2.4, 10.4 Hz, 1H), 4.76 - 4.67 (m, 1H), 3.98 - 3.87 (m, 1H), 3.77 - 3.57 (m, 4H), 3.49 (dd, *J* = 4.7, 11.5 Hz, 1H), 3.34 (s, 2H), 2.76 - 2.70 (m, 2H), 2.40 - 2.29 (m, 1H), 2.06 - 1.96 (m, 1H), 1.75 (t, *J* = 10.7 Hz, 2H), 1.07 (d, *J* = 6.3 Hz, 6H). Full characterisation for this compound is described in a later section.

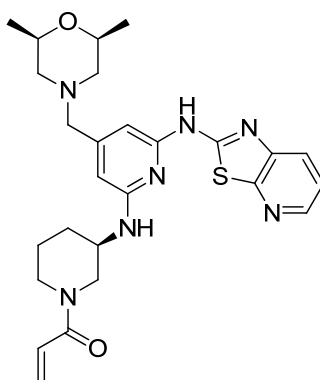
1-((*S*)-3-((4-((*cis*-2,6-Dimethyl-4-morpholino)methyl)-6-(thiazolo[5,4-*b*]pyridin-2-ylamino)pyridin-2-yl)amino)piperidin-1-yl)prop-2-en-1-one (102)



A microwave vial was charged with *N*-(6-chloro-4-((*cis*-2,6-dimethyl-4-morpholino)methyl)pyridin-2-yl)thiazolo[5,4-*b*]pyridin-2-amine **99** (50 mg, 0.13 mmol), (*S*)-*tert*-butyl 3-aminopiperidine-1-carboxylate (38.5 mg, 0.192 mmol), 2-(dicyclohexylphosphino)-3,6-dimethoxy-2',4',6'-tri-*iso*-propyl-1,1'-biphenyl **L¹** (6.9 mg, 0.013 mmol), chloro[2-(dicyclohexylphosphino)-3,6-dimethoxy-2'-4'-6'-tri-*iso*-propyl-1,1'-biphenyl][2-(2-aminoethyl)phenyl]palladium(II) **86** (10.2 mg, 0.0128 mmol) and tetrahydrofuran (1 mL). The vial was sealed and purged with vacuum and nitrogen (3 times). LHMDS in tetrahydrofuran (1 M, 0.412 mL, 0.412 mmol) was added and the vial was heated at 80 °C in the preheated oil bath for 1.5 hours. The vial was cooled to room temperature and the reaction mixture was partitioned between dichloromethane (10 mL) and saturated aqueous ammonium chloride (10 mL). After separation, the organic extract was dried using a hydrophobic frit and evaporated under reduced pressure. The yellow residue was dissolved in dichloromethane (3 mL) and methanol (1 mL). The solution was treated with HCl in dioxane (4 M, 0.5 mL, 2 mmol) and stirred at room temperature for 16 hours. The solvent was evaporated under reduced pressure. The yellow residue was dissolved in *N*-methyl-2-pyrrolidone (1 mL) and *N,N*-diisopropylethylamine (0.067 mL, 0.39 mmol). 2-Propenoyl chloride (0.021 mL, 0.26 mmol) was added and the reaction was stirred at room temperature for 1 hour. The mixture was purified by mass directed automated preparative HPLC to afford the title compound (16 mg, 25 % yield) as a brown solid. **LCMS** (Method D) (ES +ve) *m/z* 508 (M + H)⁺ Rt 0.94 minutes. **¹H NMR** (400 MHz, DMSO-*d*₆, 120 °C) δ 10.68 (br. s, 1H), 8.25 (dd, *J* = 1.5, 4.5 Hz,

1H), 7.81 (dd, $J = 1.5, 8.1$ Hz, 1H), 7.31 (dd, $J = 4.5, 8.1$ Hz, 1H), 6.60 (dd, $J = 10.7, 17.0$ Hz, 1H), 6.38 (s, 1H), 6.20 (s, 1H), 6.13 (d, $J = 7.8$ Hz, 1H), 5.97 (dd, $J = 2.3, 17.0$ Hz, 1H), 5.48 (dd, $J = 2.3, 10.7$ Hz, 1H), 4.19 - 4.10 (m, 1H), 4.09 - 4.02 (m, 1H), 3.87 - 3.79 (m, 1H), 3.69 - 3.59 (m, 2H), 3.34 (s, 2H), 3.32 - 3.22 (m, 2H), 2.75 - 2.70 (m, 2H), 2.21 - 2.11 (m, 1H), 1.92 - 1.81 (m, 1H), 1.75 (t, $J = 10.7$ Hz, 2H), 1.70 - 1.53 (m, 2H), 1.07 (d, $J = 6.0$ Hz, 6H).

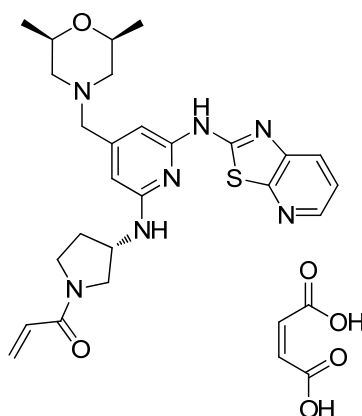
1-((*R*)-3-((4-((*cis*-2,6-Dimethyl-4-morpholino)methyl)-6-(thiazolo[5,4-*b*]pyridin-2-ylamino)pyridin-2-yl)amino)piperidin-1-yl)prop-2-en-1-one (103)



A microwave vial was charged with *N*-(6-chloro-4-((*cis*-2,6-dimethyl-4-morpholino)methyl)pyridin-2-yl)thiazolo[5,4-*b*]pyridin-2-amine **99** (50 mg, 0.13 mmol), (*R*)-*tert*-butyl 3-aminopiperidine-1-carboxylate (38.5 mg, 0.192 mmol) and {1,3-bis[2,6-bis(1-methylethyl)phenyl]-2-imidazolidinyl}(chloro)(2-methyl-2-propen-1-yl)palladium **87** (22.6 mg, 0.0384 mmol). The vial was sealed and purged with nitrogen via vacuum. LHMDS in tetrahydrofuran (1 M, 0.5 mL, 0.5 mmol) was added. The vial was stirred in the preheated oil bath at 70 °C for 1 hour. The vial was cooled to room temperature and the reaction mixture was partitioned between dichloromethane (10 mL) and saturated aqueous ammonium chloride (10 mL). After separation, the organic extract was dried using a hydrophobic frit and evaporated under reduced pressure. The yellow residue was dissolved in dichloromethane (3 mL) and methanol (1 mL). The solution was treated with HCl in dioxane (4 M, 0.5 mL, 2 mmol) and stirred at room temperature overnight. The solvent was evaporated under reduced pressure. The yellow residue was dissolved in *N*-methyl-2-pyrrolidone (1 mL) and *N,N*-diisopropylethylamine (0.112 mL, 0.641 mmol). 2-Propenoyl chloride (0.021 mL, 0.26 mmol) was added and the reaction was stirred at room

temperature for 1 hour. The mixture was purified by mass directed automated preparative HPLC to afford the title compound (14 mg, 21 % yield) as a brown solid. **LCMS** (Method D) (ES +ve) m/z 508 ($M + H$)⁺ Rt 0.94 minutes. **¹H NMR** (400 MHz, DMSO- d_6 , 120 °C) δ 8.24 (dd, $J = 1.5, 4.5$ Hz, 1H), 7.79 (dd, $J = 1.5, 8.1$ Hz, 1H), 7.30 (dd, $J = 4.5, 8.1$ Hz, 1H), 6.60 (dd, $J = 10.6, 16.9$ Hz, 1H), 6.37 (s, 1H), 6.19 (s, 1H), 6.10 (d, $J = 7.8$ Hz, 1H), 5.97 (dd, $J = 2.3, 16.9$ Hz, 1H), 5.48 (dd, $J = 2.3, 10.6$ Hz, 1H), 4.20 - 4.10 (m, 1H), 4.10 - 4.02 (m, 1H), 3.88 - 3.79 (m, 1H), 3.70 - 3.59 (m, 2H), 3.33 (s, 2H), 3.32 - 3.22 (m, 2H), 2.76 - 2.70 (m, 2H), 2.22 - 2.11 (m, 1H), 1.92 - 1.81 (m, 1H), 1.75 (t, $J = 10.6$ Hz, 2H), 1.69 - 1.54 (m, 2H), 1.07 (d, $J = 6.3$ Hz, 6H).

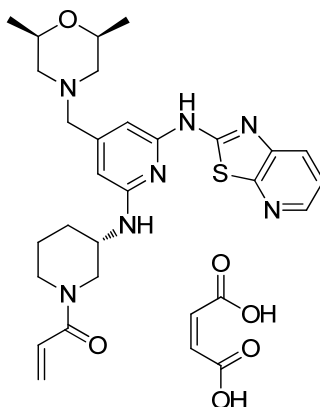
1-((S)-3-((4-((*cis*-2,6-Dimethyl-4-morpholino)methyl)-6-(thiazolo[5,4-*b*]pyridin-2-ylamino)pyridin-2-yl)amino)pyrrolidin-1-yl)prop-2-en-1-one, maleic acid salt (101a)



Maleic acid solution in water (0.1 M, 0.213 mL, 0.0213 mmol) was added to a suspension of 1-((S)-3-((4-((*cis*-2,6-dimethyl-4-morpholino)methyl)-6-(thiazolo[5,4-*b*]pyridin-2-ylamino)pyridin-2-yl)amino)pyrrolidin-1-yl)prop-2-en-1-one **100** (10 mg, 0.020 mmol) in acetonitrile (1.5 mL) and water (1.5 mL). The reaction was stirred at room temperature for 10 minutes. The solvent was concentrated under reduced pressure to give the title compound (12 mg, 97 % yield) as a yellow solid. **LCMS** (Method D) (ES +ve) m/z 494 ($M + H$)⁺ Rt 0.90 minutes. **¹H NMR** (400 MHz, DMSO- d_6 , 120 °C) δ 8.27 (dd, $J = 1.5, 4.8$ Hz, 1H), 7.83 (dd, $J = 1.5, 8.1$ Hz, 1H), 7.33 (dd, $J = 4.8, 8.1$ Hz, 1H), 6.55 (dd, $J = 10.4, 17.0$ Hz, 1H), 6.42 (s, 1H), 6.23 (s, 1H), 6.17 (s, 2H), 6.11 (dd, $J = 2.5, 17.0$ Hz, 1H), 5.61 (dd, $J = 2.5, 10.4$ Hz,

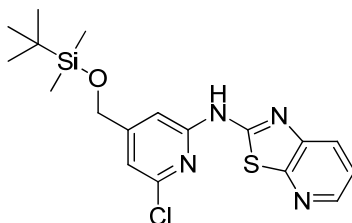
1H), 4.75 - 4.68 (m, 1H), 3.98 - 3.88 (m, 1H), 3.78 - 3.57 (m, 4H), 3.54 - 3.45 (m, 3H), 2.85 (d, $J = 11.1$ Hz, 2H), 2.41 - 2.28 (m, 1H), 2.09 - 1.97 (m, 1H), 1.93 (t, $J = 10.8$ Hz, 2H), 1.09 (d, $J = 6.3$ Hz, 6H).

1-((*S*)-3-((4-((*cis*-2,6-Dimethyl-4-morpholino)methyl)-6-(thiazolo[5,4-*b*]pyridin-2-ylamino)pyridin-2-yl)amino)piperidin-1-yl)prop-2-en-1-one, maleic acid salt (102a)



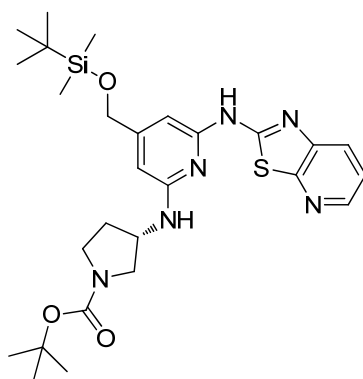
Maleic acid solution in water (0.1 M, 0.083 mL, 8.3 μmol) was added to a suspension of 1-((*S*)-3-((4-((*cis*-2,6-dimethyl-4-morpholino)methyl)-6-(thiazolo[5,4-*b*]pyridin-2-ylamino)pyridin-2-yl)amino)piperidin-1-yl)prop-2-en-1-one **102** (4 mg, 8 μmol) in acetonitrile (0.5 mL) and water (0.5 mL). The reaction was stirred at room temperature for 10 minutes. The solvent was concentrated under reduced pressure to title compound (5 mg, 100 % yield) as a yellow solid. **LCMS** (Method D) (ES +ve) m/z 508 ($M + H$)⁺ Rt 0.95 minutes. No NMR was recorded for this compound as the material was urgently submitted to the SLF assay immediately after synthesis.

***N*-[6-Chloro-4-(((1,1-dimethylethyl)(dimethyl)silyl)oxy)methyl]-2-pyridinyl][1,3]thiazolo[5,4-*b*]pyridin-2-amine (110)**



A round bottom flask was charged with 6-chloro-4-({[(1,1-dimethylethyl)(dimethyl)silyl]oxy}methyl)-2-pyridinamine **109** (7.0 g, 26 mmol) and 2-bromo[1,3]thiazolo[5,4-*b*]pyridine **31** (6.62 g, 30.8 mmol) in anhydrous *N,N*-dimethylformamide (80 mL), placed under an atmosphere of nitrogen and cooled in an ice bath. Sodium hydride (60 % w/w in mineral oil, 2.052 g, 51.30 mmol) was added portionwise over 5 minutes and the mixture stirred for 1 hour at 0 °C under a nitrogen atmosphere and at room temperature for another hour. Saturated aqueous ammonium chloride (200 mL) was added while the reaction was stirred at room temperature. The suspension was filtered under reduced pressure, the solid washed with water and with diethyl ether. The solid was dried under reduced pressure to afford the title compound (9.65 g, 89 % pure, 82 %) as a brown solid. **LCMS** (Method D) (ES +ve) *m/z* 407 (M + H)⁺ Rt 1.56 minutes. **¹H NMR** (400 MHz, DMSO-*d*₆) δ 8.37 (dd, *J* = 1.4, 4.8 Hz, 1H), 7.96 (dd, *J* = 1.4, 8.0 Hz, 1H), 7.43 (dd, *J* = 4.8, 8.0 Hz, 1H), 7.28 (s, 1H), 7.01 (s, 1H), 4.77 (s, 2H), 0.95 (s, 9H), 0.12 (s, 6H).

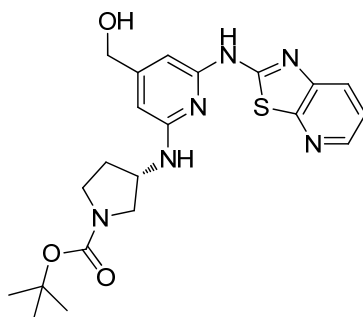
(*S*)-*tert*-Butyl 3-((4-(((*tert*-butyldimethylsilyl)oxy)methyl)-6-(thiazolo[5,4-*b*]pyridin-2-ylamino)pyridin-2-yl)amino)pyrrolidine-1-carboxylate (111**)**



A round bottom flask was charged with *N*-[6-chloro-4-({[(1,1-dimethylethyl)(dimethyl)silyl]oxy}methyl)-2-pyridinyl][1,3]thiazolo[5,4-*b*]pyridin-2-amine **110** (17.26 g, 42.41 mmol), (*S*)-*tert*-butyl 3-aminopyrrolidine-1-carboxylate (11.85 g, 63.62 mmol), and {1,3-bis[2,6-bis(1-methylethyl)phenyl]-2-imidazolidinyl}(chloro)(2-methyl-2-propen-1-yl)palladium **87** (7.50 g, 12.7 mmol). The vial was sealed and purged with nitrogen via vacuum. LHMDS in tetrahydrofuran (1 M, 200 mL, 200 mmol) was added and the vial was stirred in the

preheated oil bath at 70 °C for 2.5 hours. The reaction mixture was cooled to room temperature and partitioned between dichloromethane (300 mL) and saturated aqueous ammonium chloride (200 mL). The phases were separated and the aqueous phase was back extracted with DCM (300 mL). The organic extracts were combined, dried with magnesium sulfate, filtered and concentrated under reduced pressure to afford a brown solid. The product was purified by FlashMaster chromatography on silica using a gradient elution from 0 to 100 % ethyl acetate in dichloromethane to yield the title compound (13.2 g, 56 %) as a brown solid. **LCMS** (Method D) (ES +ve) m/z 407 / 557 ($M + H$)⁺ Rt 1.54 minutes. **¹H NMR** (400MHz, DMSO- d_6) δ 10.80 (br. s, 1H), 8.26 (dd, $J = 1.5, 4.7$ Hz, 1H), 7.82 (dd, $J = 1.5, 8.1$ Hz, 1H), 7.32 (dd, $J = 4.8, 8.1$ Hz, 1H), 6.41 (s, 2H), 6.18 (s, 1H), 4.67 - 4.61 (m, 1H), 4.59 (s, 2H), 3.78 - 3.71 (m, 1H), 3.56 - 3.47 (m, 1H), 3.45 - 3.36 (m, 1H), 3.30 - 3.21 (m, 1H), 2.35 - 2.23 (m, 1H), 1.97 - 1.87 (m, 1H), 1.43 (s, 9H), 0.97 (s, 9H), 0.14 (s, 6H).

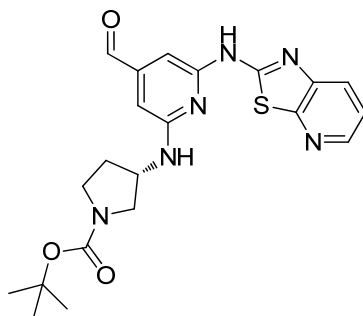
(S)-tert-Butyl 3-(((4-(hydroxymethyl)-6-(thiazolo[5,4-*b*]pyridin-2-ylamino)pyridin-2-yl)amino)pyrrolidine-1-carboxylate (112)



To a solution of (S)-tert-butyl 3-(((4-(((tert-butyl dimethylsilyl)oxy)methyl)-6-(thiazolo[5,4-*b*]pyridin-2-ylamino)pyridin-2-yl)amino)pyrrolidine-1-carboxylate **111** (13 g, 23 mmol) in tetrahydrofuran (100 mL) stirring at room temperature was added TBAF in tetrahydrofuran (1 M, 28 mL, 28 mmol). The reaction mixture was stirred at room temperature for 1 hour. The reaction was cooled in an ice bath and water (200 mL) was added. The suspension was stirred in the ice bath for 10 minutes and was filtered under reduced pressure. The solid was washed with water and dried in the oven to afford the title compound (9.0 g, 87 % yield) as a brown solid. **LCMS** (Method D) (ES +ve) m/z 443 ($M + H$)⁺ Rt 0.98 minutes. **¹H NMR** (400 MHz, DMSO- d_6) δ 11.31 (s, 1H), 8.27 (dd, $J = 1.3, 4.8$ Hz, 1H), 7.86 (dd, $J = 1.3, 8.0$ Hz,

1H), 7.35 (dd, $J = 4.8, 8.0$ Hz, 1H), 6.92 (br. s, 1H), 6.25 (s, 1H), 6.16 (s, 1H), 5.22 (t, $J = 5.6$ Hz, 1H), 4.67 - 4.54 (m, 1H), 4.36 (d, $J = 5.7$ Hz, 2H), 3.79 - 3.56 (m, 1H), 3.51 - 3.33 (m, 2H), 3.28 - 3.12 (m, 1H), 2.30 - 2.18 (m, 1H), 1.95 - 1.81 (m, 1H), 1.39 (d, $J = 18.3$ Hz, 9H). The doublet at 1.39 ppm was assigned to the Boc group and was believed to be caused by the presence of rotamers.

(*S*)-*tert*-Butyl 3-((4-formyl-6-(thiazolo[5,4-*b*]pyridin-2-ylamino)pyridin-2-yl)amino)pyrrolidine-1-carboxylate (113**)**



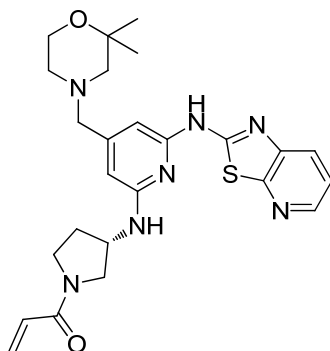
To a solution of Dess-Martin periodinane (1.98 g, 4.52 mmol) in tetrahydrofuran (30 mL), stirred at 0 °C, was added a solution of (*S*)-*tert*-butyl 3-((4-(hydroxymethyl)-6-(thiazolo[5,4-*b*]pyridin-2-ylamino)pyridin-2-yl)amino)pyrrolidine-1-carboxylate **112** (1.43 g, 3.23 mmol) in tetrahydrofuran (30 mL). The reaction mixture was warmed to room temperature and stirred for 30 minutes. The reaction mixture was partitioned between dichloromethane (100 mL) and water (100 mL). The organic phase was dried using a hydrophobic frit and evaporated under reduced pressure. The residue was purified by FlashMaster chromatography on silica using a gradient elution from 0 to 100 % ethyl acetate in cyclohexane to yield the title compound (610 mg, 43 %) as a brown solid. **LCMS** (Method D) (ES +ve) m/z 441 ($M + H$)⁺ Rt 1.09 minutes. **¹H NMR** (400 MHz, DMSO- d_6) δ 11.65 (s, 1H), 9.87 (s, 1H), 8.31 (d, $J = 4.8$ Hz, 1H), 7.92 (d, $J = 8.3$ Hz, 1H), 7.50 (d, $J = 6.3$ Hz, 1H), 7.39 (dd, $J = 4.8, 8.3$ Hz, 1H), 6.64 (s, 1H), 6.62 (s, 1H), 4.65 (br. s, 1H), 3.81 - 3.61 (m, 1H), 3.51 - 3.36 (m, 2H), 3.25 - 3.17 (m, 1H), 2.36 - 2.20 (m, 1H), 1.97 - 1.86 (m, 1H), 1.40 (d, $J = 18.3$ Hz, 9H).

General procedure J for the preparation of compounds 104-108:

A solution of (*S*)-*tert*-butyl 3-((4-formyl-6-(thiazolo[5,4-*b*]pyridin-2-ylamino)pyridin-2-yl)amino)pyrrolidine-1-carboxylate **113** in tetrahydrofuran was treated with the required amine and the reaction was stirred for 15 minutes. The mixture was then treated with dichloromethane and sodium triacetoxyborohydride. The reaction was stirred for 16 hours at room temperature. Unless stated otherwise, saturated aqueous sodium bicarbonate was added and the reaction was stirred for 30 minutes. Dichloromethane was added and the phases were separated. The organic extract was dried using a hydrophobic frit and evaporated under reduced pressure. A round bottom flask was charged with the obtained solid, HCl in dioxane (4 M), dichloromethane and methanol. The reaction was stirred at room temperature for 1 hour. A further portion of HCl in dioxane (4 M) was added and the reaction was stirred for 30 minutes. The solvent was evaporated under reduced pressure. The residue was dissolved in *N*-methyl-2-pyrrolidone and treated with *N,N*-diisopropylethylamine and 2-propenoyl chloride. The reaction was stirred at room temperature for 1 hour. The mixture was purified by mass directed automated preparative HPLC to afford the title compound.

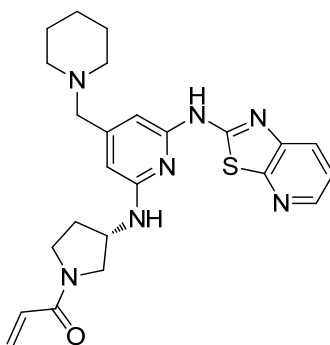
Following the general procedure J for the preparation of compounds **104-108**, data are presented as (a) amount of compound **113**, (b) volume of tetrahydrofuran, (c) amount of amine, (d) volume of dichloromethane, (e) amount of sodium triacetoxyborohydride, (f) volume of saturated aqueous sodium bicarbonate, (g) volume of HCl in dioxane (4 M) added on two separate batches, (h) volume of dichloromethane, (i) volume of methanol, (j) volume of *N*-methyl-2-pyrrolidone, (k) volume of *N,N*-diisopropylethylamine, (l) volume of 2-propenoyl chloride.

(S)-1-(3-((4-((2,2-Dimethyl-4-morpholino)methyl)-6-(thiazolo[5,4-*b*]pyridin-2-ylamino)pyridin-2-yl)amino)pyrrolidin-1-yl)prop-2-en-1-one (104)



(a) 50 mg, 0.11 mmol, (b) 0.5 mL, (c) 2,2-dimethylmorpholine (26.1 mg, 0.227 mmol), (d) 2 mL, (e) 48.1 mg, 0.227 mmol, (f) 1 mL, (g) 1.186 mL, 4.744 mmol, (h) 3 mL, (i) 2 mL, (j) 1 mL, (k) 0.104 mL, 0.593 mmol, (l) 0.019 mL, 0.24 mmol. Light brown solid. Yield: 27 mg, 48 %. **LCMS** (Method D) (ES +ve) m/z 494 ($M + H$)⁺ Rt 0.95 minutes. **¹H NMR** (400 MHz, DMSO-*d*₆, 120 °C) δ 10.84 (br. s, 1H), 8.26 (dd, $J = 1.5, 4.8$ Hz, 1H), 7.82 (dd, $J = 1.5, 8.1$ Hz, 1H), 7.32 (dd, $J = 4.8, 8.1$ Hz, 1H), 6.55 (dd, $J = 10.6, 17.0$ Hz, 1H), 6.51 (d, $J = 6.5$ Hz, 1H), 6.44 (s, 1H), 6.21 (s, 1H), 6.12 (dd, $J = 2.4, 17.0$ Hz, 1H), 5.61 (dd, $J = 2.4, 10.6$ Hz, 1H), 4.75 - 4.66 (m, 1H), 4.01 - 3.86 (m, 1H), 3.76 - 3.57 (m, 4H), 3.54 - 3.44 (m, 1H), 3.32 (s, 2H), 2.42 - 2.29 (m, 3H), 2.22 (s, 2H), 2.07 - 1.96 (m, 1H), 1.22 (s, 6H).

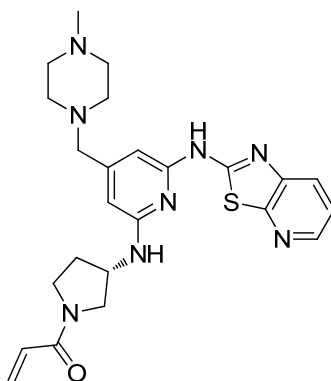
(S)-1-(3-((4-(Piperidin-1-ylmethyl)-6-(thiazolo[5,4-*b*]pyridin-2-ylamino)pyridin-2-yl)amino)pyrrolidin-1-yl)prop-2-en-1-one (105)



(a) 50 mg, 0.11 mmol, (b) 0.5 mL, (c) piperidine (0.023 mL, 0.23 mmol), (d) 2 mL, (e) 48.1 mg, 0.227 mmol, (f) 1 mL, (g) 1.177 mL, 4.708 mmol, (h) 3 mL, (i) 2 mL,

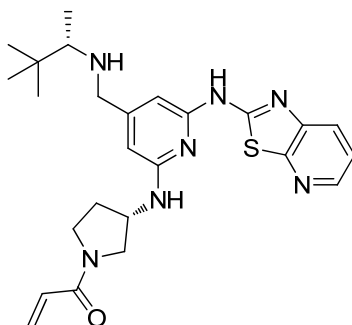
(j) 1 mL, (k) 0.103 mL, 0.589 mmol, (l) 0.019 mL, 0.24 mmol. Light brown solid. Yield: 29 mg, 55 %. **LCMS** (Method D) (ES +ve) m/z 464 ($M + H$)⁺ Rt 0.98 minutes. **¹H NMR** (400 MHz, DMSO-*d*₆, 120 °C) δ 8.26 (dd, $J = 1.5, 4.5$ Hz, 1H), 7.82 (dd, $J = 1.5, 8.1$ Hz, 1H), 7.32 (dd, $J = 4.5, 8.1$ Hz, 1H), 6.55 (dd, $J = 10.5, 16.9$ Hz, 1H), 6.50 (d, $J = 6.8$ Hz, 1H), 6.39 (s, 1H), 6.20 (s, 1H), 6.11 (dd, $J = 2.3, 16.9$ Hz, 1H), 5.61 (dd, $J = 2.3, 10.5$ Hz, 1H), 4.76 - 4.67 (m, 1H), 4.00 - 3.85 (m, 1H), 3.79 - 3.67 (m, 1H), 3.67 - 3.56 (m, 1H), 3.49 (dd, $J = 4.5, 11.3$ Hz, 1H), 3.32 (s, 2H), 2.40 (t, $J = 5.5$ Hz, 4H), 2.37 - 2.28 (m, 1H), 2.06 - 1.95 (m, 1H), 1.53 - 1.61 (m, 4H), 1.49 - 1.39 (m, 2H).

(S)-1-(3-((4-((4-Methylpiperazin-1-yl)methyl)-6-(thiazolo[5,4-*b*]pyridin-2-ylamino)pyridin-2-yl)amino)pyrrolidin-1-yl)prop-2-en-1-one (106)



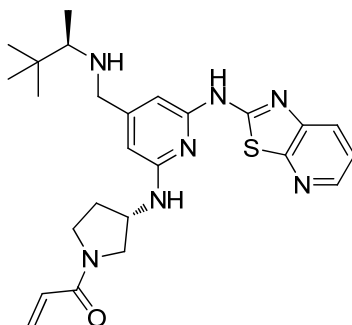
(a) 50 mg, 0.11 mmol, (b) 0.5 mL, (c) 1-methylpiperazine (0.025 mL, 0.23 mmol), (d) 2 mL, (e) 48.1 mg, 0.227 mmol, (f) 1 mL, (g) 1.201 mL, 4.804 mmol, (h) 3 mL, (i) 2 mL, (j) 1 mL, (k) 0.105 mL, 0.600 mmol, (l) 0.019 mL, 0.24 mmol. Light brown solid. Yield: 32 mg, 59 %. **LCMS** (Method D) (ES +ve) m/z 479 ($M + H$)⁺ Rt 0.78 minutes. **¹H NMR** (400 MHz, DMSO-*d*₆, 120 °C) δ 8.26 (dd, $J = 1.5, 4.7$ Hz, 1H), 7.82 (dd, $J = 1.5, 8.1$ Hz, 1H), 7.32 (dd, $J = 4.7, 8.1$ Hz, 1H), 6.55 (dd, $J = 11.1, 17.1$ Hz, 1H), 6.51 (d, $J = 6.0$ Hz, 1H), 6.38 (s, 1H), 6.20 (s, 1H), 6.12 (dd, $J = 2.3, 17.1$ Hz, 1H), 5.61 (dd, $J = 2.3, 11.1$ Hz, 1H), 4.75 - 4.67 (m, 1H), 3.99 - 3.86 (m, 1H), 3.78 - 3.67 (m, 1H), 3.67 - 3.56 (m, 1H), 3.49 (dd, $J = 4.7, 11.5$ Hz, 1H), 3.35 (s, 2H), 2.47 - 2.42 (m, 4H), 2.41 - 2.35 (m, 4H), 2.36 - 2.27 (m, 1H), 2.20 (s, 3H), 2.06 - 1.95 (m, 1H).

1-((*S*)-3-((4-(((*S*)-3,3-Dimethylbutan-2-yl)amino)methyl)-6-(thiazolo[5,4-*b*]pyridin-2-ylamino)pyridin-2-yl)amino)pyrrolidin-1-yl)prop-2-en-1-one (107)



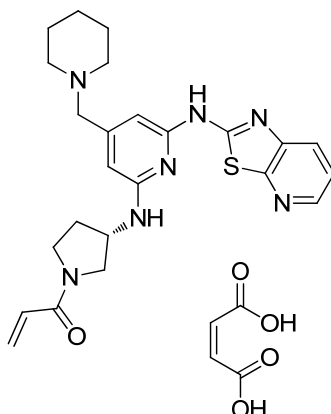
(a) 100 mg, 0.227 mmol, (b) 1 mL, (c) (*2S*)-3,3-dimethyl-2-butanamine (0.061 mL, 0.45 mmol), (d) 4 mL, (e) 96 mg, 0.45 mmol; the reaction was stirred for 14 hours at room temperature; a second portion of sodium triacetoxyborohydride (96 mg, 0.45 mmol) was added and the reaction was stirred at room temperature for 2 hours, (f) 2 mL, (g) 2.224 mL, 8.896 mmol, (h) 3 mL, (i) 2 mL, (j) 1 mL, (k) 0.198 mL, 1.13 mmol, (l) 0.022 mL, 0.27 mmol. Light brown solid. Yield: 50 mg, 46 %. **LCMS** (Method D) (ES +ve) m/z 480 ($M + H$)⁺ Rt 1.07 minutes. **¹H NMR** (400 MHz, DMSO-*d*₆, 120 °C) δ 8.25 (dd, $J = 1.5, 4.7$ Hz, 1H), 7.81 (dd, $J = 1.5, 8.1$ Hz, 1H), 7.31 (dd, $J = 4.7, 8.1$ Hz, 1H), 6.55 (dd, $J = 10.5, 16.6$ Hz, 1H), 6.43 (s, 1H), 6.42 - 6.40 (m, 1H), 6.23 (s, 1H), 6.11 (dd, $J = 2.3, 16.6$ Hz, 1H), 5.61 (dd, $J = 2.3, 10.5$ Hz, 1H), 4.74 - 4.66 (m, 1H), 3.98 - 3.85 (m, 1H), 3.73 (d, $J = 14.4$ Hz, 1H), 3.74 - 3.67 (m, 1H), 3.66 - 3.58 (m, 1H), 3.55 (d, $J = 14.4$ Hz, 1H), 3.49 (dd, $J = 4.8, 11.3$ Hz, 1H), 2.39 - 2.32 (m, 1H), 2.31 (q, $J = 6.3$ Hz, 1H), 2.06 - 1.96 (m, 1H), 1.00 (d, $J = 6.3$ Hz, 3H), 0.92 (s, 9H). Full characterisation for this compound is described in a later section.

1-((*S*)-3-((4-(((*R*)-3,3-Dimethylbutan-2-yl)amino)methyl)-6-(thiazolo[5,4-*b*]pyridin-2-ylamino)pyridin-2-yl)amino)pyrrolidin-1-yl)prop-2-en-1-one (108)



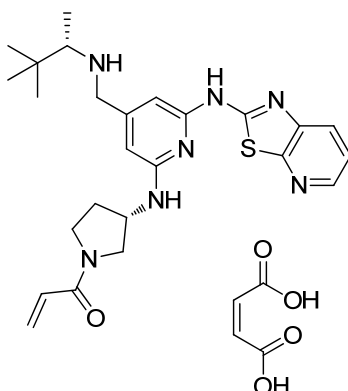
(a) 50 mg, 0.11 mmol, (b) 0.5 mL, (c) (*2R*)-3,3-dimethyl-2-butanamine (0.031 mL, 0.23 mmol), (d) 2 mL, (e) 48.1 mg, 0.227 mmol; the reaction was stirred for 4 hours at room temperature; a second portion of (*2R*)-3,3-dimethyl-2-butanamine (0.016 mL, 0.11 mmol) and sodium triacetoxyborohydride (96.2 mg, 0.454 mmol) was added and the reaction was stirred at room temperature for 14 hours, (f) 1 mL, (g) 1.121 mL, 4.484 mmol, (h) 3 mL, (i) 2 mL, (j) 1 mL, (k) 0.100 mL, 0.571 mmol, (l) 0.011 mL, 0.14 mmol. Light brown solid. Yield: 42 mg, 77 %. **LCMS** (Method D) (ES +ve) *m/z* 480 (*M* + *H*)⁺ *Rt* 1.07 minutes. **¹H NMR** (400 MHz, DMSO-*d*₆, 120 °C) δ 8.25 (dd, *J* = 1.5, 4.7 Hz, 1H), 7.81 (dd, *J* = 1.5, 8.1 Hz, 1H), 7.31 (dd, *J* = 4.7, 8.1 Hz, 1H), 6.55 (dd, *J* = 10.6, 16.9 Hz, 1H), 6.44 (s, 1H), 6.40 (d, *J* = 6.8 Hz, 1H), 6.23 (s, 1H), 6.11 (dd, *J* = 2.3, 16.9 Hz, 1H), 5.61 (dd, *J* = 2.3, 10.6 Hz, 1H), 4.75 - 4.66 (m, 1H), 3.97 - 3.88 (m, 1H), 3.74 (d, *J* = 14.4 Hz, 1H), 3.75 - 3.67 (m, 1H), 3.66 - 3.59 (m, 1H), 3.55 (d, *J* = 14.4 Hz, 1H), 3.49 (dd, *J* = 4.8, 11.3 Hz, 1H), 2.37 - 2.32 (m, 1H), 2.32 (q, *J* = 6.5 Hz, 1H), 2.06 - 1.96 (m, 1H), 1.01 (d, *J* = 6.5 Hz, 3H), 0.92 (s, 9H).

(S)-1-(3-((4-(Piperidin-1-ylmethyl)-6-(thiazolo[5,4-*b*]pyridin-2-ylamino)pyridin-2-yl)amino)pyrrolidin-1-yl)prop-2-en-1-one, maleic acid salt (105a)



Maleic acid solution in water (0.1 M, 0.181 mL, 0.0181 mmol) was added to a suspension of (S)-1-(3-((4-(Piperidin-1-ylmethyl)-6-(thiazolo[5,4-*b*]pyridin-2-ylamino)pyridin-2-yl)amino)pyrrolidin-1-yl)prop-2-en-1-one **105** (8.0 mg, 0.017 mmol) in acetonitrile (1.5 mL) and water (1.5 mL). The reaction was stirred at room temperature for 10 minutes. The solvent was concentrated under reduced pressure to give the title compound (10 mg, 100 % yield) as a yellow solid. **LCMS** (Method D) (ES +ve) m/z 464 ($M + H$)⁺ Rt 0.97 minutes. **¹H NMR** (400 MHz, DMSO-*d*₆, 120 °C) δ 8.28 (dd, $J = 1.5, 4.7$ Hz, 1H), 7.85 (dd, $J = 1.5, 8.1$ Hz, 1H), 7.34 (dd, $J = 4.7, 8.1$ Hz, 1H), 6.62 (br. s., 1H), 6.56 (dd, $J = 10.6, 16.9$ Hz, 1H), 6.44 (s, 1H), 6.25 (s, 1H), 6.12 (dd, $J = 2.3, 16.9$ Hz, 1H), 6.09 (s, 2H), 5.62 (dd, $J = 2.3, 10.6$ Hz, 1H), 4.77 - 4.66 (m, 1H), 4.00 - 3.88 (m, 1H), 3.79 (s, 2H), 3.76 - 3.68 (m, 1H), 3.68 - 3.58 (m, 1H), 3.51 (dd, $J = 4.7, 11.5$ Hz, 1H), 2.88 (br. s., 4H), 2.41 - 2.30 (m, 1H), 2.09 - 1.97 (m, 1H), 1.77 - 1.67 (m, 4H), 1.60 - 1.49 (m, 2H).

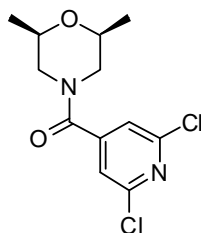
1-((*S*)-3-((4-(((*S*)-3,3-Dimethylbutan-2-yl)amino)methyl)-6-(thiazolo[5,4-*b*]pyridin-2-ylamino)pyridin-2-yl)amino)pyrrolidin-1-yl)prop-2-en-1-one, maleic acid salt (107a**)**



1-((*S*)-3-((4-(((*S*)-3,3-Dimethylbutan-2-yl)amino)methyl)-6-(thiazolo[5,4-*b*]pyridin-2-ylamino)pyridin-2-yl)amino)pyrrolidin-1-yl)prop-2-en-1-one **107** (50 mg, 0.10 mmol) was suspended in acetonitrile (1 mL) and water (1 mL). Maleic acid (12.1 mg, 0.104 mmol) was added to a suspension and the reaction mixture was shaken to obtain a clear solution. The reaction was left standing at room temperature for 30 minutes. The solvent was evaporated under nitrogen blowdown and the solid dried in the oven under reduced pressure overnight to give the title compound (55 mg, 89 % yield) as a light brown solid. **LCMS** (Method D) (ES +ve) m/z 480 ($M + H$)⁺ Rt 1.08 minutes. **¹H NMR** (400 MHz, DMSO-*d*₆, 120 °C) δ 8.28 (dd, $J = 1.5, 4.7$ Hz, 1H), 7.84 (dd, $J = 1.5, 8.1$ Hz, 1H), 7.34 (dd, $J = 4.7, 8.1$ Hz, 1H), 6.59 (br. s., 1H), 6.55 (dd, $J = 10.4, 16.9$ Hz, 1H), 6.48 (s, 1H), 6.27 (s, 1H), 6.12 (dd, $J = 2.3, 16.9$ Hz, 1H), 6.08 (s, 2H), 5.62 (dd, $J = 2.3, 10.4$ Hz, 1H), 4.75 - 4.67 (m, 1H), 3.98 (d, $J = 14.1$ Hz, 1H), 3.96 - 3.90 (m, 1H), 3.84 (d, $J = 14.1$ Hz, 1H), 3.78 - 3.69 (m, 1H), 3.68 - 3.59 (m, 1H), 3.51 (dd, $J = 4.7, 11.5$ Hz, 1H), 2.72 (q, $J = 6.8$ Hz, 1H), 2.41 - 2.31 (m, 1H), 2.08 - 1.98 (m, 1H), 1.17 (d, $J = 6.8$ Hz, 3H), 0.98 (s, 9H).

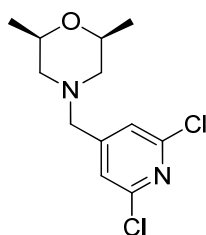
7. Synthetic procedures for the synthesis of compound 101 for toxicology assessment

***Cis*-4-[(2,6-Dichloro-4-pyridinyl)carbonyl]-2,6-dimethylmorpholine (96)**



cis-2,6-Dimethylmorpholine (45.9 mL, 371 mmol) was added dropwise to a stirred solution of 2,6-dichloro-4-pyridinecarbonyl chloride (65.0 g, 309 mmol) and DIPEA (162 mL, 927 mmol) in dichloromethane (150 mL) at 0 °C. The reaction was stirred at 0 °C for 2 hours and then at room temperature for 1 hour. Aqueous saturated ammonium chloride (400 mL) was added to the reaction and the product was extracted with dichloromethane (200 mL). The organic extract was washed with aqueous saturated sodium bicarbonate (400 mL), dried using a hydrophobic frit and concentrated under reduced pressure to give the title product (86.4 g, 97 % yield) as a yellow solid. LCMS (Method D) (ES +ve) m/z 289 ($M + H$)⁺ Rt 0.98 minutes. ¹H NMR (400 MHz, DMSO-*d*₆) δ 7.62 (s, 2H), 4.31 (d, $J = 13.1$ Hz, 1H), 3.62 - 3.48 (m, 2H), 3.34 (d, $J = 13.1$ Hz, 1H), 2.79 (t, $J = 11.5$ Hz, 1H), 2.46 (t, $J = 11.5$ Hz, 1H), 1.14 (d, $J = 6.3$ Hz, 3H), 0.99 (d, $J = 6.3$ Hz, 3H).

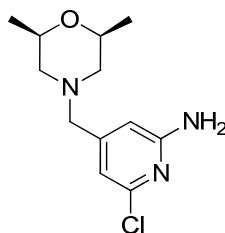
***Cis*-4-[(2,6-Dichloro-4-pyridinyl)methyl]-2,6-dimethylmorpholine (97)**



Borane in tetrahydrofuran (1 M, 235 mL, 235 mmol) was added dropwise to a cooled solution (0 °C) of *cis*-4-[(2,6-dichloro-4-pyridinyl)carbonyl]-2,6-dimethylmorpholine **96** (34 g, 12 mmol) in dichloromethane (125 mL). After the addition, the reaction

was stirred at 0 °C for 1 hour under nitrogen atmosphere. Aqueous HCl (6 M, 200 mL) was carefully added to the reaction while still stirring at 0 °C. After stirring for 2 hour while maintaining the temperature between 0 - 5 °C, the solution was left standing at room temperature overnight. The mixture was basified with aqueous NaOH (10 M, 220 mL) to reach pH 12. The phases were separated, the organic extract was dried using a hydrophobic frit and concentrated under reduced pressure. The residue was dissolved in dichloromethane (200 mL) and the solution was acidified with aqueous HCl (6 M, 200 mL). The white solid was filtered under reduced pressure. The solid was treated with aqueous NaOH (10 M, 200 mL) to reach pH 14 and then extracted with dichloromethane (200 mL). The organic extract was evaporated under reduced pressure to give the title compound (26.8 g, 83 % yield) as yellow solid. **LCMS** (Method D) (ES +ve) m/z 275 (M + H)⁺ Rt 1.2 minutes. **¹H NMR** (400 MHz, DMSO-*d*₆) δ 7.49 (s, 2H), 3.63 - 3.54 (m, 2H), 3.52 (s, 2H), 2.66 (d, J = 10.5 Hz, 2H), 1.69 (t, J = 10.5 Hz, 2H), 1.03 (d, J = 6.3 Hz, 6H).

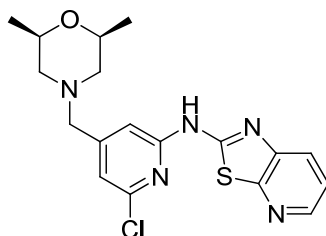
6-Chloro-4-[[*cis*-2,6-dimethyl-4-morpholinyl]methyl]-2-pyridinamine (98)



A pressure vessel was charged with *cis*-4-[(2,6-dichloro-4-pyridinyl)methyl]-2,6-dimethylmorpholine **97** (34.7 g, 126 mmol), isopropanol (30 mL) and concentrated ammonia solution (35 % in water, 55 mL, 2.8 mol). The vessel was sealed and was heated at 170 °C for 66 hours (pressure 20 bars). The reaction was cooled to room temperature. The residue was partitioned between EtOAc and aqueous NaOH (1 M). After separation, the organic layer was dried using a hydrophobic frit and concentrated under reduced pressure. The solid was suspended in diethyl ether and filtered under reduced pressure to give the title compound (28.7 g, 89 % yield) as a white solid (28.7 g, 89 % yield). **LCMS** (Method D) (ES +ve) m/z 256 (M + H)⁺ Rt 0.87 minutes. **¹H NMR** (400 MHz, DMSO-*d*₆) δ 6.43 (s, 1H), 6.33 (s, 1H), 6.30 (s,

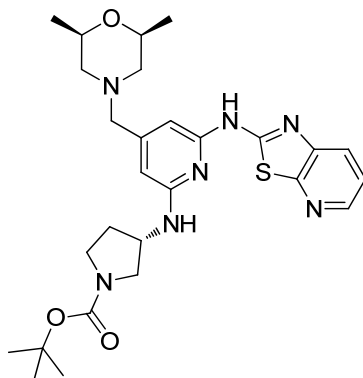
2H), 3.61 - 3.51 (m, 2H), 3.28 (br. s, 2H), 2.64 (d, $J = 10.8$ Hz, 2H), 1.64 (t, $J = 10.7$ Hz, 2H), 1.03 (d, $J = 6.3$ Hz, 6H).

***N*-(6-Chloro-4-*[(cis-2,6-dimethyl-4-morpholinyl)methyl]-2-pyridinyl*)[1,3]thiazolo[5,4-*b*]pyridin-2-amine (99)**



A round bottom flask was charged with sodium *tert*-butoxide (53.2 g, 554 mmol) in dry tetrahydrofuran (350 mL), placed in an atmosphere of nitrogen and cooled in an ice bath. A solution of 2-bromothiazolo[5,4-*b*]pyridine **31** (40.0 g, 186 mmol) and 6-chloro-4-*[(cis-2,6-dimethyl-4-morpholinyl)methyl]-2-pyridinamine* **98** (45.7 g, 179 mmol) in dry tetrahydrofuran (350 mL) was added dropwise over 5 minutes. The reaction was stirred for 1 hour keeping the temperature below 10 °C under nitrogen atmosphere. The reaction was left stirring in the water bath overnight. Saturated aqueous ammonium chloride (500 mL) was added while the reaction was stirred at room temperature. The mixture was extracted with dichloromethane (700 mL). The organic phase was dried using a hydrophobic frit and evaporated under reduced pressure to give the crude product as a brown solid. The residue was triturated with diethyl ether (100 mL). The resulting solid was filtered under reduced pressure, washed with diethyl ether (50 mL) and collected to give the title compound (58.4 g, 84 % yield) as a off-white solid. **LCMS** (Method D) (ES +ve) m/z 390 ($M + H$)⁺ Rt 1.16 minutes. **¹H NMR** (400 MHz, DMSO- d_6) δ 11.88 (br. s, 1H), 8.36 (dd, $J = 1.3, 4.5$ Hz, 1H), 7.97 (dd, $J = 1.3, 8.0$ Hz, 1H), 7.42 (dd, $J = 4.5, 8.0$ Hz, 1H), 7.19 (s, 1H), 7.07 (s, 1H), 3.66 - 3.56 (m, 2H), 3.49 (s, 2H), 2.70 (d, $J = 10.5$ Hz, 2H), 1.71 (t, $J = 10.7$ Hz, 2H), 1.04 (d, $J = 6.3$ Hz, 6H).

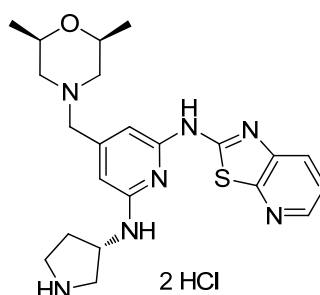
1,1-Dimethylethyl (3S)-3-[[4-[[*cis*-2,6-dimethyl-4-morpholinyl]methyl]-6-[[1,3]thiazolo[5,4-*b*]pyridin-2-ylamino)-2-pyridinyl]amino]-1-pyrrolidinecarboxylate (101i)



A three neck round bottom flask was charged with *N*-(6-chloro-4-[[*cis*-2,6-dimethyl-4-morpholinyl]methyl]-2-pyridinyl)[1,3]thiazolo[5,4-*b*]pyridin-2-amine **99** (27.5 g, 70.5 mmol), 1,1-dimethylethyl (3*S*)-3-amino-1-pyrrolidinecarboxylate (14.45 g, 77.58 mmol) and tetrahydrofuran (50 mL). {1,3-Bis[2,6-bis(1-methylethyl)phenyl]-2-imidazolidinyl}(chloro)(2-methyl-2-propen-1-yl)palladium **87** (12.45 g, 21.16 mmol) was dissolved in tetrahydrofuran (50 mL) and added into a dropping funnel. LHMDS in tetrahydrofuran (1M, 212 mL, 212 mmol) was added to the dropping funnel and the reaction was sealed. The apparatus was placed under an atmosphere of nitrogen using a vacuum purge (3 times). The reaction was heated at 50 °C and the catalyst solution was added dropwise over 15 minutes. The reaction was heated at this temperature for 30 minutes, cooled to room temperature and partitioned between dichloromethane (100 mL) and saturated aqueous ammonium chloride (100 mL). The organic extract was dried using a hydrophobic frit and concentrated under reduced pressure. The product was purified by chromatography on silica using a gradient elution from 50 to 100 % ethyl acetate in dichloromethane to give 31 g of the crude product as a brown solid. The solid was dissolved in acetonitrile (100 mL) and the suspension was heated with the heat gun to dissolve all the residue. Upon heating a white solid precipitated. The suspension was left cooling to temperature and was filtered under reduced pressure. The white solid was washed with acetonitrile (2 x 25 mL) and dried in the oven to afford the title compound (27.2 g, 71 % yield). **LCMS** (Method E) (ES +ve) *m/z* 540 (*M* + *H*)⁺ *Rt* 0.81 minutes. **¹H NMR** (400 MHz, DMSO-*d*₆) δ 11.28 (s, 1H), 8.27 (dd, *J* = 1.3, 4.8 Hz, 1H), 7.86

(dd, $J = 1.3, 8.0$ Hz, 1H), 7.36 (dd, $J = 4.8, 8.0$ Hz, 1H), 6.95 (d, $J = 6.0$ Hz, 1H), 6.26 (s, 1H), 6.15 (s, 1H), 4.65 - 4.55 (m, 1H), 3.78 - 3.69 (m, 0.5H), 3.66 - 3.53 (m, 3H), 3.51 - 3.42 (m, 1H), 3.41 - 3.33 (m, 1H), 3.27 (br. s, 2H), 3.22 - 3.14 (m, 0.5H), 2.69 (d, $J = 10.5$ Hz, 2H), 2.31 - 2.19 (m, 1H), 1.96 - 1.83 (m, 1H), 1.65 (t, $J = 10.5$ Hz, 2H), 1.42 (br. s, 4.5H), 1.37 (br. s, 4.5H), 1.04 (d, $J = 6.3$ Hz, 6H). Note that the NMR indicates the presence of rotamers (most likely due to the restricted rotation of the Boc group) hence the explanation for the reports of protons integrating for 0.5H.

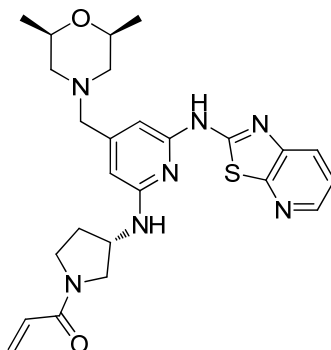
4-[[*cis*-2,6-Dimethyl-4-morpholinyl]methyl]-*N*'-[(3*S*)-3-pyrrolidinyl]-*N'*-[1,3]thiazolo[5,4-*b*]pyridin-2-yl-2,6-pyridinediamine dihydrochloride (116)



1,1-Dimethylethyl (3*S*)-3-{{4-[[*cis*-2,6-dimethyl-4-morpholinyl]methyl]-6-[[1,3]thiazolo[5,4-*b*]pyridin-2-ylamino)-2-pyridinyl]amino}-1-pyrrolidinecarboxylate **101i** (36.2 g, 67.1 mmol) was dissolved in dichloromethane (250 mL) and methanol (10 mL). The reaction mixture was stirred at 0 °C and HCl in dioxane (4M, 120 mL, 480 mmol) was added dropwise. The reaction mixture was stirred at room temperature for 16 hours. The yellow solid was filtered under reduced pressure, washed with dichloromethane (2 x 100 mL) and was dried in the oven for 16 hours at 40 °C to afford the title compound (37 g, 108 % yield). Note: the yield obtained was greater than 100 %. This was believed to be caused by the hygroscopicity of this salt (if left at room temperature under normal atmosphere, the solid becomes an oil overtime). **LCMS** (Method E) (ES +ve) m/z 440 ($M + H$)⁺ Rt 0.52 minutes. **¹H NMR** (400 MHz, DMSO-*d*₆) δ 11.79 (br. s, 1H), 9.64 (br. s, 1H), 9.37 (br. s, 1H), 8.45 (dd, $J = 1.0, 5.0$ Hz, 1H), 8.11 (d, $J = 8.1$ Hz, 1H), 7.55 (dd, $J = 5.0, 8.1$ Hz, 1H), 6.51 (s, 1H), 6.49 (s, 1H), 4.83 - 4.74 (m, 1H), 4.15 (br. s, 2H), 4.11 - 3.99 (m, 2H), 3.61 (d, $J = 6.0$ Hz, 1H), 3.45 - 3.34 (m, 2H), 3.31 (d, $J = 11.8$ Hz,

2H), 3.26 - 3.17 (m, 1H), 2.74 - 2.63 (m, 2H), 2.37 (d, $J = 6.9$ Hz, 1H), 2.09 - 1.99 (m, 1H), 1.12 (d, $J = 6.3$ Hz, 6H).

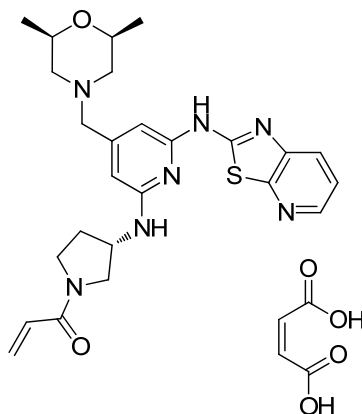
***N*-[*(3S)*-1-Acryloyl-3-pyrrolidinyl]-4-{*cis*-2,6-dimethyl-4-morpholinyl}methyl}-*N'*-[1,3]thiazolo[5,4-*b*]pyridin-2-yl-2,6-pyridinediamine (101)**



4-{*cis*-2,6-Dimethyl-4-morpholinyl}methyl}-*N*-[*(3S)*-3-pyrrolidinyl]-*N'*-[1,3]thiazolo[5,4-*b*]pyridin-2-yl-2,6-pyridinediamine dihydrochloride **116** (2.8 g, 5.5 mmol) was suspended in dichloromethane (10 mL). *N,N*-Diisopropylethylamine (3.34 mL, 19.1 mmol) was added and the suspension was stirred at 0 °C for 5 minutes. 2-Propenoyl chloride (0.488 mL, 6.01 mmol) was added dropwise and the reaction mixture was stirred at 0 °C for 30 minutes. The reaction mixture was partitioned between dichloromethane (30 mL) and water (30 mL). After separation, the organic extract was dried using a hydrophobic frit and concentrated under reduced pressure. The solid was recrystallised from acetonitrile (10 mL) (using a few drops of methanol to fully dissolve the material under heating) to afford the title compound (1.8 g, 67 % yield) as a white solid. **LCMS** (Method E) (ES +ve) m/z 494 ($M + H$)⁺ Rt 0.62 minutes. **¹H NMR** (400 MHz, DMSO-*d*₆) δ 11.29 (s, 1H), 8.27 (dd, $J = 1.1, 4.6$ Hz, 1H), 7.87 (d, $J = 8.2$ Hz, 1H), 7.36 (dd, $J = 4.6, 8.2$ Hz, 1H), 7.02 (d, $J = 6.8$ Hz, 0.5H), 6.97 (d, $J = 6.8$ Hz, 0.5H), 6.64 (dd, $J = 10.3, 16.8$ Hz, 0.5H), 6.53 (dd, $J = 10.3, 16.8$ Hz, 0.5H), 6.27 (s, 1H), 6.18 - 6.09 (m, 2H), 5.68 (dd, $J = 2.3, 10.3$ Hz, 0.5H), 5.61 (dd, $J = 2.3, 10.3$ Hz, 0.5H), 4.75 - 4.68 (m, 0.5H), 4.67 - 4.59 (m, 0.5H), 4.00 (dd, $J = 5.9, 10.4$ Hz, 0.5H), 3.81 - 3.67 (m, 1.5H), 3.65 - 3.45 (m, 4H), 3.28 (s, 2H), 2.70 (d, $J = 10.8$ Hz, 2H), 2.40 - 2.30 (m, 0.5H), 2.30 - 2.20 (m, 0.5H), 2.09 - 1.98 (m, 0.5H), 1.98 - 1.89 (m, 0.5H), 1.65 (t, $J = 10.5$ Hz, 2H), 1.04 (d, $J = 6.0$ Hz, 6H). Note that the ¹H NMR indicates the presence of rotamers (most likely due to the restricted rotation of the amide functionality) hence the explanation

for the reports of protons integrating for 0.5H. **IR** (cm^{-1}) 1523, 1574, 1611, 1630, 1652. **HRMS** (ES) calcd for $\text{C}_{25}\text{H}_{32}\text{N}_7\text{O}_2\text{S}$, $(\text{M} + \text{H})^+$ 494.2338, found 494.2333. **^{13}C NMR** (101 MHz, DMSO-d_6) δ 163.50, 163.45, 158.72, 157.17, 157.12, 155.53, 150.05, 149.91, 149.85, 143.02, 142.88, 129.69, 129.42, 126.61, 126.49, 124.89, 121.12, 101.27, 101.17, 97.84, 97.78, 70.95, 61.31, 61.29, 59.04, 52.12, 51.70, 51.53, 49.82, 44.49, 43.93, 31.73, 29.95, 18.91. Note that the ^{13}C NMR indicates the presence of rotamers. The data is reported with two decimal points to differentiate the signals. **Mp** = 217 °C. **HPLC** (Method A) Rt 1.77 minutes, 99.7 % pure. $[\alpha]_{\text{D}}^{20}$ = -112 (c = 1.031 in DMSO).

1-((S)-3-((4-((cis-2,6-Dimethyl-4-morpholino)methyl)-6-(thiazolo[5,4-b]pyridin-2-ylamino)pyridin-2-yl)amino)pyrrolidin-1-yl)prop-2-en-1-one, maleic acid salt (101a)



Maleic acid (0.249 g, 2.147 mmol) was added to a solution of 1-((S)-3-((4-((cis-2,6-dimethyl-4-morpholino)methyl)-6-(thiazolo[5,4-b]pyridin-2-ylamino)pyridin-2-yl)amino)pyrrolidin-1-yl)prop-2-en-1-one **100** (1.06 g, 2.15 mmol) in methanol (5 mL). The reaction was left standing in solution at room temperature for one hour. The solvent was concentrated under reduced pressure and the yellow solid was dried in the pistol apparatus at 35 °C under reduced pressure for 48 hours to give the title compound (1.3 g, 99 % yield). **LCMS** (Method D) (ES +ve) m/z 494 ($\text{M} + \text{H})^+$ Rt 0.91 minutes. **^1H NMR** (400 MHz, DMSO-d_6 , 120 °C) δ 8.27 (dd, J = 1.4, 4.7 Hz, 1H), 7.83 (dd, J = 1.4, 8.1 Hz, 1H), 7.33 (dd, J = 4.7, 8.1 Hz, 1H), 6.55 (dd, J = 10.3, 16.9 Hz, 1H), 6.42 (s, 1H), 6.22 (s, 1H), 6.18 (s, 2H), 6.12 (dd, J = 2.3, 16.9 Hz, 1H), 5.61 (dd, J = 2.3, 10.3 Hz, 1H), 4.71 (quin, J = 5.5 Hz, 1H), 3.98 - 3.88 (m, 1H), 3.78

- 3.58 (m, 4H), 3.52 - 3.47 (m, 3H), 2.86 (d, $J = 10.6$ Hz, 2H), 2.41 - 2.30 (m, 1H), 2.07 - 1.98 (m, 1H), 1.95 (t, $J = 10.8$ Hz, 2H), 1.10 (d, $J = 6.1$ Hz, 6H). **HPLC** (Method B) Rt 2.48 minutes, 99.4 % pure.

General procedure K for the Buchwald-Hartwig amination trial reactions – investigation of the reaction temperature.

A microwave vial was charged with *N*-[6-chloro-4-(4-morpholinylmethyl)-2-pyridinyl][1,3]thiazolo[5,4-*b*]pyridin-2-amine **72**, 1,1-dimethylethyl (3*S*)-3-amino-1-pyrrolidinecarboxylate and {1,3-bis[2,6-bis(1-methylethyl)phenyl]-2-imidazolidinyl}(chloro)(2-methyl-2-propen-1-yl)palladium **87**. The vial was sealed and placed under an atmosphere of nitrogen using a vacuum purge. LHMDS in tetrahydrofuran (1M, 3.6 equivalents) was added and the reaction was heated at the stated temperature for one hour. The advancement of the reaction was monitored by LCMS analysis (note that the % conversion refers to the formation of product relative to starting material. The % of impurities formed were not taken into account).

Data from Table 39:

Entry	72	Amine	87	LHMDS in THF (1M)	T (°C)	Conversion to 88 (%)^a
1	100 mg, 0.276 mmol	77 mg, 0.41 mmol	49 mg, 0.083 mmol	1 mL, 1 mmol	80	100
2	100 mg, 0.276 mmol	77 mg, 0.41 mmol	49 mg, 0.083 mmol	1 mL, 1 mmol	70	100
3	15 mg, 0.041 mmol	11.6 mg, 0.0623 mmol	7.3 mg, 0.012 mmol	150 μL, 0.150 mmol	50	100
4	20 mg, 0.055 mmol	15.4 mg, 0.0827 mmol	9.8 mg, 0.017 mmol	200 μL, 0.200 mmol	20	40 ^b
5	15 mg, 0.041 mmol	8.5 mg, 0.046 mmol	7.3 mg, 0.012 mmol	150 μL, 0.150 mmol	50	100

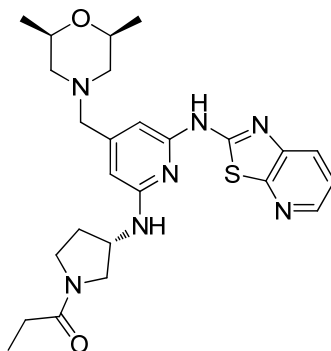
^a Determined by LCMS analysis; ^b 16 h reaction time

Data from Table 40:

Entry	72	Amine	87	LHMDS in THF (1M)	T (°C)	Conversion to 88 (%) ^a		
						1 h	3 h	18 h
1	15 mg, 0.041 mmol	11.6 mg, 0.0622 mmol	7.3 mg, 0.012 mmol	150 μL, 0.150 mmol	50	100	-	-
2	15 mg, 0.041 mmol	11.6 mg, 0.0622 mmol	4.8 mg, 0.0082 mmol	150 μL, 0.150 mmol	50	62	70 ^b	71 ^b
3	15 mg, 0.041 mmol	11.6 mg, 0.0622 mmol	2.4 mg, 0.0041 mmol	150 μL, 0.150 mmol	50	37	30 ^b	31 ^b

^a Determined by LCMS analysis; ^b more impurities observed

4-[[*cis*-2,6-Dimethyl-4-morpholinyl]methyl]-*N*-[(3*S*)-1-propanoyl-3-pyrrolidinyl]-*N'*-[1,3]thiazolo[5,4-*b*]pyridin-2-yl-2,6-pyridinediamine (117)



4-[[*cis*-2,6-Dimethyl-4-morpholinyl]methyl]-*N*-[(3*S*)-3-pyrrolidinyl]-*N'*-[1,3]thiazolo[5,4-*b*]pyridin-2-yl-2,6-pyridinediamine dihydrochloride **116** (1.0 g, 1.9 mmol) was suspended in dichloromethane (10 mL). The reaction was stirred at 0 °C and treated with *N,N*-diisopropylethylamine (1.6 mL, 9.2 mmol). Propionyl chloride (0.160 mL, 1.83 mmol) was added dropwise and the reaction was stirred at room temperature for 15 minutes. Water was added (10 mL). After separation, the organic extract was dried using a hydrophobic frit and concentrated under reduced pressure. The residue was recrystallised from acetonitrile (20 mL). The white suspension was filtered under reduced pressure. The product was purified by chromatography on

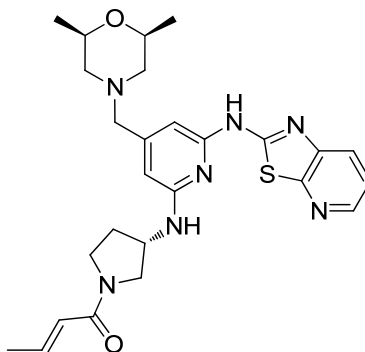
reverse phase (C18) using a gradient elution from 0 to 60 % acetonitrile (+ 0.1 % TFA) in water (+ 0.1 % TFA). The appropriate fractions were combined and evaporated under reduced pressure to remove the acetonitrile. The remaining aqueous phase was basified to pH 11 with concentrated ammonia solution. The product was extracted with dichloromethane (3 x 50 mL). The organic extracts were combined, dried using a hydrophobic frit and concentrated under reduced pressure to afford the title compound (620 mg, 64 % yield) as a white solid. **LCMS** (Method E) (ES +ve) m/z 496 (M + H)⁺ Rt 0.63 minutes. **¹H NMR** (400 MHz, DMSO-d₆, 120 °C) δ 10.79 (br. s, 1H), 8.26 (dd, J = 1.5, 4.7 Hz, 1H), 7.82 (dd, J = 1.5, 8.1 Hz, 1H), 7.32 (dd, J = 4.7, 8.1 Hz, 1H), 6.47 (d, J = 6.3 Hz, 1H), 6.39 (s, 1H), 6.20 (s, 1H), 4.75 - 4.62 (m, 1H), 3.95 - 3.75 (m, 1H), 3.69 - 3.57 (m, 3H), 3.57 - 3.47 (m, 1H), 3.39 (dd, J = 4.8, 11.1 Hz, 1H), 3.34 (s, 2H), 2.75 - 2.70 (m, 2H), 2.37 - 2.30 (m, 1H), 2.26 (q, J = 7.3 Hz, 2H), 2.04 - 1.92 (m, 1H), 1.74 (t, J = 10.7 Hz, 2H), 1.07 (d, J = 6.0 Hz, 6H), 1.05 (t, J = 7.3 Hz, 3H). **HPLC** (Method B) Rt 2.33 minutes, 99.8 % pure.

General procedure L for the amide coupling with acid chlorides (Scheme 51):

4- $\{[cis-2,6-Dimethyl-4-morpholinyl]methyl\}$ - N - $[(3S)-3-pyrrolidinyl]$ - N' - $[1,3]thiazolo[5,4-b]pyridin-2-yl$ -2,6-pyridinediamine dihydrochloride **116** (75 mg, 0.15 mmol) was suspended in N -methyl-2-pyrrolidinone (0.6 mL) and stirred at room temperature. N,N -diisopropylethylamine (0.077 mL, 0.44 mmol) was added followed by the acid chloride. The reaction was stirred for 30 minutes. The mixture was purified by mass directed automated preparative HPLC to afford the title compound.

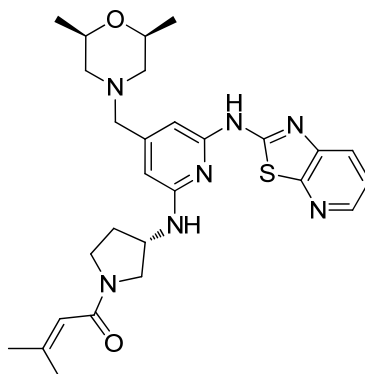
Following the general procedure L for the preparation of compounds **118** and **119**, data are presented as (a) amount of acid chloride.

***N*-{(3*S*)-1-[(2*E*)-2-Butenoyl]-3-pyrrolidinyl}-4-[[*cis*-2,6-dimethyl-4-morpholinyl]methyl]-*N'*-[1,3]thiazolo[5,4-*b*]pyridin-2-yl-2,6-pyridinediamine (118)**



(a) *Trans*-crotonyl chloride (0.014 mL, 0.15 mmol). Brown solid. Yield: 45 mg, 61 %. **LCMS** (Method E) (ES +ve) m/z 508 ($M + H$)⁺ Rt 0.65 minutes. **¹H NMR** (400 MHz, DMSO-*d*₆, 120 °C) δ 10.81 (br. s, 1H), 8.26 (dd, $J = 1.5, 4.5$ Hz, 1H), 7.82 (dd, $J = 1.5, 8.1$ Hz, 1H), 7.32 (dd, $J = 4.5, 8.1$ Hz, 1H), 6.69 (dq, $J = 6.8, 15.1$ Hz, 1H), 6.49 (d, $J = 6.8$ Hz, 1H), 6.39 (s, 1H), 6.24 (d, $J = 15.1$ Hz, 1H), 6.20 (s, 1H), 4.74 - 4.66 (m, 1H), 3.95 - 3.85 (m, 1H), 3.73 - 3.55 (m, 4H), 3.46 (dd, $J = 4.8, 11.3$ Hz, 1H), 3.34 (s, 2H), 2.76 - 2.70 (m, 2H), 2.38 - 2.27 (m, 1H), 2.04 - 1.93 (m, 1H), 1.83 (d, $J = 6.8$ Hz, 3H), 1.74 (t, $J = 10.7$ Hz, 2H), 1.07 (d, $J = 6.0$ Hz, 6H). **IR** (cm⁻¹) 1520, 1574, 1605, 1627, 1659. **HRMS** (ES) calcd for C₂₆H₃₄N₇O₂S, ($M + H$)⁺ 508.2489, found 508.2474. **¹³C NMR** (126 MHz, DMSO-*d*₆) δ 164.23, 164.21, 159.20, 157.69, 157.63, 156.02, 156.00, 150.54, 150.52, 150.40, 150.33, 143.52, 143.38, 143.37, 140.25, 140.19, 125.41, 124.11, 123.92, 121.65, 101.76, 101.68, 98.29, 98.21, 71.46, 61.82, 61.79, 59.53, 52.61, 52.11, 52.05, 50.35, 44.90, 44.34, 32.24, 30.42, 19.43, 18.13, 18.02. Note that the ¹³C NMR indicates the presence of rotamers. The data is reported with two decimal points to differentiate the signals. Decomposition temperature 171 °C.

4-{{cis-2,6-Dimethyl-4-morpholinyl}methyl}-N-[(3S)-1-(3-methyl-2-butenoyl)-3-pyrrolidinyl]-N'-[1,3]thiazolo[5,4-*b*]pyridin-2-yl-2,6-pyridinediamine (119)



(a) 3,3-Dimethylacryloyl chloride (0.016 mL, 0.15 mmol). Brown solid. Yield: 60 mg, 79 %. **LCMS** (Method E) (ES +ve) m/z 522 ($M + H$)⁺ Rt 0.70 minutes. **¹H NMR** (400 MHz, DMSO-*d*₆, 120 °C) δ 10.79 (br. s, 1H), 8.26 (dd, $J = 1.5, 4.8$ Hz, 1H), 7.82 (dd, $J = 1.5, 8.1$ Hz, 1H), 7.32 (dd, $J = 4.8, 8.1$ Hz, 1H), 6.48 (d, $J = 6.8$ Hz, 1H), 6.38 (s, 1H), 6.20 (s, 1H), 5.87 (br. s, 1H), 4.72 - 4.64 (m, 1H), 3.91 - 3.82 (m, 1H), 3.69 - 3.59 (m, 3H), 3.57 - 3.49 (m, 1H), 3.40 (dd, $J = 4.9, 11.2$ Hz, 1H), 3.34 (s, 2H), 2.75 - 2.70 (m, 2H), 2.37 - 2.26 (m, 1H), 1.99 (ddd, 3H), 1.98 - 1.92 (m, 1H), 1.81 (s, 3H), 1.74 (t, $J = 10.7$ Hz, 2H), 1.07 (d, $J = 6.3$ Hz, 6H). **IR** (cm^{-1}) 1521, 1574, 1594, 1628. **HRMS** (ES) calcd for C₂₇H₃₆N₇O₂S, ($M + H$)⁺ 522.2646, found 522.2640. **¹³C NMR** (126 MHz, DMSO-*d*₆) δ 165.63, 165.59, 159.21, 159.20, 157.70, 157.66, 156.03, 156.00, 150.54, 150.52, 150.37, 150.31, 148.92, 148.48, 143.52, 143.37, 143.35, 125.40, 121.65, 121.63, 118.43, 118.12, 101.76, 101.68, 98.29, 98.20, 71.45, 61.82, 61.79, 59.53, 52.98, 52.07, 51.84, 50.39, 45.25, 44.02, 32.34, 30.45, 27.10, 26.89, 20.18, 19.41. Note that the ¹³C NMR indicates the presence of rotamers. The data is reported with two decimal points to differentiate the signals. Decomposition temperature 148 °C.

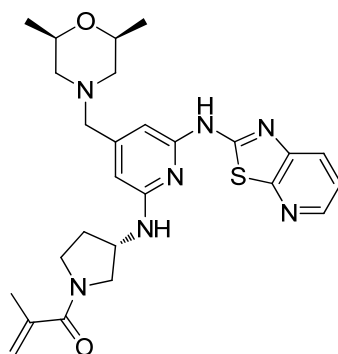
General procedure M for the amide coupling with acids and CDI (Scheme 51):

The carboxylic acid and CDI (63 mg, 0.39 mmol) were dissolved in *N*-methyl-2-pyrrolidinone (0.5 mL) and stirred at room temperature for 15 minutes. 4-{{cis-2,6-Dimethyl-4-morpholinyl}methyl}-N-[(3S)-3-pyrrolidinyl]-N'-[1,3]thiazolo[5,4-*b*]pyridin-2-yl-2,6-pyridinediamine dihydrochloride (100 mg, 0.195 mmol) was suspended in *N*-methyl-2-pyrrolidinone (0.6 mL) and stirred at room temperature.

N,N-Diisopropylethylamine (0.102 mL, 0.585 mmol) was added. This solution was added to the mixture of acid and CDI and the reaction was stirred at room temperature for 30 minutes. The mixture was purified by mass directed automated preparative HPLC to afford the title compound.

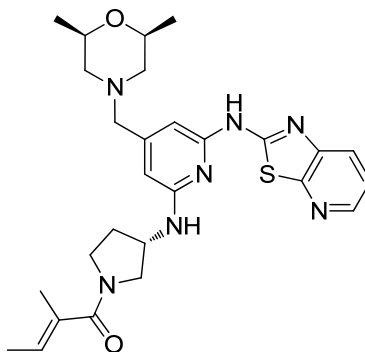
Following the general procedure M for the preparation of compounds **120** and **121**, data are presented as (a) amount of carboxylic acid.

4-[[*cis*-2,6-Dimethyl-4-morpholinyl]methyl]-*N*-[(3*S*)-1-(2-methylacryloyl)-3-pyrrolidinyl]-*N'*-[1,3]thiazolo[5,4-*b*]pyridin-2-yl-2,6-pyridinediamine (120)



(a) 2-Methyl-2-propenoic acid (34 mg, 0.40 mmol). White solid. Yield: 46 mg, 46 %. **LCMS** (Method D) (ES +ve) m/z 508 ($M + H$)⁺ Rt 0.95 minutes. **¹H NMR** (400 MHz, DMSO-*d*₆, 120 °C) δ 10.71 (br. s, 1H), 8.26 (d, $J = 4.5$ Hz, 1H), 7.81 (d, $J = 8.1$ Hz, 1H), 7.32 (dd, $J = 4.5, 8.1$ Hz, 1H), 6.44 (d, $J = 6.0$ Hz, 1H), 6.39 (s, 1H), 6.20 (s, 1H), 5.19 (br. s, 1H), 5.14 (br. s, 1H), 4.71 - 4.63 (m, 1H), 3.90 (dd, $J = 6.0, 11.3$ Hz, 1H), 3.72 - 3.59 (m, 3H), 3.58 - 3.51 (m, 1H), 3.43 (dd, $J = 4.7, 11.3$ Hz, 1H), 3.34 (s, 2H), 2.72 (d, $J = 11.3$ Hz, 2H), 2.38 - 2.26 (m, 1H), 2.03 - 1.92 (m, 1H), 1.88 (s, 3H), 1.75 (t, $J = 10.3$ Hz, 2H), 1.07 (d, $J = 6.0$ Hz, 6H). **IR** (cm⁻¹) 1521, 1575, 1604, 1627, 1652. **HRMS** (ES) calcd for C₂₆H₃₄N₇O₂S, ($M + H$)⁺ 508.2489, found 508.2484. **¹³C NMR** (126 MHz, DMSO-*d*₆) δ 169.93, 159.21, 159.07, 157.68, 156.03, 155.94, 150.51, 150.36, 143.49, 143.41, 141.89, 141.67, 125.43, 121.68, 116.45, 116.40, 101.75, 101.69, 98.32, 98.26, 71.46, 61.81, 59.52, 54.64, 52.04, 51.76, 50.48, 47.04, 44.07, 32.52, 30.27, 20.29, 20.16, 19.43. Note that the ¹³C NMR indicates the presence of rotamers. The data is reported with two decimal points to differentiate the signals. Decomposition temperature 149 °C.

4-{{cis-2,6-Dimethyl-4-morpholinyl}methyl}-N-{{(3S)-1-[(2E)-2-methyl-2-butenoyl]-3-pyrrolidinyl}-N'-[1,3]thiazolo[5,4-b]pyridin-2-yl-2,6-pyridinediamine (121)



(a) Tiglic acid (39 mg, 0.39 mmol). White solid. Yield: 51 mg, 50 %. **LCMS** (Method D) (ES +ve) m/z 522 (M + H)⁺ Rt 0.99 minutes. **¹H NMR** (400 MHz, DMSO-*d*₆, 120 °C) δ 10.52 (br. s, 1H), 8.26 (dd, J = 1.3, 4.8 Hz, 1H), 7.82 (dd, J = 1.3, 8.1 Hz, 1H), 7.32 (dd, J = 4.8, 8.1 Hz, 1H), 6.42 (d, J = 6.8 Hz, 1H), 6.39 (s, 1H), 6.20 (s, 1H), 5.74 (qd, J = 1.5, 6.8 Hz, 1H), 4.65 (sxt, J = 6.1 Hz, 1H), 3.88 (dd, J = 6.3, 11.6 Hz, 1H), 3.69 - 3.60 (m, 3H), 3.57 - 3.49 (m, 1H), 3.39 (dd, J = 5.0, 11.6 Hz, 1H), 3.34 (s, 2H), 2.73 (d, J = 10.6 Hz, 2H), 2.36 - 2.26 (m, 1H), 2.00 - 1.91 (m, 1H), 1.79 - 1.71 (m, 5H), 1.63 (d, J = 6.8 Hz, 3H), 1.07 (d, J = 6.3 Hz, 6H). **IR** (cm⁻¹) 1522, 1574, 1599, 1627. **HRMS** (ES) calcd for C₂₇H₃₆N₇O₂S, (M + H)⁺ 522.2646, found 522.2640. **¹³C NMR** (126 MHz, DMSO-*d*₆) δ 171.2, 159.1, 157.7, 156.0, 150.5, 150.3, 143.5, 143.4, 133.6, 133.3, 126.4, 126.3, 125.4, 121.6, 101.7, 98.3, 71.4, 61.8, 59.5, 54.7, 52.1, 51.7, 50.5, 47.2, 44.1, 32.5, 30.3, 19.4, 13.9, 13.6, 13.4. Note that the ¹³C NMR indicates the presence of rotamers. Decomposition temperature 155 °C.

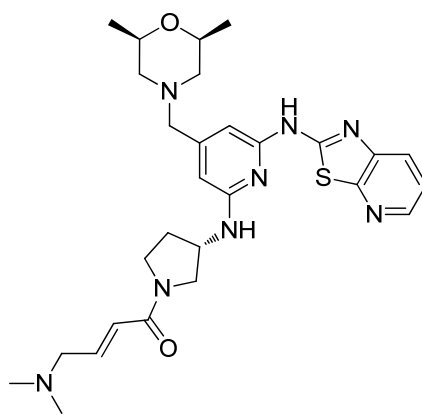
General procedure N for the amide coupling with acids and HATU (Scheme 51):

The carboxylic acid was suspended in *N*-methyl-2-pyrrolidinone (1 mL). HATU (111 mg, 0.293 mmol) was added and the solution was stirred at room temperature for 10 minutes. A solution of 4-{{cis-2,6-Dimethyl-4-morpholinyl}methyl}-N-{{(3S)-3-pyrrolidinyl}-N'-[1,3]thiazolo[5,4-b]pyridin-2-yl-2,6-pyridinediamine dihydrochloride **116** (100 mg, 0.195 mmol) and *N,N*-diisopropylethylamine (0.204

mL, 1.17 mmol) in *N*-methyl-2-pyrrolidinone (1 mL) was added to the previous acid and HATU solution and the reaction was stirred at room temperature for 3 hours. The mixture was purified by mass directed automated preparative HPLC to afford the title compound.

Following the general procedure N for the preparation of compounds **122** and **123**, data are presented as (a) amount of carboxylic acid.

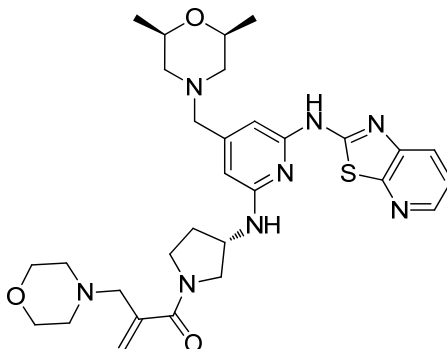
***N*-{(3*S*)-1-[(2*E*)-4-(Dimethylamino)-2-butenoyl]-3-pyrrolidinyl}-4-[[*cis*-2,6-dimethyl-4-morpholinyl]methyl]-*N'*-[1,3]thiazolo[5,4-*b*]pyridin-2-yl-2,6-pyridinediamine (**122**)**



(a) (*E*)-4-(Dimethylamino)but-2-enoic acid hydrochloride **53** (36 mg, 0.22 mmol). Brown solid. Yield: 49 mg, 46 %. **LCMS** (Method D) (ES +ve) m/z 551 ($M + H$)⁺ Rt 0.90 minutes. **¹H NMR** (400 MHz, DMSO-*d*₆, 120 °C) δ 8.24 (dd, $J = 1.3, 4.7$ Hz, 1H), 7.81 (dd, $J = 1.3, 8.0$ Hz, 1H), 7.31 (dd, $J = 4.7, 8.0$ Hz, 1H), 6.63 (dt, $J = 6.1, 15.4$ Hz, 1H), 6.45 (d, $J = 6.1$ Hz, 1H), 6.39 (s, 1H), 6.33 (d, $J = 15.4$ Hz, 1H), 6.19 (s, 1H), 4.74 - 4.66 (m, 1H), 3.98 - 3.87 (m, 1H), 3.76 - 3.55 (m, 4H), 3.47 (dd, $J = 4.5, 11.1$ Hz, 1H), 3.34 (s, 2H), 3.03 (d, $J = 5.5$ Hz, 2H), 2.73 (d, $J = 11.1$ Hz, 2H), 2.39 - 2.28 (m, 1H), 2.18 (s, 6H), 2.05 - 1.95 (m, 1H), 1.74 (t, $J = 10.6$ Hz, 2H), 1.07 (d, $J = 6.3$ Hz, 6H). **IR** (cm⁻¹) 1523, 1575, 1627, 1660. **HRMS** (ES) calcd for C₂₈H₃₉N₈O₂S, ($M + H$)⁺ 551.2911, found 551.2888. **¹³C NMR** (126 MHz, DMSO-*d*₆) δ 164.01, 163.93, 159.20, 159.18, 157.67, 157.63, 156.02, 155.98, 150.56, 150.54, 150.39, 150.33, 143.53, 143.51, 143.37, 141.84, 141.63, 125.40, 124.23, 123.98, 121.65, 101.77, 101.68, 98.32, 98.23, 71.46, 61.82, 61.79, 60.36, 60.21, 59.54, 52.68, 52.20, 52.04, 50.34, 45.57, 45.41, 44.99, 44.38, 32.24, 30.38, 19.43. Note that the ¹³C

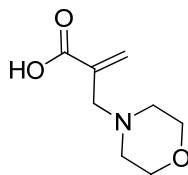
NMR indicates the presence of rotamers. The data is reported with two decimal points to differentiate the signals. Decomposition temperature 147 °C.

4-[[*cis*-2,6-Dimethyl-4-morpholinyl]methyl]-*N*-{(3*S*)-1-[2-(4-morpholinylmethyl)acryloyl]-3-pyrrolidinyl]-*N'*-[1,3]thiazolo[5,4-*b*]pyridin-2-yl-2,6-pyridinediamine (123)



(a) 2-(4-Morpholinylmethyl)-2-propenoic acid **124** (37 mg, 0.22 mmol). Brown solid. Yield: 51 mg, 44 %. **LCMS** (Method D) (ES +ve) m/z 593 (M + H)⁺ Rt 0.89 minutes. **¹H NMR** (400 MHz, DMSO-*d*₆, 120 °C) δ 10.73 (br. s, 1H), 8.26 (dd, $J = 1.4, 4.7$ Hz, 1H), 7.82 (dd, $J = 1.4, 8.2$ Hz, 1H), 7.32 (dd, $J = 4.7, 8.2$ Hz, 1H), 6.41 (d, $J = 6.8$ Hz, 1H), 6.39 (s, 1H), 6.21 (s, 1H), 5.36 (s, 1H), 5.30 (s, 1H), 4.71 - 4.62 (m, 1H), 3.89 (dd, $J = 6.0, 11.3$ Hz, 1H), 3.75 - 3.54 (m, 4H), 3.54 - 3.49 (m, 4H), 3.49 - 3.46 (m, 1H), 3.34 (s, 2H), 3.15 (d, $J = 14.1$ Hz, 1H), 3.10 (d, $J = 14.1$ Hz, 1H), 2.73 (d, $J = 10.3$ Hz, 2H), 2.41 - 2.36 (m, 4H), 2.36 - 2.28 (m, 1H), 2.03 - 1.93 (m, 1H), 1.75 (t, $J = 10.6$ Hz, 2H), 1.07 (d, $J = 6.3$ Hz, 6H). **IR** (cm⁻¹) 1521, 1575, 1626. **HRMS** (ES) calcd for C₃₀H₄₁N₈O₃S, (M + H)⁺ 593.3017, found 593.3003. **¹³C NMR** (126 MHz, DMSO-*d*₆) δ 169.24, 169.07, 159.22, 159.10, 157.69, 157.67, 156.03, 155.95, 150.54, 150.52, 150.35, 143.51, 143.39, 142.69, 142.44, 125.42, 121.68, 121.64, 118.04, 117.91, 101.73, 98.27, 71.46, 71.43, 66.68, 66.31, 61.83, 61.28, 61.10, 59.53, 59.48, 55.00, 53.81, 53.71, 52.07, 51.78, 50.47, 46.96, 44.27, 32.52, 30.03, 19.42, 19.40, 19.38. Note that the ¹³C NMR indicates the presence of rotamers. The data is reported with two decimal points to differentiate the signals. Decomposition temperature 157 °C.

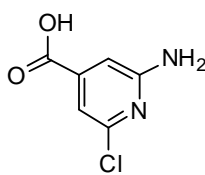
2-(4-Morpholinylmethyl)-2-propenoic acid (124)



Morpholine (8.74 mL, 100 mmol) was added to a stirred solution of malonic acid (10.4 g, 100 mmol) and paraformaldehyde (6.60 g, 220 mmol) in ethanol (150 mL) at room temperature. The suspension was heated under reflux conditions for 3 hours. The solvent was removed under reduced pressure. The oily residue was left standing at room temperature for 48 hours but no crystallisation occurred. The product was purified by chromatography on silica using isocratic elution of methanol in dichloromethane (5 % followed by 20 %) to afford the title compound (8.4 g, 49 % yield) as a white solid. $^1\text{H NMR}$ (400 MHz, CDCl_3) δ 10.68 (br. s, 1H), 6.37 (s, 1H), 5.62 (d, $J = 1.3$ Hz, 1H), 3.78 (t, $J = 4.5$ Hz, 4H), 3.37 (s, 2H), 2.67 (br. s, 4H). **Mp** = 122 °C (Note that literature reference **Mp** = 106-107 °C¹⁸⁴ and 121-125 °C.¹⁸⁵ The melting point obtained for this compound was closer to the second reference which also purified the product by column chromatography).

8. Synthetic procedures for the synthesis of compound 107 for toxicology assessment

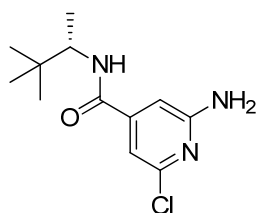
2-Amino-6-chloro-4-pyridinecarboxylic acid (126)



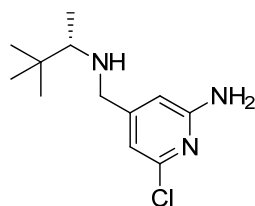
2,6-Dichloro-4-pyridinecarboxylic acid (50 g, 0.26 mol) was placed in a stainless steel autoclave and treated with concentrated ammonia (150 ml, 7.75 mol). The vessel was sealed and heated at 165 °C for 16 hours (pressure 17 bar). The solvent was removed under reduced pressure. The residue was suspended in water (1.2 L) and stirred at room temperature. Concentrated aqueous HCl was added dropwise to reach pH 3. The white suspension was filtered under reduced pressure and the solid

was dried in the oven under reduced pressure (60 °C - 48 hours) to afford the title compound (43 g, 96 % yield) as an off-white solid. **LCMS** (Method A) (ES +ve) m/z 173 (M + H)⁺ Rt 0.53 minutes. **¹H NMR** (400 MHz, DMSO-d₆) δ 6.89 (s, 1H), 6.81 (s, 1H), 6.71 (br. s, 2H). **IR** (cm⁻¹) 1549, 1634, 1686. **HRMS** (ES) calcd for C₆H₆ClN₂O₂, (M + H)⁺ 173.0118, found 173.0119. **¹³C NMR** (101 MHz, DMSO-d₆) δ 165.5, 160.6, 149.0, 142.1, 108.9, 106.7. **Mp** = 297 °C.

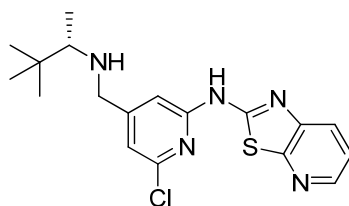
2-Amino-6-chloro-N-[(1S)-1,2,2-trimethylpropyl]-4-pyridinecarboxamide (127)



2-Amino-6-chloro-4-pyridinecarboxylic acid (intermediate 27) (10 g, 58 mmol) was suspended in tetrahydrofuran (180 ml) and *N,N*-dimethylformamide (20 ml). 1,1'-carbonyldiimidazole (11.3 g, 69.7 mmol) was added and the reaction was stirred at room temperature for 2.5 h. (2S)-3,3-dimethyl-2-butanamine (8.14 ml, 60.8 mmol) was added and stirring was continued overnight. The reaction was quenched with water (200 ml) and the product extracted with ethyl acetate (200 ml). The aqueous phase was further extracted with ethyl acetate (200 ml) and the combined organics were washed with saturated sodium carbonate solution (2 x 200 ml) followed by water (3 x 200 ml), and brine (2 x 200 ml). The organic phase was dried over magnesium sulphate and concentrated under reduced pressure. The solid was dried under reduced pressure in the oven to afford the title compound (11.5 g, 78 % yield) as a white solid. **LCMS** (Method A) (ES +ve) m/z 256 (M + H)⁺ Rt 0.90 minutes. **¹H NMR** (400 MHz, DMSO-d₆) δ 8.09 (d, *J* = 9.3 Hz, 1H), 6.82 (d, *J* = 1.0 Hz, 1H), 6.70 (d, *J* = 1.0 Hz, 1H), 6.58 (s, 2H), 3.96 - 3.85 (m, 1H), 1.05 (d, *J* = 6.8 Hz, 3H), 0.88 (s, 9H). **IR** (cm⁻¹) 1535, 1622. **HRMS** (ES) calcd for C₁₂H₁₉ClN₃O, (M + H)⁺ 256.1217, found 256.1227. **¹³C NMR** (101 MHz, DMSO-d₆) δ 164.2, 160.2, 148.5, 146.6, 107.9, 105.2, 52.4, 34.7, 26.3, 15.3. **Mp** = 168 °C. [α]_D²⁰ = -6 (c = 1.000 in DMSO).

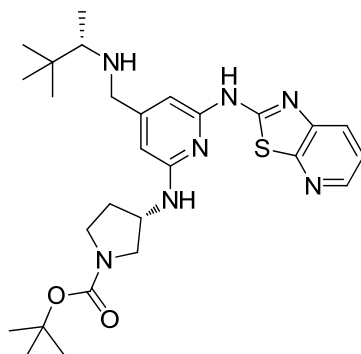
6-Chloro-4-([(1*S*)-1,2,2-trimethylpropyl]amino)methyl)-2-pyridinamine (128)

Borane in tetrahydrofuran (1 M, 860 mL, 860 mmol) was added dropwise to a solution of 2-amino-6-chloro-*N*-[(1*S*)-1,2,2-trimethylpropyl]-4-pyridinecarboxamide **127** (55.0 g, 215 mmol) in dichloromethane (100 mL) stirring at 0 °C. The reaction mixture was warmed to room temperature and stirred under an atmosphere of nitrogen for 48 hours. The reaction was then heated at 40 °C for 24 hours and left standing in solution for 72 hours. The reaction was cooled to 0 °C. Aqueous HCl (5 M, 200 mL) was added and the reaction was stirred for 3 hours. Sodium hydroxide (12 M) was then carefully added to reach pH 12. The product was extracted with dichloromethane (2 x 500 mL). The organic extracts were combined, dried using a hydrophobic frit and evaporated under reduced pressure. The product was purified by chromatography on silica using a gradient elution from 0 to 50 % ethyl acetate (+ 1 % triethylamine) in dichloromethane to afford the title compound as an off-white solid (35 g, 67 % yield). **LCMS** (Method D) (ES +ve) *m/z* 242 (*M* + *H*)⁺ *Rt* 1.13 minutes. **¹H NMR** (400 MHz, DMSO-*d*₆) δ 6.51 (s, 1H), 6.37 (s, 1H), 6.22 (br. s., 2H), 3.68 (d, *J* = 15.1 Hz, 1H), 3.45 (d, *J* = 15.1 Hz, 1H), 2.17 - 2.08 (m, 1H), 1.58 (br. s, 1H), 0.92 (d, *J* = 6.3 Hz, 3H), 0.86 (s, 9H). **IR** (cm⁻¹) 1540, 1604, 1625. **HRMS** (ES) calcd for C₁₂H₂₁ClN₃, (*M* + *H*)⁺ 242.1419, found 242.1414. **¹³C NMR** (101 MHz, DMSO-*d*₆) δ 159.9, 155.2, 148.1, 109.9, 105.2, 60.5, 50.3, 34.3, 26.4, 14.3. **Mp** = 95 °C. [α]_D²⁰ = +55 (*c* = 1.023 in DMSO).

***N*-[6-Chloro-4-([(1*S*)-1,2,2-trimethylpropyl]amino)methyl)-2-pyridinyl][1,3]thiazolo[5,4-*b*]pyridin-2-amine (129)**

A solution of 6-chloro-4-({[(1*S*)-1,2,2-trimethylpropyl]amino}methyl)-2-pyridinamine (28.0 g, 116 mmol) and 2-bromothiazolo[5,4-*b*]pyridine **128** (27.4 g, 127 mmol) in tetrahydrofuran (300 mL) was added to a solution of sodium *tert*-butoxide (34.5 g, 359 mmol) in tetrahydrofuran (250 mL), while keeping the temperature lower than 10 °C. The reaction was allowed to warm to room temperature over one hour. Saturated ammonium chloride (200 mL) and water (50 mL) were added and the aqueous phase was extracted with 2-methyltetrahydrofuran (2 x 50 mL). The combined organics were dried over magnesium sulfate, filtered and concentrated under reduced pressure. The solid was triturated with diethyl ether (200 mL) and the resultant precipitate collected by filtration, washed with diethyl ether and dried under reduced pressure to give the title compound (34.4 g, 79 % yield) as an off-white solid. **LCMS** (Method D) (ES +ve) *m/z* 376 (*M* + *H*)⁺ *Rt* 1.40 minutes. **¹H NMR** (400 MHz, DMSO-*d*₆) δ 8.36 (dd, *J* = 1.4, 4.8 Hz, 1H), 7.95 (dd, *J* = 1.4, 8.2 Hz, 1H), 7.42 (dd, *J* = 4.8, 8.2 Hz, 1H), 7.26 (s, 1H), 7.12 (s, 1H), 3.86 (d, *J* = 15.6 Hz, 1H), 3.65 (d, *J* = 15.6 Hz, 1H), 2.16 (q, *J* = 6.5 Hz, 1H), 0.94 (d, *J* = 6.5 Hz, 3H), 0.88 (s, 9H). **IR** (cm⁻¹) 1531, 1571, 1622. **HRMS** (ES) calcd for C₁₈H₂₃ClN₅S, (*M* + *H*)⁺ 376.1363, found 376.1367. **¹³C NMR** (101 MHz, DMSO-*d*₆) δ 158.5, 157.6, 155.2, 151.3, 146.8, 143.8, 142.7, 125.7, 121.4, 116.1, 108.8, 60.8, 50.1, 34.4, 26.5, 14.4. **Mp** = 210 °C. [α]_D²⁰ = +47 (*c* = 1.002 in DMSO).

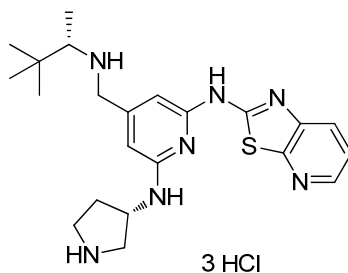
1,1-Dimethylethyl (3*S*)-3-{{6-([1,3]thiazolo[5,4-*b*]pyridin-2-ylamino)-4-({[(1*S*)-1,2,2-trimethylpropyl]amino}methyl)-2-pyridinyl]amino}-1-pyrrolidinecarboxylate (130**)**



A round-bottomed flask was charged with 1,1-dimethylethyl (3*S*)-3-amino-1-pyrrolidinecarboxylate (8.18 g, 43.9 mmol), *N*-[6-chloro-4-({[(1*S*)-1,2,2-

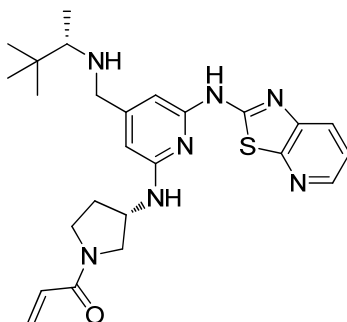
trimethylpropyl]amino)methyl)-2-pyridinyl][1,3]thiazolo[5,4-*b*]pyridin-2-amine **129** (15 g, 40 mmol) and tetrahydrofuran (130 mL) and equipped with a dropping funnel. The reaction apparatus was sealed and the reaction was placed under strict atmosphere of nitrogen by purging with nitrogen via vacuum. The reaction mixture was heated at 50 °C. A solution of LHMDS in tetrahydrofuran (1M, 120 mL, 120 mmol) was added a solution of {1,3-bis[2,6-bis(1-methylethyl)phenyl]-2-imidazolidinyl}(chloro)(2-methyl-2-propen-1-yl)palladium **87** (7.05 g, 12.0 mmol) in tetrahydrofuran (50 mL) placed in the dropping funnel. This orange solution was added dropwise over 20 minutes. The reaction was heated at 50 °C under nitrogen atmosphere for 20 minutes. The reaction was cooled to room temperature. Water (100 mL) was added and the aqueous phase was extracted with 2-methyltetrahydrofuran (2 x 100 mL). The combined organics were dried over magnesium sulfate, filtered using a celite pad and concentrated to a brown solid. The solid was dissolved in dichloromethane (70 mL). The brown compound first went into solution but a beige solid precipitated after 5 minutes stirring at room temperature. Diethyl ether (150 mL) was added and the suspension stirred in an ice bath for one hour. The solid was collected by filtration under reduced pressure, washed with cold diethyl ether and dried under reduced pressure to afford the title compound (13.6 g, 65 % yield) as an off-white solid. **LCMS** (Method D) (ES +ve) m/z 526 (M + H)⁺ Rt 1.34 minutes. **¹H NMR** (400 MHz, DMSO-*d*₆, 120 °C) δ 8.25 (dd, *J* = 1.3, 4.5 Hz, 1H), 7.81 (dd, *J* = 1.3, 8.1 Hz, 1H), 7.31 (dd, *J* = 4.5, 8.1 Hz, 1H), 6.42 (s, 1H), 6.32 (d, *J* = 6.8 Hz, 1H), 6.23 (s, 1H), 4.68 - 4.59 (m, 1H), 3.77 - 3.71 (m, 2H), 3.58 - 3.47 (m, 2H), 3.44 - 3.36 (m, 1H), 3.25 (dd, *J* = 5.0, 11.1 Hz, 1H), 2.32 (q, *J* = 6.6 Hz, 1H), 2.29 - 2.24 (m, 1H), 1.97 - 1.87 (m, 1H), 1.44 (s, 9H), 1.01 (d, *J* = 6.3 Hz, 3H), 0.92 (s, 9H). **IR** (cm⁻¹) 1523, 1576, 1629, 1668. **HRMS** (ES) calcd for C₂₇H₄₀N₇O₂S, (M + H)⁺ 526.2947, found 526.2959. **¹³C NMR** (101 MHz, DMSO-*d*₆) δ 158.83, 157.10, 155.54, 153.60, 149.81, 143.07, 142.77, 124.77, 121.10, 100.49, 97.40, 78.22, 60.66, 51.92, 51.72, 51.22, 51.04, 51.01, 50.46, 44.21, 43.96, 34.34, 31.45, 30.56, 28.17, 28.14, 26.50, 14.34. **¹³C NMR** at room temperature displays the presence of rotamers for the compound. **Mp** = 206 °C. [α]_D²⁰ = -80 (c = 1.040 in DMSO).

***N*-[(3*S*)-3-Pyrrolidinyl]-*N'*-[1,3]thiazolo[5,4-*b*]pyridin-2-yl-4-([(1*S*)-1,2,2-trimethylpropyl]amino)methyl)-2,6-pyridinediamine trihydrochloride (**131**)**



1,1-Dimethylethyl (3*S*)-3-{{6-([1,3]thiazolo[5,4-*b*]pyridin-2-ylamino)-4-([(1*S*)-1,2,2-trimethylpropyl]amino)methyl)-2-pyridinyl]amino}-1-pyrrolidinecarboxylate **130** (12.0 g, 22.8 mmol) was dissolved in dichloromethane (80 mL) and methanol (60 mL) and treated with HCl in dioxane (4 M, 110 mL, 440 mmol). After stirring at room temperature for 48 hours, the solid was filtered under reduced pressure, washed with dichloromethane, dried under reduced pressure in the oven to afford the title compound (11.44 g, 94 % yield) as a yellow solid. **LCMS** (Method E) (ES +ve) *m/z* 426 (M + H)⁺ Rt 0.58 minutes. **¹H NMR** (400 MHz, DMSO-*d*₆) δ 9.74 (br. s, 1H), 9.65 (br. s, 1H), 9.44 (br. s, 1H), 8.49 (d, *J* = 5.1 Hz, 1H), 8.37 (br. s, 1H), 8.15 (d, *J* = 8.0 Hz, 1H), 7.58 (dd, *J* = 5.1, 8.2 Hz, 1H), 6.52 (s, 1H), 6.47 (s, 1H), 4.83 - 4.75 (m, 1H), 4.15 (d, *J* = 13.8 Hz, 1H), 4.04 - 3.95 (m, 1H), 3.66 - 3.56 (m, 1H), 3.45 - 3.30 (m, 2H), 3.23 - 3.16 (m, 1H), 2.77 - 2.67 (m, 1H), 2.43 - 2.32 (m, 1H), 2.08 - 1.98 (m, 1H), 1.20 (d, *J* = 6.8 Hz, 3H), 0.96 (s, 9H). **IR** (cm⁻¹) 1526, 1557, 1582, 1631. **HRMS** (ES) calcd for C₂₂H₃₂N₇S, (M + H)⁺ 426.2434, found 426.2424. **¹³C NMR** (101 MHz, DMSO-*d*₆) δ 159.2, 156.9, 153.2, 150.2, 144.2, 143.0, 140.9, 127.0, 121.8, 102.6, 99.1, 60.7, 50.9, 49.8, 47.1, 43.5, 33.4, 30.6, 26.0, 11.3. **Mp** = 249 °C. **HPLC** (Method A) Rt 1.58 minutes, 99.6 % pure. [α]_D²⁰ = -42 (c = 1.031 in DMSO).

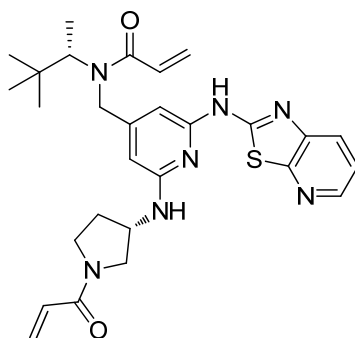
***N*-[(3*S*)-1-Acryloyl-3-pyrrolidinyl]-*N'*-[1,3]thiazolo[5,4-*b*]pyridin-2-yl-4-({[(1*S*)-1,2,2-trimethylpropyl]amino}methyl)-2,6-pyridinediamine (107)**



N-[(3*S*)-3-Pyrrolidinyl]-*N'*-[1,3]thiazolo[5,4-*b*]pyridin-2-yl-4-({[(1*S*)-1,2,2-trimethylpropyl]amino}methyl)-2,6-pyridinediamine trihydrochloride **131** (2.5 g, 4.7 mmol) was suspended in anhydrous dichloromethane (20 mL). *N,N*-Diisopropylethylamine (4.07 mL, 23.4 mmol) was added followed by acrylic acid (0.352 mL, 5.14 mmol). The reaction was stirred for 5 minutes at 0 °C. 1-Propanephosphonic acid cyclic anhydride (50 % w/w in ethyl acetate, 3.06 mL, 5.14 mmol) was added portionwise over 5 minutes and the reaction was stirred at 0 °C for 30 minutes. The reaction mixture was partitioned between dichloromethane:methanol (10:1, 50 mL) and saturated aqueous Na₂CO₃ (50 mL). The aqueous phase was back extracted with dichloromethane:methanol (10:1, 50 mL). The organic extracts were combined, dried using a hydrophobic frit and concentrated under reduced pressure. The residue was purified by chromatography on reverse phase (C18) using a gradient elution from 0 to 40 % acetonitrile (+ 0.25 % TFA) in water (+ 0.25 % TFA). The acetonitrile was removed under reduced pressure. The aqueous phase was basified with concentrated ammonia to reach pH 10. The white solid was filtered under reduced pressure, washed with water and resuspended in acetone/dichloromethane. The solvent was evaporated under reduced pressure to yield the title compound (1.45 g, 65 % yield) as an off-white solid. **LCMS** (Method D) (ES +ve) *m/z* 480 (M + H)⁺ Rt 0.67 min. **¹H NMR** (400 MHz, DMSO-*d*₆, 120 °C) δ 8.26 (dd, *J* = 1.4, 4.6 Hz, 1H), 7.81 (dd, *J* = 1.4, 8.1 Hz, 1H), 7.31 (dd, *J* = 4.6, 8.1 Hz, 1H), 6.55 (dd, *J* = 10.4, 16.7 Hz, 1H), 6.44 (s, 1H), 6.39 (d, *J* = 6.5 Hz, 1H), 6.23 (s, 1H), 6.11 (dd, *J* = 2.3, 16.7 Hz, 1H), 5.61 (dd, *J* = 2.3, 10.4 Hz, 1H), 4.75 - 4.66 (m, 1H), 3.98 - 3.88 (m, 1H), 3.77 - 3.67 (m, 2H), 3.66 - 3.59 (m, 1H), 3.56 (d, *J* = 14.4 Hz, 1H), 3.49 (dd, *J* =

4.7, 11.5 Hz, 1H), 2.39 - 2.34 (m, 1H), 2.32 (q, $J = 6.3$ Hz, 1H), 2.06 - 1.96 (m, 1H), 1.01 (d, $J = 6.5$ Hz, 3H), 0.92 (s, 9H). **IR** (cm^{-1}) 1523, 1575, 1629. **HRMS** (ES) calcd for $\text{C}_{25}\text{H}_{34}\text{N}_7\text{OS}^+$, ($\text{M} + \text{H}$) $^+$ 480.2546, found 480.2562. **^{13}C NMR** (101 MHz, DMSO-d_6) δ 163.49, 163.43, 158.83, 158.82, 157.07, 157.01, 155.54, 155.52, 153.69, 153.60, 149.81, 149.79, 143.08, 143.06, 142.82, 142.80, 129.69, 129.43, 126.64, 126.54, 124.81, 121.12, 100.58, 100.48, 97.45, 97.37, 60.70, 60.68, 52.11, 51.71, 51.56, 51.04, 51.01, 49.86, 44.50, 43.96, 34.35, 31.72, 29.95, 26.50, 14.34. ^{13}C NMR at room temperature displays the presence of rotamers for the compound. **^{13}C NMR** (101 MHz, DMSO-d_6 , 120 $^\circ\text{C}$) δ 163.5, 158.9, 156.9, 155.4, 153.4, 149.9, 142.9, 142.3, 129.6, 125.0, 124.2, 120.3, 100.3, 97.9, 61.0, 51.5, 51.1, 50.5, 43.8, 34.0, 30.7, 26.0, 14.3. Decomposition temperature (partial melt) 165 $^\circ\text{C}$. The decomposition temperature was believed to be due to the fact the solid was not crystalline. For the crystalline material **107b**, an accurate melting point was measured and confirmed by DSC. **HPLC** (Method A) Rt 1.82 minutes, 99.5 % pure. $[\alpha]_{\text{D}}^{20} = -107$ ($c = 1.034$ in DMSO).

***N*-{[2-[[*(3S)*-1-Acryloyl-3-pyrrolidinyl]amino]-6-([1,3]thiazolo[5,4-*b*]pyridin-2-ylamino)-4-pyridinyl]methyl}-*N*-[(1*S*)-1,2,2-trimethylpropyl]-2-propenamide (114)**



N-[(*3S*)-3-Pyrrolidinyl]-*N'*-[1,3]thiazolo[5,4-*b*]pyridin-2-yl-4-({[(1*S*)-1,2,2-trimethylpropyl]amino}methyl)-2,6-pyridinediamine trihydrochloride **131** (1.0 g, 1.9 mmol) was suspended in dichloromethane (10 mL), treated with *N,N*-diisopropylethylamine (1.632 mL, 9.347 mmol) and followed by acrylic acid (0.141 mL, 2.06 mmol). The mixture was cooled to 0 $^\circ\text{C}$ and 1-propanephosphonic acid cyclic anhydride (50 % w/w in ethyl acetate, 1.113 mL, 1.869 mmol) was added

dropwise. The reaction was left stirring at this temperature for 1 hour. Further portions of acrylic acid (0.013 mL, 0.19 mmol) and 1-propanephosphonic acid cyclic anhydride (50 % w/w in ethyl acetate, 0.111 mL, 0.187 mmol) were added and the reaction stirred for 30 minutes. The reaction was quenched with sodium carbonate (15 mL) and the aqueous extracted with dichloromethane:methanol (9:1, 2 x 15 mL). The organic layers were combined, dried using a hydrophobic frit and concentrated under reduced pressure. The residue was treated with a solution of fumaric acid (0.55 g, 4.7 mmol) in tetrahydrofuran:water (2:1, 6 mL). Sonication afforded a solution and 10 mL of water were added followed by seeding with pure crystalline product **107b**. The reaction was stirred for 3 hours at room temperature. The solution was stirred at 0 °C for 4 hours and left stirring overnight in the ice bath. A solid had appeared in solution and was filtered under reduced pressure and dried in the oven. HPLC analysis proved that the compound **107b** was not pure enough. The solid and the filtrate were combined and evaporated under reduced pressure. The residue was purified by chromatography on silica using a gradient elution from 0 to 10 % methanol in dichloromethane. The fractions containing the sideproduct **109** were combined and evaporate under reduced pressure to afford the title compound (5 mg, 0.5 % yield). **LCMS** (Method E) (ES +ve) m/z 534 (M + H)⁺ Rt 0.88 minutes. **¹H NMR** (400 MHz, DMSO-*d*₆, 120 °C) δ 10.79 (br. s, 1H), 8.26 (d, J = 4.6 Hz, 1H), 7.82 (d, J = 8.1 Hz, 1H), 7.32 (dd, J = 4.6, 8.1 Hz, 1H), 6.64 - 6.49 (m, 3H), 6.32 (s, 1H), 6.15 - 6.08 (m, 2H), 6.07 (s, 1H), 5.59 (t, J = 11.6 Hz, 2H), 4.74 - 4.65 (m, 1H), 4.58 (d, J = 17.6 Hz, 1H), 4.46 - 4.35 (m, 1H), 4.31 (d, J = 17.6 Hz, 1H), 3.98 - 3.85 (m, 1H), 3.76 - 3.66 (m, 1H), 3.66 - 3.55 (m, 1H), 3.48 (dd, J = 4.3, 11.3 Hz, 1H), 2.39 - 2.27 (m, 1H), 2.06 - 1.94 (m, 1H), 1.20 (d, J = 6.8 Hz, 3H), 0.97 (s, 9H).

General procedure O for the investigation of the amide coupling reaction – investigation of the coupling reagent.

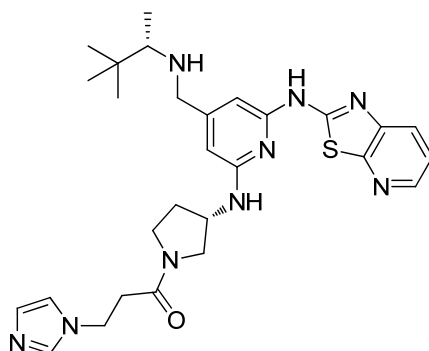
A round bottom flask was charged with *N*-[(3*S*)-3-pyrrolidinyl]-*N'*-[1,3]thiazolo[5,4-*b*]pyridin-2-yl-4-({[(1*S*)-1,2,2-trimethylpropyl]amino}methyl)-2,6-pyridinediamine trihydrochloride **131** (50 mg, 0.093 mmol), *N,N*-diisopropylethylamine (0.082 mL, 0.47 mmol), acrylic acid (6.41 μ L, 0.0935 mmol) and dichloromethane (2 mL). The coupling agent (see table) was added and the reaction stirred at room temperature for

30 minutes. The advancement of the reaction was monitored by HPLC analysis. The results were recorded in Table 45.

Data from Table 45:

Entry	Coupling agent	Amount of coupling agent	Comment
1	T3P [®]	0.056 mL 0.093 mmol	T3P [®] (50 % w/w in EtOAc)
2	PyBOP [®]	49 mg 0.093 mmol	
3	COMU	40 mg 0.093 mmol	

***N*-[(3*S*)-1-[3-(1*H*-Imidazol-1-yl)propanoyl]-3-pyrrolidinyl]-*N'*-[1,3]thiazolo[5,4-*b*]pyridin-2-yl-4-([(1*S*)-1,2,2-trimethylpropyl]amino)methyl)-2,6-pyridinediamine (132)**



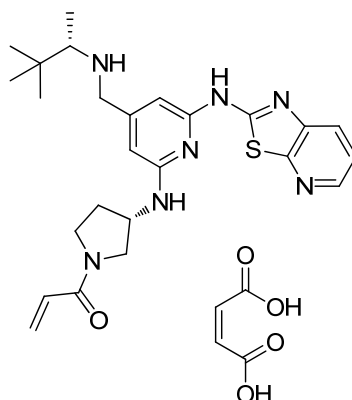
N-[(3*S*)-3-Pyrrolidinyl]-*N'*-[1,3]thiazolo[5,4-*b*]pyridin-2-yl-4-([(1*S*)-1,2,2-trimethylpropyl]amino)methyl)-2,6-pyridinediamine trihydrochloride **131** (50 mg, 0.093 mmol) was suspended in dichloromethane (1 mL) and then treated with *N,N*-diisopropylethylamine (0.082 mL, 0.47 mmol). A solution of CDI (15 mg, 0.093 mmol), acrylic acid (7.06 μ L, 0.103 mmol) in *N,N*-diisopropylethylamine (0.082 mL, 0.47 mmol) in dichloromethane (1 mL) was stirred for 10 minutes before being added dropwise to the pyrrolidine starting material mixture. The solution was stirred for 30 minutes. The mixture was partitioned between dichloromethane (2.5 mL) and saturated sodium carbonate (2.5 mL). The aqueous phase was back extracted with

dichloromethane (2.5 mL). The combined organic layers were dried using a hydrophobic frit and concentrated under reduced pressure. The mixture was purified by mass directed automated preparative HPLC to afford the title compound (30 mg, 59 % yield) as an off-white solid. **LCMS** (Method E) (ES +ve) m/z 548 (M + H)⁺ Rt 0.59 minutes. **¹H NMR** (400 MHz, DMSO-*d*₆) δ 11.31 (br. s, 1H), 8.27 (d, J = 4.6 Hz, 1H), 7.86 (dd, J = 1.0, 8.2 Hz, 1H), 7.62 (s, 0.5H), 7.57 (s, 0.5H), 7.35 (dd, J = 4.6, 8.2 Hz, 1H), 7.19 (s, 0.5H), 7.12 (s, 0.5H), 6.92 (d, J = 7.0 Hz, 0.5H), 6.86 (d, J = 7.0 Hz, 0.5H), 6.86 (s, 0.5H), 6.81 (s, 0.5H), 6.30 (s, 1H), 6.19 (s, 1H), 4.71 - 4.63 (m, 0.5H), 4.62 - 4.55 (m, 0.5H), 4.20 (t, J = 6.8 Hz, 1H), 4.17 (t, J = 6.8 Hz, 1H), 3.85 (dd, J = 5.8, 10.5 Hz, 0.5H), 3.73 - 3.64 (m, 1.5H), 3.61 - 3.37 (m, 4H), 2.88 - 2.69 (m, 2H), 2.35 - 2.14 (m, 2H), 2.04 - 1.84 (m, 1H), 0.93 (d, J = 6.3 Hz, 3H), 0.87 (s, 9H). Note that the ¹H NMR indicates the presence of rotamers hence the explanation for the reports of protons integrating for 0.5H.

General procedure P for the investigation of the amide coupling reaction - effect of the solvent.

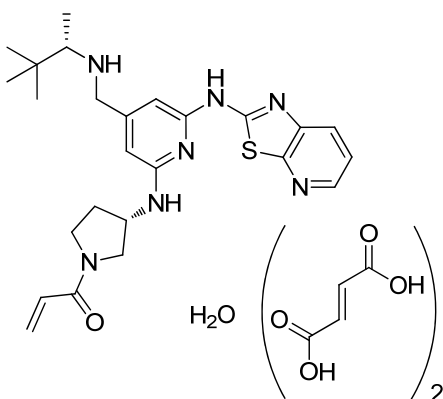
A round bottom flask was charged with *N*-[(3*S*)-3-pyrrolidinyl]-*N'*-[1,3]thiazolo[5,4-*b*]pyridin-2-yl-4-({[(1*S*)-1,2,2-trimethylpropyl]amino} methyl)-2,6-pyridinediamine trihydrochloride **131** (25 mg, 0.047 mmol), *N,N*-diisopropylethylamine (0.041 mL, 0.23 mmol), acrylic acid (3.2 μ L, 0.047 mmol) and solvent (2 mL). 1-Propanephosphonic acid cyclic anhydride (50 % w/w in ethyl acetate, 0.028 mL, 0.047 mmol) was added and the reaction stirred at room temperature for 30 minutes. The advancement of the reaction was monitored by HPLC analysis. The results are as shown in Table 46.

***N*-[(3*S*)-1-Acryloyl-3-pyrrolidinyl]-*N'*-[1,3]thiazolo[5,4-*b*]pyridin-2-yl-4-({[(1*S*)-1,2,2-trimethylpropyl]amino}methyl)-2,6-pyridinediamine (2*Z*)-2-butenedioate (107a)**



N-[(3*S*)-1-Acryloyl-3-pyrrolidinyl]-*N'*-[1,3]thiazolo[5,4-*b*]pyridin-2-yl-4-({[(1*S*)-1,2,2-trimethylpropyl]amino}methyl)-2,6-pyridinediamine **107** (714 mg, 1.49 mmol) was dissolved in methanol (10 mL) and was treated with maleic acid (0.173 g, 1.49 mmol). The solution was stirred at room temperature for 30 minutes. The solvent was removed under reduced pressure to afford the title compound (890 mg, 100 % yield) as an off-white solid. **LCMS** (Method F) (ES +ve) *m/z* 480 (*M* + *H*)⁺ *Rt* 2.89 minutes. **¹H NMR** (400 MHz, DMSO-*d*₆, 120 °C) δ 8.28 (dd, *J* = 1.5, 4.7 Hz, 1H), 7.84 (dd, *J* = 1.5, 8.1 Hz, 1H), 7.34 (dd, *J* = 4.7, 8.1 Hz, 1H), 6.55 (dd, *J* = 10.4, 16.7 Hz, 1H), 6.58 (br. s, 1H), 6.48 (s, 1H), 6.27 (s, 1H), 6.12 (dd, *J* = 2.3, 16.7 Hz, 1H), 6.09 (s, 2H), 5.62 (dd, *J* = 2.3, 10.4 Hz, 1H), 4.74 - 4.67 (m, 1H), 3.98 (d, *J* = 14.1 Hz, 1H), 3.98 - 3.90 (m, 1H), 3.84 (d, *J* = 14.1 Hz, 1H), 3.78 - 3.68 (m, 1H), 3.68 - 3.59 (m, 1H), 3.51 (dd, *J* = 4.7, 11.5 Hz, 1H), 2.72 (q, *J* = 6.5 Hz, 1H), 2.41 - 2.31 (m, 1H), 2.08 - 1.98 (m, 1H), 1.17 (d, *J* = 6.5 Hz, 3H), 0.98 (s, 9H).

N-[(3*S*)-1-Acryloyl-3-pyrrolidinyl]-*N'*-[1,3]thiazolo[5,4-*b*]pyridin-2-yl-4-({[(1*S*)-1,2,2-trimethylpropyl]amino}methyl)-2,6-pyridinediamine di[(2*E*)-2-butenedioate] hydrate (**107b**)¹⁸⁷



N-[(3*S*)-1-Acryloyl-3-pyrrolidinyl]-*N'*-[1,3]thiazolo[5,4-*b*]pyridin-2-yl-4-({[(1*S*)-1,2,2-trimethylpropyl]amino}methyl)-2,6-pyridinediamine **107** (33.4 g, 69.6 mmol) was treated with a solution of fumaric acid (16.49 g, 142.1 mmol) in tetrahydrofuran (134 mL)/water (67 mL). Sonication with heating afforded a solution. Water (335 mL) was added followed by seeding with some crystalline material of **107b**. The reaction was stirred for 1.5 hour, water (335 mL) was added and stirring continued overnight. The solid was filtered under reduced pressure and dried in a vacuum oven at 40 °C for 4 hours. The solid was ground down to a free-flowing powder and was dried in a vacuum oven at 40 °C over the weekend to afford the title compound (46.19 g, 91 % yield) as a pale yellow solid. **LCMS** (Method A) (ES +ve) *m/z* 480 (*M* + *H*)⁺ *Rt* 0.67 minutes. **¹H NMR** (400 MHz, DMSO-*d*₆) δ 8.27 (dd, *J* = 1.4, 4.6 Hz, 1H), 7.87 (d, *J* = 7.8 Hz, 1H), 7.36 (dd, *J* = 4.5, 7.8 Hz, 1H), 7.03 (dd, *J* = 6.8, 15.1 Hz, 1H), 6.63 (dd, *J* = 10.3, 17.1 Hz, 0.5H), 6.60 (s, 4H), 6.53 (dd, *J* = 10.3, 16.8 Hz, 0.5H), 6.34 (s, 1H), 6.22 (d, *J* = 1.8 Hz, 1H), 6.16 (dd, *J* = 2.5, 10.0 Hz, 0.5H), 6.11 (dd, *J* = 2.5, 10.0 Hz, 0.5H), 5.68 (dd, *J* = 2.5, 10.0 Hz, 0.5H), 5.61 (dd, *J* = 2.5, 10.0 Hz, 0.5H), 4.75 - 4.67 (m, 0.5H), 4.66 - 4.58 (m, 0.5H), 4.03 - 3.95 (m, 0.5H), 3.85 (dd, *J* = 1.8, 14.6 Hz, 1H), 3.79 - 3.46 (m, 4.5H), 2.42 - 2.30 (m, 1.5H), 2.30 - 2.20 (m, 0.5H), 2.09 - 2.00 (m, 0.5H), 1.99 - 1.90 (m, 0.5H), 1.02 (dd, *J* = 1.8, 6.5 Hz, 3H), 0.89 (s, 9H). **¹H NMR** (400 MHz, DMSO-*d*₆, 120 °C) δ 8.26 (dd, *J* = 1.5, 4.8 Hz, 1H), 7.81 (dd, *J* = 1.5, 8.0 Hz, 1H), 7.32 (dd, *J* = 4.8, 8.0 Hz, 1H), 6.65 (s, 4H), 6.55 (dd, *J* = 10.5, 16.8 Hz, 1H), 6.44 (s, 1H), 6.42 (br. s, 1H), 6.24 (s, 1H),

6.11 (dd, $J = 2.4, 16.8$ Hz, 1H), 5.61 (dd, $J = 2.4, 10.5$ Hz, 1H), 4.75 - 4.66 (m, 1H), 3.97 - 3.87 (m, 1H), 3.76 (d, $J = 14.3$ Hz, 1H), 3.76 - 3.68 (m, 1H), 3.66 - 3.58 (m, 1H), 3.58 (d, $J = 14.4$ Hz, 1H), 3.49 (dd, $J = 4.6, 11.4$ Hz, 1H), 2.36 (q, $J = 6.4$ Hz, 1H), 2.35 - 2.29 (m, 1H), 2.06 - 1.96 (m, 1H), 1.02 (d, $J = 6.4$ Hz, 3H), 0.93 (s, 9H). **IR** (cm^{-1}) 1539, 1592, 1642, 1704. **HRMS** (ES) calcd for $\text{C}_{25}\text{H}_{34}\text{N}_7\text{OS}$, ($\text{M} + \text{H}$)⁺ 480.2546, found 480.2538. **^{13}C NMR** (151 MHz, DMSO-d_6) δ 166.11, 163.48, 163.43, 158.78, 158.77, 157.11, 157.04, 155.50, 155.48, 151.53, 151.28, 149.94, 143.01, 142.88, 142.86, 134.06, 129.67, 129.42, 126.62, 126.52, 124.85, 121.13, 100.86, 100.72, 97.58, 97.50, 60.84, 60.78, 52.03, 51.64, 51.56, 50.34, 49.86, 44.48, 43.93, 34.13, 31.67, 29.92, 26.34, 13.75, 13.71. **^{13}C NMR** at room temperature displays the presence of rotamers for the compound. The data is reported with two decimal points to differentiate the signals. **Mp** = 220 °C (confirmed by DSC, Figure 80). **HPLC** (Method B) Rt 3.05 minutes, 99.7 % pure. $[\alpha]_{\text{D}}^{20} = -82$ ($c = 1.038$ in DMSO). **Chiral HPLC** Rt 22.2 mins, >99 % pure.

9. Synthetic procedures for the investigation of the Buchwald-Hartwig coupling

General procedure Q for the investigation of the Buchwald-Hartwig coupling with 20 % of precatalyst 87.

Method A: a microwave vial was charged with *N*-[6-chloro-4-({[(1*S*)-1,2,2-trimethylpropyl]amino}methyl)-2-pyridinyl][1,3]thiazolo[5,4-*b*]pyridin-2-amine **129** (25 mg, 0.067 mmol), 1,1-dimethylethyl (3*S*)-3-amino-1-pyrrolidinecarboxylate, {1,3-bis[2,6-bis(1-methylethyl)phenyl]-2-imidazolidinyl}(chloro)(2-methyl-2-propen-1-yl)palladium **87** and tetrahydrofuran (0.5 mL). The vial was sealed, placed under an atmosphere of nitrogen using a vacuum purge (3 times) and heated at the stated temperature. LHMDS in tetrahydrofuran (1M) was added dropwise and the reaction was heated at the stated temperature for the stated time. The advancement of the reaction was monitored by LCMS analysis (note that the % conversion refers to the formation of product relative to starting material. The % of impurities formed were not taken into account).

Method B: a microwave vial was charged with *N*-[6-chloro-4-({[(1*S*)-1,2,2-trimethylpropyl]amino}methyl)-2-pyridinyl][1,3]thiazolo[5,4-*b*]pyridin-2-amine **129** (25 mg, 0.067 mmol), 1,1-dimethylethyl (3*S*)-3-amino-1-pyrrolidinecarboxylate and tetrahydrofuran (0.5 mL). The vial was sealed, placed under an atmosphere of nitrogen using a vacuum purge (3 times) and heated at the stated temperature. A solution of {1,3-bis[2,6-bis(1-methylethyl)phenyl]-2-imidazolidinyl}(chloro)(2-methyl-2-propen-1-yl)palladium **87** and LHMDS in tetrahydrofuran (1M) was added dropwise and the reaction was heated at the stated temperature for the stated time. The advancement of the reaction was monitored by LCMS analysis (note that the % conversion refers to the formation of product relative to starting material. The % of impurities formed were not taken into account).

Data from Table 49

Entry	Method	Amine	87	LHMDS in THF (1 M)	T (°C)	Heating time	% Conversion ^a
1	A	14 mg 0.075 mmol	8 mg 0.01 mmol	0.2 mL 0.2 mmol	50 °C	1 h	61 %
2	A	14 mg 0.075 mmol	8 mg 0.01 mmol	0.2 mL 0.2 mmol	50 °C	16 h	62 %
3	B	14 mg 0.075 mmol	8 mg 0.01 mmol	0.2 mL 0.2 mmol	50 °C	1 h	72 %
4	B	28 mg 0.15 mmol	8 mg 0.01 mmol	0.2 mL 0.2 mmol	50 °C	1 h	61 %
5	B	14 mg 0.075 mmol	8 mg 0.01 mmol	0.1 mL 0.1 mmol	50 °C	1 h	No product
6	B	14 mg 0.075 mmol	8 mg 0.01 mmol	0.4 mL 0.4 mmol	50 °C	1 h	45 %
7	B	14 mg 0.075 mmol	8 mg 0.01 mmol	0.2 mL 0.200 mmol	50 °C	30 mins	72 %
8	A	14 mg 0.075 mmol	8 mg 0.01 mmol	0.2 mL 0.2 mmol	70 °C	30 mins	75 %

^a Determined by LCMS analysis

General procedure R for the investigation of the Buchwald-Hartwig coupling with the substrate 128.

A microwave vial was charged with 6-chloro-4-({[(1*S*)-1,2,2-trimethylpropyl]amino}methyl)-2-pyridinamine **128** (50 mg, 0.21 mmol), 1,1-dimethylethyl (3*S*)-3-amino-1-pyrrolidinecarboxylate (154 mg, 0.827 mmol), {1,3-bis[2,6-bis(1-methylethyl)phenyl]-2-imidazolidinyl}(chloro)(2-methyl-2-propen-1-yl)palladium **87** and tetrahydrofuran (0.5 mL). The vial was sealed, placed under an atmosphere of nitrogen using a vacuum purge (3 times) and heated at the stated temperature. LHMDS in tetrahydrofuran (1M) was added and the reaction was heated at the stated temperature for the stated time. The advancement of the reaction was monitored by LCMS analysis (note that the % conversion refers to the formation

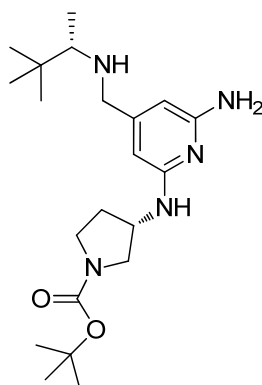
of product relative to starting material. The % of impurities formed were not taken into account).

Data from Table 50:

Entry	87	LHMDS in THF (1 M)	Heating time	T (°C)	% Conversion ^a	Isolated yield ^b
1	12 mg 0.020 mmol	0.65 mL 0.65 mmol	1 h	70 °C	43 %	
2	12 mg 0.020 mmol	0.65 mL 0.65 mmol	20 h	70 °C	100 %	43 %
3	12 mg 0.020 mmol	0.65 mL 0.65 mmol	3 h	50 °C	66 %	
4	12 mg 0.020 mmol	0.65 mL 0.65 mmol	8 h	50 °C	91 %	
5	12 mg 0.020 mmol	0.65 mL 0.65 mmol	24 h	50 °C	100 %	38 %
6	6 mg 0.01 mmol	0.65 mL 0.65 mmol	24 h	50 °C	65 %	
7	6 mg 0.01 mmol	0.65 mL 0.65 mmol	48 h	50 °C	80 %	17 %
8	6 mg 0.01 mmol	0.65 mL 0.65 mmol	24 h	70 °C	100 %	24 %

^a Determined by LCMS analysis. ^b Product isolated by MDAP.

Entry 2 - 1,1-Dimethylethyl (3S)-3-{{6-amino-4-({[(1S)-1,2,2-trimethylpropyl]amino}methyl)-2-pyridinyl}amino}-1-pyrrolidinecarboxylate
134



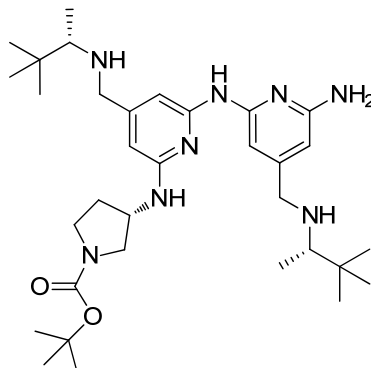
The reaction mixture was partitioned between dichloromethane (20 mL) and saturated aqueous Na₂CO₃ (20 mL). The organic extract was dried using a hydrophobic frit and concentrated under reduced pressure. The residue was purified by mass directed automated preparative HPLC to afford the title compound (35 mg, 43 % yield). **LCMS** (Method D) (ES +ve) m/z 392 (M + H)⁺ Rt 1.17 minutes. **¹H NMR** (400 MHz, DMSO-d₆) δ 6.01 (d, *J* = 6.5 Hz, 1H), 5.68 (s, 1H), 5.65 (s, 1H), 5.25 (s, 2H), 4.29 - 4.13 (m, 1H), 3.59 - 3.47 (m, 2H), 3.44 - 3.29 (m, 2H), 3.27 - 3.21 (m, 1H), 3.07 - 2.98 (m, 1H), 2.17 (q, *J* = 6.3 Hz, 1H), 2.11 - 1.98 (m, 1H), 1.84 - 1.69 (m, 1H), 1.39 (s, 9H), 0.91 (d, *J* = 6.3 Hz, 3H), 0.85 (s, 9H).

Entry 5, 7 and 8 - Isolation of compound 134:

The reaction mixture was partitioned between dichloromethane (5 mL) and water (5 mL). The organic extract was dried using a hydrophobic frit and concentrated under reduced pressure. The residue was purified by mass directed automated preparative HPLC to afford the title compound (entry 5 - 31 mg, 38 % yield; entry 7 - 14 mg, 17 % yield; entry 8 - 17 mg, 24 % yield).

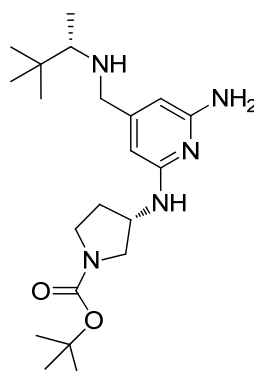
Entry 5 – Isolation of the side product 1,1-dimethylethyl (3S)-3-{{6-{{6-amino-4-(((1S)-1,2,2-trimethylpropyl)amino)methyl)-2-pyridinyl}amino}-4-(((1S)-1,2,2-trimethylpropyl)amino)methyl)-2-pyridinyl}amino}-1-pyrrolidinecarboxylate

136



The reaction mixture was partitioned between dichloromethane (5 mL) and water (5 mL). The organic extract was dried using a hydrophobic frit and concentrated under reduced pressure. The residue was purified by mass directed automated preparative HPLC to afford the title compound (8 mg, 6 % yield). **LCMS** (Method D) (ES +ve) m/z 597 ($M + H$)⁺ Rt 1.51 minutes. **¹H NMR** (400 MHz, DMSO- d_6) δ 8.40 (s, 1H), 7.16 (d, $J = 8.5$ Hz, 1H), 6.54 (d, $J = 6.0$ Hz, 1H), 6.39 (d, $J = 6.3$ Hz, 1H), 5.98 (s, 2H), 5.43 (s, 2H), 4.45 - 4.27 (m, 1H), 3.69 - 3.54 (m, 3H), 3.48 - 3.35 (m, 3H), 3.31 - 3.25 (m, 1H), 3.16 - 3.06 (m, 1H), 2.24 - 2.06 (m, 3H), 1.90 - 1.75 (m, 1H), 1.39 (d, $J = 10.3$ Hz, 9H), 0.92 (dd, $J = 1.9, 6.4$ Hz, 6H), 0.85 (d, $J = 7.0$ Hz, 18H). Note that some of the signals appear as doublets because of the presence of rotamers.

1,1-Dimethylethyl (3S)-3-{{6-amino-4-(((1S)-1,2,2-trimethylpropyl)amino)methyl)-2-pyridinyl}amino}-1-pyrrolidinecarboxylate
134 (scale up reaction)



A microwave vial was charged with 6-chloro-4-({[(1*S*)-1,2,2-trimethylpropyl]amino}methyl)-2-pyridinamine **128** (540 mg, 2.23 mmol), 1,1-dimethylethyl (3*S*)-3-amino-1-pyrrolidinecarboxylate (1.66 g, 8.93 mmol), {1,3-bis[2,6-bis(1-methylethyl)phenyl]-2-imidazolidinyl}(chloro)(2-methyl-2-propen-1-yl)palladium **87** (131 mg, 0.223 mmol) and tetrahydrofuran (0.5 mL). The vial was sealed, placed under an atmosphere of nitrogen using a vacuum purge (3 times) and heated at 50 °C. LHMDS in tetrahydrofuran (1M, 6.72 mL, 6.72 mmol) was added and the reaction was heated at 50 °C for 16 hours. The reaction mixture was cooled down to room temperature and partitioned between dichloromethane (50 mL) and saturated ammonium chloride (50 mL). The organic extract was washed with saturated sodium metabisulfate (50 mL), dried using a hydrophobic frit and concentrated under reduced pressure. The product was purified by silica chromatography using a 5 % methanol in dichloromethane elution to afford the title compound (510 mg, 90 % pure, 52 % yield) as a brown foam. **LCMS** (Method D) (ES +ve) *m/z* 392 (M + H)⁺ Rt 1.18 minutes. **¹H NMR** (400 MHz, DMSO-*d*₆) δ 6.01 (d, *J* = 6.5 Hz, 1H), 5.68 (s, 1H), 5.65 (s, 1H), 5.25 (s, 2H), 4.29 - 4.13 (m, 1H), 3.59 - 3.47 (m, 2H), 3.44 - 3.29 (m, 2H), 3.27 - 3.21 (m, 1H), 3.07 - 2.98 (m, 1H), 2.17 (q, *J* = 6.3 Hz, 1H), 2.11 - 1.98 (m, 1H), 1.84 - 1.69 (m, 1H), 1.39 (s, 9H), 0.91 (d, *J* = 6.3 Hz, 3H), 0.85 (s, 9H).

Attempt to prepare compound 134 in the presence of the intermediate 129

A microwave vial was charged with 6-chloro-4-({[(1*S*)-1,2,2-trimethylpropyl]amino}methyl)-2-pyridinamine **128** (50 mg, 0.21 mmol), *N*-[6-chloro-4-({[(1*S*)-1,2,2-trimethylpropyl]amino}methyl)-2-pyridinyl][1,3]thiazolo[5,4-*b*]pyridin-2-amine **129** (78 mg, 0.21 mmol), 1,1-dimethylethyl (3*S*)-3-amino-1-pyrrolidinecarboxylate (154 mg, 0.827 mmol), {1,3-bis[2,6-bis(1-methylethyl)phenyl]-2-imidazolidinyl}(chloro)(2-methyl-2-propen-1-yl)palladium **87** (12 mg, 0.020 mmol) and tetrahydrofuran (0.5 mL). The vial was sealed, placed under an atmosphere of nitrogen using a vacuum purge (3 times) and heated at the stated temperature. LHMDS in tetrahydrofuran (1M, 0.65 mL, 0.65 mmol) was added and the reaction was heated at 70 °C for the 20 hours. The advancement of the reaction was monitored by LCMS analysis. LCMS analyses of the reaction mixture

were recorded after one hour and 4 hours. Both profiles were similar with only 10 - 15 % of product **130** formed and no peaks corresponding to compound **134**.

General procedure S for the investigation of the Buchwald-Hartwig coupling in the presence of Lewis acids.

A microwave vial was charged with *N*-[6-chloro-4-({[(1*S*)-1,2,2-trimethylpropyl]amino}methyl)-2-pyridinyl][1,3]thiazolo[5,4-*b*]pyridin-2-amine **129** (25 mg, 0.067 mmol), 1,1-dimethylethyl (3*S*)-3-amino-1-pyrrolidinecarboxylate (14 mg, 0.075 mmol), the Lewis acid additives and tetrahydrofuran (0.5 mL). The vial was sealed, placed under an atmosphere of nitrogen using a vacuum purge (3 times) and heated at 50 °C. LHMDS in tetrahydrofuran (1 M, 0.2 mL, 0.2 mmol) was added and the reaction was heated at 50 °C. The advancement of the reaction was monitored by LCMS analysis after 1 hour and 16 hours (note that the % conversion refers to the formation of product relative to starting material. The % of impurities formed were not taken into account).

Data from Table S1:

Entry	Additive	Amount	% conversion to 130 at 1 h ^a	% conversion to 130 at 16 h ^a
1	None		30 % MF111156-1	24 % MF111165-1
2	LiCl	3 mg 0.07 mmol	35 % MF111156-2	35 % MF111165-2
3	CuI	13 mg 0.07 mmol	44 % MF111094-2	41 % MF111123-2
4	Fe(acac) ₃	24 mg 0.07 mmol	0 % MF111094-3	0 % MF111123-3
5	ZnCl ₂	10 mg 0.07 mmol	0 % MF111156-3	0 % MF111156-3

^a Determined by LCMS analysis

General procedure T for the investigation of the Buchwald-Hartwig using the Josiphos type ligand 138.

A microwave vial was charged with bis(tris(2-methylphenyl)phosphine)palladium **139** and Josiphos **138** in tetrahydrofuran (0.5 mL). The vial was sealed and put under an atmosphere of nitrogen using a vacuum purge. The solution was stirred at room temperature for 5 minutes. A solution of *N*-[6-chloro-4-({[(1*S*)-1,2,2-trimethylpropyl]amino}methyl)-2-pyridinyl][1,3]thiazolo[5,4-*b*]pyridin-2-amine **129** (50 mg, 0.13 mmol) and 1,1-dimethylethyl (3*S*)-3-amino-1-pyrrolidinecarboxylate in tetrahydrofuran (1 mL) was added to the reaction mixture. LHMDS in tetrahydrofuran (1 M, 0.4 mL, 0.4 mmol) was added and the reaction mixture was stirred at the stated temperature. The advancement of the reaction was monitored by LCMS analysis after the stated time (note that the % conversion refers to the formation of product relative to starting material. The % of impurities formed were not taken into account).

Entry 1 was performed differently (the amine was added last as described by Hartwig *et al.*):²²⁰

A microwave vial was charged with bis(tris(2-methylphenyl)phosphine)palladium **139** and Josiphos **138** in toluene (0.5 mL). The vial was sealed and put under an atmosphere of nitrogen using a vacuum purge. The solution was stirred at room temperature for 5 minutes. A solution of *N*-[6-chloro-4-({[(1*S*)-1,2,2-trimethylpropyl]amino}methyl)-2-pyridinyl][1,3]thiazolo[5,4-*b*]pyridin-2-amine **129** (50 mg, 0.13 mmol) and base in toluene (0.5 mL) was added to the reaction mixture. Finally, 1,1-dimethylethyl (3*S*)-3-amino-1-pyrrolidinecarboxylate in toluene (0.5 mL) was added and the reaction mixture was stirred at the stated temperature. The advancement of the reaction was monitored by LCMS analysis after the stated time.

Entry 5 was performed differently (the Pd catalyst and the ligand were not premixed):

A microwave vial was charged with Pd(OAc)₂, Josiphos **138**, *N*-[6-chloro-4-({[(1*S*)-1,2,2-trimethylpropyl]amino}methyl)-2-pyridinyl][1,3]thiazolo[5,4-*b*]pyridin-2-amine **129** (50 mg, 0.13 mmol) and 1,1-dimethylethyl (3*S*)-3-amino-1-

pyrrolidinecarboxylate in tetrahydrofuran (1 mL). The vial was sealed and put under an atmosphere of nitrogen using a vacuum purge. The solution was stirred at room temperature for one minute. LHMDS in tetrahydrofuran (1 M, 0.4 mL, 0.4 mmol) was added and the reaction mixture was stirred at the stated temperature. The advancement of the reaction was monitored by LCMS analysis after the stated time.

Data from Table 52:

Entry	Amine	Pd	Ligand	Base	Solvent	T (°C)	Heating time	% conversion ^a
1	27 mg 0.15 mmol	139 (9.5 mg, 0.013 mmol)	138 (7.4 mg, 0.013 mmol)	NaOtBu (38 mg, 0.399 mmol)	Toluene	room	16 h	0 %
2	27 mg 0.15 mmol	139 (9.5 mg, 0.013 mmol)	138 (7.4 mg, 0.013 mmol)	LHMDS (1M, 0.4 mL, 0.4 mmol)	THF	room	2 h	41 %
3	27 mg 0.15 mmol	139 (9.5 mg, 0.013 mmol)	138 (7.4 mg, 0.013 mmol)	LHMDS (1M, 0.4 mL, 0.4 mmol)	THF	room	16 h	65 %
4	27 mg 0.15 mmol	139 (9.5 mg, 0.013 mmol)	138 (7.4 mg, 0.013 mmol)	LHMDS (1M, 0.4 mL, 0.4 mmol)	THF	70 °C	16 h	34 %
5	27 mg 0.15 mmol	Pd(OAc) ₂ (3 mg, 0.01 mmol)	138 (7.4 mg, 0.013 mmol)	LHMDS (1M, 0.4 mL, 0.4 mmol)	THF	70 °C	24 h	11 %
6	55 mg 0.30 mmol	139 (9.5 mg, 0.013 mmol)	138 (7.4 mg, 0.013 mmol)	LHMDS (1M, 0.4 mL, 0.4 mmol)	THF	room	24 h	100 %
7	55 mg 0.30 mmol	139 (2.85 mg, 3.99 μmol)	138 (2.2 mg, 4.0 μmol)	LHMDS (1M, 0.4 mL, 0.4 mmol)	THF	room	24 h	7 %

^a Determined by LCMS analysis

References

- ¹ Gibson, S.; Leung, B.; Squire, J. A.; Hill, M.; Arima, N.; Goss, P.; Hogg, D.; Mills, G. B. *Blood* **1993**, *82*, 1561-1572.
- ² Siliciano, J. D.; Morrow, T. A.; Desiderio, S. V. *Proc. Natl. Acad. Sci. U.S.A.* **1992**, *89*, 11194-11198.
- ³ Andreotti, A. H.; Schwartzberg, P. L.; Joseph, R. E.; Berg, L. J. *Cold Spring Harbor Perspectives in Biology* **2010**, *2*, a002287.
- ⁴ Heyeck, S. D.; Wilcox, H. M.; Bunnell, S. C.; Berg, L. J. *J. Biol. Chem.* **1997**, *272*, 25401-25408.
- ⁵ Schwartzberg, P. L.; Finkelstein, L. D.; Readinger, J. A. *Nature Rev. Immunol.* **2005**, *5*, 284-295.
- ⁶ Robinson, D. S. *J. Allergy Clin. Immunol.* **2010**, *126*, 1081-1091.
- ⁷ Holgate, S. T.; Polosa, R. *Nature Rev. Immunol.* **2008**, *8*, 218-230.
- ⁸ Fowell, D. J.; Shinkai, K.; Liao, X. C.; Beebe, A. M.; Coffman, R. L.; Littman, D. R.; Locksley, R. M. *Immunity* **1999**, *11*, 399-409.
- ⁹ Mueller, C.; August, A. *J. Immunol.* **2003**, *170*, 5056-5063.
- ¹⁰ Grasis, J. A.; Tsoukas, C. D. *J. Signal Transduction* **2011**, Article ID 297868, 23 pages.
- ¹¹ Sahu, N.; August, A. *Curr. Top. Med. Chem.* **2009**, *9*, 690-703.
- ¹² Lo, H. Y. *Expert Opin. Ther. Patents* **2010**, *20*, 459-469.
- ¹³ Barrish, J. C.; Das, J.; Kanner, S. B.; Liu, C.; Spergel, S. H.; Wityrak, J.; Doweyko, A. M. P.; Furch, J. A. *PCT Int. Appl.* **2002**, WO/2002/050071.
- ¹⁴ Das, J.; Liu, C.; Moquin, R. V.; Lin, J.; Furch, J. A.; Spergel, S. H.; McIntyre, K. W.; Shuster, D. J.; O'Day, K. D.; Penhallow, B.; Hung, C. Y.; Kanner, S. B.; Lin, T. A.; Dodd, J. H.; Barrish, J. C.; Wityak, J. *Bioorg. Med. Chem. Lett.* **2006**, *16*, 2411-2415.
- ¹⁵ Das, J.; Furch, J. A.; Liu, C.; Moquin, R. V.; Lin, J.; Spergel, S. H.; McIntyre, K. W.; Shuster, D. J.; O'Day, K. D.; Penhallow, B.; Hung, C. Y.; Doweyko, A. M.; Kamath, A.; Zhang, H.; Marathe, P.; Kanner, S. B.; Lin, T. A.; Dodd, J. H.; Barrish, J. C.; Wityak, J. *Bioorg. Med. Chem. Lett.* **2006**, *16*, 3706-3712.

-
- ¹⁶ Lin, T.-A.; McIntyre, K. W.; Das, J.; Liu, C.; O'Day, K. D.; Penhallow, B.; Hung, C.-Y.; Whitney, G. S.; Shuster, D. J.; Yang, X. X.; Townsend, R.; Postelnek, J.; Spergel, S. H.; Lin, J.; Moquin, R. V.; Furch, J. A.; Kamath, A. V.; Zhang, H.; Marathe, P. H.; Perez-Villar, J. J.; Doweiko, A.; Killar, L.; Dodd, J. H.; Barrish, J. C.; Wityak, J.; Kanner, S. B. *Biochemistry* **2004**, *43*, 11056-11062.
- ¹⁷ Cywin, C.; Pullen, S. S.; Roth, G. P.; Snow, R. J.; Fleck, R. W.; Takahashi, H.; Winters, M.; Qiao, L.; Nemoto, P. A.; Moriarity, K. J.; Wang, J.; Bentzien, J.; Cook, B.; Lo, H.-Y. *PCT Int. Appl.* **2004**, WO/2004/014905.
- ¹⁸ Roth, G. P.; Qiao, L.; Moriarity, K. J. *PCT Int. Appl.* **2005**, WO/2005/070420.
- ¹⁹ Bentzien, J. M.; Cook, B. N.; Li, X.; Lo, H. Y.; Man, C. C.; Mugge, I. A.; Pullen, S. S.; Roth, G. P.; Soleymanzadeh, F.; Takahashi, H.; Wang, J.; White, A.; Zindell, R. M.; Riether, D. E.; Nemoto, P. A.; Yao, X.; Mangette, J. E. *PCT Int. Appl.* **2005**, WO/2005/079791.
- ²⁰ Snow, R. J.; Abeywardane, A.; Campbell, S.; Lord, J.; Kashem, M. A.; Khine, H. H.; King, J.; Kowalski, J. A.; Pullen, S. S.; Roma, T.; Roth, G. P.; Sarko, C. R.; Wilson, N. S.; Winters, M. P.; Wolak, J. P.; Cywin, C. L. *Bioorg. Med. Chem. Lett.* **2007**, *17*, 3660-3665.
- ²¹ Moriarty, K. J.; Winters, M. P.; Qiao, L.; Ryan, D.; DesJarlais, R.; Robinson, D.; Cook, B. N.; Kashem, M. A.; Kapilta, J. V.; Liu, L. H.; Farrell, T. M.; Khine, H. H.; King, J.; Pullen, S. S.; Roth, G. P.; Takahashi, H. *Bioorg. Med. Chem. Lett.* **2008**, *18*, 5537-5540.
- ²² Winters, M. P.; Robinson, D.; Khine, H. H.; Pullen, S. S.; Woska Jr., J. R.; Raymond, E. L.; Sellati, R. H.; Cywin, C. L.; Snow, R. J.; Kashem, M. A.; Wolak, J. P.; King, J.; Kapilta, J. V.; Liu, L. H.; Farrell, T. M.; DesJarlais, R.; Roth, G. P.; Takahashi, H.; Moriarty, K. J.; *Bioorg. Med. Chem. Lett.* **2008**, *18*, 5541-5544.
- ²³ Moriarty, K. J.; Takahashi, H.; Pullen, S. S.; Khine, H. H.; Sellati, R. H.; Raymond, E. L.; Woska Jr., J. R.; Jeanfavre, D. D.; Roth, G. P.; Winters, M. P.; Qiao, L.; Ryan, D.; DesJarlais, R.; Robinson, D.; Wilson, M.; Bobko, M.; Cook, B. N.; Lo, H. Y.; Nemoto, P. A.; Kashem, M. A.; Wolak, J. P.; White, A.; Magolda, R. L.; Tomczuk, B. *Bioorg. Med. Chem. Lett.* **2008**, *18*, 5545-5549.
-

-
- ²⁴ Lo, H. Y.; Bentzien, J.; Fleck, R. W.; Pullen, S. S.; Khine, H. H.; Woska Jr., J. R.; Kugler, S. Z.; Kashem, M. A.; Takahashi, H. *Bioorg. Med. Chem. Lett.* **2008**, *18*, 6218-6221.
- ²⁵ Lo, H. Y.; Bentzien, J.; White, A.; Man, C. C.; Fleck, R. W.; Pullen, S. S.; Khine, H. H.; King, J.; Woska Jr., J. R.; Wolak, J. P.; Kashem, M. A.; Roth, G. P.; Takahashi, H. *Tetrahedron Lett.* **2008**, *49*, 7337-7340.
- ²⁶ Cook, B. N.; Bentzien, J.; White, A.; Nemoto, P. A.; Wang, J.; Man, C. C.; Soleymanzadeh, F.; Khine, H. H.; Kashem, M. A.; Kugler Jr., S. Z.; Wolak, J. P.; Roth, G. P.; De Lombaert, S.; Pullen, S. S.; Takahashi, H. *Bioorg. Med. Chem. Lett.* **2009**, *19*, 773-777.
- ²⁷ Riether, D.; Zindell, R.; Kowalski, J. A.; Cook, B. N.; Bentzien, J.; De Lombaert, S.; Thomson, D.; Kugler Jr., S. Z.; Skow, D.; Martin, L. S.; Raymond, E. L.; Khine, H. H.; O'Shea, K.; Woska Jr., J. R.; Jeanfavre, D.; Sellati, R.; Ralph, K. L. M.; Ahlberg, J.; Labissiere, G.; Kashem, M. A.; Pullen, S. S.; Takahashi, H. *Bioorg. Med. Chem. Lett.* **2009**, *19*, 1588-1591.
- ²⁸ Jurcak, J. G.; Barrague, M.; Gillespy, T. A.; Edwards, M. L.; Musick, K. Y.; Weintraub, P. M.; Du, Y.; Dharanipragada, R. M.; Parkar, A. A. *PCT Int. Appl.* **2005**, WO/2005/026175.
- ²⁹ Jurcak, J. G.; Barrague, M.; Gillespy, T. A.; Edwards, M. L.; Musick, K. Y.; Weintraub, P. M.; Du, Y.; Dharanipragada, R. M.; Parkar, A. A. *PCT US. Appl.* **2007**, US/2007/0254937.
- ³⁰ Alder, C. M.; Baldwin, I. R.; Barton, N. P.; Campbell, A. J.; Champigny, A. C.; Harling, J. D.; Maxwell, A. C.; Simpson, J. K.; Smith, I. E. D.; Tame, C. J.; Wilson, C.; Woolven, J. M. *PCT Int. Appl.* **2010**, WO/2010/106016.
- ³¹ Alder, C. M.; Baldwin, I. R.; Barton, N. P.; Campbell, A. J.; Champigny, A. C.; Harling, J. D.; Maxwell, A. C.; Simpson, J. K.; Smith, I. E. D.; Tame, C. J.; Wilson, C.; Woolven, J. M. *PCT Int. Appl.* **2011**, WO/2011/110575.
- ³² Heathcote, M.; Lucas, F. GlaxoSmithKline, unpublished work.
- ³³ Blood was obtained by venepuncture from human volunteers into heparin. All donors provided written informed consent for use of their samples, and the collection and use of the samples received Institutional Ethics Committee approval.
-

-
- ³⁴ Morley, J.; Felton, L. GlaxoSmithKline, unpublished work.
- ³⁵ All animal procedures were reviewed and approved by the GlaxoSmithKline Animal Care and Use Committee, and were performed in accredited facilities in accordance with institutional guidelines and the Guide for the Care and Use of Laboratory Animals (Institute of Laboratory Animal Resources, National Research Council).
- ³⁶ Grimley, R. GlaxoSmithKline, unpublished data.
- ³⁷ Graves, B.; Barrett, J. GlaxoSmithKline, unpublished work.
- ³⁸ Harling, J. D.; Smith, I. E. D.; Maxwell, A. C.; Champigny, A. C.; Tame, C. J.; Wilson, C. GlaxoSmithKline, unpublished work.
- ³⁹ Brown, K.; Long, J. M.; Vial, S. C.; Dedi, N.; Dunster, N. J.; Renwick, S. B.; Tanner, A. J.; Frantz, J. D.; Fleming, M. A.; Cheetham, G. M. *J. Biol. Chem.* **2004**, *279*, 18727-18732.
- ⁴⁰ Somers, D. GlaxoSmithKline, unpublished work.
- ⁴¹ Cozzini, P.; Fornabaio, M.; Marabotti, A.; Abraham, D. J.; Kellogg, G. E.; Mozzarelli, A. *Curr. Med. Chem.* **2004**, *11*, 1345-1359.
- ⁴² Biela, A.; Nasief, N. N.; Betz, M.; Heine, A.; Hangauer, D.; Klebe, G. *Angew. Chem. Int. Ed.* **2013**, *52*, 1822-1828.
- ⁴³ Zhang, J.; Yang, P. L.; Gray, N. S. *Nature Rev. Cancer* **2009**, *9*, 28-39.
- ⁴⁴ Discafani, C. M.; Carroll, M. L.; Floyd Jr., M. B.; Hollander, I. J.; Husain, Z.; Johnson, B. D.; Kitchen, D.; May, M. K.; Malo, M. S.; Minnick Jr., A. A.; Nilakantan, R.; Shen, R.; Wang, Y.-F.; Wissner, A.; Greenberger, L. M. *Biochemical Pharmacology* **1999**, *57*, 917-925.
- ⁴⁵ Fry, D. W.; Bridges, A. J.; Denny, W. A.; Doherty, A.; Greis, K. D.; Hickes, J. L.; Hook, K. E.; Keller, P. R.; Leopold, W. R.; Loo, J. A.; McNamara, D. J.; Nelson, J. M.; Sherwood, V.; Smaill, J. B.; Trumpp-Kallmeyer, S.; Dobrusin, E. M. *Proc. Natl. Acad. Sci. USA* **1998**, *95*, 12022-12027.
- ⁴⁶ Bose, P.; Ozer, H. *Expert Opin. Investig. Drugs* **2009**, *18*, 1735-1751.
- ⁴⁷ Smaill, J. B.; Palmer, B. D.; Rewcastle, G. W.; Denny, W. A.; MacNamara, D. J.; Dobrusin, E. M.; Bridges, A. J.; Zhou, H.; Showalter, H. H. D.; Winters, T.; Leopold,
-

-
- W. R.; Fry, D. W.; Nelson, J. M.; Slintak, V.; Elliot, W. L.; Roberts, B. J.; Vincent, P. W.; Patmore, S. J. *J. Med. Chem.* **1999**, *42*, 1803-1815.
- ⁴⁸ Singh, J.; Petter, R. C.; Baillie, T. A.; Whitty, A. *Nature Rev. Drug Discov.* **2011**, *10*, 307-317.
- ⁴⁹ Johnson, D. S.; Weerapana, E.; Cravatt, B. F. *Future Med. Chem.* **2010**, *2*, 949-964.
- ⁵⁰ Potashman, M. H.; Duggan, M. E. *J. Med. Chem.* **2009**, *52*, 1231-1246.
- ⁵¹ Robertson, J. G. *Biochemistry* **2005**, *44*, 5561-5571.
- ⁵² Van Der Ouderaa, F. J.; Buytenhek, M.; Nugteren, D. H.; Van Dorp, D. A. *Eur. J. Biochem.* **1980**, *109*, 1-8.
- ⁵³ Roth, G. J.; Stanford, N.; Majerus, P. W. *Proc. Natl. Acad. Sci. USA* **1975**, *72*, 3073-3076.
- ⁵⁴ Dewitt, D. L.; El-Harith, E. A.; Kraemer, S. A.; Andrews, M. J.; Yao, E. F.; Armstrong, R. L.; Smith, W. L. *J. Biol. Chem.* **1990**, *265*, 5192-5198.
- ⁵⁵ Jeffreys, D. *Aspirin: The Remarkable story of a Wonder Drug*, Bloomsbury, New York, **2004**.
- ⁵⁶ Fleming, A. *Br. J. Exp. Pathol.* **1929**, *10*, 226-236.
- ⁵⁷ Waxman, D. J.; Strominger, J. L. *Annu. Rev. Biochem.* **1983**, *52*, 825-869.
- ⁵⁸ Yocum, R. R.; Rasmussen, J. R.; Strominger, J. L. *J. Biol. Chem.* **1980**, *255*, 3977-3986.
- ⁵⁹ Olbe, L.; Carlsson, E.; Lindberg, P. *Nature Rev. Drug Discov.* **2003**, *2*, 132-139.
- ⁶⁰ Jarvis, L. *AstraZeneca Introduces Next Generation Prilosec* **2000**, <http://www.icis.com/Articles/2000/09/18/121771/astrazeneca-introduces-next-generation-prilosec.html> (accessed April 2013).
- ⁶¹ Besancon, M.; Simon, A.; Sachs, G.; Shin, J. M. *J. Biol. Chem.* **1997**, *272*, 22438-22446.
- ⁶² Shin, J. M.; Cho, Y. M.; Sachs, G. *J. Am. Chem. Soc.* **2004**, *126*, 7800-7811.
- ⁶³ Bhatt, D. L.; Topol, E. J. *Nature Rev. Drug Discov.* **2003**, *2*, 15-28.
- ⁶⁴ Savi, P.; Pereillo, J. M.; Uzabiaga, M. F.; Combalbert, J.; Picard, C.; Maffrand, J. P.; Pascal, M.; Herbert, J. M. *Thromb. Haemost.* **2000**, *84*, 891-896.
-

-
- ⁶⁵ Pereillo, J. M.; Maftouh, M.; Andrieu, A.; Uzabiaga, M. F.; Fedeli, O.; Savi, P.; Pascal, M.; Herbert, J. M.; Maffrand, J. P.; Picard, C. *Drug Metab. Dispos.* **2002**, *30*, 1288-1295.
- ⁶⁶ Dansette, P. M.; Libraire, J.; Bertho, G.; Mansuy, D. *Chem. Res. Toxicol.* **2009**, *22*, 369-373.
- ⁶⁷ Yusuf, S.; Zhao, F.; Mehta, S. R.; Chrolavicius, S.; Tognoni, G.; Fox, K. K. *N. Engl. J. Med.* **2001**, *345*, 494-502.
- ⁶⁸ Data retrieved from <http://www.drugs.com/top200.html> (accessed in April 2013).
- ⁶⁹ Kalgutkar, A. S.; Dalvie, D. K. *Expert Opin. Drug. Discov.* **2012**, *7*, 561-581.
- ⁷⁰ Bond, G. R. *Clin. Toxicol.* **2009**, *47*, 2-7.
- ⁷¹ Evans, D. C.; Watt, A. P.; Nicoll-Griffith, D. A.; Baillie, T. A. *Chem. Res. Toxicol.* **2004**, *17*, 3-16.
- ⁷² Kumar, S.; Kassahun, K.; Tschirret-Guth, R. A.; Mitra, K.; Baillie, T. A. *Curr. Opin. Drug Discov. Devel.* **2008**, *11*, 43-52.
- ⁷³ Penning, T. M. *Trends Pharmacol. Sci.* **1983**, *4*, 212-217.
- ⁷⁴ Rando, R. R. *Trends Pharmacol. Sci.* **1980**, *1*, 168-171.
- ⁷⁵ Walsh, C. *Tetrahedron* **1982**, *38*, 871-909.
- ⁷⁶ Jencks, W. P. *Adv. Enzymol. Relat. Areas Mol. Biol.* **1975**, *43*, 219-410.
- ⁷⁷ Menger, F. M. *Acc. Chem. Res.* **1985**, *18*, 128-134.
- ⁷⁸ Garuti, L.; Roberti, M.; Bottegoni, G. *Curr. Med. Chem.* **2011**, *18*, 2981-2994.
- ⁷⁹ Singh, J.; Petter, R. C.; Kluge, A. F. *Curr. Opin. Chem. Biol.* **2010**, *14*, 475-480.
- ⁸⁰ Barf, T.; Kaptein, A. *J. Med. Chem.* **2012**, *55*, 6243-6262.
- ⁸¹ Zhou, W.; Ecran, D.; Chen, L.; Yun, C. H.; Li, D.; Capelletti, M.; Cortot, A. B.; Chirieac, L.; Iacob, R. E.; Padera, R.; Engen, J. R.; Wong, K. K.; Eck, M. J.; Gray, N. S.; Janne, P. A. *Nature* **2009**, *462*, 1070-1074.
- ⁸² Denny, W. A. *Pharmacology & Therapeutics* **2002**, *93*, 253-261.
- ⁸³ Yun, C. H.; Mengwasser, K. E.; Toms, A. V.; Woo, M. S.; Greulich, H.; Wong, K. K.; Meyerson, M.; Eck, M. J. *Proc. Natl. Acad. Sci. U.S.A.* **2008**, *105*, 2070-2075.
- ⁸⁴ Smaill, J. B.; Rewcastle, G. W.; Loo, J. A.; Greis, K. D.; Chan, H. O.; Reyner, E. L.; Lipka, E.; Showalter, H. H. D.; Vincent, P. W.; Elliott, W. L.; Denny, W. A. *J. Med. Chem.* **2000**, *43*, 1380-1387.
-

-
- ⁸⁵ Li, D.; Ambrogio, L.; Shimamura, T.; Kubo, S.; Takahashi, M.; Chirieac, L. R.; Padera, R. F.; Shapiro, G. I.; Baum, A.; Himmelsbach, F.; Rettig, W. J.; Meyerson, M.; Solca, F.; Greulich, H.; Wong, K. K. *Oncogene* **2008**, *27*, 4702-4711.
- ⁸⁶ Tsou, H.-R.; Mamuya, N.; Johnson, B. D.; Reich, M. F.; Gruber, B. C.; Ye, F.; Nilakantan, R.; Shen, R.; Discafani, C.; DeBlanc, R.; Davis, R.; Koehn, F. E.; Greenberger, L. M.; Wang, Y.-F.; Wissner, A. *J. Med. Chem.* **2001**, *44*, 2719-2734.
- ⁸⁷ Kwak, E. L.; Sordella, R.; Bell, D. W.; Godin-Heymann, N.; Okimoto, R. A.; Brannigan, B. W.; Harris, P. L.; Driscoll, D. R.; Fidias, P.; Lynch, T. J.; Rabindran, S. K.; McGinnis, J. P.; Wissner, A.; Sharma, S. V.; Isselbacher, K. J.; Settleman, J. Haber, D. A. *Proc. Natl. Acad. Sci. USA* **2005**, *102*, 7665-7670.
- ⁸⁸ Heymach, J. V.; Nilsson, M.; Blumenschein, G.; Papadimitrakopoulou, V.; Herbst, R. *Clin. Cancer Res.* **2006**, *12*, 4441s-4445s.
- ⁸⁹ Felip, E.; Santarpia, M.; Rosell, R. *Expert Opin. Emerg. Drugs* **2007**, *12*, 449-460.
- ⁹⁰ Pan, Z.; Scheerens, H.; Li, S. J.; Schultz, B. E.; Sprengeler, P. A.; Burrill, L. C.; Mendonca, R. V.; Sweeney, M. D.; Scott, K. C. K.; Grothaus, P. G.; Jeffrey, D. A.; Spoerke, J. M.; Honigberg, L. A.; Young, P. R.; Dalrymple, S. A.; Palmer, J. T. *ChemMedChem* **2007**, *2*, 58-61.
- ⁹¹ Honigberg, L. A.; Smith, A. M.; Sirisawad, M.; Verner, E.; Loury, D.; Chang, B.; Li, S.; Pan, Z.; Thamm, D. H.; Miller, R. A.; Buggy, J. J. *Proc. Natl. Acad. Sci. USA* **2010**, *107*, 13075-13080.
- ⁹² Kluge, A. F.; Petter, R. C.; Tester, R. W.; Qiao, L.; Niu, D.; Westlin, W. F.; Singh, J.; Mazdinyasni, H. *PCT Int. Appl.* **2009**, WO2009/158571.
- ⁹³ Sheridan, C. *Nature Biotechnol.* **2012**, *30*, 199-200.
- ⁹⁴ Henise, J. C.; Taunton, J. *J. Med. Chem.* **2011**, *54*, 4133-4146.
- ⁹⁵ Perez, D. I.; Palomo, V.; Perez, C.; Gil, C.; Dans, P. D.; Luque, F. J.; Conde, S.; Martinez, A. *J. Med. Chem.* **2011**, *54*, 4042-4056.
- ⁹⁶ Perez, D. I.; Conde, S.; Perez, C.; Gil, C.; Simon, D.; Wandosell, F.; Moreno, F. J.; Gelpi, J. L.; Luque, F. J.; Martinez, A. *Bioorg. Med. Chem.* **2009**, *17*, 6914-6925.
- ⁹⁷ Cohen, M. S.; Zhang, C.; Shokat, K. M.; Taunton, J. *Science* **2005**, *308*, 1318-1321.
- ⁹⁸ Barton, N. P. GlaxoSmithKline, unpublished work.
-

-
- ⁹⁹ Version 2012.10 of the MOE software was used for the molecular modelling.
- ¹⁰⁰ Copeland, R. A. *Enzymes, A Practical Introduction to Structure, Mechanism and Data Analysis*, Ed. Wiley-VCH, New York, USA, 2nd edn, **2000**.
- ¹⁰¹ HTRF[®] KinEASE website. <http://www.htrf.com/htrf-kinase> (accessed April 2013).
- ¹⁰² Final compounds in this thesis were tested in the enzyme assays at a replicate level from 1 to 39.
- ¹⁰³ Freeman, H. N. M. GlaxoSmithKline, unpublished work.
- ¹⁰⁴ Crankshaw, M. W; Grant, G. A. *Current Protocols in Protein Science* **2001**, 15.1.1-15.1.18.
- ¹⁰⁵ Marks, B.; Lebakken, C.; Riddle, S.; Somberg, R.; Hereley, S.: http://tools.invitrogen.com/content/sfs/posters/Determination_of_Drug-Kinase_Residence_Time_in_a_Homogenous_Low-Volume_Format_v2.pdf, accessed the 4th of April 2011.
- ¹⁰⁶ Chaudry, L.; Nye, C. GlaxoSmithKline, unpublished work.
- ¹⁰⁷ Kitz, R.; Wilson, I. B. *J. Biol. Chem.* **1962**, 237, 3245-3249.
- ¹⁰⁸ Deakin, A. GlaxoSmithKline, unpublished work.
- ¹⁰⁹ Chromatographic logD at pH = 7.4 measured by HPLC, Analytical Department, GlaxoSmithKline, unpublished work.
- ¹¹⁰ Sabota, C.; Kumara, K. A.; Meuniera, S.; Mioskowski, C. *Tetrahedron Lett.* **2007**, 48, 3863-3866.
- ¹¹¹ Compound **31** is commercially available from companies such as Fluorochem (CAS 412923-40-1).
- ¹¹² Huheey, J. E. *J. Phys. Chem.* **1965**, 69, 3284-3291.
- ¹¹³ Huheey, J. E. *J. Phys. Chem.* **1966**, 70, 2086-2092.
- ¹¹⁴ One replicate returned a pIC₅₀ value of < 4.56.
- ¹¹⁵ The structure has been deposited in the Protein Data Bank with accession number 4KIO.
- ¹¹⁶ Carmi, C.; Cavazzoni, A.; Vezzosi, S.; Bordi, F.; Vacondio, F.; Silva, C.; Rivara, S.; Lodola, A.; Alfieri, R. R.; La Monica, A.; Galletti, M.; Ardizzoni, A.; Petronini, P. G.; Mor, M. *J. Med. Chem.* **2010**, 53, 2038-2050.
-

-
- ¹¹⁷ Wissner, A.; Overbeek, E.; Reich, M. F.; Floyd, M. B.; Johnson, B. D.; Mamuya, N.; Rosfjord, E. C.; Discafani, C.; Davis, R.; Shi, X.; Rabindran, S. K.; Gruber, B. C.; Ye, F.; Hallett, W. A.; Nilakantan, R.; Shen, R.; Wang, Y.-F.; Greenberger, L. M.; Tsou, H.-R. *J. Med. Chem.* **2003**, *46*, 49-63.
- ¹¹⁸ Considine, J. L.; Daigneault, S.; Chew, W.; Iera, S.; Duncan, S. M.; Ren, J. *PCT Int. Appl.* **2004**, WO2004/066919A2.
- ¹¹⁹ pKa calculated *in silico* using the ACD pKa calculator software version 11.
- ¹²⁰ LogD calculated *in silico* using the ACD software version 11.
- ¹²¹ Ring, R. N.; Tesoro, G. C.; Moore, D. R. *J. Org. Chem.* **1967**, *32*, 1091-1094.
- ¹²² Similar data were observed for compound **47b** - data not shown.
- ¹²³ Wolfe, J. P.; Ahman, J.; Sadighi, J. P.; Singer, R. A.; Buchwald, S. L. *Tetrahedron Lett.* **1997**, *38*, 6367-6370.
- ¹²⁴ Brodbeck, B.; Pullmann, B.; Schmitt, S.; Nettekoven, M. *Tetrahedron Lett.* **2003**, *44*, 1675-1678.
- ¹²⁵ Guram, A. S.; Rennels, R. A.; Buchwald, S. L. *Angew. Chem., Int. Ed.* **1995**, *34*, 1348-1350.
- ¹²⁶ Wolfe, J. P.; Buchwald, S. L. *J. Org. Chem.* **1996**, *61*, 1133-1135.
- ¹²⁷ Louie, J.; Hartwig, J. F. *Tetrahedron Lett.* **1995**, *36*, 3609-3612.
- ¹²⁸ Surry, D. S.; Buchwald, S. L. *Angew. Chem., Int. Ed.* **2008**, *47*, 6338-6361.
- ¹²⁹ Kantchev, E. A. B.; O'Brien, C. J.; Organ, M. G. *Angew. Chem., Int. Ed.* **2007**, *46*, 2768-2813.
- ¹³⁰ Kataoka, N.; Shelby, Q.; Stambuli, J. P.; Hartwig, J. F. *J. Org. Chem.* **2002**, *67*, 5553-5566.
- ¹³¹ For a review of amination reaction conditions using phosphine ligands, see: Surry, D. S.; Buchwald, S. L. *Chem. Sci.* **2011**, *2*, 27-50.
- ¹³² Old, D. W.; Wolfe, J. P.; Buchwald, S. L. *J. Am. Chem. Soc.* **1998**, *120*, 9722-9723.
- ¹³³ Huang, X. H.; Anderson, K. W.; Zim, D.; Jiang, L.; Klapars, A.; Buchwald, S. L. *J. Am. Chem. Soc.* **2003**, *125*, 6653-6655.
- ¹³⁴ Wolfe, J. P.; Tomori, H.; Sadighi, J. P.; Yin, J. J.; Buchwald, S. L. *J. Org. Chem.* **2000**, *65*, 1158-1174.
-

-
- ¹³⁵ Charles, M. D.; Schultz, P.; Buchwald, S. L. *Org. Lett.* **2005**, *7*, 3965-3968.
- ¹³⁶ Amatore, C.; Jutand, A. *Coord. Chem. Rev.* **1998**, *178-180*, 511-528.
- ¹³⁷ Mace, Y.; Kapdi, A. R.; Fairlamb, I. J. S.; Jutand, A. *Organometallics* **2006**, *25*, 1795-1800.
- ¹³⁸ Maiti, D.; Fors, B. P.; Henderson, J. L.; Nakamura, Y.; Buchwald, S. L. *Chem. Sci.* **2011**, *2*, 57-68.
- ¹³⁹ Fors, B. P.; Watson, D. A.; Biscoe, M. R.; Buchwald, S. L. *J. Am. Chem. Soc.* **2008**, *130*, 13552-13554.
- ¹⁴⁰ Anderson, K. W.; Tundel, R. E.; Ikawa, T.; Altman, R. A.; Buchwald, S. L. *Angew. Chem., Int. Ed.* **2006**, *45*, 6523-6527.
- ¹⁴¹ For a review of Pd-NHC catalysts, see: Assen, E.; Kantchev, B.; O'Brien, C. J.; Organ, M. G. *Angew. Chem., Int. Ed.* **2007**, *46*, 2768-2813.
- ¹⁴² Caddick, S.; Cloke, F. G. N.; Clentsmith, G. K. B.; Hitchcock, P. B.; McKerrecher, D.; Titcomb, L. R.; Williams, M. R. V. *J. Organomet. Chem.* **2001**, *617*, 635-639.
- ¹⁴³ Viciu, M. S.; Germameau, R. F.; Navarro, O.; Stevens, E. D.; Nolan, S. P. *Organometallics* **2002**, *21*, 5470-5472.
- ¹⁴⁴ Viciu, M. S.; Navarro, O.; Germameau, R. F.; Kelly III, R. A.; Sommer, W.; Marion, N.; Stevenas, E. D.; Cavallo, L.; Nolan, S. P. *Organometallics* **2004**, *23*, 1629-1635.
- ¹⁴⁵ Navarro, O.; Kaur, H.; Mahjoor, P.; Nolan, S. P. *J. Org. Chem.* **2004**, *69*, 3173-3180.
- ¹⁴⁶ Viciu, M. S.; Germaneau, R. F.; Nolan, S. P. *Org. Lett.* **2002**, *4*, 4053-4056.
- ¹⁴⁷ Marion, N.; Navarro, O.; Mei, J.; Stevens, E. D.; Scott, N. M.; Nolan, S. P. *J. Am. Chem. Soc.* **2006**, *128*, 4101-4111.
- ¹⁴⁸ Cawley, M. J.; Cloke, F. G. N.; Fitzmaurice, R. J.; Pearson, S. E.; Scott, J. S.; Caddick, S. *Org. Biomol. Chem.* **2008**, *6*, 2820-2825.
- ¹⁴⁹ Data is a result of 10 tests with one replicate not defined.
- ¹⁵⁰ The PBMC assay was performed following a slightly different protocol but the data reported were comparable (within experimental error) to that described for previous inhibitors.
-

-
- ¹⁵¹ Heathcote, M.; Pell, T. GlaxoSmithKline, unpublished work.
- ¹⁵² Gibbon, R. GlaxoSmithKline, unpublished work.
- ¹⁵³ Ordway, D.; Henao-Tamayo, M.; Orme, I. M.; Gonzalez-Juarrero, M. *J. Immunol.* **2005**, *175*, 3873-3881.
- ¹⁵⁴ Serajuddin, A. T. M. *Adv. Drug Deliv. Rev.* **2007**, *59*, 603-616.
- ¹⁵⁵ Reed, I. GlaxoSmithKline, unpublished work.
- ¹⁵⁶ Anderson, B. D.; Flora, K. P. in C.G. Wermuth (Ed.) *The Practice of Medicinal Chemistry*, Academic Press, London, **1996**, 739-754.
- ¹⁵⁷ Willacy, R. GlaxoSmithKline, unpublished work.
- ¹⁵⁸ Patton, J. S. *Adv. Drug Deliv. Rev.* **1996**, *19*, 3-36.
- ¹⁵⁹ Kutach, A. K.; Villasenor, A. G.; Lam, D.; Belunis, C.; Janson, C.; Lok, S.; Hong, L. N.; Liu, C. M.; Deval, J.; Novak, T. J.; Barnett, J. W.; Chu, W.; Shaw, D.; Kuglstatter, A. *Chem. Biol. Drug Des.* **2010**, *76*, 154-163.
- ¹⁶⁰ Waring, M. J.; Johnstone, C. *Bioorg. Med. Chem. Lett.* **2007**, *17*, 1759-1764.
- ¹⁶¹ Cavalli, A.; Poluzzi, E.; De Ponti, F.; Recanatini, M. *J. Med. Chem.* **2002**, *45*, 3844-3853.
- ¹⁶² Cianchetta, G.; Li, Y.; Kang, J.; Rampe, D.; Fravolini, A.; Cruciani, G.; Vaz, R. J. *Bioorg. Med. Chem. Lett.* **2005**, *45*, 3637-3642.
- ¹⁶³ Buyck, C.; Tollenaere, J.; Engels, M.; De Clerck, F. *The 14th European Symposium on Quantitative Structure-Activity Relationships*: Bournemouth, UK, 2002.
- ¹⁶⁴ Sanguinetti, M. C.; Jiang, C.; Curran, M. E.; Keating, M. T. *Cell* **1995**, *81*, 299-307.
- ¹⁶⁵ Pearlstein, R.; Vaz, R.; Rampe, D. *J. Med. Chem.* **2003**, *46*, 2017-2022.
- ¹⁶⁶ Ploemen, J. P.; Kelder, J.; Hafmans, T.; van de Sandt, H.; van Burgsteden, J. A.; Salemink, P. J.; van Esch, E. *Exp. Toxicol. Pathol.* **2004**, *55*, 347-355.
- ¹⁶⁷ Tomizawa, K.; Sugano, K.; Yamada, H.; Horii, I. *J. Toxicol. Sci.* **2006**, *31*, 315-324.
- ¹⁶⁸ Hanumegowda, U. M.; Wenke, G.; Regueiro-Ren, A.; Yordanova, R.; Corradi, J. P.; Adams, S. P. *Chem. Res. Toxicol.* **2010**, *23*, 749-755.
-

-
- ¹⁶⁹ Most of the various amines were later prepared with the 4-aminopiperidine linker and, as expected, these compounds possessed weaker irreversible ITK inhibitor profiles compared to the (*S*)-3-aminopyrrolidine linker.
- ¹⁷⁰ Data obtained for the formic acid salt of compound **107**, which was obtained by purification of compound **107** by mass directed automated preparative HPLC using a formic acid modifier.
- ¹⁷¹ Values obtained for the maleic acid salt of compound **107** (*i.e.* compound **107a**).
- ¹⁷² Valko, K.; Du, C. M.; Bevan, C.; Reynolds, D. P.; Abraham, M. H. *Curr. Med. Chem.* **2001**, *8*, 1137-1146.
- ¹⁷³ Giffen, P. S. GlaxoSmithKline, unpublished work.
- ¹⁷⁴ Mortelmans, K.; Zeiger, E. *Mutat. Res.* **2000**, *455*, 29-60.
- ¹⁷⁵ Clements, J. *Mutat. Res.* **2000**, *455*, 97-110.
- ¹⁷⁶ McCann, J.; Choi, E.; Yamasaki, E.; Ames, B. N. *Proc. Natl. Acad. Sci. U.S.A.* **1975**, *72*, 5135-5139.
- ¹⁷⁷ Hakura, A.; Suzuki, S.; Satoh, T. *Mutat. Res.* **1999**, *438*, 29-36.
- ¹⁷⁸ Hastwell, P. GlaxoSmithKline, unpublished work.
- ¹⁷⁹ Smart, K. GlaxoSmithKline, unpublished work.
- ¹⁸⁰ DEREK software predicted the Michael acceptor to be genotoxic (https://www.lhasalimited.org/derek_nexus/), accessed the 8th of April 2011.
- ¹⁸¹ Krenske, E. H.; Petter, R. C.; Zhu, Z.; Houk, K. N. *J. Org. Chem.* **2011**, *76*, 5074-5081.
- ¹⁸² These data were obtained from a slightly different PBMC assay: the PBMCs were activated with Cytostim for 30 minutes prior to adding the compounds. IFN- γ was measured in supernatants following 72 hour incubation time.
- ¹⁸³ Data is a result of two tests with one replicate not defined.
- ¹⁸⁴ Krawczyk, H. *Synth. Commun.* **1995**, *25*, 641-650.
- ¹⁸⁵ Wissner, A.; Tsou, H.-R.; Johnson, B. D.; Hamann, P. R.; Zhang, N. *European Patent Office* **2004**, EP1000039(B1).
- ¹⁸⁶ Data is a result of 8 tests with one replicate not defined.
- ¹⁸⁷ Wheeler, R. GlaxoSmithKline, unpublished work.
- ¹⁸⁸ Sneddon, H.; Fisher, G.; Inglis, G. GlaxoSmithKline, unpublished work.
-

-
- ¹⁸⁹ Klose, J.; Bienert, M.; Mollenkopf, C.; Wehle, D.; Zhang, C.-W.; Carpino, L. A.; Henklein, P. *Chem. Commun.* **1999**, *18*, 1847-1848.
- ¹⁹⁰ Escher, R.; Bünning, P. *Angew. Chem., Int. Ed.* **1986**, *25*, 277-278.
- ¹⁹¹ Dunetz, J. R.; Xiang, Y.; Baldwin, A.; Ringling, R. *Org. Lett.* **2011**, *13*, 5048-5051.
- ¹⁹² Coste, J.; Le-Nguyen, D.; Castro, B. *Tetrahedron Lett.* **1990**, *31*, 205-208.
- ¹⁹³ El-Faham, A.; Subirós-Funosas, R.; Prohens, R.; Albericio, F. *Chem. Eur. J.* **2009**, *15*, 9404-9416.
- ¹⁹⁴ Foster, G. GlaxoSmithKline, unpublished work.
- ¹⁹⁵ Taylor, K. M. G.; Pancholi, K.; Wong, D. Y. T. *Pharm. Pharmacol. Commun.* **1999**, *5*, 255-257.
- ¹⁹⁶ Timsina, M. P.; Martin, G. P.; Marriott, C.; Ganderton, D.; Yianneskis, M. *International Journal of Pharmaceutics* **1994**, *101*, 1-13.
- ¹⁹⁷ Davies, P. J.; Hanlon, G. W.; Molyneux, A. J. *J. Pharm. Pharmac.* **1976**, *28*, 908-911.
- ¹⁹⁸ Rasenack, N.; Steckel, H.; Muller, B. W. *J. Pharm. Sci.* **2003**, *92*, 35-44.
- ¹⁹⁹ GSK Stevenage Inhaled Science Group, GlaxoSmithKline, unpublished work.
- ²⁰⁰ Chaumeil J. C. *Meth. Find. Exp. Clin. Pharmacol.* **1998**, *20*, 211-215.
- ²⁰¹ Amiji, M. M.; Sandmann, B. J. *Applied Chemical Pharmacy*, McGraw-Hill Education, Europe, **2002**.
- ²⁰² Dedrick, R. L. *J. Pharmacokinet. Biopharm.* **1973**, *1*, 435-461.
- ²⁰³ Mordenti, J. *J. Pharm. Sci.* **1986**, *75*, 1028-1040.
- ²⁰⁴ Houston, J. B. *Biochem. Pharmacol.* **1994**, *47*, 1469-1479.
- ²⁰⁵ Obach, R. S.; Baxter, J. G. Liston, T. E.; Silber, B. M.; Jones, B. C.; Macintyre, F.; Rance, D. J. Wastall, P. *J. Pharmacol. Exp. Ther.* **1997**, *283*, 46-58.
- ²⁰⁶ Lave, T.; Coassolo, P.; Reigner, B. *Clin. Pharmacokinet.* **1999**, *36*, 211-231.
- ²⁰⁷ Ward, K. W.; Smith B. R. *Drug. Metab. Dispos.* **2004**, *32*, 603-611.
- ²⁰⁸ Deakin, A.; Ball, D.; Butterfield, L. GlaxoSmithKline, unpublished work.
- ²⁰⁹ Harris, M. C.; Huang, X.; Buchwald, S. L. *Org. Lett.* **2002**, *4*, 2885-2888.
- ²¹⁰ Uргаonkar, S.; Verkade, J. G. *Adv. Synth. Cat.* **2004**, *346*, 611-616.
- ²¹¹ Shen, Q.; Ogata, T.; Hartwig, J. F. *J. Am. Chem. Soc.* **2008**, *130*, 6586-6596.
-

-
- ²¹² Jean, L.; Rouden, J.; Maddaluno, J.; Lasne, M.-C. *J. Org. Chem.* **2004**, *69*, 8893-8902.
- ²¹³ Slade, D. J.; Pelz, N. F.; Bodnar, W.; Lampe, J. W.; Watson, P. S. *J. Org. Chem.* **2009**, *74*, 6331-6334.
- ²¹⁴ Beria, I.; Valsasina, B.; Brasca, M. G.; Ceccarelli, W.; Colombo, M.; Cribioli, S.; Fachin, G.; Ferguson, R. D.; Fiorentini, F.; Gianellini, L. M.; Giorgini, M. L.; Moll, J. K.; Posterl, H.; Pezzetta, D.; Roletto, F.; Sola, F.; Tesei, D.; Caruso M. *Bioorg. Med. Chem. Lett.* **2010**, *20*, 6489-6494.
- ²¹⁵ Paul, F.; Patt, J.; Hartwig, J. F. *Organometallics* **1995**, *14*, 3030-3039.
- ²¹⁶ Shen, Q.; Shekhar, S.; Stambuli, J. P.; Hartwig, J. F. *Angew. Chem., Int. Ed.* **2005**, *44*, 1371-1375.
- ²¹⁷ Strieter, E. R.; Blackmond, D. G.; Buchwald, S. L. *J. Am. Chem. Soc.* **2003**, *125*, 13978-13980.
- ²¹⁸ Strieter, E. R.; Buchwald, S. L. *Angew. Chem., Int. Ed.* **2006**, *45*, 925-928.
- ²¹⁹ Note that precatalyst **86** and **L**¹ are available from Aldrich but in small quantities and with long delivery times.
- ²²⁰ Hamann, B. C.; Hartwig, J. F. *J. Am. Chem. Soc.* **1998**, *120*, 7369-7370.
- ²²¹ Ogata, T.; Hartwig, J. F. *J. Am. Chem. Soc.* **2008**, *130*, 13848-13849.
- ²²² Klinkenberg, J. L.; Hartwig, J. F. *J. Am. Chem. Soc.* **2010**, *132*, 11830-11833.
- ²²³ Hartwig, J. F., Personal Communication, November 2011.
- ²²⁴ Vo, G. D.; Hartwig, J. F. *J. Am. Chem. Soc.* **2009**, *131*, 11049-11061.
- ²²⁵ Alvaro, E.; Hartwig, J. F. *J. Am. Chem. Soc.* **2009**, *131*, 7858-7868.
- ²²⁶ Barton, N. P.; Campos, S. A.; Carr, R. A.; Harling J. D.; Smith, I. E. D. *PCT Int. Appl.* **2012**, WO/2012/035055.
- ²²⁷ Harling, J. D.; Deakin, A. M.; Campos, S.; Grimley, R.; Chaudry, L.; Nye, C.; Polyakova, O.; Bessant, C. M.; Barton, N.; Somers, D.; Barrett, J.; Graves, R. H.; Hanns, L.; Kerr, W. J.; Solari, R. *J. Biol. Chem.* **2013**, *288*, 28195-28206.
- ²²⁸ Zapf, C. W.; Gerstenberger, B. S.; Xing, L.; Limburg, D. C.; Anderson, D. R.; Caspers, N.; Han, S.; Aulabaugh, A.; Kurumbail, R.; Shakya, S.; Li, X.; Spaulding, V.; Czerwinski, R. M.; Seth, N.; Medley, Q. G. *J. Med. Chem.* **2012**, *55*, 10047-10063.
-

²²⁹ Schirok, H.; Li-Sommer, Y.; Brands, M.; Lobell, M.; Tersteegen, A.; Himmel, H.; Schlemmer, K.-H.; Lang, D.; Petersen, K.; Renz, M.; Mumberg, D.; Hoffmann, J.; Siemeister, G.; Bomer, U. *PCT Int. Appl.* **2009**, WO/2009/033581 A1.